

INVESTIGATION OF A NOVEL SUBSET OF TNFR2 EXPRESSING REGULATORY T CELL IN LUNG DISEASES

Presented by

Rohimah Mohamud

Submitted in total fulfilment of the requirements of the degree of

Doctor of Philosophy

March 2014

Department of Immunology

Faculty of Medicine, Nursing and Health Sciences

Monash University

Principal Supervisor: Professor Magdalena Plebanski

Co-supervisors: Professor Robyn O’Hehir

Professor Jennifer Rolland

Dr. Charles Hardy

In the name of God, the Beneficent, the Merciful

By time,

Indeed, mankind is in loss,

Except for those who have believed and done righteous deeds and

Advised each other to truth and advised each other to patience.

Al-Quran 103 (1-3)

Copyright

Notice 1

Under the Copyright Act 1968, this thesis must be used only under the normal conditions of scholarly fair dealing. In particular no results or conclusions should be extracted from it, nor should it be copied or closely paraphrased in whole or in part without the written consent of the author. Proper written acknowledgement should be made for any assistance obtained from this thesis.

Notice 2

I certify that I have made all reasonable efforts to secure copyright permissions for third party content included in this thesis and have not knowingly added copyright content to my work without the owner's permission.

Rohimah Mohamud

24 March 2014

Acknowledgement

In the name of Allah, the Most Generous and the Most Merciful.

First and foremost, gratitude and appreciation are for Allah, the Most Merciful and Most Compassionate for granting me a precious opportunity to come to Australia in January 2009 until now (March 2014) for the completion of my PhD and for granting me health, strength and motivation for the realisation of this endeavour. My five years as a PhD student have been a special period of my life (and family) to remember; thanks to people around me who have motivated, inspired and encouraged me to reach my goal. I especially would like to thank:

Professor Magdalena Plebanski, my main supervisor. I feel highly indebted for your scholarly guidance and generosity in assisting me in the preparation of this thesis. I feel intense gratitude for your support throughout this five years' journey, not just in completing my study but in all aspects of life. Thank you also for always keeping your door open.

I also wish to record my sincere thanks to **Dr. Charles Hardy**, as my co-supervisor, for his comments, suggestions and support given at the beginning of the research and throughout this study. I like one of your comments: “read it aloud to yourself, does it makes sense?”, which made me think a thousand times before sending any drafts to you. Many thanks also go to **Emeritus Professor Jennifer Rolland** and **Professor Robyn O’Hehir** for their advice and endless support. It is truly a privilege to have them as my

supervisors and I am extremely grateful for their assistance. Many thanks also go to **Dr. Sue Xiang** for her advice and for sharing our motherhood skill.

I also would like to record my appreciation to my colleagues in the Allergy Research Group and Vaccine and Infectious Diseases Laboratory. My appreciation goes to **Jeanne LeMasurier** for her courage and support, to take turns on counting the cells when we had hundreds of samples, to wake me up early in the morning to acquire my FACS samples and to accompany me working at crazy hours. My appreciation goes to **John Yao** for his truly super-duper assistance in collecting mice organs for me. It took me 6 minutes to collect all organs, but he did this in less than 3 minutes; I really envy his super efficiency. Not to forget, other Allergy Research Group members, **Je Lin, Sara, Astrid, Jodie, Tracy, Neeru, Thomas** and **Angela** for all their support. For **Hong-An Nguyen**, thank you for being so helpful when working together on follistatin experiments.

I wish to acknowledge the generous support of **Chindu Govindaraj** for constant support and advice. The simple message “Hi Ima” made me realise that I have a really truly friend out there who cared for me. Thank you very much Chindu for always being so caring and helpful, and sharing our ups and downs! To **Ying Ying**, your motivation in doing experiments and writing up papers has highly inspired me. To **Mutsa**, thank you for always being so positive and for your great sense of humour bringing excitement to our group. I also would like to thank **Alison, Steph, Kristy, Gao** and **Je Lin** for being supportive lab members. To **Pin Shie**, my one and only Malaysian friend in the department, ‘terima kasih atas segala perkongsian suka duka sepanjang perkenalan kita’.

I also wish to acknowledge the generous support of all previous members of the Allergy Research Group and Vaccine and Infectious Diseases (**Karen, Anja, Tanya, Anthony**). Thank you all for creating such a nice working atmosphere and for sharing all your knowledge.

Last but not least I owe my greatest debt of gratitude to my beloved husband, **Hisham** for his patience, endurance, understanding, spiritual, and material support in accompanying me and living in Australia. In fact, no words can express his devoted sacrifices, as they are innumerable. Thank you for preparing lunches for me and the children, washing the dishes, minding our little baby Hana, folding the clothes, lots more to list; without your assistance and encouragement it would not have been possible for me to finish my study. Also gratitude to my beautiful princesses, **Fatin, Shahirah, Alissa** and **Hana**; all the charm from them makes my PhD life even more exciting and meaningful. To my little Hana, cuddling you and looking at your eyes and smile gave me strength and motivation to finish my PhD.

Nor do I forget my deepest gratitude to my parents' constant prayers and spiritual support which always motivated me to complete this work. My sincere thanks also goes to my siblings and my friends for their encouragement and support, to whom I am immensely indebted.

Finally my appreciation is extended to the staff of the Department of Immunology, Monash University, Melbourne, for their support throughout my study.

Dedication

This thesis is dedicated to:

My beloved husband, Mohd Shamsul Hisham...

For endless LOVE

My beloved children, Fatin Shahirah, Fatin Shakirah, Alissa Shafiyah and Hana

Mawaddah

For making me SMILE and extra BUSY

My parents, Mohamud Awg Kechik and Siti Bidah Loman...and my parents-in-law,

Mat Hassan Latfi Mamat and Rofiah Husin...

For continual PRAYER and SPIRITUAL support

General Declaration

Monash University

Declaration for thesis based or partially based on conjointly published or unpublished work

In accordance with Monash University Doctorate Regulation 17 Doctor of Philosophy and Research Master's regulations the following declarations are made:

I hereby declare that this thesis contains no material which has been accepted for the award of any other degree or diploma at any university or equivalent institution and that, to the best of my knowledge and belief, this thesis contains no material previously published or written by another person, except where due reference is made in the text of the thesis.

This thesis includes 4 results chapters with 1 accepted publication, 2 submitted unpublished publications and 1 traditional thesis chapter on work that is yet to be submitted for publication. The core theme of the thesis is investigation on the nature of regulatory T cells in lung diseases. The ideas, development and writing up of all the papers in the thesis were the principal responsibility of me, the candidate, working within the Department of Immunology under the supervision of Prof. Magdalena Plebanski, Dr. Charles Hardy, Prof. Robyn O'Hehir and Emeritus Prof. Jennifer Rolland.

In the case of Chapter 3, 4, 5 and 6 my contribution to the work involved the provision of all data, the analysis and compilation of that data into figure format (except where due

reference is made in the text), the writing, editing and submission of all components of the paper. Contributions of student co-authors included provision of techniques and assisting in experimental procedures.

Chapter	Publication/Chapter title	Publication status	Nature and extent of candidate's contribution	
1 (Literature Review)	'The effects of engineered nanoparticles on pulmonary immune homeostasis' (Original paper attached in Appendices)	Accepted (Manuscript attached in Appendix)	RM wrote the paper 80 %	
3 (Result Chapter 1)	'The Activin A antagonist follistatin inhibits asthmatic airway remodelling' (Original paper attached in Appendices)	Accepted (Manuscript attached in Appendix)	RM designed, performed and analysed experiments 10 %	
	Modulation of lung Treg by follistatin during allergic airway inflammation	Presented as a traditional thesis chapter	RM designed, performed and analysed experiments 80 %	
4 (Result Chapter 2)	The role of TNFR2 expressing Treg in maintaining homeostasis in the lung during allergic airway inflammation	Presented as a traditional thesis chapter		
5 (Result Chapter 3)	The effects of PS50G on TNFR2 expressing Treg in the lung during allergic airway inflammation	To be submitted by 30 th April 2014	RM wrote the paper, designed, performed and analysed experiments	80 %
6 (Result Chapter 4)	The effects of LPS on TNFR2 expressing Treg in the lung during acute lung injury	Submitted		80 %

I have renumbered sections of submitted or published papers in order to generate a consistent presentation within the thesis.

Rohimah Mohamud

24 March 2014

Presentations, Publications and Awards

Results reported in this thesis have been published, submitted for publication and presented at scientific meetings as follows:

Publications

1. Hardy C. L., H. A. Nguyen, **R. Mohamud**, J. Yao, D. Y. Oh, M. Plebanski, K. L. Loveland, C. A. Harrison, J. M. Rolland, and R. E. O'Hehir. 2012. The activin A antagonist follistatin inhibits asthmatic airway remodelling. *Thorax* 68: 9-18.
2. Hardy C. L., J. S. Lemasurier, **R. Mohamud**, J. Yao, S. D. Xiang, J. M. Rolland, R. E. O'Hehir, and M. Plebanski. 2013. Differential Uptake of Nanoparticles and Microparticles by Pulmonary APC Subsets Induces Discrete Immunological Imprints. *J Immunol* 191:5278-90
3. **Mohamud, R.**, S. D. Xiang, C. Selomulya, J. M. Rolland, R. E. O'Hehir, C. L. Hardy, and M. Plebanski. 2013. The effects of engineered nanoparticles on pulmonary immune homeostasis. *Drug Metab Rev* 1:1-15.

Submitted manuscripts

1. **Mohamud, R.**, J. L. Sieow, J. S. Lemasurier, S. D. Xiang, J. Yao, J. M. Rolland, R. E. O'Hehir, C. L. Hardy, and M. Plebanski. Synthetic nanoparticles which promote persistently enhanced TNF receptor 2 expressing regulatory T cell levels in the lung generate resistance to allergic airways inflammation. *Submitted*.

2. **Mohamud, R.**, J. S. Lemasurier, S. D. Xiang, J. Yao, J. M. Rolland, R. E. O’Hehir, C. L. Hardy, and M. Plebanski. Exposure to lipopolysaccharide alters the proliferative and suppressor function of TNFR2⁺ and TNFR2⁻ regulatory T cells in the lung. *Submitted.*

Other manuscripts (Attached in Appendix)

1. **Mohamud, R.**, J. S. Lemasurier, S. D. Xiang, J. Yao, R. M. Slattery, J. M. Rolland, R. E. O’Hehir, C. L. Hardy, and M. Plebanski. Instillation of lipopolysaccharides locally in the lung alters TNFR2⁺Foxp3⁺ Treg that involve in inhibition of allergic asthma in a mouse model. *In preparation.*

2. **Mohamud, R*.**, Y.Y. Kong*, J. S. Lemasurier, J. L. Seiow, T. D. Karlson, S. D. Xiang, J. Yao, J. M. Rolland, R. E. O’Hehir, C. L. Hardy, and M. Plebanski. The lack of inflammatory effects of engineered nanoparticles in *in vitro* and *in vivo* models shows potential as disease therapeutics. *To be submitted by 30th April.*

* Equal contribution.

Conference presentations (poster)

1. ‘Follistatin treatment alters regulatory T cells proportions during chronic allergic airway inflammation’ was presented as a poster presentation at the Alfred Week 2009 (19-23 October 2009; Alfred Hospital, Melbourne, Australia) and at the Australasian Society for Immunology (6-10 December 2009; Gold Coast, Queensland, Australia).

Authors: Hong-An Nguyen, **Rohimah Mohamud**; John Yao, Jennifer Rolland, Robyn O’Hehir, Magdalena Plebanski, Charles Hardy.

2. 'Airway instillation with LPS induces a dose-dependent increase in CD25⁺Foxp3⁺ Treg in the lung and draining lymph node of naïve mice' was presented as a poster presentation at the International Congress of Immunology, Kobe, Japan (22-27 August 2010) and at the Alfred Week 2010 (18-22 October 2010; Alfred Hospital, Melbourne, Australia).

Authors: **Rohimah Mohamud**, Jeanne LeMasurier, John Yao, Jennifer Rolland, Robyn O'Hehir, Charles Hardy, Magdalena Plebanski.

3. 'LPS-induced airway inflammation transiently alters the distribution of TNF receptor II-positive Foxp3⁺ regulatory T cells in the lung' was presented as a poster presentation at the Keystone Symposium: Immunoregulation Networks (1-5 April 2011, Breckenridge, Colorado, U.S.A).

Authors: **Rohimah Mohamud**, Jeanne LeMasurier, John Yao, Jennifer Rolland, Robyn O'Hehir, Charles Hardy, Magdalena Plebanski.

4. 'Engineered 50 nm nanoparticles alter lung TNFR2⁺Foxp3⁺ regulatory T cells and might be responsible for inhibition of lung inflammation' was presented as a poster presentation at the Alfred Week 2013 (19-23 October 2013; Alfred Hospital, Melbourne, Australia) and 50th Immunology Symposium (4 October 2013; Melbourne, Australia).

Authors: **Rohimah Mohamud**, Jeanne LeMasurier, Je L. Sioew, John Yao, Jennifer Rolland, Robyn O'Hehir, Charles Hardy, Magdalena Plebanski.

5. 'Lipopolysaccharides and PS50G exhibit their therapeutics effects on allergic asthma mouse model that act via modulation on TNFR2⁺Foxp3⁺ Treg' will be presented as a poster at the 5th Australasian Vaccine and Immunotherapeutics Development Meeting (7-9 May 2014, Burnet Institute, Melbourne, Australia).

Authors: **Rohimah Mohamud**, Jeanne S. LeMasurier, John Yao, Jennifer M. Rolland, Robyn E. O’Hehir, Charles L. Hardy, Magdalena Plebanski.

Conference presentations (poster and oral)

1. ‘Regulatory T cells expressing TNFR2 in the lung have altered proliferative and suppressor function in LPS treated mice’ was presented as an oral presentation at the IgV Roadshow- AMREP/Monash Clayton (10 September 2012; Melbourne, Australia) and as a poster and oral presentation at the Australasian Society for Immunology (2-5 December 2012; Melbourne, Australia).

Authors: **Rohimah Mohamud**, Jeanne LeMasurier, John Yao, Jennifer Rolland, Robyn O’Hehir, Charles Hardy, Magdalena Plebanski.

2. ‘Engineered 50 nm nanoparticles alter lung TNFR2+Foxp3+ regulatory T cells and might be responsible for inhibition of lung inflammation’ was presented as a poster and oral presentation at the 4th International NanoMedicine Conference, Sydney, Australia (1-3 June 2013) and Australasian Society for Immunology (2-5 December 2013; Wellington, New Zealand)

Authors: **Rohimah Mohamud**, Jeanne LeMasurier, Je L. Sioew, John Yao, Jennifer Rolland, Robyn O’Hehir, Charles Hardy, Magdalena Plebanski.

Awards/Scholarships

1. January 2009 - July 2012: PhD Scholarship from Ministry of Higher Education Malaysia and Universiti of Sains Malaysia.

2. January 2010 - January 2011: PhD Top-up Scholarship from CRC - Asthma and Airways Australia.
3. August 2010: *Postgraduate International Travel Award* from CRC - Asthma and Airways to attend the International Congress of Immunology, Kobe, Japan (22-27 August 2010)
4. August 2010: *Travel Bursary* from International Congress of Immunology Travel Committee to attend the International Congress of Immunology, Kobe, Japan (22-27 August 2010).
5. April 2011: *Postgraduate International Travel Award* from CRC- Asthma and Airways to attend Keystone Symposium: Immunoregulation Networks, Breckenridge, Colorado, U.S.A (1-5 April 2011).
6. December 2012: *Conference Bursary* from Immunology Group of Victoria (IgV) to attend the Australasian Society for Immunology, Melbourne, Australia (2-5 December 2012).
7. June 2013: *Conference Bursary* from the Australian Nanotechnology Network (ANN) to attend the 4th International NanoMedicine Conference, Sydney, Australia (1-3 June 2013).

Table of Contents

Copyright	iv
Acknowledgement	v
Dedication	viii
General Declaration.....	ix
Presentations, Publications and Awards.....	xii
List of Abbreviations	xxii
Abstract.....	xxv
Chapter 1	1
Literature review.....	1
1.1 Overview	2
1.2 Acute lung injury.....	2
1.3 Allergic asthma	3
1.4 Development of mouse models of lung diseases	5
1.4.1 LPS-induced ALI mouse model.....	7
1.4.2 Acute allergic asthma mouse model	8
1.4.3 Chronic allergic asthma mouse model.....	9
1.5 Pulmonary immune homeostasis: Lung inflammation and immunity	10
1.6 Treg mediated modulation of immune responses.....	11
1.6.1 Identification and mechanisms of action of Treg.....	12
1.6.2 Regulation of Treg frequency and function during lung diseases	22
1.6.3 TNF-TNFR2 interaction on Treg.....	25
1.7 The effects of LPS, nanoparticles and follistatin on lung immune responses.....	28
1.7.1 The effects of LPS on immune responses in the lung.....	29

1.7.2	The effects of engineered nanoparticles on lung immune responses.....	31
1.7.3	The effects of follistatin on lung immune responses	34
1.8	Summary	36
1.9	Project hypothesis and aims	37
2	Chapter 2.....	39
	Materials and methods	39
2.1	Materials.....	40
2.1.1	Mice	40
2.1.2	Chemicals and reagents.....	40
2.1.3	Sterilized, deionized distilled water	42
2.1.4	Fluorochrome-labelled antibodies	42
2.1.5	RPMI medium.....	43
2.2	Methods.....	44
2.2.1	OVA immunisation and challenge protocol	46
2.2.2	Recombinant follistatin.....	46
2.2.3	Follistatin treatment in chronic AAI model	47
2.2.4	Preparation of nanoparticles	47
2.2.5	Blood and tissue collection	48
2.2.6	Cytospins.....	49
2.2.7	ELISA for TGF- β , IL-4, IL-5 and IL-13	49
2.2.8	OVA-specific IgE ELISA	50
2.2.9	Cytokine ELISPOT	51
2.2.10	FlowCytomix assay.....	52
2.2.11	Cell surface and intracellular staining.....	52

2.3	Statistical analysis	53
3	Chapter 3.....	55
	Modulation of lung Treg by follistatin during allergic airway inflammation	55
3.1	Introduction	56
3.2	Experimental Procedures.....	58
3.3	Results	60
3.3.1	Follistatin treatment altered cells numbers in BAL fluid, lung-draining LN and lung 60	
3.3.2	Follistatin treatment decreased serum OVA-specific IgE but not eosinophil absolute numbers	62
3.3.3	Follistatin treatment did not alter the cytokine profile of LN cells.....	64
3.3.4	Follistatin treatment altered Activin A and TGF- β levels in the BAL fluid.....	66
3.3.5	High dose follistatin decreased lung CD4 ⁺ CD25 ⁺ Treg (at week 3), but did not alter Foxp3 expression.....	68
3.3.6	High dose follistatin increased lung-draining LN CD4 ⁺ CD25 ⁺ Treg (at all time points), but did not alter Foxp3 expression	70
3.3.7	Follistatin treatment increased BAL IL-10 at week 5.....	72
3.4	Discussion	74
3.5	Summary	78
4	Chapter 4.....	79
	The role of TNFR2 expressing regulatory T cells in maintaining homeostasis in the lung during allergic airway inflammation	79
4.1	Introduction	80
4.2	Experimental Procedures.....	81

4.2.1	Immunisation	81
4.2.2	CD25 and TNFR2 cell sorting	82
4.2.3	Treg functional assays.....	82
4.3	Results	83
4.3.1	TNFR2 ⁺ Foxp3 ⁺ Treg in the steady state in the lung	83
4.3.2	TNFR2 ⁺ Foxp3 ⁺ Treg in resolving AAI.....	91
4.4	Discussion	103
4.5	Summary	107
5	Chapter 5.....	109
	The effects of PS50G on TNFR2 expressing regulatory T cells in the lung during allergic airway inflammation	109
5.1	Manuscript.....	111
5.2	Summary	144
6	Chapter 6.....	145
	The effects of LPS on TNFR2 expressing regulatory T cells in the lung during lung injury.....	145
6.1	Manuscript.....	147
6.2	Summary	177
7	Chapter 7.....	179
	General Discussion.....	179
7.1	Introduction	180
7.2	Main outcomes of this thesis.....	180
7.3	The importance of Treg in the lung.....	183
7.3.1	Treg mechanisms in maintaining lung homeostasis	184

7.3.2	Altered Treg numbers and function lead to imbalanced lung immunological responses.....	187
7.4	Differences in the effects of LPS and nanoparticles on lung immunity.....	188
7.5	The role of follistatin, nanoparticles and LPS on Treg in preventive and therapeutic treatments of lung inflammation.....	191
7.5.1	Follistatin as a therapeutic treatment of lung inflammation	191
7.5.2	LPS as a therapeutic treatment of lung inflammation.....	192
7.5.3	Nanoparticles as a therapeutic treatment of lung inflammation	193
7.6	Final conclusion	195
8	References	197
9	Appendices	221
	(Published and unpublished Manuscripts)	221
9.1	Unpublished manuscript 1	222
9.2	Unpublished manuscript 2.....	268

List of Abbreviations

AAI	Allergic airway inflammation
AHR	Airway hyperresponsiveness
Alum	Aluminium hydroxide gel
ALI	Acute lung injury
APC	Antigen presenting cell(s)
ARDS	Acute respiratory distress syndrome
AMP	Adenosine monophosphate
ATP	Adenosine triphosphate
BAL	Broncho-alveolar lavage
BFA	Brefeldin A
CD	Cluster of differentiation
CFSE	Carboxyl fluorescein diacetate succinimidyl ester
CNT	Carbon nanotube
Con A	Concanavalin A
COPD	Chronic obstructive pulmonary disease
cpm	counts per minute
CTLA-4	Cytotoxic T lymphocyte antigen 4
DC	Dendritic cells
DTH	Delayed-type hypersensitivity
EDAC	1-ethyl (3-dimethylaminopropyl) carbodiimide
EDTA	Ethylenediaminetetraacetic acid
ELISA	Enzyme-linked immunosorbent assay
EliSpot	Enzyme-linked immunospot assay
ENP	Engineered nanoparticles
FCS	Foetal calf serum
Foxp3	Forkhead box transcription factor 3
FS	Follistatin
FSH	Follicle stimulating hormone
GARP	Glycoprotein A repetitions predominant
GITR	Glucocorticoid-induced TNF-related protein
H&E	Haematoxylin and eosin

HBSS	Hanks Balanced Salt Solution
HDM	House dust mite
HEPES	4-(2-hydroxyethyl)-1-piperazineethanesulfonic acid
ICOS	Inducible T cell co-stimulator
IFN- γ	Interferon-gamma
IgE	Immunoglobulin E
IgG	Immunoglobulin G
IHC	Immunohistochemistry
IL	Interleukin
i.n.	Intranasal
i.p.	Intraperitoneal
i.t.	Intratracheal intubation
iTreg	Induced regulatory T cells
LAP	Latency associated peptide
LN	Lymph node(s)
LPS	lipopolysaccharides
mAb	Monoclonal antibody
NLR	Nucleotide-binding domain leucine-rich repeat
NK cells	Natural killer cells
nTreg	Naturally occurring regulatory T cells
OVA	Ovalbumin
PAS	Periodic Acid Schiff
PBS	Phosphate-buffered saline
PD-1	Programmed cell death protein 1
ROS	Reactive oxygen species
RPMI	Roswell Park Memorial Institute
RT	Room temperature
Sal	Saline
SMA	Smooth muscle actin
TACI	TNF-alpha-converting enzyme
TCR	T-cell receptor
Teff	Effector T cell(s)
TGF- β	Transforming growth factor- β

Th cell	T-helper cell
TiO ₂	Titanium dioxide
TLR	Toll-like receptor
TNF	Tumor necrosis factor
TNFR1	Tumor necrosis factor receptor 1
TNFR2	Tumor necrosis factor receptor 2
TNFRSF	Tumor necrosis factor receptor super family
Treg	Regulatory T cell(s)
WT	Wild type

Abstract

The immune system in the lung employs various mechanisms to maintain and restore lung homeostasis and protect the host against exacerbated responses to various environmental stimuli. The existence of CD3⁺CD4⁺CD25⁺ regulatory T cells (Treg) that actively suppress the function of T effector cells (Teff) is a key mechanism by which the immune system limits inappropriate or excessive inflammatory responses. In acute and chronic airway inflammation (e.g. allergen induced airway inflammation), Teff secreted various pro-inflammatory cytokines including activin A, TGF- β , IL-4, IL-5 and IL-13 that skew immune response towards T helper 2 cells (Th2). Lung exposure to cytokine antagonist (e.g. biological factors such as follistatin that bind activin A) decreased lung inflammatory responses with an increase in Treg, reflecting the therapeutics effects of targeting pro-inflammatory cytokines. In acute lung injury [e.g. lipopolysaccharides (LPS)-induce acute lung injury], the immune response was skewed towards Th17 cells that secreted higher levels of IL-17 together with other pro-inflammatory cytokines such as TNF, IL-1 α and IL-6. Excessive pro-inflammatory cytokines secreted in the lung modify lung equilibrium of Teff and Treg altering their characteristics (e.g. proliferative capacity and function) in that microenvironment. An imbalance in Treg/Teff ratios led to the induction of acute inflammatory responses (e.g. lung injury or allergic airway inflammation) that fully resolved a month after exposure to stimuli. After the inflammation resolved, Treg/Teff ratios returned to homeostatic levels. Lung exposure to inert engineered materials [polystyrene 50 nm nanoparticles (PS50G)] did not only induce lung immune activation, however it also pre-conditioned for an increase in the frequency and the suppressive capacity of lung TNFR2 expressing Treg (i.e. increased the levels of suppressor molecules). Experimental data suggests that lung exposure to bacterial

products (e.g. LPS) and PS50G protects individuals from developing allergic airway inflammation. PS50G facilitated an increase in the quantity and quality of lung TNFR2 expressing Treg which were perfectly positioned to respond rapidly to allergenic challenges and restored lung immune homeostasis. Therefore, targeting highly bioactive TNFR2 expressing Treg poses a new therapeutic avenue to promote healthy lung homeostasis. Overall, the novel findings of the effects of follistatin, LPS and engineered PS50G on TNFR2 expressing Treg may increase the chances that these stimuli will translate to new generic treatment for lung inflammation, particularly allergic diseases.

Chapter 1

Literature review

1.1 Overview

Lung diseases including acute lung injury (ALI), and allergic asthma, are due to a complex interplay between inflammatory cells, particularly neutrophils and eosinophils, lymphocytes and antigen presenting cells such as dendritic cells (DC), and macrophages. These cells can produce multiple pro-inflammatory mediators, including cytokines, chemokines and reactive oxygen species (ROS) in response to environmental and endogenous stimuli. During homeostasis, lung innate and adaptive immune cells are able to distinguish self from non-self, while still being able to respond appropriately to pathogens. In some diseases, diverse endogenous immune suppressor and anti-inflammatory mechanisms that amplify and perpetuate inflammation can be further engaged; resulting in an imbalance of the immune system.

1.2 Acute lung injury

Acute Lung Injury (ALI), known as Acute Respiratory Distress Syndrome (ARDS), is a life-threatening condition with an incidence of 86.2 per 100,000 person-years and an appreciable mortality (Ware and Matthay, 2000). Major characteristics of ALI in humans include neutrophil influx, microvascular protein leakage, hyaline membrane formation, and synthesis of pro-inflammatory mediators followed by severe lung damage (Goodman et al., 1996, Sibille and Reynolds, 1990, Weiland et al., 1986). The types of ALI can be differentiated into direct (pulmonary) and indirect (non-pulmonary). It was reported that 57 % of all pulmonary ALI is caused mainly by pneumonia, aspiration, and lung trauma, whereas 43 % of non-pulmonary ALI is caused by non-pulmonary sepsis and trauma (Bersten et al., 2002). In addition to lung damage, ALI and its more severe form ARDS, often lead to organ failure (Ware and Matthay, 2000) (Table 1). ARDS results from

excessive inflammation and oxidative stress, which are essential components of the body's response to infection and injury. Every year, there are an estimated 190,600 cases of ALI and 74,500 deaths in the United States, with reported 30-40 % mortality (Rubenfeld et al., 2005). This incidence in the United States overall (17-64 per 100,000 person-years) seems to be higher than in Europe, Australia, and other developed countries (17-34 per 100,000 person-years) (MacCallum and Evans, 2005). Even if death does not occur, the disruption of epithelial and endothelial integrity in the lung requires repair and this can result in lung fibrosis in the longer term. Healing requires fibrosis, but uncontrolled fibrosis can severely impair lung function, leading to chronic respiratory failure and death.

1.3 Allergic asthma

Allergic reactions can manifest clinically as anaphylaxis, allergic asthma, allergic rhinitis and atopic dermatitis. Allergic asthma, that is underpinned by allergic airway inflammation (AAI), is a complex syndrome with many clinical phenotypes in both adults and children. Major characteristics of allergic asthma include a variable degree of airflow obstruction, bronchial hyperresponsiveness and airway inflammation. Asthma “attacks” are episodic but the airway inflammation underlying this problem is typically persistent. Genetic susceptibility and environmental influences such as timing and dose of allergen and co-exposure to infection are the main factors for allergic asthma (Balkissoon, 2008).

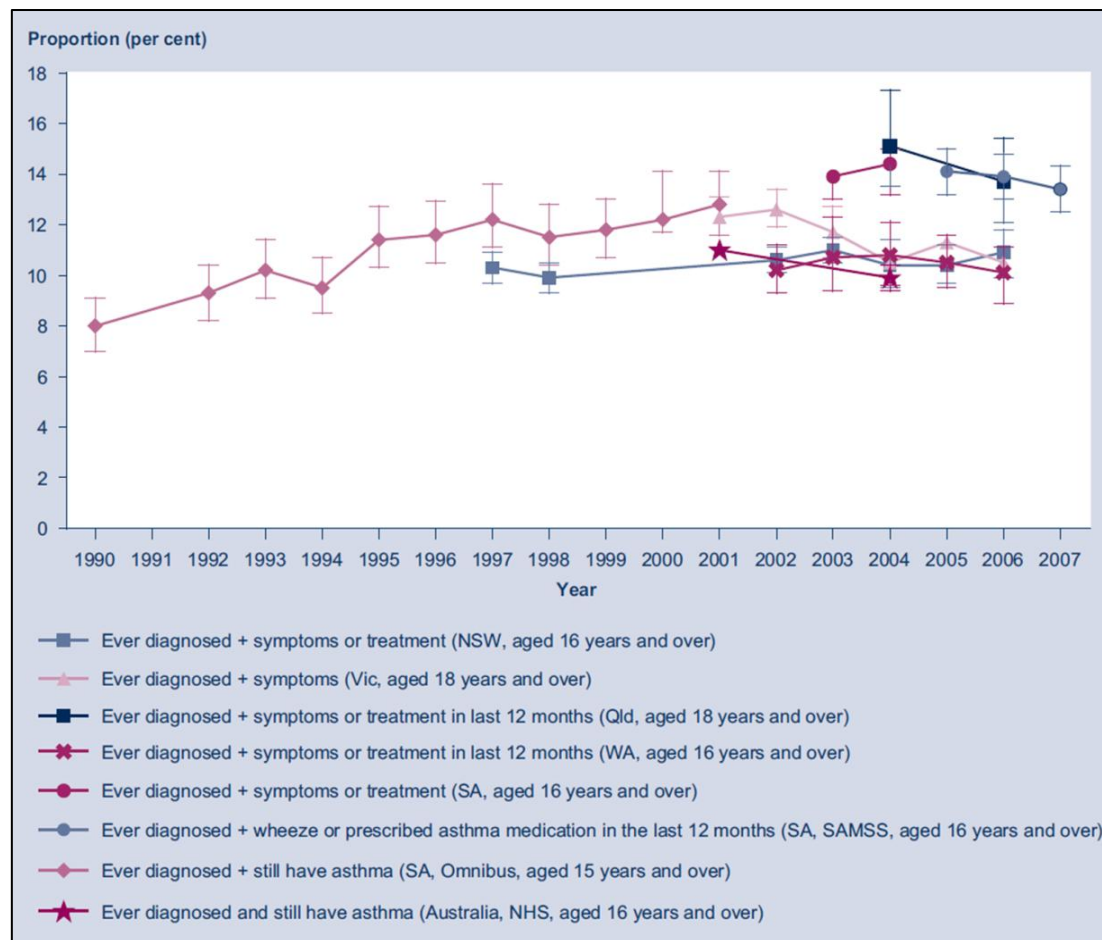
Human ALI and characteristics	Animal models of ALI
<p>Histopathological characterisations:</p> <ul style="list-style-type: none"> • Neutrophilic alveolitis • Injury of the alveolar epithelium and endothelium • Hyaline membrane formation • Microvascular thrombi <p>Clinical features:</p> <ul style="list-style-type: none"> • Acute onset • Diffuse bilateral alveolar injury • Acute oxidative phase • Repair with fibrosis 	<p>LPS-induced ALI:</p> <ul style="list-style-type: none"> • Neutrophilic inflammatory response • Increase in intrapulmonary cytokines <p>Bleomycin-induced ALI:</p> <ul style="list-style-type: none"> • Acute inflammatory injury followed by reversible fibrosis <p>Intrapulmonary bacteria-induced ALI:</p> <ul style="list-style-type: none"> • Increased permeability • Interstitial edema • Neutrophilic alveolitis

Table 1: ALI symptoms in human and animal models. No single animal model reproduces all of the characteristics of ALI/ARDS in humans. Even though LPS- and bleomycin- and intrapulmonary bacteria-induced ALI models are relevant for only limited aspects of human ALI/ARDS, the characteristics of these models are well understood, and the results are interpreted within the limits of these specific models. Adapted from (Matute-Bello et al., 2008).

Important changes in the prevalence of allergic asthma have been noted over the past 20–30 years; during the 1980s and early 1990s, there was a substantial worldwide increase in the prevalence of asthma (Pearce et al., 2007). However, in recent years, this increasing trend appears to have plateaued (Asher et al., 2006, Eder et al., 2006). Allergic asthma currently affects about 5-10 % of the world population with a rising incidence and prevalence in industrialised countries. In Australia, the prevalence is amongst the highest in the world: 10 to 15% of children and 10 to 12 % of adults have allergic asthma. In 2004-2005, the overall prevalence of allergic asthma in Australia was estimated at 10.2 % (equivalent to 2,010,212 people) (Figure 1). This prevalence decreased slightly in children and young adults, but remained unchanged in older adults, when compared to 2001. In recent years, the prevalence of allergic asthma in Australia has decreased in people aged less than 35 years old, but has remained unchanged among people aged 35 years and over [data from a survey by European Community Respiratory Health Survey (1996)]. Mortality rates of allergic asthma in Australia are relatively high on an international scale. Similar mortality rates are reported for the English- speaking countries such as United States, United Kingdom and New Zealand. However, non-English speaking countries including Japan, France, Germany, Spain and Poland have lower rates of allergic asthma mortality [data from a survey by European Community Respiratory Health Survey (1996)].

1.4 Development of mouse models of lung diseases

Although many animal species do not naturally develop human respiratory diseases, some asthma traits can be invoked by specific stimulation. Animal models have been used to elucidate the pathophysiology of lung diseases as well as to evaluate novel therapeutic targets. Much of the understanding of the laboratory animals such as guinea pigs, rats



Key points extracted from the graph:

- Among those aged 0-14 years, the prevalence of asthma is higher among boys than girls, but among those aged 15 years and over, current asthma is more prevalent in females than males.
- Among adults, there was a decrease in the proportion classified as having severe asthma between 1999 and 2006, but the majority of adults with asthma have mild or very mild forms.

Figure 1: Asthma statistics and characteristics in Australia. Asthma remains a significant health problem in Australia, with prevalence rates that are high by international standards and commonly coexists with other chronic conditions. Adapted from a report by Australian Centre for Asthma Monitoring; Asthma Series no. 3. Cat. no. ACM 14 (2008).

and mice. The main advantages of laboratory animals such as mice are their highly characterized immune systems, the availability of transgenic mice and, more importantly, the well-defined protocols and a wide array of specific reagents for analysis of the pathophysiology of this disease. The development and characteristics of these mouse models are discussed in the following sections.

1.4.1 LPS-induced ALI mouse model

Different animal models of experimental ALI have been used to investigate mechanisms of lung injury and to mimic ALI features in humans. However, none of these models completely reproduce all the features of human ALI (Matute-Bello et al., 2008). Lipopolysaccharide (LPS) that is ubiquitously present in our living environment, is a cell wall component of Gram-negative bacteria that is composed of a polar lipid head group (lipid A) and a chain of repeating disaccharides (Kelley et al., 1998). LPS has been widely used to induce lung injury and to allow examination of components of the inflammatory response (Mei et al., 2007, Rojas et al., 2005). A well-established mouse model of ALI is induced by the instillation of LPS (D'Alessio et al., 2009, Matute-Bello et al., 2008, Mei et al., 2007) with an LPS dose selected to create sufficient injury, but with an acceptable mortality to allow study of resolution. LPS can be administered to the lungs by direct intratracheal administration, aerosol form or by intranasal deposition. In general, LPS inhalation induces neutrophil recruitment, pulmonary edema and, finally, impairment of gas exchange (Matute-Bello et al., 2008), whereas recruitment of neutrophils is the key event in development of ALI (Matute-Bello et al., 2008, Ware and Matthay, 2000, Grommes et al., 2012).

1.4.2 Acute allergic asthma mouse model

Since mice do not naturally develop allergic asthma, traits of asthma need to be induced in mice. In order to sensitise the mice, allergens in the presence of T helper 2 (Th2) adjuvant, particularly aluminium hydroxide, are systemically administered to the mice, which usually takes about 14-21 days [as reviewed in (Nials and Uddin, 2008)]. This is followed by several allergen challenges for several consecutive days, to develop a challenge phase. Many key features of clinical allergic asthma are exhibited in this acute AAI model: including elevated levels of IgE, airway inflammation, goblet cell hyperplasia, epithelial hypertrophy and airway hyperresponsiveness (AHR) to specific stimuli. The development of acute AAI in mice differs between mouse strains, for different allergens, methods of sensitisation, routes and duration of challenge as well as the approach to assessing the host immune response (Kumar et al., 2008, Zosky and Sly, 2007). Although the approaches are different, and may develop some characteristic variations, the basic model is consistent. The most commonly used strain to develop this model is BALB/c as this strain is more Th2-biased (Boyce and Austen, 2005). Other strains such as C57BL/6 and A/J also have been used successfully in allergen challenge studies (as reviewed in (Kumar et al., 2008)). Different allergens have been used to induce a Th2-skewed immune response in mice. Ovalbumin (OVA) derived from chicken egg is a frequently used allergen (Hardy et al., 2012a), even though it is less implicated in human asthma (as reviewed in (Kumar et al., 2008)). Some researchers have used other allergens with greater clinical relevance in humans, such as house dust mite (HDM) and cockroach extracts (Sarpong et al., 2003, Johnson et al., 2004). However, acute model induced by their antigens are not adequate to present the features of chronic airway inflammation observed in patients with asthma, since these features develop over longer periods of allergen exposure (Kips et al., 2003, Ramos-Barbon et al., 2004). Thus, some

research groups have investigated chronic allergen exposure in mice involving repeated exposure of airways to low levels of allergen for periods up to 12 weeks (Fernandez-Rodriguez et al., 2008, Temelkovski et al., 1998).

1.4.3 Chronic allergic asthma mouse model

The development of a chronic AAI mouse model would need further to reproduce more features of clinical asthma in an established pulmonary inflammatory setting, such as airway remodeling, persistent AHR, subepithelial fibrosis, hypertrophy and hyperplasia of smooth muscle and neovascularisation (Jain et al., 2003, Kumar and Foster, 2002, Hardy et al., 2013c). As mentioned in the previous section, the development of chronic AAI mouse model would also involve sensitisation and challenge phases, but with repeated exposure to low levels of allergen up 12 weeks, to induce the changes of airway wall remodeling. The development of such a model would depend on the strain, route and dose of allergen as these are the factors for the induction of tolerance (McMillan and Lloyd, 2004, Shinagawa and Kojima, 2003). Shinagawa *et al.* have shown that A/J mice exhibited a stable chronic AAI as A/J mice do not develop T cell tolerance when challenged chronically compared to BALB/c and C57BL/6 mice (Shinagawa and Kojima, 2003). The development of T cell tolerance (only occur in animal sensitised without the presence of adjuvant) reduces the inflammatory response to repeated antigen challenges as in BALB/c and C57BL/6 mice which results in unstable chronic AAI. Kumar *et al.* suggested that T cell tolerance is induced by high mass concentrations of allergen and in their model mice were exposed to inhalation of controlled mass concentrations of aerosolised antigen to minimise tolerance (Kumar et al., 2008). Unlike acute AAI which resolves after the final allergen challenge, some of the key features of the chronic AAI such as airway remodeling have been shown to persist after the final challenge in a

number of models (Johnson et al., 2004, McMillan and Lloyd, 2004). However, in these models, discrepancies in airway remodeling and lung inflammation result from the different protocols employed, as mentioned earlier.

1.5 Pulmonary immune homeostasis: Lung inflammation and immunity

The lung is exposed to a myriad of innocuous antigens on a daily basis and must maintain a state of immune ignorance or tolerance to these stimuli to retain pulmonary homeostasis and to prevent potentially fatal immunopathology. The pulmonary immune homeostasis is controlled by a complex network of cells and molecules. The healthy airways in man and mouse are dominated by alveolar macrophages (> 95 %) (Steinmuller et al., 2000). Alveolar macrophages are functionally different from phenotypically identical counterparts elsewhere, in that they act by several suppressive pathways that, in combination, limit their responsiveness to external stimuli (Wissinger et al., 2009). The balance of innate immunity (natural or native) and adaptive immunity (specific or acquired) in the lung microenvironment is central to maintaining lung homeostasis and healthy lung function.

The lung can be confronted by a diverse range of environmental stimuli including allergens, particles and LPS. These stimuli are also taken up by antigen presenting cells (APC) in secondary peripheral lymphoid compartments, subsequently modulating immune responses (Reddy et al., 2007). Lung APC are crucial for the induction of both innate and adaptive immunities (Condon et al., 2011). Both immunities are closely interlinked, since innate immunity can stimulate, modulate and mature the subsequent antigen-specific adaptive immunity (Janeway and Bottomly, 1994). Antigen presenting

DC, the sentinels of the immune system, are found throughout the respiratory tract epithelium, and are involved in the priming and differentiation of naïve T cells in response to inhaled antigens (Condon et al., 2011, Lambrecht and Hammad, 2009). Usually, pulmonary DC that take up inhaled antigens induce tolerance to non-inflammatory substances, and initiate immunity against potentially harmful pathogens such as bacteria, viruses, fungi and parasites which trigger inflammatory ‘danger signals’. Macrophages and DC express pattern recognition receptors on their surface [e.g. Toll-like receptors (TLR); nucleotide-binding domain leucine-rich repeat (NLR) such as Nalp3; scavenger receptors etc.] which recognize bacterial ‘danger signals’ and trigger inflammatory cytokine and chemokine production. Indeed the expression of TLR2 and TLR4 on pulmonary macrophages is involved in the recognition of fine and coarse ambient particles (Shoenfelt et al., 2009). In addition, Nalp3, is also crucial for sensing asbestos fibres and particulate silica, leading to the induction of the inflammatory cytokine interleukin (IL)-1 β and activation of the innate immune response (Dostert et al., 2008). A complex network of other immune cells and molecules also exists in the lung to help maintain lung homeostasis, e.g. regulatory T cells (Treg) and B cells. Together with APC, these immunoregulatory networks are crucial in maintaining lung function and homeostasis; either induction of tolerance towards inert ‘harmless’ inhaled substances or protective immunity against invading pathogens (Randall, 2010).

1.6 Treg mediated modulation of immune responses

Most biologic systems are subject to complex regulatory controls and the immune system is not an exception. T cells play an important role in the immune response because they can function as both effector cells (cell-mediated responses) and helper cells (cell- and humoral-mediated immune response). These T cells are able to recognise antigens of

intracellular microbes and mount a response to destroy these microbes and the infected cells. ALI and allergic responses are mainly orchestrated by cytokines released from T effector cells (Teff). The magnitude of these responses must be controlled by other mechanisms mediated by other types of Teff. In addition to Teff that up-regulate immune responses, other populations down-regulate immune responses. One such population has been identified as Treg. Treg are also needed to control potentially pathogenic self-reactive cells. This is due to the fact that the immune system can also recognise self-antigens that have escaped from positive selection in the thymus and entered the periphery. A Treg is functionally defined as a T cell that inhibits an immune response by regulating the activation of other immune cells. They control the reactivity of self-aggressive T cells that are not eliminated in the thymus and potentially damaging inflammatory or toxic environmental antigens in the periphery (Sakaguchi, 2000, Belkaid, 2007, O'Garra and Vieira, 2004) Thus, these cells are responsible for keeping the immune system in homeostatic balance.

1.6.1 Identification and mechanisms of action of Treg

It is important to identify Treg surface markers for confirming purity and enrichment of viable Treg for functional studies. It was initially reported that transfer of purified CD4⁺ T cells that expressed CD25 inhibited naïve CD4-cell-mediated autoimmunity in lymphopenic mice, and the lack of CD4⁺CD25⁺ cells was also responsible for the autoimmunity developed in neonatally thymectomised mice (Sakaguchi, 2000). This shows the importance of the CD25 marker to identify functional Treg. However, utilisation of CD25 to define Treg, especially in human, is problematic as activated effector and memory cells also upregulate CD25 on their surface (Karamatsu et al., 2012). Moreover, expression of CD25 on B cells (Amu et al., 2006) and DC (Fontenot et al.,

2005a) can further confound the results obtained upon CD25-depletion by using anti-CD25 antibodies. This prompted investigators to search for more specific Treg markers. Forkhead box transcription factor 3 (Foxp3) has been identified as a master regulator of Treg function and a specific marker for murine CD4⁺ Treg (Hori et al., 2003a). As reviewed in (Chen and Oppenheim, 2011c), besides the transcription marker Foxp3, it is clear now that Treg express a panel of co-stimulatory/co-inhibitory molecules (including CD28, Cytotoxic T-Lymphocyte Antigen 4 [CTLA-4 or CD152], Inducible T-cell Co-Stimulator [ICOS or CD278] and Programmed Cell Death Protein 1 [PD-1]), Tumor Necrosis Factor (TNF) receptor super family (TNFRSF) members (TNFR2, Glucocorticoid-Induced TNFR-related Protein [GITR], OX40 [CD134], 4-1BB ligand and Fas [CD95]), chemokine receptors (C-C chemokine receptors type 2-8 [CCR2, -4, -5, -6, -7 and -8], CXC chemokine receptors [CXCR3 and -4, etc.]) and TLR (TLR including TLR1, -2, -4, -5, -6, -7, -8 and -9). Other markers that are expressed by Treg are the proliferative markers Ki67, Helios, Latency associated peptide (LAP), Glycoprotein-A Repetitions Predominant (GARP), CD39 and CD73. Some Treg markers used in this thesis are described more fully in the following section and Figure 2.

1.6.1.1 Foxp3: the key controller of Treg development and function

Foxp3 has been identified as a master regulator of Treg function and a specific marker for murine CD4⁺ Treg (Hori et al., 2003b, Khattri et al., 2003, Fontenot et al., 2005b). This intracellular marker is predominantly expressed by CD4⁺CD25⁺ Treg (Fontenot et al., 2003, Hori et al., 2003b, Pace et al., 2012, Pietruczuk et al., 2012), the population of CD4⁺ T cells that can suppress the proliferation and cytokine production of T cell receptor (TCR)-stimulated conventional CD4⁺ T cells (Sakaguchi et al., 1995, Choi et al., 2013). Other T cell subsets in the mouse do not express detectable Foxp3 expression

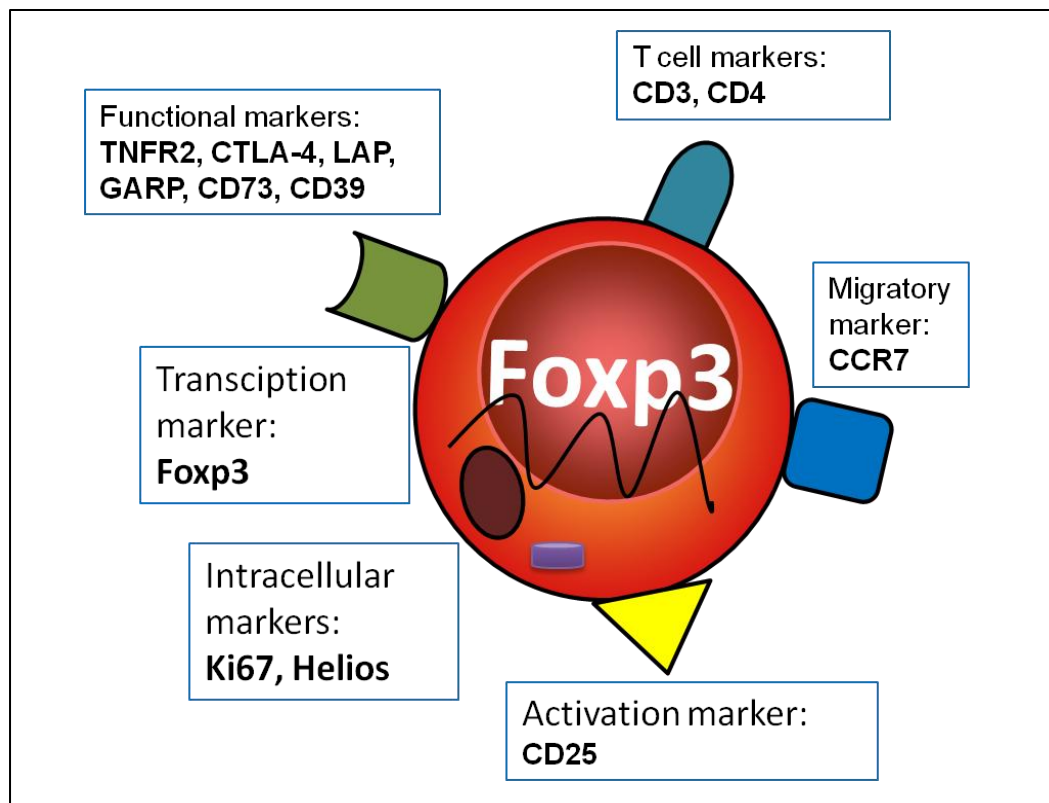


Figure 2: Phenotypic characterisation of Treg. Treg expressing different markers including T cell (CD3 and CD4), migratory marker (CCR7), Treg functional-associated markers (TNFR2, CTLA-4, LAP, GARP, CD73 and CD39) that are expressed extracellularly; proliferative marker (Ki67), Treg functional-associated markers (Helios) and Treg transcriptional marker (Foxp3) that are expressed intracellularly. TNFR2 are only expressed on specific Treg subsets (Chen et al., 2010a).

(Fontenot et al., 2003, Hori et al., 2003b). In the thymus, *Foxp3* expression starts at the late stage of double-positive cells, and *Foxp3*-expressing Treg in mice can be detected from day 3 after birth (Sakaguchi, 2004). This finding is correlated with organ-specific autoimmune disease in thymectomised mice on day 3, which can be prevented by adoptive transfer of $CD4^+CD25^+$ Treg (Sakaguchi, 2004, Fontenot et al., 2005a). Mutations in the human genome encoding *Foxp3* lead to IPEX syndrome (immune dysregulation, polyendocrinopathy, enteropathy and X-linked) which leads to severe autoimmune diseases and allergy. The IPEX syndrome and the phenotype of scurfy mice (defect in mouse *Foxp3* gene) have similar phenotypes which resemble the diseases observed following depletion of $CD4^+CD25^+$ Treg in rodents (Brunkow et al., 2001, Qu et al., 2013). This shows the central role for *Foxp3*-expressing Treg in the maintenance of peripheral tolerance. However, *Foxp3* expression is not suitable for use in isolating viable Treg, since *Foxp3* staining requires fixation and permeabilisation of the cells. Therefore, *Foxp3* expression on Treg is crucial and necessary but not easily suitable to isolate functional Treg.

1.6.1.2 TNFR2: identifies a subset of potent suppressive Treg

It has been reported that 30-40 % of splenic and lymph node (LN) Treg express TNFR2 in normal mice (Chen et al., 2008, Chen et al., 2010a). Recent studies have shown that TNFR2-expressing $CD25^+$ or $Foxp3^+$ cells defines a maximally suppressive subset of Treg in both mice and humans, while $CD25^+$ or $Foxp3^+$ cells without TNFR2 expression in normal C57BL/6 mice had only minimal or no suppressive ability (Chen et al., 2010a). However, expression of TNFR2 on $CD4^+$ T cells is not sufficient to endow $CD4^+$ T cells with immunosuppressive capacity; while expression of TNFR2 and *Foxp3* or *CD25* as a surrogate marker allows the identification of highly suppressive cells (Chen and

Oppenheim, 2010). Study in a tumor model showed that the majority of tumor infiltrating Treg is highly suppressive TNFR2⁺ cells (Chen et al., 2008), and cyclophosphamide treatment in a tumor model results in depletion of TNFR2⁺ Treg leading to eradication of tumor (van der Most et al., 2009). Furthermore, study showed that TNFR2^{-/-} Treg fail to control inflammatory responses *in vivo* (van Mierlo et al., 2008). Together, these studies suggest that TNFR2 expression on Treg identifies the potent suppressive Treg. Chen and colleagues found that TNF preferentially up-regulated TNFR2 on Treg, resulting in a self-amplification loop in the activation of Treg and proposed a new Treg mechanism based on the TNFR2 expression on Treg; Treg out-compete Teff for co-stimulation by TNF-TNFR2 (Chen and Oppenheim, 2011b). It was reported previously that Treg were able to shed large amounts of soluble TNFR2, the resultant soluble TNFR2 provide a means by which Treg inhibited the activation of Teff. Soluble TNFR2 binds and neutralises TNF, thus reducing the pro-inflammatory effects of TNF to Teff (van Mierlo et al., 2008). Treg subsets investigated in this study are shown in Figure 3.

1.6.1.3 Helios: a newly identified activation marker

Helios is a member of the Ikaros family that seems to be restricted to the T cell lineage (Kelley et al., 1998, Hahm et al., 1998). The expression of the Ikaros family in Treg has not been extensively studied, however, a few recent studies demonstrated that Helios is selectively expressed in Foxp3-expressing Treg, but not in conventional T cells (Sugimoto et al., 2006, Hill et al., 2007, Kang et al., 2007). A recent study reported that Helios is a marker to discriminate thymic-derived Treg from those peripherally induced from naïve CD4⁺ T cells with 70 % of Helios expressed on induced CD4⁺Foxp3⁺ Treg (Thornton et al., 2010). In contrast, another study demonstrated that Helios is expressed on all mouse and human activated cells, regardless of the cell subset involved, concluding

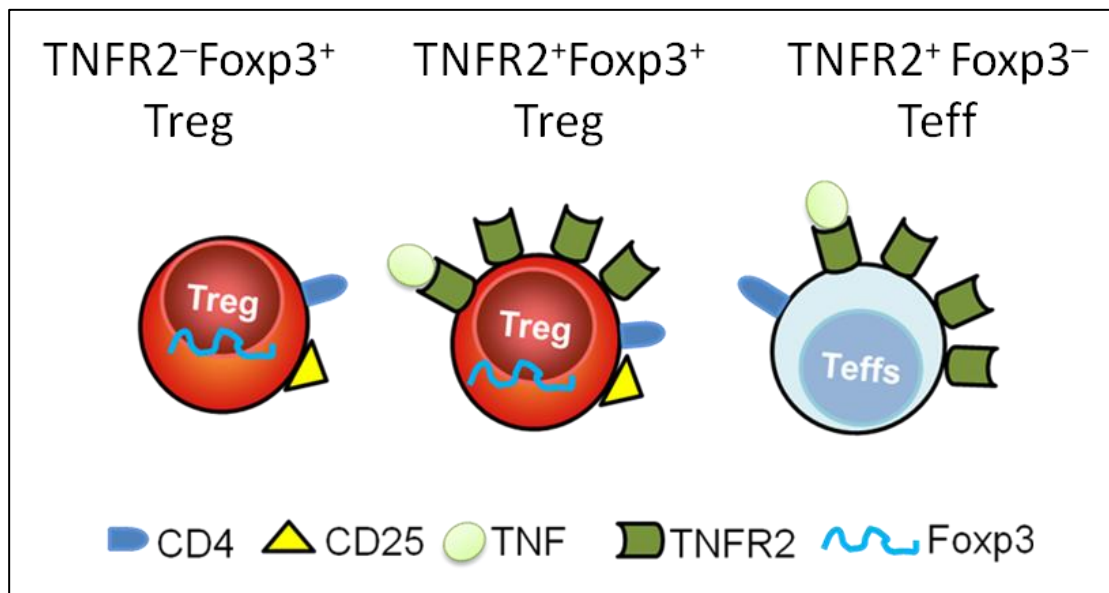


Figure 3: Treg and Teff subsets investigated in this study. Treg investigated in this study including CD4⁺CD25⁺TNFR2⁺Foxp3⁺ Treg (TNFR2⁺Foxp3⁺ Treg) and CD4⁺CD25⁺TNFR2⁻Foxp3⁺ Treg (TNFR2⁻Foxp3⁺ Treg). Treg expressed T cell markers (CD3 and CD4), activation/regulatory marker (CD25) and Treg transcriptional marker (Foxp3). TNFR2⁺Foxp3⁻ Teff investigated in this study expressed T cell markers (CD3 and CD4 without Foxp3 expression).

that Helios does not appear to be a suitable marker to distinguish between natural and induced Treg (Akimova et al., 2011).

1.6.1.4 CTLA-4: competes with CD28 during T cell activation

In rodents and humans *in vitro* suppression assays, Treg suppress Teff via a cell-cell contact mechanism. Treg suppression is abolished when Treg and responder cells are separated by a semi-permeable membrane (Takahashi et al., 1998, Thornton and Shevach, 1998). CTLA-4 (CD152) is one of the Treg surface markers that contributes to the contact-dependent suppressive mechanism (Sakaguchi, 2004). Studies showed that CTLA-4 is expressed by approximately 40 % of mouse Treg (Read et al., 2000, Takahashi et al., 2000, Zheng and Rudensky, 2007). It shares homology with CD28 and both CTLA-4 and CD28 bind to B7 molecules (CD80 and CD86) on APC. Interaction of CTLA-4 with B7 results in activation of Treg, whereas, on the other hand, CD28-B7 interaction enhances Teff activation. CTLA-4 is also transiently induced upon activation of Teff, but expression results in inhibition of cell-cycle progression and IL-2 production, thereby dampening an immune response (Krummel and Allison, 1996). CTLA-4 is reported to be critically required for functional Treg (Wing et al., 2008), at least *in vivo*, even though CTLA-4-deficient mice are still functional (Read et al., 2006). The expression level of CTLA-4 indicates the functional status of Treg. Treg with maximal function express high levels of CTLA-4, as compared with inactive CTLA-4^{low} Treg (Chen et al., 2008). CTLA-4 blockade abrogates the suppressor function of Treg in mice (Watanabe et al., 2008) and in rheumatoid arthritis CTLA-4 deficiencies are associated with abnormal Treg function (Flores-Borja et al., 2008). Another possible role for CTLA-4 is induction of the enzyme indoleamine 2,3-dioxygenase (IDO) on DC by interacting with CD80 and CD86 on their surface (Fallarino et al., 2006). IDO catalyses the

conversion of tryptophan into kynurenine and other metabolites which are cytotoxic to DC (Fallarino et al., 2006).

1.6.1.5 LAP/GARP: Modulate activity of the anti-inflammatory cytokine TGF- β

Suppressive cytokines such as IL-10 and transforming growth factor-beta (TGF- β) play important roles in controlling immune responses. One important suppressive mechanism of Treg is the secretion of these anti-proinflammatory cytokines. TGF- β is first synthesised as pro-TGF- β and is then intracellularly converted to a latent TGF- β complex that is comprised of LAP non-covalently bound to pro-TGF- β (Miyazono et al., 1993). A recent study demonstrated that the majority of mouse Foxp3⁺CD4⁺ T cells express surface LAP after activation, whereas freshly prepared murine CD4⁺CD25⁺ cells express surface LAP only weakly (Oida and Weiner, 2010). Previously, it was reported that human Foxp3-expressing Treg express surface LAP and that the surface LAP is anchored by GARP (Tran et al., 2009, Stockis et al., 2009). Another study further found that this is also the case with mouse CD4⁺ T cells (Oida and Weiner, 2010). Treg that express GARP have greater suppressive activity than Treg which do not express GARP (Fan et al., 2012).

1.6.1.6 Glucocorticoid-induced TNF receptor (GITR)

In addition to the above markers, GITR is constitutively expressed on Treg at a higher levels than on other T cells (Shevach and Stephens, 2006). GITR signaling on Treg is vital for Treg proliferation *in vitro* in the presence of IL-2 (McHugh et al., 2002, Ji et al., 2004). Suppression assays using thymidine-incorporation and carboxyfluorescein diacetate succinimidyl ester (CFSE) in which anti-GITR antibodies could only target Treg

confirmed the increase in Treg proliferation and enhanced Treg suppressive function (Stephens et al., 2004).

1.6.1.7 CD39/CD73: Adenosine converter

As mentioned earlier, Treg can suppress Teff by secreting inhibitory cytokines. However, the suppressive effect of Treg can occur even when cytokines are blocked, suggesting the presence of other inhibitory mechanisms. It has been shown that enzymatic activity of ectoapyrase CD39 and ecto-5'-nucleotidase CD73 expressed on Treg are crucial for the suppressive effect of Treg (Borsellino et al., 2007). CD39 converts extracellular nucleotides such as adenosine triphosphate (ATP) into adenosine monophosphate (AMP); AMP is further degraded by CD37 into adenosine; a known anti-inflammatory molecule that dampens Teff. Thus, Treg can induce their suppressive effects on Teff by activation of extracellular proinflammatory ATP. Furthermore, CD39 and CD73 expressed on Treg distinguish Treg from other CD4⁺ T cell populations (Deaglio et al., 2007).

1.6.1.8 CCR7: LN-homing marker

The mechanisms by which Treg dampen effector functions remain poorly understood. Studies showed that Treg predominantly suppress autoreactive T cells within secondary lymphoid organs (Sakaguchi, 2004), as well as sites of inflammation (Huehn et al., 2005, Sather et al., 2007). Accordingly, Treg constitutively express chemokine receptors (Iellem et al., 2001) and are highly sensitive to inflammatory chemokines (Bystry et al., 2001) which enhance migration to the inflamed sites in order to suppress ongoing responses (Huehn et al., 2005, Siegmund et al., 2005). CCR7 expressed on Treg binds to CCL19 and CCL21 which are constitutively expressed in the LN (Lee et al., 2007). Expression of this chemokine allows Treg to home to the LN, where they expand in

response to antigen stimulation and suppress effector cell responses. Treg lacking CCR7 accumulate in the lung and fail to traffic to the LN and leads to a significant reduction in the numbers of Treg in the LN (Schneider et al., 2007, Kocks et al., 2007). Moreover, a study by Trujillo *et al.* in a bleomycin-induced lung injury found that CD4⁺CD25^{hi}FoxP3⁺ Treg are retained in the lungs of bleomycin-treated CCR7^{-/-} mice, which is consistent with an ameliorated remodeling response in this model (Trujillo et al., 2010). Furthermore, the suppressive function of CCR7^{-/-} Treg *in vivo* is profoundly defective. This is primarily due to Treg inability to migrate toward the T cell zones within lymphoid organs (Schneider et al., 2007, Menning et al., 2007, Kocks et al., 2007).

1.6.1.9 Ki67: proliferative marker

Treg actively proliferate to maintain their numbers/pool in the periphery, especially at mucosal sites (Skrindo et al., 2011). In a steady state, Treg undergo more replication and proliferation compared to Foxp3⁻ cells (Fisson et al., 2003, Chen et al., 2010a). Proliferating cells express the Ki67 marker and studies report concomitant expression of Ki67 and TNFR2 markers (Chen et al., 2010a). Study in mice has shown that binding of TNF to TNFR2 can enhance suppressive function and *in vitro* expansion of Treg (Chen et al., 2007). Ki67^{hi} Treg are the proliferating cells that respond to antigen and increase Treg suppressive function (van der Most et al., 2009). Recent study in Foxp3 LucIDTR for specific ablation of Treg revealed that recovery of the Treg pool in the spleen, LN and blood is due to homeostatic expansion of the surviving Treg, and is not dependent on thymic output (Suffner et al., 2010). Suffner *et al.* further showed that the Foxp3⁺ Treg expanded rapidly and filled up the Treg pool both in the spleen and LN within ~2 wk (Suffner et al., 2010). Proliferating Treg acquired an activated phenotype and retained their suppressive activity (Suffner et al., 2010, Jung and Seoh, 2009) and in fact the

proliferating Treg exhibited a higher suppressive activity than Treg isolated from a nonmanipulated mouse (Suffner et al., 2010).

1.6.2 Regulation of Treg frequency and function during lung diseases

1.6.2.1 Treg in LPS-induced ALI

Research focusing on the involvement of Treg in LPS-induced ALI has been minimal. A recent study by D'Alessio *et al.* found that the severity of inflammation 4 days after LPS administration [as assessed by bronchoalveolar lavage fluid (BAL) cell counts, BAL protein, and lung histology] was similar between wild type (WT) and *Rag-I*^{-/-} mice, and concluded that lymphocytes did not play a critical role in the pathogenesis of ALI (D'Alessio et al., 2009). They however demonstrated that Treg can mediate the resolution of LPS-induced ALI through both TGF- β -dependent and -independent mechanisms (D'Alessio et al., 2009) (Figure 4). For the first time in human studies, D'Alessio *et al.* also showed that Treg are present in BAL of humans with ALI and that their Treg numbers are dynamically changed during the course of ALI (D'Alessio et al., 2009). A recent study performed by Garibaldi *et al.* showed that Treg play a central role in the resolution of ALI fibroproliferation by reducing fibrocyte recruitment along the CXCL12-CXCR4 axis (Garibaldi et al., 2013). Therefore, data from these studies demonstrated the importance of Treg in regulation ALI both in human and animal models.

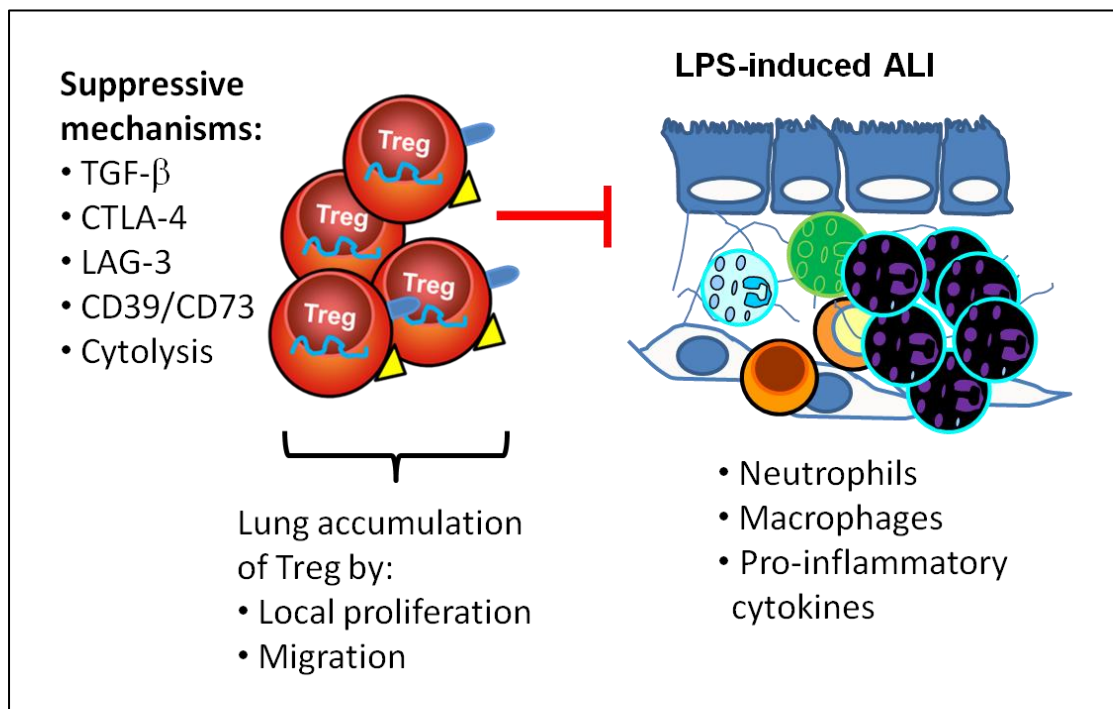


Figure 4: Regulatory pathways in the lung maintain tolerance to environmental exposure (e.g. LPS). Tolerance is maintained by an interaction of airway structural cells with the complex network of immune cells including Treg and other cells (tolerogenic DC). Administration of LPS into the airways resulted in the recruitment/induction of inflammatory cells into the airways (e.g. neutrophils, macrophages) and secreted high levels of pro-inflammatory cytokines into the BAL (e.g. TNF, IL-6). Development of lung injury resulted from the loss of tolerance and is influenced by genetic and environmental factors. Treg also accumulate in the airways and play a role in the controlling inflammation by various mechanisms including TGF- β -mediated mechanisms and other potential mechanisms (LAG-3, adenosine via modulation on CD39/CD73). Adapted from (D'Alessio et al., 2009).

1.6.2.2 Treg in allergic asthma

In allergic asthma, activation of Th2 cells is believed to orchestrate the inflammatory responses by secreting multiple pro-inflammatory cytokines including IL-4, IL-5, IL-9 and IL-13. These cytokines are responsible for the recruitment of eosinophils and other inflammatory cells into the lung surfaces which then lead to decreased lung function. Treg play a role in the maintenance of peripheral homeostasis (Sakaguchi, 2000, O'Garra and Vieira, 2004, Belkaid, 2007) and several lines of evidence suggest that Treg are also involved in the pathogenesis of allergic asthma (Ling et al., 2004, Baru et al., 2010, Thorburn and Hansbro, 2010, Thorburn et al., 2010). Treg are involved in suppression of allergen-specific T cells, playing an important function in the physiological immune response to allergens. Furthermore, a few studies have found that the induction of Th2-mediated airway inflammation in asthma may be due to defective suppression by Treg (Stiehm et al., 2013, Akdis et al., 2004, Hawrylowicz and O'Garra, 2005, Baru et al., 2010, Gupta et al., 2012, Yang and Schwartz, 2012). Studies have demonstrated that Treg involved in suppression of allergen-specific T cells dampen the activation of effector cells such as eosinophils, mast cells and basophils and have the capacity to influence B cells responses (Gri et al., 2008, Meiler et al., 2008). Moreover, transfer of Treg during the effector phase of AAI induces protection from lung inflammation and pathology (Arnold et al., 2011, D'Alessio et al., 2009, Kearley et al., 2008). A recent study has shown that Treg accumulate in the lung in allergic inflammation and efficiently suppress pulmonary T-cell proliferation but not Th2 cytokine production (Faustino et al., 2012). Findings in asthmatic patients show that the frequency of Treg is negatively correlates with clinical severity and the degree of airway inflammation (Matsumoto et al., 2009) and the ratio of Th2 cells to Treg have been implicated as a strong determinant of immune outcome to

common environmental antigens (Akdis et al., 2004). A study in pediatric asthmatics found that Treg numbers in BAL fluid are lower than those in healthy children (Hartl et al., 2007). Furthermore, suppressive effects of Treg in atopic allergic patients and patients with active allergic rhinitis during the pollen season are reduced compared to healthy individuals (Grindebacke et al., 2004). Overall, these findings demonstrated a role of Treg in controlling Th2 inflammation in allergic asthma (Figure 5).

1.6.3 TNF-TNFR2 interaction on Treg

Tumour necrosis factor (TNF) is implicated in many pulmonary diseases, including allergic asthma (Broide et al., 1992), ALI (Ward and McLeish, 1996), chronic bronchitis and chronic obstructive pulmonary disease (COPD) (Mukhopadhyay et al., 2006). The TNF is released from cells (macrophages, T cells, mast cells, granulocytes, natural killer (NK) cells, fibroblasts, neurons, keratinocytes and smooth muscle cells) as a soluble cytokine (sTNF), a homotrimer of 17-kDa monomer after being cleavage by TNF- α -converting enzyme (TACE) from its cell surface-bound precursor (tmTNF, a homotrimer of 26-kDa monomers [reviewed in (Tracey et al., 2008)]). Both sTNF and tmTNF ligands interact with either of 2 distinct receptors, namely TNF receptor 1 (TNFR1) (p55, CD102a) and TNFR2 (p75, CD120b) promoting many of the symptoms of inflammation.

A recent study has demonstrated that both TNFR1 and TNFR2 are important for antigen-induced allergic lung inflammation (Nakae et al., 2007). Although TNF is the most studied pro-inflammatory cytokine and has a wide array of immunomodulatory activities, its precise role in the pathogenesis of allergic asthma is still unclear. TNF has been implicated in several infectious and inflammatory lung diseases. In allergic asthma, TNF

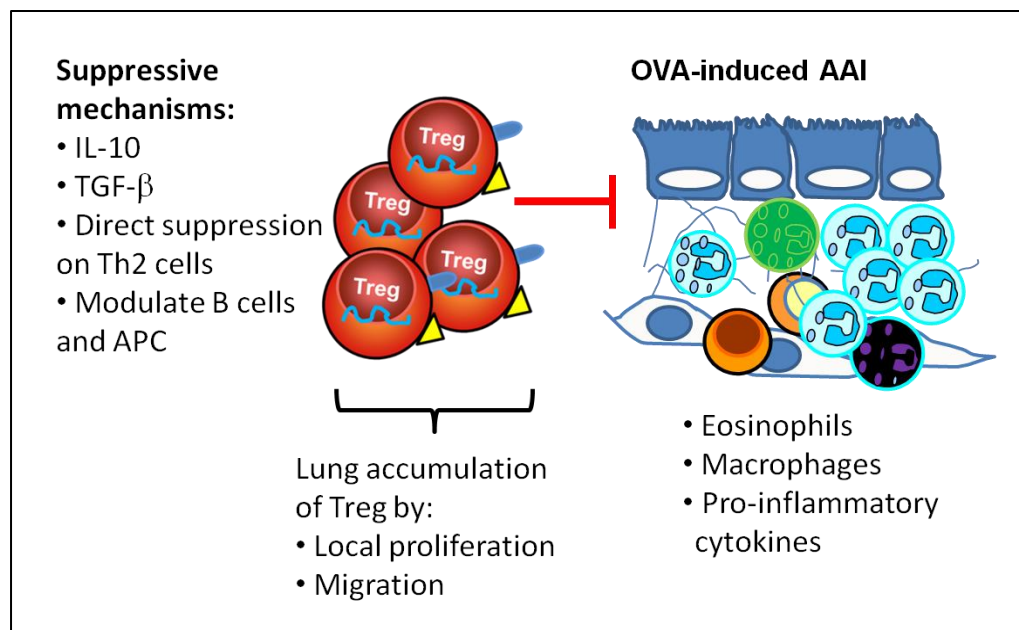


Figure 5: Regulatory pathways in the lung maintain tolerance to environmental exposure (e.g. allergen). Tolerance is maintained by an interaction of airway structural cells within the complex network of immune cells including Treg and other cells (tolerogenic DC). Airway exposure to allergen resulted in the recruitment/induction of inflammatory cells into the airways (e.g. eosinophils, macrophages) and secreted high levels of pro-inflammatory cytokines into the BAL (e.g. IL-4, IL-5). Development of inflammation resulting from the loss of tolerance is influenced by multiple factors including age, gender, obesity, infection history, atopic status, allergen exposure and nutrition which will affect the initiation and development of the allergic response. Treg also accumulate in the airways and play a role in controlling the inflammation by various mechanisms including direct suppression on Th2 cells or regulation on B cells and other potential mechanisms (anti-inflammatory cytokines, IL-10 and TGF- β). Adapted from (Lloyd and Murdoch, 2010).

has multiple effects including increased adhesion, migration and activation of inflammatory cells through the epithelial and endothelial barriers (Erzurum, 2006). An elevated level of TNF has been found in the sputum and serum of allergic asthmatic patients (Keatings et al., 1996, Silvestri et al., 2006). Furthermore, this level is also upregulated in patients with refractory asthma, as evidence by the increased expression of membrane-bound TNF, TNFR1 and TNF converting enzyme by peripheral blood monocytes (Berry et al., 2006). Ye *et al.* found increased expression of TNFR1 and TNFR2 in cryptogenic organizing pneumonia patients (Ye et al., 2011). Moreover, elevated levels of TNF and TNFR have been implicated in the pathogenesis of granulomatous and inflammatory lung diseases suggesting that these receptors play a crucial role in mediating lung inflammation (Gordon et al., 2012, Matesic et al., 2012, Bickford et al., 2012).

TNF has been shown to be implicated in LPS-induced ALI. Intranasal and intratracheal LPS from Gram-negative bacteria provoke acute pulmonary inflammation, local TNF, IL-1 β and interferon gamma (IFN- γ) production, alveolar-capillary leak and bronchoconstriction in normal C57BL/6 (Lefort et al., 2001, Schnyder-Candrian et al., 2005, Vernooy et al., 2001). A recent study in healthy volunteers showed that an inhaled LPS challenge (approximately 5 μ g) activated macrophages to secrete TNF, IL-1 β and IL-6 and induced neutrophilic inflammation (Hernandez et al., 2010). Other studies showed that TNF has the potential to modify apoptotic clearance (McPhillips et al., 2007, Borges et al., 2009). A study by Borges *et al.* demonstrated that instillation of apoptotic thymocytes into naïve mice in the presence of TNF reduces the ability of alveolar macrophages to clear apoptotic cells and enhances inflammatory responses (Borges et al.,

2009). TNF is also a neutrophil survival factor and instillation of TNF delayed neutrophil apoptosis (Ward et al., 2004).

TNF exerts pro-inflammatory effects in many autoimmune diseases and these effects are well documented. Nevertheless, increasing evidence indicates that TNF also has anti-inflammatory effects; especially after prolonged exposure (Sfikakis, 2010, So et al., 2006, Watts, 2005, Kollias and Kontoyiannis, 2002). This is supported by several lines of evidence suggesting that TNF may activate Treg (Bilate and Lafaille, 2010, Grinberg-Bleyer et al., 2010), and is also strongly supported by a number of studies (Chen et al., 2007, Chen et al., 2010a, Chen and Oppenheim, 2010, Chen and Oppenheim, 2011a, Chen and Oppenheim, 2011c, Chen and Oppenheim, 2011b, Chen et al., 2010b, Chen et al., 2008). TNF proliferatively expands Foxp3⁺ Treg in the periphery (Chen and Oppenheim, 2011a) and is critical for stabilisation of Treg in the inflammatory environment (Chen et al., 2013). Furthermore, TNF-TNFR2 interaction promotes the survival of Treg in cancer (Chen et al., 2007, Chen and Oppenheim, 2011a), and at inflammatory sites by inducing thioredoxin-1, a major antioxidative molecule, of Treg in a NFkB-dependent manner (Mougiakakos et al., 2011).

1.7 The effects of LPS, nanoparticles and follistatin on lung immune responses

The lung is exposed to a diverse range of air pollution particulates including nanoparticles and inflammatory stimulus such as LPS on a daily basis. Lung homeostasis can also be modulated by biology factors, such as follistatin that binds to activin A. Subsequent lung exposure to these stimuli resulted in either immune activation or suppression depending on the nature of stimuli (e.g. doses, characteristics), exposure route/time (e.g. inhalation)

and the lung microenvironment (e.g. host immune system) (Mohamud et al., 2013, Hardy et al., 2013c, Zhu et al., 2010). Therefore, lung must maintain a state of immune tolerance to these stimuli to retain pulmonary homeostasis and prevent potentially fatal immunopathology.

1.7.1 The effects of LPS on immune responses in the lung

LPS, a pro-inflammatory component of the gram-negative bacteria cell wall, is ubiquitously present in the environment or as a contaminant with other airborne particles and has been shown to modulate lung diseases including allergic asthma (Braun-Fahrlander et al., 2002, Eisenbarth et al., 2002, Rodriguez et al., 2003, Ege et al., 2006). Airway exposure to LPS at different doses leads to different characteristics of allergen-induced AAI (Delayre-Orthez et al., 2004, Dong et al., 2009, Gerhold et al., 2002, Zhu et al., 2010) and exposure to high dose LPS protect against the development of asthma (Braun-Fahrlander et al., 2002, Arora et al., 2011, Rodriguez et al., 2003, Arora et al., 2010, Delayre-Orthez et al., 2004, Gerhold et al., 2003) (Figure 6). Data from several models demonstrate that LPS-regulated lung inflammation is dependent on the exposure time, thus LPS exposure to the lung during allergen sensitisation or challenges might lead to different forms of asthmatic pathology (Delayre-Orthez et al., 2004, Tulic et al., 2000, Zhu et al., 2010). A study showed that in healthy volunteers, LPS inhalation activates macrophages to secrete TNF, IL-1 β and IL-6 and induces neutrophilic inflammation (Hernandez et al., 2010).

However, these various effects on cellular and molecular mechanisms, either in experimental animal models or humans have been poorly understood. This is probably because LPS favors different modulation effects on airway Treg. LPS-activated DC (e.g.

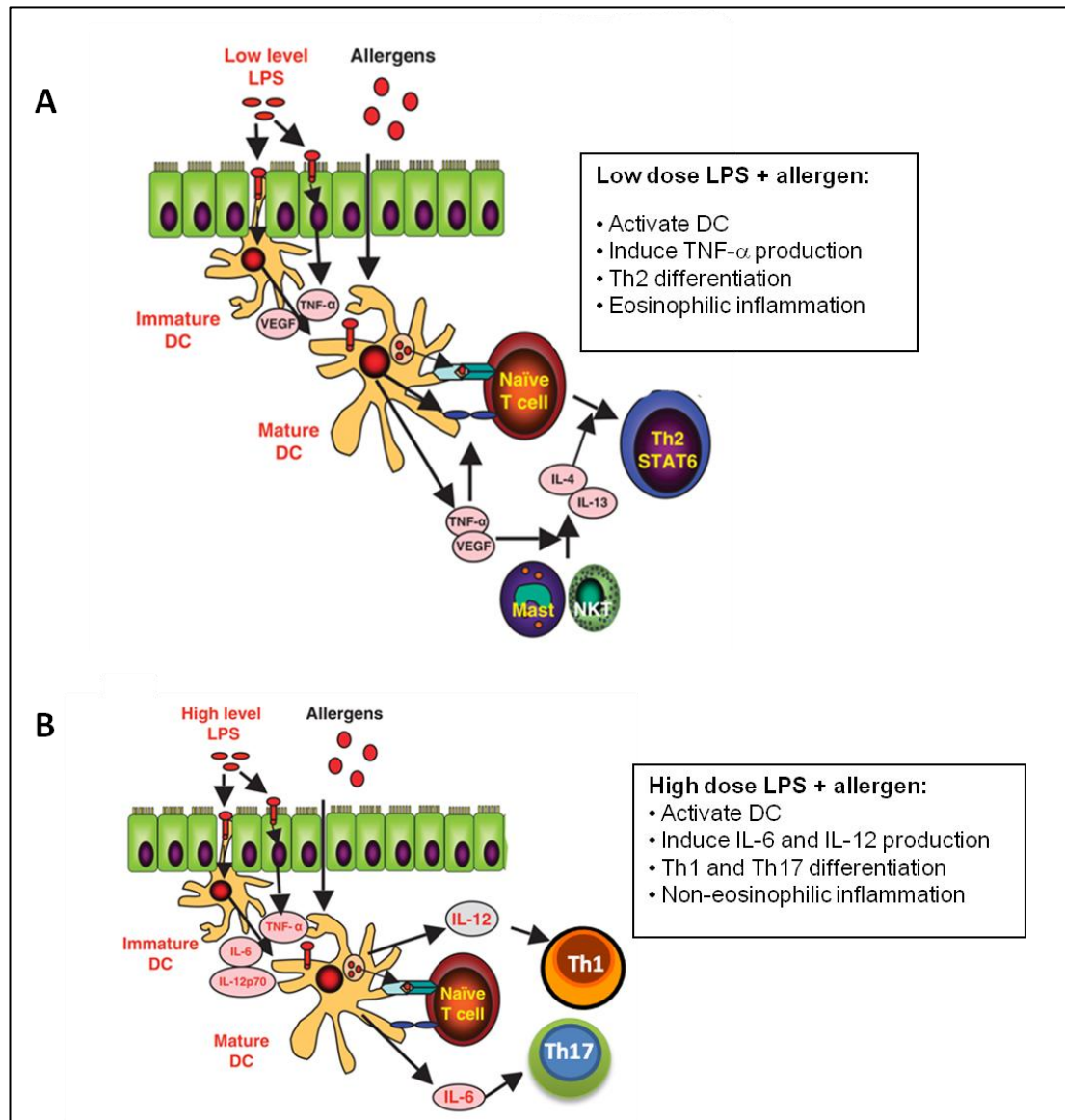


Figure 6: LPS modulates allergen exposure-induced innate immune responses, Th1, Th2, and Th17 adaptive immune responses in the lung. Administration of OVA with low-dose (100 ng) LPS-induced Th2 responses with eosinophilia and allergen-specific IgE production, whereas OVA with high-dose (10 μ g) LPS-induced Th1 inflammation with neutrophilia. Adapted from (Zhu et al., 2010).

engagement of LPS on TLR4 expressed on DC) skewed immune responses towards Th1, Th2, Th17 or Treg, depending on the airway cytokine milieu (Arora et al., 2011). TLR are pattern-recognition receptors that have a pivotal role as primary sensors of microbial products and as initiators of innate and adaptive immune responses. In naïve mice, lung exposure to high dose LPS resulted in the induction of acute lung injury (Mei et al., 2007, Rojas et al., 2005). In accordance with this, Treg are required to sustain LPS-induced pro-inflammatory responses and to increase neutrophil apoptosis, thus playing a significant role in mediating resolution of LPS-induced lung inflammation (Aggarwal et al., 2009). LPS binds to TLR-4, one of the seven TLR expressed on Treg, and can directly activate Treg and enhance their suppressive function (Caramalho et al., 2003).

Furthermore, a recent study showed that LPS exposure early in life has been suggested to induce tolerance and may be protective against allergic asthma (Lluis et al., 2013). Another study demonstrated that exposure to the environment of a farm (enrich in LPS) during pregnancy decreased allergic diseases, suggesting that exposure to LPS increased Treg numbers and function, and acted as a natural model of immunomodulation shaping a child's immune system in early life (Schaub et al., 2009).

1.7.2 The effects of engineered nanoparticles on lung immune responses

Nanoparticles (< 100 nm) can be categorised into naturally occurring (ambient) nanoparticles (e.g. forest fires), anthropogenic nanoparticles produced inadvertently as a result of human activity (e.g. combustion engines) and engineered nanoparticles (ENP) produced for various industrial applications or consumer products. Studies demonstrated that exposure to some types of nanoparticles can be associated with both mortality and morbidity, and affects lung at the cellular and molecular levels due to their unusual

physicochemical properties (Oberdorster et al., 1995, Schwartz et al., 1996, Utell and Frampton, 2000, Stone et al., 2007). Exposure of some types of nanoparticles in the lung can induce lung toxicity and exacerbation of allergic asthma in animal models (Table 2). Polystyrene ENP are inorganic, non- biodegradable, but biocompatible, and do not induce oxidative stress *in vitro* (Xia et al., 2006). Hardy *et al.* have shown that intratracheal instillation of negatively charged glycine-coated 50 nm polystyrene (PS50G) engineered nanoparticles in fact does not induce lung oxidative stress or cardiac or lung inflammation (Hardy et al., 2012a), but leaves a beneficial immunological imprint on the lung and lung-draining LN rendering mice resistant to the development of AAI (Hardy et al., 2013b, Hardy et al., 2012a). PS50G inhibit key characteristics of allergic asthma (including airway eosinophilia and production of allergen-specific IgE and Th2 cytokines), a month following instillation by inhibiting expansion of total and allergen-laden DC in the lung, and suppressing co-stimulatory function of CD11b^{hi} DC in the lung-draining LN (Hardy et al., 2012a).

Therefore, similarly to the effect of LPS in the lung, ENP also have the capability to induce detrimental or beneficial effects on lung immune homeostasis depending on the physicochemical characteristics of ENP. It should be noted that the nature of such ENP can modulate other lung-ENP interactions, such as 1) the ability to be endocytosed by APC or to stimulate cytokine secretion; 2) the ability to enter type I and II epithelial cells); 3) the ability to translocate across the epithelial cells to the blood circulation; 4) the ability to gain access to the mitochondria and nucleus prior to uptake and 5) the ability to engage the intracellular clearance mechanisms that lead to ENP clearance or local or systemic toxicity.

ENP groups	ENP types	Effects on the lung	
		Toxicity Levels	Generally depends on ENP characteristics
Organic	Lipid	Non- to low	Size, dose and functionalisation process
	Polysaccharide		
	Polymeric matrix		
Inorganic biocompatible	Polystyrene	Mild	Composition, size, dose, agglomeration, functionalisation process, surface characteristics, ions released and exposure routes and time
Inorganic	Gold and silver ENP < 5 nm		
	Gold and silver ENP > 5 nm		
	Carbon	High	Dose, surface characteristics and exposure routes and time
	Metal oxide		
	Metalloid		

Table 2: Lung exposure to different types of ENP can induce a broad range of immunological effects that might shape overall lung immune homeostasis. Whether the response to ENP is beneficial or detrimental is influenced by physicochemical characteristics (including composition, size, surface characterisation and charge), dose and timing (acute versus chronic), and route of administration (e.g. intratracheal, intranasal, whole-body exposure) of the particles. Adapted from (Mohamud et al., 2013).

Depending on their nature, ENP can exert negative adjuvant effects and can exacerbate existing allergic asthma [e.g. carbon nanotubes (CNT) (Inoue et al., 2010)], or ENP can exert positive effects, such as the ability to inhibit allergic inflammation via various mechanisms including: 1) modification of lung vascular endothelial growth [e.g. intranasal silver ENP administration, (Jang et al., 2012)], 2) decreased Th2 function [e.g. inhaled titanium dioxide (TiO₂) ENP (Rossi et al., 2010a), 3) anti-oxidant effects [e.g. inhaled silver ENP, (Park et al., 2010)] and 4) modulation of APC function towards homeostatic protection [e.g. intratracheal ENP polystyrene administration (Hardy et al., 2012a)]. Overall, the characteristic of nanoparticles determining the fate of lung homeostasis (Mohamud et al., 2013).

1.7.3 The effects of follistatin on lung immune responses

Activin A is a pleiotropic TGF- β family member involved in cell proliferation, differentiation (myeloid lineages), apoptosis, wound repair and inflammatory responses (Phillips et al., 2009). It is produced in response to inflammatory signals by various cell types, including macrophages, mast cells, monocytes and importantly Th2 cells (Phillips et al., 2009) and is thought to play an important role in various immunopathologies and systemic immune responses (Munz et al., 1999). Human DC also have been shown to produce activin A that is capable of attenuating CD40L-specific cytokine and chemokine production, and decrease antigen-specific CD8⁺ T cell expansion *in vitro* (Robson et al., 2008). Activin A can stimulate the expression of pro-inflammatory cytokines such as IL-6, TNF and IL-1 β by macrophages and plays an important role in both allergic asthma (Hardy et al., 2013c, Kariyawasam et al., 2011) and lung injury (Jones et al., 2004, Phillips et al., 2009). The abundance of activin A in the blood of asthmatic patients (Karagiannidis et al., 2006) and in the lung of mice with inflamed airways (Hardy et al.,

2013c, Hardy et al., 2006) suggests a role for this protein in allergy and asthma. The biological effects of activin A can be neutralised by follistatin, a naturally occurring secreted glycoprotein with a high affinity for activin, and thus prevents the interaction of activin A with its receptor complex (Phillips et al., 2009). Neutralisation of activin A *in vivo* reduced: 1) serum antigen-specific IgE production, 2) activin A concentrations in BAL fluid, 3) Th2-LN cells frequency and 4) blocked allergen-specific Th2 response (Ogawa et al., 2008, Hardy et al., 2013c). In a bleomycin-induced lung injury mouse model, follistatin injection inhibits fibrosis development (Aoki et al., 2005). Pre-administration of follistatin in an LPS-induced lung injury mouse model, does not prevent the acute release of activin A in response to LPS, but follistatin can dose-dependently modulate the profile of pro-inflammatory cytokines released, such as TNF, IL-1 β and IL-6 (Jones et al., 2007).

Interestingly, other studies show that activin A can inhibit inflammation and have immunosuppressive effects (Hedger et al., 2011, de Kretser et al., 2012). The immunosuppression effects of activin A are complex and dependent on the experimental settings (*in vitro* versus *in vivo*), anatomical location, cell type, phase of the immune response and the dose. Nonetheless, activin A has dual immunosuppressive effects exhibited by activin A, (1) it directly inhibits immune cell responses, and (2) it induces the generation of Treg. Activin A can enhance the conversion of mouse peripheral naïve T cells to Treg *in vivo* and increase TGF- β 1-induced Foxp3 expression on T cells *in vitro* (Huber et al., 2009). Kariyawasam *et al.* proposed that during the responses to inflammatory stimuli (i.e. allergen, pollutants, LPS), activin A modulates the suppression of airway epithelial and Th2 cells, concomitant with an induction and/or expansion of Treg. In addition, activin A promotes epithelial cell proliferation and repair; thus normal

airway architecture is restored. However, in the strong inflammatory milieu (e.g. allergic asthma), dysregulation in activin A signaling occurs and fails to induce immunoregulatory effects. This leads to excessive remodelling events and uncontrolled inflammation that exacerbates AHR (Kariyawasam et al., 2011). Thus, targeting activin A as an immunoregulator and anti-inflammatory agent has a potential to treat and prevent the induction of lung diseases (e.g. allergic asthma) and lung injury.

1.8 Summary

The lung develops tolerance towards innocuous antigens to which it is frequently exposed as well as particulates present in the environment, so it can retain pulmonary homeostasis, whilst still being able to induce immune responses towards harmful pathogens (Gereda et al., 2000, Akbari et al., 2002). Inhalation particulates and other stimuli present in the environment are epidemiologically linked to reduced lung function and exacerbation of AAI. However, experimental data showed that lung exposure to bacterial products (e.g. LPS) and PS50G protect individual from developing AAI. Furthermore, study demonstrated that treatment of chronic AAI with biological factor, follistatin improve AAI. In these cases it is a reasonable assumption that, given the major role that Treg play in the prevention and control of AAI, exposure to these stimuli may have changed Treg levels or function. Therefore, investigating on highly bioactive TNFR2 expressing Treg (i.e. levels and function) on various lung disease models poses a new therapeutic avenue to promote healthy lung homeostasis.

1.9 Project hypothesis and aims

The aim of this thesis is to investigate the regulation of Treg that are capable of inhibiting Teff function both in allergic airway inflammation and LPS-induced acute lung injury mouse models. This study also sought to identify different subsets of Treg involved in the prevention of airway inflammation, particularly focusing on TNFR2 expressing Treg.

The specific aims were divided based on murine models:

- Unmanipulated mice
 - To investigate Treg at lung homeostasis (Chapter 4)
 - To analyse the effects of nanoparticles in the modulation of lung Treg (Chapter 5)
- Allergic airway inflammation mouse model
 - To investigate the effects of follistatin treatment on the modulation of lung Treg (Chapter 3)
 - To investigate the kinetics of Treg during the induction and resolution of allergic airway inflammation (Chapter 4)
 - To investigate the effects of nanoparticles in the prevention of allergic airway inflammation (Chapter 5)
- Acute lung injury mouse model
 - To investigate Treg during the peak of LPS-induced acute lung injury (Chapter 6)

The hypotheses of this study are:

- Treg are important in controlling airway inflammation (Chapter 3).
- The reversal of airway inflammation is related to the increase of proportions of TNFR2 expressing Treg (Chapter 4 and 5).
- Airway inflammation and injury induced by allergen and LPS alters the ratios of Treg and Teff (Chapter 4, 5 and 6).
- Nanoparticles have an imprint effect on lung cells and can alter the balance of lung immune response which possibly modulates allergic asthma (Chapter 5).
- Treg fail to suppress Teff during the peak of airway inflammation (Chapter 6).

Chapter 2

Materials and methods

2.1 Materials

2.1.1 Mice

Female BALB/c mice aged 6-8 weeks old were obtained from Walter and Eliza Hall Institute Animal Services (WEHI, Kew, Victoria, Australia) and housed under specific-pathogen free conditions in the Precinct Animal Centre, the Alfred Medical Research and Education Precinct (AMREP). All experiments had ethics approval by the Animal Ethics Committee of AMREP under ethics numbers E/0709/2008/M and E/0821/2009/M.

2.1.2 Chemicals and reagents

Chemicals and reagents used in this study are listed below (Table 1):

Chemicals/Reagents	Company
1-ethyl (3-dimethylaminopropyl) carbodiimide (EDAC)	Sigma-Aldrich, USA
Aluminium hydroxide gel (alum)	Rehydragel HPA, USA
4-(2-hydroxyethyl)-1-piperazineethanesulfonic acid (HEPES)	Sigma Chemical Company, USA
Anti-mouse CD3	eBioScience, USA
Anti-mouse CD28	eBioScience, USA
Biotinylated IgE-specific antibody	BD Pharmingen, USA
Biotinylated IL-4, IL-5 antibody (ELISPOT)	BD Pharmingen, USA
Biotinylated IL-13 antibody (ELISPOT)	R&D Systems, USA
Brefeldin A	Sigma Chemical Company, USA

Collagenase Type IV	Biochemical Corporation ,USA
Concanavalin A (Con A)	Amersham Pharmacia, UK
Developed buffer AP colour (ELISPOT)	Bio-Rad, Australia
DNase type I recombinant	Roche Diagnostics, Australia
Ethylenediaminetetraacetic acid (EDTA)	R&D Systems, USA
ExtrAvidin®–alkaline phosphatase	Sigma-Aldrich, USA
Fetal Calf Serum (FCS)	Gibco BRL, USA
Follistatin	Produced ‘in house’ at Monash University
Foxp3 staining buffer kit	eBioScience, USA
Giemsa-stain	Merck, Kilsyth, Australia
Glycine	Sigma Chemical Company, USA
Hanks Balanced Salt Solution (HBSS)	Gibco BRL, USA
IL-4 and IL-5 antibody (ELISA and ELISPOT)	BD Pharmingen, USA
IL-13 antibody (ELISA and ELISPOT)	R&D Systems, USA
Isofluorane	ISOFLU; Abbott Australasia
Lipopolysaccharides (LPS)	Sigma Aldrich, USA
Mouse anti-human CD3	PharMingen, USA
Mouse anti-human CD28	PharMingen, USA
o-phenylene-diamine	Sigma-Aldrich, USA
Ovalbumin	Sigma Aldrich, USA
Paraformaldehyde	Sigma Chemical Company, USA
PBS (1x)	Gibco BRL Life Technologies, USA
Penicillin, Streptomycin and L-glutamine	Gibco BRL Life Technologies, USA
Polybead carboxylate microspheres	Polysciences, Warrington, USA

Protein G Sepharose beads	Amersham Pharmacia, UK
Ready-SET-Go! ELISA Kit	eBioScience, USA
Red Blood cell lysis buffer	Sigma Chemical Company, USA
RPMI 1640	Gibco BRL Life Technologies, USA
Sodium chloride	Pfizer, Australia
Sodium hydroxide (NaOH)	Sigma Chemical Company, USA
Streptavidin-horse radish peroxidase	Jackson ImmunoResearch, USA
TGF- β 1 DuoSet ELISA	R&D Systems, USA
Th1/Th2 10plex kit FlowCytomix	eBioscience, USA
3H-thymidine	Amersham BioSciences, UK
Trypan blue solution	Sigma Chemical Company, USA

Table 1: Chemicals and reagents used in this study.

2.1.3 Sterilized, deionized distilled water

The water used in the preparation of buffers and solutions was purified through a multistage ion-exchange system to remove extraneous salts and minerals after distillation.

2.1.4 Fluorochrome-labelled antibodies

Fluorochrome-labelled antibodies used in this study are listed below (Table 2):

Antibody	Fluochrome	Company, Catalogue number
CD3	V500	BD Horizon, # 560771
CD3	APC-Cy7	BD Pharmingen, # 557596
CD3	Q-dot 605	Invitrogen, # Q10090

CD4	V450	BD Pharmingen, # 550468
CD4	Q-dot 605	Invitrogen, # Q10092
CD25	Pe-Cy7	BD Pharmingen, # 552880
CD25	APC-Cy7	eBiosciences, # 47-0251-82
CD120b	PE	BD Pharmingen, # 550086
Foxp3	APC	eBiosciences, # 17-5773-82
Ki67	FITC	BD Pharmingen, # 51-36524x
CCR7	Per-CP	eBiosciences, # 25-1971-82
Helios	Pacific Blue	BioLegend, # 137210
CTLA-4	Biotin	eBiosciences, # 13-1522-82
LAP	Per-CP	eBiosciences, # 46-9821-82
GARP	V450	eBiosciences, # 48-9891-82
GITR	Pe-Cy7	eBiosciences, # 25-5874-82
CD39	Pe-Cy7	eBiosciences, # 25-0391-82
CD73	Biotin	eBiosciences, # 13-0731-82

Table 2: Fluorochrome-labelled antibodies used in this study.

2.1.5 RPMI medium

Ten percent FCS/RPMI medium was prepared by adding 50 ml of heated-inactivated FCS into 500 ml of RPMI and stored at 4 °C. This medium was used for tissue samples collection and single cell preparation including washings steps. Complete RPMI medium was prepared by adding 100 U/ml penicillin-G, 100 µg/ml streptomycin and 10 mM HEPES to the ‘10 % FCS/RPMI’ medium for cell culture.

2.2 Methods

In this section, general and specific methods that were used throughout the project are explained in detail and summarised in Table 3 and Table 4, respectively.

Methods	Purposes
Cytospin	BAL differential counts.
Giemsa staining	BAL differential counts.
³ [H]-thymidine assay	Proliferation assay of T cells using ³ [H]-thymidine incorporation and scintillation measurement.
Depletion assay	Determines Treg suppressive function.
ELISA	Quantitative technique to measure cytokines in BAL fluid.
ELISPOT	Antibody and enzyme based detection of cytokines release on a per cell basis.
FACS sorting	Cell separation based on FACS staining.
Flow cytometry (FACSAria and LSRII)	Laser based analysis of cells in flow using fluorochrome conjugated antibodies.
FlowCytomic assay	Determines Th1/Th2 cytokines in cell culture supernatant and BAL fluid

Table 3: Summary of general methods used throughout the project.

Chapters	<i>In vitro</i> assays		<i>In vivo</i> mouse models	
	<i>In vitro</i>	Treg subsets	Disease model	Treg subsets
3	-NA-	-NA-	Chronic AAI	CD4 ⁺ CD25 ⁺
4	Proliferation and depletion assays	Unmanipulated mice: CD25 ⁺ TNFR2 ⁺ and CD25 ⁺ TNFR2 ⁻	Acute AAI during induction and resolution phase	TNFR2 ⁺ Foxp3 ⁺ and TNFR2 ⁻ Foxp3 ⁺
5	-NA-	-NA-	PS50G-AAI prevention mouse model	TNFR2 ⁺ Foxp3 ⁺ and TNFR2 ⁻ Foxp3 ⁺
6	Proliferation and depletion assays	Unmanipulated mice: CD4 ⁺ CD25 ⁺ and CD4 ⁺ CD25 ⁻ ALI mouse model: CD25 ⁺ TNFR2 ⁺ and CD25 ⁺ TNFR2 ⁻	ALI mouse model	CD25 ⁺ TNFR2 ⁺ and CD25 ⁺ TNFR2 ⁻

Table 4: Summary of *in vitro* assays and *in vivo* mouse models used throughout the project.

2.2.1 OVA immunisation and challenge protocol

Mice were sensitised by intraperitoneal (i.p) injection with 50 µg ovalbumin (OVA; diluted in saline from 10 mg/ml stock solution) adsorbed in 10 % alum. Mice received 100 µl of OVA solution in both sides of the abdomen. Mice were sensitised twice for either the acute or chronic challenge model 10 days apart. The control group received 200 µl of saline mixed with 10 % alum on each injection. Ten days after sensitisation, mice were anaesthetised by isoflurane inhalation and challenged by intranasal (i.n) instillation with 25 µg OVA (in 50 µl from 10 mg/ml stock solution) or saline. In the AAI mouse model, mice were challenged every day for a total of 3 or 4 challenges and sacrificed 24 h after the final allergen challenge. In the kinetics AAI mouse model (induction and resolution phase), mice were challenged every day for a total of 3 or 4 challenges and sacrificed 24 h (day 1), and on days 4 and 10 after the final allergen challenge. To investigate the long term effects of nanoparticles in naïve mice, saline or PS50G were intratracheally (i.t.) administered and tissue samples collected on days 1, 3, 7 and 30. To investigate the effects of pre-exposure to nanoparticles in AAI mouse model, saline or PS50G were administered i.t before sensitisation phase and samples were collected after the final challenge. For LPS-induced ALI, samples were collected on day 3 post i.t instillation. The outline and details for each model used in this study is given in the respective chapters.

2.2.2 Recombinant follistatin

Follistatin (FS288) was produced ‘in house’ by Dr Hong-An Nguyen (Hardy et al., 2013c) using the follistatin expressing plasmid (pSV2HF288), a gift from Professor Shunichi Shimasaki (University of California, San Diego, USA). The FS288 gene was amplified from pSV2HF288 by PCR and sub-cloned into pAPEX3P vector. The

pAPEX3P-FS288 plasmid was transfected into 293EBNA cells, and puromycin-resistant cells expanded to form the stable 293EBNA FS cell line. FS288 was purified from conditioned media of cultured 293EBNA FS cells by successive rounds of chromatography through heparin-Sepharose affinity (5 ml Hi-Trap Heparin column, GE Healthcare Bio-Sciences), size exclusion (Superdex 200 prep grade, Hi-load 16/60) and RPHPLC (Reversed Phase, OD-300, Aquapore ODS, C-18, 7 μ m, 300 Å, 10 cm, 2.1 mm i.d. Brownlee Cartridge Column; PerkinElmer) columns (Hardy et al., 2013c).

2.2.3 Follistatin treatment in chronic AAI model

The effect of follistatin (also known as FS288) on chronic airways inflammation and remodelling was investigated by i.n treating OVA-sensitised mice with follistatin (0.05, 0.5 or 5 μ g per mouse) concurrently with OVA challenge 3 times/week for 5 weeks; controls received saline. Groups of mice were sacrificed after 1, 3 and 5 weeks of allergen (\pm follistatin) challenge. Blood, BAL fluid, LN and lungs were collected for further analysis.

2.2.4 Preparation of nanoparticles

Polybead carboxylate microspheres were glycine coated as described (Fifis et al., 2004). Briefly, EDAC was added to polybeads (40-50 nm, 1 % solids) at 4 mg/ml, the pH was adjusted to 6.5 with 1 M NaOH, and preparations rocked for 2 h at RT. Glycine was added to 100 mM for 30 min before overnight dialysis in cold PBS using a 12-kDa membrane cut-off. After dialysis, the volume was adjusted to maintain 1 % solids and the suspension was sonicated for 10 min before being administered to mice.

2.2.5 Blood and tissue collection

Mice were sacrificed by asphyxiation with CO₂ and blood and tissues collected. Following collection of blood from the inferior vena cava, lungs were lavaged 3 x with 0.4 ml (a total of 1.2 ml) 1 % FCS in PBS for collection of BAL fluid. The lung, lung draining LN and spleen were collected into 10% FCS RPMI 1640. For morphological assessment, lungs were collected and fixed in 10 % neutral buffered formalin for histology and/or frozen for collagen content determination. Lungs were chopped with a McIlwain tissue chopper (Mickle Laboratory Engineering Co. Ltd, Gomshall, Surrey, U.K.), while lung-draining LN were finely minced using a surgical blade (Swann-Morton, UK). Tissue fragments were digested in collagenase type IV (1 mg/ml) and DNase type I (0.025 mg/ml) in a volume of 7 ml at 25 °C by manual pipetting for 20 min. The reaction was stopped by adding one 10th volume of 0.01 M EDTA and mixing for 5 min. The cell suspension was filtered through a 70 µm cell strainer (BD Falcon, Techno Plus, Australia) and underlaid with 1 ml 0.01 M EDTA in FCS prior to centrifugation (350 x g, 8 min, 4 °C). Spleen was gently pressed onto the cell strainer (BD Falcon, Techno Plus, Australia) by using a syringe plunger (Terumo[®] Syringe, Belgium) and cells collected in a tissue culture plate (GmBh, Germany). Lung, lung-draining LN and spleen cells were RBC-lysed with 0.5 ml, 0.2 ml and 5 ml RBC lysis buffer (respectively) for 5 min at RT. Single cell suspensions were then centrifuged as above and cells resuspended in FACS staining buffer [3 % FCS, 3 % pooled normal mouse serum, 5 mM EDTA (pH 7.2) and 0.1% Na-Azide in Ca²⁺/Mg²⁺-free HBSS], and viable cells counted in a haemocytometer. In some experiments, lung-draining LN cells were resuspended in complete RPMI medium for overnight culture after cell counts.

2.2.6 Cytospins

Cells were separated from BAL fluid by centrifugation (350 x g, 5 min, 4 °C). Aliquots of BAL fluid were stored at -80 °C until required for analysis. BAL cells were resuspended in PBS 1 x (50-200 µl dependent on cell pellets) and centrifuged (300 x g, 5 min, RT) onto slides (SuperFrost White, Lomb Scientific Pty. Ltd. Australia) using a cytocentrifuge (Grale Scientific, Australia). Cytospin slides were air-dried, fixed with methanol (1-2 min) and Giemsa-stained for 8 min. Approximately 200 cells were identified by standard morphology criteria using a microscope at x1000 magnification. The absolute lymphocyte, macrophage, eosinophil and neutrophil number, for each mouse, were calculated by multiplying the percentage with the BAL total viable cell count.

2.2.7 ELISA for TGF- β , IL-4, IL-5 and IL-13

BAL fluid samples were analysed for levels of TGF- β , IL-4, IL-5 and IL-13 using TGF- β 1 DuoSet ELISA Development System and IL-4, IL-5 and IL-13 Ready-SET-Go! ELISA Kit. Costar 96-well EIA/RIA plates (Corning Incorporated, Australia) were coated with antibodies against TGF- β (4 µg/ml), IL-4 (1:500), IL-5 (1:500) and IL-13 (1:250) in (1mM) carbonate buffer (coating buffer) overnight at RT. Plates were blocked for 1 h with 200 µl/well 1 x blocking buffer (5 % Tween 20 in PBS with 0.05% NaN₃) for 1 hr at RT. For TGF- β 1 ELISA, latent TGF- β 1 in samples was first acid activated with 1 N HCl (1:5 dilution with sample) for 10 min and neutralized with 1.2 N NaOH/0.5 M HEPES; samples were adjusted to pH 7.2-7.6 as required. An 8-point TGF- β , IL-4, IL-5 and IL-13 standard was made by serial dilutions in reagent diluent (1.4 % FCS in PBS-Tween); with concentrations ranging from 7.81 - 1000 pg/ml. Blocking buffer was discarded and the

plates were washed in PBS-Tween. Samples or activated samples (TGF- β) and standards (50 μ l) were added to their appropriate wells for incubation for 2 h at RT. After incubation, samples and standards were discarded and the plates washed. Biotinylated TGF- β -, IL-4-, IL-5- and IL-13-specific antibody [TGF- β : 200 ng/ml, IL-4 (1:500), IL-5 (1:500) and IL-13 (1:250)] was added for 2 h (TGF- β) and 1 h for other cytokines. Plates were washed and streptavidin-horse radish peroxidase (1:250) added for 1 h. Washes with PBS-Tween and PBS were performed and plates were developed by addition of 100 μ l substrate solution (1x) for 30 min at 37 °C. Development for TGF- β was stopped by adding 4 M HCl and 2N H₂SO₄ for other cytokines and the plate was read at 490 nm on the Microplate reader (Model 3550, Bio-Rad) and data analysed. Final results for each sample were calculated by subtracting background (no antigen) readings from sample readings. Standards were used as positive controls and blank wells containing no antigen as negative controls.

2.2.8 OVA-specific IgE ELISA

Serum samples were used to measure OVA-specific IgE in the AAI mouse model. Costar 96-well EIA/RIA plates were coated with OVA (10 μ g/ml) in carbonate buffer (50 mM) overnight at 4 °C followed by blocking with 5 % blocking buffer (skim milk powder in PBSTween) for 1 h at 37 °C. Blocking solution was discarded and the plates were washed in 1 x PBS-Tween, then 40 μ l Protein G-treated serum (to deplete IgG) was added and incubated for 1.5 h at RT. Samples were discarded and plates washed. Biotinylated anti-mouse IgE-specific antibody diluted in 1 % blocking buffer was added for 1 h. Plates were washed and streptavidin-horse radish peroxidase (1:1000) was added for 45 min. Washes of PBS-Tween followed by PBS were performed followed by incubation with o-phenylene-diamine [dissolved in phosphate citrate buffer(0.05 M)] for 20 min at 37 °C.

Development was stopped by adding 4 M HCl and the plate was read at 490 nm on a Microplate reader (Model 3550, Bio-Rad). Serum from OVA-immunized mice with known high OVA-specific IgE titre acted as a positive control and the negative control was normal mouse serum from naïve mice. Final results for each sample were calculated by subtracting background (no antigen) readings from sample readings.

2.2.9 Cytokine ELISPOT

ELISPOT allows the frequency of cells secreting the specified cytokine to be determined. ELISPOT plates (MAHAS4510) were coated with IL-4 and IL-5 antibody at 5 µg/ml in PBS or IL-13 antibody (10 µg/ml) in PBS overnight at 4°C. Plates were washed before blocking with 10 % FCS in RPMI 1640 for 2-3 h at 37 °C. Blocking solution was discarded, and 0.5×10^6 cells (resuspended in complete RPMI 1640 medium) in 100 µl added to the wells with 10 µl of appropriately diluted antigen/mitogen (final concentration: 25 µg/ml OVA or 2 µg/ml Con A). For the negative control, cells were cultured in medium alone. Following culture for 16-17 h at 37 °C, cells were discarded by flicking off the plate. Plates were soaked in distilled water for 10 min and washed before addition of biotinylated IL-4 (1:500), IL-5 (1:500) or IL-13 (1:100) antibodies for 1.5 h. Plates were washed followed by addition of ExtrAvidin®–alkaline phosphatase for 1.5-2 h at RT. Washes were in 0.05 % Tween 20/PBS followed by PBS. Reaction product was developed by ELISPOT development buffer followed by an additional 2 washes with distilled water. Plates were air-dried overnight and read on an ELISPOT reader (Autoimmun Diagnostika, Strassberg, Germany).

2.2.10 FlowCytomix assay

The concentration of cytokines in BAL fluid (IL-1 α , IL-2, IL-4, IL-5, IL-6, IL-10, IFN- γ , TNF, and IL-17, GM-CSF) was detected by mouse Th1/Th2 10plex kit FlowCytomix (eBioScience, Austria). Assay buffer was prepared by adding 50 ml assay buffer concentrate (10 x) to 450 ml ddH₂O and mixing gently to avoid foaming. The lyophilized standard was reconstituted by adding ddH₂O according to the label on the standard vial. The highest standard was prepared by adding 10 μ l of each reconstituted standard to a vial labeled standard 1 and filled up to the final volume of 200 μ l with assay buffer (1 x). This is a 1:20 dilution of the reconstituted standard. Other standards were prepared by serial dilution as per the manufacturer's protocol. Blank, standards and samples (25 μ l each) were mixed with 25 μ l beads and 50 μ l biotin-conjugated antibodies for 2 hr at RT. Beads were washed 2 x by adding 0.5 ml of assay buffer and centrifuged at 200 x g for 5 min. Fifty μ l streptavidin-PE was added to the tubes and incubated for 1 hr at RT. The mixture was washed 2 x by adding 0.5 ml of assay buffer and centrifuged at 200 x g for 5 min. Finally, 500 μ l assay buffer (1 x) was added to the tubes before analysis by flow cytometry. Results were analysed by FlowCytomix Pro2.4 program (eBioScience, Austria).

2.2.11 Cell surface and intracellular staining

All fluorochrome-labelled monoclonal antibodies used in surface and intracellular staining were titrated prior to use to determine the optimal antibody dilution for detection by flow cytometry. Lung, lung-draining LN, BAL and spleen cells (1×10^6) were surface-stained in a 96 well-round bottom plate (on ice for 20 min) with combinations of the antibodies (Table 2) or their respective immunoglobulin isotypes. Cells were washed with

FACS staining buffer and incubated with 50 μ l Fix/Perm buffer (1:4 ratio concentrate: diluent) for 30 min on ice to allow the permeabilisation of cell membranes. Cells were washed with 1 x Perm buffer (10 % Perm buffer in distilled water). At this stage, compensation controls and blank controls (non-stained cells) required no additional staining and were resuspended in 150 μ l 1 % paraformaldehyde. All other cells were stained with intracellular antibodies [Foxp3 (APC), Ki67 (FITC) and Helios (V450)] by 30 min incubation (on ice) or with their respective immunoglobulin isotypes. Cells were washed twice with 1 x Perm buffer followed by resuspension in 150 μ l 1 % paraformaldehyde. Acquisition was on a LSRII flow cytometer (BD BioSciences) and analysis was performed using FlowJo Software (Tree Star, USA).

2.3 Statistical analysis

Data were analysed for normality, and log-transformed as necessary prior to analysis by independent samples *t* test to compare between two groups, and one or two-way ANOVAs with Tukey or Bonferroni post-tests, respectively, to compare between multiple groups and different time points. Spearman's correlations were used for the comparison of continuous variables. The Spearman's *r* value for the correlation between the two variables was stated in each result. Statistical analysis was performed using Graph Pad Prism v5.02 software (GraphPad, San Diego, USA). Differences were considered statistically significant if $p < 0.05$. All values are mean \pm SEM.

-This page intentionally left blank-

Chapter 3

Modulation of lung Treg by follistatin during allergic airway inflammation

3.1 Introduction

Regulatory T cells are a population of CD4⁺ T cells expressing CD25 (α chain of the IL-2 receptor) and the transcription factor FoxP3 (Boissier et al., 2009). They play a crucial role in the maintenance of self-tolerance and immune balance (Jonuleit and Schmitt, 2003, Murakami et al., 2002) and are involved in the modulation of immune responses to alloantigens, cancer cells, and pathogens (Belkaid et al., 2002). The major populations of Treg that have been characterised in disease models are CD4⁺CD25⁺Foxp3⁺ Treg, which are classified as natural or adaptive; the latter subset are IL-10 and TGF- β -secreting Tr1 and Th3 cells, respectively. Previous studies have demonstrated that CD4⁺CD25⁺Foxp3⁺ Treg play an important role in controlling the initiation of lung inflammation (Baru et al., 2010). However, as shown by others, and also demonstrated in this study (Chapter 4, 5 and 6), the expression and percentage of lung Foxp3⁺ cells within CD4⁺CD25⁺ Treg decreases during lung inflammation (both in the AAI and ALI mouse models), but increases to normal levels in the resolution phase (Baru et al., 2010, D'Alessio et al., 2009). In this context, the question arises whether CD4⁺CD25⁺ Treg that are Foxp3⁺ might play a role in the resolution of AAI.

Treg numbers increase in the lung and BAL fluid and remain elevated through day 10 after the induction of lung inflammation, representing Treg recruitment, proliferation, or a combination of these two factors (D'Alessio et al., 2009). This chapter aimed to investigate the effects of follistatin treatment on Treg frequencies during AAI. As introduced in Chapter 1, activin A is a pleiotropic TGF- β family member that regulates AAI and is expressed in response to inflammatory signals. Various cell types secrete activin A including peritoneal macrophages, monocytes, vascular endothelial cells and

other immune cell types (Ogawa et al., 2006). Studies show that activin A participates in various biological processes, such as development, hematopoiesis, wound repair and fibrosis (Werner and Alzheimer, 2006). Previous studies by our group showed that activin A is also increased in the lung and BAL fluid of mice during acute AAI (Hardy et al., 2006, Hardy et al., 2010) and chronic AAI (Hardy et al., 2013c). Another study also found increased activin A in BAL fluid of chronic AAI and airway remodeling (Le et al., 2007).

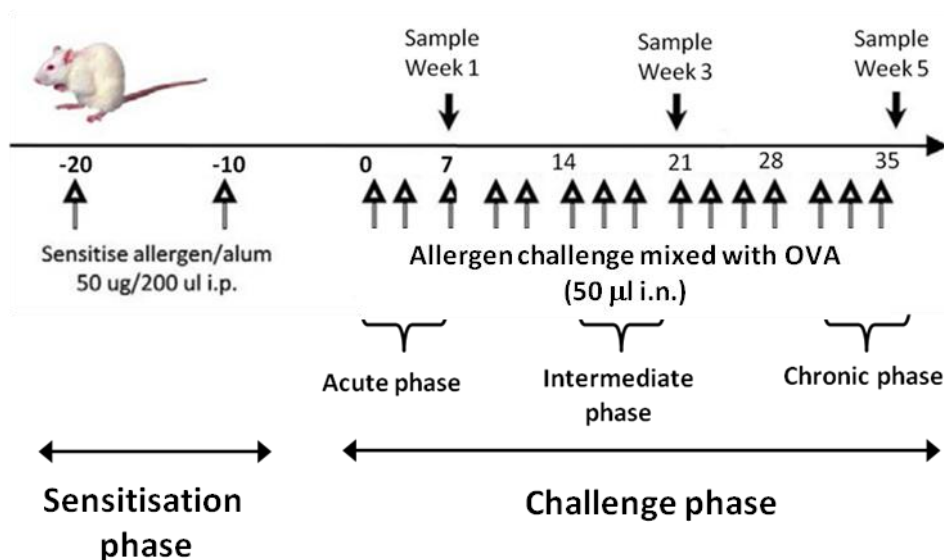
Similar to TGF- β , activin A, a pleiotropic cytokine also regulates multiple steps in the response to inflammation. In addition, they share the same signaling Smad2/3 pathway. However, unlike TGF- β , activin A is not secreted in a latent form. Activin A enhances the conversion of mouse peripheral naïve T cells to Foxp3⁺ Treg *in vivo* and increases TGF- β -induced Treg *in vitro* (Huber et al., 2009). Data regarding the role of TGF- β for the *in vivo* suppression function of CD4⁺CD25⁺ Treg are controversial. Studies have shown that TGF- β is required for conversion of CD4⁺CD25⁻ cells to CD4⁺CD25⁺ induced Treg and expansion of CD4⁺CD25⁺ Treg; suggesting a crucial role for TGF- β in the homeostatic regulation of the immune system (Huber et al., 2004, Marie et al., 2005).

As an immunomodulatory cytokine, activin A can directly inhibit immune responses and induce generation of Treg. The biological effects of activin A are neutralised or inhibited by follistatin, a natural secreted glycoprotein with high affinity binding to activin A (Krummen et al., 1993). Activin A is secreted in airway inflammation, together with follistatin, in both human asthma and experimental asthma models (Hardy et al., 2006, Karagiannidis et al., 2006, Rosendahl et al., 2001) which further suggests the importance of follistatin and activin A in modulating acute and chronic AAI.

In accordance with this, the general aim of this chapter was to investigate the frequencies and characteristics of Treg in the lung and lung-draining LN of AAI and whether blocking of activin A by follistatin has a role in modulating AAI, in the context of frequencies and characteristics of Treg.

3.2 Experimental Procedures

The effect of follistatin treatment on AAI was investigated by intranasally treating OVA-sensitised mice with 0.05 µg and 0.5 µg [based on our previous studies, (Hardy et al., 2006)] and 5 µg of follistatin (which binds endogenous activin A), concurrently with OVA challenge 3 times/week for 5 weeks; control groups received saline treatment in lieu of follistatin with the same challenge regimen as the treatment groups (Figure 3.1). Blood, BAL fluid, lung-draining LN and lung were collected for investigations into allergic disease phenotypes and the induction of CD4⁺CD25⁺ Treg, both in the lung and lung-draining LN after follistatin treatment. Part of the lung-draining LN and lung cell suspensions were provided to Dr. Hong-An Nguyen for investigation on antigen presenting cell. Some of these results are now published as an article in Thorax entitled ‘The activin A antagonist follistatin inhibits asthmatic airway remodelling’ (Hardy et al., 2012b). However, the results presented in this chapter comprise those from all time points (weeks 1, 3 and 5), whereas only results on week 5 were published (Hardy et al., 2012b).



#	Groups	Sensitisation (i.p.)	Challenge (i.n.)
1	Negative	Saline	Saline
2	Negative	Saline	Saline + Ovalbumin
3	Positive	Ovalbumin	Saline + Ovalbumin
4	Test 0.05 µg FS	Ovalbumin	Saline + Ovalbumin + 0.05 µg FS
5	Test 0.5 µg FS	Ovalbumin	Saline + Ovalbumin + 0.5 µg FS
6	Test 5 µg FS	Ovalbumin	Saline + Ovalbumin + 5 µg FS

Figure 3.1: Schedule of allergen immunisations and follistatin treatment for chronic OVA-induced allergic airway inflammation model. Groups of mice (6-7 mice/group) were sensitised i.p. with OVA/alum, while control groups received saline/alum (Sensitisation phase). Negative controls were challenged i.n either with saline (Sal/Sal = group 1) or OVA (Sal/Sal+OVA = group 2) and positive control mice were challenged i.n. with OVA (OVA/Sal+OVA = group 3) and follistatin treatment groups received different doses of follistatin (mixed with OVA and saline: 0.05 µg (OVA/Sal+OVA+0.05µg FS = group 4), 0.5 µg (OVA/Sal+OVA+0.5µg FS = group 5) or 5 µg (OVA/Sal+OVA+5µg FS = group 6). Tissue sampling was performed on day 36 after the final lung allergen challenge. FS, follistatin.

3.3 Results

3.3.1 Follistatin treatment altered cells numbers in BAL fluid, lung-draining LN and lung

Follistatin treatment at 0.05 μg during the OVA challenge period significantly increased BAL total cell counts in weeks 1 and 5, whereas instillation of 0.5 μg follistatin increased BAL total cell numbers in week, 3 compared to the OVA positive control group. In contrast, instillation on 5 μg follistatin did not cause any significant differences compared to the OVA positive control group. BAL total cell numbers in Sal/Sal and Sal/Sal+OVA negative control groups remained at the lower levels on week 1-5 (Figure 3.2A). Lung-draining LN total cell numbers were significantly increased on week 5 after instillation of 5 μg follistatin, but no changes were observed for the other follistatin doses compared to the OVA positive control group. Interestingly, in week 3 and 5, total lung-draining LN cell numbers in the Sal/Sal+OVA negative group were significantly higher than for the Sal/Sal negative control group (Figure 3.2B). Follistatin treatment did not alter lung total cell numbers at any time point, except the numbers were markedly decreased in the 0.5 μg follistatin group in week 5. Sal/Sal+OVA group showed increased total lung cell numbers to almost the same levels as the OVA positive control group at week 5, and this was significantly higher than for the Sal/Sal negative control group (Figure 3.2C).

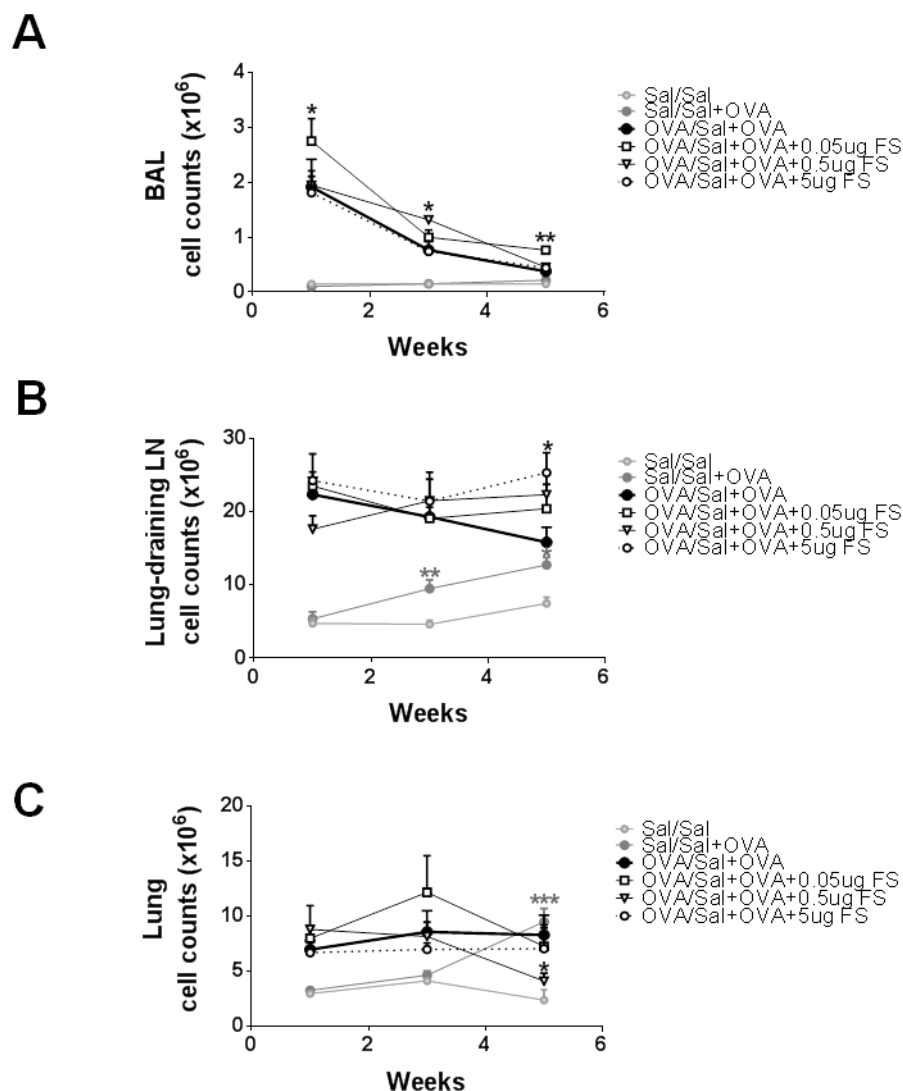


Figure 3.2: Follistatin treatment altered cell numbers in BAL fluid, lung-draining LN and lung. Mice were sensitised as described in Figure 3.1, and challenged with OVA, or OVA+follistatin (different doses); control mice received saline instead of OVA or follistatin. Time points analysis of cell numbers in the **(A)** BAL fluid, **(B)** lung-draining LN and **(C)** the lung after follistatin treatment. Mean \pm SEM, 6-7 mice/group per time-point. * $p < 0.05$, ** $p < 0.01$, and *** $p < 0.001$ (grey- compared to Sal/Sal and black- compared to OVA/Sal+OVA group).

3.3.2 Follistatin treatment decreased serum OVA-specific IgE but not eosinophil absolute numbers

Serum OVA-specific IgE concentration after 5 µg follistatin treatment was significantly decreased at week 3 and remained at a lower level in week 5 compared to the OVA positive control group. However, the serum OVA-IgE concentration in Sal/Sal+OVA mice was significantly higher compared to the saline negative control group over the time points. Eosinophil absolute numbers were decreased over time in all treatment groups, paralleling the reduction in total BAL cell counts, except 0.05 µg follistatin treatment increased eosinophil absolute numbers in week 5. However, there was no difference between the Sal/Sal+OVA group compared to the negative control group (Figure 3.3).

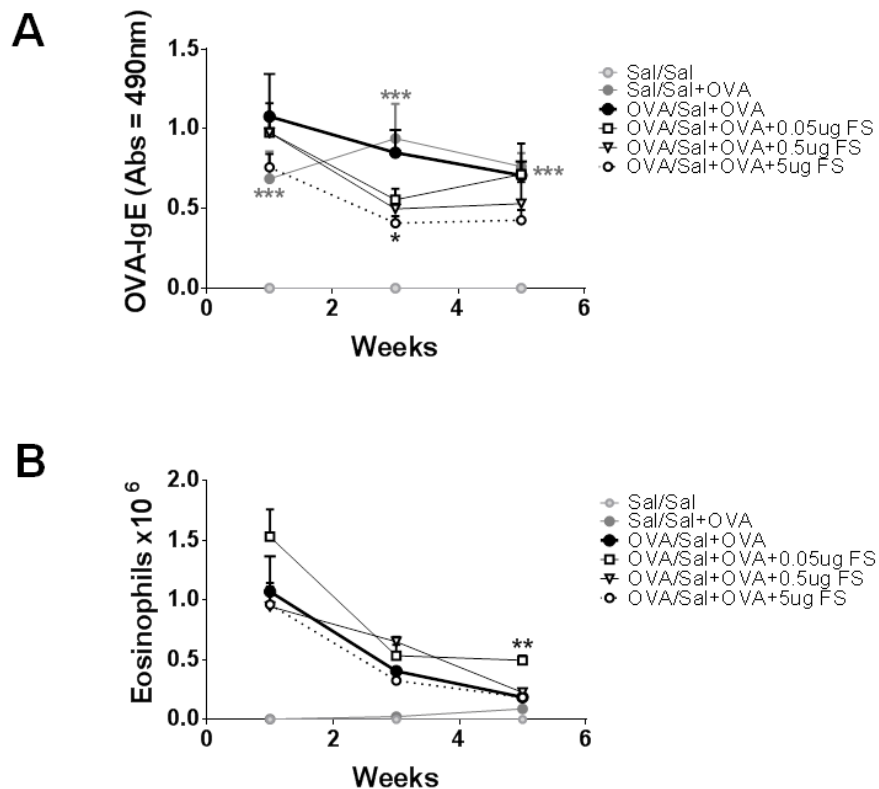


Figure 3.3: Follistatin treatment decreased serum OVA-specific IgE but not eosinophil absolute numbers. Mice were sensitised as described in Figure 3.1, and challenged with OVA, or OVA+follistatin (different doses); controls received saline instead of OVA or follistatin. Time points analysis of levels of **(A)** serum OVA-specific IgE and **(B)** BAL eosinophil numbers. Mean \pm SEM, 6-7 mice/group per time-point. ** $p < 0.01$, and *** $p < 0.001$ (grey- compared to Sal/Sal and black- compared to OVA/Sal+OVA group). Data were collected and analysed by Dr. Hong-An Nguyen.

3.3.3 Follistatin treatment did not alter the cytokine profile of LN cells

Th2-producing LN cells were analysed after follistatin treatment to determine the effects of follistatin-activin A binding on chronic AAI. Follistatin treatment did not alter the frequency of IL-4, IL-5 and IL-13 producing cells in the lung-draining LN (Figure 3.4). There was no difference between the two negative control groups (Sal/Sal and Sal/Sal+OVA). Th2-producing LN cell numbers in these negative control groups were at the basal level across all time points. Overall, Th2-producing LN cells in follistatin treatment and positive control groups were higher at week 1, and decreased at week 3 and week 5 although remaining above the negative control groups (Figure 3.4).

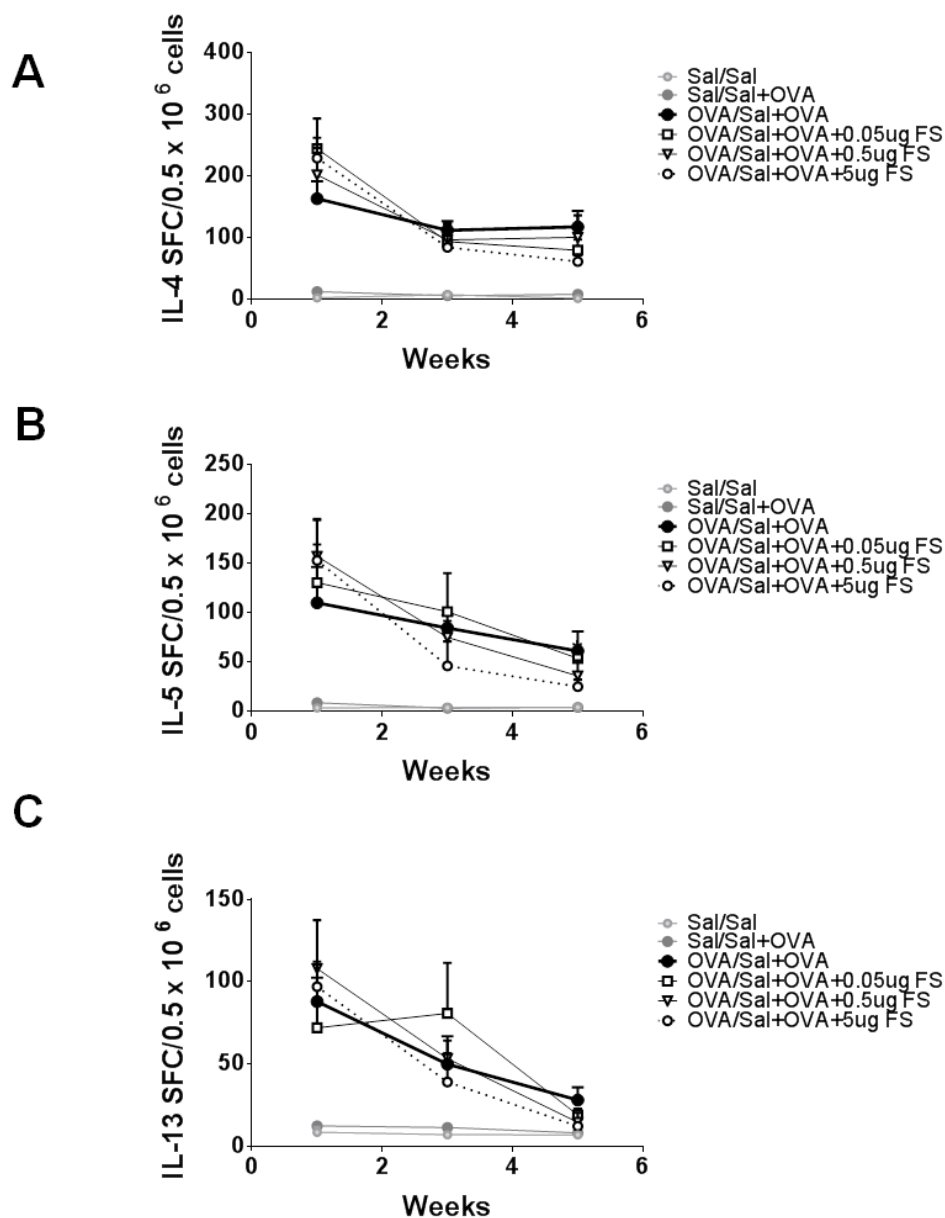


Figure 3.4: Follistatin treatment did not alter numbers of cytokine producing LN cells. Mice were sensitised as described in Figure 3.1, and challenged with OVA, or OVA+follistatin (different doses); controls received saline instead of OVA or follistatin. Time points analysis of OVA-specific (A) IL-4, (B) IL-5 and (C) IL-13 producing cells in the lung-draining LN. Mean \pm SEM, 6-7 mice/group per time-point. Data were obtained and analysed by Dr. Hong-An Nguyen.

3.3.4 Follistatin treatment altered Activin A and TGF- β levels in the BAL fluid

To further investigate the effects of follistatin on chronic AAI, the secretion of activin A in BAL fluid was examined. Instillation of 5 μ g follistatin induced a significant reduction of activin A in BAL fluid, compared to the OVA positive control group. Other follistatin doses reduced the secretion of activin A, but not significantly compared to the OVA positive control group. As it has been previously found in our laboratory that there was a close relationship between activin A and TGF- β levels (Hardy et al., 2010), this cytokine was also analysed. In accordance with a significant decrease of activin A secretion into BAL fluid, TGF- β was also significantly decreased compared to the OVA positive control group (Figure 3.5). Activin A secretion in the Sal/Sal+OVA group did not differ compared to the Sal/Sal negative control group. However, secretion of TGF- β in the Sal/Sal+OVA group was significantly higher than that in Sal/Sal negative control group in week 1 and week 3 and returned to basal level in week 5 (Figure 3.5).

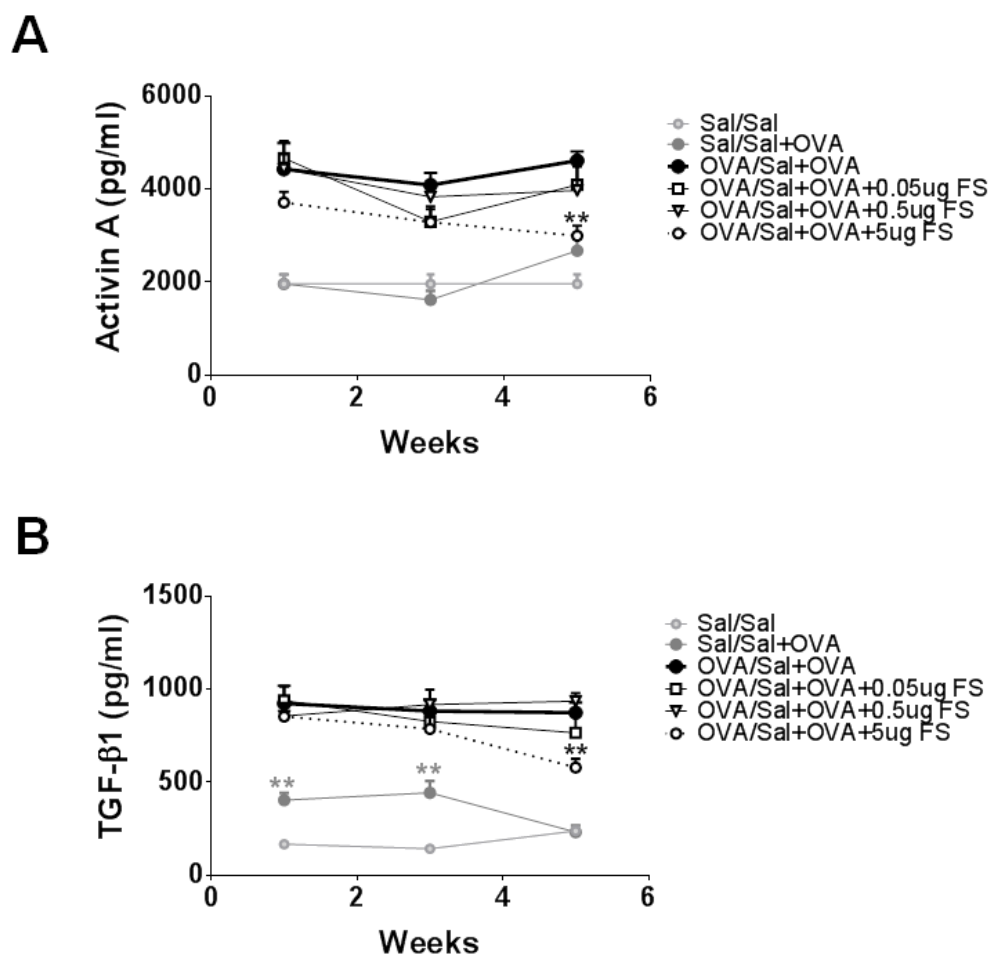


Figure 3.5: Follistatin treatment altered Activin A and TGF- β levels in the BAL fluid. Mice were sensitised as described in Figure 3.1, and challenged with OVA, or OVA+follistatin (different doses); control mice received saline instead of OVA or follistatin. Time points analysis of BAL fluid (A) activin A and (B) TGF- β concentrations. Mean \pm SEM, 6-7 mice/group per time-point. ** $p < 0.01$ compared to OVA/Sal+OVA group. Data were obtained and analysed by Dr. Hong-An Nguyen.

3.3.5 High dose follistatin decreased lung CD4⁺CD25⁺ Treg (at week 3), but did not alter Foxp3 expression

As shown in Figure 3.5, 5 µg follistatin treatments decreased activin A and TGF-β in the BAL fluid compared to the OVA positive control group at week 5. Recent studies showed that activin A plays a pivotal role in the induction of CD4⁺CD25⁺ Treg expressing Foxp3 to suppress Th2 responses through the actions of IL-10 and TGF-β (Semitekolou et al., 2009, Huber and Schramm, 2011). Thus, the frequency of CD4⁺CD25⁺ Treg after follistatin treatment in the lung was studied to assess the effects of follistatin-activin A binding on lung cells. The percentages of lung CD4⁺CD25⁺ Treg from the Sal/Sal negative control group were similar to the percentages in naïve mice, approximately 5 - 10 %. However, in the other negative control group, Sal/Sal+OVA, the percentage of these cells was significantly increased at week 3 and week 5. After treatment with 5 µg follistatin, there was a significant reduction of CD4⁺CD25⁺ Treg at week 3 compared to the OVA positive control group. Overall, the percentage of these cells in all groups decreased over time, as airway inflammation decreased, but the percentages remained at higher levels compared to the Sal/Sal negative group. Analysis of Foxp3 expression within this population showed that over the time points, when the inflammation is slightly resolved at week 5, Foxp3 expression in OVA positive and follistatin treatment groups was decreased. However, there were no significant differences between these groups. Interestingly, Foxp3 expression in the Sal/Sal+OVA negative control group was significantly less than in the Sal/Sal negative control group and dropped to the same level as in the OVA positive and follistatin treatment groups in week 5. Foxp3 expression within CD4⁺CD25⁺ Treg in the Sal/Sal negative control group was higher over the time points (Figure 3.6).

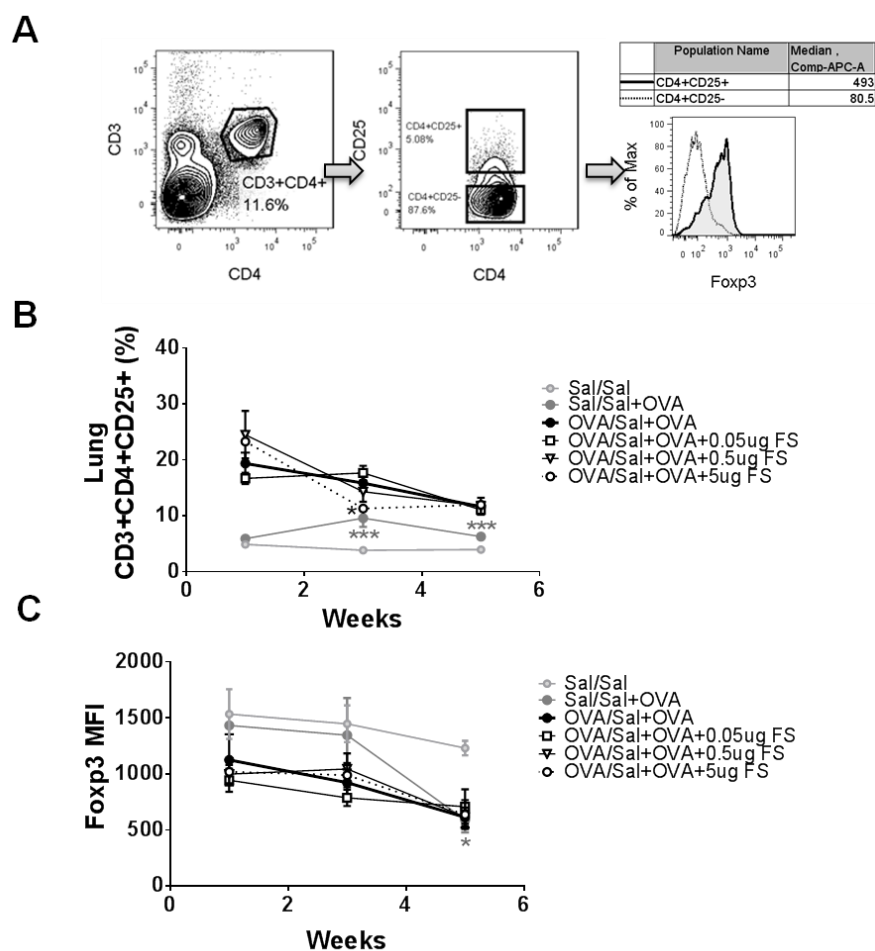


Figure 3.6: Treatment with high dose of follistatin decreased $CD4^+CD25^+$ Treg percentages only in week 3. No effects of follistatin treatment on Foxp3 expression at all time points. Mice were sensitised as described in Figure 3.1, and challenged with OVA, or OVA+follistatin (different doses); controls received saline instead of OVA or follistatin. Lung leukocytes were isolated by collagenase/DNAse digestion and gated on viable $CD3^+CD4^+CD25^+$ cells, followed by gating on (A) Foxp3 within $CD4^+CD25^+$ (thick black line, open histogram) and $CD4^+CD25^-$ (grey line, filled histogram). Plot is representative of Week 1. Time points analysis of the percentages of (B) $CD4^+CD25^+$ Treg and (C) Foxp3 expression in the lung. Mean \pm SEM, 6-7 mice/group per time-point. * $p < 0.05$, and *** $p < 0.001$ (grey- compared to Sal/Sal and black- compared to OVA/Sal+OVA group).

3.3.6 High dose follistatin increased lung-draining LN CD4⁺CD25⁺ Treg (at all time points), but did not alter Foxp3 expression

The percentages of CD4⁺CD25⁺ Treg in the lung-draining LN were also examined. There were approximately 5 - 7 % CD4⁺CD25⁺ Treg in follistatin treatment and control groups. No significant differences were observed at week 3 in all groups. However, at week 5, the percentages of CD4⁺CD25⁺ Treg in the lung-draining LN were significantly increased in all follistatin treatment groups compared to the OVA positive control group. Yet, when the expression of Foxp3 within these cell populations were analysed, there were no significant differences between any of the groups at any time point (Figure 3.7). CD4⁺CD25⁺ Treg suppress Teff and inflammation via various mechanisms, including secretion of anti-inflammatory cytokines such as TGF- β and IL-10. As shown in Figure 3.5B, BAL of AAI mice treated with high follistatin dose had decreased TGF- β at week 5, suggesting that CD4⁺CD25⁺ Treg possibly did not improve AAI via a TGF- β pathway.

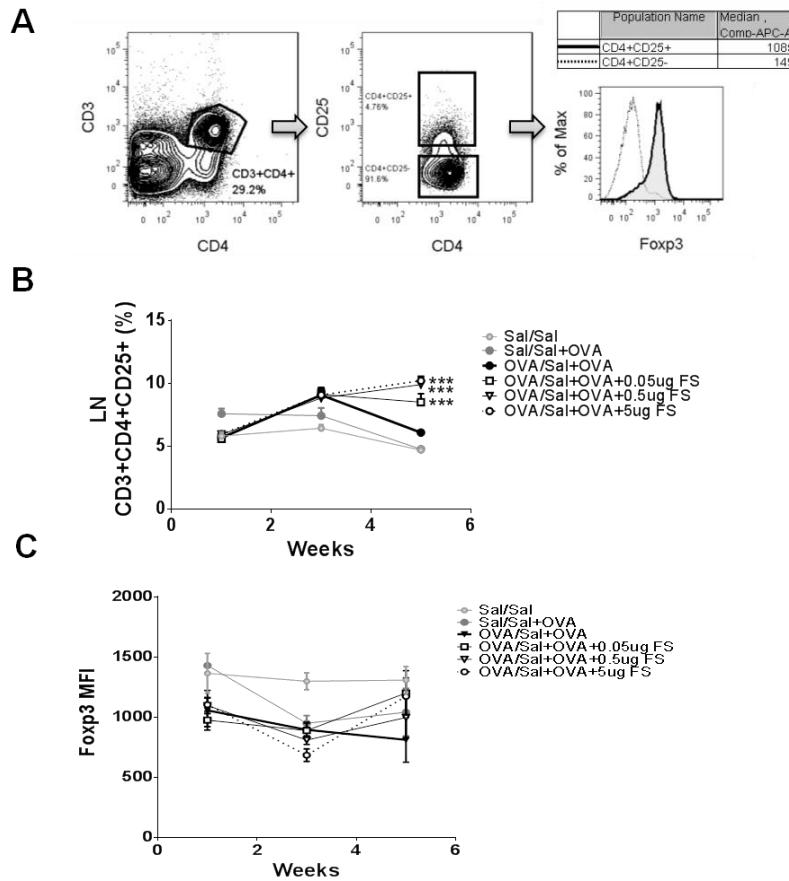


Figure 3.7: Follistatin treatment increased $CD4^+CD25^+$ Treg percentages only in week 5. No effects of follistatin treatment on Foxp3 expression at all time points. Mice were sensitised as described in Figure 3.1, and challenged with OVA, or OVA+follistatin (different doses); control received saline instead of OVA or follistatin. Stained lung-draining LN cells were gated on viable $CD3^+CD4^+CD25^+$ cells, followed by gating on (A) Foxp3 within $CD4^+CD25^+$ (thick black line, open histogram) and $CD4^+CD25^-$ (grey line, filled histogram). Plot is representative of Week 1. Time points analysis of the percentages of (B) $CD4^+CD25^+$ Treg and (C) Foxp3 expression in the lung. Mean \pm SEM, 6-7 mice/group per time-point. *** $p < 0.001$ compared to OVA/Sal+OVA group.

3.3.7 Follistatin treatment increased BAL IL-10 at week 5

To gain further insight into the effect of follistatin treatment on the concentration of BAL cytokines at week 5, a series of multiplex analyses on IL-1 α , IL-2, IL-5, IL-6, IL-10, IFN- γ , TNF, GM-CSF, IL-4 and IL-17 were performed (Table 3.1). Analysis of BAL from naïve mice revealed that at the steady state, BAL cytokines exhibited high levels of IL-1 α , IL-2, IL-10 and GM-CSF, whilst during AAI, these cytokines were decreased. In contrast, IL-4, IL-5 and IL-6 were at the highest level during AAI, but lower at the steady state. Follistatin treatment at 0.5 and 5 μ g increased IL-10 in BAL from < 0.5 pg/ml to > 5 pg/ml in both treatment groups. Other cytokines such as IL-1 α , IL-2, IFN- γ and IL-17 were not detected (below the level of detection) suggesting that immune responses of the AAI model were not skewed towards Th1 or Th17 responses (Table. 3.1).

BAL Cytokines (pg/ml)	Naïve mice	Sal negative control group	OVA positive control group	0.05 µg follistatin treatment	0.5 µg follistatin treatment	5 µg follistatin treatment
IL-1 α	64.8 \pm 10.8	52.7 \pm 6.8	BLOD	BLOD	BLOD	BLOD
IL-2	45.2 \pm 2.98	38.4 \pm 2.52	BLOD	BLOD	BLOD	BLOD
IL-5	4.8 \pm 2.58	6.1 \pm 4.9	9.6 \pm 8.49	BLOD	20.1 \pm 10.3	12.3 \pm 11.2
IL-6	1.51 \pm 1.1	BLOD	9.1 \pm 6.3	2.4 \pm 2.0	BLOD	4.7 \pm 2.74
IL-10	15.27 \pm 0.14	4.8 \pm 3.0	0.55 \pm 0.39	0.48 \pm 0.31	10.14 \pm 5.6*	4.1 \pm 2.6*
IFN- γ	BLOD	BLOD	BLOD	BLOD	BLOD	BLOD
TNF	8.23 \pm 3.5	BLOD	7.8 \pm 3.4	17.08 \pm 5.2	5.8 \pm 2.3	10.8 \pm 5.9
GM-CSF	49.15 \pm 3.34	38.73 \pm 4.5	16.5 \pm 6.7	18.5 \pm 6.9	22.1 \pm 6.24	26.23 \pm 7.6
IL-4	0.37 \pm 0.03	0.06 \pm 0.01	1.57 \pm 0.49	0.69 \pm 0.6	1.58 \pm 0.9	1.3 \pm 0.51
IL-17	BLOD	BLOD	BLOD	BLOD	BLOD	BLOD

Table 3.1: Concentrations of BAL fluid cytokines from naïve mice and at week 5 of follistatin treatment in AAI model. BAL fluid was subjected to Multiplex assay for measurement of IL-1 α , IL-2, IL-5, IL-6, IL-10, IFN- γ , TNF, GM-CSF, IL-4 and IL-17. Limits of detection were 29.86, 30.65, 1.12, 0.34, 0.16, 0.54, 2.38, 0.59, 0.04 and 0.45 pg/ml, respectively. Mean \pm SEM. *p<0.05 compared to OVA positive control group. BLOD- below limit of detection.

3.4 Discussion

The balance of innate and adaptive immunity in the lung microenvironment is central to maintaining lung homeostasis and healthy lung function. At lung homeostasis, the level of pro-inflammatory BAL cytokines (e.g. IL-6, TNF) is relatively low, cellularity at normal levels (total cell counts/numbers for naïve lung: $5 - 10 \times 10^6$ cells; lung-draining LN: $3 - 5 \times 10^6$ cells and BAL: $0.01 - 0.05 \times 10^6$ cells) and no accumulation of pro-inflammatory cells (e.g. eosinophils for Th2-skewed immune response). Nevertheless, the lung can be confronted by a diverse range of environmental substances that could induce allergic asthma in susceptible individuals. However, Treg and other complex networks of immune cells (e.g. DC) co-exist in the lung to help maintain lung homeostasis (Afshar et al., 2008). Treg are crucial in maintaining lung function and homeostasis; either induction of tolerance towards inert ‘harmless’ inhaled substances or protective immunity against invading pathogens (Randall, 2010). At lung homeostasis (Sal/Sal negative control groups of this study), Treg exhibit a higher expression level of Foxp3 suggesting their important role in downregulating the function of Teff (e.g. Th2) for the maintenance of lung immune homeostasis (Huehn et al., 2005, Sather et al., 2007).

As presented in this chapter, disruption of lung immune homeostasis (skewed towards a Th2 response) by repeated instillation of OVA for 5 weeks lead to imbalance of innate and adaptive immune responses which result in the induction of AAI at week 1 and chronic airway inflammation at week 5. The airway inflammation peaking at week 1 gradually declined over the following weeks such that by week 5 there was only low grade chronic inflammation. As reported previously, repeated allergen exposure (OVA or environmentally relevant allergens such as house dust mite or grass pollen) leads to the

development of tolerance and downregulation of airway inflammation (Kumar and Foster, 2002, Jungsuwadee et al., 2004, McMillan and Lloyd, 2004, Shinagawa and Kojima, 2003). In this study, total BAL cell counts were decreased over time after OVA challenges regardless of treatment group. The reduction in total BAL cell count was in parallel with the reduction of eosinophils, serum OVA-IgE, and LN-producing Th2 cells. This result showed that after 5 weeks of repeated OVA challenges, major features of airway inflammation were downregulated. Kumar *et al.* hypothesised that the development of tolerance in animal models of allergic inflammation was related to the high concentrations of aerosolised allergen used, which would have overwhelmed respiratory clearance mechanisms (Kumar et al., 2008). Thus, tolerance induction in the present model might result from the high concentration of OVA that was used to induce disease. Nevertheless, the reduction in airways inflammation at week 5 is parallel with an increase in Treg proportions, as seen in the lung draining LN for follistatin treatment groups. In addition, treatment with high dose of follistatin not only increased Treg proportions, but lead to the decrease in activin A and TGF- β concentrations in the BAL fluid. Treg play an important role in airway tolerance (Larche, 2007); hence the increase in CD4⁺CD25⁺ Treg in the lung-draining LN might be correlated with the development of tolerance to allergens and immune suppression (Illustrated in Figure 3.8). Future studies could address this directly by considering more sophisticated assays, such as by *in vivo* adoptive transfer of follistatin-induced Treg into compromised mice (i.e. chronic AAI) and other multivariate panels describing the cell's regulatory state (e.g. *in vitro* Treg suppression assay). I did not perform investigations on the cellular interactions between Treg and other cell types (e.g. innate and adaptive cell types such as DC and Teff, respectively), but I do know that these populations do interact one another intimately (Khare et al., 2013, Lee et al., 2012). These will be important parameters to be addressed

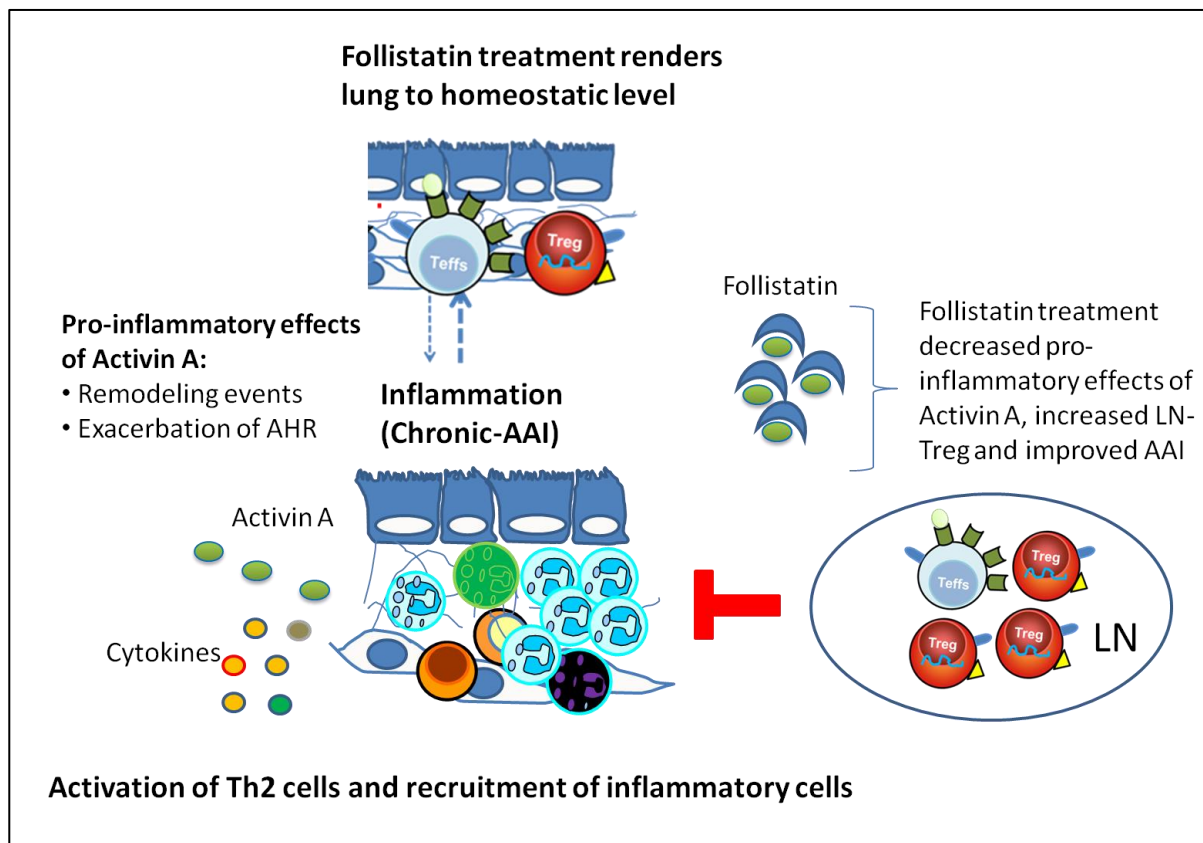


Figure 3.8: Follistatin treatment improved chronic AAI. Activin A exhibited pro-inflammatory effects during chronic AAI and exacerbates AHR and lung remodelling (Hardy et al., 2006, Hardy et al., 2013c). Treatment with high dose of follistatin decreased the concentrations of activin A and TGF- β in the BAL and increased Treg proportions in the lung-draining LN. Follistatin-activin A axis might be involved in the development of tolerance to allergens and immune suppression.

in the future. Studies have shown that activin A and TGF- β display pro- and anti-inflammatory effects depending on the cytokine microenvironment under which T cell activation occurs (Ogawa et al., 2008). Another group reported that blocking of endogenous activin A *in vivo* during allergic responses exacerbates airway inflammation (Semitekolou et al., 2009), suggesting an anti-inflammatory role for activin A. However, this anti-inflammatory trend was not observed in this study that rather showed a pro-inflammatory role since blockade of activin A with follistatin attenuated some inflammatory parameters (e.g. decreased BAL activin A concentration). This is in agreement with another study that demonstrated that activin A can be considered as a novel Th2 cytokine that can be released by activated CD4⁺ T cells (Ogawa et al., 2006).

The differences observed between this study and (Semitekolou et al., 2009) can be partly explained by 1) local vs systemic inhibition; 2) doses/timing of activin A depletion and 3) follistatin versus monoclonal antibody for activin A depletion. Moreover, *in vivo* blockade of activin A not only resulted in an increase of the percentages of Treg, but concomitantly, follistatin at 0.5 μ g and 5 μ g increased IL-10 concentrations in BAL fluid indicating that follistatin treatment alter the cytokine microenvironment in the lung. Future studies may test whether follistatin-induced Treg mediated airway suppression is directly dependent on IL-10 by utilising IL-10^{-/-} mice; or partly via other mechanism/s such as an activation of tolerogenic DC as demonstrated by Huang and colleagues (Huang et al., 2010). They showed that DC that is exposed to IL-10 (IL-10-differentiated DC) induces allergen tolerance in asthmatic mice via inducing Teff to differentiate into Treg. Hardy *et al.* showed that high dose follistatin inhibited mucus hypersecretion and subepithelial collagen deposition otherwise seen during chronic allergen challenge (Hardy et al., 2013c), indicating potential allergy-therapeutic effects of follistatin on activin A.

Overall, data from this chapter and Hardy et al. (Hardy et al., 2013c, Hardy et al., 2006) and support from future studies could answer whether follistatin can be used for optimal induction of immunologic tolerance in the lung, particularly in improving lung acute and chronic airways diseases.

3.5 Summary

In vivo blockade of activin A with its binding protein, follistatin modifies certain characteristics of inflammatory responses i.e. follistatin dose dependently inhibits activin A and TGF- β secretion into the airway lumen during chronic allergen challenge (Hardy et al., 2013c). Follistatin has been shown to ameliorate airway inflammation (Hardy et al., 2006), and here one additional possible mechanism by which follistatin can ameliorate airway inflammation is shown, by illustrating a substantial increase in Treg frequencies at critical times that would drive disease resolution. Thus, Treg appear to be an important regulator of airway inflammation. We therefore investigated in more detail the potential role of Treg subsets in lung homeostasis, and the onset of inflammation in the next chapter.

Chapter 4

**The role of TNFR2 expressing regulatory
T cells in maintaining homeostasis in the
lung during allergic airway inflammation**

4.1 Introduction

The lung is maintained in a state of homeostasis by a complex network of cells. Treg play a central role in the maintenance of the lung immune responses to infectious organisms, as well as to maintain tolerance to harmless, inhaled aeroallergens. Major populations of Treg studied in the context of lung homeostasis and airway diseases are: the natural thymic-derived $CD4^{+}Foxp3^{+}$ Treg (nTreg) and the peripherally antigen-induced adaptive $CD4^{+}$ Treg (iTreg) (Hawrylowicz and O'Garra, 2005, Roncarolo et al., 2006). To date, there are no specific markers that can completely differentiate between nTreg and iTreg that are induced *in vivo*, although many have been proposed (Akimova et al., 2011).

Distinct Treg subsets displaying different functional markers can mediate immune suppression or immune tolerance in diverse animal models of lung diseases, (Ito et al., 2008, Siegmund et al., 2005). As introduced in Chapter 1, TNFR2 is a unique marker that is used to identify highly functional Treg and TNFR2 expressing Treg are potentially reactive to an inflammatory environment (van Mierlo et al., 2008, Chen et al., 2010b, Chen et al., 2008). As shown in Figure 3 (Chapter 1), three functionally distinct T cell populations identified by the surface marker TNFR2 were investigated in this study; namely $TNFR2^{+}Foxp3^{+}$ Treg, $TNFR2^{-}Foxp3^{+}$ Treg and $TNFR2^{+}Foxp3^{-}$ Teff. $CD4^{+}CD25^{+}$ Treg in the periphery represent a stable proportion of the $CD3^{+}CD4^{+}$ T cells. As shown in other studies (Shevach, 2002, Sakaguchi, 2005, Curiel et al., 2004) and confirmed in Chapter 3 of this thesis, lung-draining LN and lung Treg constitute ~ 5-10 % of $CD3^{+}CD4^{+}$ T cells. Spleen and BAL Treg also constitute ~ 5-10 % of $CD3^{+}CD4^{+}$ T cells (data not shown). However, whether a distinct subset of $TNFR2^{+}$ Treg may be present in the lung and whether they would play a role in mediating immunosuppression

has yet to be demonstrated. Previous studies investigating the role of Foxp3 expressing TNFR2 (TNFR2⁺Foxp3⁺ Treg) have solely focused on the Treg in the spleen and LN (Chen et al., 2008, van der Most et al., 2009, Chen et al., 2010a, Chen et al., 2010b, Chen and Oppenheim, 2010) and so little information is available on the activity of this population in the lung.

The lifespan and recirculation properties of Treg are important aspects of the proper functioning of the immune system, especially in the lung. Studies have shown that TNFR2 expression is positively correlated with the proliferative capacity of Treg (Chen et.al, 2008). In accordance with this, the present study investigated the proliferative potential and suppressive activity of CD25⁺TNFR2⁺ Treg and CD25⁺TNFR2⁻ Treg, as well as proliferative capacity of CD25⁻TNFR2⁺ Teff in the healthy lung. This chapter focuses on characterising the role of Treg in maintaining lung homeostasis in unmanipulated mice and in the function of Treg in an inflammatory setting, in a model of OVA-induced acute allergic airway inflammation (AAI).

4.2 Experimental Procedures

4.2.1 Immunisation

Mice were sensitised i.p. with saline or OVA (50 µg; Sigma-Aldrich, St. Louis, MO) in aluminum hydroxide on days 0 and 10 and challenged i.n with saline or OVA (25 µg) on days 20, 21, 22, and 23 and samples were collected on days 24, 27 and 33 (d1, d4 and d10 after allergen challenges) (Figure 4.3).

4.2.2 CD25 and TNFR2 cell sorting

Lung cells pooled from 15-20 mice (1×10^8 cells) were stained with CD4 (V450), CD25 (Pe-Cy7) and CD120b/TNFR2 (PE). Stained lung cells were sorted (FACSAria) into CD25⁺TNFR2⁻ (Q1), CD25⁺TNFR2⁺ (Q2), CD25⁻TNFR2⁻ (Q3) and CD25⁻TNFR2⁺ (Q4). The purity of these sorted TNFR2 populations was > 97%.

4.2.3 Treg functional assays

To assess proliferation of TNFR2 populations from saline- and LPS-treated mice, cells (5×10^4) were cultured in duplicate (Q2, CD25⁺TNFR2⁺), triplicate (Q1, CD25⁺TNFR2⁻ and Q4, CD25⁻TNFR2⁺), or quadruplicate (Q3, CD25⁻TNFR2⁻), depending on the number of cells recovered after sorting. In TNFR2⁺ Treg depletion assay, total CD25⁻ cells (Q3+Q4) were cultured without Treg [depleted all CD25⁺ cells (Q1+Q2) and labeled as 'no Treg'], depleted only CD25⁺TNFR2⁺ (Q2) (labeled as 'CD25⁺TNFR2⁻ Treg') or without Treg depletion (labeled as 'all Treg'). As the percentages of CD25⁺TNFR2⁺ (Q2) in the lung were only less than 0.5 % from 10-15 % of lung CD3⁺CD4⁺ T cells, therefore because of these limited cell numbers, I could not rule out the suppressive function of these cells. However, in another study, the suppressive functions of CD25⁺TNFR2⁺ Treg and CD25⁺TNFR2⁻ Treg from the spleen were sorted based on Foxp3 expression (Foxp3-GFP mice) were further investigated (Mohamud *et al.*, in preparation).

All cultured cells were stimulated with plate-bound anti-CD3 (1 μ g/ml) and soluble anti-CD28 (2 μ g/ml) mAbs for 72 h. Cells were then pulsed with [³H]-thymidine (1 μ Ci/well) for an additional 18 h. Incorporation of [³H]-thymidine was measured by liquid scintillation counting. Data are presented as mean counts per min (cpm) and are shown for one of three separate experiments with similar results.

4.3 Results

4.3.1 TNFR2⁺Foxp3⁺ Treg in the steady state in the lung

4.3.1.1 TNFR2⁺ Foxp3⁺ Treg are present in the lung and lung-draining LN

To investigate the proportions and total numbers of TNFR2⁺Foxp3⁺ Treg during lung homeostasis in unmanipulated mice, cells expressing TNFR2 with/without Foxp3 were gated from CD25⁺ cells within the CD3⁺CD4⁺ T cell population (Figure 4.1). It was found that subsets of TNFR2⁺Foxp3⁺ Treg, TNFR2⁻Foxp3⁺ Treg and TNFR2⁺Foxp3⁻ Teff were present in both lung and lung-draining LN (Table 4.1). The proportions/percentages of T cells during lung homeostasis are shown in Table 4.1. The numbers of TNFR2-expressing cells (TNFR2⁺Foxp3⁺ Treg and TNFR2⁺Foxp3⁻ Teff) were similar ($\sim 0.9 \times 10^4$ and $\sim 0.7 \times 10^4$ cells, respectively), whilst TNFR2⁻Foxp3⁺ Treg and TNFR2⁻Foxp3⁻ Teff at $\sim 5 \times 10^4$ and $\sim 65 \times 10^4$ cells, respectively (Table 4.1). *In vitro* functional characteristics of these cells were analysed based on the co-expression of CD25 and TNFR2 as it was not possible to stain these cells intracellularly for Foxp3 as this requires cell fixation, rendering the cells non-functional. Analyses on Foxp3 marker showed that the highest percentages of Foxp3-positive cells were within the CD25⁺ population (TNFR2⁻ and TNFR2⁺; Q1 and Q2 respectively), but not in the CD25⁻ population (Figure 4.2). Therefore, *in vitro* functional analysis of CD25⁺ populations with high level of Foxp3 was based on the combined expression of CD25 and TNFR2.

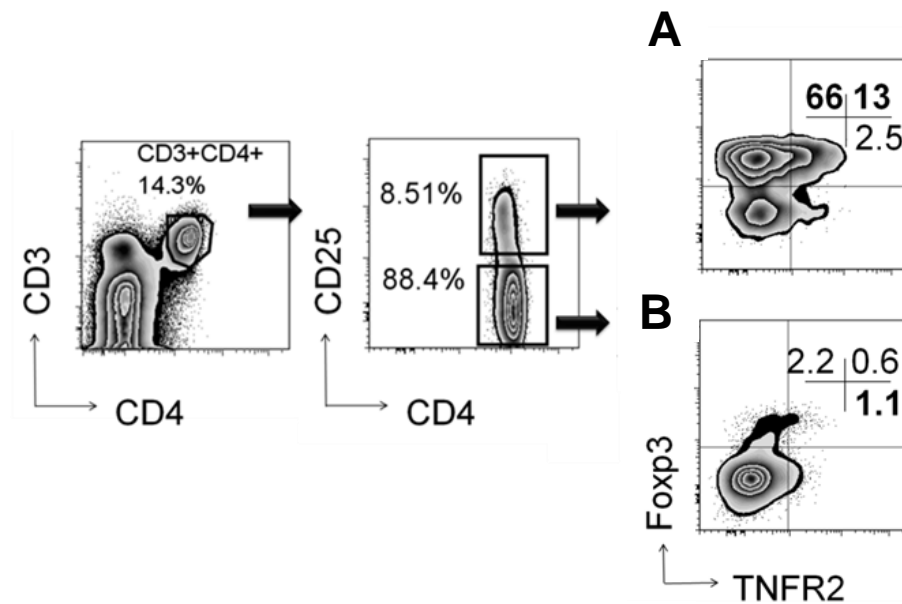


Figure 4.1: Gating strategy for characterisation of TNFR2 populations.

Representative FACS contour plots showing TNFR2⁺ cells in the lung of naïve mice.

Lung cells were processed for intracellular staining with Foxp3. (A) CD3⁺CD4⁺CD25⁺

and (B) CD3⁺CD4⁺CD25⁻ T cell populations were assessed for Foxp3 and TNFR2

expression. Percentages for each population are shown. Bold numbers indicate Treg

(TNFR2⁺ and TNFR2⁻ populations) and Teff (TNFR2⁺ population) gating of

CD3⁺CD4⁺CD25⁺ and CD3⁺CD4⁺CD25⁻ respectively.

Organs	Lung		Lung-draining LN	
	%	Numbers (10 ⁴)	%	Numbers (10 ⁴)
Total cell numbers	-	902 ± 309	-	603 ± 321
CD3⁺CD4⁺ cells	12.5 ± 1.65	5324 ± 1043	45.7 ± 4.13	504 ± 721
CD3⁺CD4⁺CD25⁺ Treg	6.7 ± 3.54	5.87 ± 2.54	9.8 ± 1.09	53.7 ± 3.5
TNFR2⁺Foxp3⁺ Treg	12.4 ± 1.53	0.97 ± 0.12	15.7 ± 2.65	8.9 ± 3.6
TNFR2⁻Foxp3⁺ Treg	79.4 ± 5.2	5.43 ± 2.13	80.3 ± 3.2	38.3 ± 6.32
CD4⁺CD25⁻ Teff	86.7 ± 7.54	68.3 ± 5.8	88.5 ± 7.2	470.4 ± 13
TNFR2⁺Foxp3⁻ Teff	1.05 ± 0.43	0.7 ± 0.54	1.87 ± 0.04	9.32 ± 2.6
TNFR2⁻Foxp3⁻ Teff	86.5 ± 4.7	65.4 ± 6.5	83.4 ± 7.8	395.2 ± 12.4

Table 4.1: The percentages and numbers of Treg and Teff at homeostasis. Analyses were performed following FACS staining on surface markers CD3, CD4, CD25, TNFR2 and intracellular Foxp3 both for lung and lung-draining LN of naïve mice. Treg (TNFR2⁺ and TNFR2⁻ populations) and Teff (TNFR2⁺ population) gating of CD3⁺CD4⁺CD25⁺ and CD3⁺CD4⁺CD25⁻, respectively. The percentages showed for Treg (TNFR2⁺ and TNFR2⁻ populations) and Teff (TNFR2⁺ population) are as a proportion of CD3⁺CD4⁺CD25⁺ and CD3⁺CD4⁺CD25⁻, respectively. Data shown are representative of more than 5 experiments. Mean ± SEM, n=4-5.

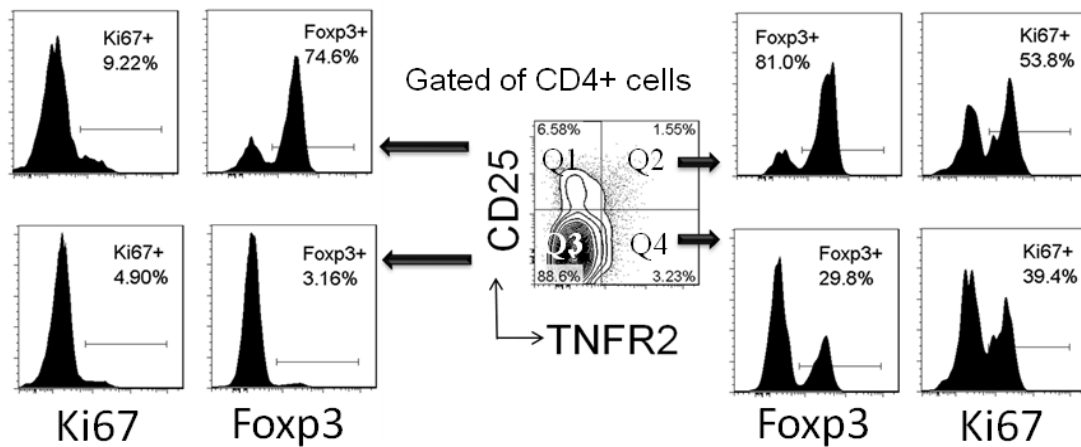


Figure 4.2: Gating strategy for functional characterisation of TNFR2 populations.

Representative plots showing CD25⁺TNFR2⁺ cells in the lung of naïve mice. Lung cells were processed and stained with surface T cell markers; CD4, CD25 and TNFR2. Percentages for Foxp3 and proliferative marker, Ki67 gated from TNFR2⁺ (Q2, Q4) and TNFR2⁻ cells (Q1, Q3) were shown. Q1-Q4 populations were isolated for functional assays. Data shown are representative of more than 3 experiments. Mean \pm SEM, n=4-5.

4.3.1.2 Ki67 expression by lung CD25⁺TNFR2⁺ cells from naïve mice was positively correlated with *in vitro* proliferative capacity

All proliferating cells express the Ki67 marker. Therefore, in this study, Ki67 expression on CD25 and TNFR2 expressing populations was further investigated to gain insight on the proliferative capacity of TNFR2 populations. The highest frequency of Ki67⁺ cells was seen among CD3⁺CD4⁺CD25⁺TNFR2⁺ (Q2; CD25⁺TNFR2⁺) cells, while CD25⁻TNFR2⁺ cells (Q4) also expressed Ki67 at a high frequency (Figure 4.2). The lowest expression levels of Ki67 and Foxp3 were observed in CD25⁻TNFR2⁻ (Q3) (Figure 4.2). Similar patterns of Ki67 expressions were observed in the lung-draining LN, but with lower percentages (data not shown).

To examine if the correlation between TNFR2 and Ki67 expression in the lung translated into enhanced *in vitro* proliferative capacity, flow cytometer-sorted TNFR2-positive and TNFR2-negative cell populations (Figure 4.2) were co-cultured with combinations of anti-CD3 and anti-CD28 mAbs. Consistent with the Ki67 expression data, irrespective of CD25 status, TNFR2⁺ cells showed significantly greater proliferation than either of the TNFR2⁻ populations (Figure 4.3A). Furthermore, CD25⁻TNFR2⁻ cells proliferated significantly more than CD25⁺TNFR2⁻ cells (Figure 4.3A). Overall, the frequency of Ki67⁺ cells within TNFR2⁺ cells correlated positively with *in vitro* proliferative capacity (Figure 4.3B). Thus, these data show that in the steady state, both lung Treg and Teff contain TNFR2⁺ fractions with high proliferative capacity *in vitro* and *in vivo*.

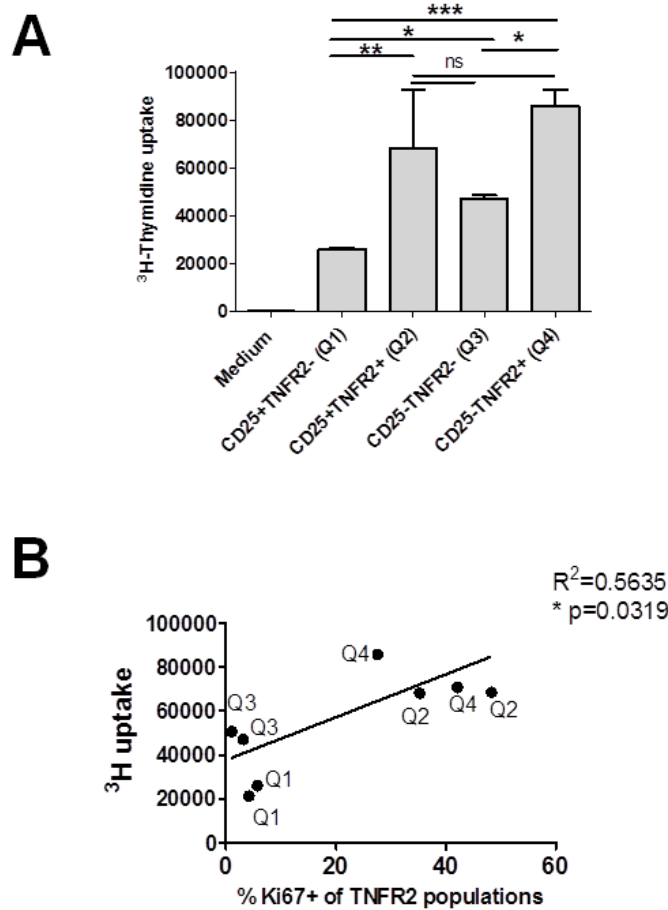


Figure 4.3: Functional characterisation of TNFR2 populations (proliferative capacity). TNFR2⁺ cells (both CD25⁺ and CD25⁻) from naïve mice proliferate more than TNFR2⁻ cells. **(A)** Proliferation of FACS sorted TNFR2 populations stimulated with combinations of anti-CD3 and anti-CD28 mAbs. **(B)** Correlation of Ki67⁺ in all TNFR2 populations with *in vitro* proliferation of respective TNFR2 populations. Mean ± SEM, n=2-4. *p < 0.05, **p < 0.01, and ***p < 0.001, ns= not significant; 1 x 10⁵ cells/well. Data are representative of 3 experiments.

4.3.1.3 CD25⁺TNFR2⁺ Treg enhances the suppressive effects of CD25⁺TNFR2⁻ cells

Recent studies in peripheral tissues have shown that TNFR2-expressing mouse Treg are maximally suppressive (Chen and Oppenheim, 2010), highly proliferative (van der Most et al., 2009) and rarely produce pro-inflammatory cytokines (Herrath et al., 2011). Consistent with a suppressor phenotype, proliferation of total CD25⁻ cells (TNFR2⁺ and TNFR2⁻ cells) in response to combinations of anti-CD3 and anti-CD28 mAbs was significantly suppressed by addition of CD25⁺TNFR2⁻ cells (Figure 4.4A). This suppression was further significantly increased by addition of CD25⁺TNFR2⁺ cells ('All Treg' group in Figure 4.4A), suggesting both populations are suppressive (i.e. Treg) and can act together to maintain homeostasis (Figure 4.4A). IL-2 and IL-4 levels in the cell culture supernatants reflected an overall similar suppressor activity pattern of these cells (Figure 4.4B-C), albeit under my experimental conditions, suppression was already maximal using CD25⁺TNFR2⁻ Treg and further enhancements by addition of CD25⁺TNFR2⁺ Treg were not significant. Cultures of CD25⁻ cell populations (either TNFR2⁺ or TNFR2⁻) secreted the highest level of IL-4 as compared to CD25⁺ cells (TNFR2⁺ and TNFR2⁻ cells) suggesting that CD25⁻ cells (TNFR2⁺ and TNFR2⁻ cells) exerted the effector cells phenotype (i.e. Teff) (Figure 4.4C).

Overall, lung CD25⁺TNFR2⁺ Treg exhibited the highest levels of suppressive marker (Foxp3) and proliferative marker (Ki67) indicating that they are both suppressive and actively proliferate at lung homeostasis. To determine potential involvement of TNFR2⁺Foxp3⁺ Treg in resolving AAI, we went on to use a mouse model of acute allergic asthma induced by injection OVA allergen and monitored airway inflammation up to 10 days after the final allergen challenges as previously performed by (Hardy et al., 2006).

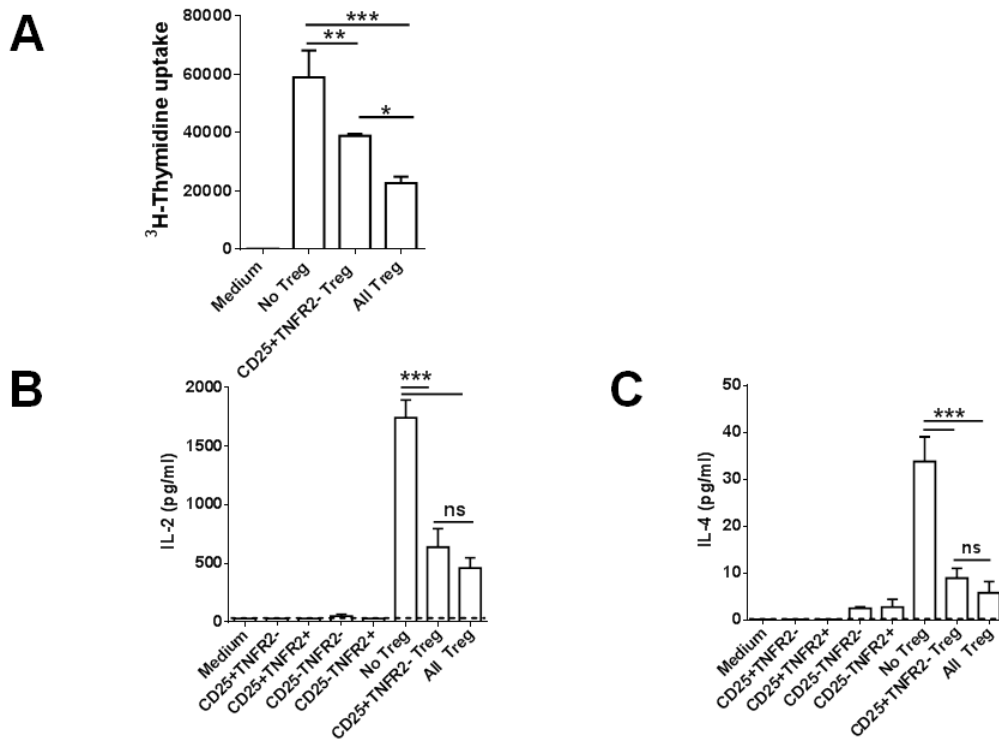


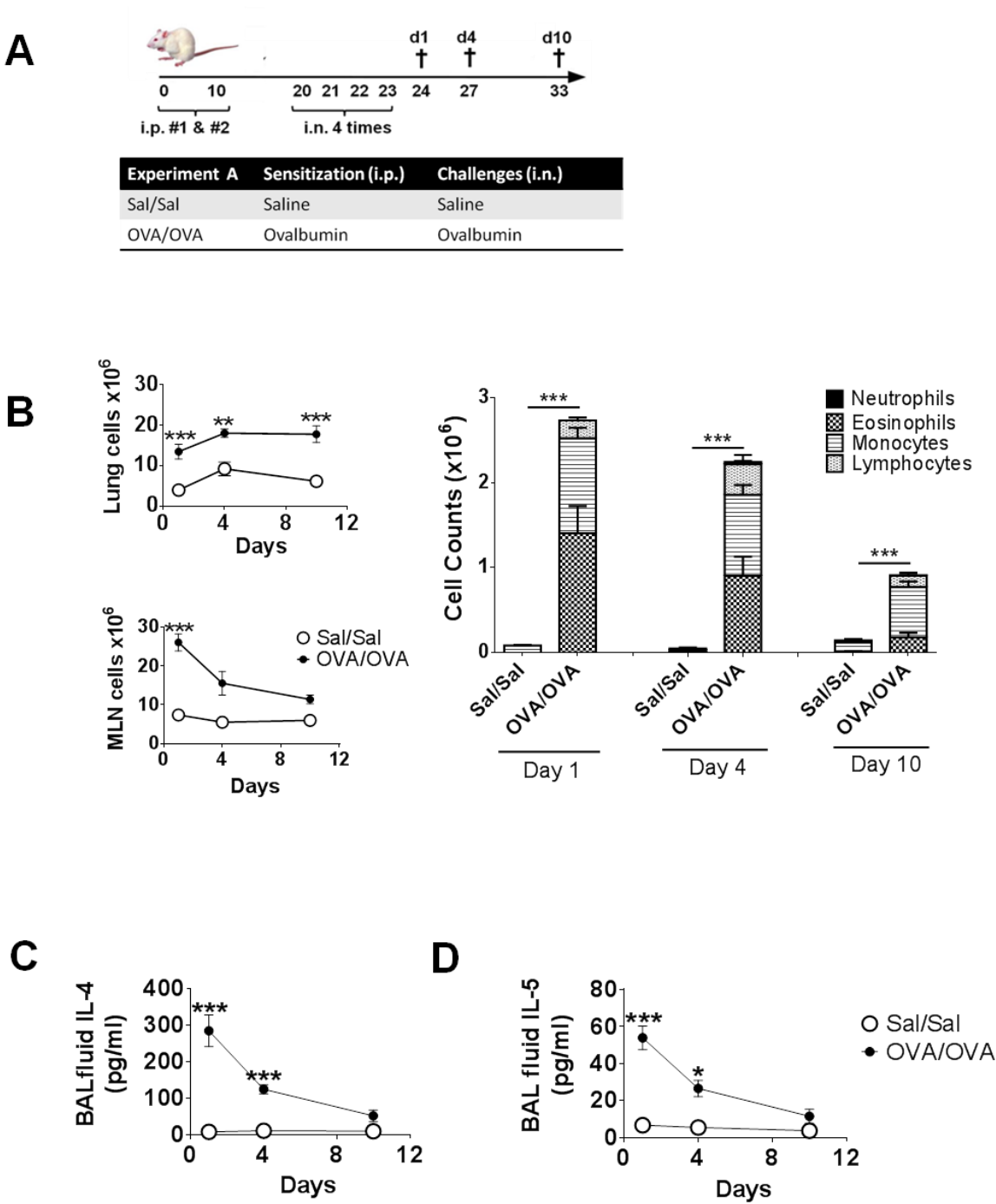
Figure 4.4: Analysis of suppressive capacity of TNFR2 populations. TNFR2⁺ and TNFR2⁻CD25⁺ Treg suppress proliferation of CD25⁻ Teff and decrease IL-2 and IL-4 concentrations in culture supernatant. Proliferation of FACS isolated TNFR2 populations cultured with/without TNFR2⁺ Treg stimulated with the combination of anti-CD3 and anti-CD28 mAbs. **(A)** Treg depletion assay. Total CD25⁻ cells (labeled as ‘no Treg’) were co-cultured with either CD25⁺TNFR2⁻ alone (labeled as ‘CD25⁺TNFR2⁻Treg’) or with total CD25⁺ Treg (labeled as ‘All Treg’). **(B)** IL-2 and **(C)** IL-4 concentration in cell culture supernatants of saline treated mice. Dashed line denotes lower limit of detection. Mean \pm SEM. n=2-4, 5×10^4 cells/well. *p < 0.05, **p < 0.01, and ***p < 0.001; ns= not significant.

4.3.2 TNFR2⁺Foxp3⁺ Treg in resolving AAI

4.3.2.1 Characterisation of the inflammatory response in the mouse model of AAI

Mice were sensitised and challenged with OVA allergen and Treg proportions analysed at 1, 4 and 10 days after the final challenge (Figure 4.5A). As expected and as seen in (Hardy et al., 2006), there was a significant increase in total lung cell numbers in on d1, d4 and d10 (Figure 4.5B, top left panel). There was also an increase in cell numbers in the lung-draining LN on d1, although this declined gradually to d10 (Figure 4.5B, below left panel). Infiltrations of total cells in BAL fluid (data not shown) and different cells type in BAL fluid were also decreased on d10, also in agreement with (Hardy et al., 2006). Recruitments of eosinophils were at the highest level on d1 and gradually decreased on d4 and returned to saline levels on d10 (Figure 4.5B, right panel). In contrast, macrophage and lymphocyte numbers remained relatively steady. Neutrophils were not detected in BAL indicating that this is a model of eosinophilic allergic asthma. Total BAL cells numbers remained very low in the Sal/Sal group, as expected, and consisted almost exclusively of macrophages, while eosinophils or neutrophils were not detected (Figure 4.5B, right panel).

Analyses in the BAL fluid showed that Th2-associated cytokines, IL-4 and IL-5 concentrations were at the highest levels in the OVA/OVA group on d1 and gradually decreased to saline levels on d10 (Figure 4.C-D). The concentrations of IL-6, TGF- β and IL-13 increased during the peak of airway inflammation (d1 after the final allergen challenge), whereas there was no difference in IL-2, IL-10, TNF, IL-1 α and GM-CSF concentrations (Table 4.2). IFN- γ and IL-17 concentrations were below the limit of detection.



Cont.....

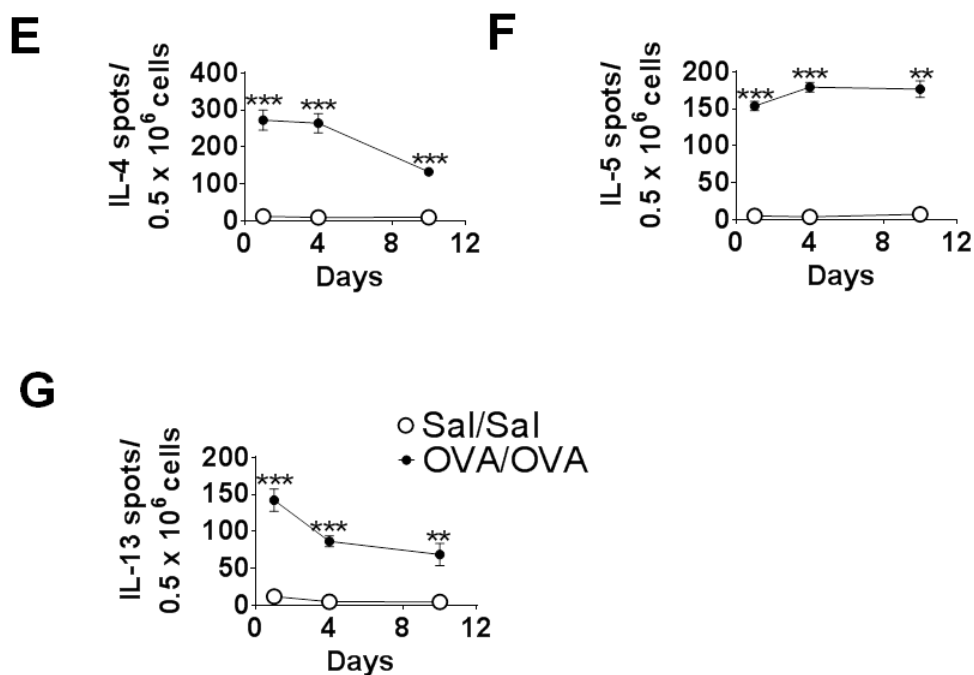


Figure 4.5: Induction and resolution of AAI mouse model. (A) Mice received OVA/alum sensitisation and OVA challenge at the indicated times to induce AAI. Negative control received saline. Tissue sampling was performed on days 1, 4 and 10 after the final lung allergen challenge. (B) Differential analysis of absolute BAL cell numbers and lung and lung-draining LN cell numbers (left upper and lower panel, respectively). (C) IL-4 and (D) IL-5 in BAL fluid. Frequency of (E) IL-4-, (F) IL-5-, and (G) IL-13-producing lung-draining LN cells stimulated with OVA. Mean \pm SEM. $n=4-5$, * $p < 0.05$, ** $p < 0.01$; *** $p < 0.001$. Data are representative of more than 3 experiments.

Cytokines	Sal/Sal d1	Peak of airway inflammation (OVA/OVA group d1 after challenge)
IL-2	38.6 ± 7.7	BLOD
IL-10	3.6 ± 2.5	2.6 ± 0.4
TNF	5.6 ± 3.4	2.6 ± 1.3
IL-1-α	45.3 ± 5.5	BLOD
GM-CSF	20.1 ± 3.2	17.9 ± 3.2
IL-6	2.9 ± 2.1	22.4 ± 8.4***
[#]TGF-β	12.2 ± 3.7	865.3 ± 25.8***
[#]IL-13	2.4 ± 1.8	80.3 ± 12.4***

Table 4.2: Concentrations of BAL fluid cytokines during the peak of airway inflammation. BAL fluid was subjected to Multiplex assay for measurement of IL-2, IL-10, TNF-α, IL-1α, GM-CSF and IL-6. Limit of detection for IL-2, IL-10, TNF-α, IL-1α, GM-CSF and IL-6 is 30.65, 0.16, 2.38, 29.86, 0.59 and 0.34, respectively. TGF-β and IL-13 were measured by ELISA[#]. Mean ± SEM. n=4-5, ***p<0.001. Data are representative of more than 3 experiments. BLOD, below limit of detection.

Detailed examination of AAI development on pulmonary allergen specific Th2 cell responses revealed that mice with AAI had a marked increase in allergen-specific IL-4, IL-5 and IL-13 production in the lung draining LN over time points (d1, d4 and d10) (Figure 4.5E-F), and these results were similar to those previously reported (Hardy et al., 2003, Hardy et al., 2006).

4.3.2.2 Lung $\text{TNFR2}^+\text{Foxp3}^+$ Treg and $\text{TNFR2}^+\text{Foxp3}^-$ Teff frequencies were positively correlated with AAI

Studies showed that Treg are responsible for the resolution of acute AAI (Burchell et al., 2009, Baru et al., 2010, Carson et al., 2008, Faustino et al., 2013). To study the involvement of $\text{TNFR2}^+\text{Foxp3}^+$ Treg in AAI, proportions of $\text{TNFR2}^+\text{Foxp3}^+$ Treg and $\text{TNFR2}^-\text{Foxp3}^+$ Treg and $\text{TNFR2}^+\text{Foxp3}^-$ Teff were examined on days 1, 4, and 10 after the final lung allergen challenge in lung and lung-draining LN (Figure 4.6A). We found that the proportions of lung $\text{TNFR2}^+\text{Foxp3}^+$ and lung $\text{TNFR2}^-\text{Foxp3}^+$ Treg in saline control group were ~ 10 % and ~ 60 %, respectively (Figure 4.6B left and middle panel). The proportions of lung $\text{TNFR2}^+\text{Foxp3}^+$ Treg in AAI mice were elevated above the saline level on d1 and d4 (~ 20 %) and returned to saline levels on d10 (Figure 4.6B, left panel). However, lung $\text{TNFR2}^-\text{Foxp3}^+$ Treg proportions were lower than saline levels from d1-d10 (30-40 %) (Figure 4.6B, middle panel). On the other hand, $\text{TNFR2}^+\text{Foxp3}^-$ Teff levels were highest on d1 and gradually decreased on d10, but remained significantly higher than saline control group (Fig 4.6B, right panel).

To better understand the balance between Treg and Teff during AAI we examined the ratio of Treg ($\text{TNFR2}^+\text{Foxp3}^+$ Treg and $\text{TNFR2}^-\text{Foxp3}^+$ Treg) to $\text{TNFR2}^+\text{Foxp3}^-$ Teff. We focused our investigations on Teff that express TNFR2 as TNFR2 expression on

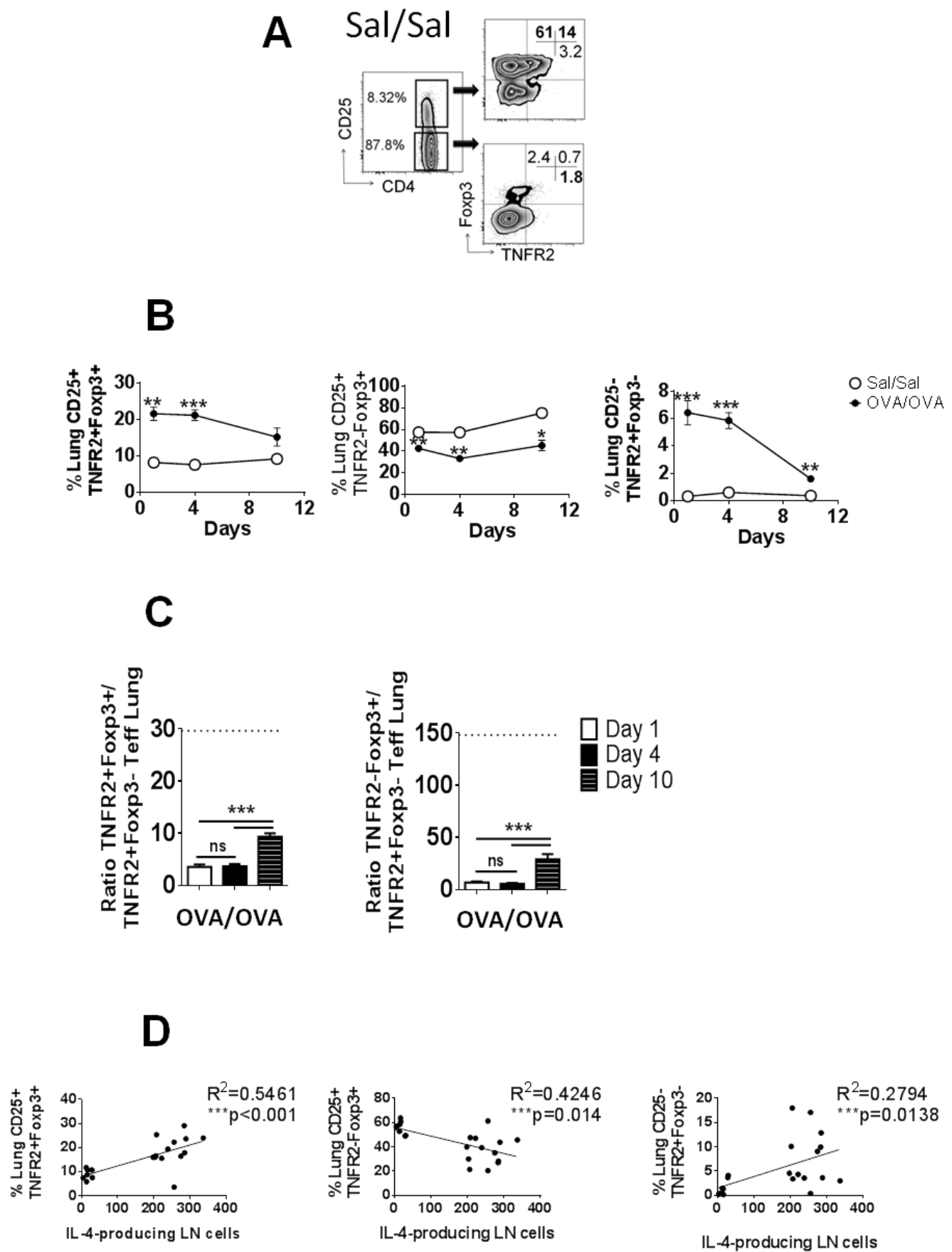


Figure 4.6: Characterisation of TNFR2 populations in lung during AAI. Mice were sensitised and challenged with OVA allergen as per Figure 4.5 and tissue sampling was performed on days 1, 4 and 10 after the final lung allergen challenge. Negative control received saline. **(A)** Representative FACS contour plots showing TNFR2⁺ cells in the lung of Sal/Sal treated mice. Gating strategy was applied as in Fig 4.1. **(B)** Percentages of TNFR2⁺Foxp3⁺ Treg, TNFR2⁻Foxp3⁺ Treg and TNFR2⁺Foxp3⁻ Teff. **(C)** Ratios of TNFR2⁺Foxp3⁺ Treg and TNFR2⁻Foxp3⁺ Treg to TNFR2⁺Foxp3⁻ Teff (left and right panel, respectively). Dotted lines indicated ratios in Sal/Sal treated mice. **(D)** Correlations of TNFR2⁺Foxp3⁺ Treg (left panel), TNFR2⁻Foxp3⁺ Treg (middle panel) and TNFR2⁺Foxp3⁻ Teff (right panel) to IL-4-producing LN cells. Mean \pm SEM. n=4-5, *p < 0.05, **p < 0.01; ***p < 0.001. Data are representative of more than 3 experiments.

CD25⁺Foxp3⁻ effector T cells confer resistance to Treg suppression. For both Treg populations the ratio was lowest on days 1 and 4, and significantly increased on d10 (Figure 4.6C). These ratios are lower than Sal/Sal negative control group (Figure 4.6C, shown as dotted line in the graph). Using linear regression analysis, a positive correlation was found between the proportions of TNFR2⁺Foxp3⁺ Treg with airway inflammation assessed by total BAL cell counts, whilst TNFR2⁻Foxp3⁺ Treg were negatively correlated with airway inflammation (Figure 4.6D, left and middle panel). TNFR2⁺Foxp3⁻ Teff were positively correlated with total BAL cell counts, followed similar pattern as TNFR2⁺Foxp3⁺ Treg (Figure 4.6D, right panel).

4.3.2.3 Lung-draining LN TNFR2⁺Foxp3⁻ Teff frequencies were positively correlated with AAI

Analyses in the lung-draining LN revealed that the percentages of TNFR2⁺Foxp3⁺ Treg were decreased on d1 in AAI mice, while the percentages of TNFR2⁻Foxp3⁺ Treg and TNFR2⁺Foxp3⁻ Teff increased on d1 and returned to saline level on d10 (Figure 4.7A). Ratios of Treg (TNFR2⁺Foxp3⁺ Treg and TNFR2⁻Foxp3⁺ Treg) to TNFR2⁺Foxp3⁻ Teff followed a similar pattern to the lung, being lowest on days 1 and 4, and increasing on d10. However, these ratios were lower than in saline control mice (Figure 4.7B). There was no correlation between TNFR2⁺Foxp3⁺ Treg and frequency of IL-4 producing cells in the lung-draining LN, whereas a positive correlation was observed for TNFR2⁻Foxp3⁺ Treg (Figure 4.7C, left and middle panel). Similar to findings in the lung, TNFR2⁺Foxp3⁻ Teff proportions positively correlated with airway inflammation suggesting that these cells were partly responsible for the inflammatory effects in the lung (Figure 4.7C, right panel).

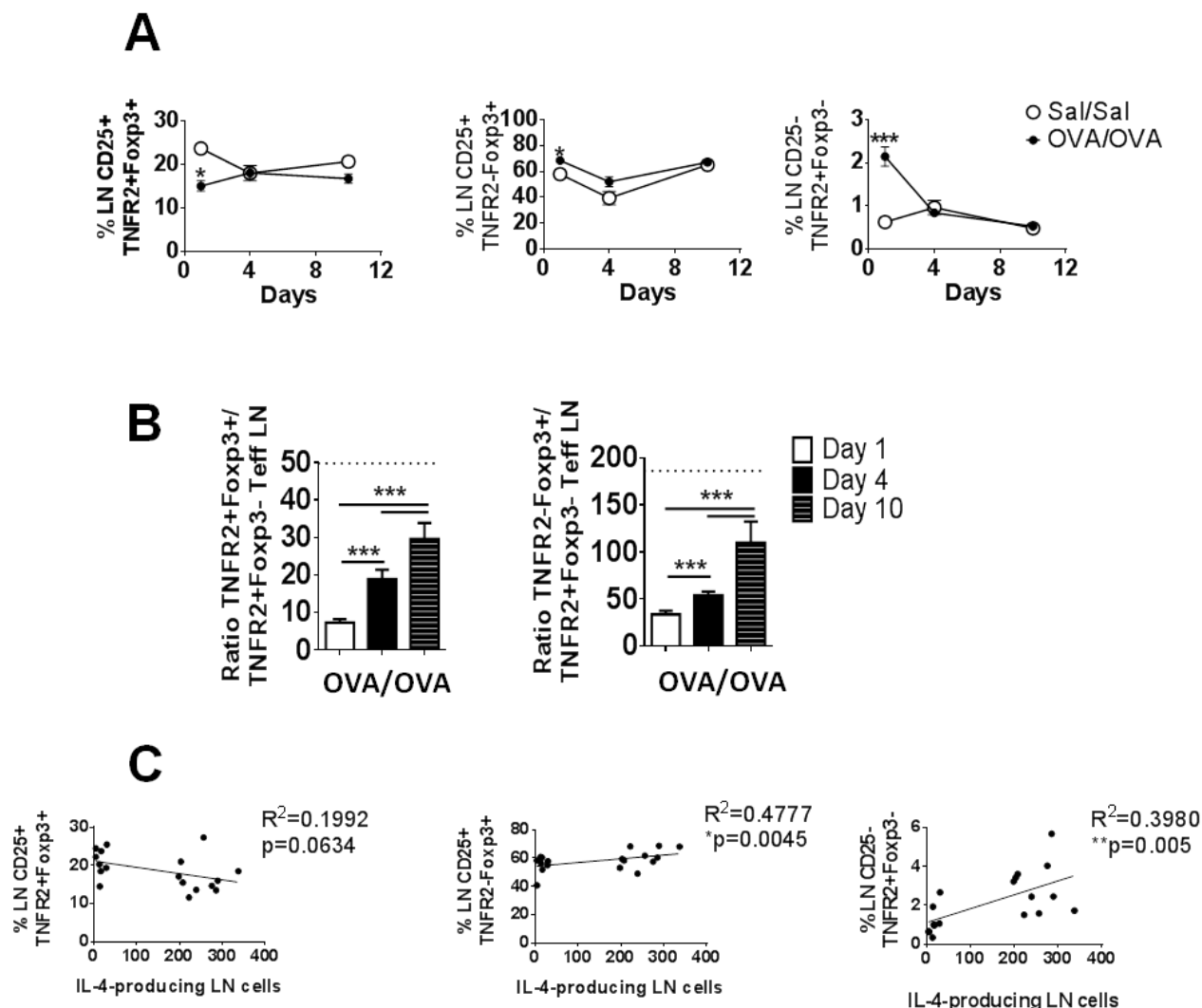


Figure 4.7: Characterisation of TNFR2 populations in lung-draining LN of AAI.

Mice were sensitised and challenged with OVA allergen as per Figure 4.5 and tissue sampling was performed on days 1, 4 and 10 after the final lung allergen challenge. Negative control received saline. Gating strategy was applied as in Figure 4.1. **(A)** Percentages of TNFR2⁺Foxp3⁺ Treg, TNFR2⁻Foxp3⁺ Treg and TNFR2⁺Foxp3⁻ Teff. **(B)** Ratios of TNFR2⁺Foxp3⁺ Treg and TNFR2⁻Foxp3⁺ Treg to TNFR2⁺Foxp3⁻ Teff (left and right panel, respectively). Dotted lines indicated ratios in Sal/Sal. **(C)** Correlations of TNFR2⁺Foxp3⁺ Treg (left panel), TNFR2⁻Foxp3⁺ Treg (middle panel) and TNFR2⁺Foxp3⁻ Teff (right panel) to IL-4-producing LN cells. Mean \pm SEM. n=4-5, *p < 0.05; ***p<0.001. Data are representative of more than 3 experiments.

4.3.2.4 Proliferative capacity of lung TNFR2⁻Foxp3⁺ Treg increased during the peak of AAI

Ki67 expression was then analysed to identify the proliferative capacity of these cells (Figure 4.8 A, B). There were no differences in the proportions of Ki67⁺ cells within TNFR2⁺Foxp3⁺ Treg and TNFR2⁺Foxp3⁻ Teff in mice with AAI over the time points (Figure 4.8C and Figure 4.8E, respectively). However, the proportions of Ki67⁺ cells within TNFR2⁻Foxp3⁺ Treg were greatest on d1 and d4, being significantly higher than the saline control group, but had returned to saline level on d10 (Figure 4.8D).

4.3.2.5 Proliferative capacity of lung-draining LN TNFR2⁺Foxp3⁺ Treg, TNFR2⁻Foxp3⁺ Treg and TNFR2⁺Foxp3⁻ Teff increased during the peak of AAI

To gain a deeper insight into the factors regulating Treg numbers in the pulmonary compartment, a similar analysis of Ki67 was performed in the lung-draining LN (Figure 4.9A, B). The frequency of Ki67⁺ cells within TNFR2⁺Foxp3⁺ Treg in mice with AAI increased on d1 and d4, whereas the frequency within TNFR2⁻Foxp3⁺ Treg and TNFR2⁺Foxp3⁻ Teff increased only on d1; all populations had returned to saline levels by d10 (Figure 4.9C, D, E).

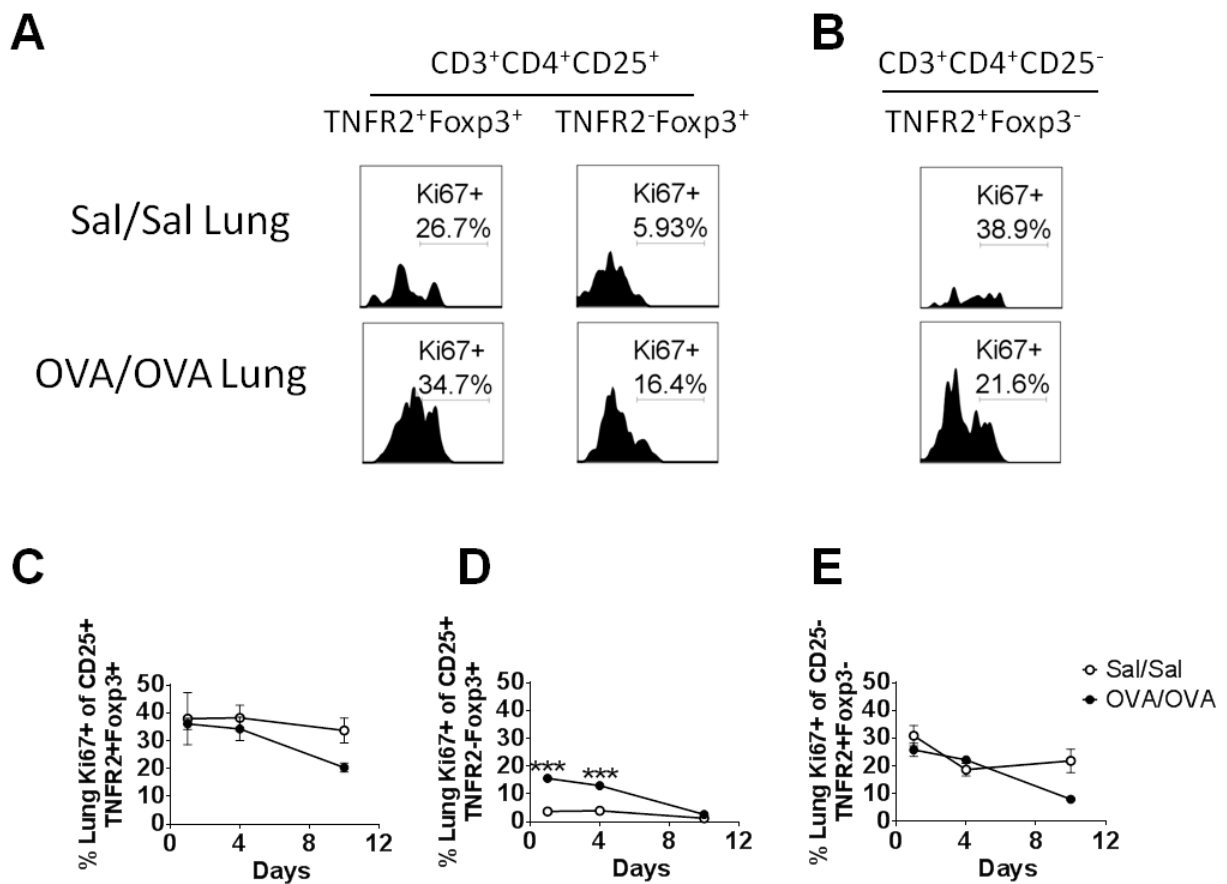


Figure 4.8: Characterisation of proliferative capacity of TNFR2 populations in lung of AAI. Mice were sensitised and challenged with OVA allergen as per Figure 4.5 and tissue sampling was performed on days 1, 4 and 10 after the final lung allergen challenge. Negative control received saline. Plots representative at day 1 after the final allergen challenge. **(A)** Ki67 histogram gated within TNFR2⁺Foxp3⁺ Treg and TNFR2⁻Foxp3⁺ Treg and **(B)** TNFR2⁺Foxp3⁻ Teff. Numbers indicate the percentages of Ki67-positive populations. Frequency of Ki67⁺ of **(C)** TNFR2⁺Foxp3⁺ Treg, **(D)** TNFR2⁻Foxp3⁺ Treg and **(E)** TNFR2⁺Foxp3⁻ Teff. Mean ± SEM. n=4-5, ***p<0.001. Data are representative of more than 3 experiments.

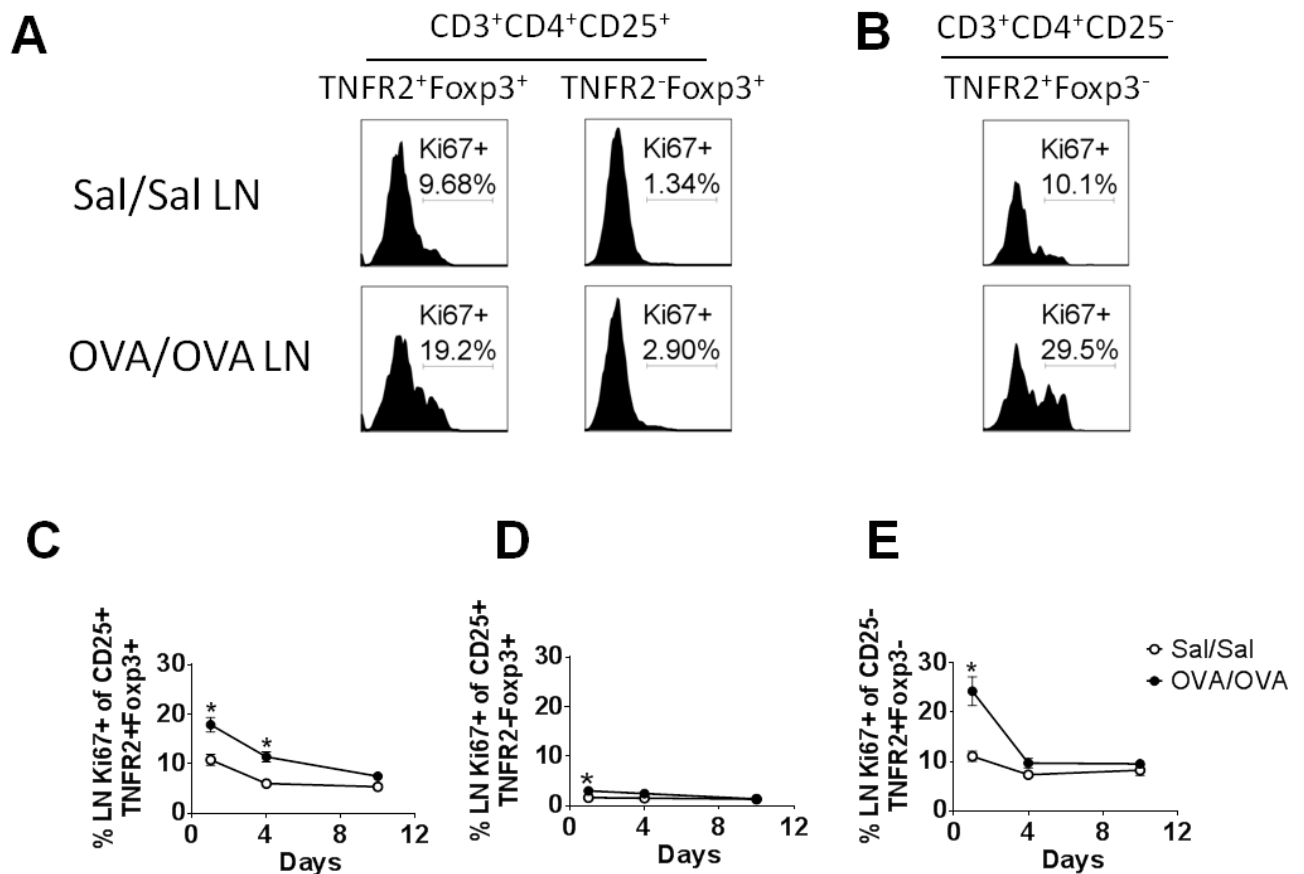


Figure 4.9: Characterisation of proliferative capacity of TNFR2 populations in lung-draining LN of AAI. Mice were sensitised and challenged with OVA allergen as per Figure 4.5 and tissue sampling was performed on days 1, 4 and 10 after the final lung allergen challenge. Negative control received saline. Plots representative at day 1 after the final allergen challenge. (A) Ki67 expression by TNFR2⁺Foxp3⁺ and TNFR2⁻Foxp3⁺ Treg and (B) TNFR2⁺Foxp3⁻ Teff. Numbers indicate the percentage Ki67-positive populations. Frequencies of Ki67⁺ of (C) TNFR2⁺Foxp3⁺ Treg, (D) TNFR2⁻Foxp3⁺ Treg and (E) TNFR2⁺Foxp3⁻ Teff. Mean ± SEM. n=4-5, *p < 0.05. Data are representative of more than 3 experiments.

4.4 Discussion

In this study, I investigated the phenotype and characteristics of TNFR2 populations (including Treg and Teff) in the lung during homeostasis and AAI. Earlier in Chapter 3, I demonstrated the importance of Foxp3 expression in maintaining lung function and homeostasis; and that disruption of lung immune homeostasis by OVA challenge leads to an imbalance in innate (e.g. APC such as DC and macrophages) and adaptive (e.g. T cells) immune responses that result in the induction of airway inflammation.

A murine model of AAI induced by the OVA allergen was established to investigate the involvement of Treg and Teff during the peak and resolution of airway inflammation. Firstly, I characterised the allergic inflammatory responses. Airway eosinophilia (assessed from BAL cells), BAL cytokine secretion, lung and lung-draining LN cell counts and frequency of Th2 cytokine producing-LN cells (IL-4, IL-5 and IL-13) were elevated in this model. Although BAL cytokines concentration in AAI had returned to saline level by d10, the frequency of Th2 producing-LN cells remained elevated compared to the saline control group, suggesting that inflammation was not fully resolved. These results were similar to what was seen in our previous studies (Hardy et al., 2003, Hardy et al., 2012a, Hardy et al., 2010).

At lung homeostasis, CD25⁺TNFR2⁺ Treg and CD25⁺TNFR2⁻ Treg expressed high levels of Foxp3, and suppressed proliferation and cytokines production by Teff (both TNFR2⁺ and TNFR2⁻), suggesting a role in controlling the activation of Teff. Further analyses showed that TNFR2⁺ cells (Treg and Teff) have higher levels of Ki67⁺ cells compared to TNFR2⁻ cells (Treg and Teff) showing that they have higher proliferative capacity in the

lung. This is parallel to previous study that showed CD4⁺CD25⁺ Treg constitute two different populations; Treg that stably expression CD25 *in vivo* with long lifespan and Treg which have a rapid turnover (continuously activated) and express multiple activation markers (Fisson et al., 2003). Indeed, my study further confirmed this by *in vitro* assay and Ki67 expression, and added here that TNFR2-expressing cells (Treg and Teff) are the subsets that are preferentially activated and have a rapid turnover *in vivo*.

The maintenance of total Treg pool is achieved by replenishing their number from existing Treg (i.e. proliferation), existence of long-lived Treg, and/or by periphery conversion of Teff to Treg (Fisson et al., 2003, van der Most et al., 2009, Chen et al., 2007). Interestingly, *in vitro* proliferation of CD25⁺TNFR2⁺ Treg positively correlated with the proliferative potential, as reflected by Ki67 expression. A recent study showed that TNFR2 expression on cell surface is positively correlates with Treg expansion *in vivo* (Chen et al., 2010a). Studies on Treg in the spleen and LN also confirmed that TNFR2-expressing cells (Treg and Teff) have higher rapid turnover and are maximally functional subsets (i.e. maximally functional Treg and Teff that are most refractory to Treg suppression) (Chen et al., 2007, van der Most et al., 2009). Chen *et al.* found that although CD25⁺TNFR2⁻ Treg exerted a weaker but detectable inhibitory effect on CD25⁻ TNFR2⁻ Teff, this subset of Treg had no suppressive activity when cocultured with CD25⁻TNFR2⁺ Teff, suggesting the enhanced functional subsets of TNFR2-expressing Treg and Teff (Chen et al., 2007). A recent study demonstrated that proliferating Treg are able to maintain Foxp3 expression (Akimova et al., 2011). Concomitantly, another study by van der Most *et al.* showed that successful chemotherapy in a mouse model is achieved after depleting Foxp3⁺TNFR2^{hi} cells, which were highly proliferative *in vivo* (van der Most et al., 2009). They further suggest that the cycling Ki67^{hi} cells are the

active suppressors that respond to antigen by increasing their suppressive function (van der Most et al., 2009).

In an allergic asthma mouse model, analyses showed that the proportions of TNFR2-positive Teff were markedly increased and at the highest levels in the lung and draining LN during the peak airway inflammation, leading to a change in the ratios of Treg/Teff. As expected, the ratios of Treg/Teff decreased during inflammation and increased towards the saline level by d10 as the inflammation improved, albeit the ratios were ~ 3-fold lower than saline level in the lung and lung-draining LN suggesting that at this stage, the inflammation was not fully resolved.

This study did not rule out the suppressive function of Treg ($CD4^+CD25^+$ or TNFR2-expressing Treg) during the peak or resolution of airway inflammation. However, some studies in asthmatic patients and allergic asthma mouse models showed that there is a functional insufficiency of Treg in controlling Th2 cells (Lin et al., 2008, Ling et al., 2004, Shi and Qin, 2005, Grindebacke et al., 2004, Curotto de Lafaille et al., 2001, Faustino et al., 2012, Carson et al., 2008). Instead, this chapter focused on the proliferative capacity of TNFR2-expressing Treg and Teff; as TNFR2 expression identifies Treg that are maximally suppressive and Teff with the capacity to resist suppression (van der Most et al., 2009, Chen et al., 2007). Additionally, studies showed that in inflammatory settings, the inflammation prevails due to: 1) Treg being outnumbered by Teff; or 2) Teff becoming refractory to Treg suppression (Herrath et al., 2011, Schneider et al., 2008). In line with this, during lung homeostasis, the numbers of TNFR2 expressing Treg and Teff exist at a similar level (Table 4.1), however, during the peak of airway inflammation, the proportions of $TNFR2^+Foxp3^+$ Treg increased ~ 2-fold,

whereas $\text{TNFR2}^+\text{Foxp3}^-$ Teff increased ~ 4 -fold, suggesting that $\text{TNFR2}^+\text{Foxp3}^+$ Treg were being outnumbered by $\text{TNFR2}^+\text{Foxp3}^-$ Teff. Similarly, $\text{TNFR2}^+\text{Foxp3}^+$ Treg were being outnumbered by $\text{TNFR2}^+\text{Foxp3}^-$ Teff in the lung-draining LN as the proportions of $\text{TNFR2}^+\text{Foxp3}^+$ Treg decreased to ~ 2 -fold, whilst $\text{TNFR2}^+\text{Foxp3}^-$ Teff increased to ~ 2 -fold. This result was concomitant with the increase in Th2-producing LN cells during the peak of airway inflammation.

The second hypothesis on Teff becoming refractory to Treg suppression during the peak of airway inflammation was not investigated in this study. Instead, the expansion capacity of TNFR2 expressing Treg and Teff was investigated at homeostasis and during the peak and resolution of airway inflammation. In this model, no differences in Ki67 proportions within these cells were observed, suggesting that airway inflammation did not alter their expansion capacity. Chen *et al.* demonstrated that TNF promotes the expansion and function of TNFR2 expressing Treg (Chen et al., 2007). Indeed, in our model there was a lack of TNF in the lung microenvironment suggesting there were inadequate stimuli to promote the expansion of TNFR2 expressing Treg. Nevertheless, an increase in Ki67⁺ cells within $\text{TNFR2}^-\text{Foxp3}^+$ Treg was observed, suggesting that different Treg subsets acted in various ways during ongoing inflammation, in order to keep the lung at homeostasis level. In contrast, all investigated cells in the lung-draining LN increased their proliferative capacity (preferentially TNFR2 expressing cells), and the expansion capacity of $\text{TNFR2}^+\text{Foxp3}^-$ Teff was even greater than $\text{TNFR2}^+\text{Foxp3}^+$ Treg. As previously mentioned, the suppressive function of lung $\text{TNFR2}^+\text{Foxp3}^+$ Treg in this model was not tested due to low cell numbers ($\text{TNFR2}^+\text{Foxp3}^+$ Treg were only $< 0.1\%$ from lung $\text{CD3}^+\text{CD4}^+$ T cells) and thus cannot be ruled out whether highly proliferative $\text{TNFR2}^+\text{Foxp3}^-$ Teff were becoming refractory to Treg suppression during the peak of

airway inflammation. However, the expansion capacity of $\text{TNFR2}^+\text{Foxp3}^-$ Teff markedly decreased by d4 of allergen challenges, whilst $\text{TNFR2}^+\text{Foxp3}^+$ Treg maintained their expansion capacity, suggesting that during the peak of airway inflammation, highly proliferative $\text{TNFR2}^+\text{Foxp3}^-$ Teff might be refractory to Treg suppression. Overall, to maintain lung homeostasis, the existence of highly proliferative $\text{TNFR2}^+\text{Foxp3}^+$ Treg is important in controlling the overwhelming activation of $\text{TNFR2}^+\text{Foxp3}^-$ Teff (Illustrated in Figure 4.10).

4.5 Summary

This chapter investigated Treg and Teff during the peak and resolution phase of inflammation in a model of AAI. The data suggest that an imbalance in the numbers of Teff and Treg arises due to differential proliferative capacity of these subsets, and specifically, the TNFR2 expressing subsets which were found to have most of the proliferative capacity within each subset.

The mechanisms driving these changes have not been explored and will be an important area for future studies. These findings however suggest that environmental stimuli which can imprint the lung to become resistant to AAI may also act to alter the Treg/Teff balance, and specifically act on the cells with higher potential to react by proliferation: the TNFR2^+ T cell subsets. Our previous studies have shown that nanoparticles such as PS50G ameliorate subsequent susceptibility to AAI (Hardy et al., 2012a, Hardy et al., 2013b); in the next chapter (presented as a manuscript), the effects of PS50G on Treg/Teff ratios were investigated.

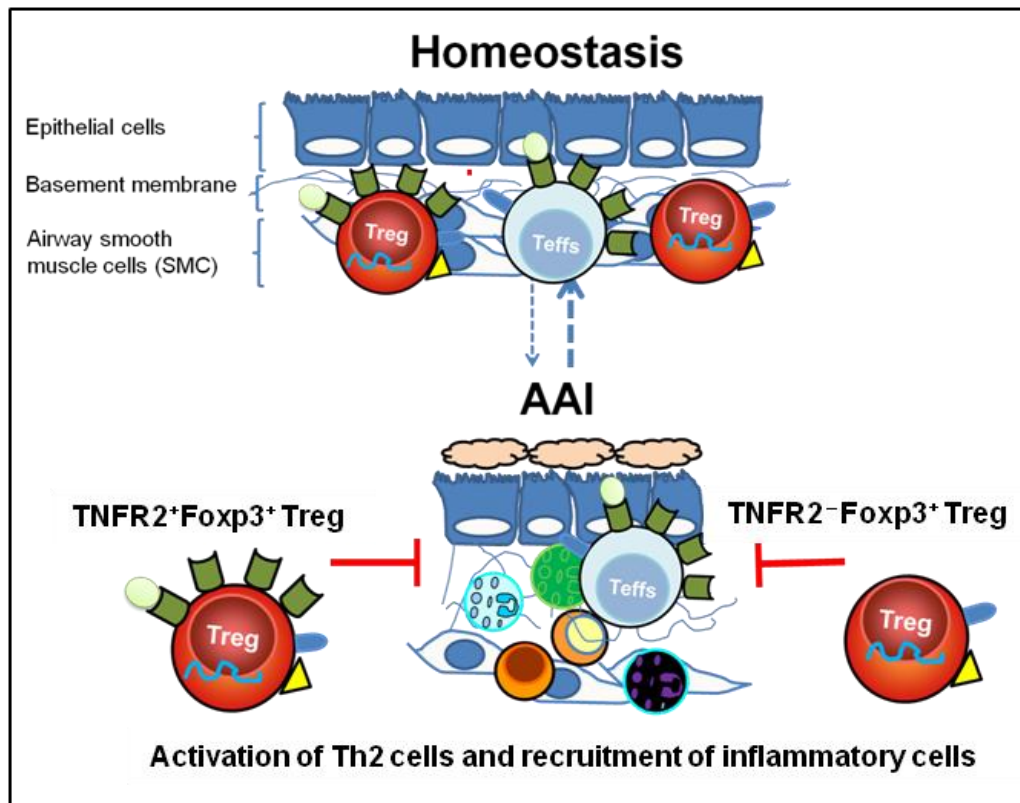


Figure 4.10: TNFR2⁺Foxp3⁺ Treg and TNFR2⁻Foxp3⁺ Treg are important in maintaining lung homeostasis and might be responsible for resolution of airway inflammation. AAI induced by OVA resulted in the recruitment of eosinophils into the BAL, increased BAL Th2 cytokines, lung and lung-draining LN cellularity and Th-2-producing LN cells. Inflammation peaked on day 1 after a series of allergen challenges and was reduced by d10. The percentages of TNFR2⁺Foxp3⁻ Teff in lung and lung-draining LN increased and positively correlated with IL-4-producing LN cells. *In vitro* data showed that CD25⁻TNFR2⁺ Teff secrete IL-4 suggesting that CD25⁻TNFR2⁺ Teff play a role in the induction of airway inflammation. An increased in TNFR2⁺Foxp3⁻ Teff in the lung and lung-draining LN altered the ratio to Treg (TNFR2⁺Foxp3⁺ Treg and TNFR2⁻Foxp3⁺ Treg) and this is partly explained by the modulation of their proliferative capacity. Thus, high levels of TNFR2⁺Foxp3⁺ Treg in the lung with higher proliferative capacity are important in controlling the overwhelming activation of TNFR2⁺Foxp3⁻ Teff.

Chapter 5

**The effects of PS50G on TNFR2 expressing
regulatory T cells in the lung during allergic
airway inflammation**

PART B: Declaration for Thesis Chapter 5**Declaration by candidate**

In the case of Chapter 5, the nature and extent of my contribution to the work was the following:

Nature of contribution	Extent of contribution (%)
In this study, I conceived, designed and performed all experiments, and I was responsible for interpretation of the data for all experiments. I played a major role in the preparation of figures, writing and editing manuscript.	80 %

The following co-authors contributed to the work. If co-authors are students at Monash University, the extent of their contribution in percentage terms must be stated:

Name	Nature of contribution	Extent of contribution (%) for student co-authors only
Jeanne LeMasurier	Technical assistance	10 %
Je Lin Sieow	Technical assistance	10 %
Sue Xiang	Editing manuscript	NA
John Yao	Technical assistance	NA
Jennifer M. Rolland	Intellectual input and editing manuscript	NA
Robyn E. O'Hehir	Intellectual input and editing manuscript	NA
Charles L. Hardy	Experimental design, editing manuscript, data interpretation and intellectual input	NA
Magdalena Plebanski*	Experimental design, editing manuscript, data interpretation and intellectual input	NA

The undersigned hereby certify that the above declaration correctly reflects the nature and extent of the candidate's and co-authors' contributions to this work*.

**Candidate's
Signature**

		Date 24. 03. 2014
--	--	-----------------------------

**Main
Supervisor's
Signature***

		Date 24. 03. 2014
--	--	-----------------------------

*Note: Where the responsible author is not the candidate's main supervisor, the main supervisor should consult with the responsible author to agree on the respective contributions of the authors.

5.1 Manuscript

Synthetic nanoparticles which promote persistently increased TNF receptor 2 expressing regulatory T cell levels in the lung and generate resistance to allergic airways inflammation

Rohimah Mohamud^{ac}, Je Lin Sieow^a, Jeanne S. LeMasurier^{ac}, Sue Xiang^a, John Yao^{abc}, Jennifer M. Rolland^{ac}, Robyn E. O’Hehir^{abc}, Charles L. Hardy^{abc*}, Magdalena Plebanski^{acd*}

** Equal contribution*

^a Department of Immunology, Monash University, Melbourne, VIC, Australia

^b Department of Allergy, Immunology and Respiratory Medicine, The Alfred Hospital and Monash University, Melbourne, VIC, Australia

^c CRC for Asthma and Airways, Sydney, NSW, Australia

^d Corresponding author:

Professor Magdalena Plebanski

[REDACTED]

[REDACTED]

Fax: + 61 3 9903 0038

This research was funded by the Cooperative Research Centre for Asthma and the National Health & Medical Research Council of Australia. RM is the recipient of Malaysian Postgraduate Scholarship Scheme and CRC-Asthma and Airways top-up Scholarship.

Abstract

Engineered nanoparticles (ENP) are increasingly being developed for vaccine and drug delivery applications. Although it has been proposed that ENP could be designed to regulate lung inflammation, to date nothing is known about the effect of ENP on lung regulatory T cells (Treg). We recently showed that glycine coated 50 nm polystyrene ENP (PS50G), unlike other ambient nanoparticles, did not promote pulmonary inflammation, but instead rendered lungs resistant to development of allergic airway inflammation. Herein we show PS50G have the unexpected capacity to modulate the frequency and the functional markers associated with Treg function, specifically on $\text{TNFR2}^+\text{Foxp3}^+$ Treg, a recently identified Treg subset with potent regulatory function. Our study show that exposure to ENP, such as PS50G, can lead to an effective elicitation of highly bioactive $\text{TNFR2}^+\text{Foxp3}^+$ Treg which had further enhanced levels of LAP and CTLA-4 upon allergen challenge, thereby promoting lung homeostasis. These findings offer the first evidence of ENP promote $\text{TNFR2}^+\text{Foxp3}^+$ Treg induction, suggesting that further that ENP (i.e., devoid of adsorbed chemicals or added immunomodulators) could be engineered to promote healthy lung homeostasis.

Keywords: TNFR2, asthma, PS50G, lung, lymph nodes, animal model

Introduction

Nanoparticles, defined as particles with a diameter less than 100 nm, comprise the dominant particles in ambient airborne particulate matter (Donaldson et al., 2001). Nanoparticles can be divided into 3 categories; naturally occurring, anthropogenic and engineered (ENP) that are manufactured for industrial or consumer applications (Mohamud et al., 2013). The increasing use of nanoparticles for pulmonary drug delivery is driving debate about their potential to negatively or positively modulate lung immune homeostasis (Verma et al., 2013, Jensen et al., 2012, Kaur et al., 2012).

The lung can be confronted by a diverse range of environmental nanoparticles including ENP on a daily basis and must maintain a state of immune ignorance or ‘tolerance’ to these stimuli to retain pulmonary homeostasis and prevent potentially fatal immunopathology. As nanotechnology develops it is clear that it will also be important to understand the impact of ENP on the lung. It has been shown previously that ENP by themselves have the capability to induce beneficial or detrimental effects on lung immune homeostasis, depending on their characteristics (Mohamud et al., 2013). For example, single-walled carbon nanotubes (SWCNT) (Inoue et al., 2010) and titanium oxide (TiO₂) (Larsen et al., 2010) can exacerbate existing allergic airway inflammation (AAI). However, we demonstrated that inert glycine-coated polystyrene 50-nm nanoparticles (PS50G) behave differently from most of the ubiquitous particles in the environment, *in vivo* and *in vitro* (Hardy et al., 2012a, Hardy et al., 2013b, Xiang et al., 2013, Karlson et al., 2013). PS50G induced the secretion of chemokines involved in recruitment and/or maturation of monocytes and dendritic cells (DC), and transiently induce lower levels of pro-inflammatory cytokines (e.g. IL-1 α , IL-1 β , IFN- γ and TNF) (Hardy et al., 2013b).

It is now understood that a primary immune response in the lung can modify the nature a subsequent pulmonary immune response in a process called innate imprinting (Hardy et al., 2013b) via various mechanisms including impairment of pulmonary antigen presenting cells (APC) function (Hardy et al., 2013b, Williams et al., 2004) or mechanisms of antigen delivery (Abadie et al., 2009), and induction of regulatory myeloid-derived suppressor cells (Arora et al., 2010). In regards to ENP exposure to the lung, we demonstrated that PS50G nanoparticles not only negatively imprint inflammatory CD11b^{hi} DC, but also increase the frequency of CD103⁺ DC in the lung (Hardy et al., 2013b), a population that recently been shown to be involved in the induction of airway tolerance (Khare et al., 2013). CD103⁺ DC has been shown closely linked to CD3⁺CD4⁺CD25⁺ regulatory T cells (Treg), for example, CD103⁺ DC in the gut has been shown to induce Treg, a function further enhanced by retinoid acid secretion (Housley et al., 2009). Treg play a major role in controlling the induction of AAI in mice (Chen et al., 2003a, Faustino et al., 2012, Grindebacke et al., 2004) and in atopic allergic patients (Ling et al., 2004, Cavani et al., 2003, Karlsson et al., 2004). We hypothesised that such ENP would substantially change the homeostatic and allergen induced migration and proliferative expansion capacity of Treg in the lung, particularly Treg expressing tumor necrosis factor (TNF) receptor 2 (TNFR2⁺Foxp3⁺ Treg) that exert maximal suppressive function (Chen et al., 2010a, van der Most et al., 2009). Thus, we propose that exposure to PS50G modifies lung immune homeostasis at two levels: with innate imprinting via DC and with adaptive imprinting via Treg.

Methods

Mice

Female BALB/c mice aged 6–8 weeks were obtained from the Walter and Eliza Hall Institute of Medical Research, Melbourne, Victoria, Australia and housed in the Alfred Medical Research and Education Precinct animal house. All studies with mice were approved by the AMREP Animal Ethics Committee.

Particles preparations, instillations and immunisations

Polybead carboxylate microspheres (unlabeled, nominally 0.05 mm; no. 15913; Polysciences, Warrington, PA) were glycine coated as described (Fifis et al., 2004), hereafter referred to as PS50G (Hardy et al., 2012a, Hardy et al., 2013b). To investigate the long term effects of PS50G on innate immune response, mice received saline or PS50G (200 µg / 50 µl) intratracheally on day 0 and samples were collected on days 1, 3, 7 and 31 post instillation. In some experiment, FITC-labeled-PS50G and 10 µg LPS were used as means of tracking particle uptake or as a positive ‘inflammatory’ control, respectively. PS50G effects on acute allergic asthma were investigated as described previously [Fig. 1 in (Hardy et al., 2012a) and Fig. 10A in (Hardy et al., 2013b)].

Bronchoalveolar lavage fluid, tissue sampling and cell isolation

Bronchoalveolar lavage fluid, tissue sampling and cell isolation were conducted as described previously (Hardy et al., 2003). Tissue digestion was performed as described previously (Hardy et al., 2013b).

Antibodies, surface and intracellular cells staining

Cells (1×10^6) were stained on ice for 20 minutes with combinations of the following antibodies (all eBioscience unless noted): CD3 (APC-Cy7, Qdot 605 from Lifetechnologies), CD4 (V450 and V500 from BDBiosciences), CD25 (PE-Cy7, APC-Cy7), CCR7 (Per-CP), CD120b/TNFR2 (PE), LAP (Per-CP), CTLA-4 biotin or their respective immunoglobulin isotypes. For intracellular staining of Foxp3 (APC) and Ki67 (FITC), cells were permeabilized according to the manufacturer's instructions. Acquisition was on a LSR II (BD) and analysis was performed on FlowJo (Tree Star, Ashland, OR, USA).

Measurement of BAL fluid cytokines and chemokines

The concentration of cytokines and chemokines in BAL fluid (IL-1 α , IL-2, IL-4, IL-5, IL-6, IL-10, IL-17, IFN- γ , TNF and IL-17) were detected Th1/Th2 10-plex kit FlowCytomix (BMS820FF, eBioscience); TGF- β was detected by mouse Simplex kit (BMS8608FF, eBioscience); IL-3, GM-CSF, G-CSF, IL-12p40 and MCP-1/CCL2 were detected by Bio-plex (Bio-Red, Hercules, CA). Protocols were as specified in the manufacturer's instructions.

Microscopy analyses for particles uptake and distribution

The superior lobe of the right lung was collected in 1 ml 2 % PFA and stored in the dark at 4 °C overnight. The lung tissue was transferred to 70 % ethanol and sliced into 1 mm – 2 mm thick transverse sections. Non-specific antibody binding was blocked in 100 μ l confocal staining buffer (3 % FCS in 1 X PBS) with CD16/CD32 block (BD Biosciences) in the dark on ice for 4 hours. Tissues were washed in 200 μ l 1 X PBS twice. Antibody staining cocktail was prepared with the following antibodies: Hoechst 33342 (Invitrogen),

MHC Class II–Alexa Fluor 647 (BioLegend) and Phalloidin–Rhodamine (Invitrogen) in 100 μ l confocal staining buffer and incubated in the dark at 4 °C overnight. Lung tissues were washed in 200 μ l 1 X PBS twice and kept in 1x PBS prior to confocal imaging to avoid drying of fixed tissue. All lung tissue sections were viewed and captured on the Nikon A1r Plus confocal microscope, operated by the NIS Elements Viewer software (Nikon, Melville, NY). Data were analyzed with FIJI (ImageJ, USA).

Statistical analysis

Data were analysed for normality and log-transformed as necessary prior to analysis by Student's *t* test or ANOVA with Bonferroni post tests, depending on the number of experimental groups. Spearman's correlations were used for the comparison of continuous variables. The Spearman's *r* value for the correlation between the two variables was stated in each result. Statistical analysis was performed using Graph Pad Prism v5.02 software. Group sizes are indicated in the figure legends. Data are expressed as mean \pm SEM. * $p < 0.05$, ** $p < 0.01$, and *** $p < 0.001$.

Results

PS50G instillation causes mild transient lung inflammation and increased cell numbers in the BAL, lung and lung-draining LN

To investigate the long term effects of PS50G on lung immunity, naïve mice were intratracheally instilled with PS50G; LPS was used as positive control. We showed that even though the total cell numbers increased on day 3 following particle instillation, a time at which maximal particle-induced effects on immune parameters (BAL and lung total cell numbers: $0.34 \pm 0.06 \times 10^6$ cells; $20.43 \pm 3.2 \times 10^6$ cells, respectively) were previously observed (Hardy et al., 2013b). These numbers were much lower compared to those found during LPS-induced acute lung injury (BAL and lung total cell numbers: $3.84 \pm 1.46 \times 10^6$ cells; $40.56 \pm 5.1 \times 10^6$ cells, respectively) suggesting that PS50G are a relatively weak inflammatory stimuli in the lung (Fig. 1A). Neutrophils and eosinophils were not detected in the BAL of saline group, whilst there were about $0.027 \pm 0.014 \times 10^6$ neutrophils and $0.0156 \pm 0.009 \times 10^6$ eosinophils found in PS50G group, as previously found (Hardy et al., 2013b). However, these numbers were much lower compared to those during LPS-induced ALI (neutrophils) and ovalbumin-induced AAI (eosinophils) ($1.56 \pm 0.54 \times 10^6$ cells and $2.43 \pm 0.6 \times 10^6$, respectively) also suggesting that PS50G are non-toxic to the lung. All BAL cell composition returned to saline levels at day 30 as reflected by BAL total cell counts (Fig.1B). Total cell numbers in the lung, BAL fluid and lung-draining LN returned to basal level on day 30 (Fig. 1A). We also instilled fluorescent-labeled PS50G to determine the uptake of PS50G by lung cells, and indeed our data showed that PS50G were taken up by lung MHC II⁺ cells showing that PS50G were not just adhering to the cell surface (Fig. 2). We next determined the capability of PS50G to modulate lung inflammation as compared to a potent inflammation mediator LPS.

PS50G instillation selectively increased BAL cytokines/chemokines secretion

Based on the above data showing that PS50G instillation only caused a small increase of BAL, lung and lung-draining LN cellularity as compared to 10 µg LPS instillation, we predicted that PS50G would not increase levels of inflammatory mediators in the lung. As expected, PS50G did not induce substantial amounts of TNF and IL-17 overtime compared to 10 µg LPS instillation, whereas the concentration of IL-1 α significantly increased compared to saline control group on day 1 and 3, and returned to saline levels on days 7 and 30. However, this level was 10-fold lower as compared to 10 µg LPS instillation, suggesting that PS50G did not induce inflammation (Fig. 3A). We previously showed that IL-12p40 and MCP-1/CCL2 concentrations were induced by PG50G to a higher level overtime than that in saline control group (Hardy et al., 2013b), and here we showed that the latter was even induced to a higher level compared to 10 µg LPS on day 3 (Fig. 3B). This is not surprising as the instillation of PS50G served as an activating stimulus, which induced immune responses to increase cell activation/recruitment through chemokine signalling and cytokine secretions.

In addition, PS50G did not increase the concentration of other effector cytokines such as IL-2, IL-3, IL-4, IL-5, IL-10 and IFN- γ in comparison to saline and 10 µg LPS 3 days post instillation (Table 1). However, the concentrations of IL-6, TGF- β , GM-CSF and G-CSF were higher compared to saline control group, but lower compared to 10 µg LPS on day 3 (Table 1). The ratio of TGF- β to pro-inflammatory IL-6 cytokine in PS50G and LPS group was ~ 10 and ~ 2-fold, respectively suggesting that PS50G might have skewed towards immunoregulation possibly orchestrated by Treg, as TGF- β has been shown previously to promote Foxp3 induction in CD4⁺ T cells (Liu et al., 2008) . Therefore, in

this study, we would predict that PS50G would be capable of promoting an increase in Treg frequencies in the lung and lung-draining LN to modulate lung homeostasis.

PS50G instillation alters the proportions and numbers of lung $CD3^+CD4^+$ T cells, $CD4^+CD25^+$ Treg, $CD4^+CD25^-$ Teff and $Foxp3^+TNFR2^+$ Treg in the lung

The above data clearly showed that PS50G selectively altered BAL cytokines and might skew the response towards immunoregulation. Therefore, we investigated the effects of PS50G on Treg frequencies. The proportion of lung $CD3^+CD4^+CD25^+$ Treg gradually increased, peaking at day 7 and remained at a significantly higher levels than the saline control group by day 30 (Fig. 4A, B). As we were interested to look at the effects of PS50G on the maximally suppressive $TNFR2^+$ Treg (Chen et al., 2010a, van der Most et al., 2009), we further analysed $TNFR2$ expression by $CD3^+CD4^+CD25^+Foxp3^+$ Treg. We simultaneously examined $TNFR2^+Foxp3^-$ population within the $CD3^+CD4^+CD25^-$ subset Teff for the identification of maximally functional effector cells expressing $TNFR2$ (Chen et al., 2010a). Instillation of PS50G increased the proportion of $TNFR2^+Foxp3^+$ Treg within total Treg (which is $CD3^+CD4^+CD25^+$) from ~ 9 % to ~ 20 % at day 1 and 3, peaking at day 7 (> 30 %), remaining significantly elevated above saline control group at day 30 (Fig. 4C). In stark contrast, the percentages of $TNFR2^-Foxp3^+$ Treg gradually decreased from days 3, 7 and remained at lower level compared to saline control group at day 30 (Fig. 4D). PS50G did not change the proportion of $TNFR2^+Foxp3^-$ Teff, (Fig. 4E). The total numbers of $TNFR2^+Foxp3^+$ Treg in the lung were also increased following PS50G instillation (Table 2), and these numbers were positively correlated with the BAL total numbers (data not shown). Absolute numbers of the other subsets discussed above remained unaltered.

Activated CD103⁺ DC were positively correlated with the proportion of TNFR2⁺Foxp3⁺ Treg and TNFR2⁺Foxp3⁺ Treg that were expanded (Ki67⁺)

The expression levels of CD86 on CD103⁺ DC is positively correlate with PS50G uptake (Hardy et al., 2013b). To investigate the possible relationship between PS50G uptake by CD103⁺ DC and Treg in the lung, we analysed the correlation between activated CD103⁺ DC (based on CD86 expression capacity) with TNFR2⁺Foxp3⁺ Treg. We demonstrated that the proportions of activated CD103⁺ DC were positively correlated with TNFR2⁺Foxp3⁺ Treg (Fig. 5A) and TNFR2⁺Foxp3⁺ Treg that proliferated (based on Ki67 expression) (Fig. 5B), but negatively correlated with TNFR2⁻Foxp3⁺ Treg (data not shown). All proliferating cells express the mitotic marker Ki67, and TNFR2⁺Foxp3⁺ Treg are predominantly Ki67-positive in peripheral lymphoid organs (Chen et al., 2010a). The proportions of total CD103⁺ DC (both activated or not) were also positively correlated with total Treg (TNFR2⁺Foxp3⁺ and TNFR2⁻Foxp3⁺) (data not shown). Thus, CD103⁺ DC might promote the increases in Treg frequencies, and their proliferative capacity.

PS50G instillation increased the percentages of TNFR2⁺Foxp3⁺ Treg in the lung-draining LN

To investigate the effects of PS50G on Treg in the lung-draining LN, we applied a similar gating strategy as we did for lung Treg (Fig. 6A). Instillation of PS50G did not significantly affect the percentages of CD3⁺CD4⁺CD25⁺ Treg at day 1 and 3, but increased the frequency from ~ 9 % to ~ 15 % at day 7, returning to saline control levels at day 30 (Fig. 6B). A similar pattern was observed in the percentages of TNFR2⁺Foxp3⁺ Treg (increased from ~ 20 % to ~ 30 % at day 7) (Fig. 6C). In contrast, the percentages of TNFR2⁻Foxp3⁺ Treg were significantly increased as early as day 1 and returned to saline control levels from day 3 to day 30 (Fig. 6D). PS50G instillation did not affect the

frequency of TNFR2⁺Foxp3⁻ Teff, being < 2 % for all time points in both saline and PS50G groups (Fig. 6E). Absolute numbers of CD3⁺CD4⁺ T cells, CD4⁺CD25⁺ Treg, TNFR2⁺Foxp3⁺ Treg, TNFR2⁻Foxp3⁺ Treg and TNFR2⁺Foxp3⁻ Teff increased on day3 (Table 2), as reflected by the ~ 5-fold increased in total lung-draining LN numbers (Fig. 1A, right panel). These numbers were positively correlated with the BAL total numbers (data not shown). Unlike in the lung, we did not observe any correlation between CD103⁺ DC (total or activated) and Treg (TNFR2⁺Foxp3⁺ or TNFR2⁻Foxp3⁺) (data not shown), even though previously we found an increase in the percentages of CD103⁺ DC in the lung-draining LN (Hardy et al., 2013b). Overall, we saw an increase in the percentages of CD3⁺CD4⁺CD25⁺ Treg, and TNFR2⁺Foxp3⁺ Treg but not TNFR2⁻Foxp3⁺Treg on day 7 in the lung-draining LN after instillation of PS50G.

PSG50-induced inhibition of allergic airway inflammation is associated with increased local efficiency in the induction of TNFR2⁺Foxp3⁺ Treg upon allergen challenge

To investigate the ability of PS50G to maintain TNFR2⁺Foxp3⁺ Treg at high level (preferentially in the lung) and thus render the lung homeostatically resistant to AAI induction, we then utilised our AAI-PS50G prevention model (Hardy et al., 2012a, Hardy et al., 2013b). We previously confirmed that PS50G inhibit development of allergic lung responses in atopic mice, as previously reported (Hardy et al., 2012a, Hardy et al., 2013b). Then we tested the hypothesis that the induction of different T cell subsets upon an allergenic lung challenge would be altered following PS50G instillation, and would result in more efficient induction of TNFR2 expressing Treg (TNFR2⁺Foxp3⁺ Treg). Moreover, this induction would be more efficient compared to the induction of potentially damaging inflammation reactive effector T cells (TNFR2⁺Foxp3⁻ Teff). Foxp3 and TNFR2 expressing populations were identified amongst CD3⁺CD4⁺CD25⁺ (Fig. 7A).

Consistent with the hypothesis that PS50G instillation promoted the induction of $\text{TNFR2}^+\text{Foxp3}^+$ Treg, we showed that the percentages of lung $\text{TNFR2}^+\text{Foxp3}^+$ Treg were significantly increased in PS50G/OVA/OVA group compared to control groups (Sal/Sal/Sal and Sal/OVA/OVA) (Fig.7B). Whilst, the percentages of lung $\text{TNFR2}^-\text{Foxp3}^+$ Treg in PS50G/OVA/OVA and Sal/OVA/OVA groups decreased from $\sim 60\%$ to $\sim 30\%$, an approximately 3-fold decreased as compared to saline negative control group (Sal/Sal/Sal) (Fig. 7C). On the other hand, the percentages of $\text{TNFR2}^+\text{Foxp3}^-$ Teff were significantly increased to ~ 4 -fold in AAI model, whether PS50G-treated or not (8%) compared to saline negative control group (Sal/Sal/Sal; $\sim 2\%$) (Fig. 7D). Thus, PS50G selectively increased $\text{TNFR2}^+\text{Foxp3}^+$ Treg proportions, without affecting $\text{TNFR2}^-\text{Foxp3}^+$ Treg or $\text{TNFR2}^+\text{Foxp3}^-$ Teff, resulting in increased ratio of $\text{TNFR2}^+\text{Foxp3}^+$ Treg: $\text{TNFR2}^+\text{Foxp3}^-$ Teff as compared to the Sal/OVA/OVA group. However, this ratio was significantly lower than saline negative control group (Fig. 7E). No differences were observed in the ratio of $\text{TNFR2}^-\text{Foxp3}^+$ Treg: $\text{TNFR2}^+\text{Foxp3}^-$ Teff in PS50G/OVA/OVA versus Sal/OVA/OVA groups; although this ratio was significantly lower than the saline negative control (Sal/Sal/Sal) (Fig. 7F). These results suggested that PSG50-induced inhibition of allergic airway inflammation was associated with increased lung $\text{TNFR2}^+\text{Foxp3}^+$ Treg upon allergen challenge.

PSG50-induced inhibition elicitation of allergic airway inflammation is associated with increased of $\text{TNFR2}^+\text{Foxp3}^+$ Treg in lung-draining LN of AAI mouse model

Previously in naïve mice, we demonstrated that PS50G were preferentially taken up by lung APC and migrated to the lung-draining LN (Hardy et al., 2013b), thus we performed analyses on Treg in the lung-draining LN to further understand the effects of PS50G on Treg in the lung-draining LN during AAI. The induction of AAI (Sal/OVA/OVA)

resulted in a decrease in frequency of $\text{TNFR2}^+\text{Foxp3}^+$ Treg relative to the saline control group (Sal/Sal/Sal), and this decreased was prevented by PS50G pre-treatment (PS50G/OVA/OVA) (Fig. 8A, B). No differences were observed in the frequencies of $\text{TNFR2}^-\text{Foxp3}^+$ Treg and $\text{TNFR2}^+\text{Foxp3}^-$ Teff (Fig. 8C, D), and neither PS50G instillation nor induction of AAI affected ratios of $\text{TNFR2}^+\text{Foxp3}^+$ Treg and $\text{TNFR2}^-\text{Foxp3}^+$ Treg to $\text{TNFR2}^+\text{Foxp3}^-$ Teff (Fig. 8E, F respectively). Thus, PS50G treatment increased $\text{TNFR2}^+\text{Foxp3}^+$ Treg proportions in lung-draining LN and might associate with the inhibition of allergic airway inflammation.

PS50G treatment increased Ki67⁺ cells within TNFR2⁺Foxp3⁺ Treg in lung of AAI mouse model

To determine whether the increase in $\text{TNFR2}^+\text{Foxp3}^+$ Treg proportions and numbers in the lung and lung-draining LN was driven by proliferation, we analysed the proliferative marker, Ki67. Given the pattern of proliferative expansion capacity was different in the lung and the lung-draining LN, we also analysed expression of CCR7 on T cell subsets after treatment, to gain insight into their capacity to migrate to the draining LN. We proposed that PS50G would increase the proliferative capacity of $\text{TNFR2}^+\text{Foxp3}^+$ Treg in order to maintain their pool/cell number in the lung during AAI, and thus render mice resistant to AAI. In addition, CD103^+ DC found in the lung after PS50G instillation (Hardy et al., 2013b) would promote the proliferative expansion of Treg, and we proposed that this is true only for TNFR2 expressing Treg as this population is concomitantly express Ki67 (Chen et al., 2010a, van der Most et al., 2009). Indeed, we found that PS50G pre-treatment (PS50G/OVA/OVA) significantly increased the percentages of Ki67^+ cells within $\text{TNFR2}^+\text{Foxp3}^+$ Treg as compared to the Sal/OVA/OVA. The percentages of Ki67^+ cells within $\text{TNFR2}^+\text{Foxp3}^+$ Treg in PS50G

pre-treatment (PS50G/OVA/OVA) were similar to saline negative control group (~ 30 %) (Sal/Sal/Sal) (Fig. 9A). The mean percentage of Ki67⁺ cells within TNFR2⁻Foxp3⁺ Treg was < 10 %, whilst that of Ki67⁺ cells in TNFR2⁺Foxp3⁻ Teff was ~ 20 % (Fig. 9A). No significant differences of the Ki67⁺ cells within TNFR2⁻Foxp3⁺ Treg and TNFR2⁺Foxp3⁻ Teff were found between PS50G/OVA/OVA and Sal/OVA/OVA groups, showing that PS50G preferentially induced proliferative expansion of TNFR2⁺Foxp3⁺ Treg. PS50G treatment did not affect CCR7 expression on Treg and Teff subsets in the lung (Fig. 9B). The CCR7 expression was highest in the TNFR2⁻Foxp3⁺ Treg (Fig. 9B). The percentages of CCR7⁺ cells in the lung draining LN were only < 2 % in Treg or Teff subsets (data not shown). PS50G did not affect the frequency of Ki67⁺ cells in any of the populations examined in the lung-draining LN. We observed that the frequency of Ki67⁺ cells in the TNFR2⁻Foxp3⁺ Treg was approximately 3-4-fold lower than the TNFR2⁺Foxp3⁺ Treg and TNFR2⁺Foxp3⁻ Teff (Fig. 9C), suggesting that Treg comprise cells that are actively proliferate in the periphery (TNFR2⁺Foxp3⁺ Treg) and actively migrate (TNFR2⁻Foxp3⁺ Treg) to the lymphoid organs.

PS50G pre-treatment increased LAP⁺ and CTLA-4⁺ cells within TNFR2⁺Foxp3⁺ Treg in lung and lung-draining LN of AAI mouse model

We hypothesised that if PS50G-induced inhibition of AAI was mediated by increased Treg this would be manifested in increased expression of suppressor molecules on Treg. To investigate this, we analysed the TGF-β binding molecule LAP and CTLA-4, molecules thought to be involved in Treg suppressive function (Duan et al., 2011, Schmidt et al., 2009). We found that PS50G treatment significantly increased the proportion of LAP⁺ within TNFR2⁺Foxp3⁺ Treg subset, but not within TNFR2⁻Foxp3⁺ Treg and TNFR2⁺Foxp3⁻ Teff (Fig. 10A). PS50G did not alter the proportion of LAP⁺

cells in any cell population the in the lung-draining LN (Fig. 10B). Consistent with the finding that LAP expression is not associated with Teff, we found the lowest frequency of LAP⁺ cells were within TNFR2⁺Foxp3⁻ Teff both in the lung and in the lung-draining LN (< 0.3 %) (Fig. 10A, B). Although PS50G did not alter the proportion of CTLA-4-positive Treg (TNFR2⁺Foxp3⁺ Treg and TNFR2⁻Foxp3⁺ Treg) in the lung, they caused a 2-fold increased the percentages of CTLA-4⁺ exclusively within TNFR2⁺Foxp3⁺ Treg in the lung-draining LN (Fig.10 C, D). Therefore, we demonstrated that PS50G altered molecules associated with suppressive function of TNFR2⁺Foxp3⁺ Treg in lung and lung-draining LN, suggesting that might increase the suppressive capacity of TNFR2⁺Foxp3⁺ Treg.

Discussion

A number of ambient, anthropogenic and engineered nanoparticles have been described that exert detrimental effects on lung immune homeostasis and exacerbate the symptoms' of asthma and lung inflammation upon allergen challenge in susceptible individuals (Inoue et al., 2010, Hussain et al., 2011). However, our recent studies suggest a radically different role of inert nontoxic PS50G; promoting homeostasis and preventing the elicitation of inflammation upon allergen challenge in atopic animals (Hardy et al., 2012a, Hardy et al., 2013b). Our initial studies suggested that PS50G can modulate pulmonary DC function (Hardy et al., 2012a, Hardy et al., 2013b). Here, we further reveal a novel role of PS50G, leading to the effective elicitation of lung $\text{TNFR2}^+\text{Foxp3}^+$ Treg upon local allergen re-challenge in sensitised animals that might mediate an effective inhibition of lung airway inflammation. Elevated levels of $\text{TNFR2}^+\text{Foxp3}^+$ Treg were maintained up to day 30 after PS50G administration. Interestingly, Hardy *et al.* found that PS50G induced CD103^+ DC on day 3 with sustained high levels up to day 30 (Hardy et al., 2013b). Given CD103^+ DC are Treg inducing APC, together our data suggests a novel mechanism to maintain lung homeostasis (Fig. 11) where PS50G: 1) increases macrophage numbers in the lung; 2) selectively alter cytokines/chemokines in the lung microenvironment, including CCL2; 3) increase CD103^+ DC numbers; 4) when internalised by lung resident CD103^+ DC and macrophages causes their activation (Hardy et al., 2013b). These changes might enhancing CD103^+ DC ability to prime naïve T cells to become Treg in the lung and lung-draining LN, and are specifically efficient at amplifying $\text{TNFR2}^+\text{Foxp3}^+$ Treg in the lung. We suggest here that the above mechanism plays a key role helping maintain lung immune homeostasis and inhibiting development of allergic airway inflammation.

Tolerogenic and migratory CD103⁺ DC travel towards lung-draining LN to prime naïve CD4⁺ T cells into Treg (Khare et al., 2013) whereas lung macrophages are involved in maintaining Foxp3 in Treg, once these cells populate in the lung tissue (Soroosh et al., 2013). As this is the first study investigating the effects of non-toxic ENP on TNFR2⁺Foxp3⁺ Treg in the lung, further studies are needed to evaluate the role of CD103⁺ DC in the priming and/or inducing TNFR2⁺Foxp3⁺ Treg both in the lung and lymphoid organs independent of TNF. Increased frequencies of Treg in the periphery and lymphoid organs indicate Treg have either proliferated or migrated into the tissue (Fisson et al., 2003). *In vitro*, Treg are usually considered anergic (Takahashi et al., 1998). However, an addition of TNF, IL-2, anti-CD28 antibody, or LPS (Chen et al., 2007, Takahashi et al., 1998, Caramalho et al., 2003) in culture can overcome the profound anergic state of TCR-stimulated Treg, and in combination with IL-2 (Chen et al., 2007), can increase their suppressive activity. Moreover, studies in co-transfer model with disease-inducing T cells have shown that Treg also can actively proliferate *in vivo* (Walker et al., 2003, Klein et al., 2003). In line with these studies, during homeostasis, we further showed that Treg and Teff that expressed TNFR2 in our system exhibited higher proliferative capacity than non-TNFR2 subsets. This would suggest that TNFR2⁺Foxp3⁺ Treg with high proliferative capacity are important in controlling the overwhelming activation of TNFR2⁺Foxp3⁻ Teff, as TNFR2⁻Foxp3⁺ Treg are not highly proliferative and are therefore less capable of suppressing Teff that expressed TNFR2 (Chen et al., 2007, Chen et al., 2010a, van der Most et al., 2009). Importantly, in another study, we showed that Teff could be divided into two distinct subsets; TNFR2 expressing Teff (TNFR2⁺Foxp3⁻ Teff) that are highly proliferative *in vivo* but do not preferentially produce cytokines and non TNFR2 expressing Teff (TNFR2⁻Foxp3⁻ Teff) that are programmed as cytokine producers, with lower proliferative capacity *in vivo* (Mohamud

et. al., in preparation). This is an important finding suggesting that, TNFR2⁺Foxp3⁺ Treg proliferate in the lung to maintain homeostasis and limit the inflammatory responses while maintaining ‘proper’ responses to harmless airborne stimulus.

Interestingly, PS50G both increased the ratio of TNFR2⁺Foxp3⁺ Treg: TNFR2⁺Foxp3⁻ Teff, and increased the proliferative expansion capacity of TNFR2⁺Foxp3⁺ Treg to the levels found during homeostasis. During allergic airway inflammation, the proliferative expansion capacity of TNFR2⁺Foxp3⁺ Treg decreased and this was prevented by pre-treatment with PS50G. Such a mechanism would be important to maintain the Treg pool/cell numbers in the system, since loss of tolerance and insufficient regulation by Treg might lead to Th2-skewed immune responses at mucosal surfaces (Lin et al., 2008, Ling et al., 2004, Shi and Qin, 2005, Grindebacke et al., 2004, Curotto de Lafaille et al., 2001, Faustino et al., 2012, Carson et al., 2008). However, the ratio of TNFR2⁺Foxp3⁺ Treg: TNFR2⁺Foxp3⁻ Teff was significantly lower than saline negative control group (Sal/Sal/Sal) as PS50G selectively increased TNFR2⁺Foxp3⁺ Treg proportions, neither lowering the proportions of TNFR2⁺Foxp3⁻ Teff to the homeostasis levels nor change the proliferative expansion capacity of TNFR2⁺Foxp3⁻ Teff. Even though previously it has been shown that CCR7⁺ T cells actively migrate to the lymphoid organs (Bromley et al., 2005), our data showed that PS50G did not alter migratory pattern of Treg. Thus, the increased frequency of TNFR2⁺Foxp3⁺ Treg in our study is potentially dependent on the proliferative expansion capacity of these cells, and this might be preferentially induced by CD103⁺ DC. We also showed that PS50G further enhanced levels of the TGF- β binding molecule LAP and CTLA-4 on TNFR2⁺Foxp3⁺ Treg in the lung and lung-draining LN, respectively. Together with the effects on DC (Hardy et al., 2012a, Hardy et al., 2013b), these results further suggest that PS50G altered the quantity and quality of lung TNFR2

expressing Treg to respond rapidly to allergenic challenges and restored lung immune homeostasis.

As reviewed in Mohamud *et al.*, besides modulation of APC functionality, nanoparticles modulate other lung-nanoparticles interactions, including the ability to interact with lung structural cells, and the ability to engage the intracellular clearance mechanisms that lead to nanoparticles clearance or local or systemic toxicity (Mohamud et al., 2013). Previously, we demonstrated that PS50G leave an innate immunological imprint in the lung. The present study extends these findings by showing that PS50G alter the frequency and suppressor phenotype of TNFR2⁺Foxp3⁺ Treg, further defining the immunological imprint exerted by PS50G. We speculate that such modulation (i.e. immunological imprint) has important consequences on adaptive immune responses in the lung, especially in controlling allergen-induced Th2 cells in allergic airway inflammation. In summary, the present study proposes a novel mechanism by which PS50G modulates the adaptive immune response by altering TNFR2⁺Foxp3⁺ Treg homeostasis, thereby decreasing susceptibility to allergic disease.

Acknowledgments

We gratefully acknowledge the expert assistance of Geza Paukovics with flow cytometry.

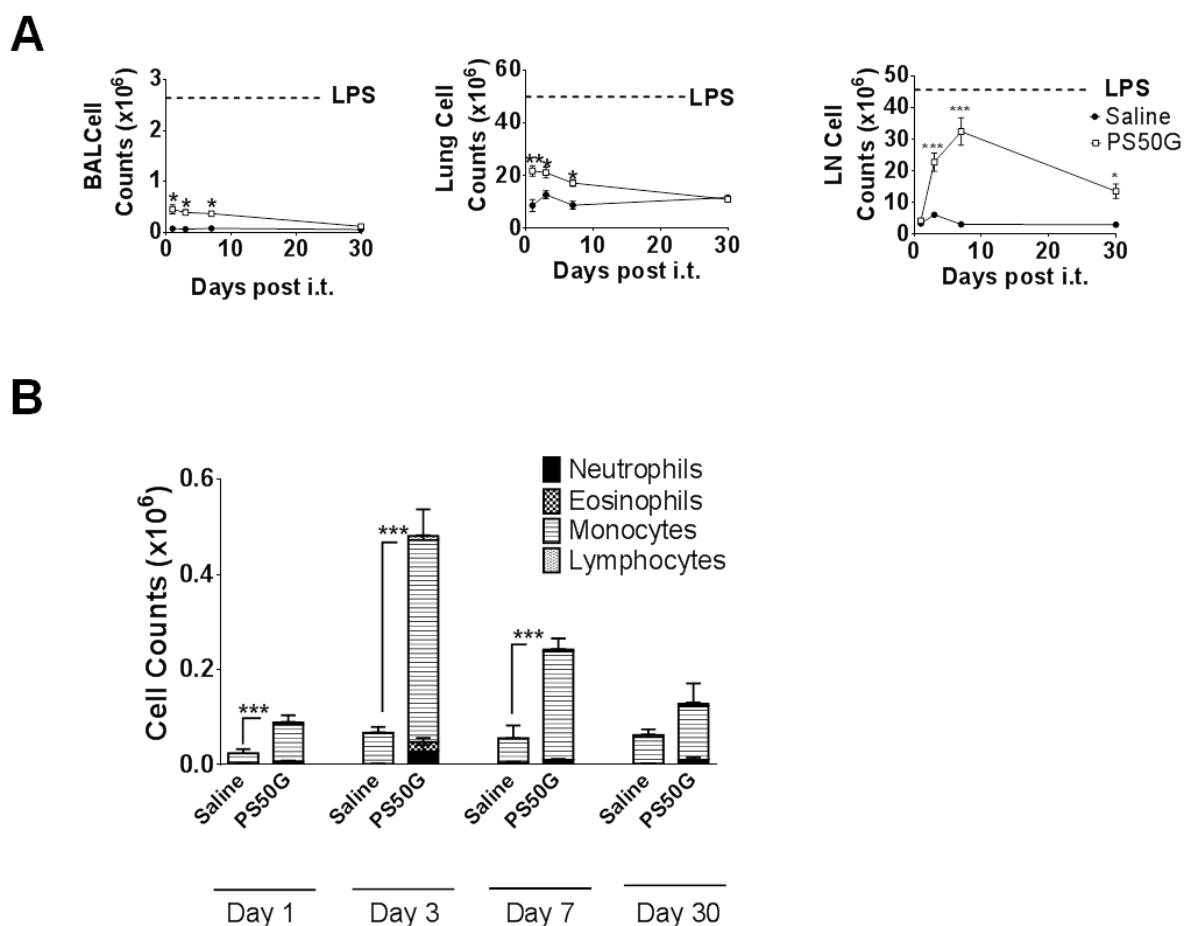


Fig. 1: PS50G instillation causes mild transient lung inflammation and increased cell numbers in the BAL, lung and lung-draining LN. Naïve mice (n=5-7 per group per time point) were received PS50G i.t. on day 0 or saline as control. Samples were collected on days 1, 3, 7 and 30 after i.t. **(A)** BAL, lung and lung-draining LN cell counts. Line denoted the total cell counts from day 3 post 10 µg LPS administration. BAL fluid were stained with Giemsa stain, counted for at least 200 cells per mouse and identified by morphological criteria for **(B)** neutrophils, eosinophils, monocytes and lymphocytes. Data represent the mean ± SEM. *p<0.05, **p<0.01, and ***p< 0.001.

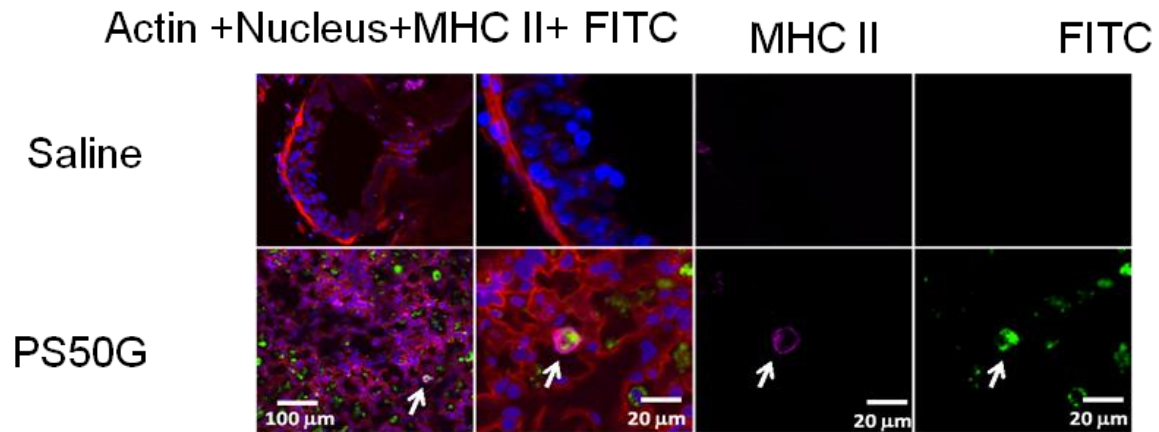


Fig. 2: PS50G are taken up by MHCII⁺ cells. Mice (n=5-7 per group per time point) were intratracheally administered with FITC-labeled PS50G on day 0, or saline as control. Lungs were fixed in 2 % paraformaldehyde and stained with appropriate antibodies and analysed on confocal on day 3 post-instillation. Cells were analysed based on their expressions of MHCII and FITC uptake. Representative lung airway and parenchyma were captured at a magnification of 400 x. Nucleus - blue; Actin- red; FITC-labeled PS50G - green; MHCII - pink.

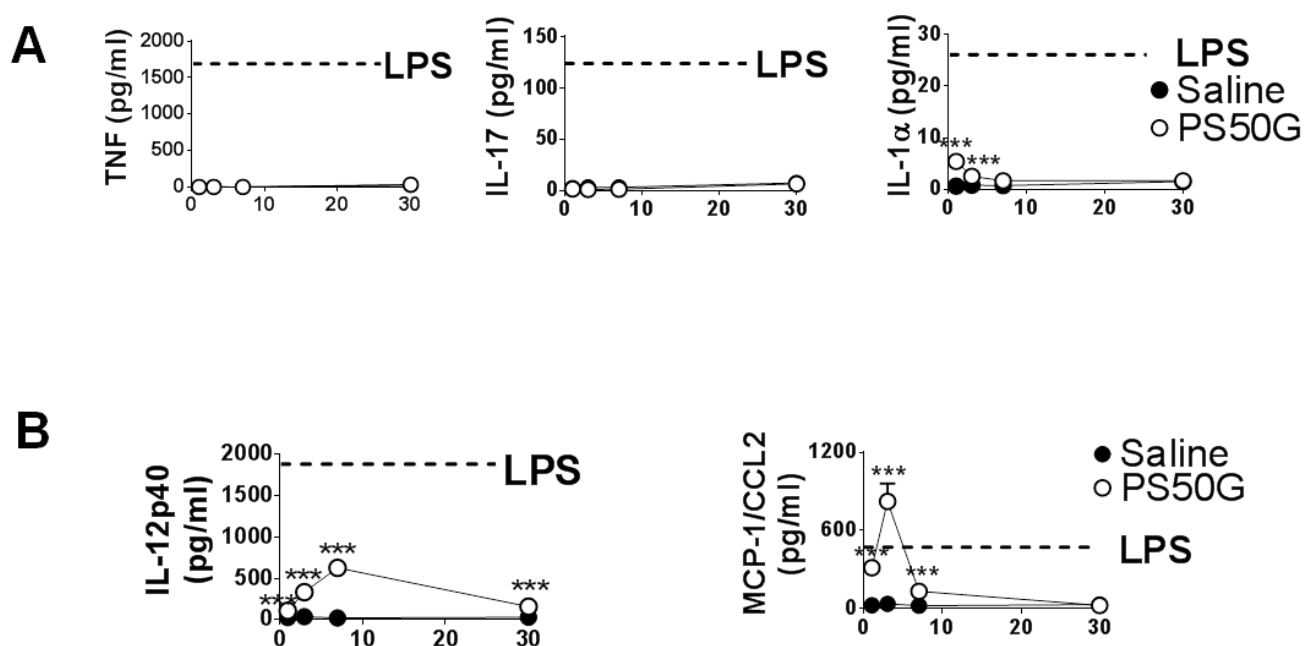


Fig. 3: PS50G instillation selectively increases BAL cytokines/chemokines secretion.

Naïve mice (n=5-7 per group per time point) were received PS50G i.t on day 0 or saline as control. BAL fluid was collected on days 1, 3, 7 and 30 after i.t. Kinetics of **(A)** inflammatory cytokines TNF, IL-17, IL-1α and **(B)** cytokines related to antigen presenting cells IL-12p40 and CCL2. Line denoted the concentration of cytokines/chemokines from day 3 post 10 μg LPS instillation. Limit of detection for TNF, IL-17, IL-1α, IL-12p40 and MCP-1/CCL2, was 13.62, 2.99, 0.75, 0.84 and 13.6, respectively. Data represent the mean ± SEM. ***p< 0.001.

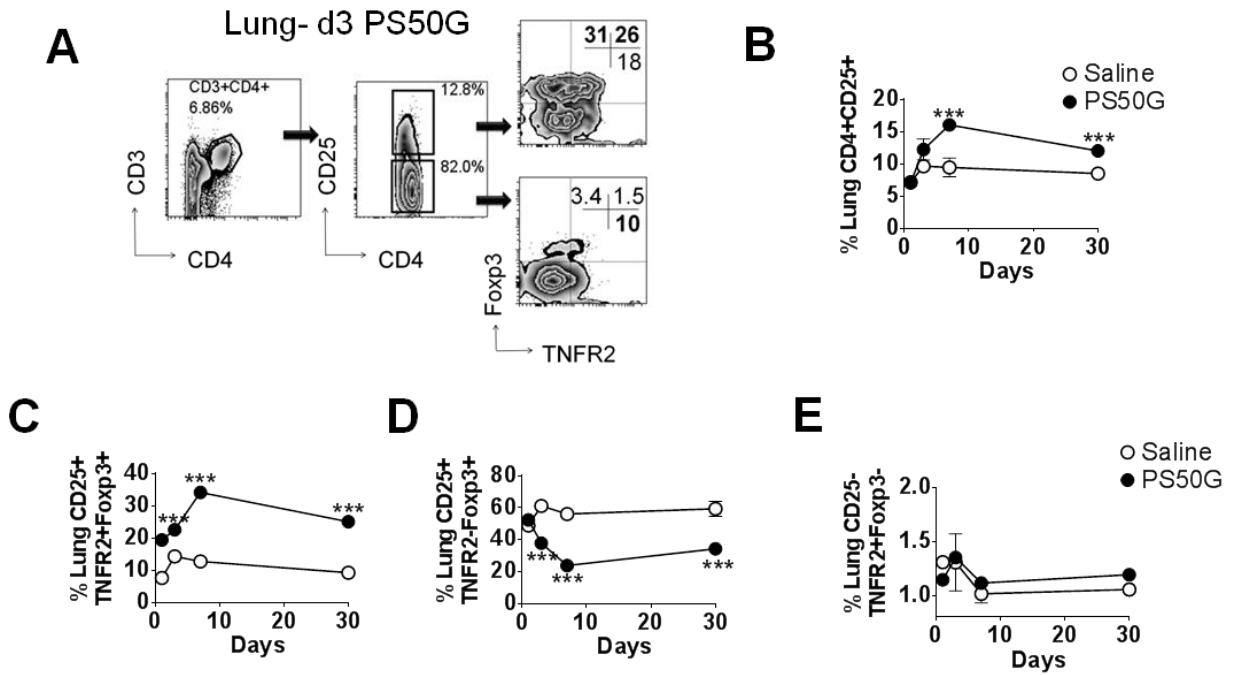


Fig. 4: PS50G instillation selectively increases lung $CD3^+CD4^+CD25^+$ that are $TNFR2^+Foxp3^+$. Naïve mice ($n=5-7$ per group per time point) were received PS50G i.t. on day 0 or saline as control. Samples were collected on days 1, 3, 7 and 30 after i.t. **(A)** Stained lung cells were gated on viable $CD3^+CD4^+CD25^+$ and $CD3^+CD4^+CD25^-$ cells, followed by gating on $TNFR2$ co-expressed $Foxp3$. Representative FACS contour plots showing $TNFR2^+$ cells in the lung of day 3 from PS50G treated mice. Percentages of **(B)** $CD3^+CD4^+CD25^+$ cells; **(C)** $TNFR2^+Foxp3^+$ Treg; **(D)** $TNFR2^-Foxp3^+$ Treg and **(E)** $TNFR2^-Foxp3^-$ Teff. Data represent the mean \pm SEM. *** $p < 0.001$.

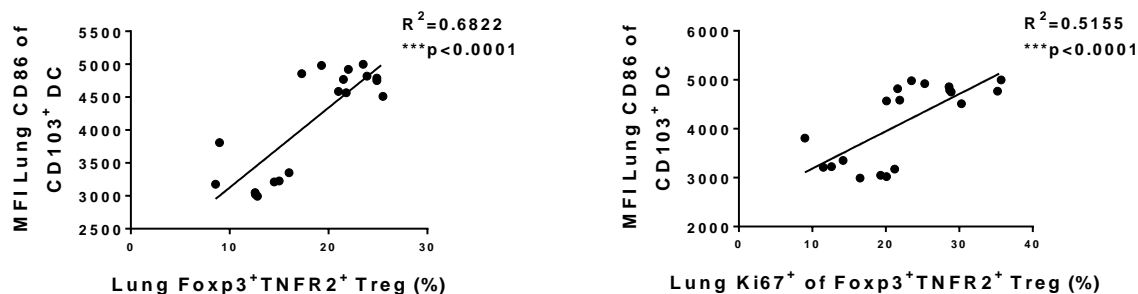


Fig. 5: Activated CD103⁺ DC positively correlates with the proportion of TNFR2⁺Foxp3⁺ Treg and TNFR2⁺Foxp3⁺ Treg that are expanded (Ki67⁺). Naïve mice (n=5-7 per group per time point) were received PS50G i.t on day 0 or saline as control. Samples were collected on days 1, 3, 7 and 30 after i.t. The percentages of TNFR2⁺Foxp3⁺ Treg (left panel) and TNFR2⁺Foxp3⁺Ki67⁺ Treg (right panel) were correlated with MFI of CD86 within CD103⁺ DC (MHCII⁺CD11c⁺CD11b⁻) (left and right panel, respectively).

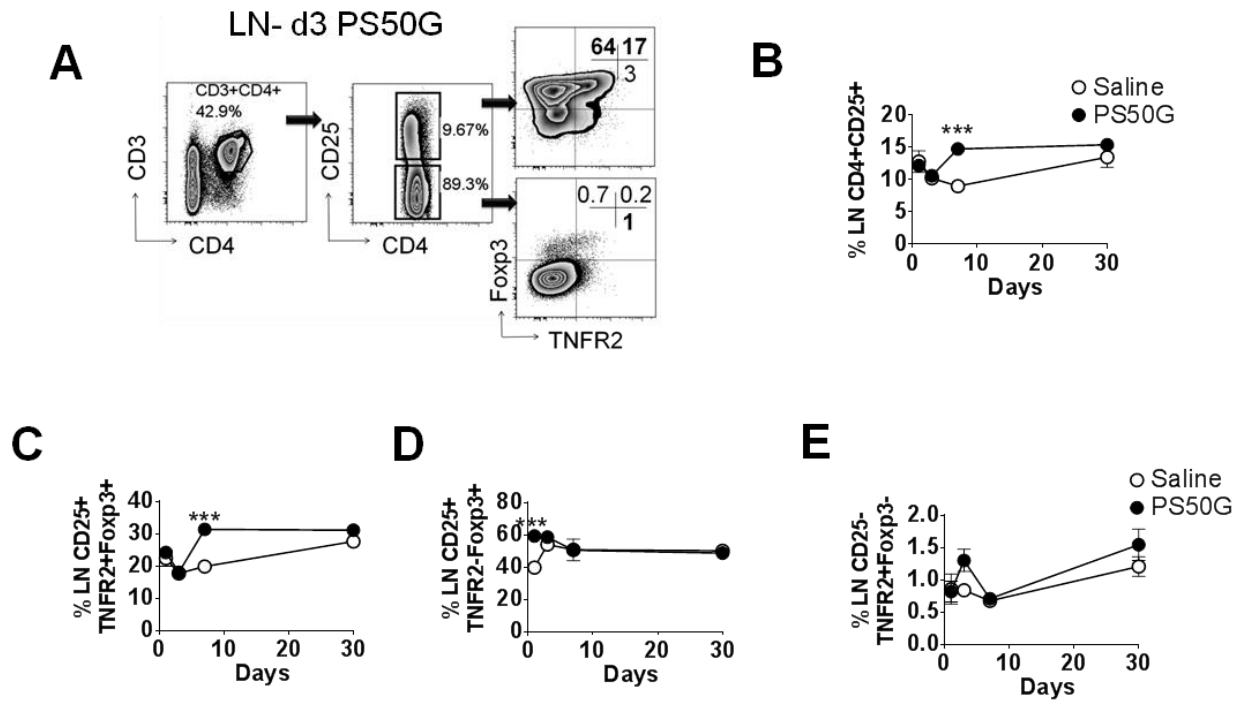


Fig. 6: PS50G instillation selectively increases lung-draining LN CD3⁺CD4⁺CD25⁺ that are TNFR2⁺Foxp3⁺ on day 7. Naïve mice (n=5-7 per group per time point) were received PS50G i.t on day 0 or saline as control. Samples were collected on days 1, 3, 7 and 30 after i.t. **(A)** Stained lung-draining LN cells were gated on viable CD3⁺CD4⁺CD25⁺ and CD3⁺CD4⁺CD25⁻ cells, followed by gating on TNFR2 co-expressed Foxp3. Representative FACS contour plots showing TNFR2⁺ cells in the lung-draining LN of day 3 from PS50G treated mice. Percentages of **(B)** CD3⁺CD4⁺CD25⁺ cells; **(C)** TNFR2⁺Foxp3⁺ Treg; **(D)** TNFR2⁻Foxp3⁺ Treg and **(E)** TNFR2⁺Foxp3⁻ Teff. Data represent the mean \pm SEM. ***p<0.001.

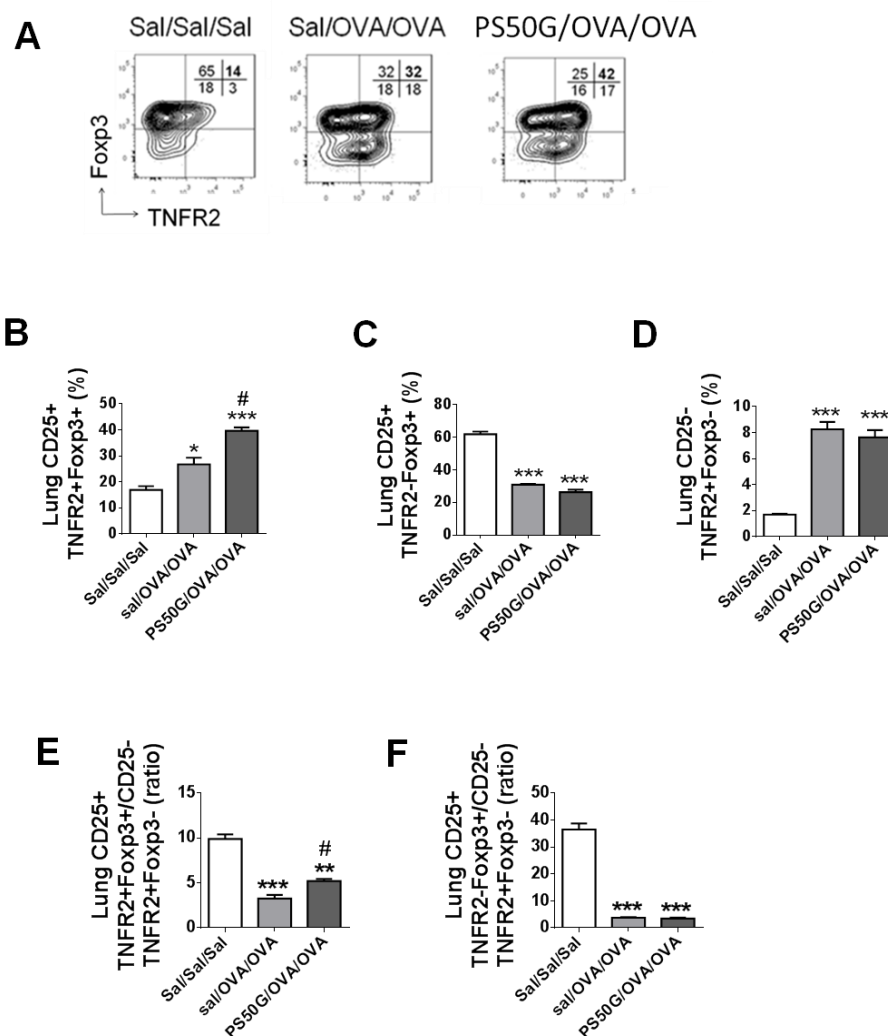


Fig. 7: PS50G instillation selectively increases lung CD3⁺CD4⁺CD25⁺ that are TNFR2⁺Foxp3⁺ in AAI mouse model. The effects PS50G on acute allergic asthma were investigated as described previously [Fig. 1 in (Hardy et al., 2012a) and Fig. 10A in (Hardy et al., 2013b)]. **(A)** Stained lung cells were gated on viable CD3⁺CD4⁺CD25⁺ and CD3⁺CD4⁺CD25⁻ cells, followed by gating on TNFR2 co-expressed Foxp3. Percentages of **(B)** TNFR2⁺Foxp3⁺ Treg; **(C)** TNFR2⁻Foxp3⁺ Treg and **(D)** TNFR2⁺Foxp3⁻ Teff. Ratios of **(E)** TNFR2⁺Foxp3⁺ Treg and **(F)** TNFR2⁻Foxp3⁺ Treg to TNFR2⁺Foxp3⁻ Teff. Data represent the mean \pm SEM. *p<0.05, **p<0.01, and ***p<0.001 compared with saline negative control group (Sal/Sal/Sal); #p<0.01, compared with OVA positive control group (Sal/OVA/OVA).

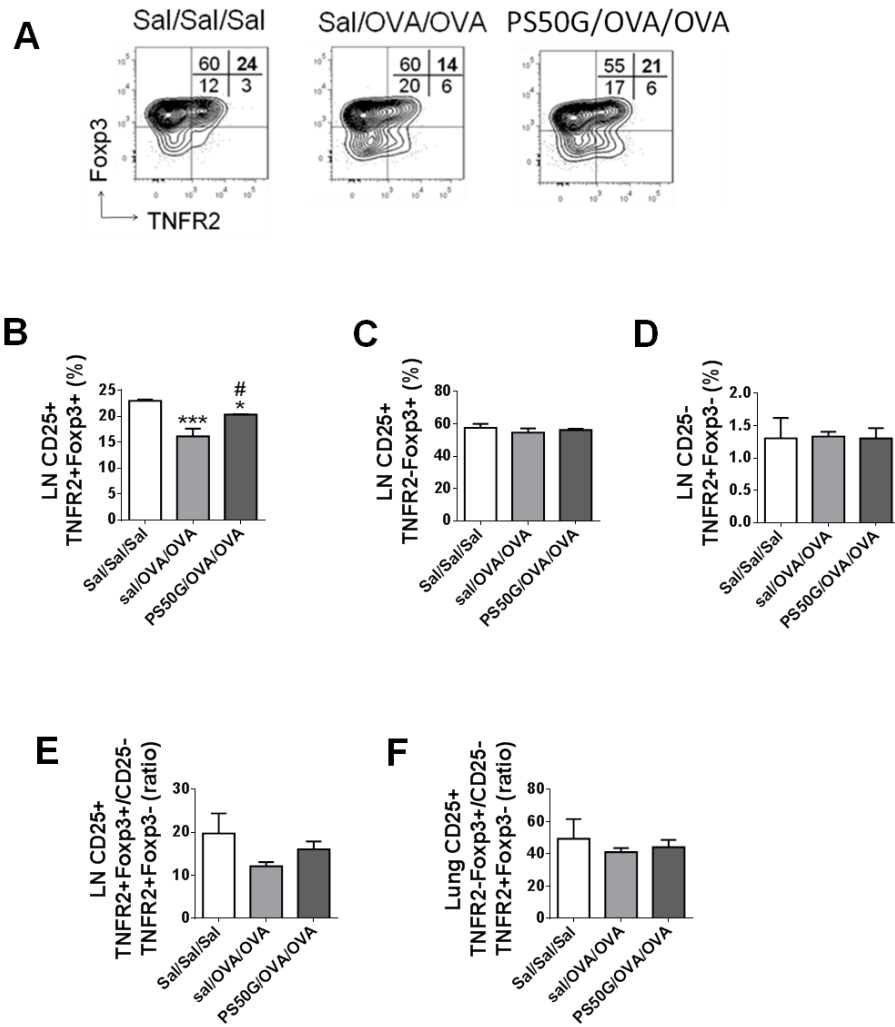


Fig. 8: PS50G instillation selectively increases lung-draining LN CD3⁺CD4⁺CD25⁺ that are TNFR2⁺Foxp3⁺ in AAI mouse model. The effects PS50G on acute allergic asthma were investigated as described previously [Fig. 1 in (Hardy et al., 2012a) and Fig. 10A in (Hardy et al., 2013b)]. **(A)** Stained lung cells were gated on viable CD3⁺CD4⁺CD25⁺ and CD3⁺CD4⁺CD25⁻ cells, followed by gating on TNFR2 co-expressed Foxp3. Percentages of **(B)** TNFR2⁺Foxp3⁺ Treg; **(C)** TNFR2⁻Foxp3⁺ Treg and **(D)** TNFR2⁺Foxp3⁻ Teff. Ratios of **(E)** TNFR2⁺Foxp3⁺ Treg and **(F)** TNFR2⁻Foxp3⁺ Treg to TNFR2⁺Foxp3⁻ Teff. Data represent the mean \pm SEM. *p<0.05, ***p<0.001 compared with saline negative control group (Sal/Sal/Sal); #p<0.05, compared with OVA positive control group (Sal/OVA/OVA).

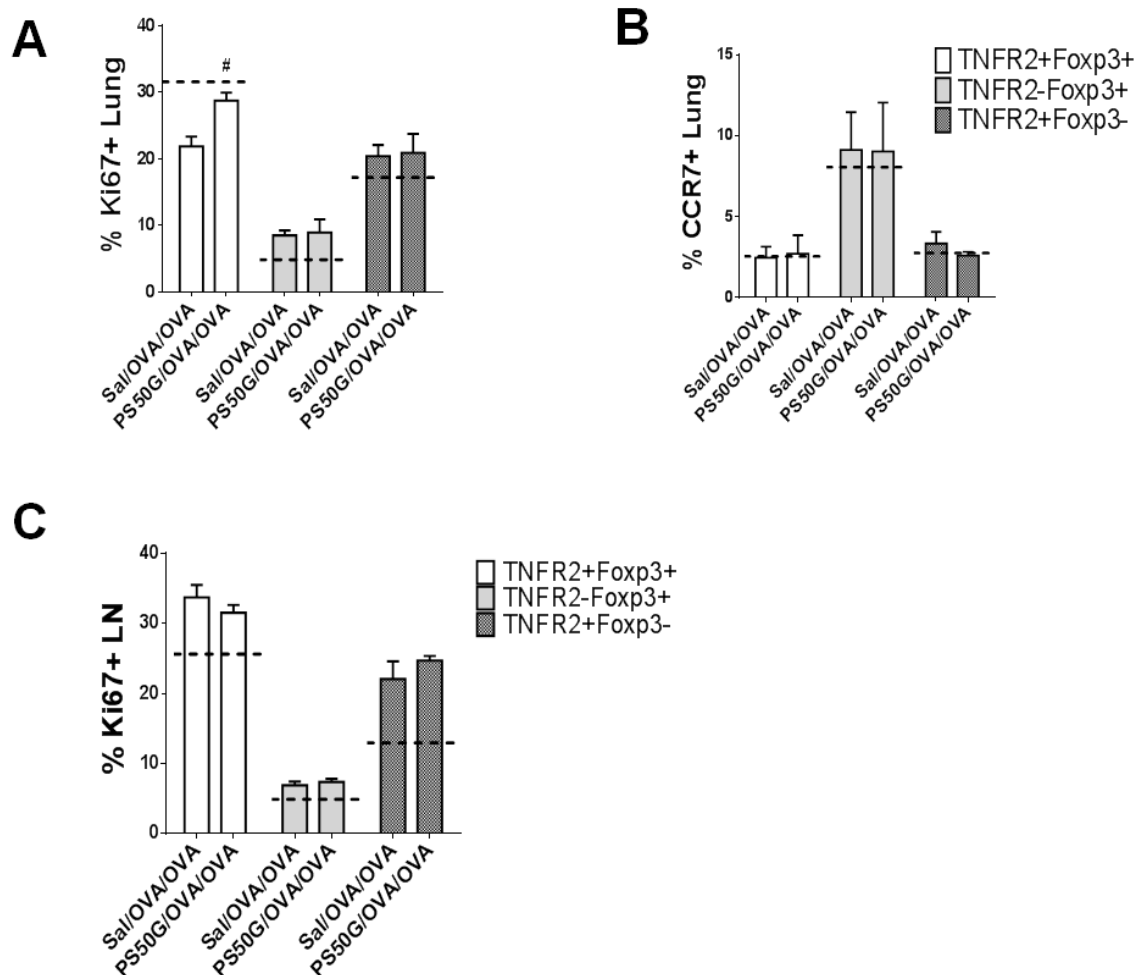


Fig. 9: PS50G instillation increases the percentages of lung Ki67⁺ within TNFR2⁺Foxp3⁺ Treg in AAI mouse model. The effects PS50G on acute allergic asthma were investigated as described previously [Fig. 1 in (Hardy et al., 2012a) and Fig. 10A in (Hardy et al., 2013b)]. Stained lung cells were gated as in Fig. 7A, followed by gated on Ki67 and CCR7. Percentages of **(A)** lung Ki67⁺ **(B)** lung CCR7⁺ and **(C)** lung-draining LN Ki67⁺ within TNFR2⁺Foxp3⁺ Treg; TNFR2⁻Foxp3⁺ Treg and TNFR2⁺Foxp3⁻ Teff. Data represent the mean \pm SEM. [#]p<0.05, compared with OVA positive control group (Sal/OVA/OVA). Line denoted the percentages of respective markers derived from saline negative control group (Sal/Sal/Sal).

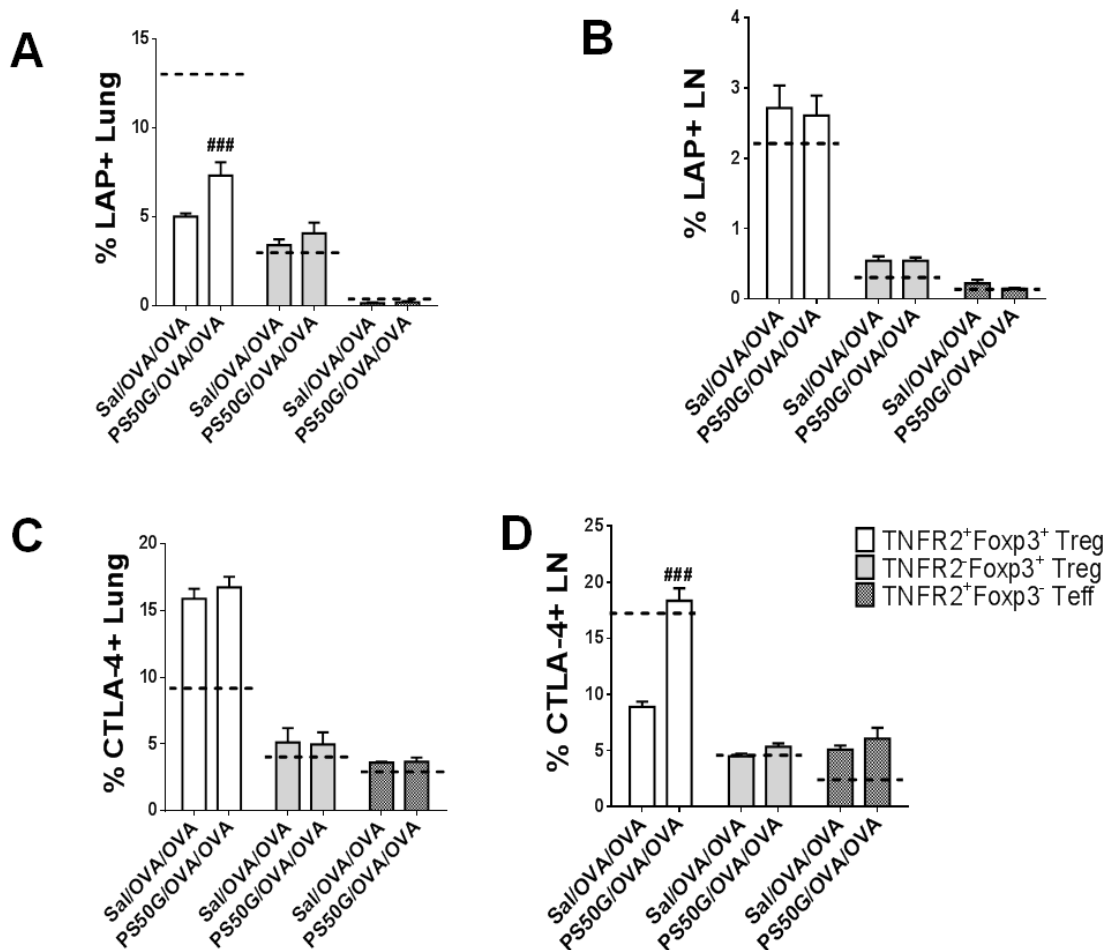


Fig. 10: PS50G increased the percentages of lung LAP⁺ and lung-draining LN CTLA-4⁺ within TNFR2⁺Foxp3⁺ Treg in AAI mouse model. The effects PS50G on acute allergic asthma were investigated as described previously [Fig. 1 in (Hardy et al., 2012a) and Fig. 10A in (Hardy et al., 2013b)]. Stained lung cells were gated as in Fig. 7A, followed by gated on LAP and CTLA-4. Percentages of (A) lung LAP⁺; (B) lung CTLA-4⁺; (C) lung-draining LN LAP⁺ and (D) lung-draining LN CTLA-4⁺ within TNFR2⁺Foxp3⁺ Treg; TNFR2⁺Foxp3⁺ Treg and TNFR2⁺Foxp3⁻ Teff. Data represent the mean \pm SEM. ^{###}p<0.001, compared with OVA positive control group (Sal/OVA/OVA). Line denoted the percentages of respective markers derived from saline negative control group (Sal/Sal/Sal).

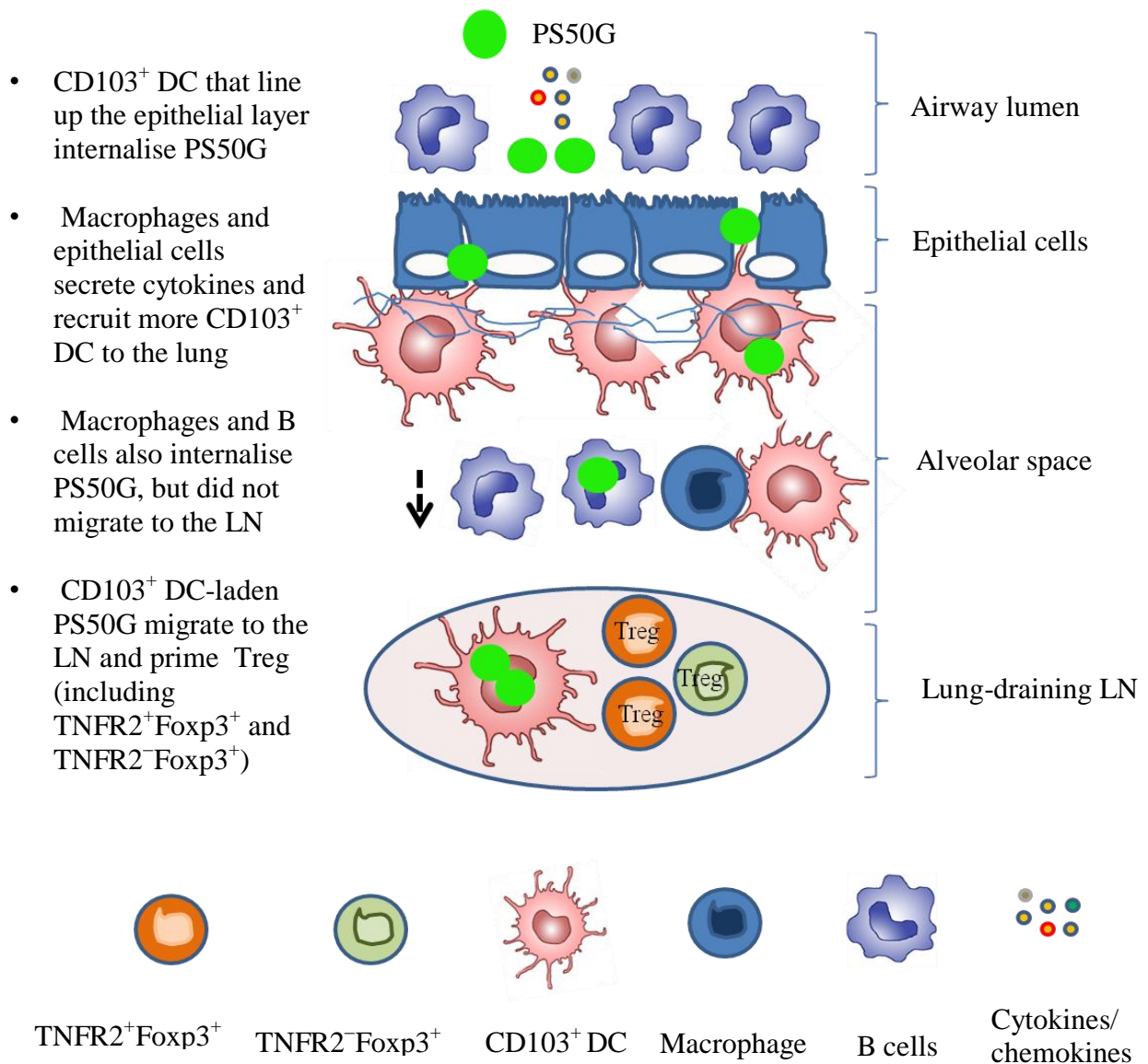


Figure 11: Proposed mechanisms on the effects of PS50G in maintaining lung immune homeostasis. PS50G increase macrophages numbers triggering them to secrete CCL2 into the airways, which causes recruitment of tolerogenic CD103⁺ DC. Lung-resident- and newly recruited-CD103⁺ DC internalise PS50G and preferentially migrate towards lung-draining LN to prime naive T cells into Treg (both TNFR2⁺Foxp3⁺ Treg and TNFR2⁻Foxp3⁺ Treg subsets). PS50G increase the proliferative expansion capacity and suppressive capacity of TNFR2⁺Foxp3⁺ Treg to render them to resistant to subsequent allergen challenges.

BAL Cytokines (pg/ml)	Sal negative control group (day 3)	PS50G instillation (day 3)	10 µg LPS instillation (day 3)	BLOD
IL-2	BLOD	BLOD	BLOD	1.56
IL-3	1.53 ± 0.33	0.88 ± 0.10	0.72 ± 0.14	0.15
IL-4	BLOD	BLOD	BLOD	4.02
IL-5	2.25 ± 0.3	1.9 ± 0.11	1.83 ± 0.24	0.25
IL-6	BLOD	7.8 ± 0.89***	165.3 ± 55.4***	1.04
IL-10	3.24 ± 0.5	2.40 ± 0.6	3.1 ± 0.4	0.03
IFN-γ	BLOD	BLOD	4.69 ± 1.9	0.76
TGF-β	45 ± 1.7	70.2 ± 2.3*	254 ± 16.2***	10.22
GM-CSF	3.33 ± 0.89	7.02 ± 1.38***	13.14 ± 0.97***	1.70
G-CSF	7.99 ± 2.4	78.6 ± 12.4***	2788 ± 1008***	4.12

Table 1: Comparative cytokines concentration in the BAL fluid at day 3 post saline, PS50G and 10 µg LPS instillation. Naïve mice (n=5-7 per group per time point) were received PS50G i.t on day 0 or saline as control. BAL was collected on day 3 after i.t. Mean ± SEM. *p<0.05, ***p<0.001 compared to saline negative control group (Sal/Sal/Sal). BLOD- below limit of detection.

Cells	Groups	Cell numbers (10 ⁴) Lung	Cell numbers (10 ⁴) LN
Total cell numbers	Saline	1054 ± 252	593 ± 207
	PS50G	2030 ± 162	2085 ± 109***
CD3⁺CD4⁺ cells	Saline	72.1 ± 5.0	476 ± 29.8
	PS50G	70.2 ± 8.2	867 ± 73.2***
CD3⁺CD4⁺CD25⁺ Treg	Saline	8.84 ± 0.36	59.6 ± 6.1
	PS50G	8.32 ± 2.1	105.8 ± 14.3***
TNFR2⁺Foxp3⁺ gated of CD3⁺CD4⁺CD25⁺ Treg	Saline	0.87 ± 0.23	9.2 ± 2.3
	PS50G	2.43 ± 0.91***	16.2 ± 2.9***
TNFR2-Foxp3⁺ gated of CD3⁺CD4⁺CD25⁺ Treg	Saline	5.1 ± 0.9	28.0 ± 6.4
	PS50G	5.01 ± 1.09	54.4 ± 7.21***
CD3⁺CD4⁺CD25⁻ Teff	Saline	60.7 ± 2.87	501.4 ± 20.5
	PS50G	62.3 ± 11.2	902 ± 13.6***
TNFR2⁺Foxp3⁻ gated of CD3⁺CD4⁺CD25⁻ Teff	Saline	0.89 ± 0.32	11.02 ± 3.3
	PS50G	1.12 ± 0.82	20.09 ± 3.6***

Table 2: PS50G alters the numbers of CD3⁺CD4⁺ T cells, total Treg and TNFR2 cells. Naïve mice (n=5-7 per group per time point) were received PS50G i.t on day 0 or saline as control. Samples were collected on day 3 after i.t. Lung and lung-draining LN were analysed for cell numbers and percentages. Data represent the mean ± SEM. ***p< 0.001.

5.2 Summary

The results detailed suggest that Treg are involved in controlling lung homeostasis in mice. Altered Treg/Teff ratios might result in an imbalance of immune responses [i.e. induction of allergic airway inflammation, recruitment and activation of Teff (e.g. Th2 cells) and inflammatory cells (e.g. eosinophils)] that lead to the secretion of pro-inflammatory cytokines in the lung. However, PS50G exhibited the capacity to restore lung immune responses to a homeostatic level, potentially by not only modifying innate imprinting in the lung as shown before, but also by unexpectedly initiating expansion of TNFR2⁺Foxp3⁺ Treg to prevent the induction of allergic airway inflammation.

The above studies suggest TNFR2 expressing Treg are important in regulating airway inflammation and can be expanded by a non-inflammatory imprint such as PS50G. The question addressed in the next chapter is whether a classic inflammatory imprint such as LPS would also preferentially promote increases in TNFR2⁺ Treg. The next chapter (presented as manuscript) investigated whether TNFR2⁺ and TNFR2⁻ Treg are altered during the induction of inflammation in an LPS-induced acute lung injury mouse model.

Chapter 6

The effects of LPS on TNFR2 expressing regulatory T cells in the lung during lung injury

PART B: Declaration for Thesis Chapter 6**Declaration by candidate**

In the case of Chapter 6, the nature and extent of my contribution to the work was the following:


Nature of contribution	Extent of contribution (%)
In this study, I conceived, designed and performed all experiments, and I was responsible for interpretation of the data for all experiments. I played a major role in the preparation of figures, writing and editing manuscript.	80 %

The following co-authors contributed to the work. If co-authors are students at Monash University, the extent of their contribution in percentage terms must be stated:

Name	Nature of contribution	Extent of contribution (%) for student co-authors only
Jeanne LeMasurier	Technical assistance	20 %
John Yao	Technical assistance	NA
Jennifer M. Rolland	Intellectual input and editing manuscript	NA
Robyn E. O’Hehir	Intellectual input and editing manuscript	NA
Charles L. Hardy	Experimental design, editing manuscript, data interpretation and intellectual input	NA
Magdalena Plebanski*	Experimental design, editing manuscript, data interpretation and intellectual input	NA

The undersigned hereby certify that the above declaration correctly reflects the nature and extent of the candidate’s and co-authors’ contributions to this work*.

**Candidate’s
Signature**

	Date 24. 03. 2014
---	-----------------------------

**Main
Supervisor’s
Signature***

	Date 24. 03. 2014
---	-----------------------------

*Note: Where the responsible author is not the candidate’s main supervisor, the main supervisor should consult with the responsible author to agree on the respective contributions of the authors.

6.1 Manuscript

LPS alters proliferative and suppressor function of TNFR2⁺ and TNFR2⁻ Tregs in the lung

Rohimah Mohamud^{ac}, Jeanne S. LeMasurier^{ac}, John Yao^{abc}, Jennifer M. Rolland^{abc}, Robyn E. O’Hehir^{abc}, Charles L. Hardy^{abc*}, Magdalena Plebanski^{acd*}

** Equal contribution*

^a Department of Immunology, Monash University, Melbourne, VIC, Australia

^b Department of Allergy, Immunology and Respiratory Medicine, The Alfred Hospital and Monash University, Melbourne, VIC, Australia

^c CRC for Asthma and Airways, Sydney, NSW, Australia

^d Corresponding author:

Professor Magdalena Plebanski

[REDACTED]

[REDACTED]

Fax: + 61 3 9903 0038

This research was funded by the Cooperative Research Centre for Asthma and the National Health & Medical Research Council of Australia.

Abstract

Administration of lipopolysaccharide (LPS) into the lung induces acute lung injury (ALI) with secretion of multiple cytokines. Tumor necrosis factor (TNF) plays an important role in mediating this inflammation. A study showed that co-expression of TNF receptor 2 (TNFR2) on CD25⁺ regulatory T cells (TNFR2⁺ Treg) isolated from the C57BL/6 mice splenocytes is associated with enhanced Treg suppressive function, whilst expression of TNFR2 on CD25⁻ effector T cells (TNFR2⁺ Teff) confers resistance to suppression. However, it is not known if TNFR2⁺ Treg are present in the lung and whether they play a role in regulating lung inflammation. To address this question, we studied TNFR2⁺ Treg at the peak of inflammation following LPS instillation into the lungs of naïve BALB/c mice. We show that instillation of LPS decreases the homeostatic *in vivo* proliferative capacity of TNFR2⁺ Treg, as reflected by a lowered proportion of Ki67⁺ cells, without altering their *in vitro* proliferative capacity following TCR stimulation. Lung TNFR2⁺ Treg in unmanipulated mice showed suppressor activity, which was then compromised in LPS treated animals. The proliferative capacity of TNFR2⁺ Treg was also reduced following LPS instillation. Mechanistically the observed impaired suppressive capacity correlated with decreased expression of key transcription factors (Foxp3, Helios) and, consistent with these changes, decreased expression of surface molecules associated with Treg suppressive capacity, namely, CTLA-4, LAP and GARP. These findings highlight the complex relationship between TNFR2⁺ Treg and inflammation and suggest that boosting lung TNFR2⁺ Treg function might offer alternative approaches to treat patients with inflammatory lung diseases.

Key words: Treg, Lipopolysaccharide, Lung, TNFR2

Introduction

Lipopolysaccharide (LPS) is a pro-inflammatory component of gram-negative bacteria cell walls that is released into the circulation during bacterial infection (Doyle et al., 1995). A recent study in healthy volunteers showed that an inhaled LPS challenge (approximately 5 µg) activated macrophages to secrete TNF, IL-1β and IL-6 and induced neutrophilic inflammation (Hernandez et al., 2010). Intratracheal LPS exposure in mice was shown to induce acute lung injury (ALI) and production of pro-inflammatory cytokines such as TNF, IL-1β and IFN-γ (Vernooy et al., 2001). However, LPS effects on immunoregulatory responses in experimental animal models and humans remain poorly understood. LPS modulates both airway innate (particularly macrophages (Vernooy et al., 2001) and neutrophils (D'Alessio et al., 2009) and adaptive immune cells [(including regulatory T cells (Treg)] (D'Alessio et al., 2009, Loures et al., 2010). Accumulating evidence shows that Treg play important roles in maintaining the balance between protective and pathogenic immune responses (Strickland et al., 2006, Lewkowich et al., 2005, Jonuleit and Schmitt, 2003). In accordance with this, recent studies in a mouse model of LPS-induced ALI showed that adoptive transfer of isolated CD4⁺CD25⁺Foxp3⁺ Treg restored lung immune homeostasis, indicating that Treg play a significant role in LPS-induced ALI (D'Alessio et al., 2009, Aggarwal et al., 2009).

Studies by Chen *et al.* and van der Most *et al.* showed that Treg that express TNFR2 on their surface (TNFR2⁺ Treg) exert maximal suppressive capacity and actively proliferate (Chen et al., 2007, Chen et al., 2010a, van der Most et al., 2009). All proliferating cells express the mitotic marker Ki67 and TNFR2⁺ Treg are predominantly Ki67-positive in peripheral lymphoid organs (Chen et al., 2010a). Nevertheless, nothing is known about the proportions and functional capacities of TNFR2⁺ Treg in LPS-induced ALI. In this

study, we assessed expression of Ki67 and the LN-homing marker CCR7 on TNFR2⁺ and TNFR2⁻ lung T cells to shed light on how the lung maintains its relative balance of Treg and T effectors (Teff). Our data show that LPS can decrease proliferation of TNFR2⁺ Treg and TNFR2⁺ Teff *in vivo*. However, LPS does not alter proliferation of TNFR2⁻ Treg, but decreases their expression of CCR7, suggesting a decreased capacity to migrate to the lung-draining LN. Furthermore, we show for the first time that lung Treg (either the TNFR2⁻ Treg subset alone or a combination of TNFR2⁺ and TNFR2⁻ Treg) fail to suppress CD25⁻ Teff after LPS instillation. Mechanistically, LPS decreased the proportions of Treg expressing transcription factors (Foxp3, Helios) and markers associated with their suppressive capacity (CTLA-4, LAP and GARP), and decreased their suppressive effects. Overall, our data suggest that local airway LPS instillation induces striking changes in TNFR2 expressing lung Treg and Teff, with significant implications for understanding lung immune function during inflammatory conditions such as bacterial infections and ALI.

Methods

Mice

Female BALB/c mice aged 6–8 weeks were obtained from the Walter and Eliza Hall Institute of Medical Research, Melbourne, Victoria, Australia and housed in the Alfred Medical Research and Education Precinct animal house. All studies with mice were approved by the AMREP Animal Ethics Committee (E/0821/09/M).

LPS instillation

Mice were anaesthetised by intraperitoneal (i.p.) injection of ketamine and xylazine as described previously (Hardy et al., 2010). Mice were intubated intratracheally (i.t.) with 10 µg LPS (Lipopolysaccharides from *Escherichia coli* # K-235, Sigma-Aldrich) diluted in saline; or saline alone as a control (Hardy et al., 2010). Three days after LPS treatment, the bronchoalveolar lavage (BAL) fluid, lung-draining LN and lung tissues were collected.

Bronchoalveolar lavage fluid and differential counts

Methods were as described previously (Hardy et al., 2003). To obtain BAL fluid, lungs were lavaged with 0.4 ml of 1% fetal calf serum (FCS) in phosphate-buffered saline (PBS) followed by 3 further lavages of 0.3 ml. For differentials, total cell counts were determined for each BAL sample and 100 µl of fluid was cytopun at 350 x g for 4 min onto glass slides. BAL cytopots were air dried, fixed in methanol for 2 minutes, and Giemsa stained for 8 minutes (Merck, Kilsyth, Victoria, Australia). At least 200 cells per mouse were counted and identified by morphological criteria.

Tissue sampling and cell isolation

Tissue digestion was performed as described previously (Vremec et al., 1992) with modifications. Lung and lung-draining LN were chopped with a tissue chopper (Mickle Laboratory Engineering Co. Ltd, Gomshall, Surrey, UK). Tissue fragments from lung were digested in collagenase type IV (1 mg/ml; Worthington, Lakewood, NJ, USA) and DNase type I (0.025 mg/ml; Roche Diagnostics, Sydney NSW #1284932) in a volume of 7 ml at 25°C by manual pipetting for 20 minutes, followed by 5 minutes mixing with one 10th volume of 0.01 M EDTA. The cell suspension was filtered [70 µm cell strainer (BD Falcon)] and underlaid with 1 ml 0.01 M EDTA in FCS prior to centrifugation (350 x g, 4°C). The cell supernatant was discarded and red cells lysed with red blood cell lysis solution for 3–5 min (#R7757, Sigma-Aldrich). The cell suspension was diluted to 10 ml in incomplete media (10% FCS RPMI), underlaid with EDTA/FCS and centrifuged as above. Cells were resuspended in FACS staining buffer [3% FCS, 5 mM EDTA (pH 7.2) and 0.1% Na-Azide in Ca²⁺/Mg²⁺-free HBSS], and viable cells were counted in a haemocytometer.

Antibodies and flow cytometry

Cells (1×10^6) were stained on ice for 20 minutes with combinations of the following antibodies (all eBioscience unless noted): CD3 (APC-Cy7, Qdot 605 from Lifetechnologies), CD4 (V450 and V500 from BDBiosciences), CD25 (PE-Cy7, APC-Cy7), CCR7 (Per-CP), CD120b/TNFR2 (PE), LAP (Per-CP), GARP (V450), CD39 (Pe-Cy7), CD73 biotin, GITR (Pe-Cy7), CTLA-4 biotin or their respective immunoglobulin isotypes. For intracellular staining of Foxp3 (APC), Ki67 (FITC) and Helios (V450 from BioLegend), cells were permeabilized according to the manufacturer's instructions.

Acquisition was on a LSRII flow cytometer (BD) and analysis was performed using FlowJo (Tree Star, Ashland, OR, USA).

CD25 and TNFR2 cell sorting

Lung cells pooled from 15-20 mice (1×10^8 cells) were stained with CD4 (V450), CD25 (Pe-Cy7) and sorted (BD FACS Aria) into CD4⁺CD25⁺ (Treg) and CD4⁺CD25⁻ (Teff) populations. For TNFR2⁺ Treg depletion assay, cells were stained with the above antibodies and CD120b/TNFR2 (PE) and sorted into CD25⁺TNFR2⁻ (Q1), CD25⁺TNFR2⁺ (Q2), CD25⁻TNFR2⁻ (Q3) and CD25⁻TNFR2⁺ (Q4). These cells (Q1, Q2, Q3 and Q4) will herein be called 'TNFR2 populations'. The purity of these sorted TNFR2 populations was > 97%.

Treg functional assays

For proliferation assay of CD4⁺CD25⁺ cells, CD4⁺CD25⁻ cells and TNFR2 populations from naïve mice, 1×10^5 of each cell population were cultured in triplicate in 200 μ l of complete medium in 96-well plates. To assess proliferation of TNFR2⁺ and TNFR2⁻ populations from saline- and LPS-treated mice, cells (5×10^4) were cultured in duplicate (Q2, CD25⁺TNFR2⁺), triplicate (Q1, CD25⁺TNFR2⁻ and Q4, CD25⁻TNFR2⁺), or quadruplicate (Q3, CD25⁻TNFR2⁻), depending on the number of cells recovered after sorting. For TNFR2⁺ Treg depletion assay, total CD25⁻ cells (Q3+Q4) were co-cultured with either CD25⁺TNFR2⁻ cells (Q1) alone or with total Tregs (Q1+Q2). All cultured cells were stimulated with plate-bound anti-CD3 (OKT3; 1 μ g/ml) and soluble anti-CD28 (2 μ g/ml) mAbs for 72 h. Cells were then pulsed with [³H]-thymidine (1 μ Ci/well, Perkin Elmer) for an additional 18 h. Incorporation of [³H]-thymidine was measured by liquid

scintillation counting. Data are presented as mean counts per min (cpm) and are shown for one of three separate experiments with similar results.

Measurement of BAL fluid and culture supernatant cytokines

The concentration of cytokines in BAL fluid (IL-2, IL-6, IL-10, IFN- γ , TNF, and IL-17) and culture supernatant (IL-2, IL-4, IL-10, IFN- γ) were detected by mouse Th1/Th2 10plex kit FlowCytomix (BMS820FF, eBioscience). Protocols were as specified in the manufacturer's instructions.

Statistical analysis

Data were analysed for normality and log-transformed as necessary prior to analysis by Student's *t* test or ANOVA with Bonferroni post tests, depending on the number of experimental groups. Spearman's correlations were used for the comparison of continuous variables. The Spearman's *r* value for the correlation between the two variables was stated in each result. Statistical analysis was performed using Graph Pad Prism v5.02 software. Group sizes are indicated in the figure legends. Data are expressed as mean \pm SEM. $p < 0.05$ was considered significant.

Results

Lung CD4⁺CD25⁺ cells from unmanipulated mice preferentially express Foxp3, TNFR2, and Ki67 and have impaired responses to TCR stimulation

To determine how LPS-induced ALI may potentially alter pulmonary Treg and Teff proliferation and activation status, we initially analysed the expression of TNFR2, Foxp3 and Ki67 on T cells in the lungs and lung-draining LN of unmanipulated mice. Analyses revealed that lung CD4⁺CD25⁺ cells (Treg) contain a significantly higher proportion of Foxp3⁺, TNFR2⁺ and Ki67⁺ cells than CD4⁺CD25⁻ cells (Teff) (Fig. 1A). Analyses of lung-draining LN also showed that the proportions of Foxp3⁺ and TNFR2⁺ cells as well as Ki67⁺ cells were significantly higher within CD4⁺CD25⁺ cells than CD4⁺CD25⁻ cells (data not shown). The increased proportion of Ki67⁺ cells within CD4⁺CD25⁺ Treg indicates that they are actively proliferating *in vivo*. We also further studied the capacity of Treg and Teff to respond to a *de novo* proliferative stimulus *in vitro*. Our results show that purified lung CD4⁺CD25⁺ cells isolated by flow cytometry had significantly decreased ability to respond to stimulation by anti-CD3 and anti-CD28 mAbs crosslinking than CD4⁺CD25⁻ cells (Fig. 1B). CD4⁺CD25⁺ cells did proliferate significantly after stimulation with the combination of anti-CD3 together with anti-CD28 mAbs, but not anti-CD3 alone (Fig. 1B). Analyses of culture supernatants from the above stimulated proliferation cultures showed that CD4⁺CD25⁻ cells produced significantly higher levels of IL-2, IL-4 and IFN- γ than CD4⁺CD25⁺ cells, consistent with an effector cell phenotype. No difference in IL-10 production was observed between CD4⁺CD25⁻ and CD4⁺CD25⁺ cells (Fig. 1C). There were no detectable cytokine levels in supernatants of cultures stimulated with anti-CD3 alone (data not shown). These results together

suggest that lung $CD4^+CD25^+$ cells meet the criteria for Treg, as shown by others (Walker, 2004).

LPS instillation causes lung inflammation and alters proportions of lung $CD3^+CD4^+$ T cells and Treg

In the previous study (Mohamud *et al.*, unpublished), we showed that both lung Treg and Teff contain $TNFR2^+$ fractions that are rapidly proliferating *in vitro* and *in vivo*. We hypothesised that an environmental insult such as LPS may alter lung homeostasis, modifying the capacity of $TNFR2^+$ cells to proliferate locally, thereby compromising the suppressive effect of $TNFR2^+$ Treg on Teff leading to the induction of airway inflammation. To test our hypothesis, we utilised a well-characterized model of LPS-induced airway inflammation. Instillation of low dose LPS (0.1 μ g) caused only mild airway inflammation, compared to the saline control group d3 post instillation as reflected in BAL cell counts, whereas administration of high dose LPS (10 μ g) caused acute airway inflammation peaking on d3 post LPS instillation [as reflected by total BAL cells counts (Suppl. Fig. 1)]. Thus, we focused our investigation on lung $TNFR2^+$ cells from 10 μ g LPS-induced ALI on d3. We first showed that LPS administration significantly increased lung total leukocyte numbers (Fig. 2A), and also caused a significant increase in total BAL cells, primarily neutrophils and lymphocytes (Fig. 2B). This inflammation was associated with a dramatic increase in pro-inflammatory BAL fluid cytokines compared to naïve and saline-treated mice (Fig. 2C). Although the frequency of $CD3^+CD4^+$ T cells among total lung leukocytes was decreased in LPS-treated mice, the percentage of $CD3^+CD4^+CD25^+$ cells was increased (Suppl. Fig. 2A, B). LPS instillation also increased the frequencies of $CD25^+TNFR2^+$, $CD25^+TNFR2^-$, $CD25^-TNFR2^+$ subpopulations, but decreased the frequency of $CD25^-TNFR2^-$ cells (Suppl. Fig. 2C). Increased frequencies

of lung Treg and other inflammatory cells during inflammation could be due to recruitment, proliferation, or a combination of these two factors (D'Alessio et al., 2009), and these possibilities are further examined below.

LPS instillation decreased proliferation of TNFR2⁺ cells (Treg and Teff) and decreased CCR7⁺ proportions of TNFR2⁻ Treg

Next, we examined local proliferative and migratory capacity of TNFR2⁺ cells to further understand how they maintained their proportions in the lung during inflammation. To investigate this, we analysed expression of Ki67 and CCR7, a chemokine receptor involved in homing of lung-derived cells to the lung-draining LN (Schneider et al., 2007). We found that the highest frequencies of proliferating cells (Ki67⁺) were seen in the CD25⁺TNFR2⁺ and CD25⁻TNFR2⁺ subsets in both saline- and LPS-treated groups (Fig. 2D). However, although proportions of CD25⁺TNFR2⁺ and CD25⁻TNFR2⁺ subsets increased after LPS instillation (Supp. Fig. 2C), the frequency of Ki67 expressing cells (within CD25⁺TNFR2⁺ and CD25⁻TNFR2⁺) was significantly lower than in the saline group (Fig. 2D). There were no differences in proportions of Ki67⁺ cells in either of the TNFR2⁻ subsets between saline- and LPS-treated mice (Fig. 2D). The frequency of Ki67⁺ cells among lung TNFR2⁺ cells in both saline and LPS groups correlated positively with *in vitro* proliferative capacity (Suppl. Fig. 3A). Moreover, the frequencies of TNFR2⁺ cells (either Treg or Teff) which expressed Ki67 were negatively correlated with lung inflammation (Suppl. Fig. 3B). LPS administration significantly decreased the frequency of CCR7⁺ lung CD25⁺TNFR2⁻ cells (Fig. 2D). The frequency of CCR7⁺ cells in the lung-draining LN was less than 2% for all gated TNFR2⁺ cells (data not shown). Together, these findings suggest the existence of a homeostatic mechanism to limit the size of the pool of Treg and Teff in the lung under inflammatory conditions.

LPS alters Foxp3 expression by CD25⁺ cells (TNFR2⁺ and TNFR2⁻ cells)

Previous studies have shown that LPS-induced ALI decreases Foxp3 expression by CD4⁺CD25⁺ T cells (D'Alessio et al., 2009, Lewkowicz et al., 2006). However, so far, there has been no investigation solely focusing on TNFR2⁺ Treg in this model. We hypothesised that LPS instillation may lead to decreased proportions of Foxp3⁺ expressing TNFR2⁺ Treg. The frequency of Foxp3⁺ cells in saline-treated mice was slightly higher in CD25⁺TNFR2⁺ cells than CD25⁺TNFR2⁻ cells (Fig. 2D), similar to the finding in unmanipulated mice (data not shown). By contrast, LPS administration consistently decreased the proportion of Foxp3⁺ cells by approximately 30-40% within the CD25⁺ fraction, regardless of TNFR2 expression (Fig. 2D). Moreover, proportions of Foxp3 expressing CD25⁺ cells whether TNFR2⁺ or TNFR2⁻ cells, were negatively correlated with lung inflammation (Suppl. Fig. 3C) consistent with the idea that CD25⁺ Foxp3⁺ cells inhibit lung inflammation. As expected, CD25⁻TNFR2⁻ cells expressed Foxp3 at the lowest levels, both in the LPS and control groups (Fig. 2D).

TNFR2⁺ Treg proliferate more than TNFR2⁻ Treg and are required for maximal suppressive capacity

Recent studies in peripheral tissues have shown that TNFR2-expressing mouse Treg are maximally suppressive (Chen and Oppenheim, 2010), highly proliferative (van der Most et al., 2009) and rarely produce pro-inflammatory cytokines (Herrath et al., 2011). Similarly, our data show that the proliferative capacity of flow sorted TNFR2⁺ cells from the lungs of saline-treated mice (Fig. 3A) was similar to that seen in unmanipulated mice (data not shown). Consistent with a suppressor phenotype, proliferation of total CD25⁻ cells (TNFR2⁺ and TNFR2⁻ cells) in response to combinations of anti-CD3 and anti-CD28 mAbs was significantly suppressed by addition of TNFR2⁻ Treg (Fig. 3B) and this

suppression was further increased by addition of TNFR2⁺ Treg, showing that both populations are suppressive and can act together to maintain homeostasis (Fig. 3B). Reassuringly, IL-2 levels in the cell culture supernatants reflected suppressor activity patterns of these cells (Fig. 3C). We hypothesised that decreases in proliferative capacity and Foxp3 expression (Fig. 2D) by TNFR2⁺ Treg would compromise the ability of TNFR2⁺ Treg to maintain lung homeostasis and that this would not be compensated by the activity of TNFR2⁻ Treg. Surprisingly, despite decreased Ki67⁺ proportions compared to the saline control group (Fig. 2D), proliferation of flow sorted TNFR2⁺ Treg and other cell populations from LPS-treated mice (Fig. 3D) was similar to that for unmanipulated (data not shown) and saline-treated mice (Fig. 3A). We therefore investigated the effects of LPS on the ability of TNFR2⁺ Treg to suppress proliferation of CD25⁻ cells (both TNFR2⁺ and TNFR2⁻) in response to combinations of anti-CD3 and anti-CD28 mAbs. TNFR2⁻ Treg alone or in combination with TNFR2⁺ Treg (all Treg) in the LPS group failed to suppress proliferation of total CD25⁻ cells (Fig. 3E), suggesting that the suppressive capacity of Treg was reduced after LPS challenge. In contrast to saline-treated mice, there was no difference in IL-2 secretion between any of these groups (data not shown).

TNFR2⁺ Treg from LPS-treated mice have lower percentages of CTLA-4⁺, Helios⁺ and LAP⁺GARP⁺ cells

To gain insight into the reason why lung TNFR2⁺ Treg may lose their suppressive activity, we analysed expression of the functional markers associated with suppressive capacity. A recent study showed that antagonising TNF with the anti-human TNF Ab (infliximab) increased the Treg frequency and upregulated CTLA-4, leading to enhancement of suppressor activity (Biton et al., 2011). Another study showed that only

proliferating Treg maintained Foxp3 expression and co-expressed Helios, while non-dividing Treg rapidly lost Foxp3 and Helios expression (Akimova et al., 2011). Concomitantly, in saline-treated mice, we found that CTLA-4 and Helios were expressed at the highest frequency by TNFR2⁺ Treg, with CD25⁻TNFR2⁻ cells expressing the lowest frequency of these functional markers (Fig. 4A). As expected, we found that the percentages of CTLA-4⁺ cells among TNFR2⁺ Treg were slightly decreased after LPS administration, but percentages of CTLA-4⁺ in other populations were unchanged (Fig. 4A). Interestingly, the frequency of Helios⁺ cells was halved after LPS administration in TNFR2⁺ cells (both CD25⁺ and CD25⁻). Another molecule that is important in controlling Treg suppressive function is the co-stimulatory molecule glucocorticoid-induced TNF receptor (GITR) (McHugh et al., 2002). Consistent with this, TNFR2⁺ Treg contained the highest proportion of GITR-expressing cells. However, frequencies of GITR⁺ cells were not significantly altered in LPS-treated mice (Fig. 4A). Treg functionality is strongly related to TGF- β signaling (Liu et al., 2008, Marie et al., 2005, Bettelli et al., 2006, Dardalhon et al., 2008), as TGF- β directly controls Treg activation and proliferation status (Li et al., 2006). GARP (glycoprotein-A repetitions predominant) is a receptor for TGF- β expressed on activated Treg that directly binds to TGF- β latency-associated peptide (LAP) and GARP expression is strongly correlated with LAP expression (Battaglia and Roncarolo, 2009, Oida and Weiner, 2010). Treg expressing GARP have greater suppressive function than Treg which do not express GARP (Fan et al., 2012). The ecto-apyrase CD39 and ecto-5'-nucleotidase CD73 are expressed on Treg and distinguish Treg from other CD4⁺ T cell populations (Deaglio et al., 2007). It has been shown that enzymatic activity of CD39 and CD73 expressed on Treg is crucial for the suppressive effect of Treg (Borsellino et al., 2007). Interestingly, our analyses showed that TNFR2⁺ Treg contain a higher proportion of cells expressing LAP, GARP, CD39 and

CD73 than TNFR2⁻ Treg. The proportions of double positive CD39⁺CD73⁺ cells were unchanged after LPS administration but interestingly, LAP⁺GARP⁺ percentages were decreased at least 10-fold in all cell populations examined (Fig. 4B). Overall, the changes in the expression of functional Treg markers after LPS administration are consistent with a molecular basis for the observed compromised Treg suppressive capacity.

Discussion

This study characterises for the first time TNFR2⁺ Treg in the lung comparatively during homeostasis and during an acute inflammatory response. Our data show that at homeostasis, about 1 to 2 % of lung CD3⁺CD4⁺ T cells that express CD25 co-express TNFR2, and show evidence of having recently proliferated *in vivo* (as assessed by expression of Ki67). Moreover, lung TNFR2⁺ Treg and TNFR2⁻ Treg suppressed the proliferation of Teff and this suppressive activity was significantly reduced after LPS challenge. Mechanistically this correlated with decreased expression of key transcription factors (Foxp3, Helios) and surface molecules associated with suppressive capacity (CTLA-4, LAP, and GARP).

Studies in a co-transfer model with disease-inducing T cells have shown that Treg actively proliferate *in vivo* (Walker et al., 2003, Klein et al., 2003). A recent study showed that the expression of TNFR2 on the cell surface is related to the expansion of Treg (Chen et al., 2010a) and enabled Teff to expand despite the presence of Treg (Chen et al., 2007). In agreement with this, we observed that *in vitro* proliferative capacity of TNFR2⁺ cells (both Treg and Teff) positively correlated with Ki67⁺ expression. This is an important finding showing that during the steady state in the lung, both TNFR2⁺ Treg and TNFR2⁺ Teff are proliferating, presumably maintaining a balance between tolerance and immunity and thereby maintaining lung homeostasis. Our study also shows that in the steady state, lung TNFR2⁻ Treg are suppressive, and that their combination with TNFR2⁺ Treg maximised the suppressive activity. As TNFR2⁺ Treg represent less than 2 % of total CD4⁺ T cells in the lung, we were unable to show that sort-purified TNFR2⁺ Treg are more suppressive than TNFR2⁻ Tregs due to limited cell numbers. However, a study using CD4⁺Foxp3/gfp⁺ cells from spleen and LN (inguinal, axillary, and mesenteric

regions) of C57BL/6 mice showed that TNFR2⁺ Treg are more suppressive than the corresponding TNFR2⁻ Treg population (Chen et al., 2008, Chen et al., 2010a), consistent with our recent findings (Mohamud *et al.*, in preparation). In support of this, a recent study in adults with severe malaria revealed that TNFR2⁺Foxp3^{hi} Treg induced by *P.falciparum*-infected red blood cells had greater suppressive activity than TNFR2⁻ Treg (Minigo et al., 2009). In agreement with this, it was recently shown that successful chemotherapy in a mouse model was achieved after depleting Foxp3⁺TNFR2^{hi} cells, which were highly proliferative *in vivo* (van der Most et al., 2009). It was further shown that the cycling Ki67^{hi} cells are the active suppressors that respond to antigen by increasing their suppressive function (van der Most et al., 2009).

TNF signaling through TNFR2 increases Treg *in vitro* suppressive function (Chen et al., 2007) and promotes Treg survival (Ware, 2008). The findings of our study and others (Chen et al., 2010a) show that TNFR2 expression on Treg is positively correlated with Ki67 expression. Thus, TNFR2 expression by Treg might be a crucial mechanism for Treg in the lung to maintain their proportions and functions, especially during acute inflammatory episodes. Furthermore, a recent study showed a reduced ability of TNFR2-deficient Treg to prevent colitis *in vivo* demonstrating a critical role for TNFR2 expression on Treg (Housley et al., 2011). Given that TNF secretion is higher at sites of inflammation than in lymphoid organs, the findings of Housley *et al.* suggest that natural Treg are initially activated locally at sites of inflammation, whereas adaptive Treg are activated and generated in LN (Housley et al., 2011). Several groups have found that Treg do not require TNF for maintenance of immune homeostasis under steady state conditions, but rather require TNF to “boost” Treg function in the context of autoimmunity (Housley et al., 2011, Grinberg-Bleyer et al., 2010). In broad agreement

with these studies, we found that TNF secretion in the BAL fluid was undetectable in the steady state (naïve and saline treated mice), but that TNFR2⁺ Treg nevertheless suppressed *in vitro* proliferation of Teff. This finding suggests that functional (i.e. suppressive) TNFR2⁺ and TNFR2⁻ Treg populations can be maintained in the lung under steady state conditions in the absence of TNF signaling.

TNFR2⁺ Treg and TNFR2⁺ Teff proportions were markedly increased in LPS-treated mice. These increased proportions are likely due to the increase in BAL fluid TNF levels following LPS instillation, similar to findings by Chen *et al.* on tumor-infiltrating lymphocytes (Chen et al., 2010a). We suggest that TNFR2⁺ Teff are profoundly involved in the pathogenesis of ALI compared to TNFR2⁻ Teff as TNFR2⁺ Teff directly interact with TNF that lead to their expansion. This is consistent with the increased and decreased of TNFR2⁺ Teff and TNFR2⁻ Teff, respectively. Pro-inflammatory cytokines produced at sites of inflammation might also affect the generation of Treg and inhibit the function of previously existing Treg (Awasthi et al., 2008). We demonstrated that LPS treatment increased levels of IL-17 in the BAL fluid, suggesting that Th17 cells are enriched at the inflammation site and might play a role in driving airway inflammation, as showed previously in neutrophilic inflammation (Laan et al., 1999). IL-17 does not directly activate the differentiation and expansion of Th17 cells, rather, synergistic activation by IL-6 and TGF- β lead to Th17 cell differentiation (Bettelli et al., 2006, Awasthi et al., 2008). In our LPS model, we found that IL-6 levels in BAL fluid are also increased. IL-6 production at sites of inflammation inhibits the induction of Foxp3 and generation of Treg (Awasthi et al., 2008), and stimulation of Treg in the presence of IL-6 results in loss of Foxp3 expression and acquisition of a Th17 phenotype (Zheng et al., 2008, Xu et al., 2007). Similarly, IL-6 secretion via activation of the TLR-9 on antigen presenting cells

was shown to block the suppressive effect of Treg on Teff activation (Pasare and Medzhitov, 2003). Interestingly, IL-6 not only directly affects Treg, but also has an ability to render Teff resistant to Treg-mediated suppression (Pasare and Medzhitov, 2003). Thus, the observed LPS-induced induction of IL-6 and TNF in the lung might antagonise lung TNFR2⁺ Treg suppressive function, consistent with our findings.

Overall, our study suggests a critical central role for TNFR2⁺ Treg in maintaining pulmonary immune homeostasis, given their ability to proliferate locally to maintain cell numbers, and their ability to suppress immunity. We showed that the suppressive capacity of TNFR2⁺ Treg is turned off by LPS, a common component of gram-negative bacteria, suggesting this capacity may lead to uncontrolled inflammatory reactions, consistent with ALI, and as showed by others (D'Alessio et al., 2009, Aggarwal et al., 2009) that Treg are central in orchestrating a complex series of events to mediate resolution of ALI. As this is the first study of TNFR2⁺ Treg in the ALI mouse model, our findings open the door for further studies by highlighting the complex and vital relationship between TNFR2⁺ Treg and inflammation. We suggest that boosting TNFR2⁺ Treg function (e.g. by increase the proliferative capacity) in the lung might offer alternative approaches to treat patients with inflammatory lung disease, such as ALI which there are no specific therapies currently available.

Acknowledgments

We gratefully acknowledge the expert assistance of Geza Paukovics with flow cytometry.

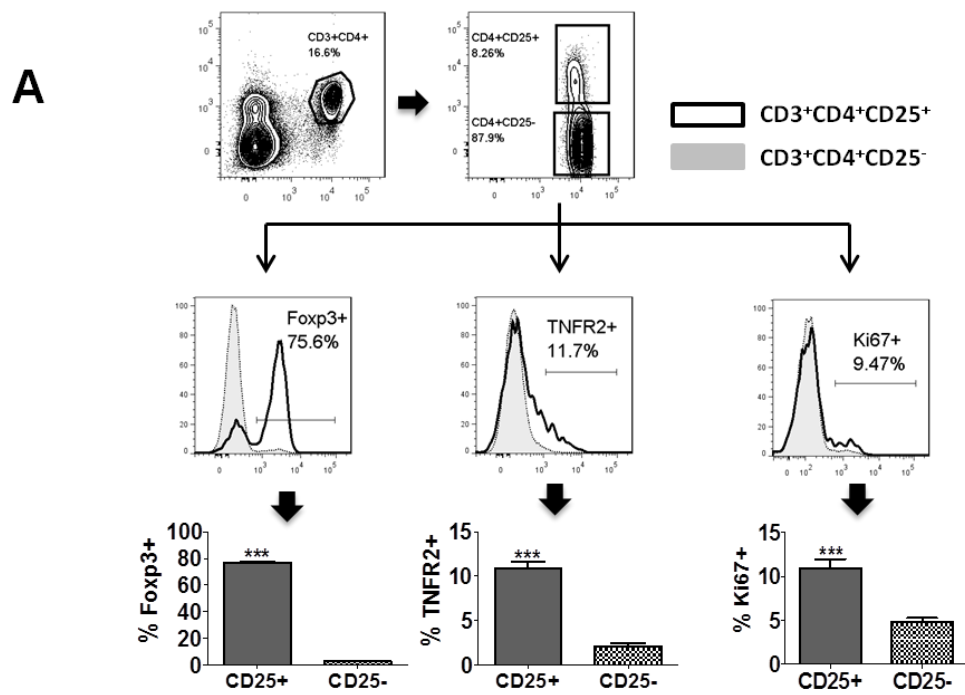
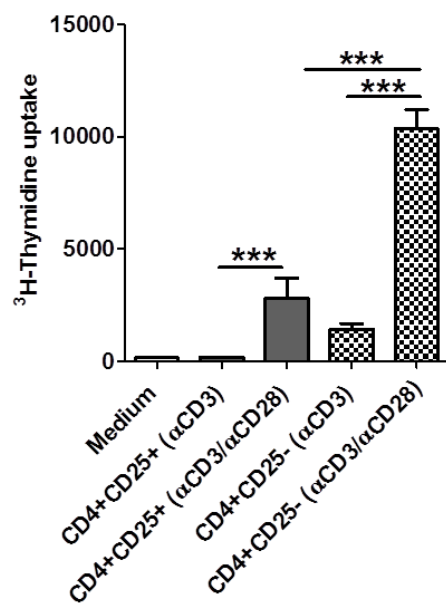
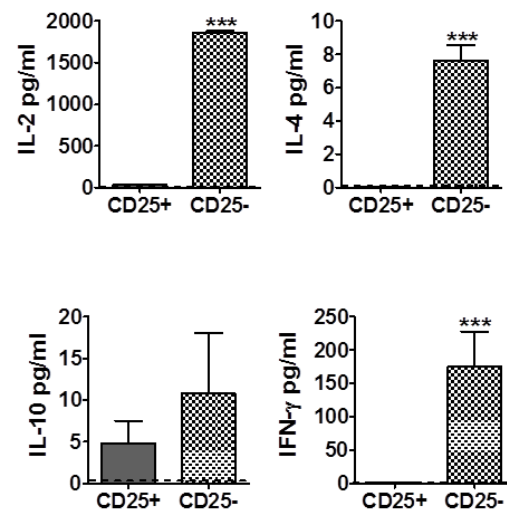
**B****C**

Figure 1: CD4⁺CD25⁺ cells from the lung of unmanipulated mice express more Foxp3, TNFR2 and Ki67, do not proliferate *in vitro* and secrete less cytokines than CD4⁺CD25⁻ cells. Lung leukocytes were isolated by collagenase/DNAse digestion and gated on viable CD3⁺CD4⁺CD25⁺ or CD25⁻ T cells. **(A)** Plots show Foxp3⁺, TNFR2⁺ and Ki67⁺ expression and percentages of positive cells by CD4⁺CD25⁺ (black line, open histogram) and CD4⁺CD25⁻ (grey line, filled histogram) cells. **(B)** Proliferation of FACS sorted CD4⁺CD25⁺ and CD4⁺CD25⁻ cells stimulated with anti-CD3 alone or combinations of anti-CD3 and anti-CD28 mAbs. **(C)** IL-2, IL-4, IL-10 and IFN- γ concentrations in culture supernatant from CD4⁺CD25⁺ and CD4⁺CD25⁻ cell stimulated with combinations of anti-CD3 and anti-CD28 mAbs. Dashed line denotes below limit of detection. Data are representative of 3 experiments. Mean \pm SEM, n=3-6. ***p<0.001.

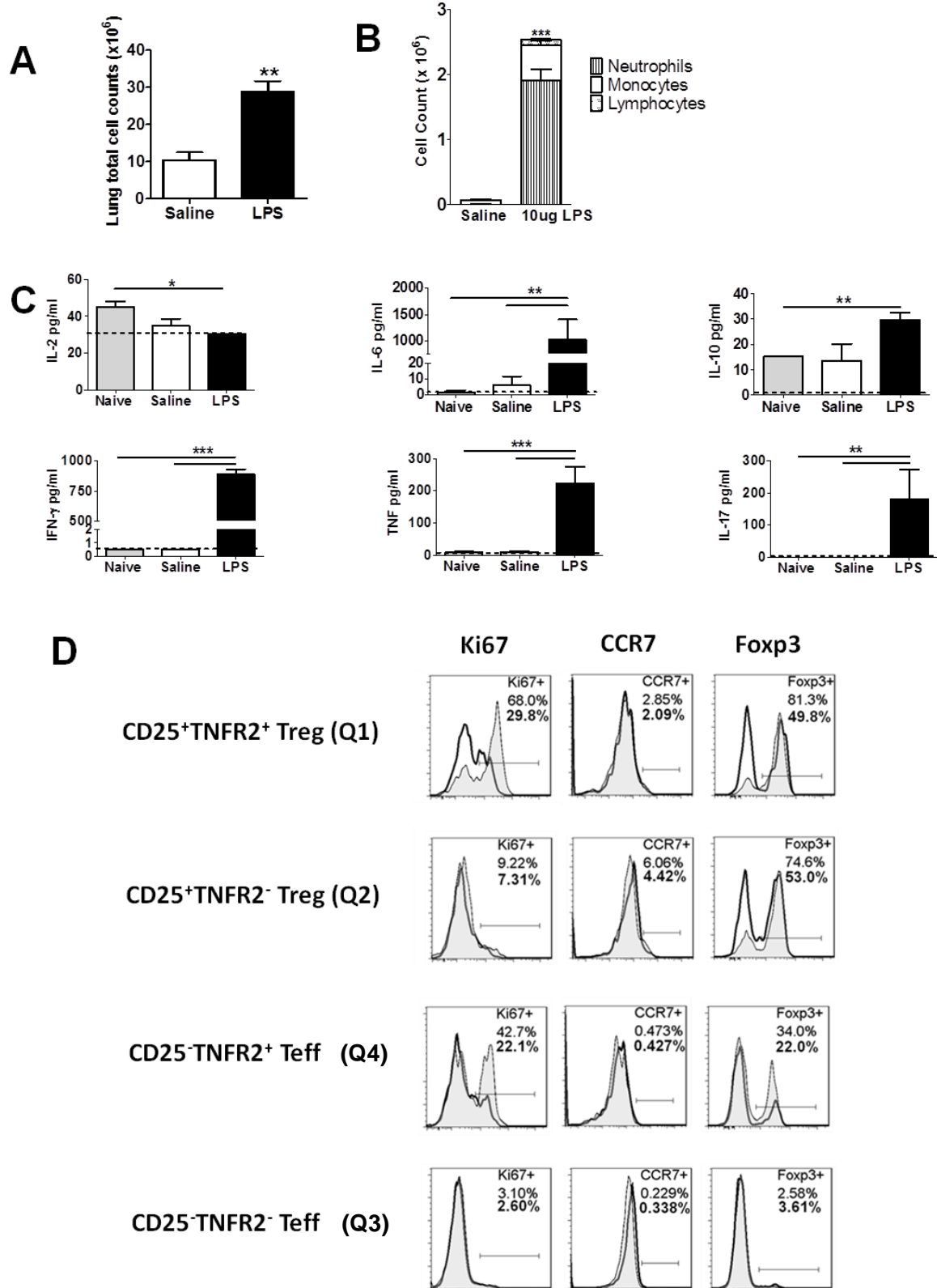


Figure 2: LPS administration induces airway inflammation, alters proinflammatory cytokines and modulates proportions of Ki67⁺, CCR7⁺ and Foxp3⁺ TNFR2 populations. Mice received saline or 10 µg LPS intratracheally and samples were collected 3 days later. **(A)** Viable cells recovered from lung homogenate. **(B)** Differential analysis of BAL cells. **(C)** Concentration of BAL fluid cytokines. **(D)** Expression of Ki67, CCR7 and Foxp3 on TNFR2 populations in saline (grey line, filled histogram) and LPS group (black line, open histogram). Percentages of positive populations for saline and LPS groups (bold) are shown. Dashed line denotes lower limit of detection. Mean ± SEM. n=5-7. *p<0.05, **p<0.01, and ***p<0.001. Data are representative of more than 3 experiments.

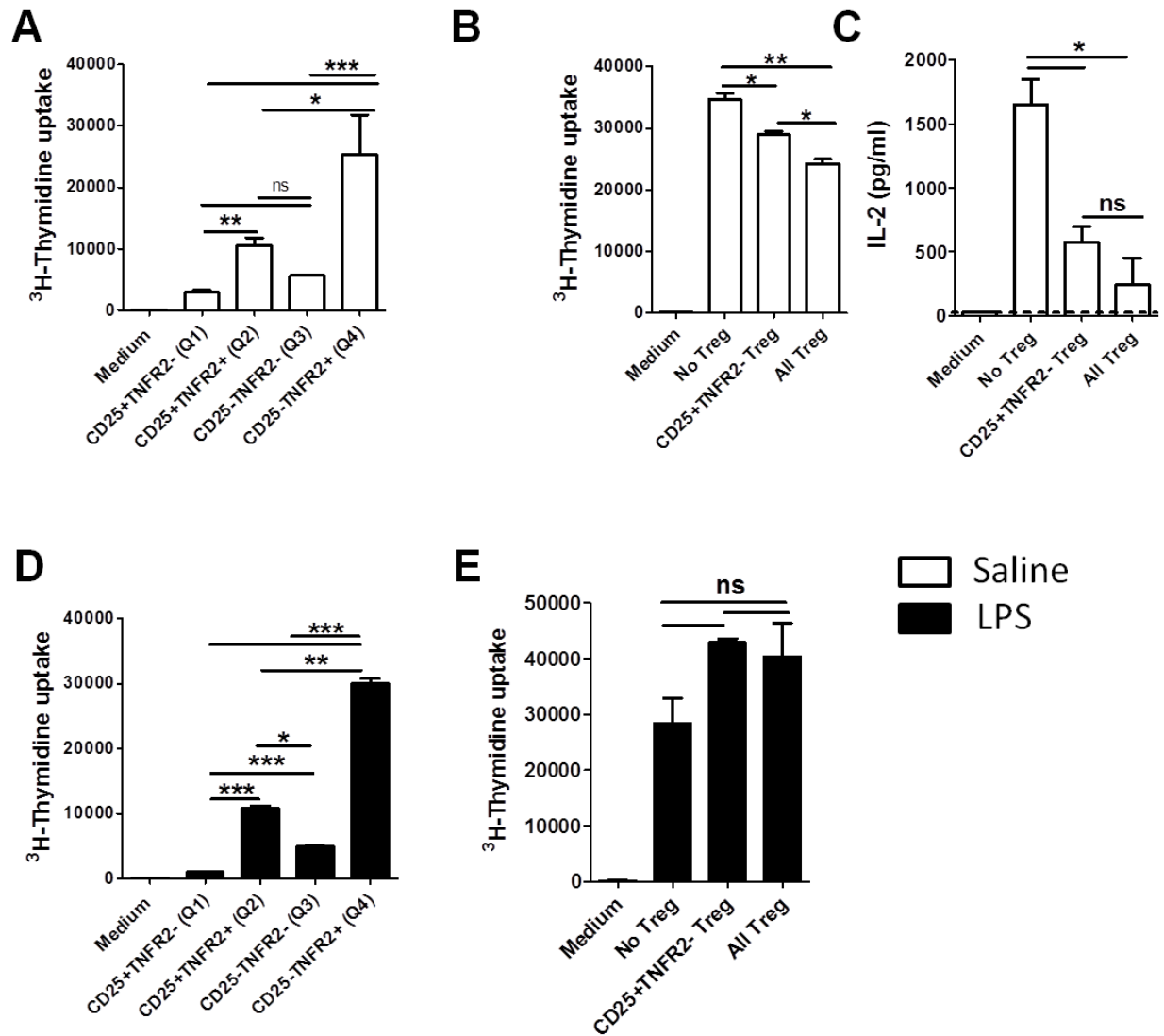


Figure 3: TNFR2 populations in saline and LPS treated mice exert similar proliferative capacity, but Treg from LPS treated mice fail to suppress proliferation of CD25⁻ Teff. Proliferation of FACS sorted TNFR2 populations cultured with/without TNFR2⁺ Treg stimulated with the combination of anti-CD3 and anti-CD28 mAbs. **(A, D)** Proliferation of FACS sorted TNFR2 populations (Q1, Q2, Q3 and Q4). **(B, E)** Treg depletion assay. Total CD25⁻ cells (Q3+Q4) were co-cultured with either CD25⁺TNFR2⁻ (Q1) alone or with total Treg (Q1+Q2). **(C)** IL-2 secretions in cells culture supernatants of saline treated mice. Dashed line denotes lower limit of detection. Mean \pm SEM. n=2-4, 5 x 10⁴ cells/well. *p<0.05, **p<0.01, and ***p<0.001; ns= not significant. Data are representative of 3 experiments.

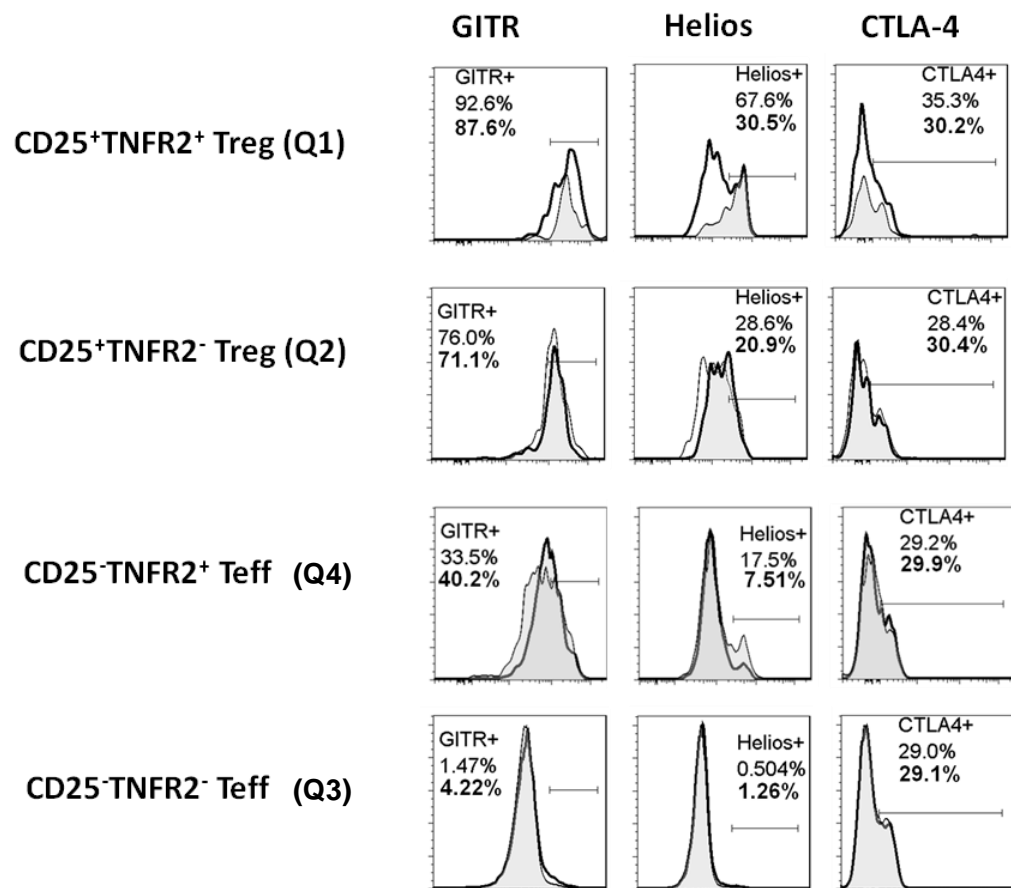
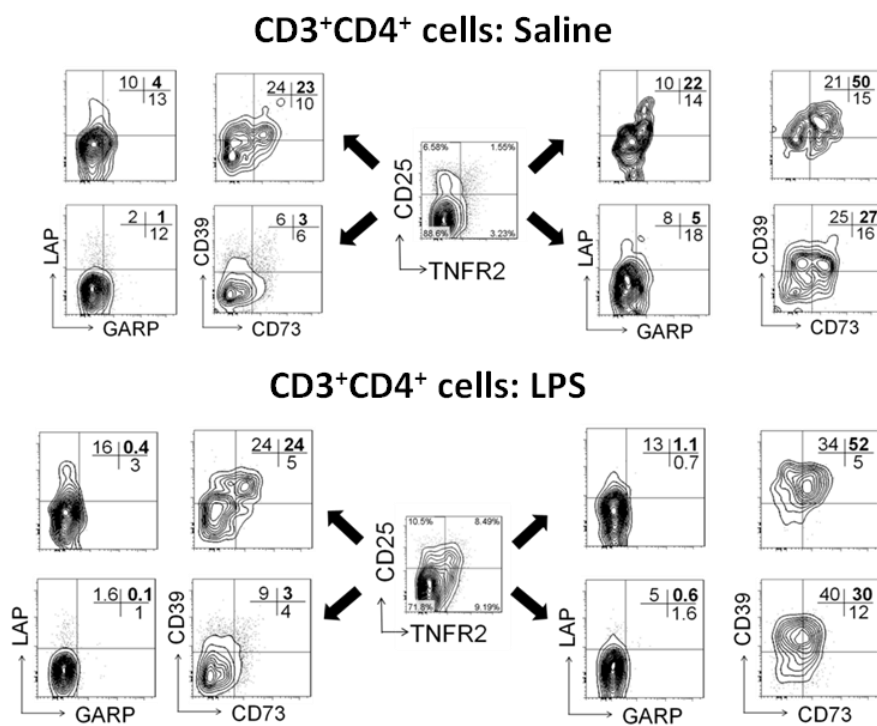
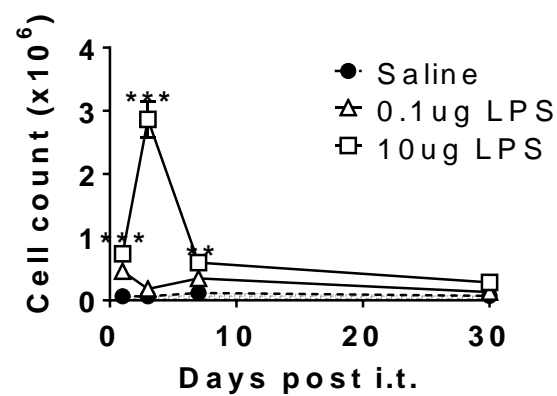
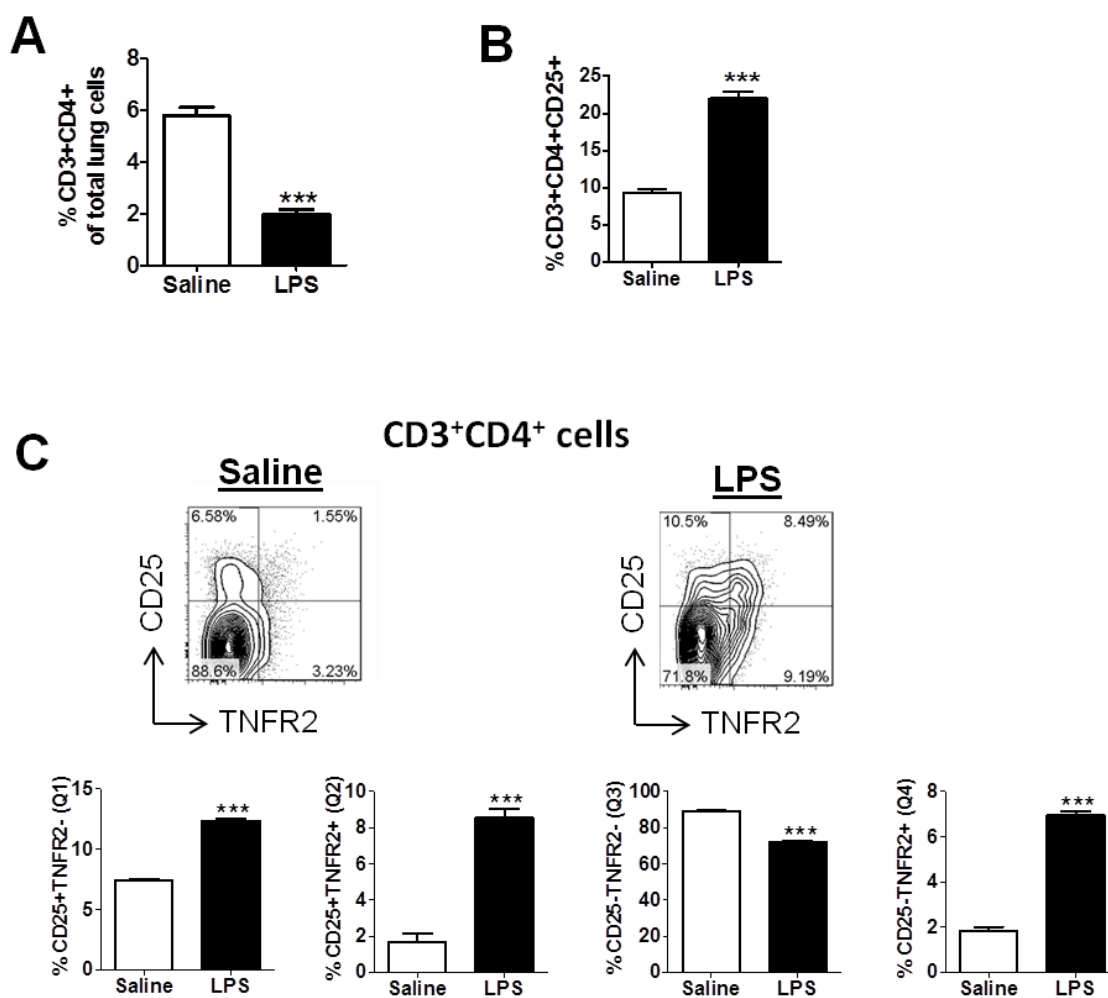
A**B**

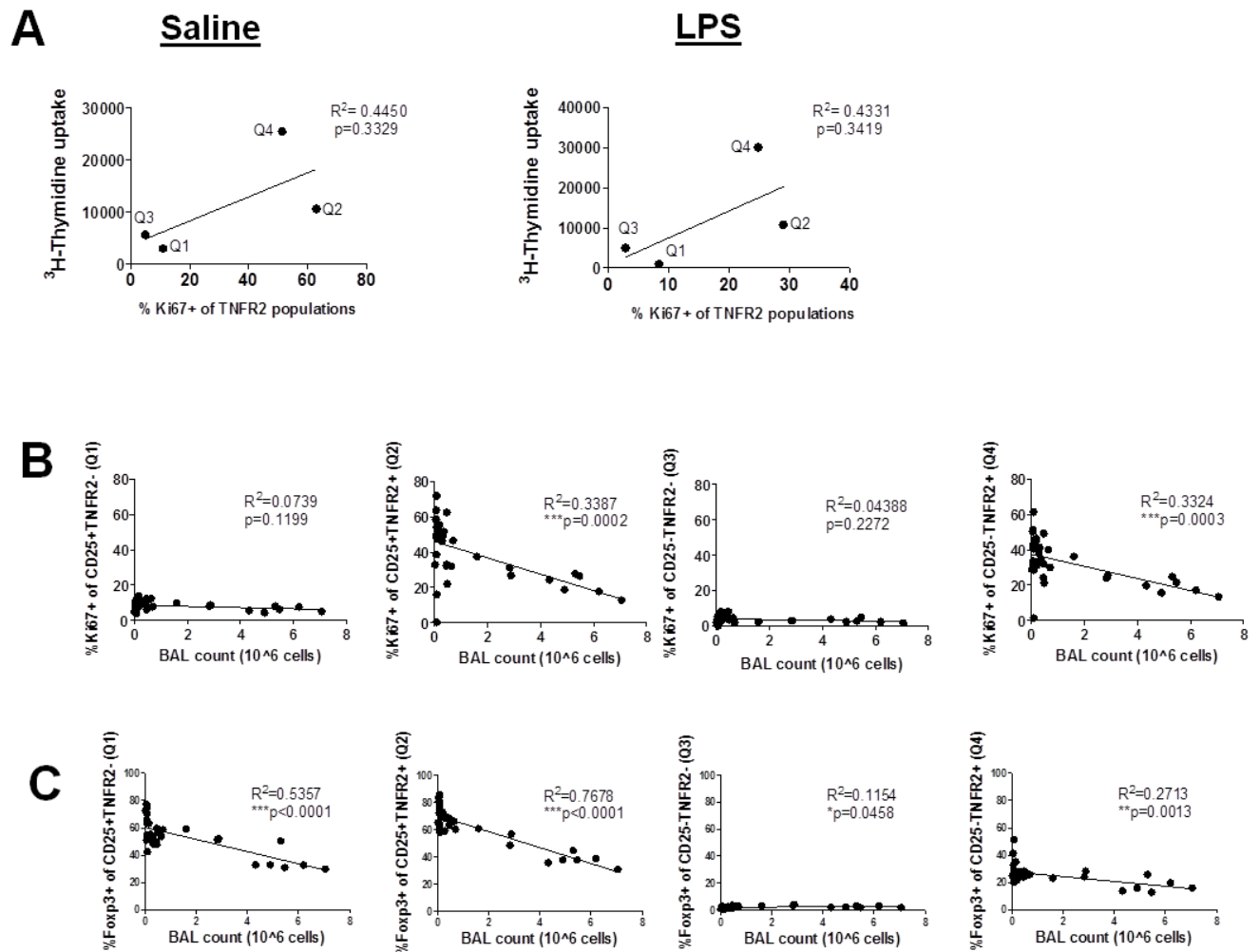
Figure 4: LPS alters the percentages of CTLA-4⁺, Helios⁺ and LAP⁺GARP⁺ cells within TNFR2 populations. (A) CD3⁺CD4⁺ T cells were gated as shown in Fig. 1, followed by gating on co-expression of CD25 and TNFR2. Expression of GITR, Helios and CTLA-4 and (B) LAP/GARP and CD39/CD73 cells within TNFR2 subpopulations in saline (grey line, filled histogram) and LPS group (black line, open histogram). Percentages of double-positive populations for saline and LPS groups (bold) are shown. Data are representative of more than 3 experiments.



Suppl. Fig. 1: High dose LPS (10 μ g) instillation caused acute airway inflammation that peaked on d3, whereas low dose LPS (0.1 μ g) caused only mild-airway inflammation compared to saline treated mice. Mice were intratracheally administered with saline, 0.1 μ g or 10 μ g LPS and samples were collected on d1, d3, d7 and d30. Viable cells recovered from BAL fluid. Mean \pm SEM. n=5-12. **p<0.01, and ***p<0.001.



Suppl. Fig. 2: LPS instillation decreased the proportions of CD3⁺CD4⁺ T cells but increased CD3⁺CD4⁺CD25⁺ Treg and TNFR2⁺ cell populations in the lung, whilst CD25⁻TNFR2⁻ cells decreased. Mice were intratracheally administered with either saline or 10 μ g LPS and samples were collected on d3. **(A)** Percentages of CD3⁺CD4⁺ T cells of total live cells, **(B)** percentages of CD4⁺CD25⁺ and **(C)** TNFR2 populations of CD3⁺CD4⁺ T cells. Mean \pm SEM. *** p <0.001. Data are representative of more than 3 experiments.



Suppl. Fig. 3: Percentages of Ki67⁺ cells in saline and LPS groups positively correlated with *in vitro* proliferation, whereas Ki67⁺ and Foxp3⁺ percentages negatively correlated with lung inflammation. (A) Proliferation of FACS sorted TNFR2 populations stimulated with combinations of anti-CD3 and anti-CD28 mAbs. Correlation of Ki67 expression with *in vitro* proliferation in saline and LPS treated mice (left and right panel, respectively). (B, C) Correlation of Ki67 and Foxp3 gated of TNFR2 populations with lung inflammation. Data are representative of 3 experiments.

6.2 Summary

This chapter shows that at lung homeostasis, lung TNFR2⁺ Treg proliferate locally (in the lung) to maintain cell numbers and have suppressor activity. The suppressive capacity of TNFR2⁺ Treg is turned off by LPS at the peak of inflammation, which may permit enhanced inflammatory reactions to occur, and potentially result in lung injury.

-This page intentionally left blank-

Chapter 7

General Discussion

7.1 Introduction

The immune system in the lung employs numerous mechanisms to maintain immunologic self-tolerance and to protect the host against exacerbated responses to diverse environmental stimuli. The existence of Treg that actively suppress the function of Teff is a key mechanism by which the immune system limits inappropriate or excessive inflammatory responses. In this project, the effects of an endogenous biological factor (follistatin) and external environmental stimuli (LPS and PS50G) in controlling allergic airway inflammation and acute lung injury were investigated in mouse models, to gain insight into their potential modulation of lung Treg frequencies and function, and explore the possible development of new therapeutic agents that target lung Treg that preferentially express the TNFR2.

7.2 Main outcomes of this thesis

The results in my thesis suggest that Treg quality (i.e. suppressive potential and proliferative capacity) and abundance are important in the maintenance of lung homeostasis, and treatments with follistatin (Chapter 3) and PS50G (Chapter 5) increased the numbers and/or suppressive capacity of Treg. Foxp3 expression and ratios of Treg/Teff decreased during airway inflammation (Chapter 3, 4 and 5) and lung injury (Chapter 6). Furthermore, the suppressive function of Treg was turned off during the peak of lung injury (Chapter 6). As the numbers of Treg are tightly regulated by the expression of TNFR2, which drives the proliferative expansion capacity of TNFR2 expressing Treg (Chen et al., 2007), Chapter 4, 5 and 6 further studied the involvement of TNFR2 expressing Treg in lung homeostasis. In comparison to inflamed lung (e.g. LPS-induced ALI and allergen-induced AAI), at lung homeostasis, CD25⁺TNFR2⁺ Treg and

CD25⁺TNFR2⁻ Treg inhibited CD4⁺CD25⁻ Teff and exhibited a higher level of Treg/Teff ratio, whilst, decreased Treg/Teff ratios were associated with imbalanced immune responses, i.e. the induction of AAI. This relative deficit in Treg numbers was paralleled by a failure to control secretions of pro-inflammatory cytokines in the lung such as IL-4 and IL-5 (Chapter 4 and 5) and IL-17 and IL-6 (Chapter 6). Treatment with PS50G increased the quality (i.e. suppressive potential and proliferative capacity) and quantity of TNFR2 expressing Treg and inhibited the subsequent development of allergic asthma (Chapter 5). Furthermore, the results in Chapter 6 showed that the suppressive capacity of TNFR2 expressing Treg was turned off by instillation of LPS suggesting this may have led to the observed uncontrolled inflammatory reactions. These results together demonstrate that Treg, preferentially TNFR2 expressing Treg, frequencies and function in the lung can be affected dramatically by encounter with diverse stimuli that can be found in the lung microenvironment, such as bacterial products and environmental particles.

Overall, the results presented in this study support all my hypotheses (as outlined in Section 1.9, Chapter 1). Experimental questions, hypotheses and findings of this thesis are summarised in Figure 7.1. It remains to be determined to what extent my findings on TNFR2 expressing Treg as a biological therapy to maintain and restore lung immune homeostasis will be applicable and/or translate to humans. Future studies will be necessary to fill gaps in this thesis by providing details on the capacity of lung stimuli (e.g. PS50G) in inducing functional TNFR2 expressing Treg and the efficacy of these cells in reverting active diseases *in vivo* (i.e. to suppress airways inflammation). However, it would not be possible to address these gaps by adoptive transferring freshly

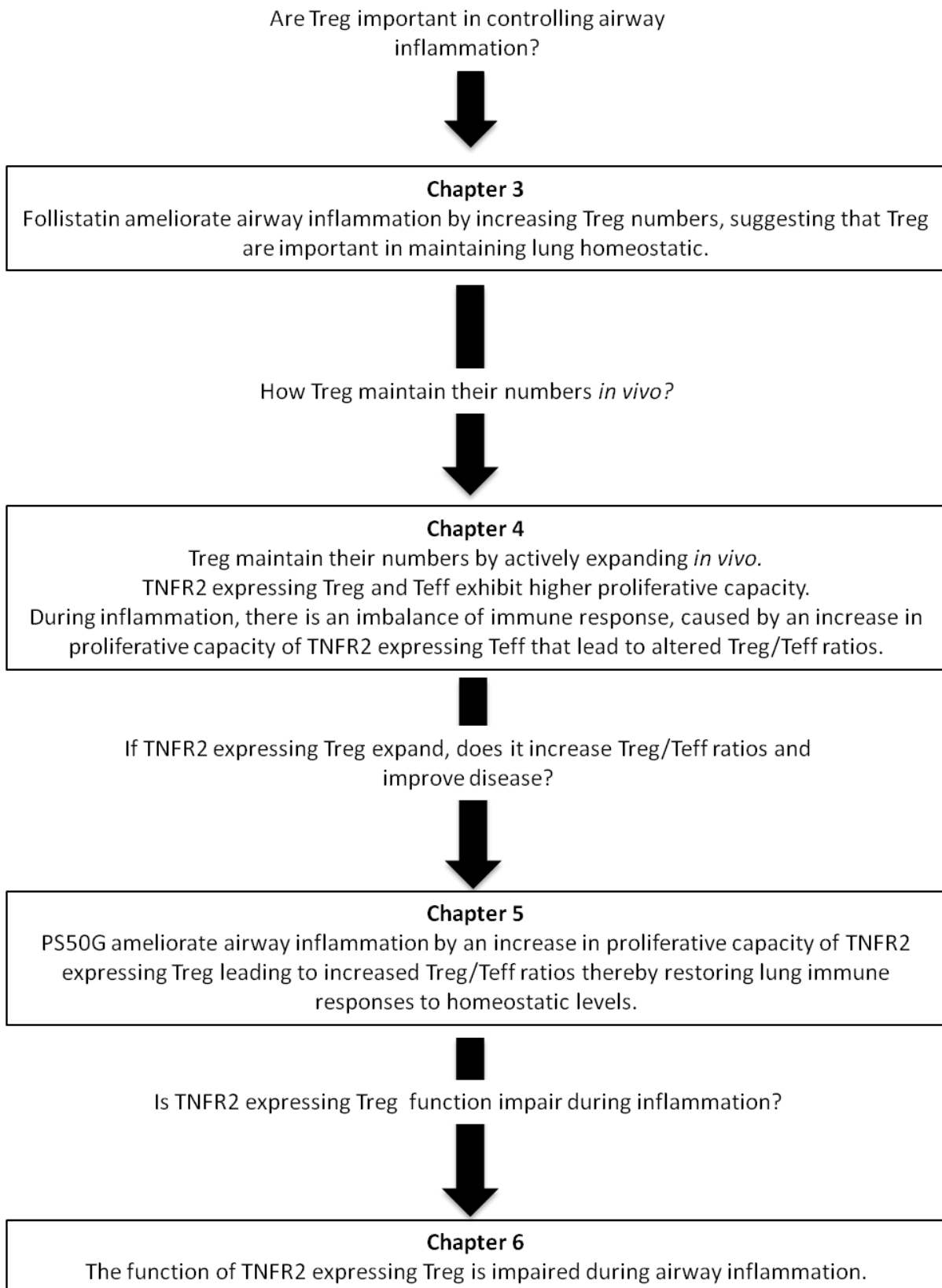


Figure 7.1: Main outcomes of this thesis.

isolated TNFR2 expressing Treg into allergen-challenged or LPS-induced ALI mouse models, the major hurdle being their very low numbers, especially in the lung (there are only 1-2 % TNFR2 expressing Treg of 10-15 % lung CD3⁺CD4⁺ T cells). One possible method is to isolate/select, expand and/or generate TNFR2 expressing Treg *in vitro* and transfer into disease models; though it is unclear whether the characteristics of these cells (i.e. the phenotype, expansion capacity and their regulatory properties) would accurately reflect that found *in vivo*. Therefore, these obstacles have to be overcome before TNFR2 expressing Treg can enter clinical practice as a biological therapy, especially for lung therapeutics.

7.3 The importance of Treg in the lung

Treg are responsible for controlling responses to allergens and/or lung infections while also maintaining peripheral tolerance by suppressing potential autoimmune responses to self-antigen. As shown in Chapter 3, Foxp3 expression levels within CD4⁺CD25⁺ Treg, in healthy mice, were higher than those in inflamed mice, whilst in Chapter 6, the data demonstrated that the suppressive capacity of CD25⁺TNFR2⁺ Treg and CD25⁺TNFR2⁻ Treg was turned off during the peak of acute lung injury. These results are in broad agreement with other studies, which demonstrate the importance of Treg during airway inflammation and in the maintenance of lung homeostasis (Aggarwal et al., 2009, D'Alessio et al., 2009). In healthy individuals, Treg play an essential role in modulating and regulating immune responses by promoting tolerance, counter-balancing aggressive inflammatory reactions, maintaining and restoring homeostasis (Thorburn and Hansbro, 2010). This thesis further suggests for the first time that TNFR2 expressing Treg and Teff play a significant role in maintaining lung homeostasis and driving lung inflammatory responses, respectively. An increase in expansion capacity of TNFR2 expressing Teff was

associated with an imbalance of the lung immune system, leading to altered Treg/Teff ratios and lung inflammatory responses. Data from this thesis suggest that Treg/Teff ratios are corrected by the expansion of TNFR2 expressing Treg restoring lung immune responses to homeostatic levels.

7.3.1 Treg mechanisms in maintaining lung homeostasis

The effector function of T helper cells, including Th2 (e.g. Chapter 4; as reflected by high levels of BAL IL-4, IL-5 and IL-13 cytokines) that are involved in allergic asthma is tightly regulated by Treg (Burchell et al., 2009). Therefore, Treg need to maintain their pool size, to ensure protection and maintain homeostatic suppression of Teff. As shown in Chapter 3, administration of follistatin at high dose increased the percentages of CD4⁺CD25⁺ Treg in the lung-draining LN and retained a higher Foxp3 expression concomitant with inhibition of the development of Th2-driven allergic asthma. This result is in agreement with Tian *et al.* who showed that the size of the Treg pool is critical for maintaining immunological balance; even relatively minor modulation of Treg numbers alters immunity (Tian et al., 2011). This further suggests that the Treg pool size can be modified to ensure protection from such diseases. In addition to the conversion of Foxp3⁻ Teff to Foxp3⁺ Treg (Chen et al., 2003b, Kim et al., 2010, Huber et al., 2009), Treg also maintain their cell numbers by actively proliferating *in vivo* (Lu et al., 2011, Pierson et al., 2013, Liston and Rudensky, 2007). Although previous studies showed that Treg are anergic (Gavin et al., 2002, Takahashi et al., 1998), a recent study has shown that during homeostatic conditions, Treg proliferate at a substantially faster rate than conventional T cells (CD4⁺ or CD8⁺) to drive rapid restoration of Treg cell numbers *in vivo* (Pierson et al., 2013). In this regards, as demonstrated in Chapter 4, 5 and 6, Treg proliferate *in vivo* and this is only true for the TNFR2⁺Foxp3⁺ Treg subset, not TNFR2⁻Foxp3⁺ Treg.

However, Chen *et al.* showed that the Foxp3^- (non-Treg) fraction within $\text{CD25}^+\text{TNFR2}^+$ Treg was more proliferative *in vitro* compared to Foxp3^+ counterparts (Chen et al., 2007). This would explain why $\text{CD25}^+\text{TNFR2}^+$ Treg sorted from unmanipulated lung (Chapter 4, Figure 4.3) exhibited a higher proliferative rate *in vitro*.

My data further extended to $\text{TNFR2}^+\text{Foxp3}^-$ Teff that have more capacity to proliferate *in vivo* as compared to non TNFR2 expressing Teff (Chapter 4 and 5). However, I did not rule out the possibility that highly proliferative TNFR2 expressing Teff may become refractory to Treg suppression in the lung, which warrants further investigations. It has previously been demonstrated that Treg fail to suppress TNFR2 expressing Teff and only TNFR2 expressing Treg are able to suppress proliferation of TNFR2 expressing Teff (Chen et al., 2007). Future studies could investigate in depth to what extent TNFR2 expressing Teff become refractory to Treg suppression in the lung and whether the higher proliferative capacity of TNFR2 expressing Teff aids the refractory setting by utilising $\text{TNFR2}^{-/-}$ mice. Future studies utilising $\text{TNFR2}^{-/-}$ mice could also dissect the effects of TNF-TNFR2 interaction on the functionality of TNFR2^+ Treg and Teff. This could be done by adoptive transfer of TNFR2 expressing Treg sorted from the lung into inflamed $\text{TNFR2}^{-/-}$ mice (either allergen- or LPS-induced airway inflammation). Even though previous studies have investigated the TNF-TNFR2 interaction in $\text{TNFR2}^{-/-}$ mice, none of these studies focused on lung disease models (Chen et al., 2007, Chen et al., 2013). Chen *et al.* showed that the proportion of Treg in the thymus and peripheral lymphoid tissues of $\text{TNFR2}^{-/-}$ mice was reduced, suggesting a potential role of TNFR2 in promoting the sustained expression of Foxp3 (Chen et al., 2013). Therefore, it is beneficial for future studies to focus on the interaction of TNF-TNFR2 in airway inflammation mouse models. In the colon inflammation model, the disease could be inhibited by cotransfer of wild-

type Treg, but not by cotransfer of Treg sorted from TNFR2^{-/-} mice (Chen et al., 2013). Investigation conducted in my study on TNFR2 subsets is crucial especially in the lung microenvironment enriched in TNF (i.e. high levels of TNF concentration in BAL from LPS-induced ALI, Chapter 6), given that the TNF-TNFR2 axis likely plays a crucial role in the development/expansion of TNFR2-expressing Treg and Teff (Chen et al., 2007, Chen and Oppenheim, 2010) and the likelihood that alteration of the Treg/Teff ratio results in dysregulated immune responses. As stated above, the major hurdle in my study is to acquire enough cell numbers for subsequent *in vivo* and *in vitro* studies (e.g. *in vivo* adoptive transfer). Therefore, I could not demonstrate that TNFR2 expressing Teff sorted from the inflammatory environment (e.g. LPS-induced ALI) favored TNFR2 expressing Teff to become refractory to Treg suppression in the lung by restraining their plasticity and promoting effector functional stability.

In this thesis, my data suggests that a high frequency of highly proliferative TNFR2⁺Foxp3⁺ Treg is important in controlling the overwhelming activation of TNFR2⁺Foxp3⁻ Teff, and in doing so maintaining immunological tolerance and control the development of lung inflammation. I demonstrated that TNFR2 expressing Treg express surface molecules associated with suppression (e.g. LAP/GARP and CTLA-4) at higher levels than non-TNFR2 expressing Treg, suggesting maximal suppressive capacity of TNFR2 expressing Treg. Nevertheless, I did not rule out whether the suppressive mechanism/s of TNFR2 expressing Treg on Teff are in antigen- or non-antigen-specific manners. Previous studies demonstrated that Treg control immune responses in an antigen-specific manner (Yamaguchi et al., 2007, Addey et al., 2011, Brincks et al., 2013), however, following activation, Treg can also suppress unrelated immune responses in a non-antigen-specific manner (e.g. cell contact and anti-inflammatory cytokines); a

mechanism known as bystander suppression (Hu et al., 2010, Joetham et al., 2009, Belkaid, 2007). I propose that TNFR2 expressing Treg can suppress Teff by both mechanisms; as previously it was shown that TNF not only promoted expansion and function of Treg, but played a critical role in the induction of antigen-specific Treg by tolerogenic DC (Kleijwegt et al., 2010). Furthermore, TNFR2 can be shed by Treg and once shed by Treg, soluble TNFR2 further reduces the pro-inflammatory effects of TNF to Teff by binding and neutralising TNF, showing the mechanism of suppression is in a non-antigen-specific manner (Chen and Oppenheim, 2011b, van Mierlo et al., 2008).

7.3.2 Altered Treg numbers and function lead to imbalanced lung immunological responses

Airway inflammation may result from dysregulated immunity to common environmental stimuli and is characterised by a lack of Treg and a pathological expansion of effector cells (e.g. activation of Th2 cells in AAI) [reviewed in (Andreev et al., 2012)]. Additionally, during asthma exacerbations, patients with asthma have greater Treg deficiency compared to patients with food allergy and severe eczema (Hartl et al., 2007, Mamessier et al., 2008). In this thesis, I demonstrated that TNFR2 expressing Teff that are highly proliferative *in vivo* increased their expansion capacity (greater than TNFR2 expressing Treg) at the peak of allergic airway inflammation [day 1 after allergen challenges, (Chapter 4.6B)], whilst, their expansion capacity increased at day 7 after LPS instillation in lung injury mouse model (Mohamud *et al.*, in preparation). As a result, TNFR2 expressing Teff increased their proportions during airway inflammation, outnumbering TNFR2 expressing Treg. Future studies could explore in depth the cellular interaction (e.g. Treg, Teff, APC such as DC and macrophages) during airway inflammation that assist in the preferential expansion on TNFR2 expressing Teff.

However, the question arises on whether altered Treg and Teff properties (i.e. quality and quantity) lead to an imbalance of immune responses (i.e. allergen- and LPS-induced airway inflammation) or airway inflammatory responses shape overall Treg and Teff properties. New studies are therefore needed to explore these important insights and possibly shed light into the causes and consequences of lung inflammatory responses.

Therefore, targeting the numbers of Treg, to increase the ratios of Treg:Teff towards homeostatic levels may offer a novel cellular pathway to prevent airway inflammation. In addition, targeting TNFR2 expressing Treg would give a significant outcome (e.g. prevent and/or improve an excessive inflammation) as this population is preferentially expanded in *in vivo*, compared to non TNFR2 expressing Treg. On the other hand, indirect targeting of TNFR2 expressing Treg such as by targeting tolerogenic DC (e.g. CD103⁺ DC as discussed in Chapter 5) could explain the cellular interactions between DC and Treg, as CD103⁺ DC are involved in allergen sampling and migrate to the lymphoid organs where they prime naïve T cells (Khare et al., 2013). To date, no studies have shown whether such a cellular interaction between CD103⁺ DC and TNFR2 expressing Treg exists.

7.4 Differences in the effects of LPS and nanoparticles on lung immunity

It is now understood that a primary immune response in the lung, can modify the nature and response of a subsequent pulmonary immune response, in a process called innate imprinting (Hardy et al., 2013b) via various mechanisms including impairment of pulmonary APC function (Hardy et al., 2013b, Williams et al., 2004) or mechanisms of antigen delivery (Abadie et al., 2009), induction of regulatory myeloid-derived suppressor

cells (Arora et al., 2010) and Treg (Wang and McCusker, 2006, Zuany-Amorim et al., 2002b). In this regards, as demonstrated in Chapter 5, PS50G left the immunological imprinting effects in the lung microenvironment a month after instillation. Our previous studies showed that PS50G decrease the key characteristics of allergic asthma by inhibiting expansion and suppressing co-stimulatory function of CD11b^{hi} inflammatory DC in the lung-draining LN (Hardy et al., 2012a, Hardy et al., 2013b). Recent data showed that at the molecular basis, PS50G at a wide range of particle concentration, surface coating, charges and time points of treatments did not activate MAPK ERK in DC (Karlson et al., 2013), showing the inert property of PS50G. In another study, Matsushita *et al.* showed that LPS impairs the antigen presentation capacity in DC and downregulates the capacity of DC to expand T cells (including allergen-specific Th2 and Th17 cells) thereby inducing airway tolerance and attenuating allergic airway inflammation (Matsushita et al., 2010). Thus, not surprisingly, LPS and PS50G induce different alterations on lung immunological responses although both LPS (Mohamud *et al.*, in preparation) and PS50G result in better quality of TNFR2 expressing Treg that partly play a crucial role in inhibition of the development of allergic airway inflammation.

It can be speculated that excessive pro-inflammatory cytokines secreted in the lung microenvironment after LPS instillation change the cytokine milieu in the lung, with secreted TNF binding directly on TNFR2 expressed by both Treg and Teff, priming these cells for subsequent immune responses. As inert PS50G do not elevate TNF, PS50G may exhibit other mechanism/s in the priming and/or inducing TNFR2⁺Foxp3⁺ Treg independent of TNF such as involvement of tolerogenic CD103⁺ DC (as discussed and illustrated in detailed Chapter 5). The different effects of LPS and PS50G on DC further support the idea that the original encounter of various type of antigens on lung APC

determines the quality of the subsequent immune response (Abadie et al., 2009, Hardy et al., 2013b, Hardy et al., 2012a).

However, the direct influences of nanoparticles such as PS50G on other immune cells (e.g. macrophages) and lung structural cells (e.g. endothelial cells) at the exposure site are still unknown. In Chapter 5, the source of CCL2 was not investigated, but it is proposed that CCL2 would attract tolerogenic CD103⁺ DC which may be involved in PS50G-mediated lung immune homeostasis by increasing the quantity and quality of TNFR2 expressing Treg. Macrophages might be involved in this mechanism as macrophages are the main source of CCL2 (Deshmane et al., 2009). Unpublished data from Je Lin Sieow of our group (Honours project 2013) showed that PS50G were not taken up by endothelial cells, and so it is likely that endothelial cells do not directly play a role in PS50G-lung imprinting. However, endothelial cells could indirectly be involved in this mechanism as a previous study showed that Treg modulate inflammation independently of their suppressive function on Teff by suppression of endothelial cell-mediated activation and leukocyte recruitment (Maganto-Garcia et al., 2011). On the other hand, as a potent inflammatory mediator, LPS activates alveolar macrophages (Aung et al., 2006) and endothelial cells (Alom-Ruiz et al., 2008). LPS-mediated endothelial cell activation in the lung increases expression of cellular adhesion molecules and cytokines (e.g. CCL2), and increases vascular permeability which promotes neutrophil and leukocyte influx that leads to acute lung injury (Alom-Ruiz et al., 2008). A recent study showed that LPS-mediated activation of lung endothelial cells by modulation of phosphorylation of key kinases in the TLR signaling cascade contributes to lung inflammation (Menden et al., 2013). Collectively, findings from my study and the aforementioned studies highlight the important effect of environmental stimuli (e.g LPS and PS50G) on lung cells (e.g. DC

recruitment to the inflammation site and endothelial cell activation) in shaping the lung immune responses. It will be interesting in future studies to examine the direct interactions of lung structural cells and immune cells after lung exposure to environmental stimuli (e.g. nanoparticles).

7.5 The role of follistatin, nanoparticles and LPS on Treg in preventive and therapeutic treatments of lung inflammation

Since one of the main routes of entry of environmental stimuli such as LPS and nanoparticles is via the lung, it is important to further characterise their therapeutics impact on the respiratory system. In addition to the environmental stimuli, the lung can also be regulated by biological factors, e.g. follistatin that binds to activin A. In this section, the capacity of follistatin, LPS and nanoparticles to induce/promote immunological tolerance in order to retain pulmonary homeostasis and prevent potentially fatal immunopathology will be discussed separately.

7.5.1 Follistatin as a therapeutic treatment of lung inflammation

As shown in Chapter 3 and in Hardy *et al.*, the activin-follistatin axis plays an important role in the pathogenesis of asthma (Hardy *et al.*, 2006) and is a candidate for an asthma therapeutic as follistatin inhibits asthmatic airway remodelling (Hardy *et al.*, 2013c). However, it has been found that neutralisation of activin A with a monoclonal antibody, exacerbated allergic airway disease that acted via induction of antigen-specific CD4⁺ CD25⁻ Foxp3⁻ Teff (Semitekolou *et al.*, 2009). Contradictory to this, the findings reported herein showed that blockade of activin A with follistatin ameliorated (or lessened) some inflammatory parameters (Hardy *et al.*, 2006, Hardy *et al.*, 2013c). There are few differences between my study protocol and Semitekolou's group. The major difference

was the site of follistatin exposure; my study involved activin A blockade in the lungs whereas Semitekolou's was via systemic inhibition. Furthermore, the source and/or timing of activin A administration is a contributing factor; the monoclonal antibody used by Semitekolou is specific for activin A, whilst follistatin used in my study is known to also antagonise other members of the TGF- β superfamily. Consistent with my findings, pro-inflammatory effects of activin A were also seen in another *in vivo* study; systemic administration of follistatin increases the survival of mice following a lethal dose of LPS (100 μ g) that is associated with decreased serum levels of TNF, IL-1 β and IL-6 (Jones et al., 2007). Together with Jones's study, data from this thesis indicated that activin-A modulated the release of several key pro-inflammatory cytokines, thus supporting the pro-inflammatory role of activin A. These findings demonstrated the crucial role of activin A in the inflammatory response and show that blocking its actions by the use of follistatin has significant therapeutic potential to reduce the severity of inflammatory diseases.

7.5.2 LPS as a therapeutic treatment of lung inflammation

In 2002, Zuany-Amorim *et al.* discussed the possibility of TLRs as potential therapeutic targets for multiple diseases including allergic asthma. It was suggested that activation of TLRs by bacteria/bacterial products might shift the predominantly Th2-driven inflammation into a more protective Th1 response, or might lead to the induction of Treg, and thereby prevent the development of allergic asthma (Zuany-Amorim et al., 2002a). Most of the recent studies that focused on LPS-induced TLR4 activation found that exposure to LPS inhibited allergic inflammation in a dose-dependent manner (Duan et al., 2008, Kuipers et al., 2003, Hollingsworth et al., 2006, Blumer et al., 2005, Gerhold et al., 2012) and clinical studies found that exposure to high levels of LPS in early life may protect against allergic asthma development (Ege et al., 2006, Braun-Fahrlander et al.,

2002, Schaub et al., 2009). In parallel with the aforementioned studies, data from the present study also showed that high dose LPS prevented the induction of allergic asthma, while low dose LPS failed to do so (Mohamud *et al.*, in preparation). Interestingly, a study demonstrated that farm exposure during pregnancy increased Treg cell numbers and function, and acted as a natural model of immunomodulation which shaped a child's immune system in early life (Schaub et al., 2009). Overall, the aforementioned studies showed the capacity of LPS to modulate Treg and exhibit therapeutic effects (as a natural model of immunomodulation) by controlling Th2 immune responses in an allergic asthma mouse model. As this is the first study investigating the effects of LPS on TNFR2-expressing cells, my unpublished data suggest that LPS alters the quality of TNFR2-positive Treg (e.g. acquire higher expression level of a suppression marker) (Mohamud *et al.*, in preparation).

7.5.3 Nanoparticles as a therapeutic treatment of lung inflammation

Nanoparticles are increasingly used for drug delivery and as therapeutic agents for the treatment of a variety of lung diseases, including allergic asthma (Rossi et al., 2010b). Even though many nanoparticles have adjuvant effects and can exacerbate existing allergic asthma [e.g. carbon nanotubes, (Inoue et al., 2010)], certain nanoparticles including those used in this study exhibit beneficial effects, such as the ability to inhibit allergic inflammation [reviewed in (Mohamud et al., 2013)]. A recent study showed that 6 nm silver nanoparticles substantially suppressed mucus hypersecretion in allergic asthma by modification of a vascular endothelial growth factor crucial in regulating the vascular changes associated with asthma (Jang et al., 2012). Furthermore, nanocrystalline silver particles (< 50 nm, specific size not mentioned) were also shown to have an anti-inflammatory effect, suppressing the expression of IL-1 β , IL-12, metalloproteinase-9 and

TNF (Bhol and Schechter, 2005) as well as blocking the proliferation of endothelial cells (Asharani et al., 2009, Kalishwaralal et al., 2009). However, the precise mechanisms by which silver nanoparticles exert these beneficial effects in lung diseases, such as possible effects on lung DC or Treg were not investigated in the aforementioned studies. As stated in Chapter 5, none of the studies to date have investigated the effects of nanoparticles on TNFR2 expressing Treg in an asthma model, and only a few studies have shown the effects of nanoparticles on Treg (Goldmann et al., 2012, Gustafsson et al., 2011). In an autoimmune study, Goldmann *et al.* showed the potential of chitosan-DNA nanoparticles to expand Treg that lead to a significant reduction of antigen-specific delayed-type hypersensitivity (DTH) response (Goldmann et al., 2012). In another study, Gustafsson *et al.* reported that lung exposure to titanium dioxide nanoparticles induces innate immune activation and long-lasting lymphocyte response including CD4⁺ helper T-cells with high expression of CD25 (Gustafsson et al., 2011), without examining the potential suppressive capacity of nanoparticles-induced Treg. My data further suggest that inert PS50G may inhibit allergic asthma via modulation of TNFR2 expressing Treg (Chapter 5). PS50G modify TNFR2 expressing Treg to be more proliferative and to express a higher level of suppressor molecules. Therefore PS50G may be responsible for tuning the quality of the subsequent immune response causing protection against airways inflammation. Moreover, along with previous studies in this field (Rossi et al., 2010a, John et al., 2003), my study demonstrates the potential of PS50G to translate to new preventive and therapeutic treatments, particularly against allergic diseases.

7.6 Final conclusion

Collectively, my findings emphasise the concept that follistatin, nanoparticles and LPS exhibit beneficial effects on lung inflammation partly by improving the quality and quantity of Treg via TNFR2 expression. My thesis demonstrated that TNFR2 expressing Treg play an important role at the homeostatic level and during airways inflammation in mouse models. Treg are regulated by lung cytokines or the microenvironment milieu, and this milieu can be shaped by exposure to different stimuli. The primary immune response shaped by these stimuli can modify the nature and response of subsequent pulmonary immune responses. As this is the first study investigating the characteristics and functions of TNFR2 expressing Treg and Teff in lung disease models, this thesis contributes important new knowledge in this field. Clarification of the cellular and/or molecular basis of plasticity and functional stability of TNFR2 expressing Treg in the lung microenvironment may have therapeutic benefit and will enhance our understanding of TNFR2 expressing Treg biology. Additionally, the role of TNFR2 expressing Treg is worth investigating in depth in non-inflammatory lung diseases setting, such as in a lung cancer model to explore their further possibility in improving pulmonary neoplasia. As my work has now established important criteria for lung TNFR2 expressing Treg in an inflammatory environment, targeting these cells poses a potential new therapeutic avenue to promote healthy lung immune homeostasis.

-This page intentionally left blank-

References

References

- (1996). Variations in the prevalence of respiratory symptoms, self-reported asthma attacks, and use of asthma medication in the European Community Respiratory Health Survey (ECRHS). *Eur Respir J* 9:687-95.
- (2008). Australian Centre for Asthma Monitoring AIHW Asthma Series no. 3. Cat. no. ACM 14. Canberra: AIHW.
- Abadie, V., Bonduelle, O., Duffy, D., Parizot, C., Verrier, B. & Combadiere, B. (2009). Original encounter with antigen determines antigen-presenting cell imprinting of the quality of the immune response in mice. *PLoS One* 4:e8159.
- Abdi, K., Singh, N. J. & Matzinger, P. (2012). Lipopolysaccharide-activated dendritic cells: "exhausted" or alert and waiting? *J Immunol* 188:5981-9.
- Addey, C., White, M., Dou, L., Coe, D., Dyson, J. & Chai, J. G. (2011). Functional plasticity of antigen-specific regulatory T cells in context of tumor. *J Immunol* 186:4557-64.
- Afshar, R., Medoff, B. D. & Luster, A. D. (2008). Allergic asthma: a tale of many T cells. *Clin Exp Allergy* 38:1847-57.
- Aggarwal, N. R., D'Alessio, F. R., Tsushima, K., Sidhaye, V. K., Cheadle, C., Grigoryev, D. N., et al. (2009). Regulatory T cell-mediated resolution of lung injury: Identification of potential target genes via expression profiling. *Physiol Genomics*.
- Akagi, T., Baba, M. & Akashi, M. (2007). [Development of vaccine adjuvants using polymeric nanoparticles and their potential applications for anti-HIV vaccine]. *Yakugaku Zasshi* 127:307-17.
- Akbari, M., Honma, K., Kimura, D., Miyakoda, M., Kimura, K., Matsuyama, T., et al. (2014). IRF4 in Dendritic Cells Inhibits IL-12 Production and Controls Th1 Immune Responses against *Leishmania major*. *J Immunol* 192:2271-9.
- Akbari, O., Freeman, G. J., Meyer, E. H., Greenfield, E. A., Chang, T. T., Sharpe, A. H., et al. (2002). Antigen-specific regulatory T cells develop via the ICOS-ICOS-ligand pathway and inhibit allergen-induced airway hyperreactivity. *Nat Med* 8:1024-32.
- Akdis, M., Verhagen, J., Taylor, A., Karamloo, F., Karagiannidis, C., Cramer, R., et al. (2004). Immune responses in healthy and allergic individuals are characterized by a fine balance between allergen-specific T regulatory 1 and T helper 2 cells. *J Exp Med* 199:1567-75.
- Akimova, T., Beier, U. H., Wang, L., Levine, M. H. & Hancock, W. W. (2011). Helios expression is a marker of T cell activation and proliferation. *PLoS One* 6:e24226.
- Alom-Ruiz, S. P., Anilkumar, N. & Shah, A. M. (2008). Reactive oxygen species and endothelial activation. *Antioxid Redox Signal* 10:1089-100.
- Amu, S., Gjerdtsson, I., Tarkowski, A. & Brisslert, M. (2006). B-cell CD25 expression in murine primary and secondary lymphoid tissue. *Scand J Immunol* 64:482-92.
- Andreev, K., Graser, A., Maier, A., Mousset, S. & Finotto, S. (2012). Therapeutic measures to control airway tolerance in asthma and lung cancer. *Front Immunol* 3:216.
- Aoki, F., Kurabayashi, M., Hasegawa, Y. & Kojima, I. (2005). Attenuation of bleomycin-induced pulmonary fibrosis by follistatin. *Am J Respir Crit Care Med* 172:713-20.
- Arnold, I. C., Dehzad, N., Reuter, S., Martin, H., Becher, B., Taube, C., et al. (2011). *Helicobacter pylori* infection prevents allergic asthma in mouse models through the induction of regulatory T cells. *J Clin Invest* 121:3088-93.
- Arora, M., Poe, S. L., Oriss, T. B., Krishnamoorthy, N., Yarlagadda, M., Wenzel, S. E., et al. (2010). TLR4/MyD88-induced CD11b+Gr-1 int F4/80+ non-migratory myeloid cells suppress Th2 effector function in the lung. *Mucosal Immunol* 3:578-93.

- Arora, M., Poe, S. L., Ray, A. & Ray, P. (2011). LPS-induced CD11b(+)Gr1(int)F4/80(+) regulatory myeloid cells suppress allergen-induced airway inflammation. *Int Immunopharmacol*.
- Asharani, P. V., Hande, M. P. & Valiyaveetil, S. (2009). Anti-proliferative activity of silver nanoparticles. *BMC Cell Biol* 10:65.
- Asher, M. I., Montefort, S., Bjorksten, B., Lai, C. K., Strachan, D. P., Weiland, S. K., et al. (2006). Worldwide time trends in the prevalence of symptoms of asthma, allergic rhinoconjunctivitis, and eczema in childhood: ISAAC Phases One and Three repeat multicountry cross-sectional surveys. *Lancet* 368:733-43.
- Aung, H. T., Schroder, K., Himes, S. R., Brion, K., van Zuylen, W., Trieu, A., et al. (2006). LPS regulates proinflammatory gene expression in macrophages by altering histone deacetylase expression. *FASEB J* 20:1315-27.
- Awasthi, A., Murugaiyan, G. & Kuchroo, V. K. (2008). Interplay between effector Th17 and regulatory T cells. *J Clin Immunol* 28:660-70.
- Balkissoon, R. (2008). Asthma overview. *Prim Care* 35:41-60, vi.
- Banchereau, J. & Steinman, R. M. (1998). Dendritic cells and the control of immunity. *Nature* 392:245-52.
- Baru, A. M., Hartl, A., Lahl, K., Krishnaswamy, J. K., Fehrenbach, H., Yildirim, A. O., et al. (2010). Selective depletion of Foxp3(+) Treg during sensitization phase aggravates experimental allergic airway inflammation. *Eur J Immunol* 40:2259-66.
- Battaglia, M. & Roncarolo, M. G. (2009). The Tregs' world according to GARP. *Eur J Immunol* 39:3296-300.
- Belkaid, Y. (2007). Regulatory T cells and infection: a dangerous necessity. *Nat Rev Immunol* 7:875-88.
- Belkaid, Y., Piccirillo, C. A., Mendez, S., Shevach, E. M. & Sacks, D. L. (2002). CD4+CD25+ regulatory T cells control *Leishmania* major persistence and immunity. *Nature* 420:502-7.
- Bell, B. D., Kitajima, M., Larson, R. P., Stoklasek, T. A., Dang, K., Sakamoto, K., et al. (2013). The transcription factor STAT5 is critical in dendritic cells for the development of TH2 but not TH1 responses. *Nat Immunol* 14:364-71.
- Berry, M. A., Hargadon, B., Shelley, M., Parker, D., Shaw, D. E., Green, R. H., et al. (2006). Evidence of a role of tumor necrosis factor alpha in refractory asthma. *N Engl J Med* 354:697-708.
- Bersten, A. D., Edibam, C., Hunt, T. & Moran, J. (2002). Incidence and mortality of acute lung injury and the acute respiratory distress syndrome in three Australian States. *Am J Respir Crit Care Med* 165:443-8.
- Bettelli, E., Carrier, Y., Gao, W., Korn, T., Strom, T. B., Oukka, M., et al. (2006). Reciprocal developmental pathways for the generation of pathogenic effector TH17 and regulatory T cells. *Nature* 441:235-8.
- Bhol, K. C. & Schechter, P. J. (2005). Topical nanocrystalline silver cream suppresses inflammatory cytokines and induces apoptosis of inflammatory cells in a murine model of allergic contact dermatitis. *Br J Dermatol* 152:1235-42.
- Bickford, J. S., Newsom, K. J., Herlihy, J. D., Mueller, C., Keeler, B., Qiu, X., et al. (2012). Induction of group IVC phospholipase A2 in allergic asthma: transcriptional regulation by TNFalpha in bronchoepithelial cells. *Biochem J* 442:127-37.
- Bilate, A. M. & Lafaille, J. J. (2010). Can TNF-alpha boost regulatory T cells? *J Clin Invest* 120:4190-2.

References

- Biton, J., Semerano, L., Delavallee, L., Lemeiter, D., Laborie, M., Grouard-Vogel, G., et al. (2011). Interplay between TNF and Regulatory T Cells in a TNF-Driven Murine Model of Arthritis. *J Immunol*.
- Blumer, N., Herz, U., Wegmann, M. & Renz, H. (2005). Prenatal lipopolysaccharide-exposure prevents allergic sensitization and airway inflammation, but not airway responsiveness in a murine model of experimental asthma. *Clin Exp Allergy* 35:397-402.
- Bochner, B. S., Udem, B. J. & Lichtenstein, L. M. (1994). Immunological aspects of allergic asthma. *Annu Rev Immunol* 12:295-335.
- Boissier, M. C., Assier, E., Biton, J., Denys, A., Falgarone, G. & Bessis, N. (2009). Regulatory T cells (Treg) in rheumatoid arthritis. *Joint Bone Spine* 76:10-4.
- Borges, V. M., Vandivier, R. W., McPhillips, K. A., Kench, J. A., Morimoto, K., Groshong, S. D., et al. (2009). TNF α inhibits apoptotic cell clearance in the lung, exacerbating acute inflammation. *Am J Physiol Lung Cell Mol Physiol* 297:L586-95.
- Borsellino, G., Kleinewietfeld, M., Di Mitri, D., Sternjak, A., Diamantini, A., Giometto, R., et al. (2007). Expression of ectonucleotidase CD39 by Foxp3⁺ Treg cells: hydrolysis of extracellular ATP and immune suppression. *Blood* 110:1225-32.
- Boyce, J. A. & Austen, K. F. (2005). No audible wheezing: nuggets and conundrums from mouse asthma models. *J Exp Med* 201:1869-73.
- Braun-Fahrlander, C., Riedler, J., Herz, U., Eder, W., Waser, M., Grize, L., et al. (2002). Environmental exposure to endotoxin and its relation to asthma in school-age children. *N Engl J Med* 347:869-77.
- Brincks, E. L., Roberts, A. D., Cookenham, T., Sell, S., Kohlmeier, J. E., Blackman, M. A., et al. (2013). Antigen-specific memory regulatory CD4⁺Foxp3⁺ T cells control memory responses to influenza virus infection. *J Immunol* 190:3438-46.
- Broide, D. H., Lotz, M., Cuomo, A. J., Coburn, D. A., Federman, E. C. & Wasserman, S. I. (1992). Cytokines in symptomatic asthma airways. *J Allergy Clin Immunol* 89:958-67.
- Bromley, S. K., Thomas, S. Y. & Luster, A. D. (2005). Chemokine receptor CCR7 guides T cell exit from peripheral tissues and entry into afferent lymphatics. *Nat Immunol* 6:895-901.
- Brunkow, M. E., Jeffery, E. W., Hjerrild, K. A., Paepker, B., Clark, L. B., Yasayko, S. A., et al. (2001). Disruption of a new forkhead/winged-helix protein, scurfy, results in the fatal lymphoproliferative disorder of the scurfy mouse. *Nat Genet* 27:68-73.
- Burchell, J. T., Wikstrom, M. E., Stumbles, P. A., Sly, P. D. & Turner, D. J. (2009). Attenuation of allergen-induced airway hyperresponsiveness is mediated by airway regulatory T cells. *Am J Physiol Lung Cell Mol Physiol* 296:L307-19.
- Bystry, R. S., Aluvihare, V., Welch, K. A., Kallikourdis, M. & Betz, A. G. (2001). B cells and professional APCs recruit regulatory T cells via CCL4. *Nat Immunol* 2:1126-32.
- Caramalho, I., Lopes-Carvalho, T., Ostler, D., Zelenay, S., Haury, M. & Demengeot, J. (2003). Regulatory T cells selectively express toll-like receptors and are activated by lipopolysaccharide. *J Exp Med* 197:403-11.
- Carson, W. F. t., Guernsey, L. A., Singh, A., Vella, A. T., Schramm, C. M. & Thrall, R. S. (2008). Accumulation of regulatory T cells in local draining lymph nodes of the lung correlates with spontaneous resolution of chronic asthma in a murine model. *Int Arch Allergy Immunol* 145:231-43.

- Cavani, A., Nasorri, F., Ottaviani, C., Sebastiani, S., De Pita, O. & Girolomoni, G. (2003). Human CD25⁺ regulatory T cells maintain immune tolerance to nickel in healthy, nonallergic individuals. *J Immunol* 171:5760-8.
- Chen, W., Jin, W., Hardegen, N., Lei, K. J., Li, L., Marinos, N., et al. (2003a). Conversion of peripheral CD4⁺CD25⁻ naive T cells to CD4⁺CD25⁺ regulatory T cells by TGF-beta induction of transcription factor Foxp3. *J Exp Med* 198:1875-86.
- Chen, X., Baumel, M., Mannel, D. N., Howard, O. M. & Oppenheim, J. J. (2007). Interaction of TNF with TNF receptor type 2 promotes expansion and function of mouse CD4⁺CD25⁺ T regulatory cells. *J Immunol* 179:154-61.
- Chen, X., Hamano, R., Subleski, J. J., Hurwitz, A. A., Howard, O. M. & Oppenheim, J. J. (2010a). Expression of costimulatory TNFR2 induces resistance of CD4⁺FoxP3⁻ conventional T cells to suppression by CD4⁺FoxP3⁺ regulatory T cells. *J Immunol* 185:174-82.
- Chen, X. & Oppenheim, J. J. (2010). TNF-alpha: an activator of CD4⁺FoxP3⁺TNFR2⁺ regulatory T cells. *Curr Dir Autoimmun* 11:119-34.
- Chen, X. & Oppenheim, J. J. (2011a). Contrasting effects of TNF and anti-TNF on the activation of effector T cells and regulatory T cells in autoimmunity. *FEBS Lett*.
- Chen, X. & Oppenheim, J. J. (2011b). The phenotypic and functional consequences of tumour necrosis factor receptor type 2 expression on CD4(+) FoxP3(+) regulatory T cells. *Immunology* 133:426-33.
- Chen, X. & Oppenheim, J. J. (2011c). Resolving the identity myth: Key markers of functional CD4(+)FoxP3(+) regulatory T cells. *Int Immunopharmacol*.
- Chen, X., Subleski, J. J., Hamano, R., Howard, O. M., Wiltout, R. H. & Oppenheim, J. J. (2010b). Co-expression of TNFR2 and CD25 identifies more of the functional CD4⁺FOXP3⁺ regulatory T cells in human peripheral blood. *Eur J Immunol* 40:1099-106.
- Chen, X., Subleski, J. J., Kopf, H., Howard, O. M., Mannel, D. N. & Oppenheim, J. J. (2008). Cutting edge: expression of TNFR2 defines a maximally suppressive subset of mouse CD4⁺CD25⁺FoxP3⁺ T regulatory cells: applicability to tumor-infiltrating T regulatory cells. *J Immunol* 180:6467-71.
- Chen, X., Wu, X., Zhou, Q., Howard, O. M., Netea, M. G. & Oppenheim, J. J. (2013). TNFR2 is critical for the stabilization of the CD4⁺Foxp3⁺ regulatory T. cell phenotype in the inflammatory environment. *J Immunol* 190:1076-84.
- Chen, Y., Shen, S., Gorentla, B. K., Gao, J. & Zhong, X. P. (2012). Murine regulatory T cells contain hyperproliferative and death-prone subsets with differential ICOS expression. *J Immunol* 188:1698-707.
- Chen, Z. M., O'Shaughnessy, M. J., Gramaglia, I., Panoskaltsis-Mortari, A., Murphy, W. J., Narula, S., et al. (2003b). IL-10 and TGF-beta induce alloreactive CD4⁺CD25⁻ T cells to acquire regulatory cell function. *Blood* 101:5076-83.
- Choi, M. S., Park, S., Choi, T., Lee, G., Haam, K. K., Hong, M. C., et al. (2013). Bee venom ameliorates ovalbumin induced allergic asthma via modulating CD4(+)CD25(+) regulatory T cells in mice. *Cytokine* 61:256-65.
- Coester, C., Nayyar, P. & Samuel, J. (2006). In vitro uptake of gelatin nanoparticles by murine dendritic cells and their intracellular localisation. *Eur J Pharm Biopharm* 62:306-14.
- Condon, T. V., Sawyer, R. T., Fenton, M. J. & Riches, D. W. (2011). Lung dendritic cells at the innate-adaptive immune interface. *J Leukoc Biol* 90:883-95.

References

- Curiel, T. J., Coukos, G., Zou, L., Alvarez, X., Cheng, P., Mottram, P., et al. (2004). Specific recruitment of regulatory T cells in ovarian carcinoma fosters immune privilege and predicts reduced survival. *Nat Med* 10:942-9.
- Curotto de Lafaille, M. A., Muriglan, S., Sunshine, M. J., Lei, Y., Kutchukhidze, N., Furtado, G. C., et al. (2001). Hyper immunoglobulin E response in mice with monoclonal populations of B and T lymphocytes. *J Exp Med* 194:1349-59.
- D'Alessio, F. R., Tsushima, K., Aggarwal, N. R., West, E. E., Willett, M. H., Britos, M. F., et al. (2009). CD4+CD25+Foxp3+ Tregs resolve experimental lung injury in mice and are present in humans with acute lung injury. *J Clin Invest* 119:2898-913.
- Dardalhon, V., Awasthi, A., Kwon, H., Galileos, G., Gao, W., Sobel, R. A., et al. (2008). IL-4 inhibits TGF-beta-induced Foxp3+ T cells and, together with TGF-beta, generates IL-9+ IL-10+ Foxp3(-) effector T cells. *Nat Immunol* 9:1347-55.
- de Kretser, D. M., O'Hehir, R. E., Hardy, C. L. & Hedger, M. P. (2012). The roles of activin A and its binding protein, follistatin, in inflammation and tissue repair. *Mol Cell Endocrinol* 359:101-6.
- Deaglio, S., Dwyer, K. M., Gao, W., Friedman, D., Usheva, A., Erat, A., et al. (2007). Adenosine generation catalyzed by CD39 and CD73 expressed on regulatory T cells mediates immune suppression. *J Exp Med* 204:1257-65.
- Delayre-Orthez, C., de Blay, F., Frossard, N. & Pons, F. (2004). Dose-dependent effects of endotoxins on allergen sensitization and challenge in the mouse. *Clin Exp Allergy* 34:1789-95.
- Deshmane, S. L., Kremlev, S., Amini, S. & Sawaya, B. E. (2009). Monocyte chemoattractant protein-1 (MCP-1): an overview. *J Interferon Cytokine Res* 29:313-26.
- Dinauer, N., Balthasar, S., Weber, C., Kreuter, J., Langer, K. & von Briesen, H. (2005). Selective targeting of antibody-conjugated nanoparticles to leukemic cells and primary T-lymphocytes. *Biomaterials* 26:5898-906.
- Diwan, M., Elamanchili, P., Lane, H., Gainer, A. & Samuel, J. (2003). Biodegradable nanoparticle mediated antigen delivery to human cord blood derived dendritic cells for induction of primary T cell responses. *J Drug Target* 11:495-507.
- Donaldson, K., Stone, V., Clouter, A., Renwick, L. & MacNee, W. (2001). Ultrafine particles. *Occup Environ Med* 58:211-6, 199.
- Dong, L., Li, H., Wang, S. & Li, Y. (2009). Different doses of lipopolysaccharides regulate the lung inflammation of asthmatic mice via TLR4 pathway in alveolar macrophages. *J Asthma* 46:229-33.
- Dostert, C., Petrilli, V., Van Bruggen, R., Steele, C., Mossman, B. T. & Tschopp, J. (2008). Innate immune activation through Nalp3 inflammasome sensing of asbestos and silica. *Science* 320:674-7.
- Doyle, R. L., Szaflarski, N., Modin, G. W., Wiener-Kronish, J. P. & Matthay, M. A. (1995). Identification of patients with acute lung injury. Predictors of mortality. *Am J Respir Crit Care Med* 152:1818-24.
- Duan, W., So, T. & Croft, M. (2008). Antagonism of airway tolerance by endotoxin/lipopolysaccharide through promoting OX40L and suppressing antigen-specific Foxp3+ T regulatory cells. *J Immunol* 181:8650-9.
- Duan, W., So, T., Mehta, A. K., Choi, H. & Croft, M. (2011). Inducible CD4+LAP+Foxp3- regulatory T cells suppress allergic inflammation. *J Immunol* 187:6499-507.
- Eder, W., Ege, M. J. & von Mutius, E. (2006). The asthma epidemic. *N Engl J Med* 355:2226-35.

- Ege, M. J., Bieli, C., Frei, R., van Strien, R. T., Riedler, J., Ublagger, E., et al. (2006). Prenatal farm exposure is related to the expression of receptors of the innate immunity and to atopic sensitization in school-age children. *J Allergy Clin Immunol* 117:817-23.
- Eisenbarth, S. C., Piggott, D. A., Huleatt, J. W., Visintin, I., Herrick, C. A. & Bottomly, K. (2002). Lipopolysaccharide-enhanced, toll-like receptor 4-dependent T helper cell type 2 responses to inhaled antigen. *J Exp Med* 196:1645-51.
- Erzurum, S. C. (2006). Inhibition of tumor necrosis factor alpha for refractory asthma. *N Engl J Med* 354:754-8.
- Fallarino, F., Grohmann, U., You, S., McGrath, B. C., Cavener, D. R., Vacca, C., et al. (2006). The combined effects of tryptophan starvation and tryptophan catabolites down-regulate T cell receptor zeta-chain and induce a regulatory phenotype in naive T cells. *J Immunol* 176:6752-61.
- Fan, H., Yang, J., Hao, J., Ren, Y., Chen, L., Li, G., et al. (2012). Comparative Study of Regulatory T Cells Expanded Ex Vivo from Cord Blood and Adult Peripheral Blood. *Immunology*.
- Faustino, L., da Fonseca, D. M., Takenaka, M. C., Mirotti, L., Florsheim, E. B., Guerreschi, M. G., et al. (2013). Regulatory T cells migrate to airways via CCR4 and attenuate the severity of airway allergic inflammation. *J Immunol* 190:2614-21.
- Faustino, L., Mucida, D., Keller, A. C., Demengeot, J., Bortoluci, K., Sardinha, L. R., et al. (2012). Regulatory T cells accumulate in the lung allergic inflammation and efficiently suppress T-cell proliferation but not Th2 cytokine production. *Clin Dev Immunol* 2012:721817.
- Fernandez-Rodriguez, S., Ford, W. R., Broadley, K. J. & Kidd, E. J. (2008). Establishing the phenotype in novel acute and chronic murine models of allergic asthma. *Int Immunopharmacol* 8:756-63.
- Fifis, T., Gamvrellis, A., Crimeen-Irwin, B., Pietersz, G. A., Li, J., Mottram, P. L., et al. (2004). Size-dependent immunogenicity: therapeutic and protective properties of nano-vaccines against tumors. *J Immunol* 173:3148-54.
- Fisson, S., Darrasse-Jeze, G., Litvinova, E., Septier, F., Klatzmann, D., Liblau, R., et al. (2003). Continuous activation of autoreactive CD4⁺ CD25⁺ regulatory T cells in the steady state. *J Exp Med* 198:737-46.
- Flores-Borja, F., Jury, E. C., Mauri, C. & Ehrenstein, M. R. (2008). Defects in CTLA-4 are associated with abnormal regulatory T cell function in rheumatoid arthritis. *Proc Natl Acad Sci U S A* 105:19396-401.
- Fontenot, J. D., Dooley, J. L., Farr, A. G. & Rudensky, A. Y. (2005a). Developmental regulation of Foxp3 expression during ontogeny. *J Exp Med* 202:901-6.
- Fontenot, J. D., Gavin, M. A. & Rudensky, A. Y. (2003). Foxp3 programs the development and function of CD4⁺CD25⁺ regulatory T cells. *Nat Immunol* 4:330-6.
- Fontenot, J. D., Rasmussen, J. P., Gavin, M. A. & Rudensky, A. Y. (2005b). A function for interleukin 2 in Foxp3-expressing regulatory T cells. *Nat Immunol* 6:1142-51.
- Gaajetaan, G. R., Geelen, T. H., Grauls, G. E., Bruggeman, C. A. & Stassen, F. R. (2012). CpG and poly(I:C) stimulation of dendritic cells and fibroblasts limits herpes simplex virus type 1 infection in an IFN β -dependent and -independent way. *Antiviral Res* 93:39-47.
- Garibaldi, B. T., D'Alessio, F. R., Mock, J. R., Files, D. C., Chau, E., Eto, Y., et al. (2013). Regulatory T cells reduce acute lung injury fibroproliferation by decreasing fibrocyte recruitment. *Am J Respir Cell Mol Biol* 48:35-43.

References

- Gavin, M. A., Clarke, S. R., Negrou, E., Gallegos, A. & Rudensky, A. (2002). Homeostasis and anergy of CD4(+)CD25(+) suppressor T cells in vivo. *Nat Immunol* 3:33-41.
- Geiser, M., Rothen-Rutishauser, B., Kapp, N., Schurch, S., Kreyling, W., Schulz, H., et al. (2005). Ultrafine particles cross cellular membranes by nonphagocytic mechanisms in lungs and in cultured cells. *Environ Health Perspect* 113:1555-60.
- Gereda, J. E., Leung, D. Y., Thatayatikom, A., Streib, J. E., Price, M. R., Klinnert, M. D., et al. (2000). Relation between house-dust endotoxin exposure, type 1 T-cell development, and allergen sensitisation in infants at high risk of asthma. *Lancet* 355:1680-3.
- Gerhold, K., Avagyan, A., Reichert, E., Seib, C., Van, D. V., Luger, E. O., et al. (2012). Prenatal allergen exposures prevent allergen-induced sensitization and airway inflammation in young mice. *Allergy* 67:353-61.
- Gerhold, K., Bluemchen, K., Franke, A., Stock, P. & Hamelmann, E. (2003). Exposure to endotoxin and allergen in early life and its effect on allergen sensitization in mice. *J Allergy Clin Immunol* 112:389-96.
- Gerhold, K., Blumchen, K., Bock, A., Seib, C., Stock, P., Kallinich, T., et al. (2002). Endotoxins prevent murine IgE production, T(H)2 immune responses, and development of airway eosinophilia but not airway hyperreactivity. *J Allergy Clin Immunol* 110:110-6.
- Goldmann, K., Ensminger, S. M. & Spriewald, B. M. (2012). Oral gene application using chitosan-DNA nanoparticles induces transferable tolerance. *Clin Vaccine Immunol* 19:1758-64.
- Goodman, R. B., Strieter, R. M., Martin, D. P., Steinberg, K. P., Milberg, J. A., Maunder, R. J., et al. (1996). Inflammatory cytokines in patients with persistence of the acute respiratory distress syndrome. *Am J Respir Crit Care Med* 154:602-11.
- Gordon, E. D., Sidhu, S. S., Wang, Z. E., Woodruff, P. G., Yuan, S., Solon, M. C., et al. (2012). A protective role for periostin and TGF-beta in IgE-mediated allergy and airway hyperresponsiveness. *Clin Exp Allergy* 42:144-55.
- Gould, H. J. & Sutton, B. J. (2008). IgE in allergy and asthma today. *Nat Rev Immunol* 8:205-17.
- Gri, G., Piconese, S., Frossi, B., Manfroi, V., Merluzzi, S., Tripodo, C., et al. (2008). CD4+CD25+ regulatory T cells suppress mast cell degranulation and allergic responses through OX40-OX40L interaction. *Immunity* 29:771-81.
- Grinberg-Bleyer, Y., Saadoun, D., Baeyens, A., Billiard, F., Goldstein, J. D., Gregoire, S., et al. (2010). Pathogenic T cells have a paradoxical protective effect in murine autoimmune diabetes by boosting Tregs. *J Clin Invest* 120:4558-68.
- Grindebacke, H., Wing, K., Andersson, A. C., Suri-Payer, E., Rak, S. & Rudin, A. (2004). Defective suppression of Th2 cytokines by CD4CD25 regulatory T cells in birch allergics during birch pollen season. *Clin Exp Allergy* 34:1364-72.
- Grommes, J., Morgelin, M. & Soehnlein, O. (2012). Pioglitazone attenuates endotoxin induced acute lung injury by reducing neutrophil recruitment. *Eur Respir J*.
- Gupta, A., Bush, A., Hawrylowicz, C. & Saglani, S. (2012). Vitamin D and asthma in children. *Paediatr Respir Rev* 13:236-43; quiz 243.
- Gustafsson, A., Lindstedt, E., Elfsmark, L. S. & Bucht, A. (2011). Lung exposure of titanium dioxide nanoparticles induces innate immune activation and long-lasting lymphocyte response in the Dark Agouti rat. *J Immunotoxicol* 8:111-21.
- Hahm, K., Cobb, B. S., McCarty, A. S., Brown, K. E., Klug, C. A., Lee, R., et al. (1998). Helios, a T cell-restricted Ikaros family member that quantitatively associates with Ikaros at centromeric heterochromatin. *Genes Dev* 12:782-96.

- Hardy, C. L., Kenins, L., Drew, A. C., Rolland, J. M. & O'Hehir, R. E. (2003). Characterization of a mouse model of allergy to a major occupational latex glove allergen Hev b 5. *Am J Respir Crit Care Med* 167:1393-9.
- Hardy, C. L., Lemasurier, J. S., Belz, G. T., Scalzo-Inguanti, K., Yao, J., Xiang, S. D., et al. (2012a). Inert 50-nm Polystyrene Nanoparticles That Modify Pulmonary Dendritic Cell Function and Inhibit Allergic Airway Inflammation. *J Immunol* 188:1431-41.
- Hardy, C. L., Lemasurier, J. S., Mohamud, R., Yao, J., Xiang, S. D., Rolland, J. M., et al. (2013a). Differential uptake of nanoparticles and microparticles by pulmonary APC subsets induces discrete immunological imprints. *J Immunol* 191:5278-90.
- Hardy, C. L., Lemasurier, J. S., Mohamud, R., Yao, J., Xiang, S. D., Rolland, J. M., et al. (2013b). Differential Uptake of Nanoparticles and Microparticles by Pulmonary APC Subsets Induces Discrete Immunological Imprints. *J Immunol*.
- Hardy, C. L., Lemasurier, J. S., Olsson, F., Dang, T., Yao, J., Yang, M., et al. (2010). Interleukin-13 regulates secretion of the tumor growth factor- β superfamily cytokine activin A in allergic airway inflammation. *Am J Respir Cell Mol Biol* 42:667-75.
- Hardy, C. L., Nguyen, H. A., Mohamud, R., Yao, J., Oh, D. Y., Plebanski, M., et al. (2012b). The activin A antagonist follistatin inhibits asthmatic airway remodelling. *Thorax*.
- Hardy, C. L., Nguyen, H. A., Mohamud, R., Yao, J., Oh, D. Y., Plebanski, M., et al. (2013c). The activin A antagonist follistatin inhibits asthmatic airway remodelling. *Thorax* 68:9-18.
- Hardy, C. L., O'Connor, A. E., Yao, J., Sebire, K., de Kretser, D. M., Rolland, J. M., et al. (2006). Follistatin is a candidate endogenous negative regulator of activin A in experimental allergic asthma. *Clin Exp Allergy* 36:941-50.
- Hartl, D., Koller, B., Mehlhorn, A. T., Reinhardt, D., Nicolai, T., Schendel, D. J., et al. (2007). Quantitative and functional impairment of pulmonary CD4⁺CD25^{hi} regulatory T cells in pediatric asthma. *J Allergy Clin Immunol* 119:1258-66.
- Hawrylowicz, C. M. & O'Garra, A. (2005). Potential role of interleukin-10-secreting regulatory T cells in allergy and asthma. *Nat Rev Immunol* 5:271-83.
- Hedger, M. P., Winnall, W. R., Phillips, D. J. & de Kretser, D. M. (2011). The regulation and functions of activin and follistatin in inflammation and immunity. *Vitam Horm* 85:255-97.
- Herbst, T., Sichelstiel, A., Schar, C., Yadava, K., Burki, K., Cahenzli, J., et al. (2011). Dysregulation of allergic airway inflammation in the absence of microbial colonization. *Am J Respir Crit Care Med* 184:198-205.
- Hernandez, M. L., Harris, B., Lay, J. C., Bromberg, P. A., Diaz-Sanchez, D., Devlin, R. B., et al. (2010). Comparative airway inflammatory response of normal volunteers to ozone and lipopolysaccharide challenge. *Inhal Toxicol* 22:648-56.
- Herrath, J., Muller, M., Amoudruz, P., Janson, P., Michaelsson, J., Larsson, P. T., et al. (2011). The inflammatory milieu in the rheumatic joint reduces regulatory T cell function. *Eur J Immunol*.
- Hill, J. A., Feuerer, M., Tash, K., Haxhinasto, S., Perez, J., Melamed, R., et al. (2007). Foxp3 transcription-factor-dependent and -independent regulation of the regulatory T cell transcriptional signature. *Immunity* 27:786-800.
- Hollingsworth, J. W., Whitehead, G. S., Lin, K. L., Nakano, H., Gunn, M. D., Schwartz, D. A., et al. (2006). TLR4 signaling attenuates ongoing allergic inflammation. *J Immunol* 176:5856-62.

References

- Hori, S., Nomura, T. & Sakaguchi, S. (2003a). Control of regulatory T cell development by the transcription factor Foxp3. *Science* 299:1057-61.
- Hori, S., Takahashi, T. & Sakaguchi, S. (2003b). Control of autoimmunity by naturally arising regulatory CD4⁺ T cells. *Adv Immunol* 81:331-71.
- Housley, W. J., Adams, C. O., Nichols, F. C., Puddington, L., Lingenheld, E. G., Zhu, L., et al. (2011). Natural but not inducible regulatory T cells require TNF- α signaling for in vivo function. *J Immunol* 186:6779-87.
- Housley, W. J., O'Connor, C. A., Nichols, F., Puddington, L., Lingenheld, E. G., Zhu, L., et al. (2009). PPAR γ regulates retinoic acid-mediated DC induction of Tregs. *J Leukoc Biol* 86:293-301.
- Hu, G., Liu, Z., Zheng, C. & Zheng, S. G. (2010). Antigen-non-specific regulation centered on CD25⁺Foxp3⁺ Treg cells. *Cell Mol Immunol* 7:414-8.
- Huang, H., Dawicki, W., Zhang, X., Town, J. & Gordon, J. R. (2010). Tolerogenic dendritic cells induce CD4⁺CD25^{hi}Foxp3⁺ regulatory T cell differentiation from CD4⁺CD25⁻/loFoxp3⁻ effector T cells. *J Immunol* 185:5003-10.
- Huber, S. & Schramm, C. (2011). Role of activin A in the induction of Foxp3⁺ and Foxp3⁻ CD4⁺ regulatory T cells. *Crit Rev Immunol* 31:53-60.
- Huber, S., Schramm, C., Lehr, H. A., Mann, A., Schmitt, S., Becker, C., et al. (2004). Cutting edge: TGF- β signaling is required for the in vivo expansion and immunosuppressive capacity of regulatory CD4⁺CD25⁺ T cells. *J Immunol* 173:6526-31.
- Huber, S., Stahl, F. R., Schrader, J., Luth, S., Presser, K., Carambia, A., et al. (2009). Activin a promotes the TGF- β -induced conversion of CD4⁺CD25⁻ T cells into Foxp3⁺ induced regulatory T cells. *J Immunol* 182:4633-40.
- Huehn, J., Siegmund, K. & Hamann, A. (2005). Migration rules: functional properties of naive and effector/memory-like regulatory T cell subsets. *Curr Top Microbiol Immunol* 293:89-114.
- Hussain, S., Vanoirbeek, J. A., Luyts, K., De Vooght, V., Verbeken, E., Thomassen, L. C., et al. (2011). Lung exposure to nanoparticles modulates an asthmatic response in a mouse model. *Eur Respir J* 37:299-309.
- Iellem, A., Mariani, M., Lang, R., Recalde, H., Panina-Bordignon, P., Sinigaglia, F., et al. (2001). Unique chemotactic response profile and specific expression of chemokine receptors CCR4 and CCR8 by CD4(+)CD25(+) regulatory T cells. *J Exp Med* 194:847-53.
- Inoue, K., Yanagisawa, R., Koike, E., Nishikawa, M. & Takano, H. (2010). Repeated pulmonary exposure to single-walled carbon nanotubes exacerbates allergic inflammation of the airway: Possible role of oxidative stress. *Free Radic Biol Med* 48:924-34.
- Ito, T., Hanabuchi, S., Wang, Y. H., Park, W. R., Arima, K., Bover, L., et al. (2008). Two functional subsets of FOXP3⁺ regulatory T cells in human thymus and periphery. *Immunity* 28:870-80.
- Jain, V. V., Businga, T. R., Kitagaki, K., George, C. L., O'Shaughnessy, P. T. & Kline, J. N. (2003). Mucosal immunotherapy with CpG oligodeoxynucleotides reverses a murine model of chronic asthma induced by repeated antigen exposure. *Am J Physiol Lung Cell Mol Physiol* 285:L1137-46.
- Janeway, C. A., Jr. & Bottomly, K. (1994). Signals and signs for lymphocyte responses. *Cell* 76:275-85.
- Jang, S., Park, J. W., Cha, H. R., Jung, S. Y., Lee, J. E., Jung, S. S., et al. (2012). Silver nanoparticles modify VEGF signaling pathway and mucus hypersecretion in allergic airway inflammation. *Int J Nanomedicine* 7:1329-43.

- Jensen, D. K., Jensen, L. B., Koocheki, S., Bengtson, L., Cun, D., Nielsen, H. M., et al. (2012). Design of an inhalable dry powder formulation of DOTAP-modified PLGA nanoparticles loaded with siRNA. *J Control Release* 157:141-8.
- Ji, H. B., Liao, G., Faubion, W. A., Abadia-Molina, A. C., Cozzo, C., Laroux, F. S., et al. (2004). Cutting edge: the natural ligand for glucocorticoid-induced TNF receptor-related protein abrogates regulatory T cell suppression. *J Immunol* 172:5823-7.
- Joetham, A., Takeda, K., Okamoto, M., Taube, C., Matsuda, H., Dakhama, A., et al. (2009). Antigen specificity is not required for modulation of lung allergic responses by naturally occurring regulatory T cells. *J Immunol* 183:1821-7.
- John, A. E., Lukacs, N. W., Berlin, A. A., Palecanda, A., Bargatze, R. F., Stoolman, L. M., et al. (2003). Discovery of a potent nanoparticle P-selectin antagonist with anti-inflammatory effects in allergic airway disease. *FASEB J* 17:2296-8.
- Johnson, J. R., Wiley, R. E., Fattouh, R., Swirski, F. K., Gajewska, B. U., Coyle, A. J., et al. (2004). Continuous exposure to house dust mite elicits chronic airway inflammation and structural remodeling. *Am J Respir Crit Care Med* 169:378-85.
- Jones, K. L., de Kretser, D. M., Clarke, I. J., Scheerlinck, J. P. & Phillips, D. J. (2004). Characterisation of the rapid release of activin A following acute lipopolysaccharide challenge in the ewe. *J Endocrinol* 182:69-80.
- Jones, K. L., Mansell, A., Patella, S., Scott, B. J., Hedger, M. P., de Kretser, D. M., et al. (2007). Activin A is a critical component of the inflammatory response, and its binding protein, follistatin, reduces mortality in endotoxemia. *Proc Natl Acad Sci U S A* 104:16239-44.
- Jonuleit, H. & Schmitt, E. (2003). The regulatory T cell family: distinct subsets and their interrelations. *J Immunol* 171:6323-7.
- Jung, Y. J. & Seoh, J. Y. (2009). Feedback loop of immune regulation by CD4+CD25+ Treg. *Immunobiology* 214:291-302.
- Jung, Y. W., Schoeb, T. R., Weaver, C. T. & Chaplin, D. D. (2006). Antigen and lipopolysaccharide play synergistic roles in the effector phase of airway inflammation in mice. *Am J Pathol* 168:1425-34.
- Jungsuwadee, P., Benkovszky, M., Dekan, G., Stingl, G. & Epstein, M. M. (2004). Repeated aerosol allergen exposure suppresses inflammation in B-cell-deficient mice with established allergic asthma. *Int Arch Allergy Immunol* 133:40-8.
- Kalishwaralal, K., Banumathi, E., Ram Kumar Pandian, S., Deepak, V., Muniyandi, J., Eom, S. H., et al. (2009). Silver nanoparticles inhibit VEGF induced cell proliferation and migration in bovine retinal endothelial cells. *Colloids Surf B Biointerfaces* 73:51-7.
- Kang, H. G., Zhang, D., Degauque, N., Mariat, C., Alexopoulos, S. & Zheng, X. X. (2007). Effects of cyclosporine on transplant tolerance: the role of IL-2. *Am J Transplant* 7:1907-16.
- Karagiannidis, C., Hense, G., Martin, C., Epstein, M., Ruckert, B., Mantel, P. Y., et al. (2006). Activin A is an acute allergen-responsive cytokine and provides a link to TGF-beta-mediated airway remodeling in asthma. *J Allergy Clin Immunol* 117:111-8.
- Karamatsu, K., Matsuo, K., Inada, H., Tsujimura, Y., Shiogama, Y., Matsubara, A., et al. (2012). Single systemic administration of Ag85B of mycobacteria DNA inhibits allergic airway inflammation in a mouse model of asthma. *J Asthma Allergy* 5:71-9.
- Kariyawasam, H. H., Semitekolou, M., Robinson, D. S. & Xanthou, G. (2011). Activin-A: a novel critical regulator of allergic asthma. *Clin Exp Allergy* 41:1505-14.

References

- Karlson, T. D., Kong, Y. Y., Hardy, C. L., Xiang, S. D. & Plebanski, M. (2013). The signalling imprints of nanoparticle uptake by bone marrow derived dendritic cells. *Methods*.
- Karlson Tde, L., Kong, Y. Y., Hardy, C. L., Xiang, S. D. & Plebanski, M. (2013). The signalling imprints of nanoparticle uptake by bone marrow derived dendritic cells. *Methods* 60:275-83.
- Karlsson, H. L., Cronholm, P., Gustafsson, J. & Moller, L. (2008). Copper oxide nanoparticles are highly toxic: a comparison between metal oxide nanoparticles and carbon nanotubes. *Chem Res Toxicol* 21:1726-32.
- Karlsson, M. R., Rugtveit, J. & Brandtzaeg, P. (2004). Allergen-responsive CD4+CD25+ regulatory T cells in children who have outgrown cow's milk allergy. *J Exp Med* 199:1679-88.
- Kaur, G., Narang, R. K., Rath, G. & Goyal, A. K. (2012). Advances in pulmonary delivery of nanoparticles. *Artif Cells Blood Substit Immobil Biotechnol* 40:75-96.
- Kearley, J., Robinson, D. S. & Lloyd, C. M. (2008). CD4+CD25+ regulatory T cells reverse established allergic airway inflammation and prevent airway remodeling. *J Allergy Clin Immunol* 122:617-24 e6.
- Keatings, V. M., Collins, P. D., Scott, D. M. & Barnes, P. J. (1996). Differences in interleukin-8 and tumor necrosis factor-alpha in induced sputum from patients with chronic obstructive pulmonary disease or asthma. *Am J Respir Crit Care Med* 153:530-4.
- Kelley, C. M., Ikeda, T., Koipally, J., Avitahl, N., Wu, L., Georgopoulos, K., et al. (1998). Helios, a novel dimerization partner of Ikaros expressed in the earliest hematopoietic progenitors. *Curr Biol* 8:508-15.
- Kerksiek, K. M., Niedergang, F., Chavrier, P., Busch, D. H. & Brocker, T. (2005). Selective Rac1 inhibition in dendritic cells diminishes apoptotic cell uptake and cross-presentation in vivo. *Blood* 105:742-9.
- Khare, A., Krishnamoorthy, N., Oriss, T. B., Fei, M., Ray, P. & Ray, A. (2013). Cutting Edge: Inhaled Antigen Upregulates Retinaldehyde Dehydrogenase in Lung CD103+ but Not Plasmacytoid Dendritic Cells To Induce Foxp3 De Novo in CD4+ T Cells and Promote Airway Tolerance. *J Immunol* 191:25-9.
- Khatttri, R., Cox, T., Yasayko, S. A. & Ramsdell, F. (2003). An essential role for Scurfin in CD4+CD25+ T regulatory cells. *Nat Immunol* 4:337-42.
- Khayrullina, T., Yen, J. H., Jing, H. & Ganea, D. (2008). In vitro differentiation of dendritic cells in the presence of prostaglandin E2 alters the IL-12/IL-23 balance and promotes differentiation of Th17 cells. *J Immunol* 181:721-35.
- Kim, B. S., Kim, I. K., Park, Y. J., Kim, Y. S., Kim, Y. J., Chang, W. S., et al. (2010). Conversion of Th2 memory cells into Foxp3+ regulatory T cells suppressing Th2-mediated allergic asthma. *Proc Natl Acad Sci U S A* 107:8742-7.
- Kim, Y. K., Oh, S. Y., Jeon, S. G., Park, H. W., Lee, S. Y., Chun, E. Y., et al. (2007). Airway exposure levels of lipopolysaccharide determine type 1 versus type 2 experimental asthma. *J Immunol* 178:5375-82.
- Kips, J. C., Anderson, G. P., Fredberg, J. J., Herz, U., Inman, M. D., Jordana, M., et al. (2003). Murine models of asthma. *Eur Respir J* 22:374-82.
- Kleijwegt, F. S., Laban, S., Duinkerken, G., Joosten, A. M., Zaldumbide, A., Nikolic, T., et al. (2010). Critical role for TNF in the induction of human antigen-specific regulatory T cells by tolerogenic dendritic cells. *J Immunol* 185:1412-8.
- Klein, L., Khazaie, K. & von Boehmer, H. (2003). In vivo dynamics of antigen-specific regulatory T cells not predicted from behavior in vitro. *Proc Natl Acad Sci U S A* 100:8886-91.

- Knuschke, T., Sokolova, V., Rotan, O., Wadwa, M., Tenbusch, M., Hansen, W., et al. (2013). Immunization with biodegradable nanoparticles efficiently induces cellular immunity and protects against influenza virus infection. *J Immunol* 190:6221-9.
- Ko, H. J., Brady, J. L., Ryg-Cornejo, V., Hansen, D. S., Vremec, D., Shortman, K., et al. (2014). GM-CSF-Responsive Monocyte-Derived Dendritic Cells Are Pivotal in Th17 Pathogenesis. *J Immunol* 192:2202-9.
- Kocks, J. R., Davalos-Misslitz, A. C., Hintzen, G., Ohl, L. & Forster, R. (2007). Regulatory T cells interfere with the development of bronchus-associated lymphoid tissue. *J Exp Med* 204:723-34.
- Kollias, G. & Kontoyiannis, D. (2002). Role of TNF/TNFR in autoimmunity: specific TNF receptor blockade may be advantageous to anti-TNF treatments. *Cytokine Growth Factor Rev* 13:315-21.
- Kong, Y. Y., Fuchsberger, M., Xiang, S. D., Apostolopoulo, V. & Plebanski, M. (2013). Myeloid Derived Suppressor Cells and Their Role in Diseases. *Curr Med Chem*.
- Krishnamoorthy, N., oriss, T., Paglia, M., Ray, A. & Ray, P. (2007). A critical role for IL-6 secretion by dendritic cells promoting Th2 and limiting Th1 response. *J Immunol* 178:S181-c-.
- Krummel, M. F. & Allison, J. P. (1996). CTLA-4 engagement inhibits IL-2 accumulation and cell cycle progression upon activation of resting T cells. *J Exp Med* 183:2533-40.
- Krummen, L. A., Woodruff, T. K., DeGuzman, G., Cox, E. T., Baly, D. L., Mann, E., et al. (1993). Identification and characterization of binding proteins for inhibin and activin in human serum and follicular fluids. *Endocrinology* 132:431-43.
- Kuipers, H., Hijdra, D., De Vries, V. C., Hammad, H., Prins, J. B., Coyle, A. J., et al. (2003). Lipopolysaccharide-induced suppression of airway Th2 responses does not require IL-12 production by dendritic cells. *J Immunol* 171:3645-54.
- Kumar, R. K. & Foster, P. S. (2002). Modeling allergic asthma in mice: pitfalls and opportunities. *Am J Respir Cell Mol Biol* 27:267-72.
- Kumar, R. K., Herbert, C. & Foster, P. S. (2008). The "classical" ovalbumin challenge model of asthma in mice. *Curr Drug Targets* 9:485-94.
- Laan, M., Cui, Z. H., Hoshino, H., Lotvall, J., Sjostrand, M., Gruenert, D. C., et al. (1999). Neutrophil recruitment by human IL-17 via C-X-C chemokine release in the airways. *J Immunol* 162:2347-52.
- Lambrecht, B. N. & Hammad, H. (2009). Biology of lung dendritic cells at the origin of asthma. *Immunity* 31:412-24.
- Larche, M. (2007). Regulatory T cells in allergy and asthma. *Chest* 132:1007-14.
- Larsen, S. T., Roursgaard, M., Jensen, K. A. & Nielsen, G. D. (2010). Nano titanium dioxide particles promote allergic sensitization and lung inflammation in mice. *Basic Clin Pharmacol Toxicol* 106:114-7.
- Le, A. V., Cho, J. Y., Miller, M., McElwain, S., Golgotiu, K. & Broide, D. H. (2007). Inhibition of allergen-induced airway remodeling in Smad 3-deficient mice. *J Immunol* 178:7310-6.
- Lee, J. H., Kang, S. G. & Kim, C. H. (2007). FoxP3+ T cells undergo conventional first switch to lymphoid tissue homing receptors in thymus but accelerated second switch to nonlymphoid tissue homing receptors in secondary lymphoid tissues. *J Immunol* 178:301-11.
- Lee, S. W., Park, Y., Eun, S. Y., Madireddi, S., Cheroutre, H. & Croft, M. (2012). Cutting edge: 4-1BB controls regulatory activity in dendritic cells through promoting optimal expression of retinal dehydrogenase. *J Immunol* 189:2697-701.

References

- Lefort, J., Motreff, L. & Vargaftig, B. B. (2001). Airway administration of *Escherichia coli* endotoxin to mice induces glucocorticosteroid-resistant bronchoconstriction and vasopermeation. *Am J Respir Cell Mol Biol* 24:345-51.
- Lewkowich, I. P., Herman, N. S., Schleifer, K. W., Dance, M. P., Chen, B. L., Dienger, K. M., et al. (2005). CD4+CD25+ T cells protect against experimentally induced asthma and alter pulmonary dendritic cell phenotype and function. *J Exp Med* 202:1549-61.
- Lewkowicz, P., Lewkowicz, N., Sasiak, A. & Tchorzewski, H. (2006). Lipopolysaccharide-activated CD4+CD25+ T regulatory cells inhibit neutrophil function and promote their apoptosis and death. *J Immunol* 177:7155-63.
- Li, M. O., Sanjabi, S. & Flavell, R. A. (2006). Transforming growth factor-beta controls development, homeostasis, and tolerance of T cells by regulatory T cell-dependent and -independent mechanisms. *Immunity* 25:455-71.
- Lin, Y. L., Shieh, C. C. & Wang, J. Y. (2008). The functional insufficiency of human CD4+CD25 high T-regulatory cells in allergic asthma is subjected to TNF-alpha modulation. *Allergy* 63:67-74.
- Ling, E. M., Smith, T., Nguyen, X. D., Pridgeon, C., Dallman, M., Arbery, J., et al. (2004). Relation of CD4+CD25+ regulatory T-cell suppression of allergen-driven T-cell activation to atopic status and expression of allergic disease. *Lancet* 363:608-15.
- Liston, A. & Rudensky, A. Y. (2007). Thymic development and peripheral homeostasis of regulatory T cells. *Curr Opin Immunol* 19:176-85.
- Liu, Y., Zhang, P., Li, J., Kulkarni, A. B., Perruche, S. & Chen, W. (2008). A critical function for TGF-beta signaling in the development of natural CD4+CD25+Foxp3+ regulatory T cells. *Nat Immunol* 9:632-40.
- Lloyd, C. M. & Hawrylowicz, C. M. (2009). Regulatory T cells in asthma. *Immunity* 31:438-49.
- Lluis, A., Depner, M., Gaugler, B., Saas, P., Casaca, V. I., Raedler, D., et al. (2013). Increased regulatory T-cell numbers are associated with farm milk exposure and lower atopic sensitization and asthma in childhood. *J Allergy Clin Immunol*.
- Loures, F. V., Pina, A., Felonato, M., Araujo, E. F., Leite, K. R. & Calich, V. L. (2010). Toll-like receptor 4 signaling leads to severe fungal infection associated with enhanced proinflammatory immunity and impaired expansion of regulatory T cells. *Infect Immun* 78:1078-88.
- Lu, Y., Malmhall, C., Sjostrand, M., Radinger, M., O'Neil, S. E., Lotvall, J., et al. (2011). Expansion of CD4(+) CD25(+) and CD25(-) T-Bet, GATA-3, Foxp3 and RORgammat cells in allergic inflammation, local lung distribution and chemokine gene expression. *PLoS One* 6:e19889.
- MacCallum, N. S. & Evans, T. W. (2005). Epidemiology of acute lung injury. *Curr Opin Crit Care* 11:43-9.
- Maganto-Garcia, E., Bu, D. X., Tarrio, M. L., Alcaide, P., Newton, G., Griffin, G. K., et al. (2011). Foxp3+-inducible regulatory T cells suppress endothelial activation and leukocyte recruitment. *J Immunol* 187:3521-9.
- Magram, J., Connaughton, S. E., Warriar, R. R., Carvajal, D. M., Wu, C. Y., Ferrante, J., et al. (1996). IL-12-deficient mice are defective in IFN gamma production and type 1 cytokine responses. *Immunity* 4:471-81.
- Mamessier, E., Nieves, A., Lorec, A. M., Dupuy, P., Pinot, D., Pinet, C., et al. (2008). T-cell activation during exacerbations: a longitudinal study in refractory asthma. *Allergy* 63:1202-10.

- Marie, J. C., Letterio, J. J., Gavin, M. & Rudensky, A. Y. (2005). TGF-beta1 maintains suppressor function and Foxp3 expression in CD4+CD25+ regulatory T cells. *J Exp Med* 201:1061-7.
- Matesic, D., Lenert, A. & Lenert, P. (2012). Modulating toll-like receptor 7 and 9 responses as therapy for allergy and autoimmunity. *Curr Allergy Asthma Rep* 12:8-17.
- Matsumoto, K., Inoue, H., Fukuyama, S., Kan, O. K., Eguchi-Tsuda, M., Matsumoto, T., et al. (2009). Frequency of Foxp3+CD4CD25+ T cells is associated with the phenotypes of allergic asthma. *Respirology* 14:187-94.
- Matsushita, H., Ohta, S., Shiraishi, H., Suzuki, S., Arima, K., Toda, S., et al. (2010). Endotoxin tolerance attenuates airway allergic inflammation in model mice by suppression of the T-cell stimulatory effect of dendritic cells. *Int Immunol* 22:739-47.
- Matute-Bello, G., Frevert, C. W. & Martin, T. R. (2008). Animal models of acute lung injury. *Am J Physiol Lung Cell Mol Physiol* 295:L379-99.
- McHugh, R. S., Whitters, M. J., Piccirillo, C. A., Young, D. A., Shevach, E. M., Collins, M., et al. (2002). CD4(+)CD25(+) immunoregulatory T cells: gene expression analysis reveals a functional role for the glucocorticoid-induced TNF receptor. *Immunity* 16:311-23.
- McMillan, S. J. & Lloyd, C. M. (2004). Prolonged allergen challenge in mice leads to persistent airway remodelling. *Clin Exp Allergy* 34:497-507.
- McPhillips, K., Janssen, W. J., Ghosh, M., Byrne, A., Gardai, S., Remigio, L., et al. (2007). TNF-alpha inhibits macrophage clearance of apoptotic cells via cytosolic phospholipase A2 and oxidant-dependent mechanisms. *J Immunol* 178:8117-26.
- Mei, S. H., McCarter, S. D., Deng, Y., Parker, C. H., Liles, W. C. & Stewart, D. J. (2007). Prevention of LPS-induced acute lung injury in mice by mesenchymal stem cells overexpressing angiopoietin 1. *PLoS Med* 4:e269.
- Meiler, F., Klunker, S., Zimmermann, M., Akdis, C. A. & Akdis, M. (2008). Distinct regulation of IgE, IgG4 and IgA by T regulatory cells and toll-like receptors. *Allergy* 63:1455-63.
- Menden, H., Tate, E., Hogg, N. & Sampath, V. (2013). LPS-mediated endothelial activation in pulmonary endothelial cells: role of Nox2-dependent IKK-beta phosphorylation. *Am J Physiol Lung Cell Mol Physiol* 304:L445-55.
- Menning, A., Hopken, U. E., Siegmund, K., Lipp, M., Hamann, A. & Huehn, J. (2007). Distinctive role of CCR7 in migration and functional activity of naive- and effector/memory-like Treg subsets. *Eur J Immunol* 37:1575-83.
- Michel, O., Ginanni, R., Duchateau, J., Vertongen, F., Le Bon, B. & Sergysels, R. (1991). Domestic endotoxin exposure and clinical severity of asthma. *Clin Exp Allergy* 21:441-8.
- Minigo, G., Woodberry, T., Piera, K. A., Salwati, E., Tjitra, E., Kenangalem, E., et al. (2009). Parasite-dependent expansion of TNF receptor II-positive regulatory T cells with enhanced suppressive activity in adults with severe malaria. *PLoS Pathog* 5:e1000402.
- Miyazono, K., Ichijo, H. & Heldin, C. H. (1993). Transforming growth factor-beta: latent forms, binding proteins and receptors. *Growth Factors* 8:11-22.
- Mohamud, R., Xiang, S. D., Selomulya, C., Rolland, J. M., O'Hehir, R. E., Hardy, C. L., et al. (2013). The effects of engineered nanoparticles on pulmonary immune homeostasis. *Drug Metab Rev*.

References

- Mougiakakos, D., Johansson, C. C., Jitschin, R., Bottcher, M. & Kiessling, R. (2011). Increased thioredoxin-1 production in human naturally occurring regulatory T cells confers enhanced tolerance to oxidative stress. *Blood* 117:857-61.
- Mukhopadhyay, S., Hoidal, J. R. & Mukherjee, T. K. (2006). Role of TNF α in pulmonary pathophysiology. *Respir Res* 7:125.
- Munz, B., Hubner, G., Tretter, Y., Alzheimer, C. & Werner, S. (1999). A novel role of activin in inflammation and repair. *J Endocrinol* 161:187-93.
- Murakami, M., Sakamoto, A., Bender, J., Kappler, J. & Marrack, P. (2002). CD25+CD4+ T cells contribute to the control of memory CD8+ T cells. *Proc Natl Acad Sci U S A* 99:8832-7.
- Nakae, S., Lunderius, C., Ho, L. H., Schafer, B., Tsai, M. & Galli, S. J. (2007). TNF can contribute to multiple features of ovalbumin-induced allergic inflammation of the airways in mice. *J Allergy Clin Immunol* 119:680-6.
- Nials, A. T. & Uddin, S. (2008). Mouse models of allergic asthma: acute and chronic allergen challenge. *Dis Model Mech* 1:213-20.
- O'Garra, A. & Vieira, P. (2004). Regulatory T cells and mechanisms of immune system control. *Nat Med* 10:801-5.
- Oberdorster, G., Gelein, R. M., Ferin, J. & Weiss, B. (1995). Association of particulate air pollution and acute mortality: involvement of ultrafine particles? *Inhal Toxicol* 7:111-24.
- Ogawa, K., Funaba, M., Chen, Y. & Tsujimoto, M. (2006). Activin A functions as a Th2 cytokine in the promotion of the alternative activation of macrophages. *J Immunol* 177:6787-94.
- Ogawa, K., Funaba, M. & Tsujimoto, M. (2008). A dual role of activin A in regulating immunoglobulin production of B cells. *J Leukoc Biol* 83:1451-8.
- Oida, T. & Weiner, H. L. (2010). TGF- β induces surface LAP expression on murine CD4 T cells independent of Foxp3 induction. *PLoS One* 5:e15523.
- Pace, E., Di Sano, C., La Grutta, S., Ferraro, M., Albeggiani, G., Liotta, G., et al. (2012). Multiple In Vitro and In Vivo Regulatory Effects of Budesonide in CD4+ T Lymphocyte Subpopulations of Allergic Asthmatics. *PLoS One* 7:e48816.
- Park, H. S., Kim, K. H., Jang, S., Park, J. W., Cha, H. R., Lee, J. E., et al. (2010). Attenuation of allergic airway inflammation and hyperresponsiveness in a murine model of asthma by silver nanoparticles. *Int J Nanomedicine* 5:505-15.
- Park, J. H., Szponar, B., Larsson, L., Gold, D. R. & Milton, D. K. (2004). Characterization of lipopolysaccharides present in settled house dust. *Appl Environ Microbiol* 70:262-7.
- Pasare, C. & Medzhitov, R. (2003). Toll pathway-dependent blockade of CD4+CD25+ T cell-mediated suppression by dendritic cells. *Science* 299:1033-6.
- Pearce, N., Ait-Khaled, N., Beasley, R., Mallol, J., Keil, U., Mitchell, E., et al. (2007). Worldwide trends in the prevalence of asthma symptoms: phase III of the International Study of Asthma and Allergies in Childhood (ISAAC). *Thorax* 62:758-66.
- Peek, L. J., Middaugh, C. R. & Berkland, C. (2008). Nanotechnology in vaccine delivery. *Adv Drug Deliv Rev* 60:915-28.
- Phillips, D. J., de Kretser, D. M. & Hedger, M. P. (2009). Activin and related proteins in inflammation: not just interested bystanders. *Cytokine Growth Factor Rev* 20:153-64.
- Pierson, W., Cauwe, B., Policheni, A., Schlenner, S. M., Franckaert, D., Berges, J., et al. (2013). Antiapoptotic Mcl-1 is critical for the survival and niche-filling capacity of Foxp3 regulatory T cells. *Nat Immunol*.

- Pietruczuk, M., Eusebio, M., Kraszula, L., Kupczyk, M. & Kuna, P. (2012). Phenotypic characterization of ex vivo CD4⁺CD25^{high}CD127^{low} immune regulatory T cells in allergic asthma: pathogenesis relevance of their FoxP3, GITR, CTLA-4 and FAS expressions. *J Biol Regul Homeost Agents* 26:627-39.
- Pugin, J., Schurer-Maly, C. C., Leturcq, D., Moriarty, A., Ulevitch, R. J. & Tobias, P. S. (1993). Lipopolysaccharide activation of human endothelial and epithelial cells is mediated by lipopolysaccharide-binding protein and soluble CD14. *Proc Natl Acad Sci U S A* 90:2744-8.
- Qu, S. Y., Ou-Yang, H. F., He, Y. L., Wan, Q., Shi, J. R. & Wu, C. G. (2013). Der p 2 Recombinant Bacille Calmette-Guerin Targets Dendritic Cells to Inhibit Allergic Airway Inflammation in a Mouse Model of Asthma. *Respiration* 85:49-58.
- Radstake, T. R., van Lent, P. L., Pesman, G. J., Blom, A. B., Sweep, F. G., Ronnelid, J., et al. (2004). High production of proinflammatory and Th1 cytokines by dendritic cells from patients with rheumatoid arthritis, and down regulation upon FcγR triggering. *Ann Rheum Dis* 63:696-702.
- Ramos-Barbon, D., Ludwig, M. S. & Martin, J. G. (2004). Airway remodeling: lessons from animal models. *Clin Rev Allergy Immunol* 27:3-21.
- Randall, T. D. (2010). Pulmonary dendritic cells: thinking globally, acting locally. *J Exp Med* 207:451-4.
- Read, S., Greenwald, R., Izcue, A., Robinson, N., Mandelbrot, D., Francisco, L., et al. (2006). Blockade of CTLA-4 on CD4⁺CD25⁺ regulatory T cells abrogates their function in vivo. *J Immunol* 177:4376-83.
- Read, S., Malmstrom, V. & Powrie, F. (2000). Cytotoxic T lymphocyte-associated antigen 4 plays an essential role in the function of CD25⁽⁺⁾CD4⁽⁺⁾ regulatory cells that control intestinal inflammation. *J Exp Med* 192:295-302.
- Reddy, S. T., van der Vlies, A. J., Simeoni, E., Angeli, V., Randolph, G. J., O'Neil, C. P., et al. (2007). Exploiting lymphatic transport and complement activation in nanoparticle vaccines. *Nat Biotechnol* 25:1159-64.
- Revets, H., Pynaert, G., Grooten, J. & De Baetselier, P. (2005). Lipoprotein I, a TLR2/4 ligand modulates Th2-driven allergic immune responses. *J Immunol* 174:1097-103.
- Robson, N. C., Phillips, D. J., McAlpine, T., Shin, A., Svobodova, S., Toy, T., et al. (2008). Activin-A: a novel dendritic cell-derived cytokine that potently attenuates CD40 ligand-specific cytokine and chemokine production. *Blood* 111:2733-43.
- Rodriguez, D., Keller, A. C., Faquim-Mauro, E. L., de Macedo, M. S., Cunha, F. Q., Lefort, J., et al. (2003). Bacterial lipopolysaccharide signaling through Toll-like receptor 4 suppresses asthma-like responses via nitric oxide synthase 2 activity. *J Immunol* 171:1001-8.
- Rojas, M., Woods, C. R., Mora, A. L., Xu, J. & Brigham, K. L. (2005). Endotoxin-induced lung injury in mice: structural, functional, and biochemical responses. *Am J Physiol Lung Cell Mol Physiol* 288:L333-41.
- Roncarolo, M. G., Gregori, S., Battaglia, M., Bacchetta, R., Fleischhauer, K. & Levings, M. K. (2006). Interleukin-10-secreting type 1 regulatory T cells in rodents and humans. *Immunol Rev* 212:28-50.
- Rosendahl, A., Checchin, D., Fehniger, T. E., ten Dijke, P., Heldin, C. H. & Sideras, P. (2001). Activation of the TGF-β/activin-Smad2 pathway during allergic airway inflammation. *Am J Respir Cell Mol Biol* 25:60-8.
- Rossi, E. M., Pylkkanen, L., Koivisto, A. J., Nykasenoja, H., Wolff, H., Savolainen, K., et al. (2010a). Inhalation exposure to nanosized and fine TiO₂ particles inhibits features of allergic asthma in a murine model. *Part Fibre Toxicol* 7:35.

References

- Rossi, E. M., Pylkkanen, L., Koivisto, A. J., Vippola, M., Jensen, K. A., Miettinen, M., et al. (2010b). Airway exposure to silica-coated TiO₂ nanoparticles induces pulmonary neutrophilia in mice. *Toxicol Sci* 113:422-33.
- Rubenfeld, G. D., Caldwell, E., Peabody, E., Weaver, J., Martin, D. P., Neff, M., et al. (2005). Incidence and outcomes of acute lung injury. *N Engl J Med* 353:1685-93.
- Sakaguchi, S. (2000). Regulatory T cells: key controllers of immunologic self-tolerance. *Cell* 101:455-8.
- Sakaguchi, S. (2004). Naturally arising CD4⁺ regulatory t cells for immunologic self-tolerance and negative control of immune responses. *Annu Rev Immunol* 22:531-62.
- Sakaguchi, S. (2005). Naturally arising Foxp3-expressing CD25⁺CD4⁺ regulatory T cells in immunological tolerance to self and non-self. *Nat Immunol* 6:345-52.
- Sakaguchi, S., Sakaguchi, N., Asano, M., Itoh, M. & Toda, M. (1995). Immunologic self-tolerance maintained by activated T cells expressing IL-2 receptor alpha-chains (CD25). Breakdown of a single mechanism of self-tolerance causes various autoimmune diseases. *J Immunol* 155:1151-64.
- Sallusto, F., Nicolo, C., De Maria, R., Corinti, S. & Testi, R. (1996). Ceramide inhibits antigen uptake and presentation by dendritic cells. *J Exp Med* 184:2411-6.
- Sarpong, S. B., Zhang, L. Y. & Kleeberger, S. R. (2003). A novel mouse model of experimental asthma. *Int Arch Allergy Immunol* 132:346-54.
- Sather, B. D., Treuting, P., Perdue, N., Miazgowiec, M., Fontenot, J. D., Rudensky, A. Y., et al. (2007). Altering the distribution of Foxp3(+) regulatory T cells results in tissue-specific inflammatory disease. *J Exp Med* 204:1335-47.
- Schaub, B., Liu, J., Hoppler, S., Schleich, I., Huehn, J., Olek, S., et al. (2009). Maternal farm exposure modulates neonatal immune mechanisms through regulatory T cells. *J Allergy Clin Immunol* 123:774-82 e5.
- Schmidt, E. M., Wang, C. J., Ryan, G. A., Clough, L. E., Qureshi, O. S., Goodall, M., et al. (2009). Ctla-4 controls regulatory T cell peripheral homeostasis and is required for suppression of pancreatic islet autoimmunity. *J Immunol* 182:274-82.
- Schneider, A., Rieck, M., Sanda, S., Pihoker, C., Greenbaum, C. & Buckner, J. H. (2008). The effector T cells of diabetic subjects are resistant to regulation via CD4⁺ FOXP3⁺ regulatory T cells. *J Immunol* 181:7350-5.
- Schneider, J., Gilbert, S. C., Blanchard, T. J., Hanke, T., Robson, K. J., Hannan, C. M., et al. (1998). Enhanced immunogenicity for CD8⁺ T cell induction and complete protective efficacy of malaria DNA vaccination by boosting with modified vaccinia virus Ankara. *Nat Med* 4:397-402.
- Schneider, M. A., Meingassner, J. G., Lipp, M., Moore, H. D. & Rot, A. (2007). CCR7 is required for the in vivo function of CD4⁺ CD25⁺ regulatory T cells. *J Exp Med* 204:735-45.
- Schnyder-Candrian, S., Quesniaux, V. F., Di Padova, F., Maillet, I., Noulin, N., Couillin, I., et al. (2005). Dual effects of p38 MAPK on TNF-dependent bronchoconstriction and TNF-independent neutrophil recruitment in lipopolysaccharide-induced acute respiratory distress syndrome. *J Immunol* 175:262-9.
- Schulz, C., Farkas, L., Wolf, K., Kratzel, K., Eissner, G. & Pfeifer, M. (2002). Differences in LPS-induced activation of bronchial epithelial cells (BEAS-2B) and type II-like pneumocytes (A-549). *Scand J Immunol* 56:294-302.
- Schwartz, J., Dockery, D. W. & Neas, L. M. (1996). Is daily mortality associated specifically with fine particles? *J Air Waste Manag Assoc* 46:927-39.

- Semitekolou, M., Alissafi, T., Aggelakopoulou, M., Kourepini, E., Kariyawasam, H. H., Kay, A. B., et al. (2009). Activin-A induces regulatory T cells that suppress T helper cell immune responses and protect from allergic airway disease. *J Exp Med* 206:1769-85.
- Sfikakis, P. P. (2010). The first decade of biologic TNF antagonists in clinical practice: lessons learned, unresolved issues and future directions. *Curr Dir Autoimmun* 11:180-210.
- Shevach, E. M. (2002). CD4⁺ CD25⁺ suppressor T cells: more questions than answers. *Nat Rev Immunol* 2:389-400.
- Shevach, E. M. & Stephens, G. L. (2006). The GITR-GITRL interaction: co-stimulation or contrasuppression of regulatory activity? *Nat Rev Immunol* 6:613-8.
- Shi, H. Z. & Qin, X. J. (2005). CD4CD25 regulatory T lymphocytes in allergy and asthma. *Allergy* 60:986-95.
- Shima, F., Uto, T., Akagi, T. & Akashi, M. (2013). Synergistic stimulation of antigen presenting cells via TLR by combining CpG ODN and poly(gamma-glutamic acid)-based nanoparticles as vaccine adjuvants. *Bioconjug Chem* 24:926-33.
- Shinagawa, K. & Kojima, M. (2003). Mouse model of airway remodeling: strain differences. *Am J Respir Crit Care Med* 168:959-67.
- Shoenfelt, J., Mitkus, R. J., Zeisler, R., Spatz, R. O., Powell, J., Fenton, M. J., et al. (2009). Involvement of TLR2 and TLR4 in inflammatory immune responses induced by fine and coarse ambient air particulate matter. *J Leukoc Biol* 86:303-12.
- Sibille, Y. & Reynolds, H. Y. (1990). Macrophages and polymorphonuclear neutrophils in lung defense and injury. *Am Rev Respir Dis* 141:471-501.
- Siegmund, K., Feuerer, M., Siewert, C., Ghani, S., Haubold, U., Dankof, A., et al. (2005). Migration matters: regulatory T-cell compartmentalization determines suppressive activity in vivo. *Blood* 106:3097-104.
- Silvestri, M., Bontempelli, M., Giacomelli, M., Malerba, M., Rossi, G. A., Di Stefano, A., et al. (2006). High serum levels of tumour necrosis factor-alpha and interleukin-8 in severe asthma: markers of systemic inflammation? *Clin Exp Allergy* 36:1373-81.
- Skrindo, I., Scheel, C., Johansen, F. E. & Jahnsen, F. L. (2011). Experimentally induced accumulation of Foxp3(+) T cells in upper airway allergy. *Clin Exp Allergy* 41:954-62.
- So, T., Lee, S. W. & Croft, M. (2006). Tumor necrosis factor/tumor necrosis factor receptor family members that positively regulate immunity. *Int J Hematol* 83:1-11.
- Soppimath, K. S., Aminabhavi, T. M., Kulkarni, A. R. & Rudzinski, W. E. (2001). Biodegradable polymeric nanoparticles as drug delivery devices. *J Control Release* 70:1-20.
- Soroosh, P., Doherty, T. A., Duan, W., Mehta, A. K., Choi, H., Adams, Y. F., et al. (2013). Lung-resident tissue macrophages generate Foxp3⁺ regulatory T cells and promote airway tolerance. *J Exp Med* 210:775-88.
- Steinman, R. M. (2001). Dendritic cells and the control of immunity: enhancing the efficiency of antigen presentation. *Mt Sinai J Med* 68:160-6.
- Steinman, R. M. & Banchereau, J. (2007). Taking dendritic cells into medicine. *Nature* 449:419-426.
- Steinmuller, C., Franke-Ullmann, G., Lohmann-Matthes, M. L. & Emmendorffer, A. (2000). Local activation of nonspecific defense against a respiratory model

References

- infection by application of interferon-gamma: comparison between rat alveolar and interstitial lung macrophages. *Am J Respir Cell Mol Biol* 22:481-90.
- Stephens, G. L., McHugh, R. S., Whitters, M. J., Young, D. A., Luxenberg, D., Carreno, B. M., et al. (2004). Engagement of glucocorticoid-induced TNFR family-related receptor on effector T cells by its ligand mediates resistance to suppression by CD4⁺CD25⁺ T cells. *J Immunol* 173:5008-20.
- Stiehm, M., Bufe, A. & Peters, M. (2013). Proteolytic activity in cowshed dust extracts induces C5a release in murine bronchoalveolar lavage fluids which may account for its protective properties in allergic airway inflammation. *Thorax* 68:31-8.
- Stockis, J., Colau, D., Coulie, P. G. & Lucas, S. (2009). Membrane protein GARP is a receptor for latent TGF-beta on the surface of activated human Treg. *Eur J Immunol* 39:3315-22.
- Stone, V., Johnston, H. & Clift, M. J. (2007). Air pollution, ultrafine and nanoparticle toxicology: cellular and molecular interactions. *IEEE Trans Nanobioscience* 6:331-40.
- Strickland, D. H., Stumbles, P. A., Zosky, G. R., Subrata, L. S., Thomas, J. A., Turner, D. J., et al. (2006). Reversal of airway hyperresponsiveness by induction of airway mucosal CD4⁺CD25⁺ regulatory T cells. *J Exp Med* 203:2649-60.
- Suffner, J., Hochweller, K., Kuhnle, M. C., Li, X., Krocze, R. A., Garbi, N., et al. (2010). Dendritic cells support homeostatic expansion of Foxp3⁺ regulatory T cells in Foxp3.LuciDTR mice. *J Immunol* 184:1810-20.
- Sugimoto, N., Oida, T., Hirota, K., Nakamura, K., Nomura, T., Uchiyama, T., et al. (2006). Foxp3-dependent and -independent molecules specific for CD25⁺CD4⁺ natural regulatory T cells revealed by DNA microarray analysis. *Int Immunol* 18:1197-209.
- Takahashi, T., Kuniyasu, Y., Toda, M., Sakaguchi, N., Itoh, M., Iwata, M., et al. (1998). Immunologic self-tolerance maintained by CD25⁺CD4⁺ naturally anergic and suppressive T cells: induction of autoimmune disease by breaking their anergic/suppressive state. *Int Immunol* 10:1969-80.
- Takahashi, T., Tagami, T., Yamazaki, S., Uede, T., Shimizu, J., Sakaguchi, N., et al. (2000). Immunologic self-tolerance maintained by CD25(+)CD4(+) regulatory T cells constitutively expressing cytotoxic T lymphocyte-associated antigen 4. *J Exp Med* 192:303-10.
- Temelkovski, J., Hogan, S. P., Shepherd, D. P., Foster, P. S. & Kumar, R. K. (1998). An improved murine model of asthma: selective airway inflammation, epithelial lesions and increased methacholine responsiveness following chronic exposure to aerosolised allergen. *Thorax* 53:849-56.
- Thorburn, A. N. & Hansbro, P. M. (2010). Harnessing regulatory T cells to suppress asthma: from potential to therapy. *Am J Respir Cell Mol Biol* 43:511-9.
- Thorburn, A. N., O'Sullivan, B. J., Thomas, R., Kumar, R. K., Foster, P. S., Gibson, P. G., et al. (2010). Pneumococcal conjugate vaccine-induced regulatory T cells suppress the development of allergic airways disease. *Thorax* 65:1053-60.
- Thornton, A. M., Korty, P. E., Tran, D. Q., Wohlfert, E. A., Murray, P. E., Belkaid, Y., et al. (2010). Expression of Helios, an Ikaros transcription factor family member, differentiates thymic-derived from peripherally induced Foxp3⁺ T regulatory cells. *J Immunol* 184:3433-41.
- Thornton, A. M. & Shevach, E. M. (1998). CD4⁺CD25⁺ immunoregulatory T cells suppress polyclonal T cell activation in vitro by inhibiting interleukin 2 production. *J Exp Med* 188:287-96.

- Thornton, A. M. & Shevach, E. M. (2000). Suppressor effector function of CD4+CD25+ immunoregulatory T cells is antigen nonspecific. *J Immunol* 164:183-90.
- Tian, L., Altin, J. A., Makaroff, L. E., Franckaert, D., Cook, M. C., Goodnow, C. C., et al. (2011). Foxp3(+) regulatory T cells exert asymmetric control over murine helper responses by inducing Th2 cell apoptosis. *Blood* 118:1845-53.
- Tracey, D., Klareskog, L., Sasso, E. H., Salfeld, J. G. & Tak, P. P. (2008). Tumor necrosis factor antagonist mechanisms of action: a comprehensive review. *Pharmacol Ther* 117:244-79.
- Tran, D. Q., Andersson, J., Wang, R., Ramsey, H., Unutmaz, D. & Shevach, E. M. (2009). GARP (LRRC32) is essential for the surface expression of latent TGF-beta on platelets and activated FOXP3+ regulatory T cells. *Proc Natl Acad Sci U S A* 106:13445-50.
- Tritto, E., Muzzi, A., Pesce, I., Monaci, E., Nuti, S., Galli, G., et al. (2007). The acquired immune response to the mucosal adjuvant LTK63 imprints the mouse lung with a protective signature. *J Immunol* 179:5346-57.
- Trujillo, G., Hartigan, A. J. & Hogaboam, C. M. (2010). T regulatory cells and attenuated bleomycin-induced fibrosis in lungs of CCR7-/- mice. *Fibrogenesis Tissue Repair* 3:18.
- Tulic, M. K., Wale, J. L., Holt, P. G. & Sly, P. D. (2000). Modification of the inflammatory response to allergen challenge after exposure to bacterial lipopolysaccharide. *Am J Respir Cell Mol Biol* 22:604-12.
- Umetsu, D. T. & DeKruyff, R. H. (2006). The regulation of allergy and asthma. *Immunol Rev* 212:238-55.
- Utecht, M. J. & Frampton, M. W. (2000). Acute health effects of ambient air pollution: the ultrafine particle hypothesis. *J Aerosol Med* 13:355-59.
- Uto, T., Akagi, T., Hamasaki, T., Akashi, M. & Baba, M. (2009). Modulation of innate and adaptive immunity by biodegradable nanoparticles. *Immunol Lett* 125:46-52.
- Uto, T., Akagi, T., Toyama, M., Nishi, Y., Shima, F., Akashi, M., et al. (2011a). Comparative activity of biodegradable nanoparticles with aluminum adjuvants: antigen uptake by dendritic cells and induction of immune response in mice. *Immunol Lett* 140:36-43.
- Uto, T., Akagi, T., Yoshinaga, K., Toyama, M., Akashi, M. & Baba, M. (2011b). The induction of innate and adaptive immunity by biodegradable poly(gamma-glutamic acid) nanoparticles via a TLR4 and MyD88 signaling pathway. *Biomaterials* 32:5206-12.
- Uto, T., Toyama, M., Nishi, Y., Akagi, T., Shima, F., Akashi, M., et al. (2013). Uptake of biodegradable poly(γ -glutamic acid) nanoparticles and antigen presentation by dendritic cells in vivo. *Results in Immunology* 3:1-9.
- Uto, T., Wang, X., Sato, K., Haraguchi, M., Akagi, T., Akashi, M., et al. (2007). Targeting of antigen to dendritic cells with poly(gamma-glutamic acid) nanoparticles induces antigen-specific humoral and cellular immunity. *J Immunol* 178:2979-86.
- van der Most, R. G., Currie, A. J., Mahendran, S., Prosser, A., Darabi, A., Robinson, B. W., et al. (2009). Tumor eradication after cyclophosphamide depends on concurrent depletion of regulatory T cells: a role for cycling TNFR2-expressing effector-suppressor T cells in limiting effective chemotherapy. *Cancer Immunol Immunother* 58:1219-28.
- van Mierlo, G. J., Scherer, H. U., Hameetman, M., Morgan, M. E., Flierman, R., Huizinga, T. W., et al. (2008). Cutting edge: TNFR-shedding by CD4+CD25+

References

- regulatory T cells inhibits the induction of inflammatory mediators. *J Immunol* 180:2747-51.
- Verma, N. K., Crosbie-Staunton, K., Satti, A., Gallagher, S., Ryan, K. B., Doody, T., et al. (2013). Magnetic core-shell nanoparticles for drug delivery by nebulization. *J Nanobiotechnology* 11:1.
- Vernooy, J. H., Dentener, M. A., van Suylen, R. J., Buurman, W. A. & Wouters, E. F. (2001). Intratracheal instillation of lipopolysaccharide in mice induces apoptosis in bronchial epithelial cells: no role for tumor necrosis factor-alpha and infiltrating neutrophils. *Am J Respir Cell Mol Biol* 24:569-76.
- von Delwig, A., Hilkens, C. M., Altmann, D. M., Holmdahl, R., Isaacs, J. D., Harding, C. V., et al. (2006). Inhibition of macropinocytosis blocks antigen presentation of type II collagen in vitro and in vivo in HLA-DR1 transgenic mice. *Arthritis Res Ther* 8:R93.
- Vremec, D., Zorbas, M., Scollay, R., Saunders, D. J., Ardavin, C. F., Wu, L., et al. (1992). The surface phenotype of dendritic cells purified from mouse thymus and spleen: investigation of the CD8 expression by a subpopulation of dendritic cells. *J Exp Med* 176:47-58.
- Walker, L. S. (2004). CD4⁺ CD25⁺ Treg: divide and rule? *Immunology* 111:129-37.
- Walker, L. S., Chodos, A., Eggena, M., Dooms, H. & Abbas, A. K. (2003). Antigen-dependent proliferation of CD4⁺ CD25⁺ regulatory T cells in vivo. *J Exp Med* 198:249-58.
- Wan, Y. Y. & Flavell, R. A. (2007). Regulatory T-cell functions are subverted and converted owing to attenuated Foxp3 expression. *Nature* 445:766-70.
- Wang, Y. & McCusker, C. (2006). Neonatal exposure with LPS and/or allergen prevents experimental allergic airways disease: development of tolerance using environmental antigens. *J Allergy Clin Immunol* 118:143-51.
- Ward, C., Walker, A., Dransfield, I., Haslett, C. & Rossi, A. G. (2004). Regulation of granulocyte apoptosis by NF-kappaB. *Biochem Soc Trans* 32:465-7.
- Ward, R. & McLeish, K. R. (1996). Soluble TNF alpha receptors are increased in chronic renal insufficiency and hemodialysis and inhibit neutrophil priming by TNF alpha. *Artif Organs* 20:390-5.
- Ware, C. F. (2008). The TNF Superfamily-2008. *Cytokine Growth Factor Rev* 19:183-6.
- Ware, L. B. & Matthay, M. A. (2000). The acute respiratory distress syndrome. *N Engl J Med* 342:1334-49.
- Watanabe, K., Rao, V. P., Poutahidis, T., Rickman, B. H., Ohtani, M., Xu, S., et al. (2008). Cytotoxic-T-lymphocyte-associated antigen 4 blockade abrogates protection by regulatory T cells in a mouse model of microbially induced innate immune-driven colitis. *Infect Immun* 76:5834-42.
- Watkins, A. C., Caputo, F. J., Badami, C., Barlos, D., Xu da, Z., Lu, Q., et al. (2008). Mesenteric lymph duct ligation attenuates lung injury and neutrophil activation after intraperitoneal injection of endotoxin in rats. *J Trauma* 64:126-30.
- Watts, T. H. (2005). TNF/TNFR family members in costimulation of T cell responses. *Annu Rev Immunol* 23:23-68.
- Weiland, J. E., Davis, W. B., Holter, J. F., Mohammed, J. R., Dorinsky, P. M. & Gadek, J. E. (1986). Lung neutrophils in the adult respiratory distress syndrome. Clinical and pathophysiologic significance. *Am Rev Respir Dis* 133:218-25.
- Werner, S. & Alzheimer, C. (2006). Roles of activin in tissue repair, fibrosis, and inflammatory disease. *Cytokine Growth Factor Rev* 17:157-71.
- Williams, A. E., Edwards, L., Humphreys, I. R., Snelgrove, R., Rae, A., Rappuoli, R., et al. (2004). Innate imprinting by the modified heat-labile toxin of *Escherichia coli*

- (LTK63) provides generic protection against lung infectious disease. *J Immunol* 173:7435-43.
- Williams, A. E., Edwards, L. & Hussell, T. (2006). Colonic bacterial infection abrogates eosinophilic pulmonary disease. *J Infect Dis* 193:223-30.
- Williams, L. M. & Rudensky, A. Y. (2007). Maintenance of the Foxp3-dependent developmental program in mature regulatory T cells requires continued expression of Foxp3. *Nat Immunol* 8:277-84.
- Wing, K., Onishi, Y., Prieto-Martin, P., Yamaguchi, T., Miyara, M., Fehervari, Z., et al. (2008). CTLA-4 control over Foxp3+ regulatory T cell function. *Science* 322:271-5.
- Wissinger, E., Goulding, J. & Hussell, T. (2009). Immune homeostasis in the respiratory tract and its impact on heterologous infection. *Semin Immunol* 21:147-55.
- Xia, T., Kovochich, M., Brant, J., Hotze, M., Sempf, J., Oberley, T., et al. (2006). Comparison of the abilities of ambient and manufactured nanoparticles to induce cellular toxicity according to an oxidative stress paradigm. *Nano Lett* 6:1794-807.
- Xiang, S. D., Wilson, K., Day, S., Fuchsberger, M. & Plebanski, M. (2013). Methods of effective conjugation of antigens to nanoparticles as non-inflammatory vaccine carriers. *Methods* 60:232-41.
- Xu, L., Kitani, A., Fuss, I. & Strober, W. (2007). Cutting edge: regulatory T cells induce CD4+CD25-Foxp3- T cells or are self-induced to become Th17 cells in the absence of exogenous TGF-beta. *J Immunol* 178:6725-9.
- Yamaguchi, T., Hirota, K., Nagahama, K., Ohkawa, K., Takahashi, T., Nomura, T., et al. (2007). Control of immune responses by antigen-specific regulatory T cells expressing the folate receptor. *Immunity* 27:145-59.
- Yang, I. V. & Schwartz, D. A. (2012). Epigenetic mechanisms and the development of asthma. *J Allergy Clin Immunol* 130:1243-55.
- Ye, Q., Dai, H., Sarria, R., Guzman, J. & Costabel, U. (2011). Increased expression of tumor necrosis factor receptors in cryptogenic organizing pneumonia. *Respir Med* 105:292-7.
- Zhang, X., Dong, Y., Zeng, X., Liang, X., Li, X., Tao, W., et al. (2014). The effect of autophagy inhibitors on drug delivery using biodegradable polymer nanoparticles in cancer treatment. *Biomaterials* 35:1932-43.
- Zheng, S. G., Wang, J. & Horwitz, D. A. (2008). Cutting edge: Foxp3+CD4+CD25+ regulatory T cells induced by IL-2 and TGF-beta are resistant to Th17 conversion by IL-6. *J Immunol* 180:7112-6.
- Zheng, Y. & Rudensky, A. Y. (2007). Foxp3 in control of the regulatory T cell lineage. *Nat Immunol* 8:457-62.
- Zhu, Z., Oh, S. Y., Zheng, T. & Kim, Y. K. (2010). Immunomodulating effects of endotoxin in mouse models of allergic asthma. *Clin Exp Allergy* 40:536-46.
- Zosky, G. R. & Sly, P. D. (2007). Animal models of asthma. *Clin Exp Allergy* 37:973-88.
- Zuany-Amorim, C., Hastewell, J. & Walker, C. (2002a). Toll-like receptors as potential therapeutic targets for multiple diseases. *Nat Rev Drug Discov* 1:797-807.
- Zuany-Amorim, C., Sawicka, E., Manlius, C., Le Moine, A., Brunet, L. R., Kemeny, D. M., et al. (2002b). Suppression of airway eosinophilia by killed Mycobacterium vaccae-induced allergen-specific regulatory T-cells. *Nat Med* 8:625-9.

-This page intentionally left blank-

Appendices

(Published and unpublished Manuscripts)

9.1 Unpublished manuscript 1

Instillation of lipopolysaccharides locally in the lung alters TNFR2⁺Foxp3⁺ Treg that involve in inhibition of allergic asthma in a mouse model

Rohimah Mohamud^a, Jeanne S. LeMasurier^a, John Yao^{ab}, Robyn M. Slattery^a, Sue Xiang^a, Jennifer M. Rolland^{ab}, Robyn E. O’Hehir^{ab}, Charles L. Hardy^{ab*}, Magdalena Plebanski^{ac*}

** Equal contribution*

^a Department of Immunology, Monash University, Melbourne, VIC, Australia

^b Department of Allergy, Immunology and Respiratory Medicine, The Alfred Hospital and Monash University, Melbourne, VIC, Australia

^c Corresponding author:

Professor Magdalena Plebanski

[REDACTED]

[REDACTED]

Fax: + 61 3 9903 0038

This research was funded by the Cooperative Research Centre for Asthma and the National Health & Medical Research Council of Australia. RM is the recipient of Malaysian Postgraduate Scholarship Scheme and CRC-Asthma and Airways top-up Scholarship.

Abstract

Epidemiological and experimental data suggest that infections or exposure to bacteria/bacterial products protect individuals from developing allergic diseases. Regulatory T cells (Treg) are the key player in this phenomenon and play a crucial role in early shaping of the immune system and suppression of the development of Th2-driven allergic immune responses. In this study, low and high doses of bacterial products lipopolysaccharides (LPS) were intratracheally instilled into naïve mice, and samples were collected on d1, d3, d7 and d30 to investigate the inflammatory responses and kinetics of Treg. We analysed the Treg fractions that are most capable of proliferating by the expression of TNF receptor 2 (TNFR2⁺Foxp3⁺ Treg). LPS instillation into naïve mice resulted in the development of acute lung injury on day 3 that fully resolved on day 30. In allergic airways inflammation mouse model, we found that exposure to high dose LPS rendered mice resistant to the development of allergic airways inflammation upon subsequent allergen challenge after 30 days. Lung TNFR2⁺Foxp3⁺ Treg pre-conditioned by LPS express higher levels of suppressor effector molecules, as well as having higher proliferative capacity, and hence are perfectly positioned to respond rapidly to allergenic challenges and restore lung immune homeostasis. These results show that high dose LPS promote a long term imprint in the lung rendering it resistant to allergen challenge, which is further associated with changes in the ‘quality’ of persistent TNFR2⁺Foxp3⁺ Treg. We propose childhood exposure to gram negative bacteria may promote similar qualitative changes, useful to limit over-reactivity in high burden environments, which then would provide a feasible mechanism to support the ‘hygiene hypothesis’.

Keywords: Treg, Lung, Lipopolysaccharides, Inflammation, Asthma

Introduction

The lungs develop tolerance towards the frequently exposed innocuous antigens and particulates present in the environment to retain pulmonary homeostasis (Gereda et al., 2000, Akbari et al., 2002). In asthmatics, these innocuous antigens elicit a skewed antigen-specific Th2 immune response, resulting eosinophilic lung inflammation (Umetsu and DeKruyff, 2006, Gould and Sutton, 2008). Lipopolysaccharide (LPS), a gram-negative bacteria cell wall, is ubiquitously present in the environment and has been shown to modulate lung diseases including allergic asthma when co-administered with allergen (Braun-Fahrlander et al., 2002, Eisenbarth et al., 2002, Rodriguez et al., 2003, Ege et al., 2006). Airway exposure to LPS in diverse allergic asthma animal models alters multiple aspects of allergen-induced allergic asthma, such as IgE hyperproduction, airway eosinophilia and airway hyperresponsiveness (Bochner et al., 1994) in a dose-dependent manner (Delayre-Orthez et al., 2004, Gerhold et al., 2002, Kim et al., 2007). Data from several models demonstrated that LPS regulates allergic airways inflammation is dependent on the exposure time and dose. Therefore, LPS exposure to the lung during allergen sensitisation or challenges might lead to different forms of asthmatic pathology (Delayre-Orthez et al., 2004, Tulic et al., 2000, Zhu et al., 2010). On the other hand, different doses of LPS would determine whether Th1 or Th2 immunity will be induced (Park et al., 2004); low dose LPS work in synergy with antigen to induce airway inflammation and asthma exacerbation through the TLR4 signaling pathway (Jung et al., 2006), whereas high dose LPS inhibit asthma development in a mouse model (Dong et al., 2009, Wang and McCusker, 2006). However, in naïve animals, LPS itself induced acute lung injury that is mediated by inflammatory changes in the lung (Vernooy et al., 2001, D'Alessio et al., 2009), whilst in healthy volunteers, LPS inhalation activated

macrophages to secrete pro-inflammatory cytokines and induced neutrophilic inflammation (Hernandez et al., 2010).

Interestingly, a study on prenatal farm exposure that is rich in LPS is related to a long-lasting upregulation of receptors of the innate immune system [eg. Toll-like receptor 4 (TLR4)] and showed a protection against the development of allergic asthma (Ege et al., 2006). In addition, children growing up on a farm exhibited lower risk to develop allergic diseases in later childhood and adulthood (Braun-Fahrlander et al., 2002). Various mechanisms involved in this protection, including the modulation effects on airway innate and adaptive immune components, preferentially regulatory T cells (Treg). Treg play an important role in maintaining the balances between protective and pathogenic responses in the lung (Strickland et al., 2006, Lewkowich et al., 2005). More interestingly, a study demonstrated that farm exposures during pregnancy increased Treg cell numbers and function, and acted as a natural model of immunomodulation which shaping a child's immune system in early life (Schaub et al., 2009). Overall, the aforementioned studies showed that environmental exposure left an immunological imprint in the lung (including Treg) of neonates which are beneficial for later stage of their life. Furthermore, Treg are important for the long-lasting allergy-protective effect upon subsequent allergen exposure in older children and adults (Schaub et al., 2009, Lewkowich et al., 2005, Akbari et al., 2002, Wang and McCusker, 2006).

Major populations of Treg studied in the context of lung homeostasis and airway diseases are the natural thymic-derived $CD4^{+}Foxp3^{+}$ Treg (nTreg) and peripherally antigen-induced adaptive $CD4^{+}$ Treg (iTreg), the latter comprise both Foxp3-positive and -negative populations (Hawrylowicz and O'Garra, 2005, Roncarolo et al., 2006). In this

study, we investigated the maximally suppressive Treg that are identified by the expression of TNFR2 on their surface (van Mierlo et al., 2008, Chen et al., 2010b, Chen et al., 2008) in acute lung injury and allergic airways inflammation mouse models.

In this regards, we investigated the effects of LPS on lung TNFR2⁺Foxp3⁺ Treg in the respective of proliferative and migration (as reflected by the expressions of intracellular Ki67 and CCR7 marker, respectively) and whether LPS provided the protection against allergen challenges in ovalbumin-induced allergic asthma. Other functional markers on Treg such as TGF- β latency associated peptide (LAP) and cytotoxic T-lymphocytes antigen 4 (CTLA-4) were also investigated to understand the mechanism of Treg in mediating the suppressive effect. We showed that in naïve mice, LPS affected lung TNFR2⁺Foxp3⁺ Treg to be actively proliferated and migrated to the lung-draining LN faster, thus we proposed that mice exposed to LPS be resistant to allergic asthma. TNFR2⁺Foxp3⁺ Treg tend to stay in the lung and exhibited lower proliferative capacity during lung inflammation (in both models), but acquire massive migration and proliferative capacity on day 30 in naïve mice; which we believe that these cells might be responsible for the protection upon allergen challenges. Treg not only maintained their capacity to proliferate, but also increased LAP⁺ cells within TNFR2⁺Foxp3⁺ Treg in allergic asthma mouse model that was pre-exposed to LPS. Consistent with other study (Dong et al., 2009), we showed that LPS altered the ratio of Th1/Th2 cells in allergic asthma mouse model in a dose-dependent manner. Overall, our data suggest that local airway LPS instillation imprinted TNFR2 expressing lung Treg, and modulated their capacity to proliferate and migrate to the LN, to modulate the outcome of subsequent lung immune responses.

Methodology

Mice

Female BALB/c and DREG mice aged 7–8 weeks were obtained from Monash Animal Research Platform Melbourne, Victoria, Australia and housed in the Alfred Medical Research and Education Precinct animal house. All studies with mice were approved by the AMREP Animal Ethics Committee.

LPS instillations and allergen immunisations

To investigate the effects of LPS on airway inflammation, BALB/c mice were intratracheally instilled with 0.1 µg and 10 µg LPS from *Escherichia Coli* K (Sigma–Aldrich, Louis, MO, USA) and samples were collected on days 1, 3, 7 and 30. To determine LPS effects on allergic airway inflammation, BALB/c mice received saline (control) (50 µl) or LPS with different doses (0.1 and 10 µg in 50 µl) intratracheally on day 0 and day 2. The trachea was intubated with a soft plastic 20-gauge catheter and guide wire, and saline or LPS were delivered via a 50-µl microsyringe (SGE International Pty., Melbourne, Australia) attached to a blunted 20-gauge needle (Hardy et al., 2003, Hardy et al., 2012a). Mice were then sensitised i.p. with saline or ovalbumin (Sigma–Aldrich, St. Louis, MO) (50 µg) on days 11 and 21 and challenged with 25 µg ovalbumin on days 31, 32, 33 and 34 (Fig. 6). Samples were collected on day 35.

BAL fluid, differential counts and Treg staining

Methods were as described previously (Hardy et al., 2003). To obtain BAL fluid, lungs were lavaged with 0.4 ml of 1% fetal calf serum (FCS) in phosphate-buffered saline (PBS) followed by 3 further lavages of 0.3 ml. The concentration of cytokines in BAL

Appendices

fluid (IL-1 α , IL-2, IL-5, IL-6, IL-10, IFN- γ , TNF, TGF- β , GM-CSF, IL-4 and IL-17) were detected by mouse Th1/Th2 10plex kit FlowCytomix (BMS820FF, eBioscience). Protocols were as specified in the manufacturer's instructions. For differentials, total cell counts were determined for each BAL sample and 100 μ l of fluid was cytopun at 350 x g for 4 min onto glass slides. BAL cytopots were air dried, fixed in methanol for 2 minutes, and Giemsa stained for 8 minutes (Merck, Kilsyth, Victoria, Australia). At least 200 cells per mouse were counted and identified by morphological criteria.

Tissue sampling and cell isolation

Tissue digestion was performed as described previously (Hardy et al., 2003) with modifications. Lung and lung-draining LN were chopped with a tissue chopper (Mickle Laboratory Engineering Co. Ltd, Gomshall, Surrey, UK). Tissue fragments from lung were digested in collagenase type IV (1 mg/ml; Worthington, Lakewood, NJ, USA) and DNase type I (0.025 mg/ml; Roche Diagnostics, Sydney NSW #1284932) in a volume of 7 ml at 25 °C by manual pipetting for 20 minutes, followed 5 minutes mixing with one-tenth volume of 0.01 M EDTA. The cell suspension was filtered (70 μ m cell strainers) (BD Falcon) and underlaid with 1 ml 0.01 M EDTA in FCS prior to centrifugation (350 x g, 4°C). The cell supernatant was discarded and red cells lysed with red blood cell lysis solution (#R7757, Sigma-Aldrich) for 3–5 min. The cell suspension was diluted to 10 ml in incomplete media (10% FCS RPMI), underlaid with EDTA/FCS and centrifuged as above. Cells were resuspended in FACS staining buffer [3% FCS, 5 mM EDTA (pH 7.2) and 0.1% Na-Azide in Ca²⁺/Mg²⁺-free HBSS], and viable cells were counted in a haemocytometer.

Antibodies and flow cytometry

Cells (1×10^6) were stained on ice for 20 minutes with combinations of the following antibodies (all eBioscience unless noted): CD3 (APC-Cy7, Qdot 605 from Lifetechnologies), CD4 (APC and V500 from BDBiosciences), CD25 (PE-Cy7, APC-Cy7), CCR7 (Per-CP), CD120b/TNFR2 (PE), LAP (Per-CP), CTLA-4-biotin or their respective immunoglobulin isotypes. For intracellular staining of Foxp3 (APC) and Ki67 (FITC), cells were permeabilized according to the manufacturer's instructions. Acquisition was on a LSR II (BD) and analysis was performed on FlowJo (Tree Star, Ashland, OR, USA).

CD25 and TNFR2 cell sorting from the lungs of Balb/c mice

Lung cells pooled from 15-20 BALB/c naïve mice (1×10^8 cells) were stained with CD4 (APC), CD25 (Pe-Cy7) and sorted (BD FACS Aria) into $CD4^+CD25^+$ (Treg) and $CD4^+CD25^-$ (Teff) populations. For assessment of TNFR2 populations, cells were stained with the above antibodies and CD120b/TNFR2 (PE) and sorted into $CD25^+TNFR2^-$, $CD25^+TNFR2^+$, $CD25^-TNFR2^-$ and $CD25^-TNFR2^+$. The purity of these sorted populations was $> 97\%$.

Treg cytokines inhibition assays on lungs cells of Balb/c mice

For proliferation assay of $CD4^+CD25^+$ cells, $CD4^+CD25^-$ cells and TNFR2 populations from naïve mice, 1×10^5 of each cell population were cultured in triplicate in 200 μ l of RPMI complete medium (containing 100 U/ml penicillin-G, 100 μ g/ml streptomycin, 10 mM HEPES) in 96-well plates. To assess proliferation of TNFR2 populations from naïve mice, cells (5×10^4) were cultured in duplicate ($CD25^+TNFR2^+$), triplicate ($CD25^+TNFR2^-$ and $CD25^-TNFR2^+$), or quadruplicate ($CD25^-TNFR2^-$), depending on

Appendices

the number of cells recovered after FACS sorting. For TNFR2⁺ Treg depletion assay, total CD25⁻ cells (both TNFR2⁺ and TNFR2⁻) were co-cultured with either CD25⁺TNFR2⁻ cells alone or with total Tregs (CD25⁺TNFR2⁺ and CD25⁺TNFR2⁻). All cultured cells were stimulated with plate-bound anti-CD3 (OKT3; 1 µg/ml) and soluble anti-CD28 (Clone 37.51; 2 µg/ml) for 72 hours. Cells were then pulsed with [³H]-thymidine (1 µCi/well, Perkin Elmer) for an additional 18 hours. Incorporation of [³H]-thymidine was measured by liquid scintillation counting. Cytokines concentrations of culture supernatant (IL-2, IL-4, IFN-γ) were detected by mouse Th1/Th2 10plex kit FlowCytomix (BMS820FF, eBioscience). Protocols were as specified in the manufacturer's instructions.

CD25, TNFR2 and Foxp3 cells sorting from the spleen of DEREg mice

Spleen cells were pooled from 3 DEREg mice (2 x 10⁸ cells) were stained with CD4 (APC), CD25 (Pe-Cy7) and CD120b/TNFR2 (PE) were sorted (BD FACS Aria) into Q1: CD4⁺CD25⁺TNFR2⁻GFP⁺ (TNFR2⁻Foxp3⁺ Treg); Q2: CD4⁺CD25⁺TNFR2⁺GFP⁺ (TNFR2⁺Foxp3⁺ Treg), Q3: CD4⁺CD25⁻TNFR2⁻GFP⁻ (TNFR2⁻Foxp3⁻ Teff) and Q4: CD4⁺CD25⁻TNFR2⁺GFP⁻ (TNFR2⁺Foxp3⁻ Teff) populations. The purity of these sorted populations was > 97%.

Treg-IL-4⁺ Teff inhibition assay of DEREg mice

To determine the percentages of IL-4⁺ producing Teff from each sorted populations (Q1-Q4), cells (2.5 x 10⁴) were cultured in duplicate (Q2), triplicate (Q2, Q4), or quadruplicate (Q4), depending on the number of cells recovered after sorting. To determine the suppressive function of Treg in inhibition of IL-4⁺ Teff, sorted Q3: CD4⁺CD25⁻TNFR2⁻GFP⁻ (TNFR2⁻Foxp3⁻ Teff) cells were labeled with V450 proliferation dye (eBioScience, # 65-0842-85). Q1, Q2 and Q4 were co-cultured with

V450-labeled Q3. All cultured cells were stimulated with plate-bound anti-CD3 (OKT3; 1 µg/ml) and soluble anti-CD28 (Clone 37.51; 2 µg/ml) for 72 hours. Brefeldin A (eBioScience, # 00-4506-51) was added to the culture for the final 5 hours of incubation.

ELISPOT assay

IL-4, IL-5, and IL-13 ELISPOT assays were performed as described (Hardy et al., 2006). IFN-γ ELISPOT assay was performed using AN18 capture and R4-6A2 biotinylated detection Abs (no. 3321-3-1000 and no. 3321-6-1000; Mabtech, Mossman, Australia) and hydrophobic membrane plates (no. MAIPS4510; Millipore).

Statistical analysis

Data were analysed for normality and log-transformed as necessary prior to analysis by Student's *t* test or ANOVA with Bonferroni post tests, depending on the number of experimental groups. Spearman's correlations were used for the comparison of continuous variables. The Spearman's *r* value for the correlation between the two variables was stated in each result. Statistical analysis was performed using Graph Pad Prism v5.02 software. Group sizes are indicated in the figure legends. Data are expressed as mean ± SEM. * *p* < 0.05, ** *p* < 0.01, and *** *p* < 0.001 compared to positive control group and representative of 3-4 experiments.

Results

Lung CD4⁺CD25⁺TNFR2⁺ cells from unmanipulated mice are non-cytokines producer, suppressed cytokines production of Teff and have higher proliferative capacity than CD4⁺CD25⁺TNFR2⁻ cells

Expression of TNFR2 on Treg is reported to play a critical role in sustaining Foxp3 expression and consequently maintaining the phenotypic and functional stability of Treg (Chen et al., 2013), and subsequently maintaining Treg pool (Chen et al., 2007). CD4⁺CD25⁺ Treg is reported as anergic to TCR activation *in vitro* (Takahashi et al., 1998, Gavin et al., 2002, Thornton and Shevach, 2000), but they are actively proliferate *in vivo* (Walker et al., 2003, Klein et al., 2003, Chen et al., 2012). CD4⁺CD25⁺ Treg that co-expressed TNFR2 exert the maximum proliferative capacity (Chen et al., 2010a) and are maximally suppressive than non-TNFR2 expressing Treg (Chen et al., 2010a, van der Most et al., 2009). In regards with this, we investigated the ability of CD25⁺TNFR2⁺ and CD25⁺TNFR2⁻ Treg to secrete cytokines and/or to inhibit cytokines production by CD4⁺CD25⁻ Teff (Fig. 1A). We analysed IL-2, IL-4 and IFN- γ concentration prior activation of T-cell receptor on Treg and Teff to show the functionality of these cells.

As expected, FACS sorted CD4⁺CD25⁻ cells secreted the highest concentration of IL-2, which was parallel as seen in the combination of total CD4⁺CD25⁻ cells (CD4⁺CD25⁻ TNFR2⁺ and CD4⁺CD25⁻TNFR2⁻ cells) (~ 2000 pg/ml) (Fig. 1B). On the other hand, CD4⁺CD25⁺ cells (either with or without TNFR2 co-expression) did not increase the concentration of IL-2 cytokines in the culture supernatant (Fig. 1B, C, left panel). CD4⁺CD25⁻TNFR2⁻ cells by themselves secreted only ~ 50 pg/ml (Fig. 1C, left panel), but showed the synergistic effects when co-cultured with CD4⁺CD25⁻TNFR2⁺ cells,

which the latter did not increase the concentration of IL-2 cytokines by themselves (below lower detection level: 30.42 pg/ml) (Fig. 1C, left panel). Interestingly, we showed that co-cultured of total $CD4^+CD25^-$ cells with either $CD4^+CD25^+TNFR2^+$ or $CD4^+CD25^+TNFR2^-$ cells significantly lowered the concentration of IL-2 by total $CD4^+CD25^-$ cells (~ 500 pg/ml) (Fig. 1C, left panel). Similar pattern were observed for IL-4 concentration. However, the synergistic effect of $CD4^+CD25^-TNFR2^+$ and $CD4^+CD25^-TNFR2^-$ cells produced almost 2-fold increased in IL-4 concentration (~ 30 pg/ml) compared to the culture of sorted on $CD4^+CD25^-$ cells (~ 10 pg/ml). Similar to what seen in the reduction of IL-2 concentration, $CD25^+TNFR2^+$ or $CD25^+TNFR2^-$ Treg were significantly lowered the concentration of IL-4 by total $CD25^-$ cells (< 10 pg/ml) (Fig. 1C, right panel). Similar pattern was observed for IFN- γ (data not shown). Overall, this showed that $CD4^+CD25^+$, $CD4^+CD25^+TNFR2^-$ and $CD4^+CD25^+TNFR2^+$ cells were non-cytokine producers. However, these cells showed an ability to lower the cytokines concentration in co-culture of $CD4^+CD25^-$ cells suggesting their regulatory functional relevance. On the other hand, $CD4^+CD25^-$, $CD4^+CD25^-TNFR2^-$ and $CD4^+CD25^-TNFR2^+$ cells were cytokine producers suggesting that they involve in effector function.

Spleen $CD4^+CD25^-TNFR2^-GFP^-$ cells from unmanipulated DERE mice are IL-4⁺ producing cells that suppressed after co-cultured with $TNFR2^+Foxp3^+$ Treg and $TNFR2^-Foxp3^+$ Treg

Sustained Foxp3 expression in Treg is required for their maintenance and suppressive function (Wan and Flavell, 2007, Williams and Rudensky, 2007, Hori et al., 2003a, Fontenot et al., 2003, Khattri et al., 2003), thus it is crucial to focus our investigation on $CD4^+CD25^+TNFR2^+$ Treg expressing Foxp3 ($TNFR2^+Foxp3^+$ Treg). To overcome our

problems in getting enough T cell numbers from the lungs, we sorted T cells from the spleen, as we sought to get ~3-4 folds more T cells in the spleen than the lung. In this experiment, we utilized DERE mice that express eGFP-Foxp3 which can be easily isolated by FACS sorting on the basis of eGFP expression for their functional analysis, and for determination of Teff based on eGFP-negative. Following data observed in the lungs, we further demonstrated that Treg (both TNFR2⁺Foxp3⁺ Treg and TNFR2⁻Foxp3⁺ Treg) were the least produced IL-4⁺ cells (< 2 %), followed by TNFR2⁺Foxp3⁻ Teff (9.54 %) and as expected, TNFR2⁻Foxp3⁻ Teff exhibited the highest IL-4⁺ cells (23.3 %) (Fig. 2A). Interestingly, IL-4⁺ cells within TNFR2⁻Foxp3⁻ Teff was suppressed after co-cultured with Treg, both TNFR2⁻Foxp3⁺ Treg and TNFR2⁺Foxp3⁺ Treg with the latter suppressed with maximal capacity than non-TNFR2 expressing Treg (TNFR2⁻Foxp3⁺ Treg), whilst co-culture of TNFR2⁻Foxp3⁻ Teff and TNFR2⁺Foxp3⁻ Teff did not change the proportion of IL-4⁺ cells (Fig. 2C).

As previous studies demonstrated a close relationship of proliferative capacity with TNFR expressing cells (Treg and Teff) (Chen et al., 2007) and that maximally functional Treg have higher proliferative capacity (van der Most et al., 2009), we then focus our investigations on the expression of Ki67 marker on Treg- and Teff-expressing TNFR2 in the lung and lung-draining LN from naïve mice. We demonstrated that TNFR2⁺Foxp3⁺ Treg exerted higher percentages of Ki67⁺ cells, followed by TNFR2⁺Foxp3⁻ Teff and TNFR2⁻Foxp3⁺ Treg (Suppl. Fig. 1A-E). CD4⁺CD25⁻ cells are highly proliferated *in vitro* upon TCR activation (Takahashi et al., 1998, Gavin et al., 2002, Thornton and Shevach, 2000), and interestingly, we showed here that TNFR2⁺Foxp3⁺ gated from CD4⁺CD25⁻ cells exerted the highest Ki67⁺ cells (60.2 % ± 4.5 %), suggesting that they expand at the highest rate than any other cell populations (Suppl. Fig. 1B-C). On the other hand, as

mention above, the expansion capacity of $\text{TNFR2}^-\text{Foxp3}^-$ Teff was lowered than $\text{TNFR2}^+\text{Foxp3}^-$ Teff, suggesting that Teff also comprised population that actively proliferated. In contrast, the expansion capacity of all gated cells in the lung-draining LN was lower than lung cells (Suppl. Fig. 1D-E), paralleling that lung cells are continuously exposed to environmental stimuli. Similar to what seen in the lung, the highest percentages of Ki67^+ were observed in $\text{TNFR2}^+\text{Foxp3}^+$ cells gated from $\text{CD4}^+\text{CD25}^+$ and $\text{CD4}^+\text{CD25}^-$ cells (Suppl. Fig. 1B-C), which were in agreement with Chen *et al.* that Ki67 expression was higher in TNFR2 -positive cells regardless of CD25 expression (Chen *et al.*, 2010a). Overall, *in vitro* studies from the spleen and lungs suggested that Treg contain 2 populations, TNFR2 expressing Treg with maximal capacity in suppressing Teff and are highly proliferative; whilst TNFR2 expressing Teff are not cytokines producers, albeit highly proliferative than non- TNFR2 expressing Teff.

The next studies investigating the effects of LPS on lung cells (focusing on the Treg and Teff) in naïve mice and how different doses of LPS exposure in allergic airway inflammation mouse model altered Treg and/or Teff and subsequently modified lung immunological responses. A previous study demonstrated that mice that lack any exposure to microorganisms (germ-free) failed to protect against allergic asthma suggesting that bacterial exposure is critical for ensuring normal cellular maturation, recruitment and control of allergic asthma (Herbst *et al.*, 2011). In addition, newborn mice exposed to LPS and/or allergen activated Treg and Th1-type cellular responses upon subsequent allergen sensitisation and inhibited allergic response (Wang and McCusker, 2006). Together with a natural model of immunomodulation which shaping a child's immune system in early life (Schaub *et al.*, 2009) and aforementioned studies (Wang and McCusker, 2006, Herbst *et al.*, 2011), we proposed that LPS exposure would imprint lung

immunological responses that are beneficial for later protection against allergic development.

Administration of LPS induced acute lung injury in a dose and time dependent manner

To determine whether LPS induced cellularity in the BAL, lung and lung-draining LN in a time- and dose-dependent manner, mice were i.t. with 0.1 μg and 10 μg LPS and samples were collected on days 1, 3, 7, and 30. Analyses on the different cells type in BAL fluid revealed that the recruitments of monocytes and lymphocytes in high dose 10 μg LPS group were peaked on d3 and d7. In contrast, neutrophils were recruited as early as d1, peaked on d3 and significantly increased compared to saline control group on both days (Fig. 3A). Interestingly, accumulation of neutrophils in 10 μg LPS group were completely abolished on d7 and d30, whilst there were detectable levels of lymphocytes and monocytes on these days (Fig. 3A). On the contrary, infiltration of neutrophils and monocytes in low dose 0.1 μg LPS group was less pronounced compared to 10 μg LPS group, with significant increased on d1 and d7, respectively compared to saline control group. Lymphocytes recruitment in low dose 0.1 μg LPS group was under detectable levels throughout the course of study (Fig. 3A). Administration of high dose 10 μg LPS gave a significant increase of total cell numbers in lung tissues on d1, d3 and d7 (Fig.3B). Infiltrations of total cells are substantially increased on d3 in both compartments, and greatly decreased on d7, but remained elevated above low dose 0.1 μg LPS and saline control group. Low dose 0.1 μg LPS has comparable cell numbers with saline control group, both in the BAL and lung d7 (Fig.3B). Similar kinetics was observed in lung-draining LN for high and low dose 0.1 μg LPS, which were significantly increased in high dose 10 μg LPS on d3 and d7, compared to saline control group. Total cell numbers

returned to saline levels on d30 d7 (Fig. 3C). All cell numbers returned to saline levels on d30, as reflected by total cell counts. Overall, we showed that inflammation induced by LPS were dose- and time-dependent as higher LPS dose induced higher inflammation that peak on d3. Our results were consistent with others that intratracheal LPS (3.75 µg/g mouse) induced peak lung injury 4 days after the challenge, with resolution by d10 (D'Alessio et al., 2009, Aggarwal et al., 2009).

We next investigated the cytokines secretion in the BAL fluid after treatment with high dose 10 µg LPS. Analyses in the BAL fluid revealed that administration of 10 µg LPS significantly increased the secretion of TNF, IL-1 α , IL-17 and IL-6 as early as d1, peaked on d3 for IL-1 α and IL-17 and all the cytokines levels were sharp decreased on d7 and returned to baseline on d30 (Fig. 3D). On the other hand, other cytokines such as IL-2, IL-4, IL-5 and IL-10 were not prominent increased compared to saline control group for all timepoints (data not shown). IFN- γ concentration was also increased during the peak of inflammation, whereas GM-CSF decreased compared to saline negative control group and naïve mice (Table 1). Cytokine concentrations returned to normal level on day 30 post LPS exposure (Fig. 3D) suggesting that the inflammatory responses completely resolved by day 30. Previous studies demonstrated that the induction and resolution of acute lung injury was modulated by Treg, and that Treg played a crucial role at the resolution phase (Aggarwal et al., 2009, D'Alessio et al., 2009). In this regards, we further analysed the effects of LPS exposure on Treg both in the lung and lung-draining LN.

LPS instillation increased the percentages of TNFR2 expressing cells (Treg and Teff) and were positively correlated with airway inflammation

Further analyses were performed to investigate the effects on T cells in the lung and lung-draining LN of LPS induced acute lung injury. We first demonstrated that majority of CD4⁺CD25⁺Foxp3⁺ Treg in the lung during homeostasis (saline treated mice) were TNFR2⁻ (60.4 ± 5.7 %) and a small portion that expressed TNFR2 (12.7 ± 4.6 %) (Fig. 4C), and this observation was consistent with the data obtained from naïve mice (Suppl. Fig. 1B). High dose LPS increased the percentages of CD4⁺CD25⁺ Treg on d3 and resolved to a basal level on days 7 and 30 (Fig. 4B). We then showed that instillation of 10 µg LPS significantly increased the percentages of TNFR2⁺Foxp3⁺ Treg to ~ 20 % at days 1 and 3 compared to saline control group (Fig. 4A), whereas TNFR2⁻Foxp3⁺ Treg decreased to ~ 25 % on day 3 (Fig. 4D). Previously, D'Alessio showed that the percentage of CD4⁺CD25⁺ alveolar cells expressing Foxp3⁺ was approximately 60 % at d1 after i.t. LPS (3.75 µg/g mouse), fell to 38 % on the peaked of lung inflammation on d4, and increased to about 80 % by d10 (D'Alessio et al., 2009). Interestingly, in our present study, we further showed that CD4⁺CD25⁺ alveolar cells expressing Foxp3⁺ that do not express TNFR2 followed this pattern, but not TNFR2 expressing Treg (TNFR2⁺Foxp3⁺ Treg) (Fig. 4C-D).

Interestingly, TNFR2⁺Foxp3⁻ Teff proportion was strikingly increased at day 3 to approximately 3-fold to reach ~ 6 %, and had returned to ~ 1 % at days 7 and 30, which was the same level observed in saline negative control group (Fig. 4E). The percentages of TNFR2⁺Foxp3⁺ Treg and TNFR2⁺Foxp3⁻ Teff were positively correlated with airway inflammation (Fig. 4C-E, lower panel). The kinetics of these cells returned to saline level at day 30 (Fig. 4C-E). However, cell numbers of lung TNFR2⁺Foxp3⁺ Treg, TNFR2⁻

Foxp3⁺ Treg and TNFR2⁺Foxp3⁻ Teff increased 3 days after LPS instillation, in parallel with the increased of total lung cells (data not shown). Diverse kinetics of these populations both in the lung and lung-draining LN lead us to further analysed Ki67 and CCR7 markers to understand the capacity of these cells to expand and migrate in maintaining lung homeostasis.

LPS instillation altered proliferative and migration capacity of TNFR2⁺ cells during the peak of airway inflammation and at day 30

Further analyses revealed that the percentages of lung Ki67⁺ cells gated from TNFR2⁺Foxp3⁺ Treg was significantly decreased to below than 20 % in LPS induced acute lung injury (Fig. 5A). The percentages of lung Ki67⁺ cells from both Treg (TNFR2⁺Foxp3⁺ Treg and TNFR2⁻Foxp3⁺ Treg) were steadily increase at day 7 and remained at the higher levels than saline treated mice at day 30. This result suggests that during excessive lung inflammations, TNFR2⁺Foxp3⁺ Treg lowered their expansion capacity, whereas TNFR2⁻Foxp3⁺ Treg proliferated at the same level as in saline treated mice (Fig. 5A, B). However, LPS altered both Treg to expand at the highest level at day 30, suggesting these Treg are able to respond more efficiently later to any exposed antigen in the lung (Fig. 5A, B). Surprisingly, LPS also lowered the percentages of Ki67⁺ cells within TNFR2⁺Foxp3⁻ Teff, but did not alter these cells to expand more at day 30 (Fig. 5C). On the other hand, analyses in the lung-draining LN demonstrated that no differences were observed in the proliferative capacity for TNFR2⁺Foxp3⁺ Treg and TNFR2⁻Foxp3⁺ Treg (Suppl. Fig. 2). In contrast, Ki67⁺ cells within TNFR2⁺Foxp3⁻ Teff in the lung-draining LN increased on day 7 and returned to saline level on day 30 (Suppl. Fig. 2).

Appendices

Besides Treg proliferation, the increased of percentages and numbers of Treg (TNFR2⁺Foxp3⁺ Treg and TNFR2⁻Foxp3⁺ Treg) might also represent recruitment, or a combination of these two factors. To investigate further into the capacity of cell to migrate to the lung-draining LN, the expression of CCR7 on Treg and Teff was analysed. There were < 2 % of CCR7⁺ in Treg and Teff, with TNFR2⁺Foxp3⁺ Treg exerted significantly lower CCR7⁺ percentages than saline negative control group, which suggesting that TNFR2⁺Foxp3⁺ Treg were tissue-dwelling cells during the peak of acute lung injury (Fig. 5D, E). On the other hand, the percentages of CCR7⁺ cells within both Treg populations were steadily increase on d7 and stayed at the higher levels than saline treated mice on day 30 (Fig. 5D, E), suggesting that LPS altered Treg to actively migrated to the lung-draining LN on day 30. No differences were observed for CCR7⁺ cells within TNFR2⁻Foxp3⁺ Teff (Fig. 5F). The expression of CCR7 on Treg and Teff was downregulated as they arrived in the lung-draining LN (data not shown).

LPS that is ubiquitously present in environmental allergens is known to induce the production of IFN- γ and IL-12 (Gereda et al., 2000, Michel et al., 1991) and skewed towards Th1 response and thus reduced Th2 cell priming to allergens (Magram et al., 1996, Kuipers et al., 2003). Studies also showed that low dose LPS (0.1 μ g) and high dose LPS (100 μ g) induced Th2 and Th1 responses, respectively; the latter inhibited the induction of allergic asthma (Eisenbarth et al., 2002, Kim et al., 2007). In addition, the natural model of allergy protection by maternal exposure to rich LPS environment suggest that neonatal immune mechanisms modulate through the increase the number and function of Treg (Schaub et al., 2009). Thus, we hypothesised that high dose LPS would inhibit allergic airway inflammation pathogenesis by modulation on Treg and that these cells might be partially responsible for the controlling of allergic inflammation in a mouse

model. To confirm this hypothesis, we then analyse Treg in mice that were administered with LPS 30 days before OVA challenge in OVA-induced AAI mouse model.

LPS pre-treatment improved AAI in a dose-dependent manner

Previous study has indicated the potential of LPS in inhibit AAI induction in a dose-dependent manner, high dose LPS (1 µg) was responsible in inhibition of AAI whereas low dose LPS (0.01 µg) exacerbated AAI (Dong et al., 2009). Nevertheless, LPS exposure in allergic asthma mediated immunity in a time-dependent manner. For instance, airway exposure to high dose LPS (1 µg) during sensitisation phase exacerbated noneosinophilic-allergic asthma (characterized by high levels of airway hyperresponsiveness) (Kim et al., 2007). Therefore, the study on LPS pre-exposure prior to AAI induction (administered 10 days before the sensitisation phase) in a mouse model was designed to mimic a natural model of immunotherapy (Fig. 6). In this LPS-prevention AAI mouse model, mice that were pre-treated with high dose 10 µg LPS, sensitised and challenged with OVA (LPS 10 µg/OVA/OVA) dramatically decreased the frequency and number of lung, lung-draining LN and airway eosinophils compared with the positive control group (Sal/OVA/OVA) (Fig. 7A-C). Moreover, mice with AAI had significantly increased concentrations of BAL fluid IL-4 and IL-5 (Sal/OVA/OVA), and this was significantly inhibited by LPS (LPS 10 µg/OVA/OVA) (Fig. 7D-E). Elevated IgE levels in mice with AAI (Sal/OVA/OVA) were also inhibited by LPS (LPS 10 µg/OVA/OVA) (Fig. 7F). Mice that were pre-treated with low dose 0.1 µg LPS and sensitised and challenged with OVA (LPS 0.1 µg/OVA/OVA) failed to inhibit the induction of AAI (Fig. 7A-F), suggesting that different doses of LPS play a crucial role in

inhibiting the induction of allergic airways inflammation, similar observed in others (Dong et al., 2009, Eisenbarth et al., 2002, Kim et al., 2007).

LPS treatment did not changed the percentages of Treg and Teff in the lung and lung-draining LN of AAI model but altered their proliferative and migration capacity

Previous studies demonstrated that LPS modify Th1/Th2 ratios that lead to the inhibition of the induction of allergic asthma (Revets et al., 2005, Eisenbarth et al., 2002). Another study showed that LPS inhibit allergic asthma by inducing endotoxin tolerance resulted from the unresponsiveness of dendritic cells (DC) and monocytes to subsequent LPS exposure (Matsushita et al., 2010). Our analyses revealed that LPS instillation in AAI did not change the numbers (data not shown) or percentages of $\text{TNFR2}^+\text{Foxp3}^+$ Treg, $\text{TNFR2}^-\text{Foxp3}^+$ Treg and $\text{TNFR2}^+\text{Foxp3}^-$ Teff in the lung (Fig. 8A-C) and lung-draining LN (Fig. 8D-F) compared to positive control group (Sal/OVA/OVA).

We hypothesised that LPS would alter the quality of Treg and/or Teff (as LPS did not alter the proportions/frequencies of Treg), thus to understand the effects of LPS on Treg and/or Teff quality, we analysed Ki67 and CCR7 on Treg and Teff in lung and lung-draining LN of AAI model (Fig. 9A-E). Results in naïve mice showed that $\text{TNFR2}^+\text{Foxp3}^+$ Treg lower their proliferative and migration capacity (Fig. 5A, D), but dramatically increased at day 30, which was the day that allergen challenge was performed in AAI model (Fig. 5A, D). Interestingly, as expected, only high dose LPS increased the proliferative capacity of $\text{TNFR2}^+\text{Foxp3}^+$ Treg to almost the same level as Sal/Sal/Sal group, and significantly higher than Sal/OVA/OVA group; whilst proliferative capacity of $\text{TNFR2}^+\text{Foxp3}^-$ Teff was unchanged (Fig. 9C). However, high dose LPS

treatment did not change Treg migration capacity to the lung-draining LN, rather decreased the percentages of CCR7⁺ within TNFR2⁺Foxp3⁻ Teff suggesting that they accumulated more in the lung (Fig.9D). Analyses on the expansion capacity of Treg in the lung-draining LN revealed that LPS treatment decreased the percentages of Ki67⁺ cells within TNFR2⁺Foxp3⁻ Teff (Fig. 9E). Overall, high dose LPS increased the capacity of Treg to expand in the lung, but decreased the expansion capacity of Teff in the lung-draining LN, whilst increased their accumulation capacity in the lung. Similar to what observed in naïve mice, CCR7 expression in the lung-draining LN were downregulated (data not shown).

LPS treatment increased the percentages of LAP⁺ within Treg in the lung and lung-draining LN of allergic asthma mouse model

Treg functionality is strongly related to TGF- β signalling (Liu et al., 2008, Marie et al., 2005, Bettelli et al., 2006, Dardalhon et al., 2008). TGF- β binds LAP is important in controlling Treg activation and proliferation status (Li et al., 2006). Besides LAP, CTLA-4 is another suppressor molecule that was reported to involve in the suppressive function of Treg (Duan et al., 2011, Schmidt et al., 2009). Therefore, to further understand the suppressive capacity of Treg, the percentages of LAP⁺ and CTLA-4⁺ cells within Treg in the lung and lung-draining LN were analysed (Fig. 10A, B). We demonstrated here that treatment with high dose LPS significantly increased the proportions of LAP⁺ cells within TNFR2⁻Foxp3⁺ Treg and TNFR2⁺Foxp3⁺ Treg the lung and lung-draining LN, respectively to a higher level than that in Sal/OVA/OVA group (Fig. 10C, E). On the other hand, there were no differences observed for CTLA-4⁺ cells within Treg in all groups both in the lung and lung-draining LN (Fig. 10D, F).

High dose 10 µg LPS inhibited Th2-producing LN cells

A more detailed examination on pulmonary allergen-specific Th2 cell responses revealed that mice with AAI had a marked increase in allergen-specific IL-4-, IL-5-, and IL-13-producing cells in the draining LN, as expected, and this was significantly inhibited by high dose 10 µg LPS treatment, whereas IFN- γ showed a decreased pattern with no significance decreased (Fig. 11A-D). The decreased frequencies of Th2 cytokine-producing cells in LPS 10 µg/OVA/OVA mice translated into 2- to 3-fold reduction in the total numbers of IL-4-, IL-5-, and IL-13-producing cells in the draining LN. Even though total IFN- γ -producing LN cells did not significantly decreased after high dose LPS treatment, the ratio of IFN- γ - /IL-4-producing cells was increased to almost 10-fold compared to Sal/OVA/OVA mice (data not shown). These results are in agreement as in the previous results, that high dose LPS increased the accumulation of Teff in the lung (Fig. 9D), and lowered the expansion capacity in the lung-draining LN (Fig. 9E). Despite altering Treg proportions/characteristics both in the lung and lung-draining LN, these results suggest that high dose LPS exposure might skew towards Th1 cells activation in the lung-draining LN, thus altering the balance between Th1 and Th2 cells.

Discussion

This study investigated the kinetics of Treg during the induction and resolution of LPS-induced acute lung injury and the modulation of different doses of LPS on Treg in allergic airways inflammation mouse model. We first showed that sorted $CD4^+CD25^-$ Teff (including $CD4^+CD25^-TNFR2^+$ and $CD4^+CD25^-TNFR2^-$ Teff) from naïve lung are the source of IL-2 and IL-4 cytokines, and we further showed that co-cultured of these cells with $CD4^+CD25^+$ Treg (including $CD4^+CD25^+TNFR2^+$ and $CD4^+CD25^+TNFR2^-$ Treg) decreased the concentration of the cytokines, which demonstrated the suppressive ability of $CD4^+CD25^+TNFR2^+$ and $CD4^+CD25^+TNFR2^-$ Treg to decrease IL-2 and IL-4 cytokines secretion from Teff.

Next, we further differentiated the functional characteristic of Treg and Teff based on eGFP-Foxp3. We suggested here that Teff could be divided into two distinct subsets; TNFR2 expressing Teff ($TNFR2^+Foxp3^-$ Teff) that are highly proliferative *in vivo* but not preferentially as cytokines producer and non TNFR2 expressing Teff ($TNFR2^-Foxp3^-$ Teff) that are programmed as cytokine producers, with less proliferative capacity *in vivo*. Chen *et al.* found that TNFR2 expressing Teff are maximally functional subset than non TNFR2 expressing Teff; and only TNFR2 expressing Treg are able to suppress TNFR2 expressing Teff (Chen et al., 2007, Chen and Oppenheim, 2011b). Additionally, TNFR2 expressing cells (Treg and Teff) are positively correlated Ki67 suggesting that TNFR2 cells are highly proliferative *in vivo* (Chen et al., 2010a, van Mierlo et al., 2008). Therefore, here we targeted highly functional $TNFR2^+Foxp3^+$ Treg as these cells were able to suppress maximally functional TNFR2 expressing Teff. To our knowledge, this is the first study indentifying TNFR2 expressing Treg and Teff in lung inflammatory setting.

We then sought to understand the effects of low and high doses of LPS on Treg (with or without TNFR2 expression) in the lung and lung-draining LN, and modulation of Treg by high dose LPS for the induction of a protective lung microenvironment to inhibit allergic asthma. The primary lung immune response can modify the nature of a subsequent immune responses in a process called innate imprinting (Hardy et al., 2013b) via various mechanisms including 1) impairment of pulmonary APC function (Hardy et al., 2013b, Williams et al., 2004, Hardy et al., 2012a) or mechanisms of antigen delivery (Abadie et al., 2009) and 2) induction of regulatory myeloid-derived suppressor cells (Arora et al., 2010) and Treg (Wang and McCusker, 2006, Zuany-Amorim et al., 2002b). Paralleling, we found that high dose LPS altered the primary immune response in the lung (preferentially on the quality of Treg) to respond more efficiently upon subsequent allergen exposure.

Others have also shown that exposure of mouse lungs to LPS prior to or concomitant with allergen sensitisation inhibits development of allergic asthma following allergen challenge (Eisenbarth et al., 2002, Arora et al., 2010). In regards to Treg induction, studies demonstrate that LPS or a killed *Mycobacterium vaccae* suspension induces IL-10⁺ Treg or CD4⁺CD45RB^{lo} cells producing IL-10 and TGF- β , which could inhibit allergic responses (Wang and McCusker, 2006, Zuany-Amorim et al., 2002b). We showed that Treg in mice treated with high dose LPS had higher proportions of TGF- β binding protein, LAP suggesting that immunosuppression observed in this system was partly mediated by TGF- β . In animal models, few studies reported that LPS exposure during sensitisation and allergen challenges decreased allergen-induced allergic asthma (Delayre-Orthez et al., 2004, Tulic et al., 2000, Rodriguez et al., 2003). However, in this

study, we exposed LPS without an encounter of allergen or any adjuvant for immunological imprinting effects in the lung, yet we also showed inhibition effects of LPS on the development of allergic asthma in a dose-dependent manner.

We observed that during the peak of airway inflammation in acute lung injury mouse model, the proportions of $\text{TNFR2}^+\text{Foxp3}^+$ Treg and $\text{TNFR2}^+\text{Foxp3}^-$ Teff increased to ~ 2 and ~ 3 fold, respectively suggesting that high levels of TNF concentrations in lung microenvironment play a role in driving the induction of TNFR2 expressing cells (Treg and Teff). However, we showed that highly proliferative TNFR2 expressing cells decreased their proliferative capacity in the inflamed lung microenvironment, but surprisingly, their expansion and migration capacity was gradually increased after inflammation resolved, a month after high dose LPS instillation. We proposed that LPS altered the lung homeostatic profile and re-programming the lung immune system to behave in a qualitatively different manner for subsequent responses. This is in agreement with Lloyd and Hawrylowicz, 2009, that they showed the importance of early life events in programming the lung immune system and effect on disease development (Lloyd and Hawrylowicz, 2009). Our study also is in parallel with a study that demonstrated *E. coli* endotoxin, LTK63 not only alters lung innate and adaptive immune responses by itself, but establishes lung protection by innate immune mechanisms and by improving adaptive responses to invading pathogens and/or infections (Williams et al., 2004, Tritto et al., 2007). More interestingly, the protective lung microenvironment limiting inflammatory responses or respiratory infection not only seen after prior immune activation in the lung, but events in the gut impact lung immunity (Williams et al., 2006, Watkins et al., 2008). Thus, not surprisingly that the lungs response to upon subsequent allergen exposure or

Appendices

infection will depend on each individual's position on the innate immune rheostat, supporting 'hygiene hypothesis' (Wissinger et al., 2009).

We showed that low dose LPS did not induce acute inflammation in the lung 3 days after exposure in naïve mice and unable to offer protection against allergic asthma. This suggests that subsequent responses of the lung in the absence or small magnitude (e.g. low dose LPS) of prior immune activation will produce a different nature of responses to the subsequent allergen challenges in the lungs (un-protective lung microenvironment). Overall, we proposed that exposure of high dose LPS into the lung microenvironment leave a long-lasting lung immunological imprinting, preferentially on the actively replicating cells (TNFR2⁺Foxp3⁺ Treg). TNFR2⁺Foxp3⁺ Treg exhibited active migration to the lung-draining LN and highly proliferative that were pre-conditioned by high dose LPS may have an essential role in restoring the lung immune homeostasis to reduce allergic asthma. Thus, targeting TNFR2⁺Foxp3⁺ Treg in inhibition of allergic asthma may offer advantages to new asthmatic therapeutics.

Acknowledgments

We gratefully acknowledge the expert assistance of Geza Paukovics with flow cytometry. MP is a Senior Research Fellow supported by National Health & Medical Research Council (NHMRC) of Australia and a non-executive director of PX Biosolutions. RM is a fellow of the Academic Staff Training Scheme at Universiti Sains Malaysia and a recipient of a Malaysian Government PhD Scholarship and CRC-Airways and Asthma top-up Scholarship.

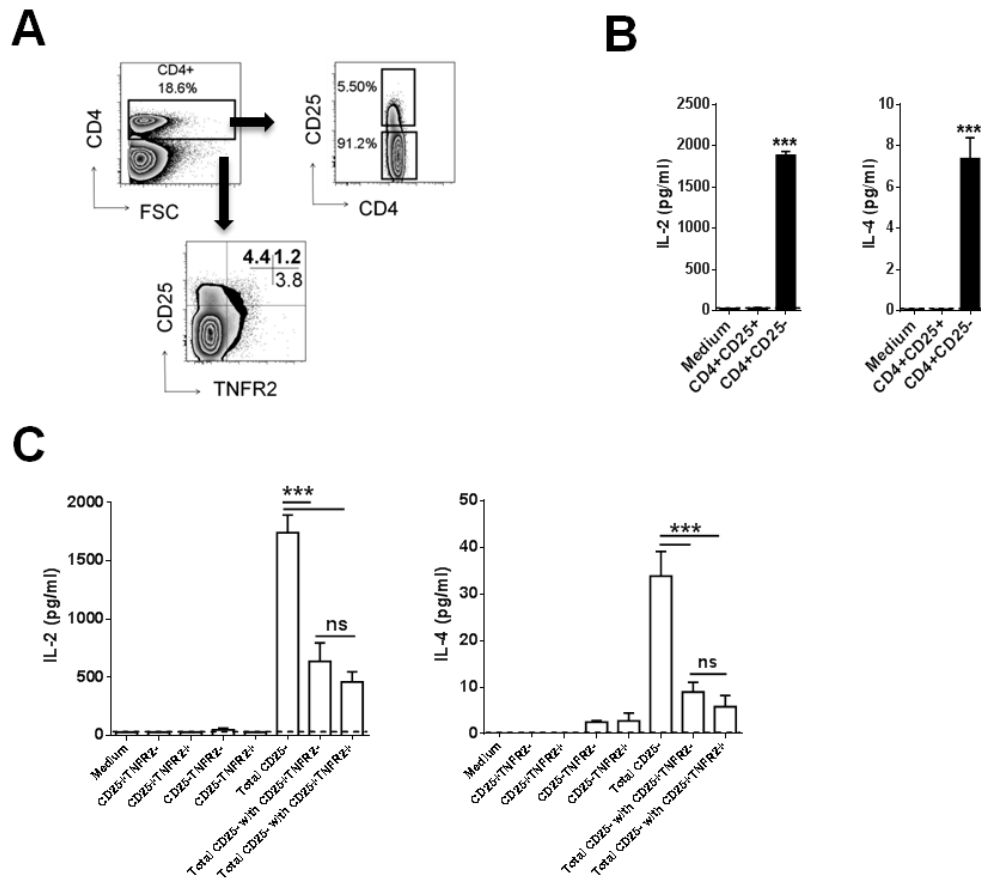


Fig. 1: Lung $CD4^+CD25^+$ ($TNFR2^+$ and $TNFR2^-$) cells from the lungs of unmanipulated mice are non-cytokines producer, exhibited suppressive function and express more Ki67.

Lung leukocytes were isolated by collagenase/DNase digestion. **(A)** Cells were sorted based on viable $CD3^+CD4^+CD25^+$ or $CD25^-$ T cells. $TNFR2$ cells were then gated and sorted on $CD4^+$ cells followed by gating on $CD25$ co-expressed $TNFR2$. FACS sorted $CD4^+CD25^+$ cells, $CD4^+CD25^-$ cells and $TNFR2$ populations were stimulated with the combination of $\alpha CD3$ and $\alpha CD28$. IL-2 and IL-4 secretions in cells culture supernatants of sorted cells were analysed by multiplex. **(B)** IL-2 and IL-4 secretions in $CD4^+CD25^+$ and $CD4^+CD25^-$ cells culture supernatants. **(C)** Cytokines inhibition assay. Dashed line denotes lower limit of detection. Mean \pm SEM. ns, not significant. *** $p < 0.001$.

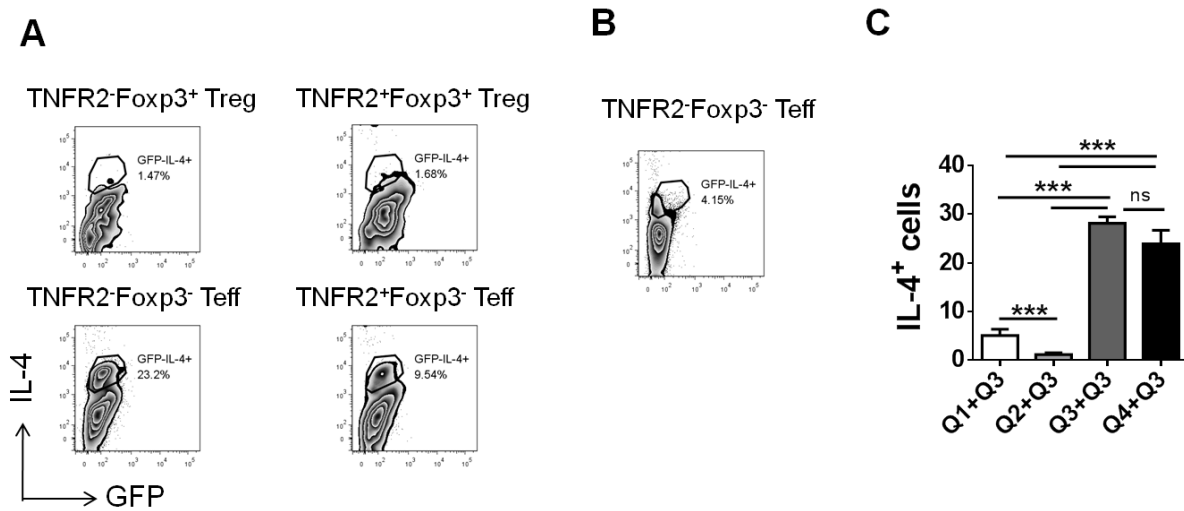


Fig. 2: Sorted spleen Teff (CD25⁻TNFR2⁺Foxp3⁻/GFP⁻ and CD25⁻TNFR2⁻CD25⁺TNFR2⁺Foxp3⁻/GFP⁻ Foxp3⁻/GFP⁻) exhibited higher IL-4⁺ cells, whereas TNFR2 expressing Treg were more suppressive than non-TNFR2 expressing Treg (CD25⁺TNFR2⁻Foxp3⁺/GFP⁺)

FACS sorted spleen cells from naïve mice were subjected to proliferation assay by culturing with the combination of anti-CD3 and anti-CD28 for 72 hrs, Brefeldin A was added to the culture for the final 5 hours. Cells were stained with Dead cells stain and intracellular cytokine staining was performed for IL-4. Live cells were then gated based on IL-4 co-expressed GFP. GFP⁻IL-4⁺ cells gated from (A) TNFR2⁻Foxp3⁺ Treg (Q1), TNFR2⁺Foxp3⁺ Treg (Q2), TNFR2⁻Foxp3⁻ Teff (Q3) and TNFR2⁺Foxp3⁻ Teff (Q4). (B) GFP⁻IL-4⁺ cells gated from TNFR2⁻Foxp3⁻ Teff (Q3) cultured without α CD3 and α CD28 (negative control). (C) Treg suppression assay on IL-4⁺ cells Teff. IL-4⁺ cells within TNFR2⁻Foxp3⁻ Teff (Q3) were suppressed after co-cultured with TNFR2⁺Foxp3⁺ Treg (Q2) and TNFR2⁻Foxp3⁺ Treg (Q1).

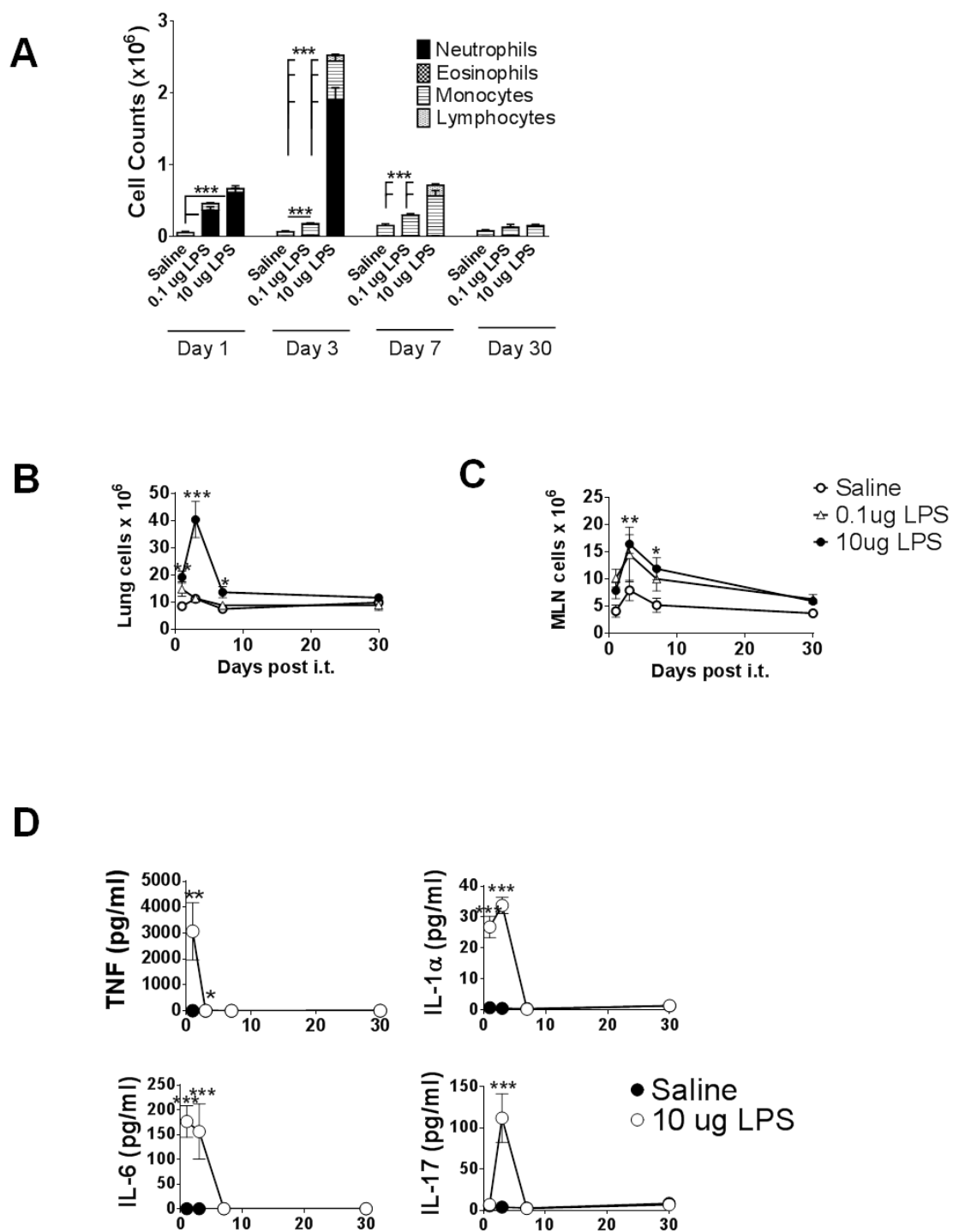


Fig. 3: Analysis of pulmonary inflammatory responses on airway inflammation induced by LPS.

Mice (n=5-7 per group per time point) were intratracheally administered with saline, 0.01 μ g, and 10 μ g LPS. Samples were collected on d1, d3, d7 and d30 after LPS administration. **(A)** Cells from BAL fluid were stained with Giemsa stain, counted for at least 200 cells per mouse and identified by morphological criteria for lymphocytes, monocytes, eosinophils and neutrophils. Total cell counts from **(B)** lung and **(C)** lung-draining LN. **(D)** BAL fluid was subjected to multiplex for the detection of TNF, IL-1 α , IL-6 and IL-17 concentration. Limit of detection was 2.38, 29.86, 0.34 and 0.45 pg/ml, respectively. Data represent the mean \pm SEM. * $p < 0.05$, ** $p < 0.01$, and *** $p < 0.001$.

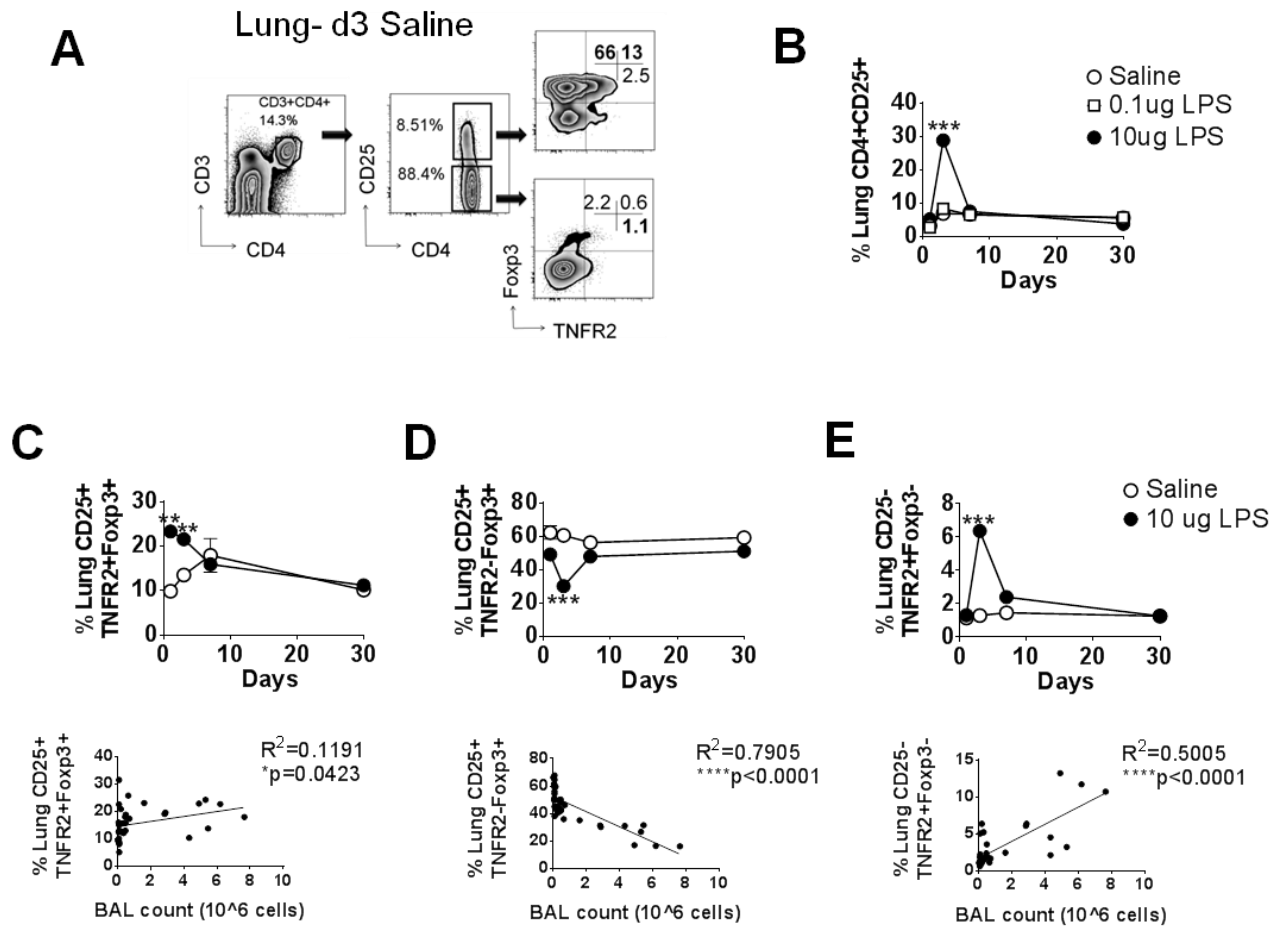
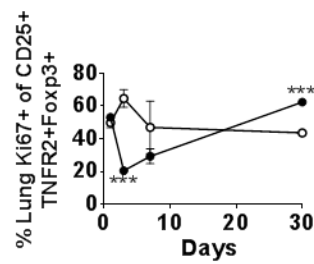
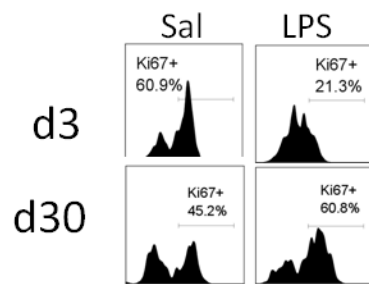


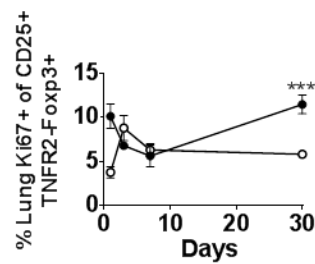
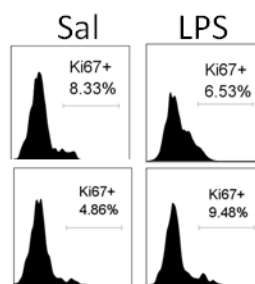
Fig. 4: Analysis of lung Treg and Teff in LPS induced acute lung injury mouse model.

Mice (n=5-7 per group per time point) were intratracheally administered with saline and 10 ug LPS. Samples were collected on d1, d3, d7 and d30 after LPS administration. (A) Lung cells were gated on viable CD3⁺CD4⁺CD25⁺ and CD3⁺CD4⁺CD25⁻ cells, followed by gating on TNFR2 co-expressed Foxp3. Percentages for each populations and respective correlation with BAL counts for (B) CD4⁺CD25⁺ (C) TNFR2⁺Foxp3⁺ Treg; (D) TNFR2⁻Foxp3⁺ Treg and (E) TNFR2⁺Foxp3⁻ Teff. Data represent the mean \pm SEM. * p < 0.5, ** p< 0.01, and *** p < 0.001.

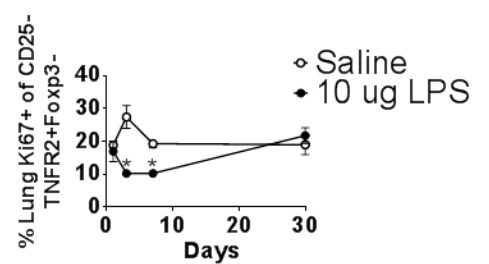
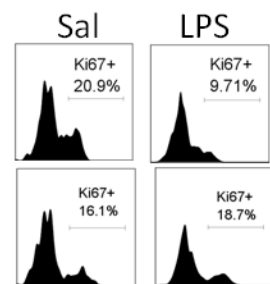
A



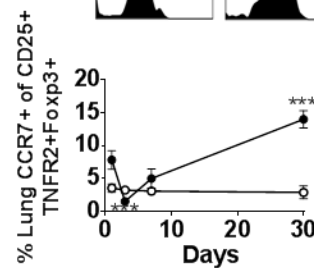
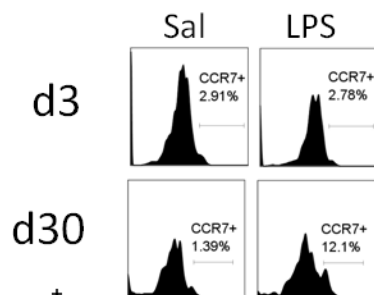
B



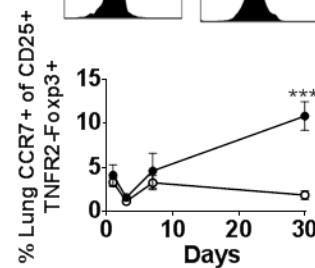
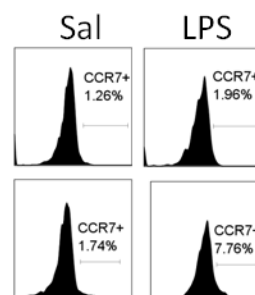
C



D



E



F

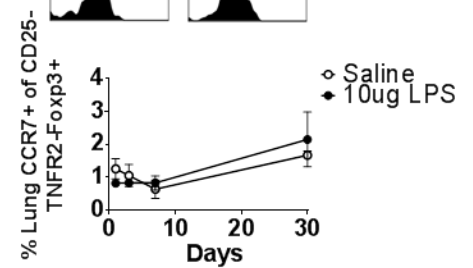
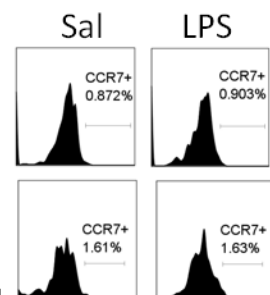
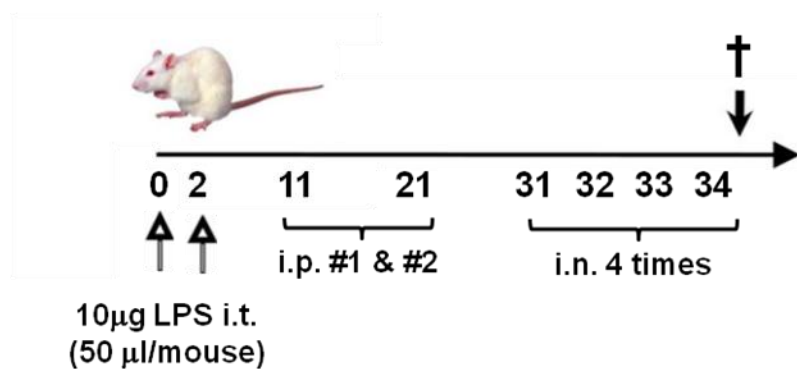


Fig. 5: Analysis on the proliferative and migration capacity of lung Treg and Teff in LPS induced acute lung injury mouse model.

Mice (n=5-7 per group per time point) were intratracheally administered with saline and 10 µg LPS. Samples were collected on d1, d3, d7 and d30 after LPS administration. Representative FACS plots showing Ki67⁺ cells and CCR7⁺ in the lung at day 3 and day 30 post saline and 10 µg LPS administration. Percentages of Ki67⁺ cells and CCR7⁺ cells within (A, D) TNFR2⁺Foxp3⁺ Treg; (B, E) TNFR2⁻Foxp3⁺ Treg and (C, F) TNFR2⁺Foxp3⁻ Teff. Data represent the mean ±SEM. * p < 0.05, ** p < 0.01, and *** p < 0.001.

LPS-AAI prevention mouse model



#	Groups	Pre-treatment (i.p.)	Sensitization (i.p.)	Challenge (i.n.)
1	S/S/S (Negative)	Saline	Saline	Saline
2	S/O/O (Postive)	Saline	Ovalbumin	Ovalbumin
3	LPS 0.1/O/O	LPS 0.1 µg	Ovalbumin	Ovalbumin
4	LPS 10/O/O	LPS 10 µg	Ovalbumin	Ovalbumin

Fig. 6: Schedule of allergen immunisations and LPS pre-treatment in AAI model.

Groups of mice (6-7 mice/group) were sensitised i.p. with OVA/alum, positive control group received saline for pre-treatment and challenged with OVA. Negative control group received saline. LPS were i.t. twice, before sensitised and challenged with OVA. Tissue sampling was performed on day 1 after the final lung allergen challenge.

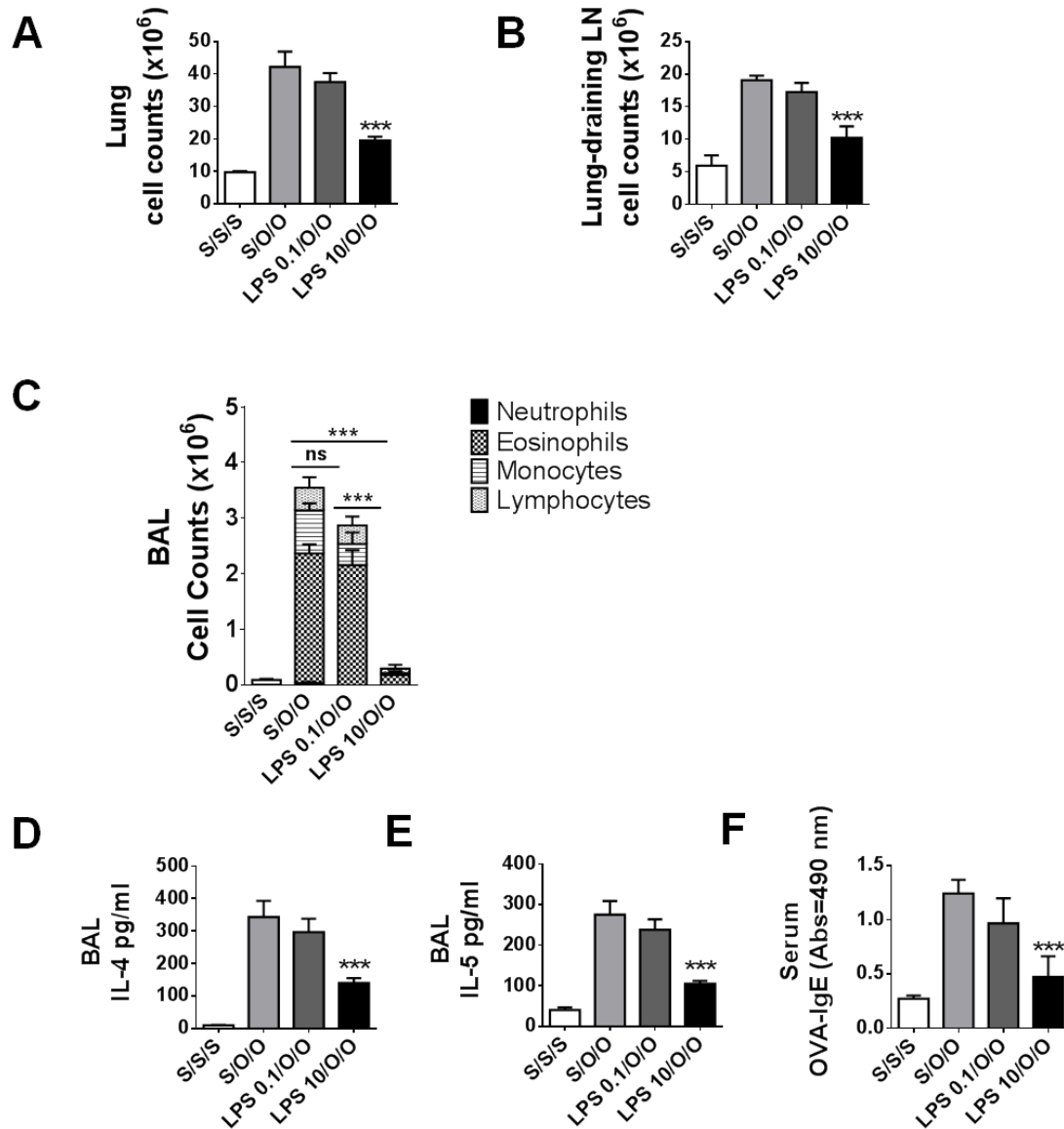


Fig. 7: LPS improved AAI in a dose-dependent manner.

Mice were treated with LPS and sensitised as described in Fig. 6 and challenged with OVA; control mice received saline instead of LPS or OVA. Total cell counts in the (A) lung and (B) lung-draining LN. (C) Cells from BAL fluid were stained with Giemsa stain, counted for at least 200 cells per mouse and identified by morphological criteria for lymphocytes, monocytes, eosinophils and neutrophils. Levels of (B) IL-4 (C) IL-5 in the BAL fluid and (D) levels of serum OVA-specific IGE. Mean \pm SEM. 6-7 mice/group. ns = not significant; ***p < 0.001.

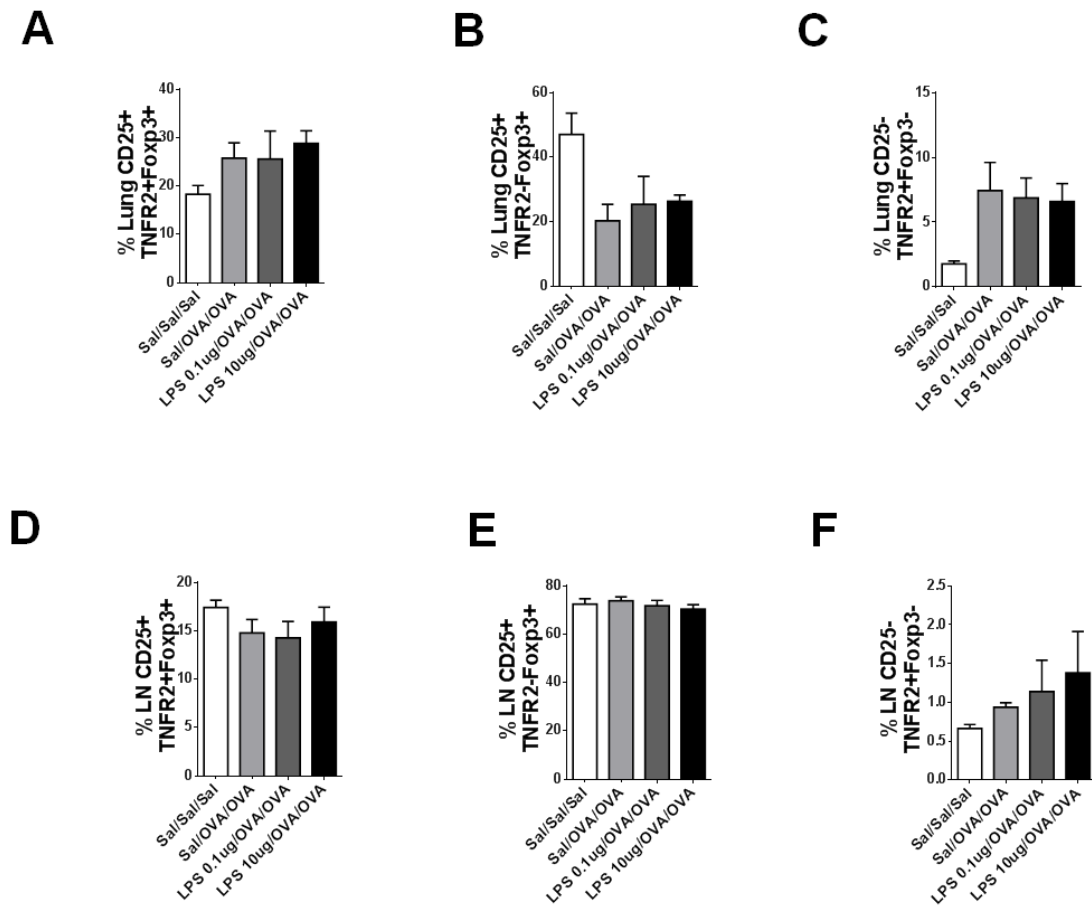


Fig. 8: LPS did not alter Treg and Teff profile in the lung and lung-draining LN of AAI mice. Mice were treated with LPS and sensitised as described in Fig. 6 and challenged with OVA; control mice received saline instead of LPS or OVA. Stained lung cells were gated on viable CD3⁺CD4⁺CD25⁺ and CD3⁺CD4⁺CD25⁻ cells, followed by gating on TNFR2 co-expressed Foxp3. Gating strategy was applied as in Fig. 2. Percentages of (A) TNFR2⁺Foxp3⁺ Treg; (B) TNFR2⁻Foxp3⁺ Treg and (C) TNFR2⁺Foxp3⁻ Teff in the lung and (D) TNFR2⁺Foxp3⁺ Treg; (E) TNFR2⁻Foxp3⁺ Treg and (F) TNFR2⁺Foxp3⁻ Teff in the lung-draining LN. Mean \pm SEM. 6-7 mice/group.

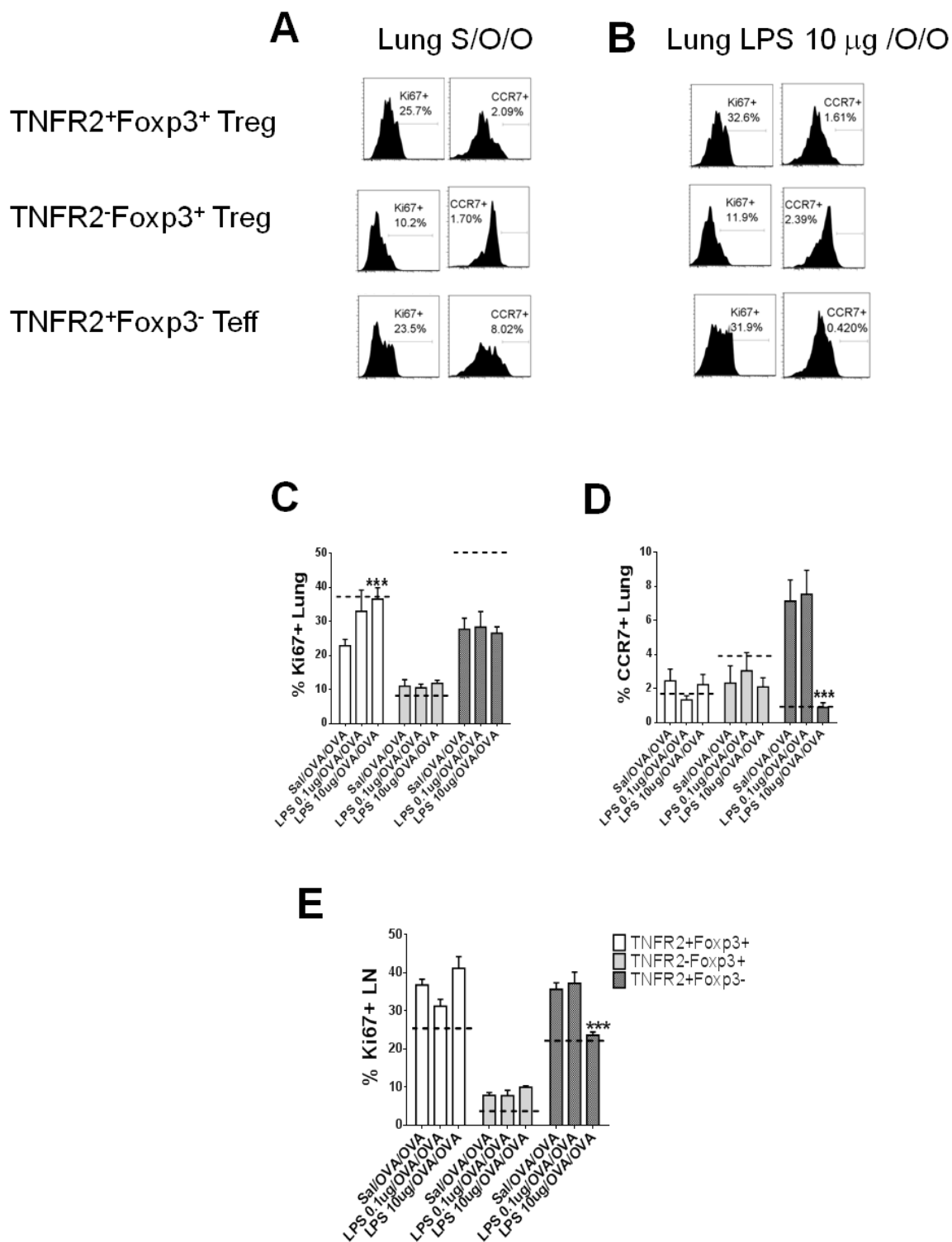


Fig. 9: LPS altered Ki67 and CCR7 of Treg and Teff in the lung-draining LN of AAI mice in a dose-dependent manner. Mice were treated with LPS and sensitised as described in Fig. 6 and challenged with OVA; control mice received saline instead of LPS or OVA. Stained lung cells were gated on viable CD3⁺CD4⁺CD25⁺ and CD3⁺CD4⁺CD25⁻ cells, followed by gating on TNFR2 co-expressed Foxp3. Further analyses were performed on Ki67 and CCR7 both in the lung and lung-draining LN. FACS plot representative of (A) Sal/OVA/OVA and (B) 10 µg LPS/OVA/OVA in the lung. Analyses on lung (C) Ki67⁺ (D) CCR7⁺ and lung-draining LN (E) Ki67⁺ cells. Mean ± SEM. 6-7 mice/group. ns = not significant; **p< 0.01 ***p< 0.001.

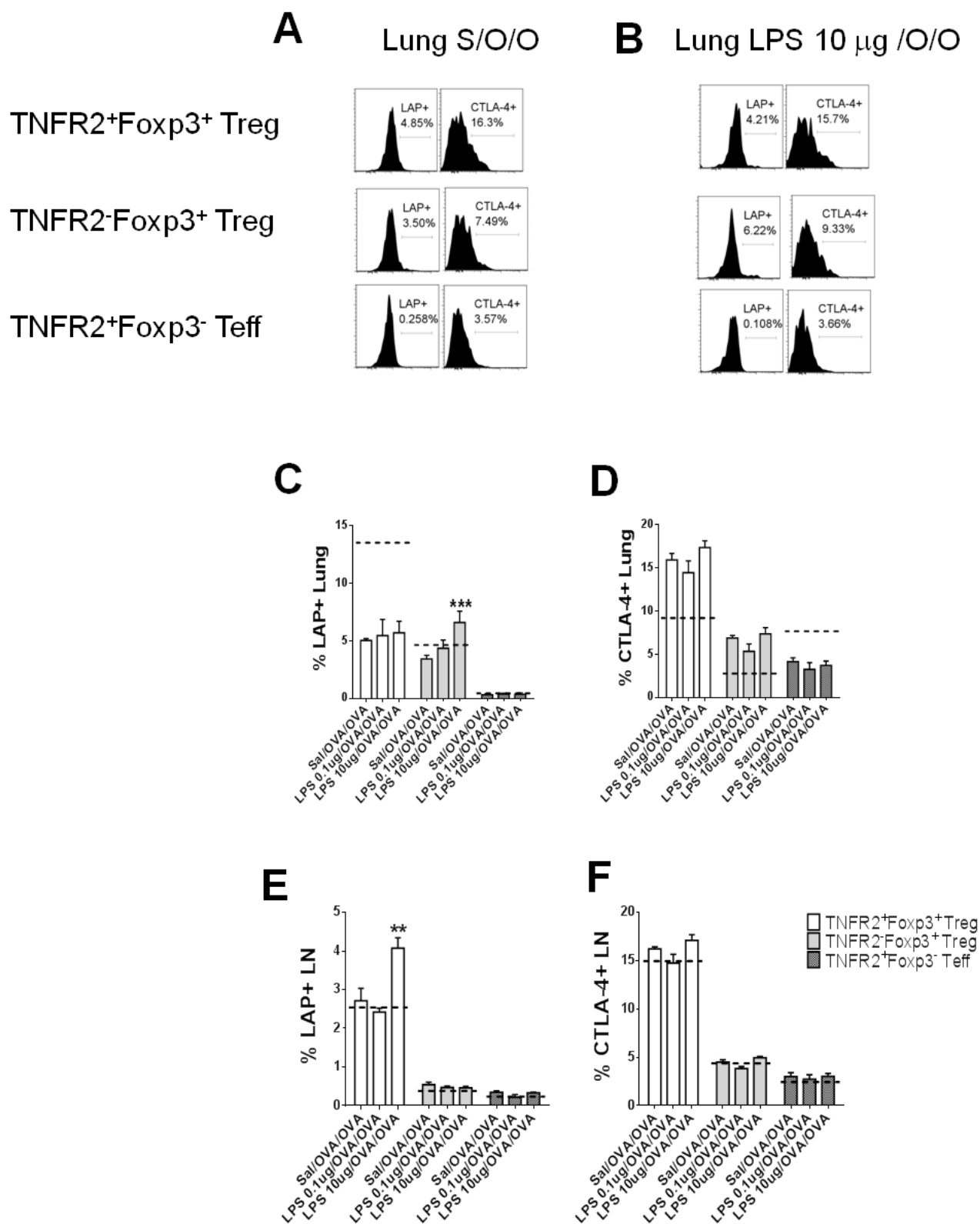


Fig. 10: LPS altered LAP of Treg in the lung-draining LN of AAI mice in a dose-dependent manner. Mice were treated with LPS and sensitised as described in Fig. 6 and challenged with OVA; control mice received saline instead of LPS or OVA. Stained lung cells were gated on viable CD3⁺CD4⁺CD25⁺ and CD3⁺CD4⁺CD25⁻ cells, followed by gating on TNFR2 co-expressed Foxp3. Further analyses were performed on LAP and CTLA-4 both in the lung and lung-draining LN. FACS plot representative of (A) Sal/OVA/OVA and (B) 10 µg LPS/OVA/OVA in the lung. Analyses on lung (C) LAP⁺ (D) CTLA-4⁺ and lung-draining LN (E) LAP⁺ (F) CTLA-4⁺ cells. Mean ± SEM. 6-7 mice/group. ns = not significant; **p< 0.01 ***p< 0.001.

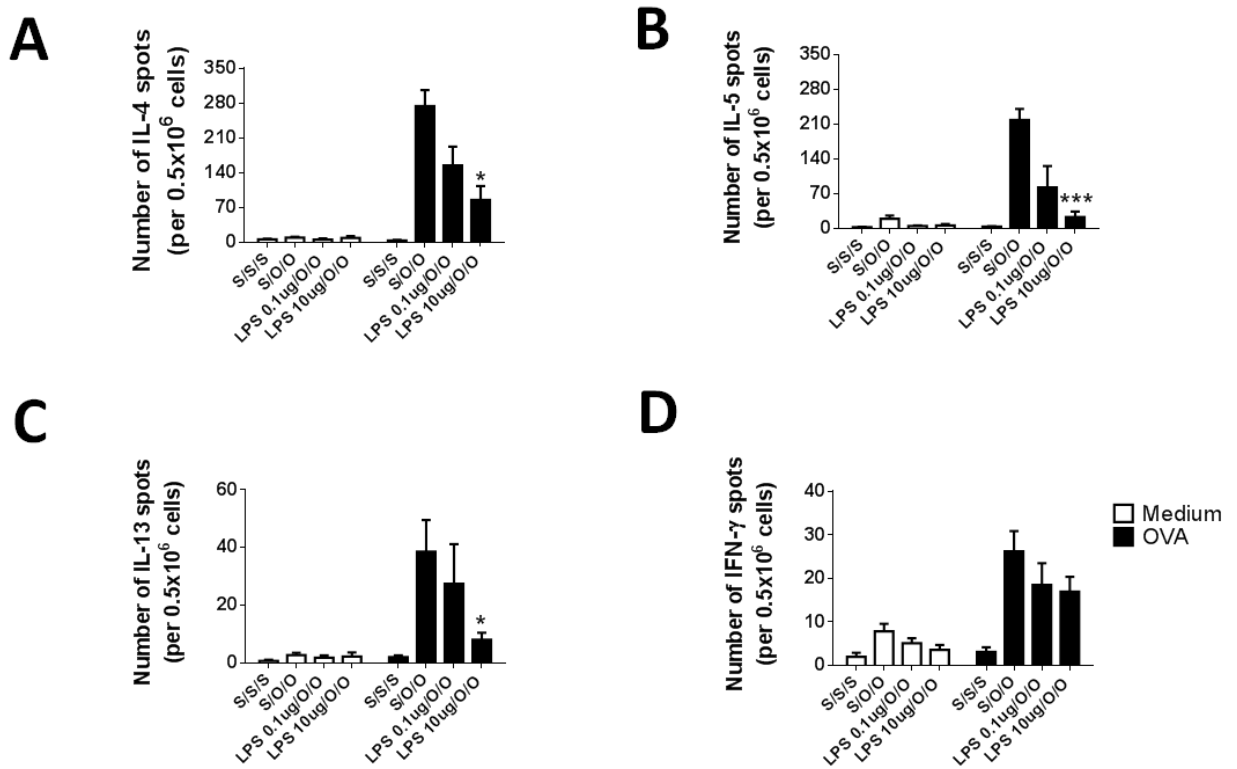
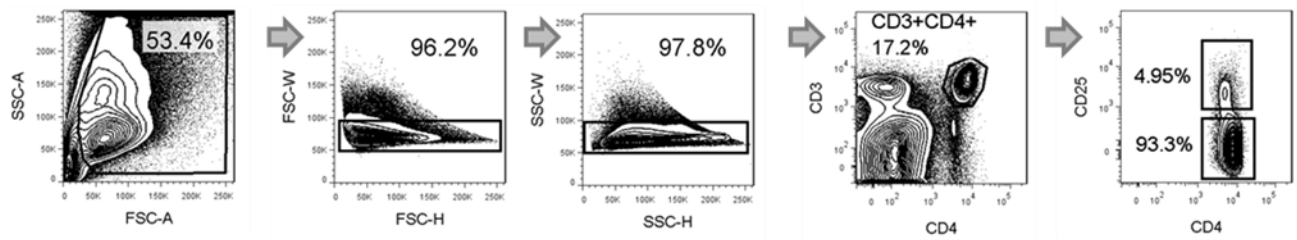


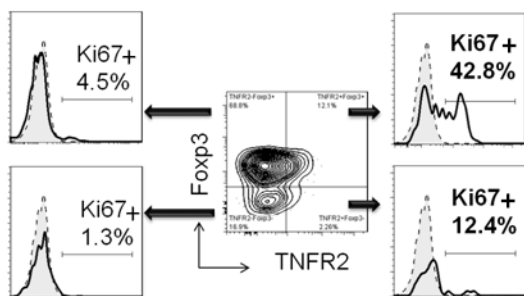
Fig. 11: LPS modulated acute AAI in a dose dependent manner . Mice were treated with LPS and sensitised as described in Fig. 6 and challenged with OVA; control mice received saline instead of LPS or OVA. **(A)** IL-4- **(B)** IL-5- **(C)** IL-13- and **(D)** IFN- γ -producing LN cells. Mean \pm SEM. * $p < 0.05$; *** $p < 0.001$.

A



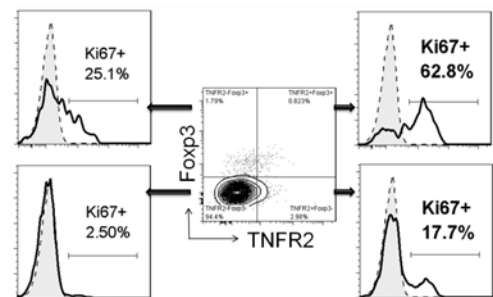
B

Lung CD3⁺CD4⁺CD25⁺ cells



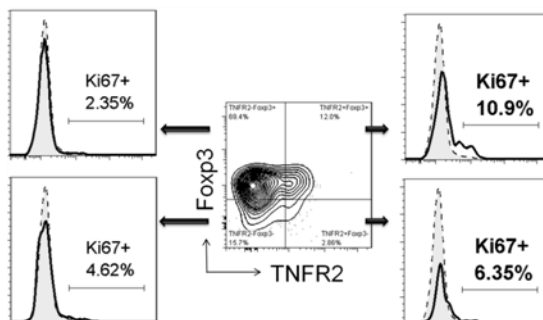
C

Lung CD3⁺CD4⁺CD25⁻ cells



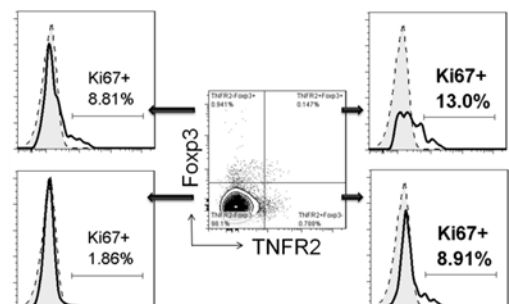
D

LN CD3⁺CD4⁺CD25⁺ cells



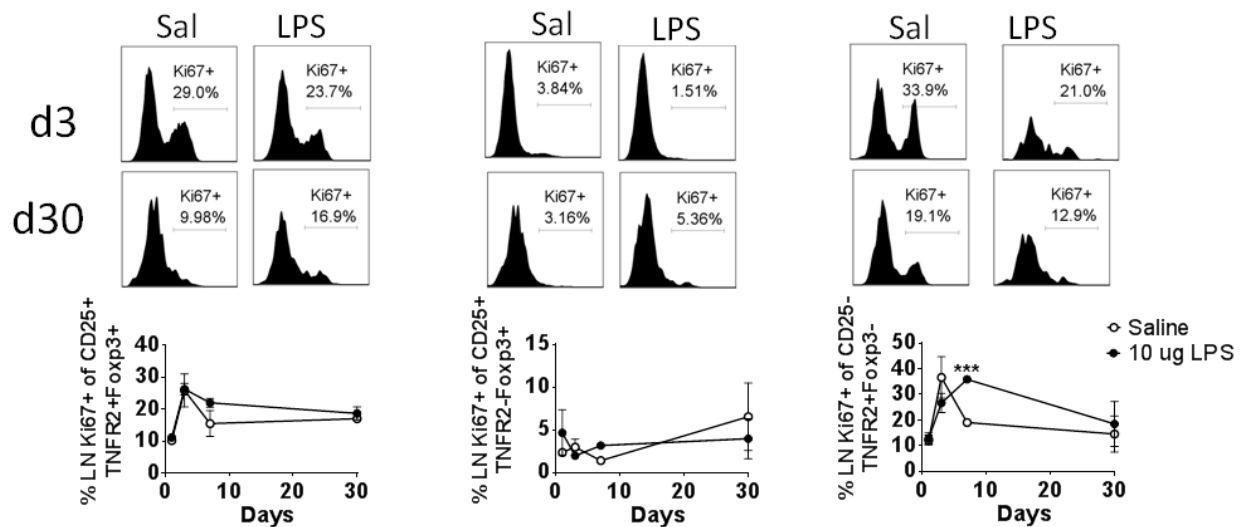
E

LN CD3⁺CD4⁺CD25⁻ cells



Suppl. Fig. 1: Lung $CD3^+CD4^+CD25^+TNFR2^+Foxp3^+$ and $CD3^+CD4^+CD25^-TNFR2^+Foxp3^-$ cells from the lungs and lung draining LN of unmanipulated mice have more Ki67 compared to $TNFR2^-$ counterparts.

(A) Gating strategy applied for $CD3^+CD4^+CD25^+$ and $CD3^+CD4^+CD25^-$ cells. Percentages of $Ki67^+$ population (black line, open histogram) and appropriate isotype control (dotted line, grey filled histogram) from lung (B) $CD3^+CD4^+CD25^+$; (C) $CD3^+CD4^+CD25^-$ cells and lung-draining LN (D) $CD3^+CD4^+CD25^+$; (E) $CD3^+CD4^+CD25^-$ cells.



Suppl. Fig. 2: Analysis on the proliferative capacity of lung-draining LN Treg and Teff in LPS induced acute lung injury mouse model. Mice (n=5-7 per group per time point) were intratracheally administered with saline and 10 μ g LPS. Samples were collected on d1, d3, d7 and d30 after LPS administration. Representative FACS plots showing Ki67⁺ cells in the lung-draining LN at day 3 and day 30 post saline and 10 μ g LPS administration. Percentages of Ki67⁺ cells within TNFR2⁺Foxp3⁺ Treg (left panel); TNFR2⁻Foxp3⁺ Treg (middle panel) and TNFR2⁺Foxp3⁻ Teff (right panel). Data represent the mean \pm SEM. * p < 0.5, ** p < 0.01, and *** p < 0.001.

BAL Cytokines (pg/ml)	Naïve mice	Sal negative control group	LPS induced lung injury
IL-1a	64.8 ± 10.8	55.76 ± 9.21	325.4 ± 33.2***
IL-2	45.2 ± 2.98	40.5 ± 5.32	LLOD
IL-5	4.8 ± 2.58	4.5 ± 1.54	LLOD
IL-6	1.51 ± 1.1	LLOD	1350 ± 46.4***
IL-10	15.27 ± 0.14	10.43 ± 3.3	32.54 ± 7.92
IFN- γ	LLOD	LLOD	867 ± 20.3***
TNF	8.23 ± 3.5	LLOD	245.5 ± 23.4***
TGF-β	40 ± 3.4	55 ± 5.43	287 ± 23.3***
GM-CSF	49.15 ± 3.34	38.73 ± 4.5	5.4 ± 1.23**
IL-4	0.37 ± 0.03	0.06 ± 0.01	LLOD
IL-17	LLOD	LLOD	196 ± 5.4***

Table 1: High dose 10 μ g LPS increased BAL pro-inflammatory cytokines.

BAL fluid was subjected to Multiplex assay for measurement of IL-1 α , IL-2, IL-5, IL-6, IL-10, IFN- γ , TNF, TGF- β , GM-CSF, IL-4 and IL-17. Limit of detection was 29.86, 30.65, 1.12, 0.34, 0.16, 0.54, 2.38, 10.56, 0.59, 0.08 and 0.45 pg/ml, respectively. Mean \pm SEM. **p<0.01; ***p<0.001 compared to OVA positive control group. LLOD- lower limit of detection.

9.2 Unpublished manuscript 2

Lack of inflammatory effects of engineered nanoparticles in *in vitro* and *in vivo* models show potential as disease therapeutics

Rohimah Mohamud^{a*}, Ying Ying Kong^{a*}, Jeanne LeMasurier^a, Je Lin Sieow^a, Tanya De L. Karlson^a, Sue D. Xiang^a, Jennifer M. Rolland^{abc}, Robyn E. O’Hehir^{abc}, Charles L. Hardy^{abc*}, Magdalena Plebanski^{acd*}

** Equal contribution*

^aDepartment of Immunology, Monash University, Melbourne, VIC, Australia

^b Department of Allergy, Immunology and Respiratory Medicine, The Alfred Hospital and Monash University, Melbourne, VIC, Australia

^c CRC for Asthma and Airways, Sydney, NSW, Australia

^d Corresponding author:

Professor Magdalena Plebanski

[REDACTED]

[REDACTED]

Fax: + 61 3 9903 0038

This research was funded by the Cooperative Research Centre for Asthma and the National Health & Medical Research Council of Australia. RM is the recipient of Malaysian Postgraduate Scholarship Scheme and CRC-Asthma and Airways top-up Scholarship.

Abstract

Engineered nanoparticles (ENP) are increasingly being developed for nanocarriers and/or vaccines. Although it has been proposed that ENP could regulate lung inflammation and induce toxicity in *in vitro* cell cultures, few ENP have been shown to be safe and being used as disease therapeutics. In this study, we investigated the toxicity effects of ENP both *in vitro* and *in vivo*. We found that PS-ENP did not induce cytotoxicity in the bone marrow dendritic cells culture, as reflected by low levels of pro-inflammatory cytokines in the culture supernatants. Whilst, in *in vivo* studies, we investigated the effects of inflammatory effects of ferum oxide-ENP (Fe₃O₄-ENP) and polystyrene-ENP (PS-ENP) in the lung 3 days post intratracheal instillation. We demonstrated that PS-ENP initiated an active immune response in the lung including recruited higher cellularity levels and increased bronchoalveolar lavage (BAL) cytokines, while Fe₃O₄-ENP failed to recruit higher cellularity levels in the lung suggesting that lung-ENP interactions are partially dependent on the ENP composition. Nevertheless, Fe₃O₄- and PS-ENP are safe to the lung, a feature that holds great potential for these ENP in the development of targeted nanocarriers and/or vaccines.

Keywords: Dendritic cells, Lung, Lipopolysaccharides, Inflammation, Toxicity

Introduction

Nanoparticles (< 100 nm) can be categorised into naturally occurring (ambient) nanoparticles (e.g. forest fires), anthropogenic nanoparticles produced inadvertently as a result of human activity (e.g. combustion engines) and engineered nanoparticles (ENP) produced for various industrial applications or consumer products (Mohamud et al., 2013). Studies demonstrated that exposure to some types of nanoparticles can be associated with both mortality and morbidity, and they affect the lungs at the cellular and molecular levels due to their unusual physicochemical properties (Oberdorster et al., 1995, Schwartz et al., 1996, Utell and Frampton, 2000, Stone et al., 2007). Polystyrene ENP are inorganic, non-biodegradable, but biocompatible, and do not induce oxidative stress *in vitro* (Xia et al., 2006). We previously showed that intratracheal instillation of 50 nm polystyrene engineered nanoparticles (PS-ENP) do not induce lung oxidative stress, cardiac or lung inflammation (Hardy et al., 2012a, Hardy et al., 2013a). Similar to PS-ENP, iron oxide-ENP (Fe₃O₄-ENP) are inorganic, non-biodegradable and exhibit biocompatibility both *in vitro* and *in vivo*. Fe₃O₄-ENP with various sizes (10-120 nm) do not induce cytotoxicity or mutagenicity in human lung epithelial cells (Karlsson et al., 2008, Verma et al., 2013). Intranasal delivery of Fe₃O₄-ENP (10 nm) into mice do not induce detectable inflammation in BAL fluid after days 1, 4 or 7 post-treatment (Verma et al., 2013). Prior exposure of ENP into the lung, antigen-presenting cells (APCs) will taken up ENP and initiates an active immune responses or inflammatory reaction. Lung-ENP interactions are influenced by the diverse biophysical and chemical characteristics of the ENP including composition, size and mode of delivery.

Dendritic cells, considered as the most potent APCs, are characterised by their unique ability to activate the adaptive immune response (Banchereau and Steinman, 1998,

Steinman and Banchereau, 2007). They are a rare cell population *in vivo* but are strategically located in tissue niches, which helps them interact with T- and B-cells efficiently. Dendritic cells consist of an extensive array of subsets with myeloid or lymphoid origins, each with specific functions within the immune system (Kong et al., 2013). Immature dendritic cells generally express low levels of activation markers such as CD80, CD86 and major histocompatibility complex (MHC) class I and II (Banchereau and Steinman, 1998). Immature dendritic cells also have a high endocytic capacity, which allows them to pick up foreign antigen and invading pathogens. Endocytosis plays an important role in downstream antigen processing and presentation such that, inhibition of endocytosis eradicates both functions in dendritic cells (Sallusto et al., 1996, Kerksiek et al., 2005, von Delwig et al., 2006). The interaction between dendritic cells and antigens initiates dendritic cell maturation, enhancing antigen presentation, activation marker expression and inflammatory cytokine production (Uto et al., 2013). For instance, Uto et al showed, in several of their studies, that by using nanoparticles coated with antigens, it increased the exposure of dendritic cells to antigens and enhanced their maturation status; inducing inflammatory cytokine secretion and long-term, antigen-specific effector and central memory T cells (Uto et al., 2007, Uto et al., 2009, Uto et al., 2011a, Uto et al., 2011b). Moreover, during antigen presentation, dendritic cells are able to shape the nature of the adaptive immune response through cytokine secretion by either skewing the immune response towards immune activation (induction of Th1, Th2, Th17) or immune regulation (induction of regulatory T cells) (Banchereau and Steinman, 1998, Krishnamoorthy et al., 2007, Radstake et al., 2004, Khayrullina et al., 2008, Akbari et al., 2014, Bell et al., 2013, Ko et al., 2014).

Appendices

Dendritic cell preferentially take up PS-ENP however this does not result in the initiation of inflammation via the ERK mediated signalling pathways (Karlson Tde et al., 2013). Furthermore, we have shown that, in the lung, pre-exposure to PS-ENP primes the immune response such that subsequent challenge with allergen does not result in allergic airway inflammation (AAI). We speculate that nanoparticles may modulate dendritic cell function by down regulating their capacity to activate an inflammatory response.

Materials & Methods

Mice

Female BALB/c and C57BL/6 mice age between 6-8 weeks old were obtained from Precinct Animal Centre (PAC) at the Alfred Medical Research and Educational Precinct (AMREP) (Melbourne, VIC) and housed in the Alfred Medical Research and Education Precinct animal house. The AMREP Animal Ethics Committee approved all studies with these mice.

Generation of in vitro dendritic cell cultures

Bone marrow cells from femurs and tibias of C57BL/6 mice were collected and treated with ACK lysis buffer (155mM NHCl₄, 0.1mM Na-EDTA, 10mM KHCO₃ pH 7.2) for 3 minutes at RT to lyse erythrocytes. Cells were washed and cultured at 5×10^5 cells/ml with complete media (RPMI 1640, 2mM L-glutamine (Sigma–Aldrich, Louis, MO, USA), 20mM HEPES (Sigma–Aldrich, Louis, MO, USA), 0.1 mM 2-mercaptoethanol (2-ME) (Sigma–Aldrich, Louis, MO, USA), 100 U/ml Penicillin, 100µg/ml of Streptomycin (Sigma–Aldrich, Louis, MO, USA) and 50 ml of heat-inactivated Foetal Calf Serum (FCS) (Sigma–Aldrich, Louis, MO, USA)) at 37°C, 6% CO₂. GM-CSF (PeproTech, Rocky Hill, NJ, USA) (10ng/ml) was added to induce dendritic cell generation for 3 days.

Preparation of particles and induction of dendritic cell activation

Fluorescent-labelled PS-ENP were dialysed in MilliQ water overnight and sonicated for 15 minutes to prevent aggregation before using. Dendritic cells were stimulated with lipopolysaccharide (LPS) (1µg/ml) derived from *Escherichia coli* (Sigma–Aldrich, Louis, MO, USA) or PS-ENP for 24 hours and harvested after stimulation.

Appendices

Particles preparations and instillations

Polybead carboxylate microspheres (unlabelled, nominally 0.05 μ m; no. 15913; Polysciences, Warrington, PA) were glycine coated as described (Fifis et al., 2004), hereafter referred to as PS-ENP (Hardy et al., 2012a, Hardy et al., 2013a). To investigate the effects of PS-ENP on lung immune response, BALB/c mice received saline PS-ENP (200 μ g / 50 μ l) or 10 μ g LPS intratracheally on day 0 and samples were collected on day 3. In some experiment, FITC-labelled-PS-ENP was used as means of tracking. Fe₃O₄-ENP (200 μ g / 50 μ l) were also used to investigate the effects on lung immune response. The trachea was intubated with a soft plastic 20-gauge catheter and guide wire, and saline or particles were delivered via a 50- μ l microsyringe (SGE International Pty., Melbourne, Australia) attached to a blunted 20-gauge needle (Hardy et al., 2003, Hardy et al., 2012a).

Bronchoalveolar lavage fluid and differential counts

Methods were as described previously (Hardy et al., 2003). To obtain BAL fluid, lungs were lavaged with 0.4 ml of 1 % foetal calf serum (FCS) in phosphate-buffered saline (PBS) followed by 3 further lavages of 0.3 ml. For differentials, total cell counts were determined for each BAL sample and 100 μ l of fluid was cytopun at 350 x g for 4 min onto glass slides. BAL cytopots were air-dried, fixed in methanol for 2 minutes, and Giemsa stained for 8 minutes (Merck, Kilsyth, Victoria, Australia). At least 200 cells per mouse were counted and identified by morphological criteria.

Confocal microscopy analysis of PS-ENP uptake by in vitro dendritic cells culture

Cultured bone marrow cells in GM-CSF were treated for 24 hours with fluorescent-labelled PS-ENP (Invitrogen, Life Technologies Australia Pty, Ltd, Australia). Cells were then harvested and stained overnight at 4 °C with biotin anti-Mouse 1-Ab (BD

Pharmingen, New Jersey, USA) anti-mouse CD11c Alexa Fluor 647 conjugated (eBioscience, Inc, San Diego, USA) to detect dendritic cells. After staining, cells were washed with PBS, streptavidin Alexa Fluor 546 (Invitrogen, Life Technologies Australia Pty, Ltd, Australia) was added and further incubated for 10 min on ice. After washing with PBS, Hoechst 33342, kindly provided by Monash Micro Imaging Center was added to the cells for 15 min at 37°C. Cells were then directly imaged on coverslip by Nikon A1r Confocal microscope, operated by the NIS Elements Viewer software (Nikon, Melville, NY). Data were analysed with FIJI (ImageJ, USA).

Microscopy analyses for particles uptake and distribution in the lung

The superior lobe of the right lung was collected in 1 ml 2 % PFA and stored in the dark at 4 °C overnight. The lung tissue was transferred to 70 % ethanol and sliced into 1 mm – 2 mm thick transverse sections. Non-specific antibody binding was blocked in 100 µl confocal staining buffer (3 % FCS in 1 X PBS) with CD16/CD32 block (BD Biosciences) in the dark on ice for 4 hours. Tissues were washed in 200 µl 1 X PBS twice. Antibody staining cocktail was prepared with the following antibodies: Hoechst 33342 (Invitrogen), MHC Class II–Alexa Fluor 647 (BioLegend) and Phalloidin–Rhodamine (Invitrogen) in 100 µl confocal staining buffer and incubated in the dark at 4 °C overnight. Lung tissues were washed in 200 µl 1 X PBS twice and kept in 1x PBS prior to confocal imaging to avoid drying of fixed tissue. All lung tissue sections were viewed and captured on the Nikon A1r Plus confocal microscope, operated by the NIS Elements Viewer software (Nikon, Melville, NY). Data were analysed with FIJI (ImageJ, USA).

Flow cytometric analysis

Appendices

Culture cells were harvested and labelled with anti-CD11c V450 (HL3) (BD Biosciences, Franklin Lakes, NJ, USA) to identify dendritic cells. To study the activation marker expression, cells were labelled with anti-CD86 PE (GL1) (BD Biosciences, Franklin Lakes, NJ, USA) and anti-MHCII APC-Cy7 (M5/114.15.2) (BD Biosciences, Franklin Lakes, NJ, USA). Dead cell were discriminated by staining harvested cells with LIVE/DEAD Fixable Aqua Dead Cell Stain Kit (Invitrogen, Life Technologies Australia Pty Ltd, Victoria Australia). Antibodies were prepared in flow cytometry staining buffer (mouse PBS, 2% FCS) and cells were stained for 20 minutes on ice. Samples were acquired with LSRII (BD Biosciences, Franklin Lakes, NJ, USA) at AMREP Flow-Cytometry Core Facility (Melbourne, Australia). Data was analysed with FlowJo Flow Cytometry Analysis Software (TreeStar).

Cytokine detection in dendritic cell culture and measurement of BAL fluid cytokines

To detect and quantify IL-6, IL-10, IL-12p70 and TNF concentrations secreted within the culture and BAL fluid, supernatant was collected at the end of each experiment and analysed by following the manufacturer's instructions in the cytometric bead array (CBA) inflammation kit (BD Biosciences, Franklin Lakes, NJ, USA). Estimated concentrations of cytokines were obtained from FCAP Array (Soft Flow) based on the level of mean fluorescence intensity (MFI).

Statistical analysis

The data generated in this study are shown in the mean \pm SD. All values were graphed and analysed with one-way ANOVA for statistical significance using Prism (GraphPad). Statistical significance was indicated by the *p*-value (* denote $p < 0.05$; ** denote $p < 0.01$, *** denote $p < 0.001$).

Results

Endocytic uptake of in vitro dendritic cells

Dendritic cells play a vital role in immune system and numerous studies have exploited this ability for a potential system for drug and vaccine delivery (Akagi et al., 2007, Diwan et al., 2003, Fifi et al., 2004, Knuschke et al., 2013, Shima et al., 2013, Uto et al., 2011a). To examine the endocytic uptake of our PS-ENP by *in vitro* dendritic cells, bone marrow cells were supported with GM-CSF to induce *in vitro* dendritic cell generation. Upon exposure to the PS-ENP, particles were detected within the cell membrane of the dendritic cells (labelled as CD11c⁺ MHCII⁺) (Fig 1A). This showed that the *in vitro* dendritic cells have actively taken up the PS-ENP.

PS-ENP lacks the ability to activate in vitro dendritic cells.

Following endocytosis of antigens, dendritic cells process the foreign pathogen and get activated. Dendritic cell activation can be measured by the expression of various activation markers such as CD86 and MHCII, and cytokine secretion. To investigate the effects of activation capacity of dendritic cell by PS-ENP, dendritic cells generated from bone marrow cells supported with GM-CSF were incubated with fluorescent-labelled PS-ENP for 24 hours, a time-point at which was previously observed to have maximal effects of PS-ENP on dendritic cells (Kong Y. Y. et. al., unpublished observations). In this study, we benchmarked the effects of PS-ENP to LPS, well-known inflammatory stimulant. While exposure to LPS significantly increased expression of activation markers such as CD86 and MHCII on the dendritic cells, exposure to PS-ENP did not affect the expression levels of those markers (Fig 1B). These results suggest that PS-ENP lacks the capability to activate dendritic cell cultures.

PS-ENP selectively altered cytokine secretion in in vitro dendritic cell cultures

To investigate the capacity of PS-ENP in the induction of cytotoxic effects in dendritic cell cultures, we further analysed the cytokines secreted by dendritic cells in the culture supernatant (Fig. 1C). We found that there was no increase in the pro-inflammatory cytokines, IL-6, IL-12p70 and TNF in the supernatants from dendritic cell cultures exposed to PS-ENP. Furthermore, we noted a significant decrease in TNF and significant increase in IL-10 secretions when compared to the untreated cultures, suggesting that the immune response maybe skewed towards immunosuppression. LPS induced secretion of all the cytokines mentioned. Although PS-ENP instigated IL-10 secretion within the culture, it was still significantly lower than that of LPS. These observations demonstrated that PS-ENP does not activate dendritic cell cultures.

In vivo uptake of PS-ENP by MHCII-positive cells

To further investigate the effects of PS-ENP *in vivo*, intratracheal instillation of the PS-ENP was done on mice. Studies have shown that epithelial cells (type I and II) and alveolar macrophages are capable of taking up nanoparticles (Geiser et al., 2005). However, our data showed that the lung MHCII⁺ cells, and not the epithelial cells, took up the PS-ENP (Fig. 2A). Lung immune cells such as macrophages, B cells and dendritic cells express MHCII on their surfaces. This was in line with our previous studies, where we showed that these cells (i.e. macrophages, B cells and dendritic cells) took up PS-ENP, and the proportions of the cells that took up PS-ENP depends on the location/niches (i.e. lung or lung-draining lymph nodes) (Hardy et al., 2012a, Hardy et al., 2013a).

PS-ENP instillation increased BAL, lung and lung-draining LN cell numbers to a lower magnitude than LPS

To test the hypothesis that PS-ENP is not toxic, we intratracheally instilled PS-ENP into BALB/c naïve mice and samples were collected on day 3, a time at which was previously observed to have maximal effects on immune parameters (Hardy et al., 2013a). Instillation of PS-ENP increased total cell numbers in the BAL fluid when compared to saline control group (data not shown). Further analysis of the BAL cell population showed that the infiltration of monocytes was significantly higher than saline control group (Fig. 2B, left panel). Lymphocytes and neutrophils were not detected in saline control group (similar to what seen in naïve mice, data not shown). However, we noted a low, but significant increase in lymphocyte and neutrophil infiltration upon exposure to PS-ENP (Fig. 2B, middle and right panel, respectively). Instillation of PS-ENP also gave a higher cellularity in the lung and lung-draining LN (Fig. 2C). However, these numbers were much lower compared to 10 µg LPS instillation suggesting that PS-ENP only induced lung inflammation to a lower magnitude than LPS (Fig. 2B-C).

PS-ENP instillation selectively increased BAL cytokines secretion

The low levels of cell infiltration in the BAL, lung and lung-draining LN suggested that PS-ENP might not increase the concentration of pro-inflammatory cytokines in the lung compartments. To test this, BAL fluid was collected and cytokine levels were measured. As expected, PS-ENP induced lower levels of IL-6 and TNF compared to LPS instillation, but significantly increased the concentration of IL-12p70. However, this level was significantly lower as compared to LPS instillation (Fig. 2D). The induction of IL-12p70 is not surprising as the instillation of PS-ENP served as a stimulus, which increases

Appendices

cell activation/recruitment (preferentially dendritic cells). Overall, these results showed that relative to LPS, PS-ENP did not induce acute lung injury in the lung 3 days post administration.

Fe₃O₄-ENP instillation did not increase BAL, lung and lung-draining LN cell numbers

To further investigate the toxicity level of Fe₃O₄-ENP, we intratracheally instilled Fe₃O₄-ENP into BALB/c naïve mice and samples were collected on day 3. In contrast to PS-ENP, Fe₃O₄-ENP did not increased BAL, lung and lung-draining LN cell numbers (Fig. 3). We did not perform further analysis of the BAL cell population and cytokines as the cellularity levels suggested that Fe₃O₄-ENP did not induce significant responses in the lung.

Discussion

A number of ambient, anthropogenic and engineered nanoparticles have been described that exert detrimental effects on *in vivo* lung immune homeostasis (Inoue et al., 2010, Hussain et al., 2011). However, our recent studies suggest a different role of PS-ENP, which promotes lung immune homeostasis and prevents the elicitation of inflammation upon allergen challenge in atopic animals (Hardy et al., 2012a, Hardy et al., 2013a). Dendritic cells are well known for their abilities to capture, process and present antigens to activate the adaptive immune responses. As such, they have been extensively investigated in vaccine strategies and particle-based delivery systems to induce a potent adaptive immune response (Peek et al., 2008, Schneider et al., 1998, Uto et al., 2007).

In this study, we demonstrated that GM-CSF derived bone marrow cells can efficiently take up PS-ENP. Endocytosis is the first crucial step to antigen presentation. Inhibition of endocytosis has shown to eradicate downstream antigen processing and antigen presentation in dendritic cells (Sallusto et al., 1996, Kerksiek et al., 2005, von Delwig et al., 2006). Subsequently after endocytosis, dendritic cell activation ensues. Dendritic cell activation is associated with elevated expression of activation markers such as CD40, CD80, CD86, MHCI and MHCII (Steinman, 2001). It is widely known that various mediators such as LPS, CpG and poly I:C can activate dendritic cells (Gaajetaan et al., 2012, Abdi et al., 2012). Unlike exposure to LPS, dendritic cells did not increase any activation marker expression upon exposure to PS-ENP. Furthermore, we noted that they have taken up the fluorescently labelled PS-ENP. Recently, we have also observed that these dendritic cells can take up PS-ENP as soon as 1-hour exposure (Kong Y. Y. et. al., unpublished observations). Combining these observations, we have shown strong evidence that PS-ENP does not activate dendritic cells.

In normal healthy individuals, dendritic cells that take up harmless inhaled antigens usually mediate immunoregulation or non-responsiveness (Condon et al., 2011). However, dendritic cells also initiate immunity against potentially harmful pathogens such as bacteria/bacterial components (e.g. LPS), viruses, fungi and parasites, which trigger production of pro-inflammatory cytokines (Steinman, 2001). Interestingly, our *in vitro* data showed a decrease in IL-6 and TNF secretion but undetectable IL-12p70 levels. Previously, our results showed that PS-ENP, at a wide range of particles concentration, surface coating, charges and time points of treatments, do not induce inflammatory ERK-mediated signalling pathways in bone marrow derived dendritic cells (Karlson Tde et al., 2013). Therefore, we suggest that PS-ENP is non-toxic and biocompatible. Furthermore, we detected low levels of IL-10 secretion; approximately 20 folds lower than the levels induced by LPS. The lack of pro-inflammatory cytokine secretion and the increased levels of IL-10 allow us to speculate that the PS-ENP may inhibit inflammatory Th1 response and skew towards immunosuppression. These criteria (non-toxic, biocompatible and have capacity to alter immune responses) are important as nanoparticles are widely explored for biological use in the field of medicine (Coester et al., 2006, Dinauer et al., 2005, Soppimath et al., 2001, Zhang et al., 2014).

Next, our *in vivo* investigation showed that Fe₃O₄- and PS-ENP did not induce acute inflammatory responses relative to LPS. This is consistent with our previous data that PS-ENP only induce mild inflammatory responses in the lung (Hardy et al., 2013a), and here we added that the pro-inflammatory levels (reflected by cellularity and BAL cytokines) induced by PS-ENP were significantly lower than LPS. In parallel to our *in vitro* observation, this result would suggest that PS-ENP is non-toxic and biocompatible in the lung. Furthermore, our previous studies showed that PS-ENP not only maintains lung

homeostasis, it also modulates dendritic cells (i.e. functions and numbers) to render lung resistance against allergic asthma development (Hardy et al., 2013a, Hardy et al., 2012a). In contrast to PS-ENP, despite low toxicity levels of Fe₃O₄-ENP in the lung microenvironment, no reports to date demonstrate the capability of Fe₃O₄-ENP in improving lung diseases, particularly allergic asthma.

Besides the interaction of nanoparticles with dendritic cells, Mohamud *et al.* has reviewed on other effects of nanoparticles-lung interaction. The review stated that epithelial cells release pro-inflammatory mediators (e.g. TNF, IL-6) and translocate to the blood when exposed to nanoparticles (Hardy et al., 2013a). However, we demonstrated that epithelial cells did not take up PS-ENP. Therefore, we suggest that PS-ENP do not activate epithelial cells, thus maintaining the lung homeostatic level. On the other hand, LPS poses an ability to activate epithelial cells for subsequent immune activation (Schulz et al., 2002); either by direct LPS-epithelial cell interaction, or by the cytokines released from LPS-stimulated myeloid cells (Pugin et al., 1993). Our *in vivo* data showed that PS-ENP significantly increased the concentration of IL-12p70 in BAL when compared to the control group. As mentioned earlier, this is not surprising as PS-ENP act as an activating stimulus that is able to alter immune responses in the lung (Hardy et al., 2012a, Hardy et al., 2013a).

In conclusion, our work demonstrated that PS-ENP is non-toxic and is biocompatible to the lung. These nanoparticles can be taken up by various cell subsets, particularly dendritic cells, and they are able to alter the immune response. This study reveals attractive opportunities for the use of these nanoparticles as potential prophylactic therapies for pathological conditions such as AAI.

Acknowledgments

We gratefully acknowledge the expert assistance of Geza Paukovics with flow cytometry.

MP is a Senior Research Fellow supported by National Health & Medical Research Council (NHMRC) of Australia and a non-executive director of PX Biosolutions. RM is a fellow of the Academic Staff Training Scheme at Universiti Sains Malaysia and a recipient of a Malaysian Government PhD Scholarship and CRC-Airways and Asthma top-up Scholarship.

Figure legends:

Fig. 1: PS-ENP lacks the ability to activate *in vitro* dendritic cells. Day 3 C57BL/6 dendritic cells generated from GM-CSF derived bone marrow culture were stimulated with LPS or PS-ENP for 24 hours. Cells were harvested after 24 hours and confocal microscopy was done to analyse **(A)** endocytic uptake of fluorescent-labelled PS-ENP. Flow cytometry was done to analyse **(B)** the expression of activation markers on dendritic cells (CD11c⁺ cells) and **(C)** cytokine secretions within the culture. Results shown were the average of 3-8 mice. One-way ANOVA was used. Mean \pm SD * denote $p < 0.05$; *** denote $p < 0.001$

Fig. 2: PS-ENP fails to induce toxicity in the lung. BALB/c mice were intratracheally administered with FITC-labelled PS-ENP on day 0, or saline as control; sampled were collected on day 3. **(A)** Confocal analyses of FITC-labelled PS-ENP. Representative lung airway and parenchyma were captured at a magnification of 400 x. Cells were analysed based on their expressions of MHCII and FITC uptake. Nucleus - blue; Actin- red; FITC-labelled PS-ENP - green; MHCII - pink. Samples were analysed for **(B)** BAL differential **(C)** Cellularity in the lung and lung-draining LN and **(D)** BAL cytokines. Mean \pm SD * denote $p < 0.05$; ** $p < 0.01$; *** denote $p < 0.001$, ns denote not significant.

Fig. 3: Fe3O4-ENP fails to induce toxicity in the lung. BALB/c mice were intratracheally administered with Fe3O4-ENP on day 0, or saline as control; sampled were collected on day 3. Cellularity in the BAL fluid, lung and lung-draining LN. Mean \pm SD.

Figure 1

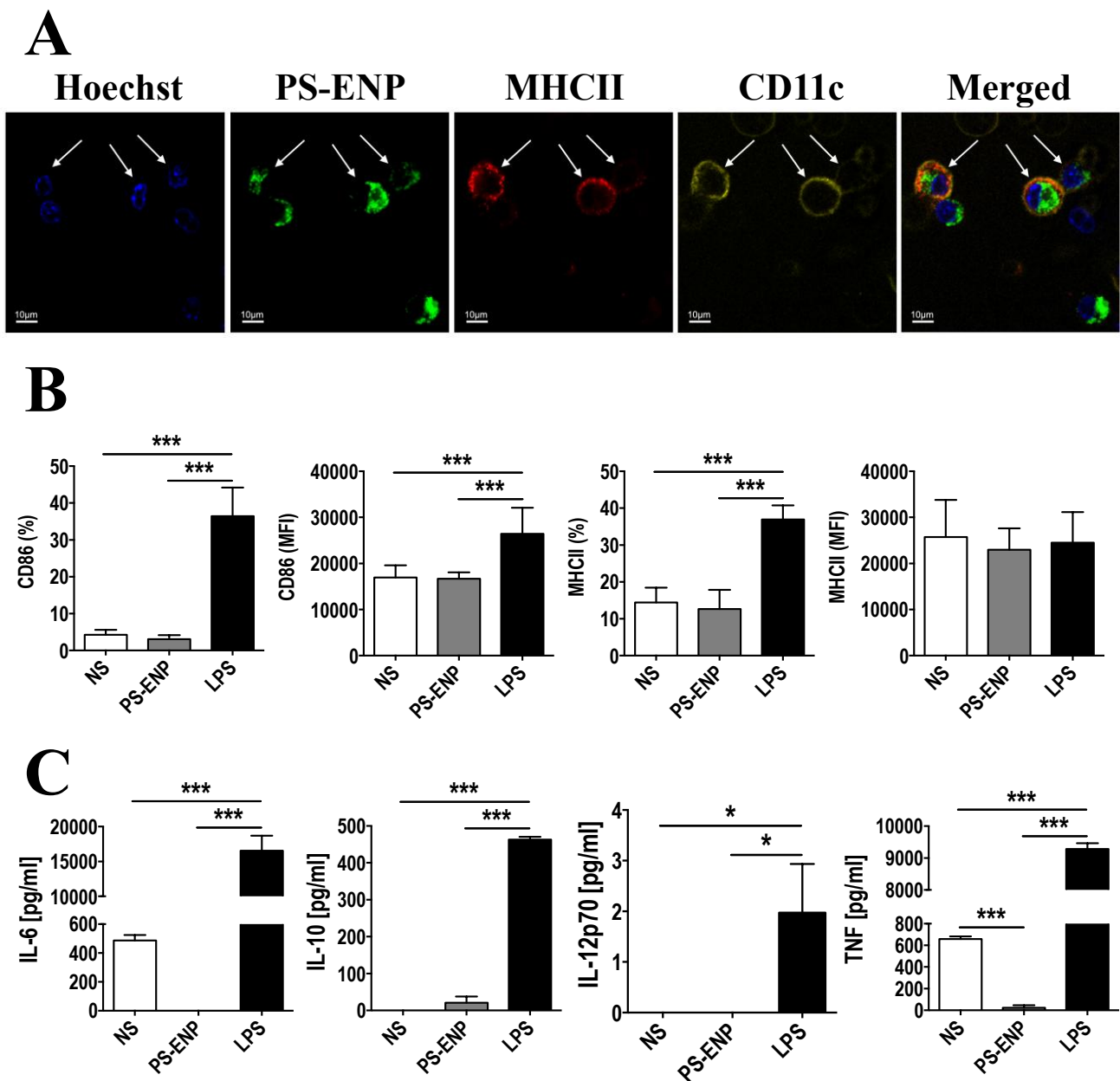


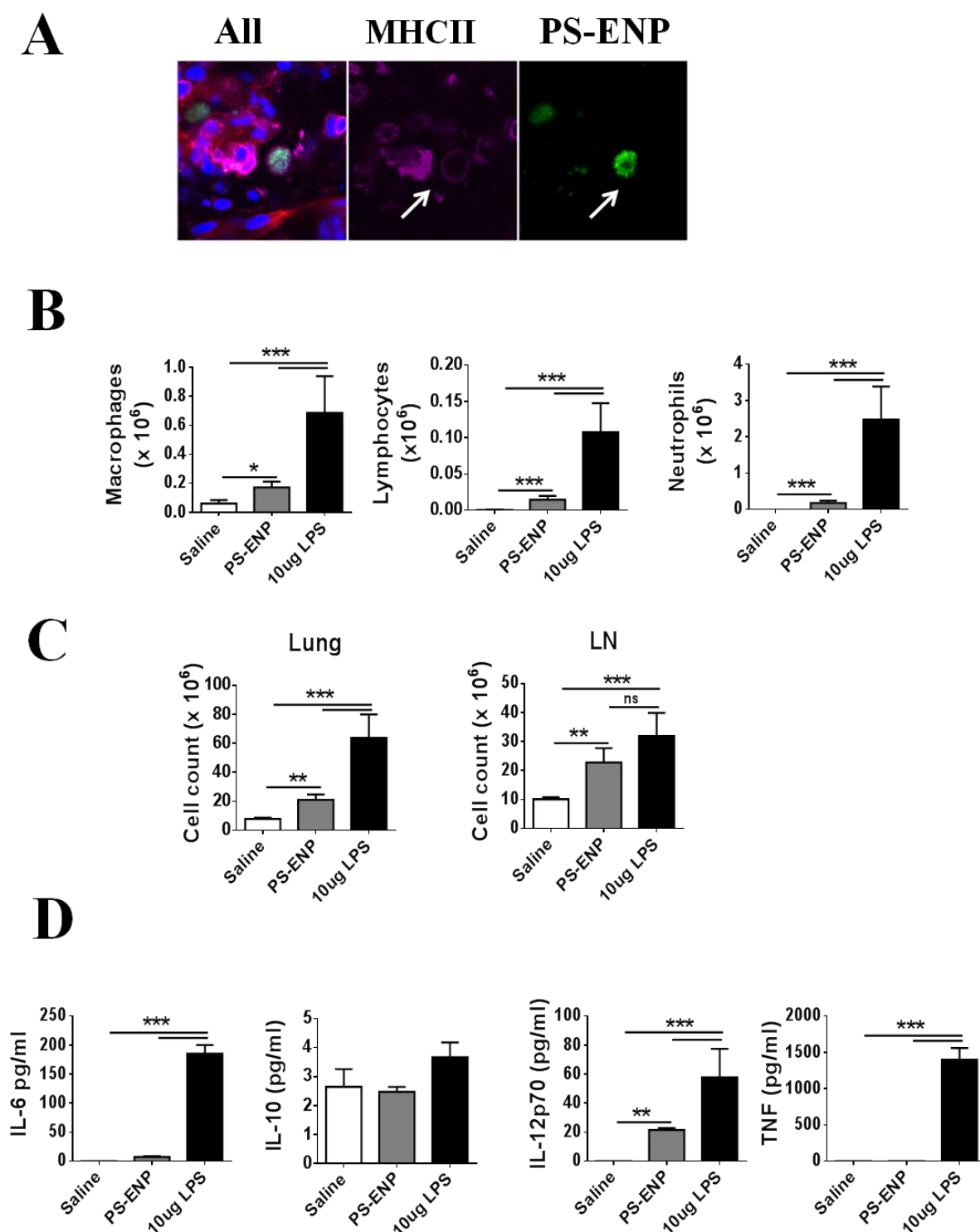
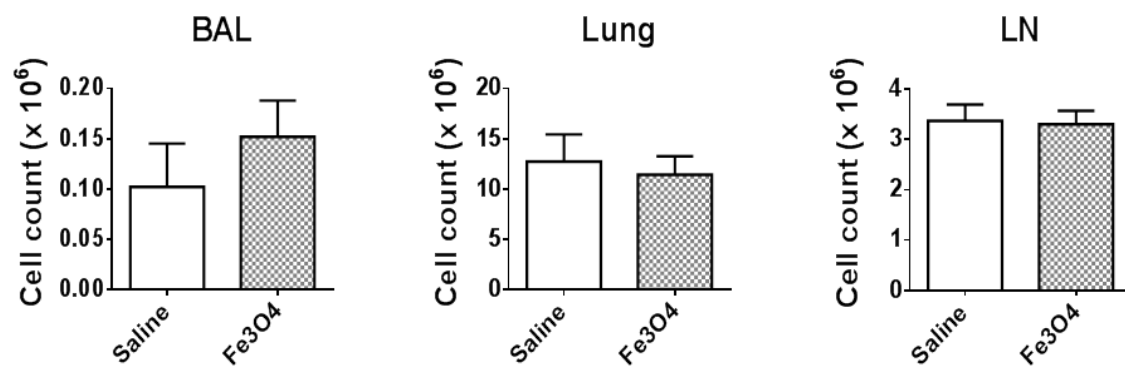
Figure 2

Figure 3



REVIEW ARTICLE

The effects of engineered nanoparticles on pulmonary immune homeostasis

Rohimah Mohamud¹, Sue D. Xiang¹, Cordelia Selomulya², Jennifer M. Rolland^{1,3}, Robyn E. O’Hehir^{1,3}, Charles L. Hardy^{1,3}, and Magdalena Plebanski¹

¹Department of Immunology and ²Department of Chemical Engineering, Monash University, Melbourne, VIC, Australia, and ³Department of Allergy, Immunology and Respiratory Medicine, The Alfred Hospital and Monash University, Melbourne, VIC, Australia

Abstract

Engineered nanoparticles (ENP), which could be composed of inorganic metals, metal oxides, metalloids, organic biodegradable and inorganic biocompatible polymers, are being used as carriers for vaccine and drug delivery. There is also increasing interest in their application as delivery agents for the treatment of a variety of lung diseases. Although many studies have shown ENP can be effectively and safely used to enhance the delivery of drugs and vaccines in the periphery, there is concern that some ENP could promote inflammation, with unknown consequences for lung immune homeostasis. In this study, we review research on the effects of ENP on lung immunity, focusing on recent studies using diverse animal models of human lung disease. We summarize how the inflammatory and immune response to ENP is influenced by the diverse biophysical and chemical characteristics of the particles including composition, size and mode of delivery. We further discuss newly described unexpected beneficial properties of ENP administered into the lung, where biocompatible polystyrene or silver nanoparticles can by themselves decrease susceptibility to allergic airways inflammation. Increasing our understanding of the differential effects of diverse types of nanoparticles on pulmonary immune homeostasis, particularly previously underappreciated beneficial outcomes, supports rational ENP translation into novel therapeutics for prevention and/or treatment of inflammatory lung disorders.

Keywords

Lung, particles, immune response, delivery vehicles, vaccine, inflammation, toxicity, animal models

History

Received 19 September 2013

Revised 17 October 2013

Accepted 18 October 2013

Published online 25 November 2013

Introduction

Nanoparticles, defined as particles with a diameter less than 100 nm, are being increasingly used as carriers for drug delivery (Kaur et al., 2012). The diminutive size of nanoparticles used in such applications facilitates their interaction and/or uptake by cells, as well as potentially enabling them to interfere with specific subcellular components, enabling less toxic and more efficient therapeutic actions. The large surface area of nanoparticles (compared to an equivalent mass of microparticles) supports enhanced bioactivity. Hence, surface modifications can effectively enhance bioactivity, facilitate targeting and circulation and can alter solubility and stability (Kaur et al., 2012). This makes them potentially ideal carriers for vaccine or drug delivery. Nanoparticles can be categorized into naturally occurring (ambient) nanoparticles (e.g. forest fires, volcanic eruptions or viruses), anthropogenic nanoparticles produced inadvertently as a result of human activity (e.g. combustion engines, grilling, welding, power plants and incinerators) and engineered nanoparticles (ENP) produced for various

industrial applications or consumer products. The use of ENP in medical applications has increased markedly in recent decades, and ENP are expected to be widely used in medical applications in the future. ENP have the potential to be utilized in a wide variety of functions, from diagnostics to disease therapy. They can infiltrate almost any tissue site due to their unique physical properties. Delivering drugs in inhalable nanoparticles for treating lung diseases is an attractive option, and currently the subject of much investigation (Jensen et al., 2012; Verma et al., 2013). The pulmonary drug delivery route is very promising due to (1) the large alveolar surface area available for drug absorption/action, (2) the easily permeable epithelial layer, (3) the extensive vascularization facilitating distribution, (4) the relatively low level of endogenous enzymatic/proteolytic activity, (5) the ability to deliver drugs directly to the site of lung diseases and (6) the avoidance of first-pass metabolism by the hepatic portal system (e.g. liver) and further extreme pH challenges by the digestive system (e.g. gut) (Bur et al., 2009; Edwards & Dunbar, 2002; Hussain et al., 2004; Patton & Byron, 2007; Pilcer & Amighi, 2010). However, to effectively utilize ENP as delivery vehicles to treat lung diseases, it is crucial to understand their effects on pulmonary immune/inflammatory regulation, in order to help minimize any potential toxic side-effects. In this review, we have

Address for correspondence: Magdalena Plebanski, Department of Immunology, Monash University, Faculty of Medicine, Nursing and Health Sciences, Level 2, 89 Commercial Road AMREP Building, Melbourne 3004, Australia. E-mail: [REDACTED]

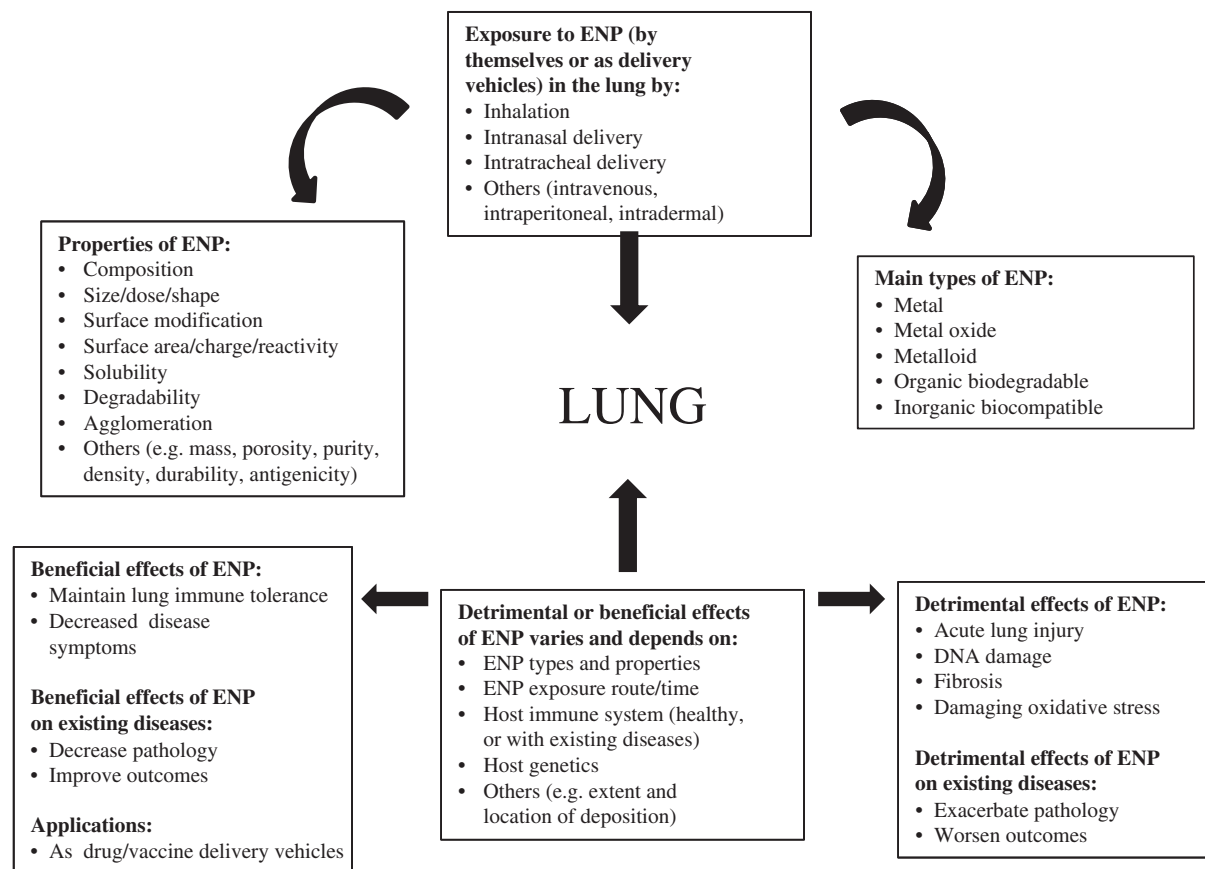


Figure 1. Properties and potential ENP effects on the lung.

focussed on the effects of ENP on lung immune homeostasis and immunity, categorizing ENP by their unique physical properties, critically by size and by composition. We provide an overview of the effects of ENP in the pulmonary compartment (Figure 1), including newly identified beneficial outcomes and the potential for the translation of well characterized ENP into novel therapeutics for prevention and/or treatment of inflammatory lung disorders.

Pulmonary immune homeostasis: lung inflammation and immunity

The lung is exposed to a myriad of innocuous agents on a daily basis and must maintain a state of immune ignorance or “tolerance” to these stimuli to retain pulmonary homeostasis and prevent potentially fatal immunopathology. The immune system is divided into two major arms: the innate and adaptive immune systems. Innate immunity (natural or native immunity) consists of cellular and biochemical defense mechanisms to provide immediate defense against microbes, but has no memory (Janeway & Medzhitov, 2002). The adaptive immune response (specific or acquired immunity) is stimulated by exposure to infectious agents and has the capacity to increase in magnitude and is accompanied by development of long lasting memory to subsequent challenges by the same infectious agents (Janeway & Bottomly, 1994). The innate and adaptive immunity are closely interlinked since the innate immunity stimulates adaptive immune responses and influences the nature of subsequent

antigen-specific adaptive immunity (Janeway & Bottomly, 1994). The balance of innate and adaptive immunity in the lung microenvironment is central to maintaining lung homeostasis and healthy lung function.

Healthy airways in man and mouse are dominated by alveolar macrophages (>90%), the remainder being dendritic cells (DC) and T cells (Holt et al., 2008; Steinmuller et al., 2000). Alveolar macrophages are functionally different from phenotypically identical counterparts elsewhere, in that they act by several suppressive pathways that, in combination, limit their responsiveness to external stimuli (Wissinger et al., 2009). DC, considered part of the innate immune system, plays a sentinel role in sensing foreign pathogens and provide a link between the innate and adaptive immune responses. DC are found throughout the respiratory tract and are involved in the priming and differentiation of naïve T cells in response to inhaled antigens (Condon et al., 2011; Lambrecht & Hammad, 2009). Macrophages and DC express pattern recognition receptors on their surface [e.g. Toll-like receptors (TLR), nucleotide-binding domain leucine-rich repeat (NLR), scavenger receptors etc.], which recognize bacterial “danger signals” and trigger the production of cytokines, which in turn promote lung inflammation *via* the production of factors (chemokines) that can attract diverse cell types into the lung environment. Indeed, the expression of TLR2 and TLR4 on pulmonary macrophages is involved in the recognition of fine and coarse ambient particles (Shoenfelt et al., 2009). In addition, a member of the NLR family, Nalp3, is crucial for sensing asbestos fibers and particulate silica, leading to the

induction of the inflammatory cytokine such as interleukin (IL)-1 β and activation of the innate immune response (Dostert et al., 2008). In normal healthy individuals, DC that take up harmless inhaled antigens usually induce immunological tolerance or non-responsiveness (Condon et al., 2011). However, DC also initiate immunity against potentially harmful pathogens such as bacteria, viruses, fungi and parasites, which trigger production of inflammatory “danger signals”. Macrophages inhibit development of inappropriate lung immune responses *via* the production of mediators that in turn can modulate the nature of the immune response (Holt et al., 2008).

The lung can be confronted by a diverse range of environmental nanoparticles including ENP. ENP can be intentionally delivered to the lung for imaging and therapeutic purposes, or accidentally inhaled as emissions in the environment, such as occupational exposure to aerosols during the production of nanoparticles. Nanoparticles are taken up by antigen presenting cells (APC) (such as DC and macrophages) in secondary peripheral lymphoid compartments (Reddy et al., 2007), subsequently modulating immune response, and such capability has been harnessed for the development of vaccines and therapeutics (Fifis et al., 2004; Mottram et al., 2007; Xiang et al., 2008). While it has been appreciated for some time that nanoparticles have a high alveolar deposition rate in the lung (Oberdorster et al., 2005), recent studies clearly show that nanoparticles are readily taken up by APC in the lung (Hardy et al., 2012, 2013; Vranic et al., 2013).

In addition to APC, lymphocytes (e.g. T and B cells) that exist in the lung also play an important role in the lung immune response because they can function as “effector” cells and/or regulatory cells to suppress the induction of inflammation. For example, allergic airway responses are orchestrated by cytokines released from T cells called “Th2” cells (e.g. IL-4, IL-5, IL-9 and IL-13). In order to maintain lung homeostasis, allergic responses must be controlled by regulatory immune cells and molecules that exist in the lung, such as regulatory T cells (Treg). Together with APC, Treg play a crucial role in inhibiting allergic airway inflammation and maintaining lung immune homeostasis (Holt et al., 2008). Mechanisms that regulate immunity affect both the induction of tolerance towards inert “harmless” inhaled agents/substances and protective immunity against invading pathogens (Randall, 2010).

ENP as potential pulmonary delivery vehicles

The application of ENP as delivery vehicles for therapeutic agents [e.g. drugs (bronchodilators, corticosteroids and antibiotics) and biologics (proteins, peptides and nucleic acids)] or vaccines would fulfill therapeutic needs (Card et al., 2008; Sung et al., 2007). Generally, ENP as drug-delivery vehicles protect conjugated drugs against degradation and prolong their release of drugs (Edwards et al., 1997). Diverse ENP have also been shown to be excellent vaccine carriers, inducing innate immune responses by complement activation (Reddy et al., 2007), and potent adaptive T cell and antibody immunity in the absence of inflammation, by selectively targeting peripheral DC (Fifis et al., 2004; Klippstein & Pozo, 2010; Reddy et al., 2007).

In addition to their role as a vehicle for drug delivery, some unmasked ENP (also known as naked, plain or non-functionalized ENP) exhibit direct effects on lung immunobiology and have potential as anti-allergen therapeutics (Park et al., 2010c), or conversely, as agents which can exert adverse effects such as fibrosis and granuloma formation in mouse lungs (Shvedova et al., 2005). The degree to which ENP exert beneficial or adverse effects is dependent on the particle elemental compositions as well as their physicochemical properties, particularly size. Thus, the broad goal for ENP-based drug or vaccine deliveries would be to also maximize the direct beneficial effects of ENP, whilst minimizing their potential adverse effects. In this review, we will focus on ENP made of inorganic metal (e.g. gold), inorganic metal oxide [e.g. iron oxide (Fe₃O₄)], inorganic metalloid (e.g. silica), organic biodegradable polymers (e.g. lipid) and inorganic non-biodegradable but biocompatible polymers (e.g. polystyrene) and further discuss the biodistribution of such ENP in the lung *in vivo* and the effect of their physical characteristics such as composition and size on pulmonary immune homeostasis.

Effects of inorganic metal-based ENP on pulmonary immune homeostasis

Gold ENP

Gold ENP are some of the most frequently used ENP in research, biological applications and industrial products. Their popularity is due to the relatively simple and well-developed synthesis procedures (Huang et al., 2007). Gold ENP are considered inert and biocompatible, and generally regarded as safe (Connor et al., 2005). Gold ENP have several advantageous physicochemical properties, including their excellent light absorbing and scattering properties (El-Sayed et al., 2005), and their adaptable surface chemistry (e.g. conjugation to peptides or antibodies) (Han et al., 2007; Sperling et al., 2008). The range of applications for gold ENP is growing rapidly, including their use in diagnostics to detect biomarkers of heart disease (Maiseyeu et al., 2012), cancer (Yang et al., 2013) and infectious agents (Zagorovsky & Chan, 2013). In addition, gold ENP have shown potential for delivering synthetic carbohydrate-based vaccines (e.g. synthetic tetrasaccharide epitope) (Safari et al., 2012) and have been used as pulmonary delivery vehicles for multiple therapeutic purposes (De Jong & Borm, 2008; Sperling et al., 2008).

The effect of gold ENP on the lung varies depending on their size, route of delivery and duration of exposure. Smaller gold ENP <5 nm generally accumulated in the lung after intravenous administration (De Jong et al., 2008; Sonavane et al., 2008), but were then rapidly excreted in the urine (Semmler-Behnke et al., 2008), perhaps due to their ability to passively pass through cell membranes (Madl & Pinkerton, 2009), and brief exposure did not induce pulmonary inflammation (Chen et al., 2009). However, long-term exposure (~90 d in a whole-body inhalation chamber) to gold ENP (4–5 nm) promoted low-level inflammation in the pulmonary alveoli in rats (Sung et al., 2011). Studies on middle-sized gold ENP (10–50 nm) indicated that such size ranged gold ENP were more active in causing lung

emphysema and death following intraperitoneal injection into mice (Chen et al., 2009). Further studies on various sizes of gold ENP showed that intratracheally instilled gold ENP of 2, 20 and 200 nm induced minimal lung inflammation (evidenced by increased numbers of alveolar macrophages) and did not induce genotoxic, systemic or local adverse effects in the lungs three days after exposure (Schulz et al., 2012). Similar studies in rats, where gold ENP were instilled intratracheally into rat lungs, showed that 50 nm gold ENP were less detrimental to lung homeostasis than 250 nm gold ENP, as reflected by lower levels of neutrophilic inflammation and pro-inflammatory cytokines [e.g. tumor necrosis factor (TNF)- α] (Gosens et al., 2010). However, these results may appear to contradict a murine study in which gold ENP of both 50 and 100 nm injected intraperitoneally were completely nontoxic to mice (Chen et al., 2009), perhaps suggesting that the mild inflammatory reaction to gold ENP was dependent on the initial route of exposure.

Notably, physicochemistry-dependent toxicity (safety) and bioincompatibility of naked gold ENP can be further minimized by modifying their surface (Chen et al., 2009; Fraga et al., 2013). Gold ENP can be functionalized with a thiolated poly(ethylene glycol) (PEG) monolayer and an active agent can be added to the PEG surface. PEG-platinum-tethered gold ENP (176 ± 25 nm) showed improved cell uptake and increased the delivery of the anti-cancer drug oxaliplatin into the nucleus of lung cancer cells, presumably releasing it intracellularly, whereupon it could bind and cross link deoxyribonucleic acid (DNA), preventing DNA replication and transcription (Brown et al., 2010). Functionalized gold ENP (e.g. with exposed peptide ligands) were shown to better escape clearance by the immune system (macrophage-mediated uptake) and thus remain in the circulation for prolonged periods of time (Huang et al., 2010). Conversely, non-functionalized gold ENP aggravated pulmonary inflammation in a mouse model of diisocyanate-induced asthma, although the size of the ENP was not reported (Hussain et al., 2011). Even though the weight of the literature therefore indicates that gold ENP are safe to administer into the lung, we propose that their effects are strongly dependent on their size, route of delivery and surface modifications.

Silver ENP

Silver ENP have the beneficial property of being antimicrobial (Oves et al., 2013). They are therefore widely utilized in medical applications (e.g. surgical instruments) and as antibacterial/antifungal agents in biotechnology and bioengineering (e.g. wound dressings and coatings in medical devices) (Johnston et al., 2010) and in water purification (Chen & Schluesener, 2008; Vigneshwaran et al., 2007). However, *in vitro* naked silver ENP (6–20 nm) can also inhibit cell proliferation, inducing cytotoxicity and genotoxicity in a time- and dose-dependent manner in human lung cell lines (AshaRani et al., 2009b). Silver ENP and silver ions found inside the cell nucleus have been suggested to be able to bind to DNA, reduce adenosine triphosphate production, induce the generation of reactive oxygen species (ROS) and damage the mitochondrial respiratory chain triggering DNA damage (AshaRani et al., 2009b). Following mouse inhalation, *in vivo*

silver ENP (5 ± 2 nm) were detected in the lung, liver, brain, olfactory bulb and blood, and induced only minimal pulmonary inflammation [reflected by mild increases in bronchoalveolar lavage (BAL) neutrophils]. Following whole-body exposure in mice, histopathologic analyzes showed no epithelial damage or fibrosis *in vivo* (Stebounova et al., 2011). However, whole-body exposure to larger silver ENP (15 nm) in rats caused alveolar inflammation characterized by alveolitis and alveolar wall thickening (Song et al., 2012; Sung et al., 2008). By contrast, when given intranasally, 25 nm silver ENP did not induce substantial inflammation in the lower respiratory tract and were taken up by phagocytic cells in the respiratory mucosa and then redistributed to kidney, spleen and brain (Genter et al., 2012). Silver ENP 42 nm can, however, induce some inflammatory cytokines in the serum after intratracheal instillation into the mouse lung (Park et al., 2011). Furthermore, following repeated oral administration in mice, silver ENP (22, 42 and 71 nm) increased serum levels of some inflammatory cytokines (e.g. IL-1) and were detected in the lung, brain, liver, kidney and testis (Park et al., 2010a). By contrast, in this study, 323 nm silver nanoparticles were not detected in tissues and did not affect cytokine levels.

Despite some potential for inducing inflammation, several studies have shown beneficial effects on lung immunobiology from the administration of silver ENP. A recent study showed that 6 nm silver ENP substantially suppressed mucus hypersecretion in allergic asthma by modification of a vascular endothelial growth factor crucial in regulating the vascular changes associated with asthma (Jang et al., 2012). In another study, administration of 6 nm silver ENP by a nebulizer 1 h before allergen challenge decreased the level of ROS production and attenuated allergic asthma (Park et al., 2010c). Furthermore, silver ENP < 50 nm were also shown to have an anti-inflammatory effect, suppressing the expression of IL- β , IL-12, metalloproteinase-9 and TNF- α (Bhol & Schechter, 2007), as well as blocking the proliferation and migration of endothelial cells (Asharani et al., 2009a; Kalishwaralal et al., 2009). The precise mechanisms by which silver ENP exert these beneficial effects in lung diseases are still unclear.

In conclusion, the literature suggests that silver ENP have no or little toxicity or inflammatory capacity when administered into the lung in short-term studies, although some inflammation is induced following chronic ENP exposure. Moreover, some studies show silver ENP can have intriguing therapeutic potential themselves in the lung. We suggest that this therapeutic potential may depend on surface charge; one of the most important factors that govern the toxicity of ENP by mediating their dynamic binding to lung cells (Hirn et al., 2011), and which was not reported in many of the above important studies.

Carbon-based ENP

Carbon-based nanomaterials (CBN) are of great interest to biomedical engineers working on nanotechnology applications. Carbon nanotubes (CNT) and fullerenes (also known as buckyballs) are the most investigated carbon-based ENP. CNT are cylindrical while fullerenes are spherical in shape.

The physical properties of CBN, including mechanical strength, electrical conductivity and optical properties are of great value for creating advanced biomaterials. There is considerable interest in using CBN for various biomedical applications.

CBN have been widely explored in biomedicine, for example, as nanoprobe for imaging (Madani et al., 2013), delivery of therapeutic agents, such as DNA, proteins, drug molecules or vaccines (Prato et al., 2008) as well as for photothermal therapy (Marches et al., 2011). It has, however, been reported that carbon ENP exposure (e.g. CNT) can induce acute inflammation and fibrosis in the lung (Shvedova et al., 2005), as well as systemic immune responses (Park et al., 2009), which are dependent on the physical characteristics of CBN (e.g. size, shape, dose and agglomeration) (Shvedova et al., 2005; Wang et al., 2010). The detailed effects of CBN on lung pulmonary immunity will be discussed below.

Carbon nanotubes. CNT are formed by the rolling of a single layer of graphite (called a graphene layer) into a seamless cylinder. There are two types of CNT; single-walled CNT (SWCNT) and multi-walled CNT (MWCNT) with different length and aspect ratios. The properties of CNT are highly dependent on the manufacturing process and their physicochemical properties including structure and surface characteristics (Foldvari & Bagonluri, 2008). SWCNT are characterized by a high aspect ratio and have unique electrical, optical, thermal and spectroscopic properties (Banerjee et al., 2003). Both naked SWCNT and MWCNT administered into the lung have been shown to exacerbate allergic asthma, either by promoting Th2 immunity (Inoue et al., 2010) or B-cell activation and production of IgE (Park et al., 2009). Naked SWCNT (1–4 nm) administered *via* the pharyngeal route caused dose- and time-dependent acute inflammation, fibrosis and granuloma in mouse lungs (Shvedova et al., 2005). MWCNT, at the size of <10 µm long, 5–10 nm in diameter and 70 nm in length, induced mild lung inflammation 24 h after intratracheal administration into mice together with increased neutrophils and enhanced peripheral thrombogenicity *via* P-selectin-mediated platelet-leukocyte conjugation (Nemmar et al., 2007). However, another study showed that MWCNT, at the size of 10–20 nm, did not cause lung inflammation or tissue damage, even at relatively high exposure concentrations (2.7 mg/kg body weight) by whole-body inhalation by aerosol for 7 or 14 d (6 h/d), despite the upregulated NAD(P)H oxidoreductase 1 and IL-10 gene expressions (Mitchell et al., 2007).

To overcome the unwanted effect of the naked CNT in lung, recent studies have been focused on chemically modifying CNT with specific surface moieties (e.g. functional groups, molecules and polymers) to impart properties suited for biological applications, including increased solubility and biocompatibility, enhanced material compatibility and cellular responsiveness (Vardharajula et al., 2012). For example, water-soluble taurine functionalized MWCNT induced less lung inflammation in mice than the insoluble raw MWCNT (Wang et al., 2010); functionalization of SWCNT with phosphatidylserine also increased their uptake by lung alveolar macrophages in mice both *in vivo* and *in vitro* (Konduru et al., 2009). It is hoped that functionalization of

CNT would improve their biocompatibility and overcome their adverse effects in the lung, thereby maximizing biotherapeutic applications (Bonner, 2011; Vardharajula et al., 2012). Furthermore, CNT are promising candidates for the delivery of poorly immunogenic antigens to target DC, serving as multifunctional biological transporters and improving cellular uptake by APC (Konduru et al., 2009). They appear to be particularly suited for antigen/drug/vaccine delivery (Prato et al., 2008).

Fullerenes (buckyballs). Fullerenes, also known as buckyballs (soccer ball-shaped) or carbon cages (C₆₀), are similar to CNT in that they can be functionalized with a wide array of surface modifications (Satoh & Takayanagi, 2006). Intratracheally administered “naked” fullerenes (160 nm) increased IL-2 and TNF-α production in BAL fluid in a time- and dose-dependent manner (Ding et al., 2011) and caused alveolar hemorrhage (Ema et al., 2012). Microarray-based gene expression profiling demonstrated that most gene expression was “inflammatory-associated” 1 week post fullerene instillation in mice (Fujita et al., 2010). Data from several groups shows that intratracheal delivery of fullerenes (160 ± 50 nm) generally induces transient pulmonary inflammation within a week (Sayes et al., 2007) whilst whole-body fullerene (96 nm) inhalation does not cause significant inflammation until three days post-exposure (Ogami et al., 2011). In rats, fullerenes (55 nm) induced only minimal changes on lung toxicological parameters (Baker et al., 2008).

Functionalization of fullerenes was shown to increase their biocompatibility and reduce their cytotoxic effects (Sayes et al., 2006a). Indeed, administration of water-soluble fullerene attenuated, rather than exacerbated, quartz-induced neutrophilic lung inflammation (Roursgaard et al., 2008). Interestingly, water-soluble fullerene derivatives (polyhydroxy C₆₀) inhibited allergic airway inflammation in mice (Ryan et al., 2007), and hence may have potential in controlling asthmatic disease. We suggest that whereas “naked” carbon-base ENP should be treated with caution for lung delivery, appropriate surface modifications render them of interest as potential new therapeutics.

Effects of inorganic metal oxide-based ENP on pulmonary immune homeostasis

Titanium dioxide

The most commonly investigated inorganic metal oxide-based ENP are made of titanium dioxide (TiO₂). TiO₂ is chemically very stable, generally nontoxic and cheap to manufacture. In nanomedicine, TiO₂ ENP are used as antimicrobials (Yuan et al., 2010), in photo-dynamic therapy (Szacilowski et al., 2005) and as smart stimulus-sensitive tumor-targeted drug delivery systems (Zhang et al., 2012). Because of its brightness and high refractive index, TiO₂ is a popular white pigment in paints and is used in human cosmetic, skincare and sunscreen products (Wiesenthal et al., 2011).

There are two tetragonal crystal structures of TiO₂, anatase and rutile, with anatase being more chemically reactive (Sayes et al., 2006b; Warheit et al., 2007b), and consequently possessing greater toxic potential than the

rutile form (Pan et al., 2009). Although TiO₂ ENP are believed to be biologically and physiologically inert (Bernard et al., 1990), some studies have demonstrated adverse effects on cells, especially in the lung, presumably because toxicity may occur at a certain ENP dose, and/or because some ENP sizes and/or types of chronic exposure may be more damaging (Shi et al., 2013). Thus, whereas anatase TiO₂ ENP 2–5 nm induced minimal lung toxicity in mice after short term whole-body exposure (4 h) (Grassian et al., 2007), daily exposure over 10 d significantly increased numbers of macrophages in the BAL, although this inflammation had resolved by three weeks post-end of treatment (Grassian et al., 2007). Even more prolonged exposure, with daily intranasal instillation of 6 nm anatase TiO₂ over 90 d induced severe pulmonary inflammation and pneumonocytic apoptosis in mice (Li et al., 2013). The stage of development of the lung may also be a susceptibility factor, since intranasal instillation of 8–10 nm anatase TiO₂ into newborn mice caused dose-dependent lung inflammation postnatally and inhibited lung development (Ambalavanan et al., 2013). Particle size may also be a factor, with studies in IL-1R- and IL-1 α -deficient mice showing that intranasally instilled larger TiO₂ ENP (20 nm anatase and 80 nm rutile) can provoke IL-1 α -dependent lung inflammation (Yazdi et al., 2010).

In murine allergic lung disease models, 28 nm rutile TiO₂ ENP were shown to exert an adjuvant effect when co-administered with allergen (ovalbumin) (Larsen et al., 2010). In this context, anatase TiO₂ ENP (40 nm) aggravated pulmonary function and inflammation in a mouse asthma model, causing increased airway hyper-reactivity (AHR), cell infiltration in the BAL by macrophages and neutrophils as well as edema and epithelial damage (Hussain et al., 2011). Interestingly, non-sensitized animals remained unaffected, reinforcing the idea of an adjuvant role rather than a direct causative effect. Overall, these studies show that, despite being generally perceived as non-toxic, both anatase and rutile TiO₂ ENP have the potential to promote pulmonary immunopathology.

Similar to other ENP, surface modifications influence the bioactivity of TiO₂ ENP. Silica-coated TiO₂ ENP (needle-like: 10 \times 40 nm in size) were shown to inhibit the induction of allergic asthma (reduced AHR to the level of the control group) in a mouse asthma model (Rossi et al., 2010). Surface coating can also prevent TiO₂ ENP from forming large agglomerates and hence reduce the cytotoxicity associated with the aggregated form of TiO₂ ENP. This was clearly demonstrated by a study showing that coating TiO₂ ENP (49 nm) with PEG eliminated aggregation in an aqueous media and significantly decreased cytotoxicity and induction of stress-related genes (IL-6 and heat shock protein 70B) in human pulmonary epithelial cells compared to uncoated TiO₂ ENP (Mano et al., 2012).

Overall, naked TiO₂ ENP can exert both positive and negative effects on lung homeostasis depending on the chronicity of exposure, capacity to aggregate and co-exposure with other stimuli such as allergens. However, surface modifications that prevent aggregation can eliminate some of the unwanted effects of naked TiO₂ ENP in the lung, warranting more investigation in this area.

Zinc oxide

Zinc oxide (ZnO) ENP are widely used in nanotechnology for the construction of solar cells (Wong et al., 2012), as gas sensor devices (Wang et al., 2011), as efficient photosensitizer carrier systems (Fakhar-e-Alam et al., 2012) and in sunscreens (Filipe et al., 2009). Inhalation of ZnO ENP is reported to cause acute systemic disease (i.e. metal fume fever) (Barceloux, 1999). *In vitro* studies showed that exposure to ZnO ENP (20–70 nm, 11–176 μ g/ml) by rat alveolar epithelial cells induced ROS-related severe injury in a dose- and time-dependent manner (Kim et al., 2010) and exposure of rodent fibroblast cells to 15 μ g/ml ZnO ENP (19 nm) induced DNA and mitochondrial damage (Brunner et al., 2006). In addition, exposure to ZnO ENP (10 nm, 5–25 μ g/ml or 71 nm, >40 μ g/ml) induced oxidative stress (Heng et al., 2010) and DNA damage (Karlsson et al., 2008) in human bronchial epithelial cells. *In vivo* studies showed that ZnO ENP (71 \pm 35 nm) delivered intratracheally into the mouse lung induced transient expression of the inflammatory genes TNF- α , IL-6, CXCL1 and the monocyte chemo-attractant protein 1 in a MyD88-dependent manner (Chang et al., 2013). Intratracheally instilled ZnO ENP (<10 nm) promoted eosinophil recruitment and caused progressive severe lung injury, aggravated by the release of metal ions, and induced a unique inflammatory footprint in the lung (Cho et al., 2012). Overall, a range of *in vitro* and *in vivo* studies show that ZnO exhibit pro-inflammatory effects and/or induce oxidative stress in the lung.

Previous studies demonstrated detrimental effects of ZnO ENP after they dissolved into Zn ions, both inside and outside the cells (Cho et al., 2012; Kao et al., 2012). Kim et al. reported that DNA damage induced by Zn ions in alveolar epithelial cells was significantly attenuated by a Zn chelator (Kim et al., 2010), suggesting that the toxicity of ZnO ENP may be reduced by lowering their solubility, coating or surface functionalization, consequently decreasing the release of Zn ions (George et al., 2010). Human lung carcinoma cells, exposed in culture to ZnO ENP (50 nm, for 30 min), showed an increase in Zn ions leading to mitochondrial dysfunction, caspase activation and cell apoptosis, whilst *in vivo* whole-body exposure to these 50 nm ZnO ENP in rats caused an increase in Zn ions in both BAL cells and white blood cells (Kao et al., 2012). Overall, exposure to ZnO ENP is usually detrimental to lung homeostasis across multiple particle sizes and modalities of exposure.

Iron oxide ENP (Fe₃O₄)

Magnetic nanoparticles, in particular iron oxide (also called magnetite or Fe₃O₄), are widely used for the development of novel drug deliveries and disease diagnostics (Akbarzadeh et al., 2012; Verma et al., 2013; Xie et al., 2011). Besides being relatively easily functionalized (e.g. with targeting ligands) and having superparamagnetic properties, Fe₃O₄ ENP are useful as nanomaterials due to (1) availability of manufacturing processes that can precisely fine-tune the physical characteristics of ENP, including scalable processes; (2) the fact that these ENP can be manipulated by an external magnetic field and (3) their biocompatibility (approved by FDA) (Verma et al., 2013).

In vitro studies show that Fe₃O₄ ENP of various sizes (10–120 nm) and at differing doses (10–250 µg/ml) did not induce cytotoxicity or mutagenicity in human lung epithelial cells (Karlsson et al., 2008; Verma et al., 2013) and other types of cell cultures, for example, rat liver cells (Hussain et al., 2005), human DC (Kunzmann et al., 2011) or HeLa cancer cells (Shen et al., 2009). Intranasal delivery of Fe₃O₄ ENP (10 nm, 50 µg/ml) into mice did not induce detectable inflammation (e.g. IL-6) in BAL fluid after 1, 4, or 7 d post-treatment (Verma et al., 2013). However, there was a dramatic increase in glutathione in lung tissue on day 1 indicative of oxidative stress induction, which decreased progressively from days 4–7 (Verma et al., 2013). Intratracheally instilled Fe₃O₄ ENP (5–36 nm, 250–5400 µg/ml) induced secretion of pro-inflammatory cytokines (e.g. TNF-α) in the BAL fluid (Cho et al., 2009; Park et al., 2010b) and increased expression of tissue damage genes (e.g. heat shock protein) in lung tissues on day 1, but in this case, these remained elevated up to day 28 post-instillation (Park et al., 2010b). Similarly, intratracheally instilled Fe₃O₄ ENP (<50 nm, 1–5 mg/ml) in rats caused weak pulmonary fibrosis and low levels of interstitial lung inflammation (Szalay et al., 2012). Overall, these studies indicate that while Fe₃O₄ ENP are safe in cell cultures and *in vivo* at lower doses, higher doses promote inflammation when delivered into the lung.

Fe₃O₄ ENP can also be functionalized, concentrated or held in position within the body with the aid of an external magnetic field, features that hold great potential for the development of targeted nanocarriers (Verma et al., 2013). An *in vitro* study showed that silica-coated superparamagnetic iron oxide ENP (SPION) (30, 50, 70 and 120 nm) were taken up and internalized by APC (macrophages and DC) to a greater extent than similar-sized iron oxide ENP with different surface coatings (e.g. dextran). It was proposed that the difference in uptake was due to differences in surface charge (the latter were positively charged, SPION were negatively charged) (Kunzmann et al., 2011). In mice, neither naked nor poly(lactic-co-glycolic) acid (PLGA)-coated Fe₃O₄ ENP significantly increased BAL IL-6 post intranasal instillation (up to seven days), consistent with the idea that Fe₃O₄ ENP are mildly inflammatory or non-inflammatory, and hence have potential as pulmonary drug carriers to treat various lung diseases (Verma et al., 2013).

Effects of inorganic metalloid-based ENP on pulmonary immune homeostasis

Crystalline silica

Crystalline silica (e.g. quartz, cristobalite, zeosils and clathrasils) has great practical importance in industrial applications such as the fabrication of electric and thermal insulators, drug vehicles or target-specific contrast agents for imaging (Barik et al., 2008; Napierska et al., 2010; Suh et al., 2009). Quartz is the most common form of crystalline silica and has been shown to promote lung injury (generating free radicals), fibrosis (silicosis) and lung cancer (Mossman & Churg, 1998). *In vitro* and *in vivo* studies have demonstrated that quartz ENP can induce dose-dependent cytotoxicity and increase the levels of ROS and pro-inflammatory mediators in the lung (Sayes et al., 2007; Wang et al., 2007).

Intratracheally instilled quartz ENP (7, 12, 9, 50, 123, 300 to 2000 nm) induced dose-dependent lung inflammation in rats (Sayes et al., 2007; Warheit et al., 2007a). Warheit et al. also reported that quartz-induced lung inflammation and cytotoxicity are independent of particle size but correlate with surface activity, particularly hemolytic potential (Warheit et al., 2007a). Intratracheal administration of cadmium-doped silica ENP (20–80 nm) to rats induced inflammation, oxidative stress (e.g. inducible nitric oxide synthase) and granuloma formation (Coccini et al., 2012). Similarly, intratracheal administration of quartz (30 or 377 nm) into mice induced lung inflammation peaking 16 h post instillation (Roursgaard et al., 2010). Together, these studies show that quartz-induced lung inflammation and toxicity are independent of particle size, but dependent on exposure dose (concentration) and surface activity. For this reason, quartz is often used as a positive control in ENP toxicity studies (Sayes et al., 2007; Warheit et al., 2007b).

Amorphous silica

Amorphous silica (e.g. colloidal silica, silica gel and mesoporous silica), also known as non-crystalline silica, is being increasingly used in several industries including cosmetics, food additives and drug delivery (Napierska et al., 2010). Despite these broad applications, there is growing evidence that amorphous silica ENP can cause an inflammatory response in the lung. *In vitro* studies demonstrated that amorphous silica ENP (10, 150 and 500 nm) increase inflammatory reactions (up-regulates the IL-6 gene) and cause death of human lung submucosal cells after exposure for 2–24 h, in a size-, time- and concentration-dependent manner, with the strongest toxic effects observed for the smallest particles (10 nm) (McCarthy et al., 2012). Similarly, amorphous silica ENP (2, 16, 60 and 104 nm) induced the release of pro-inflammatory mediators (e.g. TNF-α, IL-6 and IL-8) in co-cultures of pulmonary epithelial cells, macrophages and endothelial cells, in a surface area-dependent manner (Napierska et al., 2012b). Furthermore, larger amorphous silica ENP (250 and 500 nm) induced cytotoxic and genotoxic effects *in vitro* in murine macrophages and human epithelial lung cell lines after 4 and 24 h of treatment (Guidi et al., 2013). In addition to this extensive *in vitro* evidence of toxicity and pro-inflammatory potential, *in vivo* studies show that intravenous injection of amorphous silica ENP (15 and 55 nm) caused DNA damage in liver and lung in a dose-dependent manner in rats (Downs et al., 2012) and induced transient but very severe lung inflammation upon intratracheal instillation (14 nm amorphous silica ENP) in mice (Cho et al., 2007a). Amorphous silica ENP (50 nm) activate IL-1β release from macrophages *via* the NALP3-inflammasome complex (involved in lung inflammation) in primary lung macrophages (RAW264.7) (Sandberg et al., 2012). The chemical composition of amorphous silica ENP is a dominant factor in their ability to induce oxidative stress, as shown in a study where hemeoxygenase-1 mRNA expression was up-regulated in human endothelial cell lines treated with iron-doped amorphous silica ENP (16 nm) but not with similarly sized pure amorphous silica ENP (Napierska et al., 2012a). Together, similar to quartz-induced lung toxicity, the

total surface area (a combination of dose and particle size) of amorphous silica ENP appears to play a crucial role in determining the level of their toxicity in the lung. Collectively, the weight of the literature suggests metalloid-based ENP may not be good candidates as nanomaterials for treating pulmonary diseases given their overall highly toxic and inflammatory effects on the lung. However, further modification of such metalloid-based ENP may offer new opportunities to reassess this potential delivery vehicle.

Effects of organic biodegradable polymers ENP on pulmonary immune homeostasis

The organic biocompatible and biodegradable ENP studied in this review include lipid-based ENP [e.g. liposomes, immunostimulating complex (ISCOM) and solid lipid nanoparticles (SLN)], polysaccharide-based ENP (e.g. chitosan, alginates and Carbopol) and polymeric matrix ENP [PLGA, polylactic acid (PLA) and polycaprolactone (PCL), cyanoacrylates, gelatin]. Some of these ENP may come from natural materials, while others are synthesized (e.g. liposomes). These ENP are used for pulmonary drug delivery and as vectors to transport drugs, receptors, medical imaging chemicals or nucleic acids to specific sites (Kaur et al., 2012).

Lipid-based ENP

Liposomes are vesicular carriers with lipid bilayers alternating with aqueous compartments. In a cockroach-induced allergic asthma mouse model, administration of polymerized liposomes (73 nm) with ligand mimetics stimulating P-selectin (P-selectin antagonist) inhibited eosinophil recruitment to the lung, and attenuated both peribronchial inflammation and AHR (John et al., 2003). Liposomes have been used extensively to deliver drugs to treat cancer, including doxorubicin (Pastorino et al., 2008) and paclitaxel (Latimer et al., 2009). Liposome-mediated drug delivery has also been tested to treat lung cancer (Latimer et al., 2009; Zakharian et al., 2005) and promote lung transplantation (Monforte et al., 2009), with some success. Liposomes persist in the lung for up to 24 h after inhalation (Dhand, 2004); retain more than 65% of the incorporated drug (Zaru et al., 2009); and do not have any apparent detrimental effect on respiratory function (Nassimi et al., 2010). Another lipid-based ENP, ISCOM, has been injected intradermally as a vaccine delivery vehicle and shown to drive the production of high titer specific antibodies in sera and at mucosal sites including the lung (San Gil et al., 1999), and to provide complete protection against respiratory syncytial virus (RSV) infection in animal models (Regner et al., 2004).

SLN also offer promise as drug carriers due to their biocompatibility and the fact that they can protect the incorporated drug against degradation and control its rate of release (Farboud et al., 2011). Nassimi et al. investigated the inflammatory potential of SLN (98.4 ± 4.9 nm) on human type II pneumocyte-like cells (A549 epithelial cell line). Exposure to SLN for 24 h did not increase IL-8 and TNF- α concentrations in cell culture supernatant, but increased levels of the keratinocyte-derived chemokine (involved in neutrophil chemotaxis and activation) in tissue culture supernatant (Nassimi et al., 2010). Furthermore, SLN did not increase

lactate dehydrogenase activity (a marker for tissue damage) or total BAL fluid protein at any dose (1, 10, 35, 100, 150 and 200 μ g) or timing (days 4, 8, 12 and 16) over which mice received SLN daily administration *via* aerosol. These data suggest that biodegradable SLN possess only minimal inflammatory effects in the lung, even with chronic exposure (Nassimi et al., 2010). A recent study demonstrated that curcumin incorporated into SLN (curcumin-SLN, 190 nm) effectively suppressed AHR, inflammation and expression of Th2 cytokines in a murine allergic asthma model (Wang et al., 2012). Overall, these studies show that lipid-based ENP show great promise for the development of nanoparticle-based therapeutics for lung diseases.

Polysaccharide-based ENP

Polysaccharide-based ENP (e.g. chitosan, alginates, Carbopol, cyclodextrin, hyaluronic acid and carboxymethylcellulose) are highly stable, biocompatible and biodegradable. Chitosan (a natural polysaccharide biopolymer derived from deacetylation of chitin) is one of the most intensively studied and provides a useful building block for drug delivery systems due to its (1) low pulmonary toxicity (Choi et al., 2010); (2) unique physicochemical characteristics including bioadhesiveness (high protein-binding efficiency) (Amidi et al., 2010) and (3) excellent controlled drug release pattern (Derakhshandeh & Fathi, 2012). Chitosan ENP are also being investigated as anti-allergen therapeutics to treat allergic asthma. For example, theophylline (a drug that reduces the inflammatory effects of allergic asthma) delivered in chitosan ENP (220 ± 23 nm) efficiently blocked experimental allergic asthma by decreasing BAL eosinophilia, bronchial epithelial damage, mucus hypersecretion and lung cell apoptosis (Lee et al., 2006). Imiquimod cream (containing a penetrating agent and a TLR7 agonist that skews immune responses toward the Th1-type) mixed with chitosan ENP (220 ± 23 nm) containing small inhibitory ribonucleic acid specific for the natriuretic peptide receptor A, applied to shaved skin on the backs (above the lung) of mice inhibited AHR, airway eosinophilia, lung histopathology and the Th2 cytokines IL-4 and IL-5 in lung homogenates (Wang et al., 2008). Similarly, intranasal administration of chitosan/interferon- γ pDNA effectively inhibited airway inflammation and AHR (Kumar et al., 2003) and RSV infection (Kumar et al., 2002). Moreover, administration of chitosan ENP containing pVD (N-terminal natriuretic peptide) protected mice from experimental allergic asthma (Wang et al., 2009).

The physicochemical properties of chitosan ENP can be modified to selectively target lung cells for the delivery of therapeutic molecules to treat lung diseases (e.g. cancer and allergic asthma). Chitosan can be hydrophobically modified with bile acid analogs (Choi et al., 2010), making it an effective delivery carrier (Nafee et al., 2007). Glycol chitosan, a commercially available derivative of chitosan, has been used as a scaffold to deliver multiple therapeutic agents or for diagnostic imaging applications (Cho et al., 2007b). N-trimethyl chitosan tripolyphosphate ENP (400 nm) were shown to enhance antigen delivery to APC and promoted Th17 immune responses, and thus represent promising vaccines against infectious diseases (Keijzer et al., 2013).

Chitosan-coated PLGA ENP (172.3 ± 4.5 nm) were shown to be a flexible and efficient system for delivery of antisense oligonucleotides to lung cancer cells (Nafee et al., 2007). Overall, organic and biodegradable polysaccharide-based ENP can effectively inhibit disease in models of allergic asthma and other inflammatory lung diseases.

Polymeric matrix-based ENP

Biodegradable and biocompatible polymeric matrix-based ENP [PLA, and copolymers containing glycolide (PLGA) and PCL, cyanoacrylates and gelatin] have been extensively studied for site-specific delivery of drugs and other molecules and are widely used to engineer experimental vaccines (Kaur et al., 2012; Ungaro et al., 2012) and for tissue and bone regeneration (Alves Cardoso et al., 2012). These ENP have also shown potential for vaccine or drug delivery via the pulmonary route (Andrade et al., 2011).

PLGA formulations are the most extensively investigated polymeric matrix-based ENP, as they are stable, highly biocompatible, have high bioavailability and drug loading capability, offer a wide range of degradation/drug release rates (Pirooznia et al., 2012), protect the encapsulated drug from enzymatic degradation (Hoet et al., 2004) and have high lung deposition efficiency (Yang et al., 2012). Moreover, evidence suggests that PLGA formulations are not toxic to cells, as Cor L105 lung epithelial-like cells retained $\geq 80\%$ of their viability after treatment with PLGA and $\alpha 1$ AT (human neutrophil elastase inhibitor to protect the lungs from cellular inflammatory enzymes) – loaded PLGA (300 nm) (Pirooznia et al., 2012). Both 220 nm unconjugated PLGA and PLGA ENP which target the intercellular adhesion molecule-1 (a molecule that controls leukocyte recruitment) are non-toxic to lung epithelial cells (Chittasupho et al., 2009). Besides being widely used as drug carriers in asthma models [e.g. for betamethasone (Matsuo et al., 2009)], PLGA ENP have been used for targeted allergen delivery (e.g. to target APC) for allergen-specific immunotherapy for pollen [nano size; (Scholl et al., 2006)] and bee venom allergy *via* peripheral delivery [micro size; (Martinez Gomez et al., 2007)]. Local delivery of the drug/antibiotics/allergen is necessary for the treatment of lung diseases, and PLGA thus have excellent potential as a nanocarrier for patients suffering from lung diseases (Ungaro et al., 2012). Most studies do not report precise size ranges, but assembled PLGA ENP usually fall in the 200–400 nm range.

Effects of inorganic biocompatible ENP on pulmonary immune homeostasis

Polystyrene ENP are inorganic, non-biodegradable, but biocompatible, and do not induce oxidative stress *in vitro* (Xia et al., 2006). The applications of these ENP in nanomedicine are expanding. Polystyrene ENP have been investigated as drug carriers for the treatment of hyperviscous mucus in cystic fibrosis (Lai et al., 2011), as a vaccine carrier against tumors (Fifis et al., 2004) and to enhance DNA vaccine efficacy (Minigo et al., 2007). Polystyrene ENP can be labeled internally with fluorescent dyes, allowing tracking of their localization both *in vivo* and *in vitro* (dos Santos et al., 2011; Hardy et al., 2012, 2013).

Similar to most other ENP, the size, dose and surface charge of polystyrene ENP play a role in their effects on lung cells. Consistent with this, the toxicity of polystyrene ENP on human alveolar epithelial type 1-like cells was dependent on their surface modifications (amine- or carboxyl-modified), particle size (50 and 100 nm), surface charge (positive and negative), dose (1, 10, 25, 50, 100 and 250 $\mu\text{g}/\text{ml}$) and period of exposure (4 and 24 h) (Ruenraroengsak et al., 2012). Importantly, most of the above polystyrene forms do not cause cell damage, the one exception being the amine-surface modified polystyrene ENP, which caused membrane damage to the respiratory epithelium (Ruenraroengsak et al., 2012). In another study, neutral 50 and 100 nm polystyrene ENP showed no toxicity to a human lung adenocarcinoma cell line (Dorney et al., 2012). Moreover, consistent with the above, several studies have shown that neutral or negatively charged polystyrene ENP do not promote inflammation *in vivo*, in contrast to positively charged ENP. Thus, in naïve hamsters intratracheal instillation of 60 nm unmodified (naked) and negatively charged carboxylate-modified polystyrene ENP did not cause pulmonary inflammation or vascular thrombosis, whilst positively charged amine-modified polystyrene ENP (60 nm) induced pulmonary inflammation (Nemmar et al., 2003). Our own studies have shown that intratracheal instillation of negatively charged glycine-coated 50 nm polystyrene ENP (PS50G) did not induce lung oxidative stress or cardiac or lung inflammation (Hardy et al., 2012), but imparted a beneficial immunological imprint on the lung and lung-draining lymph nodes rendering mice resistant to the development of allergic airway inflammation (Hardy et al., 2012, 2013). Previously, we and others reported a lack of inflammatory reactions at sites of peripheral injection or in any organs up to 2 months after intradermal or subcutaneous injection of PS50G into mice and sheep (Fifis et al., 2004; Mottram et al., 2007). In addition, our recent studies show that PS50G ENP do not induce inflammatory ERK mediated signaling pathways in bone marrow derived DC (Karlson et al., 2013).

Our studies show that PS50G inhibited key characteristics of allergic asthma (including airway eosinophilia and production of allergen-specific IgE and Th2 cytokines) a month after their instillation by inhibiting expansion of total and allergen-laden DC in the lung, and suppressing co-stimulatory function of CD11b^{hi} DC in the lung-draining lymph nodes (Hardy et al., 2012). Interestingly, PS50G, but not larger 500 nm polystyrene ENP (PS500G), preferentially inhibited development of allergic asthma, likely due to the particle size-dependent effects on particle uptake by APC and induction of cytokine/chemokine production in the lung and lung-draining LN differentially modulating APC migration/recruitment and/or function (Hardy et al., 2013). In broad agreement, lung-associated DC subpopulations were shown to preferentially capture 20 nm versus 1 μm particles (Blank et al., 2013). Size-dependent effects on vaccine efficacy have also been shown for polystyrene ENP with preferential uptake by DC of 40–50 nm sizes, which was also the optimal size for induction of adaptive immune responses and protection against disease (Fifis et al., 2004; Minigo et al., 2007; Xiang et al., 2006). The preferential uptake of smaller polystyrene ENP seen in the above studies may be due to their

size similarity with many viruses, suggesting that APC may have adapted to preferentially uptake particles of this size. Overall, inorganic non-biodegradable polystyrene ENP hold great potential in nanomedicine as they generally exert minimal toxicity *in vivo*, and are easily functionalized, permitting conjugation of vaccines or probes for imaging. Nevertheless, it is clear that, as with most other ENP, the characteristics of polystyrene ENP, particularly surface charge, need to be carefully considered to determine the maximum beneficial effects that can accrue from the development of novel pulmonary carriers, both for diagnostic or therapeutic applications. Thus, similar to silver ENP, “naked” polystyrene ENP have the potential to be direct anti-inflammatory agents in the lung, and to promote a beneficial imprint promoting long-term immune homeostasis, even in the face of allergen challenge.

Mechanisms by which ENP regulate pulmonary immune homeostasis

ENP have the capability to induce detrimental or beneficial effects on lung immune homeostasis. Most inorganic metal-, metal oxide- and metalloid-based ENP tend to induce inflammation and/or cell death in the lung. In contrast, organic biodegradable and inorganic biocompatible ENP generally cause only low-level inflammation (Figure 2). Understanding of the mechanisms by which ENP alter lung immune homeostasis is needed before they can safely be used for beneficial purposes. Since lungs comprise the largest surface area of the human body that interacts with environmental ENP, they are equipped with diverse defense mechanisms including pulmonary epithelial cells (secreting surfactant proteins and lipids), pulmonary immune cells (including innate cells that endocytose particles) and the mucociliary escalator (upwards transportation/translocation of mucus and foreign material for expectoration) (Nicod, 1999). The interactions of ENP with the pulmonary defense mechanisms are influenced by the characteristics of the ENP and play a role in determining whether inflammatory/immune response or lung tolerance ensues (Table 1).

Lung epithelial cells are the major source of various pro-inflammatory mediators that affect lung immunity. For

example, interaction of ENP with lung epithelial cells induces the release of pro-inflammatory mediators (e.g. TNF- α , IL-6 and IL-8) in a size- and surface area-dependent manner (Napieriska et al., 2012b). TNF- α plays a role in mediating the transition from pulmonary inflammation to fibrosis (Oikonomou et al., 2006). Lung immune cells (e.g. APC) also secrete pro-inflammatory cytokines in response to ENP, again affected by the characteristics of the ENP (Sandberg et al., 2012). The different physicochemical characteristics of ENP affect their ability to be endocytosed by APC or to stimulate cytokine secretion. They also modulate other lung-ENP interactions, such as (1) the interaction with lung epithelial cells (ability to enter type I and II epithelial cells); (2) the ability to translocate across the epithelial cells to the blood circulation; (3) the ability to gain access to the mitochondria and nucleus prior to uptake and (4) the ability to engage the intracellular clearance mechanisms (mucociliary escalator for macrophages or migration for DC) that lead to ENP clearance or local or systemic toxicity (Muhlfeld et al., 2008). For example, lung exposure to inorganic gold and silver ENP <5 nm (Chen et al., 2009) is frequently nontoxic or induces low levels of inflammation; however, other inorganic ENP (gold and silver >5 nm, or carbon-based, metal oxide-based and metalloid-based ENP) can be highly toxic to the lung (Table 1). ENP size strongly determines the lung-ENP interaction mechanisms, primarily by affecting the uptake of ENP by APC. However, the toxic effects triggered by the administration of metalloid-based ENP (e.g. crystalline silica such as quartz) (Sandberg et al., 2012) are independent of size, but primarily dependent on the dose, surface characteristics and exposure route and time. Besides these factors, inflammatory effects of other inorganic ENP (carbon-based and metal oxide-based ENP) are also dependent on composition, size, agglomeration, functionalization process and the release of ions. These various characteristics exerted by inorganic ENP (carbon-based, metalloid-based and metal oxide-based ENP) render them more highly toxic than other ENP. On the other hand, neither naked nor modified organic biodegradable-based ENP are highly toxic to the lung, perhaps owing to their biocompatibility and biodegradability – and in this case, the effects on the lung range from no toxicity to low toxicity and are dependent on size, dose and surface chemistry.

Depending on their nature, ENP can exert negative adjuvant effects and can exacerbate existing allergic asthma [e.g. CNT, (Inoue et al., 2010)], or they can exert beneficial effects, such as the ability to inhibit allergic inflammation *via* various mechanisms including: (1) modification of lung vascular endothelial growth [e.g. intranasal silver ENP administration, (Jang et al., 2012)], (2) decreased Th2 function [e.g. inhaled TiO₂ ENP (Rossi et al., 2010), (3) anti-oxidant effects [e.g. inhaled silver ENP, (Park et al., 2010c)] and (4) modulation of APC function toward homeostatic protection [e.g. intratracheal ENP polystyrene administration (Hardy et al., 2012)]. Taken together, these data indicate that lung-ENP interactions can be harnessed to optimize safety and to promote therapeutic benefit in settings such as allergy and asthma, as well as potentially to provide long-term beneficial homeostatic imprinting.

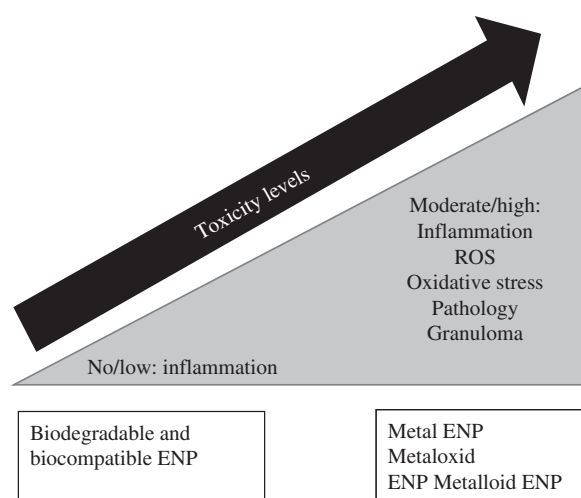


Figure 2. Overview on the effects of ENP on pulmonary immune homeostasis.

Table 1. Summary of ENP toxicity effects on pulmonary immune homeostasis.

ENP groups	ENP types	Effects on the lung	
Organic	Lipid Polysaccharide Polymeric matrix	Toxicity levels None/low	Generally depends on ENP characteristics Size, dose and functionalization process
Inorganic biocompatible Inorganic	Polystyrene Gold and silver ENP < 5 nm Gold and silver ENP > 5 nm Carbon Metal oxide Metalloid	Mild High	Composition, size, dose, agglomeration, functionalization process, surface characteristics, ions release and exposure routes and time Dose, surface characteristics and exposure routes and time

Conclusion

Lung exposure to different types of ENP can induce a broad range of immunological effects that might shape overall lung immune homeostasis. Whether the response to ENP is beneficial or detrimental is influenced by physicochemical characteristics (including composition, size, surface characterization and charge), dose and timing (acute versus chronic), and route of administration (e.g. intratracheal, intranasal and whole-body exposure). Generally, naked inorganic metal and metal oxide-based ENP induce inflammation and/or cell death in the lung. However, surface modification of those ENP can limit these adverse effects and provide scope for their use as drug delivery vehicles to the lung and in the treatment of lung diseases (e.g. allergic asthma, fibrosis and lung cancer). Metalloid-based ENP induce ROS, pulmonary fibrosis and lung inflammation at various sizes, and may therefore be unsuitable in their present form as lung drug delivery agents and therapeutics. By contrast, a range of organic biodegradable ENP, as well as inorganic biocompatible ENP, show great potential as drug carriers to treat lung diseases. They exert beneficial effects in the treatment of various lung diseases, without toxic side-effects, including allergic asthma (e.g. chitosan and polystyrene) and cancer (e.g. PLGA and polystyrene). This provides a basis for their exploration as nanocarriers for patients suffering from lung diseases. As well as being relatively safe carriers, recent studies indicate ENP can provide additional beneficial effects with anti-inflammatory properties (e.g. silver and polystyrene) and imprinting of the lung which favors the maintenance of immune homeostasis (e.g. polystyrene). Further understanding of the mechanisms underlying the direct beneficial effects of ENP on pulmonary immune homeostasis will help facilitate their development as therapeutics for the prevention and/or treatment of inflammatory lung disorders.

Declaration of interest

The authors report no declarations of interest. M. P. is a Senior Research Fellow supported by National Health & Medical Research Council (NHMRC) of Australia and a non-executive director of PX Biosolutions. R. M. is a fellow of the Academic Staff Training Scheme at Universiti Sains Malaysia and a recipient of a Malaysian Government PhD Scholarship.

References

- Akbarzadeh A, Samiei M, Davaran S. (2012). Magnetic nanoparticles: Preparation, physical properties, and applications in biomedicine. *Nanoscale Res Lett* 7:144–156.
- Alves Cardoso D, Jansen JA, Leeuwenburgh SC. (2012). Synthesis and application of nanostructured calcium phosphate ceramics for bone regeneration. *J Biomed Mater Res B Appl Biomater* 100: 2316–2326.
- Ambalavanan N, Stanishevsky A, Bulger A, et al. (2013). Titanium oxide nanoparticle instillation induces inflammation and inhibits lung development in mice. *Am J Physiol Lung Cell Mol Physiol* 304: L152–L161.
- Amidi M, Mastrobattista E, Jiskoot W, Hennink WE. (2010). Chitosan-based delivery systems for protein therapeutics and antigens. *Adv Drug Deliv Rev* 62:59–82.
- Andrade F, Videira M, Ferreira D, Sarmiento B. (2011). Nanocarriers for pulmonary administration of peptides and therapeutic proteins. *Nanomedicine (Lond)* 6:123–141.
- Asharani PV, Hande MP, Valiyaveetil S. (2009a). Anti-proliferative activity of silver nanoparticles. *BMC Cell Biol* 10:65.
- Asharani PV, Low Kah Mun G, Hande MP, Valiyaveetil S. (2009b). Cytotoxicity and genotoxicity of silver nanoparticles in human cells. *ACS Nano* 3:279–290.
- Baker GL, Gupta A, Clark ML, et al. (2008). Inhalation toxicity and lung toxicokinetics of C₆₀ fullerene nanoparticles and microparticles. *Toxicol Sci* 101:122–131.
- Banerjee S, Kahn MG, Wong SS. (2003). Rational chemical strategies for carbon nanotube functionalization. *Chemistry* 9:1898–1908.
- Barceloux DG. (1999). Zinc. *J Toxicol Clin Toxicol* 37:279–292.
- Barik TK, Sahu B, Swain V. (2008). Nanosilica-from medicine to pest control. *Parasitol Res* 103:253–258.
- Bernard BK, Osheroff MR, Hofmann A, Mennear JH. (1990). Toxicology and carcinogenesis studies of dietary titanium dioxide-coated mica in male and female Fischer 344 rats. *J Toxicol Environ Health* 29:417–429.
- Bhol KC, Schechter PJ. (2007). Effects of nanocrystalline silver (NPI 32101) in a rat model of ulcerative colitis. *Dig Dis Sci* 52: 2732–2742.
- Blank F, Stumbles PA, Seydoux E, et al. (2013). Size-dependent uptake of particles by pulmonary APC populations and trafficking to regional lymph nodes. *Am J Respir Cell Mol Biol* 49:66–77.
- Bonner JC. (2011). Carbon nanotubes as delivery systems for respiratory disease: Do the dangers outweigh the potential benefits? *Expert Rev Respir Med* 5:779–787.
- Brown SD, Nativo P, Smith JA, et al. (2010). Gold nanoparticles for the improved anticancer drug delivery of the active component of oxaliplatin. *J Am Chem Soc* 132:4678–4684.
- Brunner TJ, Wick P, Manser P, et al. (2006). In vitro cytotoxicity of oxide nanoparticles: Comparison to asbestos, silica, and the effect of particle solubility. *Environ Sci Technol* 40:4374–4381.
- Bur M, Henning A, Hein S, et al. (2009). Inhalative nanomedicine – Opportunities and challenges. *Inhal Toxicol* 21:137–143.
- Card JW, Zeldin DC, Bonner JC, Nestmann ER. (2008). Pulmonary applications and toxicity of engineered nanoparticles. *Am J Physiol Lung Cell Mol Physiol* 295:L400–L411.

- Chang H, Ho CC, Yang CS, et al. (2013). Involvement of MyD88 in zinc oxide nanoparticle-induced lung inflammation. *Exp Toxicol Pathol* 65:887–896.
- Chen X, Schluesener HJ. (2008). Nanosilver: A nanoparticle in medical application. *Toxicol Lett* 176:1–12.
- Chen YS, Hung YC, Liao I, Huang GS. (2009). Assessment of the in vivo toxicity of gold nanoparticles. *Nanoscale Res Lett* 4:858–864.
- Chittasupho C, Xie SX, Baoum A, et al. (2009). ICAM-1 targeting of doxorubicin-loaded PLGA nanoparticles to lung epithelial cells. *Eur J Pharm Sci* 37:141–150.
- Cho WS, Cho M, Kim SR, et al. (2009). Pulmonary toxicity and kinetic study of Cy5.5-conjugated superparamagnetic iron oxide nanoparticles by optical imaging. *Toxicol Appl Pharmacol* 239: 106–115.
- Cho WS, Choi M, Han BS, et al. (2007a). Inflammatory mediators induced by intratracheal instillation of ultrafine amorphous silica particles. *Toxicol Lett* 175:24–33.
- Cho WS, Duffin R, Poland CA, et al. (2012). Differential pro-inflammatory effects of metal oxide nanoparticles and their soluble ions in vitro and in vivo; zinc and copper nanoparticles, but not their ions, recruit eosinophils to the lungs. *Nanotoxicology* 6: 22–35.
- Cho YW, Park SA, Han TH, et al. (2007b). In vivo tumor targeting and radionuclide imaging with self-assembled nanoparticles: Mechanisms, key factors, and their implications. *Biomaterials* 28:1236–1247.
- Choi M, Cho M, Han BS, et al. (2010). Chitosan nanoparticles show rapid extrapulmonary tissue distribution and excretion with mild pulmonary inflammation to mice. *Toxicol Lett* 199: 144–152.
- Coccini T, Roda E, Barni S, et al. (2012). Long-lasting oxidative pulmonary insult in rat after intratracheal instillation of silica nanoparticles doped with cadmium. *Toxicology* 302:203–211.
- Condon TV, Sawyer RT, Fenton MJ, Riches DW. (2011). Lung dendritic cells at the innate-adaptive immune interface. *J Leukoc Biol* 90: 883–895.
- Connor EE, Mwamuka J, Gole A, et al. (2005). Gold nanoparticles are taken up by human cells but do not cause acute cytotoxicity. *Small* 1: 325–327.
- De Jong WH, Borm PJ. (2008). Drug delivery and nanoparticles: Applications and hazards. *Int J Nanomedicine* 3:133–149.
- De Jong WH, Hagens WI, Krystek P, et al. (2008). Particle size-dependent organ distribution of gold nanoparticles after intravenous administration. *Biomaterials* 29:1912–1919.
- Derakhshandeh K, Fathi, S. (2012). Role of chitosan nanoparticles in the oral absorption of Gemcitabine. *Int J Pharm* 437:172–177.
- Dhand, R. (2004). New frontiers in aerosol delivery during mechanical ventilation. *Respir Care* 49:666–677.
- Ding N, Kunugita N, Ichinose T, et al. (2011). Intratracheal administration of fullerene nanoparticles activates splenic CD11b+ cells. *J Hazard Mater* 194:324–330.
- Dorney J, Bonnier F, Garcia A, et al. (2012). Identifying and localizing intracellular nanoparticles using Raman spectroscopy. *Analyst* 137: 1111–1119.
- dos Santos T, Varela J, Lynch I, et al. (2011). Effects of transport inhibitors on the cellular uptake of carboxylated polystyrene nanoparticles in different cell lines. *PLoS One* 6:e24438.
- Dostert C, Petrilli V, Van Bruggen R, et al. (2008). Innate immune activation through Nalp3 inflammasome sensing of asbestos and silica. *Science* 320:674–677.
- Downs TR, Crosby ME, Hu T, et al. (2012). Silica nanoparticles administered at the maximum tolerated dose induce genotoxic effects through an inflammatory reaction while gold nanoparticles do not. *Mutat Res* 745:38–50.
- Edwards DA, Dunbar C. (2002). Bioengineering of therapeutic aerosols. *Annu Rev Biomed Eng* 4:93–107.
- Edwards DA, Hanes J, Caponetti G, et al. (1997). Large porous particles for pulmonary drug delivery. *Science* 276:1868–1871.
- El-Sayed IH, Huang X, El-Sayed MA. (2005). Surface plasmon resonance scattering and absorption of anti-EGFR antibody conjugated gold nanoparticles in cancer diagnostics: Applications in oral cancer. *Nano Lett* 5:829–834.
- Ema M, Tanaka J, Kobayashi N, et al. (2012). Genotoxicity evaluation of fullerene C₆₀ nanoparticles in a comet assay using lung cells of intratracheally instilled rats. *Regul Toxicol Pharmacol* 62: 419–424.
- Fakhar-e-Alam M, Ali SM, Ibupoto ZH, et al. (2012). Sensitivity of A-549 human lung cancer cells to nanoporous zinc oxide conjugated with Photofrin. *Lasers Med Sci* 27:607–614.
- Farboud ES, Nasrollahi SA, Tabbakhi Z. (2011). Novel formulation and evaluation of a Q10-loaded solid lipid nanoparticle cream: In vitro and in vivo studies. *Int J Nanomedicine* 6:611–617.
- Fifis T, Gamvrellis A, Crimeen-Irwin B, et al. (2004). Size-dependent immunogenicity: therapeutic and protective properties of nano-vaccines against tumors. *J Immunol* 173:3148–3154.
- Filipe P, Silva JN, Silva R, et al. (2009). Stratum corneum is an effective barrier to TiO₂ and ZnO nanoparticle percutaneous absorption. *Skin Pharmacol Physiol* 22:266–275.
- Foldvari M, Bagonluri M. (2008). Carbon nanotubes as functional excipients for nanomedicines: II. Drug delivery and biocompatibility issues. *Nanomedicine* 4:183–200.
- Fraga S, Faria H, Soares ME, et al. (2013). Influence of the surface coating on the cytotoxicity, genotoxicity and uptake of gold nanoparticles in human HepG2 cells. *J Appl Toxicol* 33:1111–1119.
- Fujita K, Morimoto Y, Endoh S, et al. (2010). Identification of potential biomarkers from gene expression profiles in rat lungs intratracheally instilled with C₆₀ fullerenes. *Toxicology* 274:34–41.
- Genter MB, Newman NC, Shertzer HG, et al. (2012). Distribution and systemic effects of intranasally administered 25 nm silver nanoparticles in adult mice. *Toxicol Pathol* 40:1004–1013.
- George S, Pokhrel S, Xia T, et al. (2010). Use of a rapid cytotoxicity screening approach to engineer a safer zinc oxide nanoparticle through iron doping. *ACS Nano* 4:15–29.
- Gosens I, Post JA, de la Fonteyne LJ, et al. (2010). Impact of agglomeration state of nano- and submicron sized gold particles on pulmonary inflammation. *Part Fibre Toxicol* 7:37–47.
- Grassian VH, O'Shaughnessy PT, Adamcakova-Dodd A, et al. (2007). Inhalation exposure study of titanium dioxide nanoparticles with a primary particle size of 2 to 5 nm. *Environ Health Perspect* 115: 397–402.
- Guidi P, Nigro M, Bernardeschi M, et al. (2013). Genotoxicity of amorphous silica particles with different structure and dimension in human and murine cell lines. *Mutagenesis* 28:171–180.
- Han G, Ghosh P, Rotello VM. (2007). Functionalized gold nanoparticles for drug delivery. *Nanomedicine (Lond)* 2:113–123.
- Hardy CL, Lemasurier JS, Belz GT, et al. (2012). Inert 50-nm polystyrene nanoparticles that modify pulmonary dendritic cell function and inhibit allergic airway inflammation. *J Immunol* 188: 1431–1441.
- Hardy CL, Lemasurier JS, Mohamud R, et al. (2013). Differential uptake of nanoparticles and microparticles by pulmonary APC subsets induces discrete immunological imprints. *J Immunol* 191:5278–5290.
- Heng BC, Zhao X, Xiong S, et al. (2010). Toxicity of zinc oxide (ZnO) nanoparticles on human bronchial epithelial cells (BEAS-2B) is accentuated by oxidative stress. *Food Chem Toxicol* 48:1762–1766.
- Hirn S, Semmler-Behnke M, Schleh C, et al. (2011). Particle size-dependent and surface charge-dependent biodistribution of gold nanoparticles after intravenous administration. *Eur J Pharm Biopharm* 77:407–416.
- Hoet PH, Bruske-Hohlfeld I, Salata OV. (2004). Nanoparticles – known and unknown health risks. *J Nanobiotechnology* 2:12–26.
- Holt PG, Strickland DH, Wikstrom ME, Jahnsen FL. (2008). Regulation of immunological homeostasis in the respiratory tract. *Nat Rev Immunol* 8:142–152.
- Huang X, Jain PK, El-Sayed IH, El-Sayed MA. (2007). Gold nanoparticles: Interesting optical properties and recent applications in cancer diagnostics and therapy. *Nanomedicine (Lond)* 2:681–693.
- Huang X, Peng X, Wang Y, et al. (2010). A reexamination of active and passive tumor targeting by using rod-shaped gold nanocrystals and covalently conjugated peptide ligands. *ACS Nano* 4:5887–5896.
- Hussain A, Arnold JJ, Khan MA, Ahsan F. (2004). Absorption enhancers in pulmonary protein delivery. *J Control Release* 94:15–24.
- Hussain S, Vanoirbeek JA, Luyts K, et al. (2011). Lung exposure to nanoparticles modulates an asthmatic response in a mouse model. *Eur Respir J* 37:299–309.
- Hussain SM, Hess KL, Gearhart JM, et al. (2005). In vitro toxicity of nanoparticles in BRL 3A rat liver cells. *Toxicol In Vitro* 19:975–983.
- Inoue K, Yanagisawa R, Koike E, et al. (2010). Repeated pulmonary exposure to single-walled carbon nanotubes exacerbates allergic inflammation of the airway: Possible role of oxidative stress. *Free Radic Biol Med* 48:924–934.

- Janeway Jr CA, Bottomly K. (1994). Signals and signs for lymphocyte responses. *Cell* 76:275–285.
- Janeway Jr CA, Medzhitov R. (2002). Innate immune recognition. *Annu Rev Immunol* 20:197–216.
- Jang S, Park JW, Cha HR, et al. (2012). Silver nanoparticles modify VEGF signaling pathway and mucus hypersecretion in allergic airway inflammation. *Int J Nanomedicine* 7:1329–1343.
- Jensen DK, Jensen LB, Koocheki S, et al. (2012). Design of an inhalable dry powder formulation of DOTAP-modified PLGA nanoparticles loaded with siRNA. *J Control Release* 157:141–148.
- John AE, Lukacs NW, Berlin AA, et al. (2003). Discovery of a potent nanoparticle P-selectin antagonist with anti-inflammatory effects in allergic airway disease. *FASEB J* 17:2296–2298.
- Johnston HJ, Hutchison G, Christensen FM, et al. (2010). A review of the *in vivo* and *in vitro* toxicity of silver and gold particulates: Particle attributes and biological mechanisms responsible for the observed toxicity. *Crit Rev Toxicol* 40:328–346.
- Kalishwaralal K, Banumathi E, Ram Kumar Pandian S, et al. (2009). Silver nanoparticles inhibit VEGF induced cell proliferation and migration in bovine retinal endothelial cells. *Colloids Surf B Biointerfaces* 73:51–57.
- Kao YY, Chen YC, Cheng TJ, et al. (2012). Zinc oxide nanoparticles interfere with zinc ion homeostasis to cause cytotoxicity. *Toxicol Sci* 125:462–472.
- Karlson TD, Kong YY, Hardy CL, et al. (2013). The signalling imprints of nanoparticle uptake by bone marrow derived dendritic cells. *Methods* 60:275–283.
- Karlsson HL, Cronholm P, Gustafsson J, Moller L. (2008). Copper oxide nanoparticles are highly toxic: A comparison between metal oxide nanoparticles and carbon nanotubes. *Chem Res Toxicol* 21:1726–1732.
- Kaur G, Narang RK, Rath G, Goyal AK. (2012). Advances in pulmonary delivery of nanoparticles. *Artif Cells Blood Substit Immobil Biotechnol* 40:75–96.
- Keijzer C, Spiering R, Silva AL, et al. (2013). PLGA nanoparticles enhance the expression of retinaldehyde dehydrogenase enzymes in dendritic cells and induce FoxP3 T-cells *in vitro*. *J Control Release* 168:35–40.
- Kim YH, Fazlollahi F, Kennedy IM, et al. (2010). Alveolar epithelial cell injury due to zinc oxide nanoparticle exposure. *Am J Respir Crit Care Med* 182:1398–1409.
- Klippstein R, Pozo D. (2010). Nanotechnology-based manipulation of dendritic cells for enhanced immunotherapy strategies. *Nanomedicine* 6:523–529.
- Konduru NV, Tyurina YY, Feng W, et al. (2009). Phosphatidylserine targets single-walled carbon nanotubes to professional phagocytes *in vitro* and *in vivo*. *PLoS One* 4:e4398.
- Kumar M, Behera AK, Lockey RF, et al. (2002). Intranasal gene transfer by chitosan-DNA nanospheres protects BALB/c mice against acute respiratory syncytial virus infection. *Hum Gene Ther* 13:1415–1425.
- Kumar M, Kong X, Behera AK, et al. (2003). Chitosan IFN- γ -pDNA nanoparticle (CIN) therapy for allergic asthma. *Genet Vaccines Ther* 1:3–12.
- Kunzmann A, Andersson B, Vogt C, et al. (2011). Efficient internalization of silica-coated iron oxide nanoparticles of different sizes by primary human macrophages and dendritic cells. *Toxicol Appl Pharmacol* 253:81–93.
- Lai SK, Suk JS, Pace A, et al. (2011). Drug carrier nanoparticles that penetrate human chronic rhinosinusitis mucus. *Biomaterials* 32:6285–6290.
- Lambrech BN, Hammad H. (2009). Biology of lung dendritic cells at the origin of asthma. *Immunity* 31:412–424.
- Larsen ST, Roursgaard M, Jensen KA, Nielsen GD. (2010). Nano titanium dioxide particles promote allergic sensitization and lung inflammation in mice. *Basic Clin Pharmacol Toxicol* 106:114–117.
- Latimer P, Menchaca M, Snyder RM, et al. (2009). Aerosol delivery of liposomal formulated paclitaxel and vitamin E analog reduces murine mammary tumor burden and metastases. *Exp Biol Med* (Maywood) 234:1244–1252.
- Lee DW, Shirley SA, Lockey RF, Mohapatra SS. (2006). Thiolated chitosan nanoparticles enhance anti-inflammatory effects of intranasally delivered theophylline. *Respir Res* 7:112.
- Li B, Ze Y, Sun Q, et al. (2013). Molecular mechanisms of nanosized titanium dioxide-induced pulmonary injury in mice. *PLoS One* 8:e55563.
- Madani SY, Shabani F, Dwek MV, Seifalian AM. (2013). Conjugation of quantum dots on carbon nanotubes for medical diagnosis and treatment. *Int J Nanomedicine* 8:941–950.
- Madl AK, Pinkerton KE. (2009). Health effects of inhaled engineered and incidental nanoparticles. *Crit Rev Toxicol* 39:629–658.
- Maiseyeu A, Badgeley MA, Kampfrath T, et al. (2012). *In vivo* targeting of inflammation-associated myeloid-related protein 8/14 via gadolinium immunonanoparticles. *Arterioscler Thromb Vasc Biol* 32:962–970.
- Mano SS, Kanehira K, Sonezaki S, Taniguchi A. (2012). Effect of polyethylene glycol modification of TiO₂ nanoparticles on cytotoxicity and gene expressions in human cell lines. *Int J Mol Sci* 13:3703–3717.
- Marches R, Mikoryak C, Wang RH, et al. (2011). The importance of cellular internalization of antibody-targeted carbon nanotubes in the photothermal ablation of breast cancer cells. *Nanotechnology* 22:095101 (1–10).
- Martinez Gomez JM, Fischer S, Csaba N, et al. (2007). A protective allergy vaccine based on CpG- and protamine-containing PLGA microparticles. *Pharm Res* 24:1927–1935.
- Matsuo Y, Ishihara T, Ishizaki J, et al. (2009). Effect of betamethasone phosphate loaded polymeric nanoparticles on a murine asthma model. *Cell Immunol* 260:33–38.
- McCarthy J, Inkielewicz-Stepniak I, Corbalan JJ, Radomski MW. (2012). Mechanisms of toxicity of amorphous silica nanoparticles on human lung submucosal cells *in vitro*: Protective effects of fisetin. *Chem Res Toxicol* 25:2227–2235.
- Minigo G, Scholzen A, Tang CK, et al. (2007). Poly-L-lysine-coated nanoparticles: A potent delivery system to enhance DNA vaccine efficacy. *Vaccine* 25:1316–1327.
- Mitchell LA, Gao J, Wal RV, et al. (2007). Pulmonary and systemic immune response to inhaled multiwalled carbon nanotubes. *Toxicol Sci* 100:203–214.
- Monforte V, Ussetti P, Lopez R, et al. (2009). Nebulized liposomal amphotericin B prophylaxis for Aspergillus infection in lung transplantation: Pharmacokinetics and safety. *J Heart Lung Transplant* 28:170–175.
- Mossman BT, Churg A. (1998). Mechanisms in the pathogenesis of asbestosis and silicosis. *Am J Respir Crit Care Med* 157:1666–1680.
- Mottram PL, Leong D, Crimeen-Irwin B, et al. (2007). Type 1 and 2 immunity following vaccination is influenced by nanoparticle size: Formulation of a model vaccine for respiratory syncytial virus. *Mol Pharm* 4:73–84.
- Muhlfeld C, Rothen-Rutishauser B, Blank F, et al. (2008). Interactions of nanoparticles with pulmonary structures and cellular responses. *Am J Physiol Lung Cell Mol Physiol* 294:L817–L829.
- Nafee N, Taetz S, Schneider M, et al. (2007). Chitosan-coated PLGA nanoparticles for DNA/RNA delivery: Effect of the formulation parameters on complexation and transfection of antisense oligonucleotides. *Nanomedicine* 3:173–183.
- Napierska D, Rabolli V, Thomassen LC, et al. (2012a). Oxidative stress induced by pure and iron-doped amorphous silica nanoparticles in subtoxic conditions. *Chem Res Toxicol* 25:828–837.
- Napierska D, Thomassen LC, Lison D, et al. (2010). The nanosilica hazard: Another variable entity. Part I. *Fibre Toxicol* 7:39–70.
- Napierska D, Thomassen LC, Vanaudenaerde B, et al. (2012b). Cytokine production by co-cultures exposed to monodisperse amorphous silica nanoparticles: The role of size and surface area. *Toxicol Lett* 211:98–104.
- Nassimi M, Schleh C, Lauenstein HD, et al. (2010). A toxicological evaluation of inhaled solid lipid nanoparticles used as a potential drug delivery system for the lung. *Eur J Pharm Biopharm* 75:107–116.
- Nemmar A, Hoet PH, Vandervoort P, et al. (2007). Enhanced peripheral thrombogenesis after lung inflammation is mediated by platelet-leukocyte activation: Role of P-selectin. *J Thromb Haemost* 5:1217–1226.
- Nemmar A, Hoylaerts MF, Hoet PH, et al. (2003). Size effect of intratracheally instilled particles on pulmonary inflammation and vascular thrombosis. *Toxicol Appl Pharmacol* 186:38–45.
- Nicod LP. (1999). Pulmonary defence mechanisms. *Respiration* 66:2–11.
- Oberdorster G, Oberdorster E, Oberdorster J. (2005). Nanotoxicology: An emerging discipline evolving from studies of ultrafine particles. *Environ Health Perspect* 113:823–839.

- Ogami A, Yamamoto K, Morimoto Y, et al. (2011). Pathological features of rat lung following inhalation and intratracheal instillation of C₆₀ fullerene. *Inhal Toxicol* 23:407–416.
- Oikonomou N, Harokopos V, Zalevsky J, et al. (2006). Soluble TNF mediates the transition from pulmonary inflammation to fibrosis. *PLoS One* 1:e108.
- Oves M, Khan MS, Zaidi A, et al. (2013). Antibacterial and cytotoxic efficacy of extracellular silver nanoparticles biofabricated from chromium reducing novel OS4 strain of *Stenotrophomonas maltophilia*. *PLoS One* 8:e59140.
- Pan Z, Lee W, Slutsky L, et al. (2009). Adverse effects of titanium dioxide nanoparticles on human dermal fibroblasts and how to protect cells. *Small* 5:511–520.
- Park EJ, Bae E, Yi J, et al. (2010a). Repeated-dose toxicity and inflammatory responses in mice by oral administration of silver nanoparticles. *Environ Toxicol Pharmacol* 30:162–168.
- Park EJ, Cho WS, Jeong J, et al. (2009). Pro-inflammatory and potential allergic responses resulting from B cell activation in mice treated with multi-walled carbon nanotubes by intratracheal instillation. *Toxicology* 259:113–121.
- Park EJ, Choi K, Park K. (2011). Induction of inflammatory responses and gene expression by intratracheal instillation of silver nanoparticles in mice. *Arch Pharm Res* 34:299–307.
- Park EJ, Kim H, Kim Y, et al. (2010b). Inflammatory responses may be induced by a single intratracheal instillation of iron nanoparticles in mice. *Toxicology* 275:65–71.
- Park HS, Kim KH, Jang S, et al. (2010c). Attenuation of allergic airway inflammation and hyperresponsiveness in a murine model of asthma by silver nanoparticles. *Int J Nanomedicine* 5:505–515.
- Pastorino F, Di Paolo D, Piccardi F, et al. (2008). Enhanced antitumor efficacy of clinical-grade vasculature-targeted liposomal doxorubicin. *Clin Cancer Res* 14:7320–7329.
- Patton JS, Byron PR. (2007). Inhaling medicines: Delivering drugs to the body through the lungs. *Nat Rev Drug Discov* 6:67–74.
- Pilcer G, Amighi K. (2010). Formulation strategy and use of excipients in pulmonary drug delivery. *Int J Pharm* 392:1–19.
- Pirooznia N, Hasannia S, Lotfi AS, Ghanei M. (2012). Encapsulation of alpha-1 antitrypsin in PLGA nanoparticles: In vitro characterization as an effective aerosol formulation in pulmonary diseases. *J Nanobiotechnol* 10:20–34.
- Prato M, Kostarelos K, Bianco A. (2008). Functionalized carbon nanotubes in drug design and discovery. *Acc Chem Res* 41:60–68.
- Randall TD. (2010). Pulmonary dendritic cells: Thinking globally, acting locally. *J Exp Med* 207:451–454.
- Reddy ST, van der Vlies AJ, Simeoni E, et al. (2007). Exploiting lymphatic transport and complement activation in nanoparticle vaccines. *Nat Biotechnol* 25:1159–1164.
- Regner M, Culley F, Fontannaz P, et al. (2004). Safety and efficacy of immune-stimulating complex-based antigen delivery systems for neonatal immunisation against respiratory syncytial virus infection. *Microbes Infect* 6:666–675.
- Rossi EM, Pytkanen L, Koivisto AJ, et al. (2010). Inhalation exposure to nanosized and fine TiO₂ particles inhibits features of allergic asthma in a murine model. *Part Fibre Toxicol* 7:35–48.
- Roursgaard M, Poulsen SS, Kepley CL, et al. (2008). Polyhydroxylated C₆₀ fullerene (fullerenol) attenuates neutrophilic lung inflammation in mice. *Basic Clin Pharmacol Toxicol* 103:386–388.
- Roursgaard M, Poulsen SS, Poulsen LK, et al. (2010). Time-response relationship of nano and micro particle induced lung inflammation. Quartz as reference compound. *Hum Exp Toxicol* 29:915–933.
- Ruenraroengsak P, Novak P, Berhanu D, et al. (2012). Respiratory epithelial cytotoxicity and membrane damage (holes) caused by amine-modified nanoparticles. *Nanotoxicology* 6:94–108.
- Ryan JJ, Bateman HR, Stover A, et al. (2007). Fullerene nanomaterials inhibit the allergic response. *J Immunol* 179:665–672.
- Safari D, Marradi M, Chiodo F, et al. (2012). Gold nanoparticles as carriers for a synthetic *Streptococcus pneumoniae* type 14 conjugate vaccine. *Nanomedicine (Lond)* 7:651–662.
- San Gil F, Turner B, Walker MJ, et al. (1999). Contribution of adjuvant to adaptive immune responses in mice against *Actinobacillus pleuropneumoniae*. *Microbiology* 145 (Pt 9):2595–2603.
- Sandberg WJ, Lag M, Holme JA, et al. (2012). Comparison of non-crystalline silica nanoparticles in IL-1β release from macrophages. *Part Fibre Toxicol* 9:32–44.
- Satoh M, Takayanagi I. (2006). Pharmacological studies on fullerene (C₆₀), a novel carbon allotrope, and its derivatives. *J Pharmacol Sci* 100:513–518.
- Sayes CM, Liang F, Hudson JL, et al. (2006a). Functionalization density dependence of single-walled carbon nanotubes cytotoxicity in vitro. *Toxicol Lett* 161:135–142.
- Sayes CM, Marchione AA, Reed KL, Warheit DB. (2007). Comparative pulmonary toxicity assessments of C₆₀ water suspensions in rats: Few differences in fullerene toxicity in vivo in contrast to in vitro profiles. *Nano Lett* 7:2399–2406.
- Sayes CM, Wahi R, Kurian PA, et al. (2006b). Correlating nanoscale titania structure with toxicity: A cytotoxicity and inflammatory response study with human dermal fibroblasts and human lung epithelial cells. *Toxicol Sci* 92:174–185.
- Scholl I, Kopp T, Bohle B, Jensen-Jarolim E. (2006). Biodegradable PLGA particles for improved systemic and mucosal treatment of Type I allergy. *Immunol Allergy Clin North Am* 26:349–364, ix.
- Schulz M, Ma-Hock L, Brill S, et al. (2012). Investigation on the genotoxicity of different sizes of gold nanoparticles administered to the lungs of rats. *Mutat Res* 745:51–57.
- Semmler-Behnke M, Kreyling WG, Lipka J, et al. (2008). Biodistribution of 1.4- and 18-nm gold particles in rats. *Small* 4:2108–2111.
- Shen S, Liu Y, Huang P, Wang J. (2009). In vitro cellular uptake and effects of Fe₃O₄ magnetic nanoparticles on HeLa cells. *J Nanosci Nanotechnol* 9:2866–2871.
- Shi H, Magaye R, Castranova V, Zhao J. (2013). Titanium dioxide nanoparticles: A review of current toxicological data. *Part Fibre Toxicol* 10:15–47.
- Shoenfelt J, Mitkus RJ, Zeisler R, et al. (2009). Involvement of TLR2 and TLR4 in inflammatory immune responses induced by fine and coarse ambient air particulate matter. *J Leukoc Biol* 86:303–312.
- Shvedova AA, Kisin ER, Mercer R, et al. (2005). Unusual inflammatory and fibrogenic pulmonary responses to single-walled carbon nanotubes in mice. *Am J Physiol Lung Cell Mol Physiol* 289:L698–L708.
- Sonavane G, Tomoda K, Makino K. (2008). Biodistribution of colloidal gold nanoparticles after intravenous administration: Effect of particle size. *Colloids Surf B Biointerfaces* 66:274–280.
- Song KS, Sung JH, Ji JH, et al. (2012). Recovery from silver-nanoparticle-exposure-induced lung inflammation and lung function changes in Sprague Dawley rats. *Nanotoxicology* 7:169–180.
- Sperling RA, Rivera Gil P, Zhang F, et al. (2008). Biological applications of gold nanoparticles. *Chem Soc Rev* 37:1896–1908.
- Stebounova LV, Adamcakova-Dodd A, Kim JS, et al. (2011). Nanosilver induces minimal lung toxicity or inflammation in a subacute murine inhalation model. *Part Fibre Toxicol* 8:5–16.
- Steinmuller C, Franke-Ullmann G, Lohmann-Matthes ML, Emmendorffer A. (2000). Local activation of nonspecific defense against a respiratory model infection by application of interferon-gamma: Comparison between rat alveolar and interstitial lung macrophages. *Am J Respir Cell Mol Biol* 22:481–490.
- Suh WH, Suslick KS, Stucky GD, Suh YH. (2009). Nanotechnology, nanotoxicology, and neuroscience. *Prog Neurobiol* 87:133–170.
- Sung JC, Pulliam BL, Edwards DA. (2007). Nanoparticles for drug delivery to the lungs. *Trends Biotechnol* 25:563–570.
- Sung JH, Ji JH, Park JD, et al. (2011). Subchronic inhalation toxicity of gold nanoparticles. *Part Fibre Toxicol* 8:16–33.
- Sung JH, Ji JH, Yoon JU, et al. (2008). Lung function changes in Sprague-Dawley rats after prolonged inhalation exposure to silver nanoparticles. *Inhal Toxicol* 20:567–574.
- Szacilowski K, Macyk W, Drzewiecka-Matuszek A, et al. (2005). Bioinorganic photochemistry: Frontiers and mechanisms. *Chem Rev* 105:2647–2694.
- Szalay B, Tatrai E, Nyiro G, et al. (2012). Potential toxic effects of iron oxide nanoparticles in vivo and in vitro experiments. *J Appl Toxicol* 32:446–453.
- Ungaro F, d'Angelo I, Miro A, et al. (2012). Engineered PLGA nano- and micro-carriers for pulmonary delivery: Challenges and promises. *J Pharm Pharmacol* 64:1217–1235.
- Vardharajula S, Ali SZ, Tiwari PM, et al. (2012). Functionalized carbon nanotubes: Biomedical applications. *Int J Nanomedicine* 7:5361–5374.
- Verma NK, Crosbie-Staunton K, Satti A, et al. (2013). Magnetic core-shell nanoparticles for drug delivery by nebulization. *J Nanobiotechnol* 11:1–12.

- Vigneshwaran N, Kathe AA, Varadarajan PV, et al. (2007). Functional finishing of cotton fabrics using silver nanoparticles. *J Nanosci Nanotechnol* 7:1893–1897.
- Vranic S, Garcia-Verdugo I, Darnis C, et al. (2013). Internalization of SiO₂ nanoparticles by alveolar macrophages and lung epithelial cells and its modulation by the lung surfactant substitute Curosurereg®. *Environ Sci Pollut Res Int* 20:2761–2770.
- Wang H, Zou C, Tian C, et al. (2011). A novel gas ionization sensor using Pd nanoparticle-capped ZnO. *Nanoscale Res Lett* 6:534–541.
- Wang JJ, Sanderson BJ, Wang H. (2007). Cytotoxicity and genotoxicity of ultrafine crystalline SiO₂ particulate in cultured human lymphoblastoid cells. *Environ Mol Mutagen* 48:151–157.
- Wang W, Zhu R, Xie Q, et al. (2012). Enhanced bioavailability and efficiency of curcumin for the treatment of asthma by its formulation in solid lipid nanoparticles. *Int J Nanomed* 7:3667–3677.
- Wang X, Xu W, Kong X, et al. (2009). Modulation of lung inflammation by vessel dilator in a mouse model of allergic asthma. *Respir Res* 10:66–73.
- Wang X, Xu W, Mohapatra S, et al. (2008). Prevention of airway inflammation with topical cream containing imiquimod and small interfering RNA for natriuretic peptide receptor. *Genet Vaccines Ther* 6:7–15.
- Wang X, Zang JJ, Wang H, et al. (2010). Pulmonary toxicity in mice exposed to low and medium doses of water-soluble multi-walled carbon nanotubes. *J Nanosci Nanotechnol* 10:8516–8526.
- Warheit DB, Webb TR, Colvin VL, et al. (2007a). Pulmonary bioassay studies with nanoscale and fine-quartz particles in rats: Toxicity is not dependent upon particle size but on surface characteristics. *Toxicol Sci* 95:270–280.
- Warheit DB, Webb TR, Reed KL, et al. (2007b). Pulmonary toxicity study in rats with three forms of ultrafine-TiO₂ particles: Differential responses related to surface properties. *Toxicology* 230:90–104.
- Wiesenthal A, Hunter L, Wang S, et al. (2011). Nanoparticles: Small and mighty. *Int J Dermatol* 50:247–254.
- Wissinger E, Goulding J, Hussell T. (2009). Immune homeostasis in the respiratory tract and its impact on heterologous infection. *Semin Immunol* 21:147–155.
- Wong KK, Ng A, Chen XY, et al. (2012). Effect of ZnO nanoparticle properties on dye-sensitized solar cell performance. *ACS Appl Mater Interfaces* 4:1254–1261.
- Xia T, Kovochich M, Brant J, et al. (2006). Comparison of the abilities of ambient and manufactured nanoparticles to induce cellular toxicity according to an oxidative stress paradigm. *Nano Lett* 6:1794–1807.
- Xiang SD, Scalzo-Inguanti K, Minigo G, et al. (2008). Promising particle-based vaccines in cancer therapy. *Expert Rev Vaccines* 7:1103–1119.
- Xiang SD, Scholzen A, Minigo G, et al. (2006). Pathogen recognition and development of particulate vaccines: Does size matter? *Methods* 40:1–9.
- Xie J, Liu G, Eden HS, et al. (2011). Surface-engineered magnetic nanoparticle platforms for cancer imaging and therapy. *Acc Chem Res* 44:883–892.
- Yang M, Yamamoto H, Kurashima H, et al. (2012). Design and evaluation of inhalable chitosan-modified poly (DL-lactic-co-glycolic acid) nanocomposite particles. *Eur J Pharm Sci* 47:235–243.
- Yang S, Damiano MG, Zhang H, et al. (2013). Biomimetic, synthetic HDL nanostructures for lymphoma. *Proc Natl Acad Sci U S A* 110:2511–2516.
- Yazdi AS, Guarda G, Riteau N, et al. (2010). Nanoparticles activate the NLR pyrin domain containing 3 (Nlrp3) inflammasome and cause pulmonary inflammation through release of IL-1alpha and IL-1beta. *Proc Natl Acad Sci U S A* 107:19449–19454.
- Yuan Y, Ding J, Xu J, et al. (2010). TiO₂ nanoparticles co-doped with silver and nitrogen for antibacterial application. *J Nanosci Nanotechnol* 10:4868–4874.
- Zagorovsky K, Chan WC. (2013). A plasmonic DNAzyme strategy for point-of-care genetic detection of infectious pathogens. *Angew Chem Int Ed Engl* 52:3168–3171.
- Zakharian TY, Seryshev A, Sitharaman B, et al. (2005). A fullerene-paclitaxel chemotherapeutic: Synthesis, characterization, and study of biological activity in tissue culture. *J Am Chem Soc* 127:12508–12509.
- Zaru M, Sinico C, De Logu A, et al. (2009). Rifampicin-loaded liposomes for the passive targeting to alveolar macrophages: In vitro and in vivo evaluation. *J Liposome Res* 19:68–76.
- Zhang H, Wang C, Chen B, Wang X. (2012). Daunorubicin-TiO₂ nanocomposites as a “smart” pH-responsive drug delivery system. *Int J Nanomed* 7:235–242.

ORIGINAL ARTICLE

The activin A antagonist follistatin inhibits asthmatic airway remodelling

Charles Linton Hardy,^{1,2,3} Hong-An Nguyen,^{1,2,3} Rohimah Mohamud,^{1,3} John Yao,^{1,2,3} Ding Yuan Oh,^{1,2} Magdalena Plebanski,^{1,3} Kate L Loveland,⁴ Craig A Harrison,⁵ Jennifer M Rolland,^{1,2,3} Robyn E O'Hehir^{1,2,3}

► Additional supplementary files are published online only. To view these files please visit the journal online (<http://dx.doi.org/10.1136/thoraxjnl-2011-201128>).

¹Department of Immunology, Monash University, Melbourne, Victoria, Australia

²Department of Allergy, Immunology and Respiratory Medicine, Monash University and The Alfred Hospital, Melbourne, Victoria, Australia

³CRC for Asthma and Airways, Sydney, Australia

⁴Department of Biochemistry, Molecular Biology, Anatomy and Developmental Biology, School of Biomedical Sciences, Monash University, Clayton, Victoria, Australia

⁵Growth Factor Signaling, Prince Henry's Institute, Clayton, Victoria, Australia

Correspondence to

Dr Charles Linton Hardy, Department of Immunology, Monash University, 89 Commercial Road, Level 2, Melbourne, VIC 3004, Australia

Received 19 September 2011
Accepted 30 August 2012

ABSTRACT

Background Current pharmacotherapy is highly effective in the clinical management of the majority of patients with stable asthma, however severe asthma remains inadequately treated. Prevention of airway remodelling is a major unmet clinical need in the management of patients with chronic severe asthma and other inflammatory lung diseases. Accumulating evidence convincingly demonstrates that activin A, a member of the transforming growth factor (TGF)- β superfamily, is a key driver of airway inflammation, but its role in chronic asthmatic airway remodelling is ill-defined. Follistatin, an endogenously produced protein, binds activin A with high affinity and inhibits its bioactivity. The aim of this study was to test the potential of follistatin as a therapeutic agent to inhibit airway remodelling in an experimental model of chronic allergic airway inflammation.

Methods BALB/c mice were systemically sensitised with ovalbumin (OVA), and challenged with OVA intranasally three times a week for 10 weeks. Follistatin was instilled intranasally during allergen challenge.

Results Chronic allergen challenge induced mucus hypersecretion and subepithelial collagen deposition which persisted after cessation of challenge. Intranasal follistatin (0.05, 0.5, 5 μ g) inhibited the airway remodelling and dose-dependently decreased airway activin A and TGF- β 1, and allergen-specific T helper 2 cytokine production in the lung-draining lymph nodes. Follistatin also impaired the loss of TGF- β 1 and activin RIB immunostaining in airway epithelium which occurred following chronic allergen challenge.

Conclusions These data demonstrate that follistatin attenuates asthmatic airway remodelling. Our findings point to the potential of follistatin as a therapeutic for prevention of airway remodelling in asthma and other inflammatory lung diseases.

INTRODUCTION

Current pharmacotherapy is highly effective in the clinical management of the majority of patients with stable asthma, however severe asthma remains inadequately treated. Prevention of airway remodelling is a major unmet clinical need in the management of patients with chronic severe asthma and other inflammatory lung diseases.¹ Increasing evidence implicates activin A, a homodimer of activin β A subunits and a member of the transforming growth factor (TGF)- β superfamily, in this process. Activin A can promote inflammation by stimulating production of inflammatory mediators including interleukin (IL)-1 β , IL-6, tumour

Key messages

What is the key question?

- To determine whether blocking activin A with its naturally occurring antagonist follistatin inhibits asthmatic airway remodelling.

What is the bottom line?

- Follistatin instillation during allergen challenge inhibited secretion of activin A and transforming growth factor β 1 in the lung, and significantly inhibited subepithelial collagen deposition and airway epithelial mucus production.

Why read on?

- Our findings provide insight into the therapeutic potential of follistatin in the control of fibrosis in lung inflammatory disease, and highlight a role for activin A in the regulation of inflammation.

necrosis factor and nitric oxide. However, other studies show that activin A can inhibit inflammation.^{2,3} Clearly, regulation of the immunoregulatory effect of activin A is complex and dependent on the anatomical site, cell type and phase of the immune response. Importantly, activin A bioactivity is inhibited by the endogenously produced high-affinity binding protein follistatin.⁴

Accumulating data suggest that activin A regulates inflammation and fibrosis in the lung.⁵⁻⁹ In vitro, activin A stimulates proliferation of human lung fibroblasts and smooth muscle cells.⁵⁻¹⁰ In vivo, activin A is upregulated in bleomycin-induced pulmonary fibrosis, and follistatin injection inhibits this fibrosis.¹¹ Furthermore, mice deficient in Smad3, common to the TGF- β /activin A signalling pathways, have decreased airway remodelling.¹² In contrast, overexpression of the TGF- β /activin signalling intermediate Smad2 in airway epithelium induced activin A secretion and airway remodelling.¹³ Remodelling was inhibited by injection of activin A neutralising antibody prior to allergen challenge, providing direct evidence of a role for activin A in remodelling. However, detailed knowledge of the effect of inhibiting activin A with follistatin in chronic asthma is lacking. In the current study we investigated whether follistatin treatment during allergen challenge inhibited development of

Asthma

airway remodelling in a model of chronic allergic asthma. Our data identify activin A as an important driver of asthmatic airway pathology and highlight the therapeutic potential of follistatin as an inhibitor of airway remodelling.

METHODS

Mice

Female BALB/c mice (7 weeks) were obtained from the Walter and Eliza Hall Institute of Medical Research, Melbourne, Victoria, Australia and housed in the Alfred Medical Research and Education Precinct (AMREP) animal house. All experimental protocols were approved by the AMREP Animal Ethics Committee.

Recombinant follistatin and follistatin luciferase bioassay

For follistatin production and assessment of bioactivity, see online supplement.

Immunisations and tissue processing

Mice were sensitised with intraperitoneal ovalbumin (OVA; A5503, Sigma-Aldrich, Saint Louis, Missouri, USA) in alum,⁶ and isoflurane-anaesthetised mice challenged intranasally (50 µl) with OVA (5 µg, 25 µg or 100 µg) three times per week.^{14–16} Groups were killed after 2, 5 or 10 weeks of allergen challenge, and 2 weeks after the final challenge (12 weeks) (see online supplementary figure S1A). For the follistatin instillation experiments, OVA-sensitised mice were challenged intranasally

with OVA (25 µg) alone or mixed with follistatin (0.05, 0.5 or 5 µg), and analysis performed after 5 weeks of challenge (see online supplementary figure S1B). Controls received saline instead of OVA or follistatin. Bronchoalveolar lavage (BAL), differentials and tissue sampling were as described¹⁷ (see online supplement).

Cytokine ELISPOT, OVA-specific IgE, activin A, TGF-β1 and IL-13 ELISA

IL-4, IL-5 and IL-13 enzyme-linked immunosorbent spot (ELISPOT) on lung-draining lymph node (LN) cells were performed as described.⁶ OVA-specific IgE was detected as described.¹⁷ Activin A was measured by a specific ELISA as described.⁶ TGF-β1 was detected using a TGF-β1 ELISA kit (#DY1679, R&D Systems, Minneapolis, MN, USA) (see online supplement). IL-13 was detected using the IL-13 Ready-SET-Go! kit (#88-7137-88; eBioscience, Inc., San Diego, California, USA).

Follistatin radioimmunoassay

Follistatin concentrations were measured using a discontinuous radioimmunoassay as described.¹⁸

Activin A, TGF-β, follistatin and activin receptor immunohistochemistry

Immunohistochemistry was performed on 3 µm formalin-fixed sections. Activin A and follistatin immunohistochemistry were performed as described.⁶ For TGF-β and activin receptor

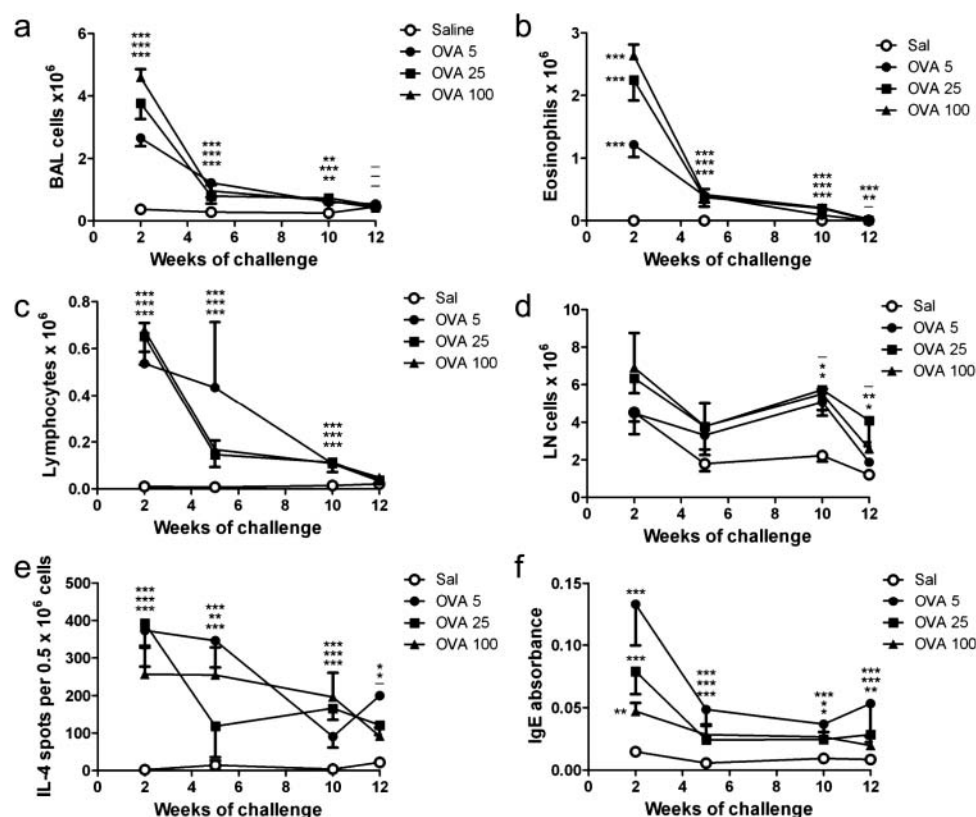


Figure 1 Chronic allergen challenge causes resolution of allergic inflammation independent of allergen challenge dose. Mice were sensitised and challenged with OVA as per online supplementary figure S1 A; controls received saline instead of OVA. (A–D) Counts of total bronchoalveolar lavage (BAL) cells, BAL eosinophils, BAL lymphocytes, and draining LN cells, and (E, F) frequency of interleukin (IL)-4-producing cells in the lung-draining LN, and levels of serum OVA-specific IgE were measured at the time points shown in (A). Mean \pm SEM, $n = 6–7$ mice/group per time point. * $p < 0.05$, ** $p < 0.01$, *** $p < 0.001$; the order of symbols from top to bottom is OVA 5, 25 and 100 µg (relative to saline).

immunostaining antigen retrieval was performed and endogenous peroxidase blocked in H_2O_2 . Sections were stained with antibodies specific for TGF- β 1 (sc-146; Santa Cruz Biotechnology, Inc. Santa Cruz, California, USA), or ActRIB/ALK4, ActRIIA and ActRIIB (N-20, sc-11984; N-17, sc-5667; and N-16, sc-5665, respectively; Santa Cruz Biotechnology, Inc.) or appropriate isotype controls. See online supplement.

Quantitative image analysis

The frequency of periodic acid Schiff (PAS), activin A, follistatin or ActRIB positive airway epithelial cells per mm basement membrane was calculated (<http://fiji.sc>). Alternatively, airway epithelial TGF- β , activin A, ActRIIA and ActRIIB immunoreactivity was expressed as integrated density ($n=5-19$ airways/mouse). The percentage of subepithelial collagen in Masson's trichrome-stained sections was calculated to a depth of 20 μ m below the basement membrane.¹⁶ Smooth muscle thickness was measured at right angles across the muscle bundle on ActRIB-stained sections ($n=2-7$ airways/mouse). See online supplement.

Statistics

Data were analysed for normality and log transformed as necessary prior to analysis by analysis of variance and Tukey post tests or t tests (GraphPad Prism V5.03). Differences were considered significant at $p<0.05$. Group sizes are indicated in the figure legends. All values in figures are mean \pm SEM.

RESULTS

Repeated allergen challenge induces acute resolving pulmonary inflammation

We investigated the effect of chronic allergen challenge on the kinetics of airway inflammation and remodelling to validate our model. Mice were challenged with 5, 25 or 100 μ g OVA to investigate the effect of allergen dose (see online supplementary figure S1A). Regardless of OVA challenge dose, BAL cell counts were markedly increased compared with saline controls after 2 weeks of challenge, with eosinophils the major infiltrating cell type (figure 1A,B). After 5–10 weeks of challenge total BAL and eosinophil counts had decreased sharply but remained significantly higher than saline controls, and returned to baseline after challenges ceased. BAL lymphocytes followed a similar pattern (figure 1C). Cell counts in the lung-draining LN were elevated from 5 weeks and trended toward control values once allergen challenges stopped (12 weeks) (figure 1D). The frequency of IL-4-producing cells in the draining LN peaked after 2 weeks of challenge, decreasing gradually thereafter, but remaining above saline levels at 12 weeks (figure 1E). OVA-specific IgE levels were significantly elevated after 2 weeks of challenge, dropping sharply by 5 weeks and remaining stable thereafter (figure 1F). Thus allergen challenge induced acute inflammation at 2 weeks, similar to other acute asthma models, but this decreased sharply upon continued OVA challenge, and decreased further once allergen challenge ceased. Airway inflammation/eosinophilia was dose dependent, with the 100 μ g group showing the greatest inflammation. The dose-dependent effect on serum OVA-specific IgE was reversed, with the 5 μ g OVA challenge group having the highest level at all time points.

Allergen challenge increases BAL fluid levels of activin A, follistatin and TGF- β 1

Next we determined the effect of chronic allergen challenge on concentrations of activin A, follistatin and TGF- β 1 in the

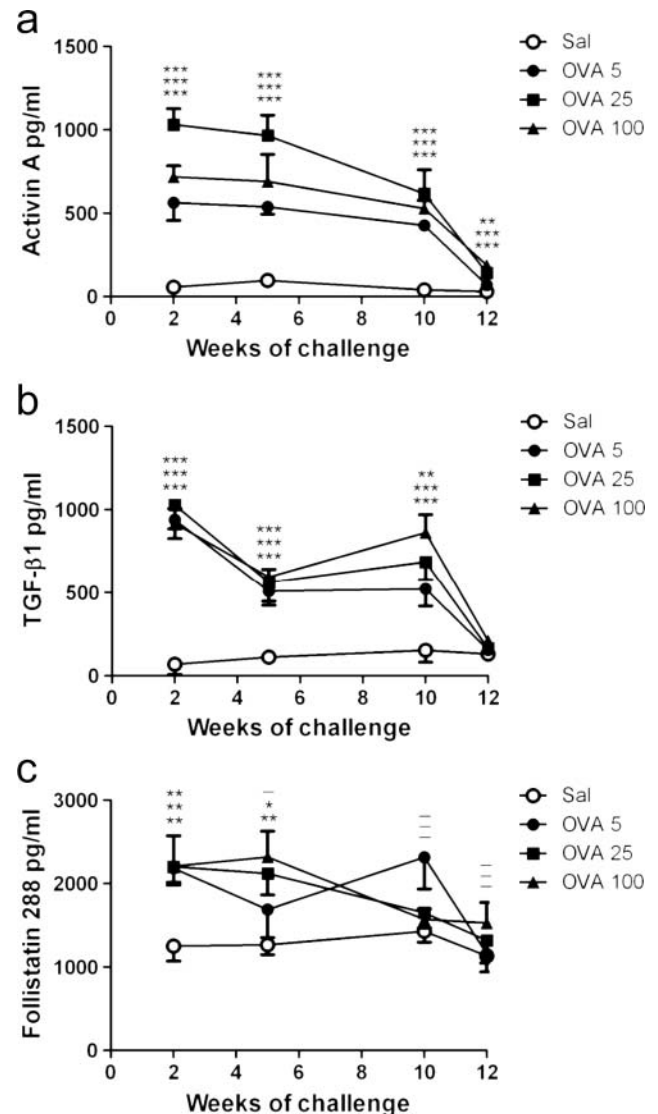


Figure 2 Activin A, TGF- β 1 and follistatin levels are increased in bronchoalveolar lavage fluid during chronic allergen challenge. Mice were sensitised and challenged as described in online supplementary figure S1A, controls received saline instead of OVA. (A–C) Concentrations of activin A, TGF- β 1 (ELISA) and follistatin (RIA) were measured at the time points shown in (A). Mean \pm SEM, $n=6-7$ mice/group per time point. * $p<0.05$, ** $p<0.01$, *** $p<0.001$; the order of symbols from top to bottom is OVA 5, 25 and 100 μ g (relative to saline).

airways. Activin A and TGF- β 1 concentrations were significantly elevated after 2 weeks of challenge, remaining high during allergen challenge, and dropping sharply once allergen challenge ceased (figure 2A,B). Follistatin concentrations showed a similar pattern, approaching control values by the 10-week time point (figure 2C). Thus, the elevated BAL fluid levels of activin A, TGF- β 1 and follistatin seen during acute challenge are dependent on continued allergen challenge.

Chronic allergen challenge decreases airway epithelial cell activin A and follistatin immunoreactivity, and induces airway remodelling

Airway epithelium in the saline group showed strong and uniform immunoreactivity for activin A and follistatin (figure 3A,C). In contrast, epithelial cell activin A and follistatin immunoreactivity were dramatically decreased during chronic

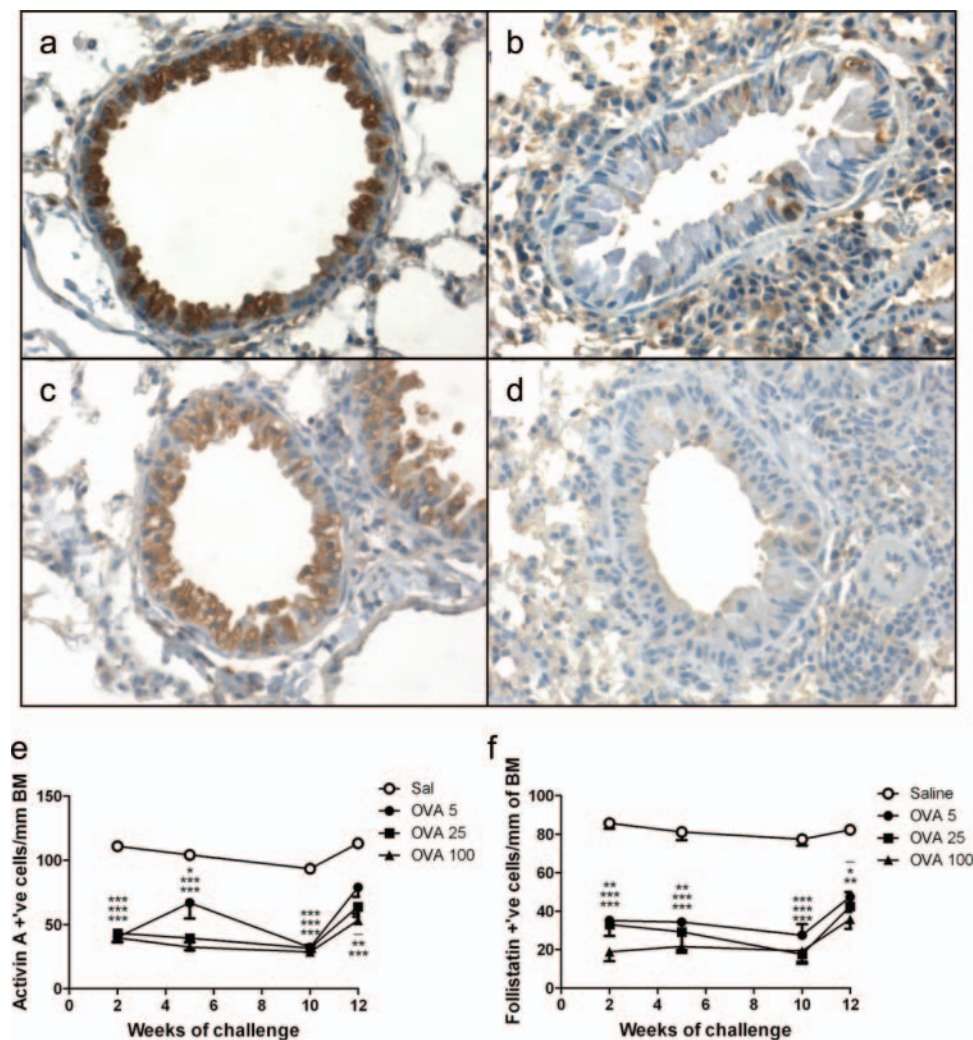


Figure 3 Activin A and follistatin expression by airway epithelium in the normal lung is lost during chronic allergen challenge. Mice were sensitised and challenged as described in online supplementary figure S1A, controls received saline instead of OVA. Representative lung tissue sections stained immunohistochemically for activin A (A, B) and follistatin (C, D) from saline control (A, C) and OVA sensitised and challenged mice (B, D). (E, F) Frequency of activin A and follistatin immunoreactive cells per millimetre basement membrane (BM) as determined by quantitative image analysis. (A–D) Original magnification $\times 400$. (E, F) Mean \pm SEM, $n=6-7$ mice/group per time point. * $p<0.05$, ** $p<0.01$, *** $p<0.001$, respectively; order of symbols from top to bottom is OVA 5, 25 and 100 μg .

allergen challenge, remaining low throughout the challenge period, and sharply increasing once allergen challenge ceased (figure 3B,D,E,F). After 5 weeks of challenge there was a significant increase in subepithelial collagen, consistent with other chronic challenge models,^{14–16} and this persisted at 10 weeks and after cessation of allergen challenge (figure 4A,B,E). The frequency of PAS-positive airway epithelial cells was significantly increased after 2 weeks of allergen challenge, remaining high throughout the challenge period, but declining sharply once allergen challenge stopped (figure 4C,D,F). Therefore, the increase in subepithelial collagen deposition persisted after cessation of allergen challenge, whereas mucus hypersecretion was dependent upon continued challenge. There was no consistent effect of allergen dose on the kinetics of these parameters.

Follistatin administration during chronic allergen challenge attenuates Th2 cytokine production

To investigate the role of activin A in the remodelling process we instilled follistatin at the time of allergen challenge. We previously showed that 0.5–1 μg FS288 instilled prior to allergen

challenge inhibits allergen-specific T helper 2 (Th2) cytokine and airway epithelial mucus production in an acute asthma model.⁶ Since activin A acts in a concentration-dependent manner¹⁹ (our own unpublished data), we tested the effect of 0.05, 0.5 and 5 μg follistatin instilled during chronic allergen challenge (see online supplementary figure S1B). Given that remodelling was independent of the OVA challenge dose (figure 4), we used 25 μg OVA per challenge for the remainder of our studies. Compared with mice challenged with OVA alone, low-dose follistatin significantly increased the number of BAL eosinophils (figure 5A) and total BAL cells (not shown). Surprisingly, however, higher follistatin doses had no effect on BAL eosinophils or total BAL cell counts. Follistatin dose-dependently increased lung-draining LN cell counts (figure 5B), but decreased the frequency of IL-4, IL-5 and IL-13 producing cells in the lung-draining LN (figure 5C–E). Thus, overall there was a marginal decrease in numbers of Th2 cytokine-producing cells (see online supplementary figure S2). In contrast, BAL fluid IL-13 concentrations were only significantly decreased in mice treated with low-dose follistatin (see online supplementary

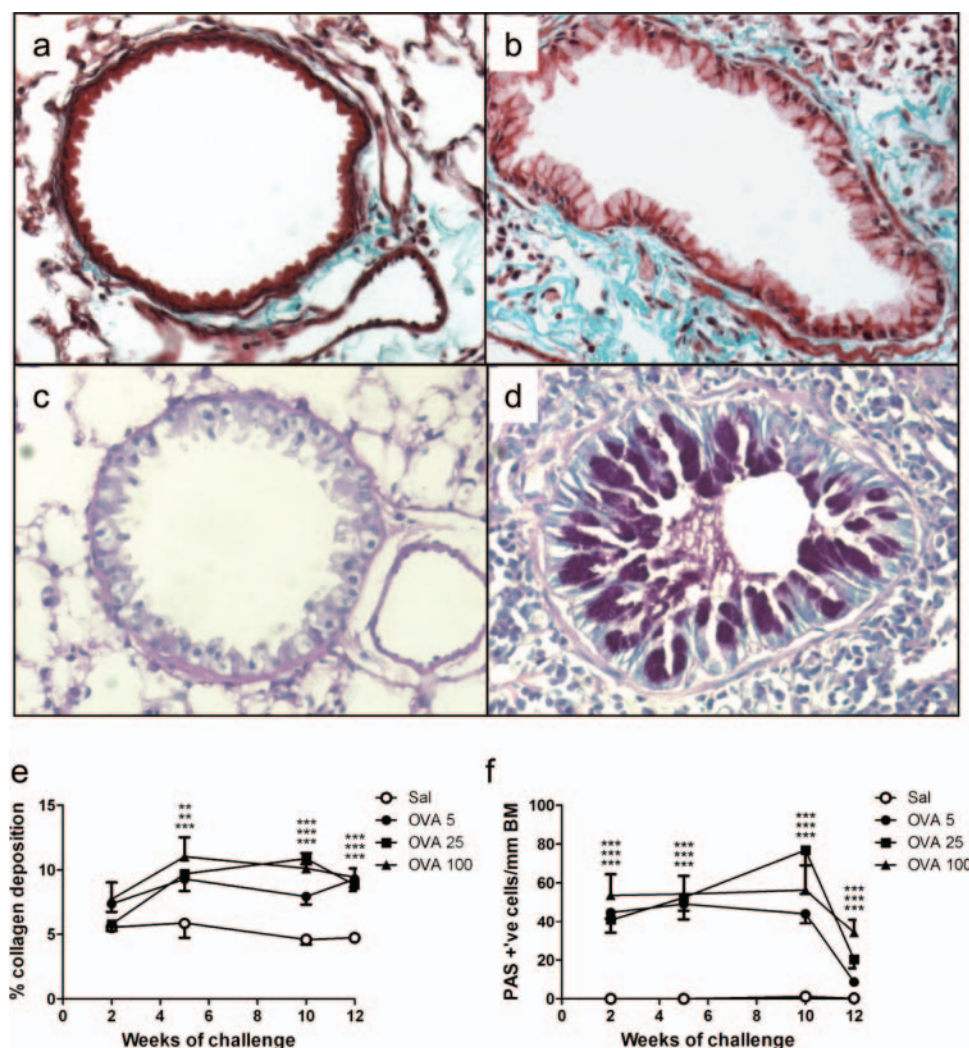


Figure 4 Chronic allergen challenge induces subepithelial collagen deposition and mucus hypersecretion. Mice were sensitised and challenged as described in online supplementary figure S1A, controls received saline instead of OVA. Representative lung tissue sections stained with Masson's Trichrome (A, B) or periodic acid Schiff (PAS) reagent (C, D) from saline control (A, C) and OVA sensitised and challenged mice (B, D). Collagen deposition in the subepithelial region (E) and frequency of PAS-positive airway epithelial cells per millimetre basement membrane (BM) (F) as determined by quantitative image analysis. (A–D) Original magnification $\times 400$. (E, F) Mean \pm SEM, $n=6-7$ mice/group per time point. ** $p<0.01$, *** $p<0.001$; order of symbols from top to bottom is OVA 5, 25 and 100 μg .

figure S3). We questioned whether the decreased frequency of Th2 cytokine-producing cells was mediated by regulatory T cells (Treg) or induction of a Th1-biased response. Lung $\text{CD4}^+\text{CD25}^+\text{Foxp3}^+$ Treg numbers and proportions were increased by chronic allergen challenge, as expected,²⁰ but were not further increased by follistatin treatment (see online supplementary figure S4). BAL fluid interferon γ levels were below the limit of detection in all treatment groups (data not shown). Follistatin instillation also dose-dependently decreased serum OVA-specific IgE levels (figure 5F). Thus follistatin exerts distinct dose-dependent effects in different pulmonary compartments, with a trend towards decreased frequency of Th2 cytokine-producing cells and serum OVA-specific IgE at the highest dose.

Follistatin during chronic allergen challenge inhibits BAL fluid activin A and TGF- $\beta 1$ concentrations, and airway remodelling

Follistatin instillation during chronic allergen challenge dose-dependently decreased BAL fluid activin A concentrations, with the 5 μg follistatin group decreased to approximately saline

levels (figure 6A). Similarly, high-dose follistatin significantly decreased BAL fluid TGF- $\beta 1$ concentrations (figure 6B). Notably, quantitative image analysis demonstrated that follistatin at all three doses significantly decreased collagen deposition in the subepithelial region (figure 6C). Furthermore, 5 μg follistatin significantly decreased the frequency of airway epithelial mucus-producing cells (figure 6D). Thus, follistatin inhibited airway activin A and TGF- $\beta 1$ levels, and mucus hypersecretion and subepithelial collagen deposition.

Follistatin inhibits the loss of airway epithelial TGF- β and ActRIB immunostaining during chronic allergen challenge

Immunohistochemistry showed strong TGF- β and ActRIB/ALK4 staining in normal (sal/sal) airway epithelium, which was significantly decreased in chronically challenged mice, and this decrease was significantly inhibited by follistatin (figures 7 and 8). There was strong immunostaining for ActRIB in the subepithelial smooth muscle of large airways in all groups. Subepithelial smooth muscle thickness was significantly increased more than twofold in OVA/OVA mice, and there was

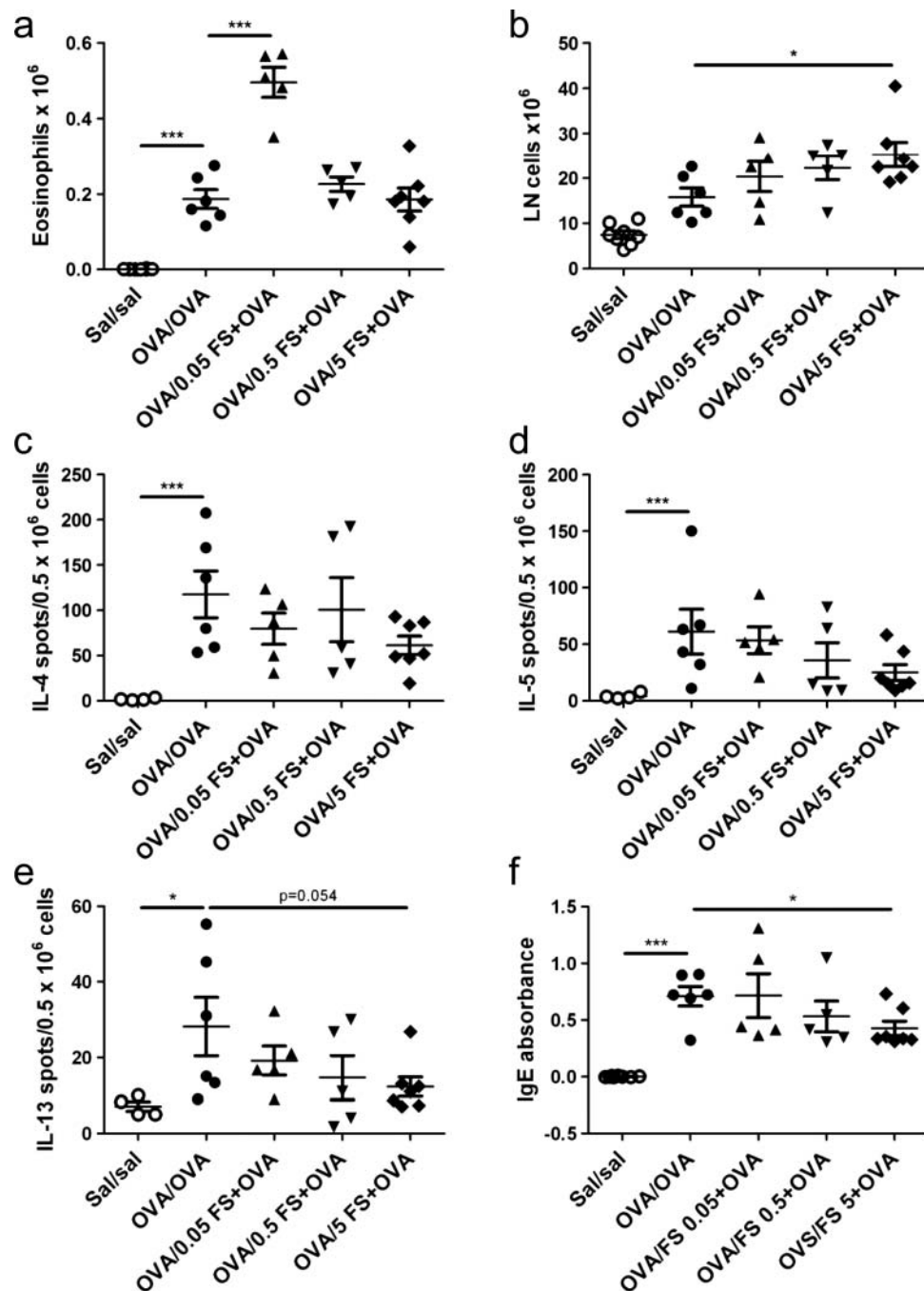


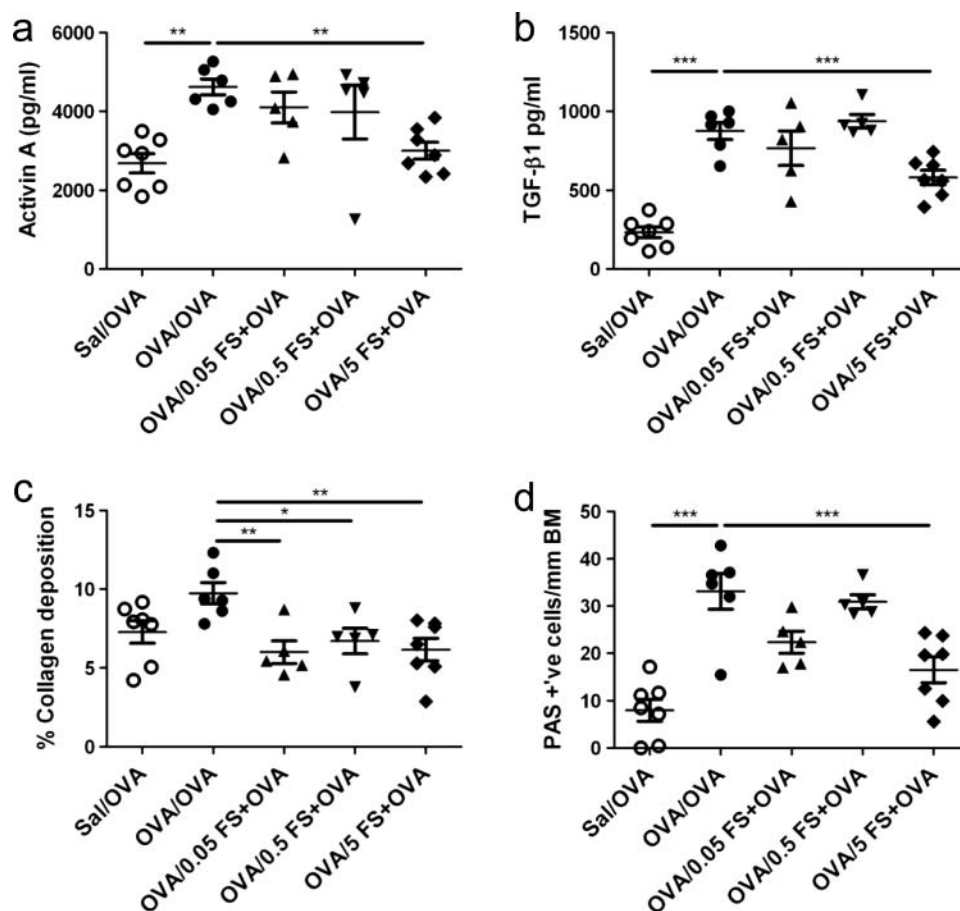
Figure 5 High-dose follistatin instillation during chronic allergen challenge inhibits allergen-specific T helper 2 cytokine production in the lung draining LN and serum allergen-specific IgE. Mice were sensitised as described in online supplementary figure S1B, and challenged with OVA, or OVA and follistatin; controls received saline instead of OVA or follistatin. Number of bronchoalveolar lavage eosinophils (A) and lung-draining LN cells (B). (C–E) Frequency of OVA-specific interleukin (IL)-4, IL-5 and IL-13 producing cells in the lung-draining LN. (F) Levels of serum OVA-specific IgE. Mean ± SEM, n=6–8 mice/group. *p<0.05, ***p<0.001. FS, follistatin; Sal, saline.

a strong trend for inhibition of this increase by 5 µg follistatin (p=0.09) (figure 8A,C). The strong immunoreactivity for activin A, ActRIIA and ActRIIB in normal airway epithelium mice was significantly decreased in chronically challenged mice, but this was not affected by follistatin treatment (see online supplementary figures S5 and S6). Apart from occasional activin A-positive macrophages in the lamina propria, there was weak and/or diffuse activin A, TGF-β and activin receptor staining of inflammatory cells in the OVA/OVA and OVA/5 FS +OVA groups.

DISCUSSION

In most patients stable asthma is well controlled on current medication but management of severe asthma remains inadequate. Despite the importance of inflammation in asthma pathogenesis, drugs targeting key inflammatory cells and inflammatory mediators show limited clinical benefit.¹ These disappointing results suggested a reappraisal of asthma pathogenesis.¹ Accumulating evidence indicates that activin A drives tissue fibrosis in a variety of organs,^{21–24} and is implicated in

Figure 6 Follistatin instillation during chronic allergen challenge inhibits bronchoalveolar lavage (BAL) fluid levels of activin A and TGF- β 1, subepithelial collagen deposition and mucus hypersecretion. Mice were sensitised as described in online supplementary figure S1B, and challenged with OVA, or OVA and follistatin; controls received saline instead of OVA or follistatin. BAL fluid concentrations of activin A (A) and TGF- β 1 (B). (C) Collagen deposition in the subepithelial region (D) and frequency of periodic acid Schiff (PAS)-positive airway epithelial cells per millimetre basement membrane as determined by quantitative image analysis. Mean \pm SEM, n=6–8 mice/group. *p<0.05, **p<0.01, ***p<0.001. FS, follistatin; Sal, saline.



airway remodelling.^{12 13} In the current study we established a murine model of chronic allergic asthma to investigate the ability of follistatin to inhibit development of airway remodelling. Our results show that high-dose follistatin decreased airway activin A and TGF- β 1 concentrations, and inhibited the decrease in TGF- β and ActRIB/ALK4 immunostaining observed in the airway epithelium of chronically challenged mice. Follistatin further inhibited mucus hypersecretion, subepithelial collagen deposition and thickening of the subepithelial smooth muscle, indicating a potential therapeutic role for follistatin in the prevention of airway remodelling.

Our data show that BAL fluid concentrations of activin A are elevated after 2 weeks of challenge, the earliest time point examined. Our previous studies show that increases in BAL fluid activin A concentrations occur within 24 h after allergen challenge,⁶ consistent with reports of increased activin A after one to three allergen challenges.^{10 13} The increased BAL fluid activin A and loss of activin A immunolocalisation in airway epithelium were rapidly reversed upon cessation of allergen challenge. These changes in airway and epithelial activin A expression mirrored the pattern seen for TGF- β 1, consistent with other reports,^{14 25} suggesting release of activin A from epithelium into the airspaces. Similar changes were observed for follistatin, supporting the idea that follistatin is rapidly released as an endogenous antagonist of activin A bioactivity.^{6 26} One factor driving altered activin A compartmentalisation is IL-13,⁹ a key instigator of airway remodelling.^{15 27 28} Our observation that BAL fluid concentrations of TGF- β 1 showed almost identical kinetics to activin A is not surprising since activin A and TGF- β 1 stimulate secretion of one another,^{5 29–31} and IL-13 stimulates production of activin A and TGF- β 1.^{9 27}

Follistatin instillation during chronic allergen challenge decreased BAL fluid activin A and TGF- β 1 concentrations. Since follistatin inhibited the loss of airway epithelial TGF- β during chronic challenge, the decreased BAL fluid TGF- β could simply reflect its decreased liberation from airway epithelium. The decreased BAL fluid activin A levels are likely due to formation of follistatin–activin A complexes. Subsequently, the decrease in available activin A would lead to decreased BAL fluid TGF- β 1.^{5 29–31} Given the key role for TGF- β 1 in airway remodelling,²⁷ a simplistic interpretation would be that follistatin attenuated airway remodelling via inhibition of TGF- β 1. However, follistatin binds to activin A with high affinity, but does not bind TGF- β 1 or TGF- β 2.^{32 33} Furthermore, activin A has been implicated in lung fibrosis via promotion of collagen and α -smooth muscle actin synthesis, and proliferation of human airway fibroblasts and smooth muscle,^{5 10 11} and follistatin decreases collagen secretion by pancreatic and hepatic stellate cells, and renal fibroblasts.^{29–31} Receptor-blocking experiments using dominant negative activin A and TGF- β type II receptors suggested that TGF- β action is partly mediated by secreted activin A.³⁰ Together, these studies suggest that follistatin inhibits airway remodelling by blocking activin A, thereby inhibiting TGF- β 1 production, positioning activin A as a central regulator of fibrosis.

We observed a general loss of activin receptor staining in airway epithelium following chronic allergen challenge. The thickened subepithelial smooth muscle showed strong ActRIB/ALK4 immunostaining but weak immunostaining for ActRIIA and ActRIIB. Subepithelial cells in the same location and with similar morphology stain with α -smooth muscle actin,¹⁶ emphasising that the ActRIB/ALK4-stained cells are smooth

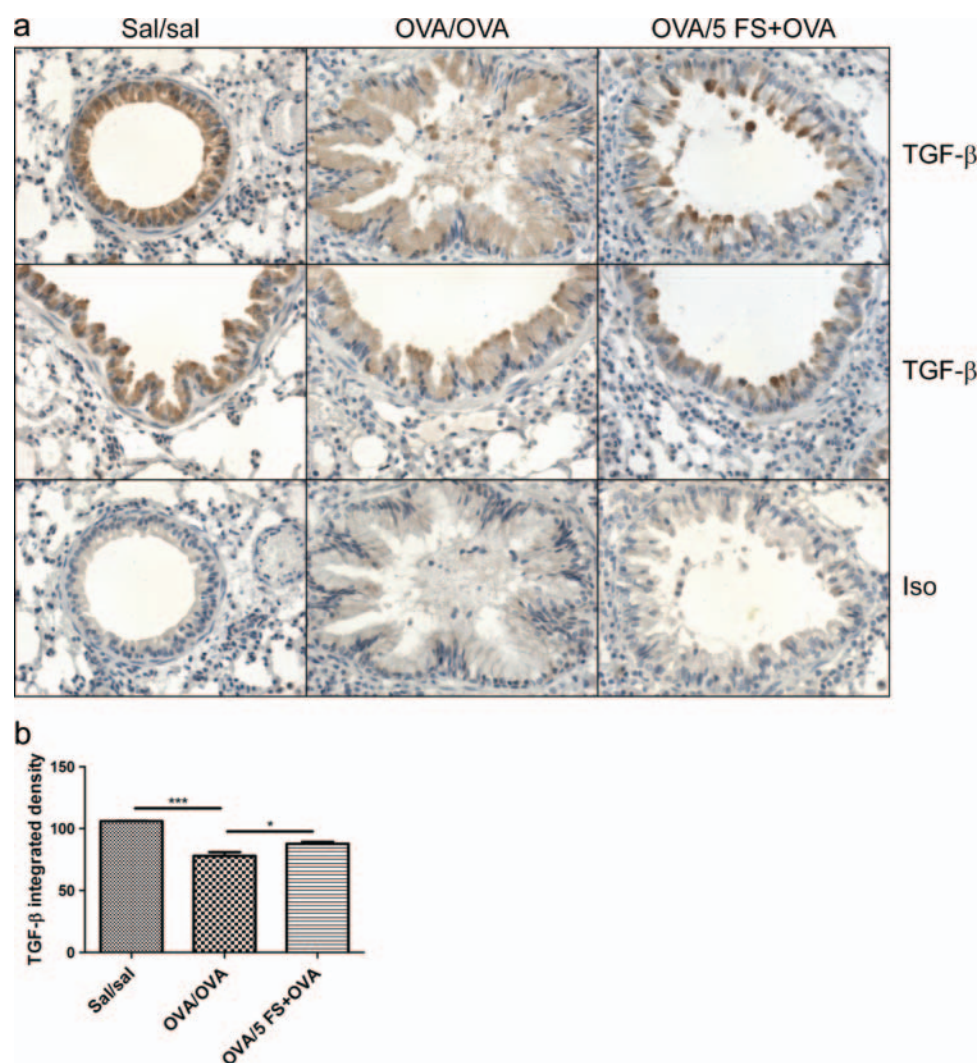


Figure 7 Follistatin treatment during chronic allergen challenge diminishes the loss of TGF- β immunoreactivity in airway epithelium. Mice were sensitised as described in online supplementary figure S1B, and challenged with OVA, or OVA and follistatin; controls received saline instead of OVA or follistatin. (A) Formalin-fixed lung sections were stained immunohistochemically with antibody to TGF- β 1. Representative micrographs, original magnification $\times 400$. (B) Airway epithelial TGF- β staining intensity in small-medium airways. Mean \pm SEM, $n=3$ mice/group. * $p<0.05$, *** $p<0.001$. FS, follistatin; Sal, saline.

muscle or myofibroblasts. Similarly, decreased activin type I and II receptor expression was observed in airway epithelium and/or subepithelial cells in patients with asthma.⁷ In contrast, increased ALK4 and ActRIIA expression was found in airway epithelium of OVA-sensitised mice following acute allergen challenge,³⁴ and increased ALK4 and ActRIIA expression was found in asthmatic airway epithelium 24 h after allergen challenge.⁸ Conceivably, differences in activin receptor expression between studies are due to different kinetics, with increased activin receptor expression occurring early after allergen challenge, decreasing at later times (ie, 5 weeks).

Chronic inflammation may be a driver of airway remodelling.¹ However, several studies report dissociation between inflammation and airway remodelling. Neutralisation of TGF- β 1 specifically, or all TGF- β isoforms, in OVA chronic allergen challenge models suppressed pulmonary fibrosis, without affecting airway inflammation, eosinophilia, or IL-5 or IL-13 production.^{25–35} Furthermore, overexpression of the activin/TGF- β 1 signalling intermediate Smad2 in airway epithelium exacerbated airway remodelling in a house dust mite allergen challenge model.¹³ Intraperitoneal injection of activin A

neutralising antibody markedly inhibited airway remodelling, but had no effect on lung inflammation, airway eosinophilia or Th2 cytokine production. Our data demonstrate that while follistatin dose-dependently modulated inflammation, the inhibition of subepithelial fibrosis was dose independent. However, BAL fluid activin A and TGF- β 1 levels were only inhibited by high-dose follistatin, suggesting that even subtle decreases in local tissue concentrations of activin A and TGF- β 1 can decrease fibrosis. Thus, while ELISA for activin A and TGF- β 1 in the BAL fluid provides insight into lung levels of these mediators, it does not exactly mirror changes in mediator concentrations in the local tissue microenvironment.

Recently, antibody-mediated neutralisation of activin A during allergen challenge was demonstrated to exacerbate acute allergic airway inflammation.⁷ However, in our model of chronic allergic inflammation, inhibiting activin A with intermediate or high-dose intranasal follistatin suppressed OVA-specific IgE and allergen-specific Th2 cytokine production, and had no effect on airway eosinophilia. The attenuated Th2 cytokine production in the draining LN was not due to follistatin-induced expansion of CD4⁺CD25⁺Foxp3⁺ Treg in

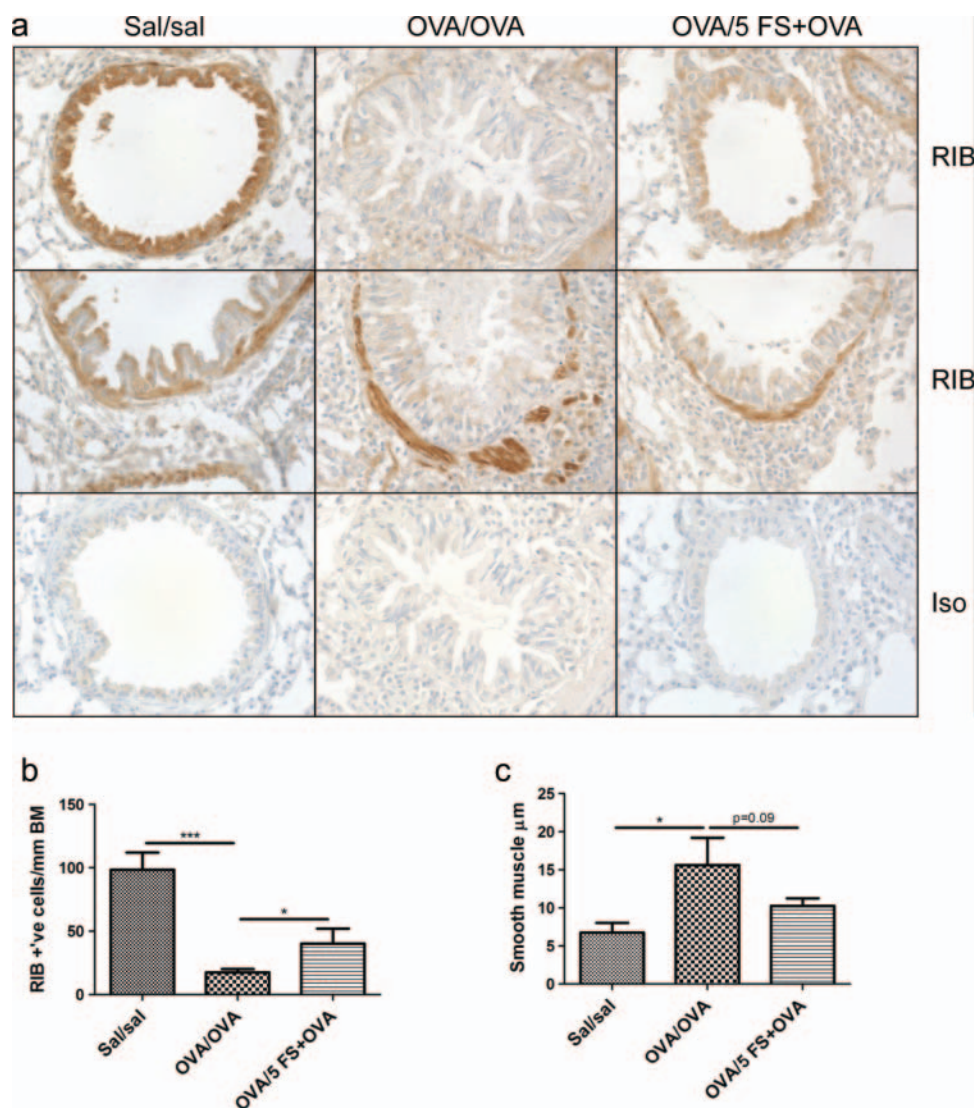


Figure 8 Follistatin treatment during chronic allergen challenge diminishes the loss of ActRIB/ALK4 immunoreactivity in airway epithelium. Mice were sensitised as described in online supplementary figure S1B, and challenged with OVA, or OVA and follistatin; controls received saline instead of OVA or follistatin. (A) Formalin-fixed lung sections were stained immunohistochemically with antibody to ActRIB. Representative micrographs, original magnification $\times 400$. Frequency of ActRIB-positive airway epithelial cells in small-medium airways (B) and subepithelial muscle thickness in large airways (C). Mean \pm SEM, $n=3$ mice/group. * $p<0.05$, *** $p<0.001$. FS, follistatin; Sal, saline.

the lung, nor was it due to a switch to a Th1-type immune response. Thus, follistatin must exert this dampening effect via the induction of an alternative suppressive mechanism, such as the selective deletion/apoptosis of Th2 cells. These data suggest that the outcome of blocking activin A depends on the method (antibody vs follistatin) and/or the site (systemic vs local) of inhibition. Our finding that the lowest follistatin dose ($0.05 \mu\text{g}$) enhanced airway eosinophilia points to concentration-dependent effects of activin A on immune function. Analogous concentration-dependent morphogen effects of activin A occur during development.¹⁹

In summary, our study shows that follistatin inhibited activin A and TGF- $\beta 1$ secretion into the airway lumen during chronic allergen challenge, and significantly decreased subepithelial fibrosis and airway epithelial mucus production. Follistatin treatment also caused a dose-dependent modulation of allergic airway inflammation, suggesting 'morphogen-like' effects of activin A on immune function. This is consistent with apparently contradictory observations of pro-inflammatory versus anti-inflammatory

effects of activin A in other systems.² Our study reinforces the idea that activin A is a key driver of inflammation and fibrosis, and indicates that follistatin represents an attractive potential therapeutic for the prevention of fibrosis in asthma.

Acknowledgements The authors thank Professor Gary Anderson (University of Melbourne) for advice on establishing the mouse chronic asthma model and Ms Genevieve Tan (Department of Immunology, Monash University) for assistance with image analysis. We are grateful to Professor Jennifer Wilkinson-Berka and Pam Tong Zhu (Department of Immunology, Monash University) for advice with the TGF- β immunohistochemistry, and Elizabeth Richards (Department of Biochemistry and Molecular Biology, Monash University) for assistance with the activin A and activin receptor immunohistochemistry.

Contributors CLH wrote the paper, designed, performed and analysed experiments. HN designed, performed and analysed experiments, and produced rhFS288. RM performed and analysed experiments. JY performed experiments. DO analysed experiments. MP provided intellectual guidance. KL provided advice and helped with techniques. CH helped produce rhFS288. JM wrote the paper and provided intellectual guidance. ROH wrote the paper and provided intellectual guidance.

Funding Supported by grants from the National Health and Medical Research Council and the Co-operative Research Centre for Asthma and Airways, Australia.

Competing interests None.

Ethics approval This study was conducted with the approval of the Alfred Medical Research and Education Precinct Animal Ethics Committee.

Provenance and peer review Not commissioned; externally peer reviewed.

REFERENCES

- Holgate ST.** Asthma: a simple concept but in reality a complex disease. *Eur J Clin Invest* 2011;**41**:1339–52.
- Hedger MP, Winnall WR, Phillips DJ, et al.** The regulation and functions of activin and follistatin in inflammation and immunity. *Vitam Horm* 2011;**85**:255–97.
- de Kretser DM, O'Hehir RE, Hardy CL, et al.** The roles of activin A and its binding protein, follistatin, in inflammation and tissue repair. *Mol Cell Endocrinol* 2012;**359**:101–6.
- Phillips DJ.** Regulation of activin's access to the cell: why is mother nature such a control freak? *Bioessays* 2000;**22**:689–96.
- Karagiannis C, Hense G, Martin C, et al.** Activin A is an acute allergen-responsive cytokine and provides a link to TGF-beta-mediated airway remodeling in asthma. *J Allergy Clin Immunol* 2006;**117**:111–18.
- Hardy CL, O'Connor AE, Yao J, et al.** Follistatin is a candidate endogenous negative regulator of activin A in experimental allergic asthma. *Clin Exp Allergy* 2006;**36**:941–50.
- Semitekolou M, Alissafi T, Aggelakopoulou M, et al.** Activin-A induces regulatory T cells that suppress T helper cell immune responses and protect from allergic airway disease. *J Exp Med* 2009;**206**:1769–85.
- Kariyawasam HH, Pegorier S, Barkans J, et al.** Activin and transforming growth factor-beta signaling pathways are activated after allergen challenge in mild asthma. *J Allergy Clin Immunol* 2009;**124**:454–62.
- Hardy CL, Lemasurier JS, Olsson F, et al.** Interleukin-13 regulates secretion of the tumor growth factor- β superfamily cytokine activin A in allergic airway inflammation. *Am J Respir Cell Mol Biol* 2010;**42**:667–75.
- Cho SH, Yao Z, Wang SW, et al.** Regulation of activin A expression in mast cells and asthma: its effect on the proliferation of human airway smooth muscle cells. *J Immunol* 2003;**170**:4045–52.
- Aoki F, Kurabayashi M, Hasegawa Y, et al.** Attenuation of bleomycin-induced pulmonary fibrosis by follistatin. *Am J Respir Crit Care Med* 2005;**172**:713–20.
- Le AV, Cho JY, Miller M, et al.** Inhibition of allergen-induced airway remodeling in Smad 3-deficient mice. *J Immunol* 2007;**178**:7310–16.
- Gregory LG, Mathie SA, Walker SA, et al.** Overexpression of Smad2 drives house dust mite-mediated airway remodeling and airway hyperresponsiveness via activin and IL-25. *Am J Respir Crit Care Med* 2010;**182**:143–54.
- McMillan SJ, Lloyd CM.** Prolonged allergen challenge in mice leads to persistent airway remodelling. *Clin Exp Allergy* 2004;**34**:497–507.
- Kumar RK, Herbert C, Yang M, et al.** Role of interleukin-13 in eosinophil accumulation and airway remodelling in a mouse model of chronic asthma. *Clin Exp Allergy* 2002;**32**:1104–11.
- Leigh R, Ellis R, Wattie J, et al.** Dysfunction and remodeling of the mouse airway persist after resolution of acute allergen-induced airway inflammation. *Am J Respir Cell Mol Biol* 2002;**27**:526–35.
- Hardy CL, Kenins L, Drew AC, et al.** Characterization of a mouse model of allergy to a major occupational latex glove allergen Hev b 5. *Am J Respir Crit Care Med* 2003;**167**:1393–9.
- O'Connor AE, McFarlane JR, Hayward S, et al.** Serum activin A and follistatin concentrations during human pregnancy: a cross-sectional and longitudinal study. *Hum Reprod* 1999;**14**:827–32.
- Gurdon JB, Dyson S, St Johnston D.** Cells' perception of position in a concentration gradient. *Cell* 1998;**95**:159–62.
- Strickland DH, Stumbles PA, Zosky GR, et al.** Reversal of airway hyperresponsiveness by induction of airway mucosal CD4+CD25+ regulatory T cells. *J Exp Med* 2006;**203**:2649–60.
- Gaedeke J, Boehler T, Budde K, et al.** Glomerular activin A overexpression is linked to fibrosis in anti-Thy1 glomerulonephritis. *Nephrol Dial Transplant* 2005;**20**:319–28.
- Patella S, Phillips DJ, Tchongue J, et al.** Follistatin attenuates early liver fibrosis: effects on hepatic stellate cell activation and hepatocyte apoptosis. *Am J Physiol Gastrointest Liver Physiol* 2006;**290**:G137–44.
- Yndestad A, Ueland T, Oie E, et al.** Elevated levels of activin A in heart failure: potential role in myocardial remodeling. *Circulation* 2004;**109**:1379–85.
- Munz B, Smola H, Engelhardt F, et al.** Overexpression of activin A in the skin of transgenic mice reveals new activities of activin in epidermal morphogenesis, dermal fibrosis and wound repair. *EMBO J* 1999;**18**:5205–15.
- Alcorn JF, Rinaldi LM, Jaffe EF, et al.** Transforming growth factor-beta1 suppresses airway hyperresponsiveness in allergic airway disease. *Am J Respir Crit Care Med* 2007;**176**:974–82.
- Jones KL, De Kretser DM, Clarke IJ, et al.** Characterisation of the rapid release of activin A following acute lipopolysaccharide challenge in the ewe. *J Endocrinol* 2004;**182**:69–80.
- Lee CG, Homer RJ, Zhu Z, et al.** Interleukin-13 induces tissue fibrosis by selectively stimulating and activating transforming growth factor beta(1). *J Exp Med* 2001;**194**:809–21.
- Zhu Z, Homer RJ, Wang Z, et al.** Pulmonary expression of interleukin-13 causes inflammation, mucus hypersecretion, subepithelial fibrosis, physiologic abnormalities, and eotaxin production. *J Clin Invest* 1999;**103**:779–88.
- Ohnishi N, Miyata T, Ohnishi H, et al.** Activin A is an autocrine activator of rat pancreatic stellate cells: potential therapeutic role of follistatin for pancreatic fibrosis. *Gut* 2003;**52**:1487–93.
- Wada W, Kuwano H, Hasegawa Y, et al.** The dependence of transforming growth factor-beta-induced collagen production on autocrine factor activin A in hepatic stellate cells. *Endocrinology* 2004;**145**:2753–9.
- Yamashita S, Maeshima A, Kojima I, et al.** Activin A is a potent activator of renal interstitial fibroblasts. *J Am Soc Nephrol* 2004;**15**:91–101.
- Iemura S, Yamamoto TS, Takagi C, et al.** Direct binding of follistatin to a complex of bone-morphogenetic protein and its receptor inhibits ventral and epidermal cell fates in early *Xenopus* embryo. *Proc Natl Acad Sci U S A* 1998;**95**:9337–42.
- Harrington AE, Morris-Triggs SA, Ruotolo BT, et al.** Structural basis for the inhibition of activin signalling by follistatin. *EMBO J* 2006;**25**:1035–45.
- Rosendahl A, Checchin D, Fehniger TE, et al.** Activation of the TGF-beta/activin-Smad2 pathway during allergic airway inflammation. *Am J Respir Cell Mol Biol* 2001;**25**:60–8.
- McMillan SJ, Xanthou G, Lloyd CM.** Manipulation of allergen-induced airway remodeling by treatment with anti-TGF-beta antibody: effect on the Smad signaling pathway. *J Immunol* 2005;**174**:5774–80.



The activin A antagonist follistatin inhibits asthmatic airway remodelling

Charles Linton Hardy, Hong-An Nguyen, Rohimah Mohamud, et al.

Thorax published online October 10, 2012
doi: 10.1136/thoraxjnl-2011-201128

Updated information and services can be found at:
<http://thorax.bmj.com/content/early/2012/10/09/thoraxjnl-2011-201128.full.html>

These include:

Data Supplement

"Web Only Data"
<http://thorax.bmj.com/content/suppl/2012/10/09/thoraxjnl-2011-201128.DC1.html>

References

This article cites 35 articles, 22 of which can be accessed free at:
<http://thorax.bmj.com/content/early/2012/10/09/thoraxjnl-2011-201128.full.html#ref-list-1>

P<P

Published online October 10, 2012 in advance of the print journal.

Email alerting service

Receive free email alerts when new articles cite this article. Sign up in the box at the top right corner of the online article.

Topic Collections

Articles on similar topics can be found in the following collections

[Asthma](#) (1297 articles)
[Inflammation](#) (701 articles)

Advance online articles have been peer reviewed, accepted for publication, edited and typeset, but have not yet appeared in the paper journal. Advance online articles are citable and establish publication priority; they are indexed by PubMed from initial publication. Citations to Advance online articles must include the digital object identifier (DOIs) and date of initial publication.

To request permissions go to:
<http://group.bmj.com/group/rights-licensing/permissions>

To order reprints go to:
<http://journals.bmj.com/cgi/reprintform>

To subscribe to BMJ go to:
<http://group.bmj.com/subscribe/>

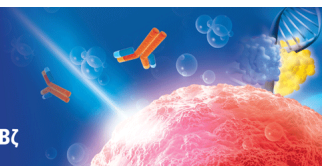
Notes

Advance online articles have been peer reviewed, accepted for publication, edited and typeset, but have not yet appeared in the paper journal. Advance online articles are citable and establish publication priority; they are indexed by PubMed from initial publication. Citations to Advance online articles must include the digital object identifier (DOIs) and date of initial publication.

To request permissions go to:
<http://group.bmj.com/group/rights-licensing/permissions>

To order reprints go to:
<http://journals.bmj.com/cgi/reprintform>

To subscribe to BMJ go to:
<http://group.bmj.com/subscribe/>

**Differential Uptake of Nanoparticles and
Microparticles by Pulmonary APC Subsets
Induces Discrete Immunological Imprints**

This information is current as
of October 15, 2013.

Charles L. Hardy, Jeanne S. LeMasurier, Rohimah
Mohamud, Jun Yao, Sue D. Xiang, Jennifer M. Rolland,
Robyn E. O'Hehir and Magdalena Plebanski

J Immunol published online 11 October 2013
<http://www.jimmunol.org/content/early/2013/10/10/jimmunol.1203131>

-
- Supplementary Material** <http://www.jimmunol.org/content/suppl/2013/10/11/jimmunol.1203131.DC1.html>
- Subscriptions** Information about subscribing to *The Journal of Immunology* is online at:
<http://jimmunol.org/subscriptions>
- Permissions** Submit copyright permission requests at:
<http://www.aai.org/ji/copyright.html>
- Email Alerts** Receive free email-alerts when new articles cite this article. Sign up at:
<http://jimmunol.org/cgi/alerts/etoc>

Differential Uptake of Nanoparticles and Microparticles by Pulmonary APC Subsets Induces Discrete Immunological Imprints

Charles L. Hardy,^{*,†,‡} Jeanne S. LeMasurier,^{*,†,‡} Rohimah Mohamud,^{*,‡}
Jun Yao,^{*,†,‡} Sue D. Xiang,^{*,‡} Jennifer M. Rolland,^{*,†,‡} Robyn E. O'Hehir,^{*,†,‡} and
Magdalena Plebanski^{*,‡}

There is increasing interest in the use of engineered particles for biomedical applications, although questions exist about their proinflammatory properties and potential adverse health effects. Lung macrophages and dendritic cells (DC) are key regulators of pulmonary immunity, but little is known about their uptake of different sized particles or the nature of the induced immunological imprint. We investigated comparatively the immunological imprints of inert nontoxic polystyrene nanoparticles 50 nm in diameter (PS50G) and 500 nm in diameter (PS500G). Following intratracheal instillation into naive mice, PS50G were preferentially taken up by alveolar and nonalveolar macrophages, B cells, and CD11b⁺ and CD103⁺ DC in the lung, but exclusively by DC in the draining lymph node (LN). Negligible particle uptake occurred in the draining LN 2 h postinstillation, indicating that particle translocation does not occur via lymphatic drainage. PS50G but not PS500G significantly increased airway levels of mediators that drive DC migration/maturation and DC costimulatory molecule expression. Both particles decreased frequencies of stimulatory CD11b⁺ MHC class II^{hi} allergen-laden DC in the draining LN, with PS50G having the more pronounced effect. These distinctive particle imprints differentially modulated induction of acute allergic airway inflammation, with PS50G but not PS500G significantly inhibiting adaptive allergen-specific immunity. Our data show that nanoparticles are taken up preferentially by lung APC stimulate cytokine/chemokine production and pulmonary DC maturation and translocate to the lung-draining LN via cell-associated transport. Collectively, these distinctive particle imprints differentially modulate development of subsequent lung immune responses. These findings support the development of lung-specific particulate vaccines, drug delivery systems, and immunomodulators. *The Journal of Immunology*, 2013, 191: 000–000.

Inhalation of air pollution particulates is epidemiologically linked to reduced lung function, bronchitis, and asthma exacerbations (1). Evidence suggests that ambient ultrafine particles (<100 nm) play a disproportionate role in asthma exacerbations compared with fine-sized microparticles (100–2500 nm) (2–5), suggesting that inhaled particle size influences their relative ability to modulate lung function. Similarly, man-made carbon black and titanium dioxide nanoparticles (6–8) and carbon nanotubes (9, 10) all promote allergic sensitization and/or allergic

airway inflammation (AAI). However, counterintuitively, we recently made the discovery that preadministration of inert nontoxic polystyrene nanoparticles 50 nm in diameter (PS50G), which do not induce oxidative stress, can inhibit development of AAI by impairing pulmonary dendritic cell (DC) expansion or stimulatory function (11). It is currently unknown if the novel beneficial immunological imprint of particle exposure in the lung that we identified using PS50G is affected by particle size.

DC and macrophages play critical roles in the induction and regulation of pulmonary immunity and AAI (12–16). However, surprisingly little is known about how different-sized particles are handled by pulmonary APC. Previous studies by our group have shown that 40–50 nm nanoparticles, when conjugated to protein Ag, are taken up by lymph node (LN) DC and potently stimulate immune responses, whereas particles >200 nm fail to do so (17). An early study suggested that 400-nm latex particles were taken up predominantly by F4/80⁺ (CD11c⁺ or CD11c^{low}) cells, consistent with a macrophage phenotype, in the lung up to 48 h after instillation (18). Further, diesel and ambient particulates were shown to promote Th2 cytokine production in the draining LN and activate lung CD11c⁺ cells (19), although these CD11c⁺ cells were not segregated into macrophage and DC subsets. Similarly, carbon black nanoparticles coadministered with allergen promote AAI by increasing costimulatory capacity of DC (20). The above would suggest nanoparticles (<100 nm) and fine-sized particles (>100 nm) could be handled differently in the lung and may have different imprinting consequences. Particle-adsorbed toxic chemicals and metallic impurities and the induction of oxidative stress are thought to play significant roles in the adjuvant and/or inflammatory

*Department of Immunology, Monash University, Melbourne, Victoria 3004, Australia; [†]Department of Allergy, Immunology and Respiratory Medicine, The Alfred Hospital, Monash University, Melbourne, Victoria 3004, Australia; and [‡]The Cooperative Research Centre for Asthma and Airways, Sydney, New South Wales 2050, Australia

Received for publication November 13, 2012. Accepted for publication August 28, 2013.

This work was supported by grants from the National Health and Medical Research Council of Australia (to C.L.H., J.M.R., R.E.O., and M.P.), the Australian Research Council (to R.E.O.), and the Cooperative Research Center for Asthma and Airways, Sydney, Australia (to C.L.H., J.M.R., R.E.O., and M.P.).

Address correspondence and reprint requests to Dr. Charles L. Hardy and Prof. Magdalena Plebanski, Department of Immunology, Monash University, 89 Commercial Road, Level 2, Melbourne, VIC 3004, Australia. E-mail addresses: [redacted] (C.L.H.) and [redacted] (M.P.)

The online version of this article contains supplemental material.

Abbreviations used in this article: AAI, allergic airway inflammation; BAL, bronchoalveolar lavage; DC, dendritic cell; FSC, forward light scatter; i.t., intratracheally; LN, lymph node; MHC II, MHC class II; pDC, plasmacytoid DC; PS50G, nontoxic polystyrene nanoparticle 50 nm in diameter; PS500G, nontoxic polystyrene nanoparticle 500 nm in diameter.

Copyright © 2013 by The American Association of Immunologists, Inc. 0022-1767/13/\$16.00

effect of ambient and diesel particulates (5, 21). However, no studies have compared the long-term effects of different-sized inert particles, which are devoid of potential toxic contaminants and do not induce oxidative stress, on pulmonary APC distribution and function and development of subsequent lung immune responses.

We investigated comparatively the uptake by different APC subsets of ultrafine PS50G nanoparticles and fine 500-nm microparticles (PS500G) in the lung and lung-draining LN, as well as the activation status of these APC at both early and late time points after exposure. We also compared the potential downstream effects of PS50G and PS500G particles in preventing the subsequent development of AAI. Use of fluorescent-labeled particles allowed us to determine the rates of particle clearance, track particle migration, and identify the subsets of particle-laden APC over time for PS50G and PS500G. Our results provide new insights into particle effects on pulmonary APC distribution and function and indicate that when engineering particles for topical lung administration, the substantial differences in biological function due to size-dependent effects of particles on APC should be taken into account.

Materials and Methods

Mice

Female BALB/c mice aged 7 to 8 wk were obtained from Laboratory Animal Services (Adelaide, South Australia) and housed in the Alfred Medical Research and Education Precinct animal facility. All experimental protocols were approved by the precinct Animal Ethics Committee.

Particle instillation and immunization

FITC-labeled carboxylate-modified microspheres (nominally 0.04 and 0.5 μm ; Invitrogen-Molecular Probes, Carlsbad, CA; #F8795 and #F8813, respectively) were glycine-coated as described previously (17). PS50G and PS500G had a narrow size distribution (58.54 ± 0.3 and 488.33 ± 7.87 nm, respectively) and carried a negative surface charge (-14.8 ± 1.65 and -38.87 ± 4.71 mV, respectively) (Supplemental Fig. 1). Mice received saline (control), PS50G, or PS500G particles (200 $\mu\text{g}/50 \mu\text{l}$) intratracheally (i.t.) (22) on day 0, and analysis was performed 2 h or on days 1, 3, 7, and 30/31 postinstillation. In experiments to test particle effects on AAI, mice received PS50G or PS500G (200 $\mu\text{g}/50 \mu\text{l}$) i.t. on days 0 and 2 prior to i.p. sensitization with OVA (50 μg ; Sigma-Aldrich, St. Louis, MO) in aluminum hydroxide on days 12 and 22 and i.n. OVA challenge (25 μg) on days 32, 34, 37, and 39 as described (Fig. 10A) (11). In experiments to test particle effects on allergen uptake, mice received particles i.t. prior to OVA-Alexa Fluor 488 (100 $\mu\text{g}/50 \mu\text{l}$) (Molecular Probes, Grand Island, NY; #O34781) on day 3, with analysis performed on days 4 or 31.

Tissue sampling and cell isolation

Methods were as described previously (22). Blood was collected from the inferior vena cava and serum collected. Bronchoalveolar lavage (BAL) was performed with 0.4 ml 1% FCS in PBS and three further lavages of 0.3 ml. For differentials, BAL cytoplots were Giemsa stained (Merck, Kilsyth, VIC, Australia) and ≥ 200 cells identified by morphological criteria. Tissue digestion was performed as described previously (11). The right ventricle was perfused with 5 ml $\text{Ca}^{2+}/\text{Mg}^{2+}$ -free HBSS (Invitrogen; #14175095) with 0.01 M EDTA (pH 7.2). Lung-draining LN were minced with a scalpel blade, whereas lung tissue was chopped with a tissue chopper (Mickle Laboratory Engineering Co. Ltd, Gomshall, Surrey, U.K.). Tissue fragments were digested in collagenase type III (1 mg/ml; Worthington, Lakewood, NJ) and DNase type I (0.025 mg/ml; Roche Diagnostics, Sydney, NSW, Australia; #1284932) at 25°C mixing continuously for 45 min (LN) or 1 h (lung). The reaction was stopped by adding one-tenth volume EDTA and 3% FCS and mixing for 5 min. The cell suspension was filtered through a 70- μm cell strainer (BD Falcon), red cells lysed, and washed in staining buffer (3% FCS, 5 mM EDTA [pH 7.2] and 0.1% Na-azide in $\text{Ca}^{2+}/\text{Mg}^{2+}$ -free HBSS). Viable cells were counted in a hemocytometer.

Flow cytometry

Nonspecific FcR binding was blocked by incubating cells in CD16/CD32 block (BD Biosciences, San Jose, CA) in staining buffer (see above) containing 3% normal mouse serum for 15 min. Cells (1×10^6) were stained on ice for 20 min with combinations of the following Abs/conjugates (all from BD Biosciences unless noted): CD11b-PE (M1/70),

CD11b-PerCP-Cy 5.5 (M1/70), CD11c-allophycocyanin (HL-3), CD45R (B220)-eFluor 450 (eBioscience; clone RA3-6B2), MHC class II (MHC II)-PE (AMS-32.1), MHC II-allophycocyanin-eFluor 780 (eBioscience; clone M5/114.15.2), F4/80-PE-Cy7 (eBioscience; clone BM8), biotinylated CD40 (3/23), CD80 (16-10A1), CD86 (PO3), CD86-Brilliant Violet 605 (BioLegend; clone GL-1), and Siglec-F-PE-CF594 (E50-2440). Appropriate isotype control Abs and/or fluorescence-minus-one controls were used. All dilutions were in staining buffer (see above). Cells were protected from light at all times. Acquisition was on an FACSCalibur, LSRII, or LSRFortessa (all BD Biosciences) and analysis performed on FlowJo (Tree Star, Ashland, OR).

Measurement of BAL fluid cytokines and chemokines

IL-5 and IL-13 were detected using IL-5 and IL-13 ELISA kits (#88-7054 and #88-7137; eBioscience). Fifty-microliter standards and samples were tested. Details were otherwise as specified in the manufacturer's instructions. IL-1 α , IL-1 β , IL-6, IL-12p40, IL-12p70, eotaxin/CCL11, G-CSF, GM-CSF, keratinocyte chemoattractant/CXCL1, MCP-1/CCL2, MIP-1 α /CCL3, MIP-1 β /CCL4, RANTES/CCL5, and TNF were detected by Bio-Plex (Bio-Rad, Hercules, CA). TGF- β 1 was detected using the TGF- β 1 ELISA DuoSet following acid activation of latent TGF- β according to the manufacturer's instructions (#DY1679; R&D Systems).

Statistical analysis

Statistics were analyzed using GraphPad Prism v5.02 software (GraphPad). Data were analyzed for normality and log-transformed as necessary prior to analysis by independent samples *t* test, ANOVA, or two-way ANOVA with Tukey or Bonferroni posttests, as appropriate. Differences were considered statistically significant at $p < 0.05$. Group sizes are indicated in the figure legends. All values are mean \pm SEM.

Results

PS50G nanoparticles cause mild transient airway inflammation and sustained increases in lung and draining LN cell numbers

To understand the broad effects of PS50G and PS500G within the pulmonary compartment, we analyzed their effects on leukocyte numbers in the airways, lung parenchyma, and lung-draining LN. Mice were exposed to an equal mass (200 μg) of PS50G or PS500G, consistent with other studies in the particulate literature (7, 23, 24). Relative to saline controls, PS50G nanoparticles induced a 5-fold expansion of BAL cells at day 3, declining rapidly to near baseline values by day 31 (Fig. 1A). PS500G microparticles induced a smaller expansion in BAL cell numbers at day 1, returning to baseline by day 31. To put these particle-induced increases in context, BAL counts in acute AAI (11, 25) are typically 6–10-fold greater ($3\text{--}5 \times 10^6$ cells) than the maximum values seen in PS50G-treated mice. PS50G nanoparticles caused an ~ 2 -fold increase in lung leukocyte counts relative to controls at all time points (Fig. 1B). PS500G microparticles caused a small expansion in lung leukocytes at day 1, although cell counts returned to control values by day 7. Nanoparticles increased draining LN cell counts 4-fold at day 7 relative to saline controls, and this was maintained at day 31, whereas PS500G did not cause any significant change (Fig. 1C). The peak PS50G-induced increases in lung and LN cell counts were ~ 2 -fold lower than those seen during acute AAI (11, 25).

Differential analysis of BAL cells showed that, relative to saline mice, PS50G treatment caused an expansion of macrophages at day 3 (routine differential analysis of BAL cells does not discriminate between macrophages and DC, and these are hereafter referred to as macrophage/DC) (Fig. 1D). There was a small expansion of eosinophils and neutrophils at day 3. These changes had markedly subsided by day 7, although macrophage/DC numbers were still elevated 2-fold in PS50G-treated mice (Fig. 1E). By day 31, macrophage/DC numbers were still slightly elevated in PS50G nanoparticle-treated mice, whereas BAL cell composition in PS500G-treated mice resembled controls (Fig. 1F).

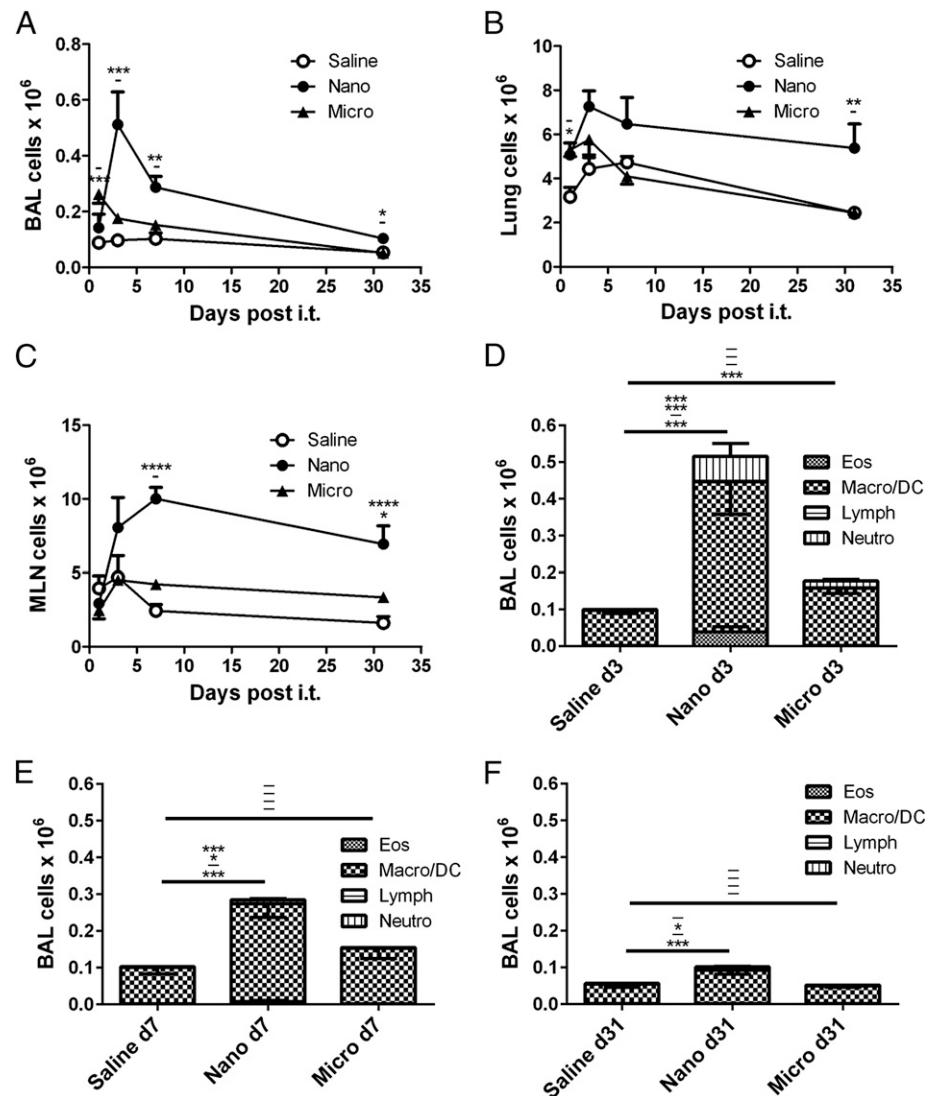


FIGURE 1. PS50G cause mild transient airway inflammation and increase lung and draining LN leukocyte counts. Naive mice received PS50G or PS500G (nano or micro, respectively) i.t. on day 0 or saline as control; groups of mice were killed for analysis at the indicated times. Total leukocyte numbers in BAL (A), lung (B), and draining LN (C). Differential analysis of Giemsa-stained BAL cells at days 3, 7, and 31 after particle instillation (D–F, respectively). Representative of three separate experiments. Mean \pm SEM, $n = 6$ –9 mice/group/time point. The order of symbols from top to bottom is nano then micro (versus saline) (A–C) and eos, macro, lymph, and neutro, respectively (D–F). * $p < 0.05$, ** $p < 0.01$, *** $p < 0.001$, **** $p < 0.0001$. MLN, Mesenteric LN.

PS50G nanoparticles increase pulmonary DC and macrophage numbers

We predicted that these broad changes in pulmonary leukocyte numbers would translate into marked alterations in pulmonary APC distribution. We performed a detailed analysis of lung APC populations at days 3 and 30 postparticle instillation, as our time-course analysis (Fig. 1A–C) showed that these represented peak and resolution phases of particle-induced inflammation, respectively. We analyzed proportions of lung CD11c⁺ alveolar macrophages (CD11c⁺CD11b⁺F4/80⁺), CD11c⁺ nonalveolar (interstitial) macrophages (CD11c⁺CD11b⁺F4/80⁺, excluding MHC II⁺CD45R⁺ B cells using Boolean gating), B cells (CD11c⁺CD11b⁺MHC II⁺CD45R⁺[B220]⁺forward light scatter [FSC]^{low}), and CD11c⁺MHC II⁺CD11b⁺CD103⁺ and CD11b⁺CD103⁺ DC (excluding F4/80⁺Siglec-F⁺ cells using Boolean gating) (Fig. 2). To validate our macrophage gating strategy, we confirmed that the majority (98 \pm 0.15%) of alveolar macrophages identified as CD11c⁺CD11b⁺F4/80⁺ expressed Siglec-F⁺, a marker of alveolar macrophages (26), and we therefore used this phenotype to identify alveolar macrophages across different time points. We also confirmed that <0.5% of nonalveolar/interstitial macrophages identified as CD11c⁺CD11b⁺F4/80⁺ (excluding MHC II⁺CD45R⁺ B cells using Boolean gating) expressed Siglec-F (data not shown).

Both PS50G and PS500G caused an ~3-fold decrease in proportions of lung CD11c⁺ alveolar macrophages at day 3, with this

decrease maintained at day 30 in the PS500G group (Supplemental Fig. 2A). In contrast, PS500G caused a small increase in frequency of CD11c⁺ nonalveolar macrophages at day 3, although proportions of this population had returned to baseline by day 30 (Supplemental Fig. 2A). PS50G and PS500G caused a small but significant decrease in proportions of B cells at day 3. Neither particle size caused a significant change in proportions of plasmacytoid DC (pDC) (CD11c^{int}MHC II^{low/int}CD11b⁺CD45R⁺, the majority confirmed to be pDC Ag-1⁺ in preliminary experiments; region 3, Supplemental Fig. 2B) (0.4–0.7% of lung leukocytes across all groups; data not shown). PS50G decreased proportions of CD11b⁺CD103⁺ lung DC over 2-fold at day 3, with PS500G having a slightly smaller effect, and this pattern was largely maintained at day 30 (Supplemental Fig. 2A). In contrast, PS50G caused an ~2-fold increase in proportions of CD11b⁺CD103⁺ lung DC at both early and late time points, whereas PS500G caused a smaller increase at day 3 only. Additional analysis showed that PS50G nanoparticles caused an ~7-fold increase in proportions of CD11c⁺MHC II⁺ lung DC at day 3 (region 1; Supplemental Fig. 2B) and increased proportions of CD11b^{hi}CD11c⁺MHC II⁺ DC by 10%, whereas PS500G similarly increased the frequency of CD11b^{hi} DC at days 3 and 7 (Supplemental Fig. 2B).

In the lung-draining LN, PS50G induced a 5-fold expansion of migratory (Ag-transporting) CD11c⁺MHC II^{hi} DC (27, 28) (region 1;

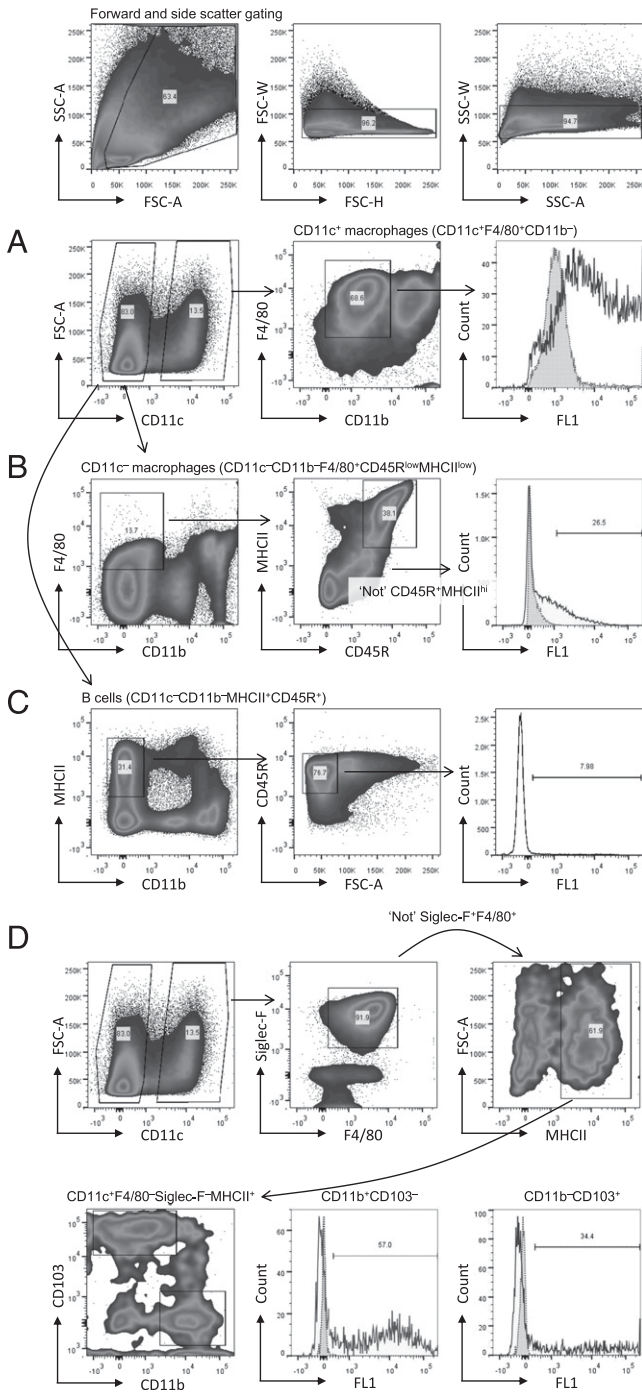


FIGURE 2. Gating strategy for analysis of particle uptake by lung macrophages, B cells, and DC. Lung cells isolated by collagenase/DNase digestion were gated on FSC/side scatter (SSC) followed by gating to exclude doublets. CD11c⁺ or CD11c⁻ gating was then applied to allow discrimination of CD11c⁺ alveolar macrophages (**A**), CD11c⁻ nonalveolar macrophages (**B**), B cells (**C**), and CD11b⁻CD103⁺ and CD11b⁺CD103⁻ DC (**D**). Histograms show representative plots of bead-positive cells in the FL1 channel. FSC-A, FSC pulse area; FSC-H, FSC height; FSC-W, FSC width; SSC-A, side scatter pulse area; SSC-W, side scatter width.

Supplemental Fig. 2C) at day 7 and caused a smaller but significant increase in proportions of CD11b^{hi}CD11c⁺MHC II^{hi} migratory DC from days 3–31 (Supplemental Fig. 2C). Neither PS50G or PS500G significantly altered proportions of tissue-resident CD11c⁺MHC II⁺ DC (27) (region 2; Supplemental Fig. 2C) relative to saline controls. Overall proportions of migratory DC in the draining LN were ~5–10-

fold greater than LN-resident DC numbers, regardless of treatment. There were no marked changes in proportions of lung-derived migratory CD11c^{int}MHC II^{int} alveolar macrophages (29) (region 3; Supplemental Fig. 2C) (0.41, 0.36, and 0.51%; saline, PS50G, and PS500G, respectively). Further analysis showed that ~60% of this minor CD11c^{int}MHC II^{int} population were CD11b⁻CD45R⁺ pDC in saline controls, and this was not altered by either particle size (data not shown). There were no significant changes in CD11c⁻MHC II⁺ cells (>99% small leukocytes by FSC/side scatter, <1% CD11b⁺, region 4; Supplemental Fig. 2C) (74.8, 72.5, and 69.1%; saline, PS50G, and PS500G, respectively) or CD11c⁺MHC II⁺ B cells (region 5; Supplemental Fig. 2C) (20.9, 23.2, and 24.4%; saline, PS50G, and PS500G, respectively) among the three groups.

Nanoparticles and microparticles are taken up and cleared from the lung and lung-draining LN with different kinetics

To gain insight into how particle size affects cellular uptake and clearance within the pulmonary compartment, we identified cells which internalized particles as fluorescent positive (Fluo⁺) (Fig. 3A). The frequency of PS50G-laden cells in the lung was significantly greater than PS500G-laden cells at day 1 (38%), dropping steadily over the next month (Fig. 3B). In contrast, whereas the frequency of PS50G- and PS500G-laden cells in the draining LN was the same at day 1, the frequency of PS50G-laden cells increased rapidly until day 7 (an 18-fold expansion of cell numbers). There was little change in the frequency of PS500G-laden cells over this time (Fig. 3C). Background frequencies (i.e., mice that received saline instead of particles) were 0.2–0.6% in the lung and lung-draining LN at all times. Thus, the frequency of nanoparticle-laden cells peaked early in the lung, dropping gradually over time, with a delayed increase in particle-laden cells seen in the lung-draining LN, whereas smaller changes were observed for PS500G.

PS50G and PS500G are taken up by distinct cell populations in the lung and lung-draining LN

Previous data from our group showed size-differential uptake of PS50G and PS500G by DC and macrophages, respectively, in the draining LN following footpad injection (17), and we speculated that a similar phenomenon would operate in the lung. We analyzed particle uptake by lung CD11c⁺ alveolar macrophages (CD11c⁺CD11b⁻F4/80⁺Siglec-F⁺), CD11c⁻ nonalveolar (interstitial) macrophages (CD11c⁻CD11b⁻F4/80⁺CD45R⁺MHCII⁺), B cells (CD11c⁻CD11b⁻F4/80⁺MHC II⁺CD45R⁺[B220]⁺), and CD11b⁻CD103⁺ and CD11b⁺CD103⁻ DC (CD11c⁺MHC II⁺F4/80⁻Siglec-F⁻) as gated in Fig. 2. PS50G were preferentially taken up by CD11c⁺ alveolar macrophages at day 3, whereas the proportion of PS500G-laden CD11c⁺ macrophages more than doubled by day 30 (Fig. 4). Similarly, nonalveolar CD11c⁻ macrophages preferentially took up PS50G nanoparticles, exceeding 30% of PS50G-laden cells at day 3 and dropping to 18% at day 30. The proportion of PS500G-laden CD11c⁻ macrophages was steady at ~5% at both time points. Approximately 10% of B cells took up PS50G at day 3, dropping to < 6% at day 30, whereas uptake of PS500G was ~3-fold lower. Approximately 60% of CD11b⁻CD103⁺ and CD11b⁺CD103⁻ DC took up PS50G at day 3, whereas uptake of PS500G microparticles was ~4-fold lower. The proportion of PS50G-laden CD103⁺ DC had decreased ~2-fold (to 30%) at day 30, whereas the proportion of PS50G-laden CD11b⁺ DC remained static. The frequency of PS500G-laden CD103⁺ and CD11b⁺ DC remained virtually unchanged from day 3 to 30.

In the draining LN, we determined particle uptake by CD11c⁺MHC II⁺ DC examining CD103/CD11b subsets (gated on total CD11c⁺MHC II⁺ and CD11c⁺MHC II⁺ cells; Fig. 5A, Supplemental Fig. 2C), lung-derived migratory CD11c^{int}MHC II^{int} al-

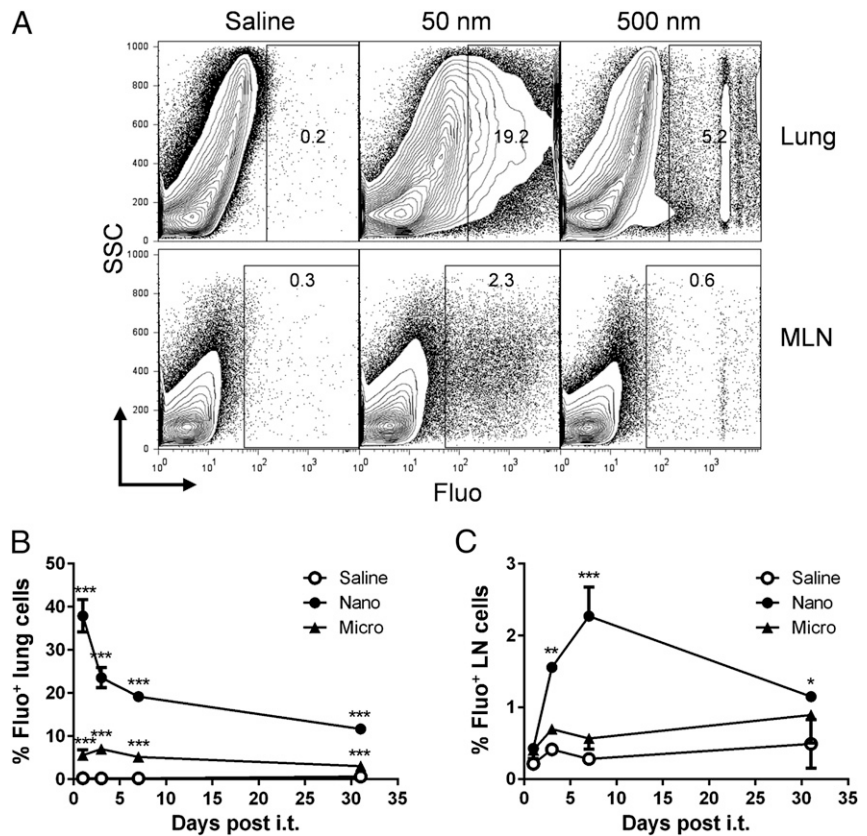


FIGURE 3. PS50G-laden cell frequencies show different kinetics in the lung and lung-draining LN. Naive mice received FITC-labeled PS50G or PS500G (nano or micro, respectively) i.t. on day 0, or saline as control; groups of mice were killed for analysis at the indicated times. **(A)** Gating strategy for identification of particle-laden (Fluo⁺) cells in lung and draining LN. Time-course analysis of frequency of particle-laden cells in lung **(B)** and draining LN **(C)**. Representative of three separate experiments. Mean \pm SEM, $n = 6$ –9 mice/group/time point. * $p < 0.05$, ** $p < 0.01$, *** $p < 0.001$ (versus saline). MLN, Mesenteric LN.

veolar macrophages (29) (region 3; Supplemental Fig. 2C), CD11c⁺MHC II⁺ cells (region 4; Supplemental Fig. 2C), and CD11c⁺MHC II⁺ B cells (region 5; Supplemental Fig. 2C). We observed strong preferential size-dependent uptake of PS50G by CD11b⁺CD103⁺, CD11b⁺CD103[−], and CD11b⁺CD103[−] DC subsets (90–95% of these three DC subsets lacked expression of the monocytic marker Ly6C; data not shown). The proportion of PS50G-laden CD11b⁺CD103⁺ DC was ~10% at day 3, increasing to 30% by day 30 (Fig. 5B). The proportion of CD11b⁺CD103[−] DC that took up PS50G remained relatively stable at ~30% across both time points. The strongest particle uptake occurred in CD11b⁺CD103⁺ DC, with ~45% of these cells containing PS50G at both time points. Overall, uptake of PS50G nanoparticles was ~3-fold greater than for PS500G microparticles for all three draining LN DC subsets (Fig. 5B). In contrast, the proportion of B cells that took up PS50G or PS500G at day 3 was 0.1–0.5% and not examined further (data not shown). Similarly, the proportion of particle-laden CD11c⁺MHC II⁺ lymphocytes was 0.01–0.03%, whereas particle uptake by CD11c^{int}MHC II^{int} migratory alveolar macrophages and CD11c^{int}MHC II^{int}CD11b[−]CD45R⁺ pDC was <1% (data not shown).

Particle trafficking to the lung-draining LN is cell associated

The above data clearly show that particles instilled into the lung subsequently appear within DC in the draining LN. However, it was unclear whether these particles were transported from the lung via migration of particle-laden DC or direct lymphatic drainage. Data from several studies suggest that migration of Ag-laden DC occurs within 6 h postinstillation of Ag to the lung, peaking at 12–24 h (27, 30–32). However, soluble tracers appear within the draining LN within minutes postinjection due to lymphatic drainage (33, 34). Therefore, to distinguish between these two particle-transport possibilities, we instilled fluorescent particles into naive mice and examined proportions of particle-laden

cells 2 h later. Our data show that the frequency of particle-laden cells in the draining LN was extremely low (~0.02%) at 2 h postinstillation for both the PS50G and PS500G groups and not significantly different from background levels in saline-treated mice (Fig. 6A). Accumulation of PS50G and PS500G within migratory CD11c⁺MHC II^{hi} draining LN DC (27, 28) was also very low and not significantly different from saline controls (0.07 ± 0.05 , 0.16 ± 0.04 , and $0.4 \pm 0.14\%$; saline, PS50G, and PS500G, respectively). In contrast, the proportion of particle-laden total lung cells (isolated from the same mice) was already >20% for both particle sizes by 2 h (Fig. 6B), confirming that particles had been instilled correctly.

PS50G nanoparticles selectively increase expression of cytokines and chemokines in BAL fluid

The above data show that PS50G and PS500G are differentially taken up by pulmonary APC, suggesting that particle size could influence cytokine/chemokine production in the lung. Indeed, instillation of PS50G nanoparticles caused a rapid induction of IL-6, G-CSF, and GM-CSF at day 1 postinstillation and IL-12p40, CCL2 (MCP-1), and CCL5 (RANTES) by day 3 postinstillation (Fig. 7). In contrast, PS500G caused smaller increases in IL-6, G-CSF, GM-CSF, and CCL5 at day 1 after instillation. Distinct from these selective PS50G effects, both PS50G and PS500G caused broadly similar increases in BAL fluid levels of IL-1 α , IL-1 β , IL-12p70, CCL3 (MIP-1 α), and TNF (Supplemental Fig. 3). PS500G caused a modest increase in TGF- β 1 levels at day 3. Neither particle size significantly increased CXCL1 (keratinocyte chemoattractant) or CCL4 (MIP-1 β) over saline control values (Supplemental Fig. 3). Overall, these data show that instillation of PS50G and PS500G into the lung rapidly increases production of selected cytokines and chemokines, with evidence for induction of both distinct (particle size-dependent), and overlapping (particle size-independent) cytokine/chemokine profiles.

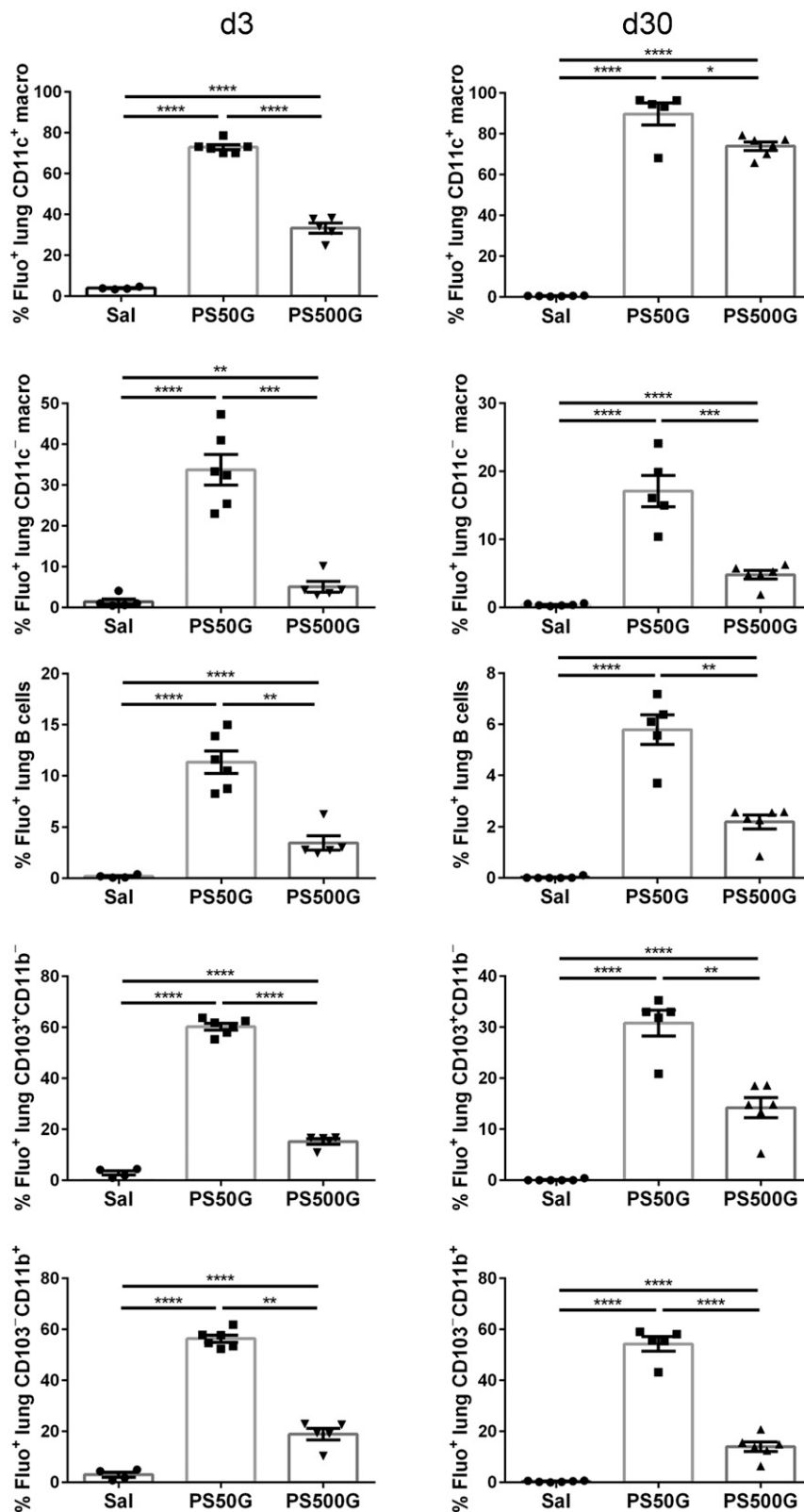


FIGURE 4. PS50G are preferentially taken up by macrophages, B cells, and DC in the lung. Naive mice received fluorescent-labeled PS50G or PS500G i.t. on day 0 or saline (Sal) as control. Particle-laden (FL1-positive) cells were gated as per Fig. 2. Proportions of bead-positive cells for each population are shown at days 3 and 30. Mean \pm SEM, $n = 6$ mice/group/time point. * $p < 0.05$, ** $p < 0.01$, *** $p < 0.001$, **** $p < 0.0001$.

PS50G nanoparticles increase costimulatory molecule expression on lung DC

The above findings show that particles induced production of chemokines involved in DC maturation, suggesting possible effects on DC costimulatory molecule expression. Flow cytometry confirmed that PS50G nanoparticles caused a marked increase in expression of CD40, CD80, and CD86 on CD11c⁺MHC II⁺ DC in the lung at day 3

after instillation, primarily in cells containing the highest number of particles (Fig. 8A, 8B). Further analysis confirmed that CD86 expression was similarly upregulated on PS50G-laden macrophages, B cells, and CD11b⁺ and CD103⁺ DC in the lung, with the degree of CD86 upregulation positively correlated with the level of particle uptake (FL1 fluorescence; data not shown). PS50G-induced costimulatory molecule expression decreased at day 7, but nevertheless

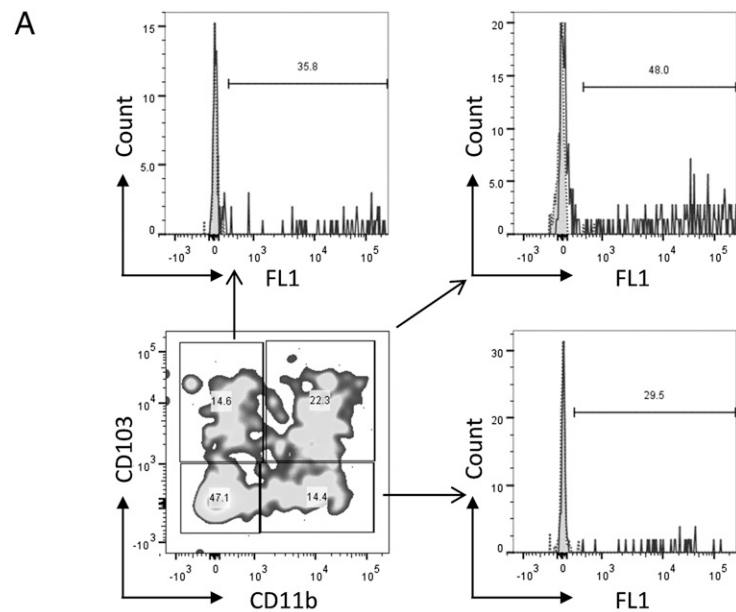
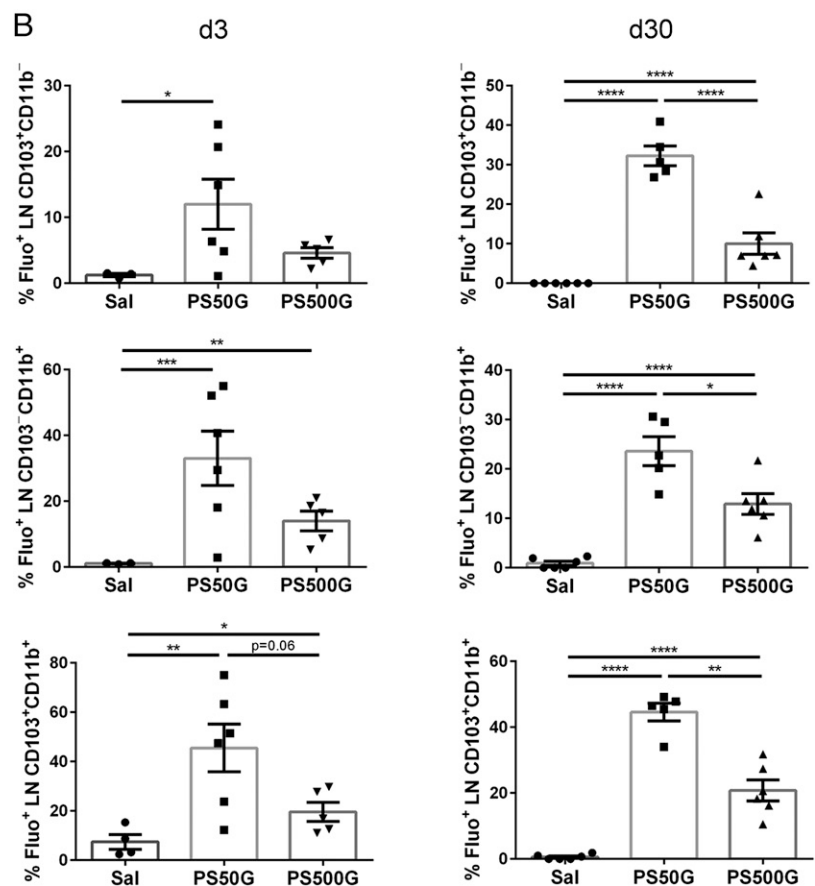


FIGURE 5. PS50G are preferentially taken up by DC in the lung-draining LN. Naive mice received fluorescent-labeled PS50G or PS500G i.t. on day 0 or saline (Sal) as control. **(A)** CD11c⁺MHC II⁺ cells were gated for identification of CD11b⁺CD103⁺, CD11b⁺CD103⁺, and CD11b⁺CD103⁺ cells in the lung-draining LN. **(B)** Proportions of bead-positive cells for the indicated populations are shown at days 3 and 30. Mean \pm SEM, $n = 6$ mice/group/time point. * $p < 0.05$, ** $p < 0.01$, *** $p < 0.001$, **** $p < 0.0001$.



remained significantly elevated over saline and PS500G levels until day 31 after instillation. PS500G had a negligible effect on costimulatory molecule expression by lung DC. In contrast to the lung, neither particle type affected CD40 expression by DC in the lung-draining LN, although CD80 expression was decreased at day 31 (Supplemental Fig. 4B, 4C). Both PS50G and PS500G increased CD86 expression at days 1 and 3 (Supplemental Fig. 4A, 4D). Overall, these data show that PS50G cause sustained increases in costimulatory molecule expression in the lung, whereas both PS50G

and PS500G caused a transient increase in CD86 expression in the draining LN.

PS50G and PS500G increase migration of allergen-laden DC from lung to draining LN in naive mice and decrease proportions of allergen-laden CD11b⁺ DC

Migration of allergen-laden DC from lung to the draining LN is an important step in the induction of allergic pulmonary inflammation. We investigated the effect of inert particles on this

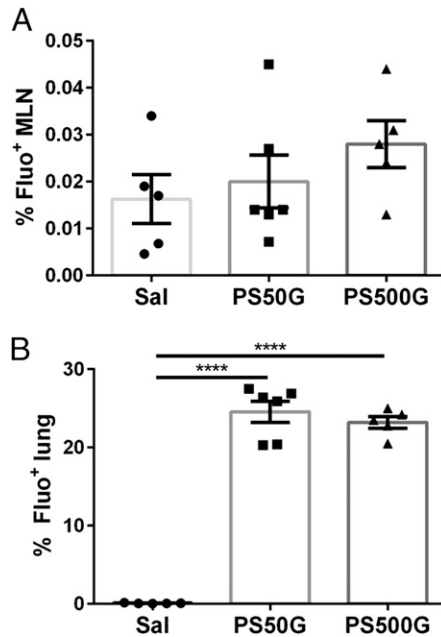


FIGURE 6. PS50G or PS500G do not accumulate in lung-draining LN cells 2 h postinstillation. Naive mice received fluorescent-labeled PS50G or PS500G i.t. on day 0 or saline (Sal) as control. Frequency of particle-laden cells among total draining LN (**A**) and lung cells (**B**) at 2 h post-particle instillation. Mean \pm SEM; $n = 6$ mice/group/time point. **** $p < 0.0001$.

pathway by instilling PS50G or PS500G into the lungs of naive, healthy, otherwise unmanipulated mice prior to instillation of fluorescent-labeled (Alexa Fluor 488) OVA and analyzed allergen-

laden cells using established methods (27, 35). Both PS50G and PS500G increased the frequency of allergen-laden (Alexa Fluor 488⁺) lung-derived DC in the draining LN by 70% (Fig. 9A). Despite this increase in total allergen laden DC, PS50G decreased the frequency of CD11b⁺MHC II⁺ DC among allergen-laden CD11c⁺ cells in the draining LN by 70% at days 3 and 31 post-instillation, whereas PS500G caused a slightly smaller decrease (Fig. 9B).

Particle-mediated inhibition of AAI is particle size dependent

Our previous studies showed that PS50G impair the induction of AAI (11). Given the above data showing dramatically different effects of PS50G versus PS500G on pulmonary APC distribution and maturation, we predicted that PS500G would have altered ability to impair AAI relative to PS50G. We investigated this by instilling PS50G or PS500G particles into the lungs of naive mice prior to OVA sensitization and OVA challenge (Fig. 10A). As expected, PS50G inhibited BAL eosinophilia and lung tissue inflammation (Fig. 10B, 10C). PS500G also partially prevented the development of lung airway and parenchymal inflammation, although this was less pronounced than for the PS50G. Of note, PS50G, but not PS500G, additionally inhibited the production of serum OVA-specific IgE (Fig. 10D), a hallmark of allergic disease. PS50G also significantly decreased BAL fluid IL-5 and IL-13 (Fig. 10E, 10F), whereas PS500G had a blunted effect, consistent with their reduced effect on BAL eosinophilia. ELISPOT analysis was performed to further confirm a differential effect of PS50G and PS500G pretreatment on production of IL-13, a key cytokine that regulates mucus production. Consistent with the BAL ELISA data, PS50G but not PS500G significantly decreased the frequency of

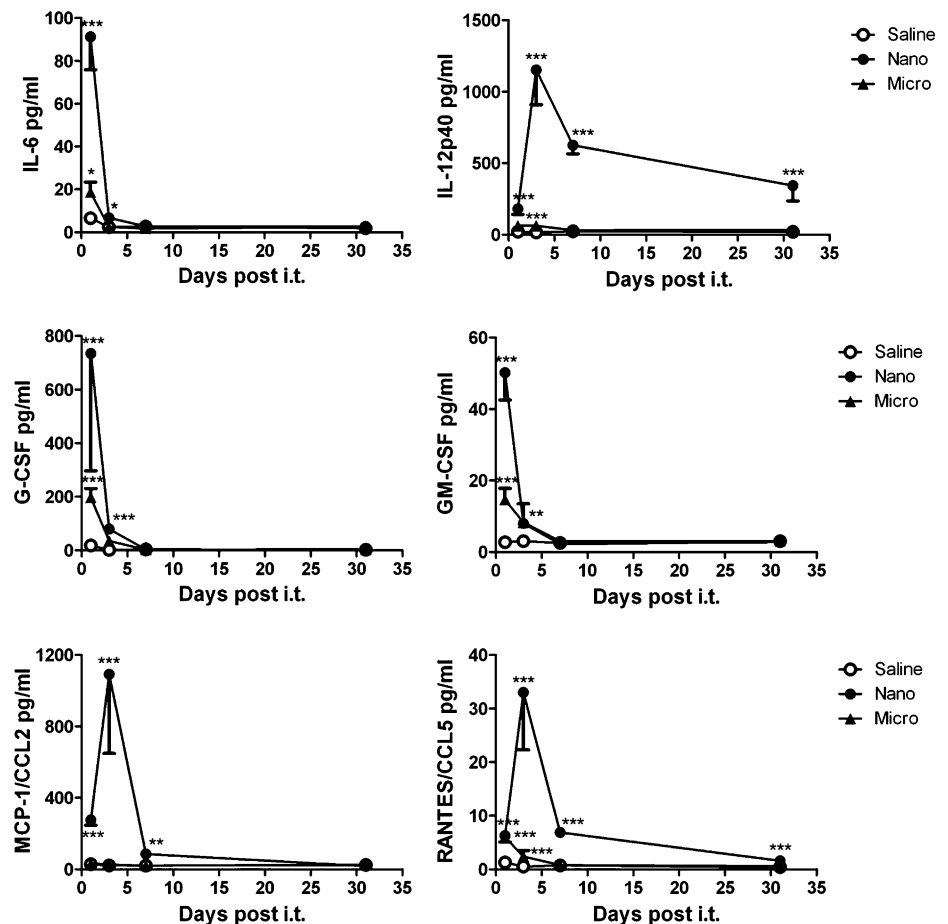


FIGURE 7. PS50G and PS500G induce distinct patterns of BAL fluid cytokines and chemokines. Naive mice received PS50G or PS500G (nano or micro, respectively) i.t. on day 0 or saline as control; groups of mice were killed for analysis at the indicated times. Data show concentrations of IL-6, IL-12p40, G-CSF, GM-CSF, CCL2, and CCL5. Representative of two separate experiments. Mean \pm SEM, $n = 3-7$ mice/group/time point. * $p < 0.05$, ** $p < 0.01$, *** $p < 0.001$ (versus saline).

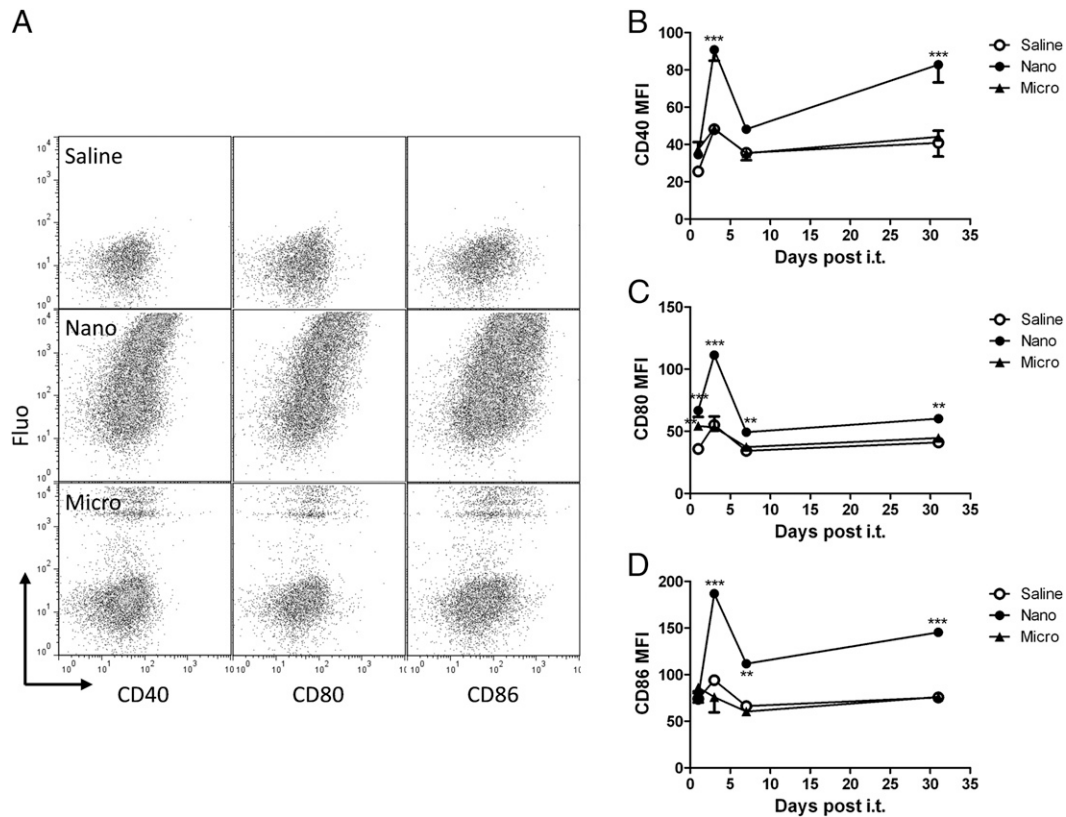


FIGURE 8. PS50G increase costimulatory molecule expression on lung DC. Naive mice received fluorescent-labeled PS50G or PS500G (nano or micro, respectively) i.t. on day 0 or saline as control. **(A)** Bead uptake (Fluo) versus CD86 expression by lung CD11c⁺MHC II⁺ DC (gated as per region 1; Supplemental Fig. 2B) on day 3 postparticles. **(B–D)** Time-course analysis of CD40, CD80, and CD86 expression by lung CD11c⁺MHC II⁺ DC. Mean \pm SEM; $n = 3$ /group (each replicate consisting of pools of two to three mice). ** $p < 0.01$, *** $p < 0.001$ (versus saline).

OVA-specific IL-13-producing cells in the lung-draining LN (Fig. 10G).

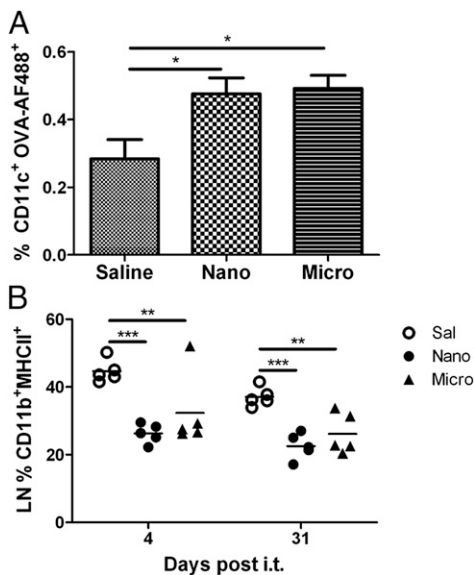


FIGURE 9. PS50G and PS500G alter migration of allergen-laden DC from lung to draining LN. Mice received PS50G or PS500G (nano or micro, respectively) i.t. on day 0 or saline (Sal) as control. On day 3 **(A, B)** or day 30 **(B)**, mice received OVA-Alexa Fluor 488 i.t.; analysis was performed 24 h later. Proportions of CD11c⁺ OVA-Alexa Fluor⁺ cells in the draining LN **(A)** and proportions of CD11b⁺ MHC II⁺ cells among gated CD11c⁺ OVA-Alexa Fluor⁺ cells in the draining LN **(B)**. Mean \pm SEM; $n = 5$ /group/time point. * $p < 0.05$, ** $p < 0.01$, *** $p < 0.001$ (versus saline).

Discussion

Ambient, pollutant, and man-made ultrafine/nanoparticles are known to promote allergic sensitization and AAI. However, our recent studies counter intuitively showed that inert nontoxic PS50G nanoparticles can inhibit AAI via modulation of pulmonary DC function, demonstrating that nanoparticles in the lung do not inherently promote pathology. However, relatively little is known of the effect of particle size on kinetics of particle uptake by APC in the pulmonary compartment and potential effects on APC distribution, maturation, and inflammatory mediator production. Our data show that PS50G were taken up in much greater proportions than PS500G by all lung APC including alveolar (CD11c⁺) and nonalveolar (CD11c⁻) macrophages, B cells, and CD11b⁺ CD103⁻ and CD11b⁻ CD103⁺ DC, with alveolar macrophages and DC showing the strongest uptake. In contrast, we only detected significant PS50G uptake by DC in the lung-draining LN. Particle uptake by total lung-draining LN cells or migratory CD11c⁺ MHC II^{hi} DC was not detected at 2 h postinstillation, suggesting that particles do not translocate to the draining LN via lymphatic flow, as drainage to LN via the lymphatics occurs within minutes. PS50G instillation was associated with markedly increased costimulatory molecule expression on lung DC and a distinct pattern of cytokine and chemokine production in the lung airways. Although both PS50G and PS500G decreased proportions of stimulatory allergen-laden DC in the draining LN, the effect was most pronounced for PS50G at the day 4 time point. Thus, PS50G and PS500G leave distinct long-lasting immunological imprints in the lung. Based on these data, we predicted that PS500G microparticles would have impaired ability to inhibit AAI relative to PS50G nanoparticles. Our studies confirmed this prediction, showing that

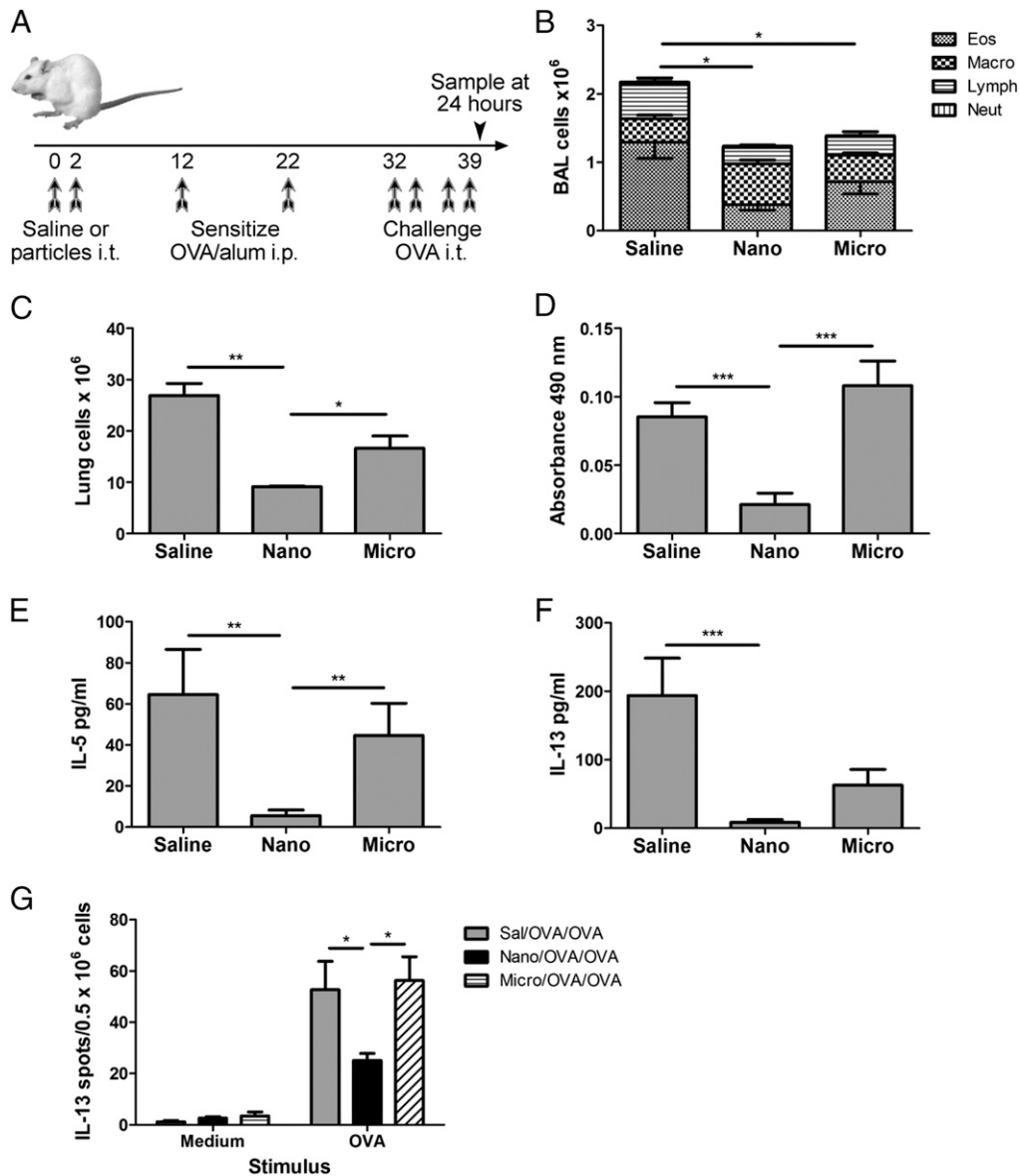


FIGURE 10. PS50G inhibit development of eosinophilic lung inflammation and allergen-specific immunity. **(A)** Mice received PS50G or PS500G (nano or micro, respectively) or saline i.t. prior to i.p. OVA/aluminum hydroxide (alum) sensitization and i.t. OVA challenge at the indicated times. Tissue sampling was performed 24 h after the final allergen challenge. **(B)** Differential analysis of absolute BAL cells numbers. **(C)** Total lung leukocyte counts. **(D)** OVA-specific serum IgE. BAL fluid concentrations of IL-5 **(E)** and IL-13 **(F)**. **(G)** Frequency of IL-13-producing lung-draining LN cells stimulated with medium or OVA. Mean \pm SEM; $n = 8$ –10 mice/group. Lung cell counts and IL-13 ELISPOT data were from $n = 2$ to 3/group (each replicate consisting of pools of three to five mice). * $p < 0.05$, ** $p < 0.01$, *** $p < 0.001$.

PS50G significantly inhibited the allergen-specific adaptive immune response, whereas PS500G failed to do so.

It has been convincingly shown that particles are taken up by cells in a size-dependent manner. Foged et al. (36) found that in vitro, DC preferentially take up polystyrene particles of 40 nm, with particle uptake decreasing for particles >100 nm in diameter. In vivo, we previously showed that 40-nm polystyrene particles injected into the footpad preferentially localize to DC in the draining LN (17). Similarly, i.v. infused 25-nm nanoparticles are rapidly transported to the draining LN via the lymphatic system, where they are taken up by DC (37). Several other studies showed that microparticles (1000 nm) are preferentially phagocytosed by macrophages in the LN or lung airways (17, 38), whereas nanoparticles (titanium dioxide, gold, and iridium) are inefficiently and nonspecifically taken up by macrophages in the lung (39–41). Our results using fluorescent particles extend these findings by show-

ing that PS50G were taken up preferentially by alveolar macrophages and both $CD11b^+CD103^-$ and $CD11b^-CD103^+$ DC in the lung, with lower uptake by nonalveolar macrophages and B cells. Uptake of larger PS500G was 2- to 3-fold lower in all lung APC at day 3. Interestingly, the proportion of alveolar $CD11c^+$ macrophages that took up PS500G increased from 33 to 74% from days 3 to 30, indicating ongoing accumulation of PS500G microparticles within these cells. Preliminary data showed that uptake of PS50G by the small population of lung pDC (~ 0.4 – 0.7%) was also significantly higher than PS500G at day 3 (26.3 ± 2.7 versus $6.1 \pm 0.7\%$; $n = 6$ /group; $p < 0.001$). The increased uptake of PS50G by lung pDC is unlikely to be functionally significant; however, future studies could explore potential changes in frequency of regulatory T cells. Despite uptake of both particle sizes by all lung APC, particle uptake in the lung-draining LN was restricted to $CD11b^+CD103^-$, $CD11b^-CD103^+$, and $CD11b^+$

CD103⁺ DC, with negligible uptake by other cells (alveolar macrophages, pDC, B cells, and CD11c⁺CD11b⁺MHC II⁺ lymphocytes). Our data show that the proportion of PS50G-laden CD11b⁺CD103⁺ DC in the draining LN increased from 12 to 32% from days 3 to 30, despite the fact that the proportion of PS50G-laden CD11b⁺CD103⁺ DC in the lung had dropped from 60 to 30% over this time, suggesting preferential migration and/or retention of PS50G-laden CD11b⁺CD103⁺ DC. We found significant PS50G uptake by CD11b⁺CD103⁺ draining LN DC, a minor population of lung-draining LN DC (e.g., Ref. 42). CD11b⁺CD103⁺ DC in the small intestine lamina propria were recently shown to play an important role in driving Th17 responses (43), although the function of these cells in the lung-draining LN has not been described. In contrast, CD11b⁺CD103⁺ DC in the lung-draining LN have been shown by us and others (11, 28, 44, 45) to play an important role in stimulating CD4⁺ T cells and driving Th2-biased inflammation, whereas CD11b⁺CD103⁺ appear to selectively stimulate cross presentation of apoptotic Ag to CD8⁺ T cells and drive antiviral immunity (44, 46, 47). Our data raise the possibility that nanoparticle-mediated delivery of appropriate Ag to diverse draining LN DC subsets could be harnessed to selectively promote Th1, Th2, or Th17 immunity.

Transport of soluble Ag and particles from lung to the lung-draining LN is mediated by active cellular transport, as evidenced by the lack of allergen accumulation in the draining LN in CCR7-deficient mice (28) and the profound inhibition of allergen and latex particle accumulation in mice treated with pertussis toxin, an inhibitor of chemokine signaling (32). The appearance of PS50G in macrophages, B cells, and DC in the lung, but only in DC in the draining LN, suggested onward migration of DC from the lung to the draining LN. The uptake of particles by lung-draining LN DC that we observed could be due to particle drainage via the lymphatics and uptake within the draining LN or by DC uptake in the lung and subsequent migration. Accumulation of allergen or particle-laden DC in the lung-draining LN is apparent within 6 h, peaking at 12–24 h after instillation (27, 30–32). However, soluble tracers can be transported to the draining LN from within minutes postinjection into peripheral sites (33, 34). Therefore, we examined particle uptake in the draining LN at 2 h postinstillation, a time preceding the known dynamics of DC accumulation. Particle accumulation within draining LN cells was undetectable at this time, suggesting that the particle uptake by DC that we observe at day 3 is due to cell-mediated transport, in agreement with studies showing DC-mediated transport of 500-nm particles to the lung-draining LN (18, 32, 47). Our studies advance these findings, showing that nano-sized particles accumulate to a greater degree than microparticles. In contrast, another study found that nanoparticles (20 nm) appear within the subcapsular region of the popliteal LN within 2 h following footpad injection and are taken up by DC (defined as CD11c⁺) as well as macrophages, B cells, and pDC (F4/80⁺, B220⁺, and pDC Ag-I⁺, respectively) at this early time (48). These findings are consistent with the idea of drainage via the lymphatics and uptake by cells within the popliteal LN, as macrophages and pDC are not considered to be migratory cell populations (28, 32). More surprisingly, this study also showed that a major portion of the 20-nm particle uptake was by macrophages in the draining LN, in contrast to our findings showing uptake exclusively by DC. The differences between this study and ours could be due to differences in the anatomical site (leg versus lung), the route of administration (footpad injection versus i.t.), or the difference in particle size.

DC migration is significantly increased by inflammatory stimuli (30, 32, 49). It is therefore likely that the minor transient inflammation induced by i.t. particle instillation helps drive DC

uptake and migration from the lung to the draining LN. The ongoing, albeit gradually decreasing, presence of PS50G in the lung (Fig. 3) would provide a sustained source of particle-laden DC. Our data also indicate that the frequency of PS50G-laden cells in the lung steadily declines to approximately one-third of the initial value, indicating ongoing clearance of PS50G from the lung. Presumably, this clearance would be via a combination of: 1) DC-mediated transport; 2) drainage of particles via the lymphatic system; and 3) clearance of PS50G-laden macrophages via the mucociliary escalator.

PS50G instillation increased BAL fluid levels of mediators involved in recruitment and/or maturation of monocytes and DC, specifically CCL2, G-CSF, GM-CSF, and RANTES/CCL5 (13, 50, 51), explaining the increase in lung DC at day 3. PS50G also increased BAL fluid IL-6 levels, explaining the transient airway neutrophilia we observed. Numerous cell types have been linked to the production of these cytokines, including lung epithelium (IL-6, G-CSF, and GM-CSF) and activated DC (IL-6, IL-12) (13, 51). PS50G instillation was also associated with increased costimulatory molecule expression by lung CD11c⁺MHC II⁺ DC, primarily within the particle-laden DC population. Notably, maximum levels of these BAL fluid cytokines/chemokines (day 1 or 3) immediately preceded or coincided with the increased costimulatory molecule expression by lung DC (day 3). This increased costimulatory molecule expression was likely due to inflammatory mediator induced DC maturation, direct effects of PS50G uptake on these cells, or a combination of these factors.

It is now understood that a primary immune response in the lung can modify the nature and/or severity of a subsequent immune response. For example, influenza virus infection protects against infection from the unrelated respiratory syncytial virus (52), and heat-labile *Escherichia coli* toxin enhances protection to subsequent influenza or respiratory syncytial virus infection (53). Furthermore, in humans, exposure to high levels of LPS inhibits allergies and allergic asthma (54), whereas exposure of mouse lungs to LPS prior to or concomitant with allergen sensitization inhibits development of AAI following allergen challenge (55, 56). This process of innate imprinting is thought to operate by various mechanisms including impairment of pulmonary APC function (53) or induction of regulatory myeloid-derived suppressor cells (56). Our previous study (11) demonstrated an analogous inhibition of AAI with PS50G nanoparticles mediated via modification of pulmonary DC function. Our new findings comparing the same mass of PS50G and PS500G show that PS50G, and to a lesser extent PS500G, decreased proportions of CD11b⁺ DC allergen-laden in the draining LN, a subset we and others (11, 44) have shown to be responsible for stimulation of allergen-specific CD4⁺ T cell responses. However, PS50G and PS500G leave distinctive immunological imprints, with PS50G but not PS500G markedly inhibiting the allergen-specific adaptive component of AAI (allergen-specific Th2 cytokines and serum IgE).

In summary, our data show that 50- and 500-nm particles leave different immunological imprints in the pulmonary compartment. PS50G were taken up by macrophages, B cells, and DC in the lung, but only by DC in the draining LN, suggesting onward migration of particle-laden DC to the draining LN. Our finding that uptake of particles (of either size) was undetectable in the lung-draining LN at 2 h postinstillation suggests that they do not translocate to the draining LN via simple lymphatic drainage, but are actively transported within DC. PS50G induced DC maturation in the lung and induced a distinct subset of cytokines and chemokines involved in DC recruitment and/or maturation. PS500G were taken up less efficiently than PS50G in the lung and draining LN, with maximal uptake seen at day 30 by lung CD11c⁺ macrophages, and induced

a more restricted subset of cytokines and chemokines in the lung. The outcome was that pretreatment with PS50G, but not PS500G, significantly inhibited the development of AAI. It is tempting to speculate that the impaired Ag-specific costimulatory capacity of CD11b⁺ DC we observed in the draining LN of PS50G-treated mice (11) is due to a state of PS50G-induced DC refractoriness, possibly occurring due to induction of DC maturation in the absence of specific Ag uptake. An analogous situation occurs during endotoxin tolerance in which refractory or exhausted DC are induced following LPS stimulation, resulting in suppression of AAI (57, 58). Overall, these data increase our understanding of how differently sized inert nontoxic particles differentially modulate pulmonary APC function and lung immune homeostasis. These findings provide new insights into particle effects on lung immunobiology and may support the development of lung-specific particulate vaccines, drug delivery systems, and immunomodulators.

Acknowledgments

We thank Je Lin Sieow (Department of Immunology, Monash University) for technical assistance. We also thank Dr. Gabrielle Belz (The Walter and Eliza Hall Institute of Medical Research, Parkville, VIC, Australia) for helpful discussions about lung-draining LN DC subsets. This article is dedicated to the memory of the late Geoffrey Linton Hardy.

Disclosures

The authors have no financial conflicts of interest.

References

1. Brunekreef, B., and S. T. Holgate. 2002. Air pollution and health. *Lancet* 360: 1233–1242.
2. Peters, A., H. E. Wichmann, T. Tuch, J. Heinrich, and J. Heyder. 1997. Respiratory effects are associated with the number of ultrafine particles. *Am. J. Respir. Crit. Care Med.* 155: 1376–1383.
3. Penttinen, P., K. L. Timonen, P. Tiittanen, A. Mirme, J. Ruuskanen, and J. Pekkanen. 2001. Ultrafine particles in urban air and respiratory health among adult asthmatics. *Eur. Respir. J.* 17: 428–435.
4. von Klot, S., G. Wölke, T. Tuch, J. Heinrich, D. W. Dockery, J. Schwartz, W. G. Kreyling, H. E. Wichmann, and A. Peters. 2002. Increased asthma medication use in association with ambient fine and ultrafine particles. *Eur. Respir. J.* 20: 691–702.
5. Li, N., M. Wang, L. A. Bramble, D. A. Schmitz, J. J. Schauer, C. Sioutas, J. R. Harkema, and A. E. Nel. 2009. The adjuvant effect of ambient particulate matter is closely reflected by the particulate oxidant potential. *Environ. Health Perspect.* 117: 1116–1123.
6. Alessandrini, F., H. Schulz, S. Takenaka, B. Lentner, E. Karg, H. Behrendt, and T. Jakob. 2006. Effects of ultrafine carbon particle inhalation on allergic inflammation of the lung. *J. Allergy Clin. Immunol.* 117: 824–830.
7. de Haar, C., I. Hassing, M. Bol, R. Bleumink, and R. Pieters. 2006. Ultrafine but not fine particulate matter causes airway inflammation and allergic airway sensitization to co-administered antigen in mice. *Clin. Exp. Allergy* 36: 1469–1479.
8. Larsen, S. T., M. Roursgaard, K. A. Jensen, and G. D. Nielsen. 2010. Nano titanium dioxide particles promote allergic sensitization and lung inflammation in mice. *Basic Clin. Pharmacol. Toxicol.* 106: 114–117.
9. Inoue, K., E. Koike, R. Yanagisawa, S. Hirano, M. Nishikawa, and H. Takano. 2009. Effects of multi-walled carbon nanotubes on a murine allergic airway inflammation model. *Toxicol. Appl. Pharmacol.* 237: 306–316.
10. Inoue, K., R. Yanagisawa, E. Koike, M. Nishikawa, and H. Takano. 2010. Repeated pulmonary exposure to single-walled carbon nanotubes exacerbates allergic inflammation of the airway: Possible role of oxidative stress. *Free Radic. Biol. Med.* 48: 924–934.
11. Hardy, C. L., J. S. LeMasurier, G. T. Belz, K. Scalzo-Inguanti, J. Yao, S. D. Xiang, P. Kanellakis, A. Bobik, D. H. Strickland, J. M. Rolland, et al. 2012. Inert 50-nm polystyrene nanoparticles that modify pulmonary dendritic cell function and inhibit allergic airway inflammation. *J. Immunol.* 188: 1431–1441.
12. Lambrecht, B. N., and H. Hammad. 2003. Taking our breath away: dendritic cells in the pathogenesis of asthma. *Nat. Rev. Immunol.* 3: 994–1003.
13. Vermaelen, K., and R. Pauwels. 2005. Pulmonary dendritic cells. *Am. J. Respir. Crit. Care Med.* 172: 530–551.
14. Thepen, T., K. Hoeben, J. Brevé, and G. Kraal. 1992. Alveolar macrophages down-regulate local pulmonary immune responses against intratracheally administered T-cell-dependent, but not T-cell-independent antigens. *Immunology* 76: 60–64.
15. Thepen, T., C. McMenamin, B. Girn, G. Kraal, and P. G. Holt. 1992. Regulation of IgE production in pre-sensitized animals: in vivo elimination of alveolar macrophages preferentially increases IgE responses to inhaled allergen. *Clin. Exp. Allergy* 22: 1107–1114.
16. Bedoret, D., H. Wallemacq, T. Marichal, C. Desmet, F. Quesada Calvo, E. Henry, R. Closset, B. Dewals, C. Thielen, P. Gustin, et al. 2009. Lung interstitial macrophages alter dendritic cell functions to prevent airway allergy in mice. *J. Clin. Invest.* 119: 3723–3738.
17. Fifis, T., A. Gamvrellis, B. Crimeen-Irwin, G. A. Pietersz, J. Li, P. L. Mottram, I. F. McKenzie, and M. Plebanski. 2004. Size-dependent immunogenicity: therapeutic and protective properties of nano-vaccines against tumors. *J. Immunol.* 173: 3148–3154.
18. Byersdorfer, C. A., and D. D. Chaplin. 2001. Visualization of early APC/T cell interactions in the mouse lung following intranasal challenge. *J. Immunol.* 167: 6756–6764.
19. Bezemer, G. F., S. M. Bauer, G. Oberdörster, P. N. Breyse, R. H. Pieters, S. N. Georas, and M. A. Williams. 2011. Activation of pulmonary dendritic cells and Th2-type inflammatory responses on instillation of engineered, environmental diesel emission source or ambient air pollutant particles in vivo. *J. Innate Immun.* 3: 150–166.
20. de Haar, C., M. Kool, I. Hassing, M. Bol, B. N. Lambrecht, and R. Pieters. 2008. Lung dendritic cells are stimulated by ultrafine particles and play a key role in particle adjuvant activity. *J. Allergy Clin. Immunol.* 121: 1246–1254.
21. Nel, A. 2005. Atmosphere. Air pollution-related illness: effects of particles. *Science* 308: 804–806.
22. Hardy, C. L., L. Kenins, A. C. Drew, J. M. Rolland, and R. E. O’Hehir. 2003. Characterization of a mouse model of allergy to a major occupational latex glove allergen Hev b 5. *Am. J. Respir. Crit. Care Med.* 167: 1393–1399.
23. Kaewamatawong, T., N. Kawamura, M. Okajima, M. Sawada, T. Morita, and A. Shimada. 2005. Acute pulmonary toxicity caused by exposure to colloidal silica: particle size dependent pathological changes in mice. *Toxicol. Pathol.* 33: 743–749.
24. Renwick, L. C., D. Brown, A. Clouter, and K. Donaldson. 2004. Increased inflammation and altered macrophage chemotactic responses caused by two ultrafine particle types. *Occup. Environ. Med.* 61: 442–447.
25. Hardy, C. L., A. E. O’Connor, J. Yao, K. Sebire, D. M. de Kretser, J. M. Rolland, G. P. Anderson, D. J. Phillips, and R. E. O’Hehir. 2006. Follistatin is a candidate endogenous negative regulator of activin A in experimental allergic asthma. *Clin. Exp. Allergy* 36: 941–950.
26. Lambrecht, B. N., and H. Hammad. 2012. Lung dendritic cells in respiratory viral infection and asthma: from protection to immunopathology. *Annu. Rev. Immunol.* 30: 243–270.
27. Vermaelen, K. Y., I. Carro-Muino, B. N. Lambrecht, and R. A. Pauwels. 2001. Specific migratory dendritic cells rapidly transport antigen from the airways to the thoracic lymph nodes. *J. Exp. Med.* 193: 51–60.
28. Plantinga, M., M. Guillemins, M. Vanheerswyngheles, K. Deswarte, F. Branco-Madeira, W. Toussaint, L. Vanhoutte, K. Neyt, N. Killeen, B. Malissen, et al. 2013. Conventional and monocyte-derived CD11b(+) dendritic cells initiate and maintain T helper 2 cell-mediated immunity to house dust mite allergen. *Immunity* 38: 322–335.
29. Kirby, A. C., M. C. Coles, and P. M. Kaye. 2009. Alveolar macrophages transport pathogens to lung draining lymph nodes. *J. Immunol.* 183: 1983–1989.
30. Vermaelen, K., and R. Pauwels. 2003. Accelerated airway dendritic cell maturation, trafficking, and elimination in a mouse model of asthma. *Am. J. Respir. Cell Mol. Biol.* 29: 405–409.
31. von Garnier, C., L. Filgueira, M. Wikstrom, M. Smith, J. A. Thomas, D. H. Strickland, P. G. Holt, and P. A. Stumbles. 2005. Anatomical location determines the distribution and function of dendritic cells and other APCs in the respiratory tract. *J. Immunol.* 175: 1609–1618.
32. Jakubczik, C., J. Helft, T. J. Kaplan, and G. J. Randolph. 2008. Optimization of methods to study pulmonary dendritic cell migration reveals distinct capacities of DC subsets to acquire soluble versus particulate antigen. *J. Immunol. Methods* 337: 121–131.
33. Gretz, J. E., C. C. Norbury, A. O. Anderson, A. E. Proudfoot, and S. Shaw. 2000. Lymph-borne chemokines and other low molecular weight molecules reach high endothelial venules via specialized conduits while a functional barrier limits access to the lymphocyte microenvironments in lymph node cortex. *J. Exp. Med.* 192: 1425–1440.
34. Sixt, M., N. Kanazawa, M. Selg, T. Samson, G. Roos, D. P. Reinhardt, R. Pabst, M. B. Lutz, and L. Sorokin. 2005. The conduit system transports soluble antigens from the afferent lymph to resident dendritic cells in the T cell area of the lymph node. *Immunity* 22: 19–29.
35. Wikstrom, M. E., E. Batanero, M. Smith, J. A. Thomas, C. von Garnier, P. G. Holt, and P. A. Stumbles. 2006. Influence of mucosal adjuvants on antigen passage and CD4⁺ T cell activation during the primary response to airborne allergen. *J. Immunol.* 177: 913–924.
36. Foged, C., B. Brodin, S. Frokjaer, and A. Sundblad. 2005. Particle size and surface charge affect particle uptake by human dendritic cells in an in vitro model. *Int. J. Pharm.* 298: 315–322.
37. Reddy, S. T., A. J. van der Vlies, E. Simeoni, V. Angeli, G. J. Randolph, C. P. O’Neil, L. K. Lee, M. A. Swartz, and J. A. Hubbell. 2007. Exploiting lymphatic transport and complement activation in nanoparticle vaccines. *Nat. Biotechnol.* 25: 1159–1164.
38. Geiser, M. 2010. Update on macrophage clearance of inhaled micro- and nanoparticles. *J. Aerosol Med. Pulm. Drug Deliv* 23: 207–217.
39. Takenaka, S., E. Karg, W. G. Kreyling, B. Lentner, W. Möller, M. Behnke-Semmler, L. Jennen, A. Walch, B. Michalke, P. Schramel, et al. 2006. Distribution pattern of inhaled ultrafine gold particles in the rat lung. *Inhal. Toxicol.* 18: 733–740.
40. Semmler-Behnke, M., S. Takenaka, S. Fertsch, A. Wenk, J. Seitz, P. Mayer, G. Oberdörster, and W. G. Kreyling. 2007. Efficient elimination of inhaled nanoparticles from the alveolar region: evidence for interstitial uptake and subsequent reentrainment onto airways epithelium. *Environ. Health Perspect.* 115: 728–733.

41. Geiser, M., M. Casaulta, B. Kupferschmid, H. Schulz, M. Semmler-Behnke, and W. Kreyling. 2008. The role of macrophages in the clearance of inhaled ultrafine titanium dioxide particles. *Am. J. Respir. Cell Mol. Biol.* 38: 371–376.
42. Nakano, H., M. E. Free, G. S. Whitehead, S. Maruoka, R. H. Wilson, K. Nakano, and D. N. Cook. 2012. Pulmonary CD103(+) dendritic cells prime Th2 responses to inhaled allergens. *Mucosal Immunol.* 5: 53–65.
43. Persson, E. K., H. Uronen-Hansson, M. Semmrich, A. Rivollier, K. Hägerbrand, J. Marsal, S. Gudjonsson, U. Håkansson, B. Reizis, K. Kotarsky, and W. W. Agace. 2013. IRF4 transcription-factor-dependent CD103(+)CD11b(+) dendritic cells drive mucosal T helper 17 cell differentiation. *Immunity* 38: 958–969.
44. del Rio, M. L., J. I. Rodriguez-Barbosa, E. Kremmer, and R. Förster. 2007. CD103- and CD103+ bronchial lymph node dendritic cells are specialized in presenting and cross-presenting innocuous antigen to CD4+ and CD8+ T cells. *J. Immunol.* 178: 6861–6866.
45. Raymond, M., M. Rubio, G. Fortin, K. H. Shalaby, H. Hammad, B. N. Lambrecht, and M. Sarfati. 2009. Selective control of SIRP- α -positive airway dendritic cell trafficking through CD47 is critical for the development of T(H)2-mediated allergic inflammation. *J. Allergy Clin. Immunol.* 124: 1333–1342.e1331.
46. Belz, G. T., S. Bedoui, F. Kupresanin, F. R. Carbone, and W. R. Heath. 2007. Minimal activation of memory CD8+ T cell by tissue-derived dendritic cells favors the stimulation of naive CD8+ T cells. *Nat. Immunol.* 8: 1060–1066.
47. Desch, A. N., G. J. Randolph, K. Murphy, E. L. Gautier, R. M. Kedl, M. H. Lahoud, I. Caminschi, K. Shortman, P. M. Henson, and C. V. Jakubzick. 2011. CD103+ pulmonary dendritic cells preferentially acquire and present apoptotic cell-associated antigen. *J. Exp. Med.* 208: 1789–1797.
48. Manolova, V., A. Flace, M. Bauer, K. Schwarz, P. Saudan, and M. F. Bachmann. 2008. Nanoparticles target distinct dendritic cell populations according to their size. *Eur. J. Immunol.* 38: 1404–1413.
49. Jakubzick, C., M. Bogunovic, A. J. Bonito, E. L. Kuan, M. Merad, and G. J. Randolph. 2008. Lymph-migrating, tissue-derived dendritic cells are minor constituents within steady-state lymph nodes. *J. Exp. Med.* 205: 2839–2850.
50. Robays, L. J., T. Maes, S. Lebecque, S. A. Lira, W. A. Kuziel, G. G. Brusselle, G. F. Joos, and K. V. Vermaelen. 2007. Chemokine receptor CCR2 but not CCR5 or CCR6 mediates the increase in pulmonary dendritic cells during allergic airway inflammation. *J. Immunol.* 178: 5305–5311.
51. Hammad, H., and B. N. Lambrecht. 2008. Dendritic cells and epithelial cells: linking innate and adaptive immunity in asthma. *Nat. Rev. Immunol.* 8: 193–204.
52. Walzl, G., S. Tafuro, P. Moss, P. J. Openshaw, and T. Hussell. 2000. Influenza virus lung infection protects from respiratory syncytial virus-induced immunopathology. *J. Exp. Med.* 192: 1317–1326.
53. Williams, A. E., L. Edwards, I. R. Humphreys, R. Snelgrove, A. Rae, R. Rappuoli, and T. Hussell. 2004. Innate imprinting by the modified heat-labile toxin of *Escherichia coli* (LTk63) provides generic protection against lung infectious disease. *J. Immunol.* 173: 7435–7443.
54. Braun-Fahrlander, C., J. Riedler, U. Herz, W. Eder, M. Waser, L. Grize, S. Maisch, D. Carr, F. Gerlach, A. Bufe, et al; Allergy and Endotoxin Study Team. 2002. Environmental exposure to endotoxin and its relation to asthma in school-age children. *N. Engl. J. Med.* 347: 869–877.
55. Eisenbarth, S. C., D. A. Piggott, J. W. Huleatt, I. Visintin, C. A. Herrick, and K. Bottomly. 2002. Lipopolysaccharide-enhanced, toll-like receptor 4-dependent T helper cell type 2 responses to inhaled antigen. *J. Exp. Med.* 196: 1645–1651.
56. Arora, M., S. L. Poe, T. B. Oriss, N. Krishnamoorthy, M. Yarlagadda, S. E. Wenzel, T. R. Billiar, A. Ray, and P. Ray. 2010. TLR4/MyD88-induced CD11b+Gr-1 int F4/80+ non-migratory myeloid cells suppress Th2 effector function in the lung. *Mucosal Immunol.* 3: 578–593.
57. Kuipers, H., D. Hijdra, V. C. De Vries, H. Hammad, J. B. Prins, A. J. Coyle, H. C. Hoogsteden, and B. N. Lambrecht. 2003. Lipopolysaccharide-induced suppression of airway Th2 responses does not require IL-12 production by dendritic cells. *J. Immunol.* 171: 3645–3654.
58. Matsushita, H., S. Ohta, H. Shiraishi, S. Suzuki, K. Arima, S. Toda, H. Tanaka, H. Nagai, M. Kimoto, A. Inokuchi, and K. Izuhara. 2010. Endotoxin tolerance attenuates airway allergic inflammation in model mice by suppression of the T-cell stimulatory effect of dendritic cells. *Int. Immunol.* 22: 739–747.